UNIVERSIDADE ESTADUAL PAULISTA “JÚLIO DE MESQUITA FILHO”

FACULDADE DE CIÊNCIAS FARMACÊUTICAS DE ARARAQUARA

**NAYLA DE SOUZA PITANGUI**

# REGULAÇÃO TRANSCRICIONAL, METABÓLICA E PERFIL DE MICRORNAs DOS BIOFILMES DE *Histoplasma capsulatum:* GENES, METABÓLITOS E RNAs NÃO CODIFICANTES COMO ALVOS TERAPÊUTICOS E/OU BIOMARCADORES

Araraquara

2017

UNIVERSIDADE ESTADUAL PAULISTA "JÚLIO DE MESQUITA FILHO"

FACULDADE DE CIÊNCIAS FARMACÊUTICAS DE ARARAQUARA

**NAYLA DE SOUZA PITANGUI**

# REGULAÇÃO TRANSCRICIONAL, METABÓLICA E PERFIL DE MICRORNAs DOS BIOFILMES DE *Histoplasma capsulatum:* GENES, METABÓLITOS E RNAs NÃO CODIFICANTES COMO ALVOS TERAPÊUTICOS E/OU BIOMARCADORES

Tese apresentada ao programa de Pós-Graduação em Biociências e Biotecnologia aplicadas à Farmácia da Faculdade de Ciências Farmacêuticas de Araraquara – UNESP como pré-requisito para obtenção do título de Doutor.

Orientadora: Profa. Dra. Ana Marisa Fusco Almeida

Coorientador: Dr. Paulo César Gomes

Araraquara

2017

**Ficha Catalográfica**
Elaborada Por Diretoria Técnica de Biblioteca e Documentação
Faculdade de Ciências Farmacêuticas
UNESP – Campus de Araraquara

**P681r**

Pitangui, Nayla de Souza
Regulação transcricional, metabólica e perfil de MicroRNAs dos biofilmes de *Histoplasma capsulatum:* genes, metabólitos e RNAs não codificantes como alvos terapêuticos e/ou biomarcadores / Nayla de Souza Pitangui. – Araraquara, 2017.
243 f. : il.

Tese (Doutorado) – Universidade Estadual Paulista. "Júlio de Mesquita Filho". Faculdade de Ciências Farmacêuticas. Programa de Pós Graduação em Biociências e Biotecnologia Aplicadas á Farmácia. Área de pesquisa em Micologia.

Orientadora: Ana Marisa Fusco Almeida.
Coorientador: Paulo César Gomes.

1. Transcriptômica. 2. Metabolômica. 3. MicroRNAs. 4. *Histoplasma capsulatum*. 5. Biofilmes. I. Almeida, Ana Marisa Fusco, orient. II. Gomes, Paulo César, coorient. III. Título.

**CAPES: 40500005**

NAYLA DE SOUZA PITANGUI

REGULAÇÃO TRANSCRICIONAL, METABÓLICA E PERFIL DE MICRORNAs DOS BIOFILMES DE *Histoplasma capsulatum*: GENES, METABÓLITOS E RNAs NÃO CODIFICANTES COMO ALVOS TERAPÊUTICOS E/OU BIOMARCADORES

Tese de Doutorado apresentada à Faculdade de Ciências Farmacêuticas da Universidade Estadual Paulista – UNESP, Campus de Araraquara como requisito para a obtenção do título de Doutor(a) em Biociências e Biotecnologia aplicadas à Farmácia

Araraquara, 24 de março de 2017.

BANCA EXAMINADORA

ANA MARISA FUSCO ALMEIDA

MARIA LÚCIA TAYLOR

MARIO SERGIO PALMA

GUILHERME TARGINO VALENTE

DANIEL GUARIZ PINHEIRO

Este trabalho foi desenvolvido na Faculdade de Ciências Farmacêuticas de Araraquara/SP – UNESP, sendo a doutoranda contemplada com bolsa da Coordenação de Aperfeiçoamento de Pessoal de Nível Superior – CAPES – e contou com auxílio financeiro da Fundação de Amparo à Pesquisa do Estado de São Paulo – FAPESP (processo nº 2013/05853-1) e do Conselho Nacional de Desenvolvimento Científico e Tecnológico - CNPq Universal (processo nº 480316/2012-0).

**"Por vezes sentimos que aquilo que fazemos não é senão uma gota de água no mar. Mas o mar seria menor se lhe faltasse uma gota".**

***Madre Teresa de Calcuta***

## Dedicatória

**A quem esteve constantemente em meus pensamentos aliviando qualquer aflição e aplaudindo as minhas vitórias: Deus, meus pais Arnaldo e Sônia, meu marido Anderson e a minha jóia preciosa Tomás.**

# Agradecimentos

**Acima de tudo, demonstro minha maior gratidão a Deus, por me capacitar física e intelectualmente para o desenvolvimento deste trabalho e por estar traçando os melhores caminhos para a minha vida.**

**Aos meus pais que, em primeiro lugar, me deram uma base sólida e me fazem viver diariamente o verdadeiro sentido de "família". Como é bom saber que tenho vocês, que sempre me incentivam com suas opiniões que nunca falham sobre os meus caminhos e com seus aplausos que enchem o coração e que fazem todo o esforço valer a pena. Vocês são os meus maiores e melhores professores da vida. A minha gratidão é eterna por tudo o que representam e fazem. Amo vocês meus exemplos!**

**Ao meu marido, Anderson, por todo seu carinho, proteção e amor. Que esteve comigo em todos os momentos desta jornada, tornou os meus dias muito mais leves com o seu carinhoso "Bom dia meu amor", enfrentou sol, chuva e frio pra que eu não ficasse sozinha e acreditou em mim quando eu mesma não acreditei. Impossível não agradecer ainda sua paciência. Amo você minha fortaleza!**

**Ao meu filho amado Tomás, que com toda certeza, tem sido a melhor experiência de toda a minha vida e que tem me incentivado a alcançar os meus maiores sonhos. "Antes deles a gente acha que não vai dar. Que não vai ter tempo, que vai sobrar cansaço. Que está com sono e então "deixa pra amanhã, não tem problema"... mas eles chegam e provam que amanhã vai ser tarde, que na verdade, o cansaço é que a gente deixa pra depois. Que o tempo se multiplica. Que a força se reproduz. Eles nos mostram que o trabalho agora é garantia de escola, viagens, alegria, brinquedos, comida, vacinas, roupinhas e leite. Eles chegam e chacoalham tudo. Eles chegam e tiram tudo do lugar, mas na verdade eles criam novos lugares para tudo. E assim a gente vai... se desdobra para que não falte nada, e não só isso; a gente se vira em mil e uma para que, além de não faltar, que ainda sobre; sobre, principalmente, alguns minutinhos ao lado deles". Amo você minha vida!**

**A minha querida irmã Camila, minha sobrinha Amelie e ao meu cunhado Fábio, que mesmo do outro lado do mundo estão presentes em meus pensamentos e me fizeram entender que quanto maior a distância, maior também é o amor e a alegria do reencontro. Amo vocês minha saudade!**

**A minha avó Amélia (*in memoriam*) que acompanha todas as etapas da minha caminhada e que acalenta meu coração nas horas mais críticas! Amo você eternamente minha companheira!**

**A minha avó Lourdes, por todo amor e carinho!**

**Aos meus sogros Beta e Silvio, aos meus cunhados Danilo, Fabiana e Gustavo, e aos meus sobrinhos Leo e Lara, por me acolherem desde sempre em sua casa e no coração. Hoje nós sabemos que nossa família é o nosso bem maior. Amo vocês minha família!**

**A minha confidente pessoal e profissional, aquela que transmite todo o seu conhecimento e experiência, aquela que não mede esforços pra me fazer o bem, que se doa de todo o coração, que passa meses sem me ver, mas não passa uma semana sem se preocupar comigo, que me deseja o melhor e que me ensinou muito sobre a vida acadêmica. Minha irmã de coração, Janaína!**

**Aquele por quem a afinidade foi imediata, que muito, mas muito mais que um co-orientador soube me ouvir em quantas situações pessoais e profissionais foram necessárias, aquele mineiro que devagar me faz repensar em minhas fraquezas e quer o meu melhor, que assumiu, junto comigo, várias das minhas preocupações e que foi fundamental para o êxito deste trabalho. Meu amigo e professor Paulo!**

**Aquela que foi meu porto seguro em Araraquara, não importa o que havia, eu sabia que poderia contar com ela a qualquer hora do dia ou da noite! Ela me trasmitiu dicas valiosas para ter sucesso em cultura de células, microscopia, citometria de fluxo e maternidade! Minha gratidão é eterna por todo o seu apoio minha grande amiga e mãe do Augusto, Claudia!**

**A quem, graças a Deus, cruzou meu caminho e embora tenha sido por pouco tempo, ocupou um lugar enorme em meu coração e em minha vida! Minha amiga e mãe exemplar Thais Bernardi!**

**A minha comadre e madrinha que me acompanha desde a faculdade! Aquela que passou comigo por muitas experiências ao longo destes 12 anos, dividindo trabalhos e preocupações! A minha amiga Fernanda Gullo!**

**A companheira das horas de almoço, café e desabafo! A quem esteve sempre presente nos últimos 4 anos e se dispôs de coração! A quem me deixou mais segura em Araraquara, minha amiga Natália!**

**A quem tenho imensa admiração e respeito pela sua dedicação incansável à carreira acadêmica. Ah como sou grata por ter conhecido este exemplo de profissional, que não mede esforços e nem distância para transmitir sua experiência e conhecimento! Com toda a certeza a colaboração com ela tornou possível a concretização deste trabalho! Meus sinceros agradecimentos a Professora Maria Lucia Taylor! Agradeço ainda a companheira científica**

**Gabriela Rodríguez-Arellanes por todo o conhecimento compartilhado e pela sua disponibilidade de ajudar em todas as necessidades!**

**A orientadora deste trabalho, que me deu a grande oportunidade de ingressar em um laboratório no qual pude contar com uma estrutura física e científica gigantesca e que, acima de tudo, confiou em meu trabalho. Agradeço a ela por ter permitido que eu fizesse parte deste time. Aquela que se desdobra em mil para que tudo possa correr bem. Com toda certeza ela foi fundamental para o meu crescimento profissional. Agradeço a professora, orientadora, mãe e mais um milhão de funções que ela agarra com unhas e dentes, Ana Marisa Fusco Almeida!**

**A profa. Maria José Soares Mendes Giannini, que me inspira tanto com sua postura pessoal e profissional. Aquela que mesmo ausente se fez tão presente e contribuiu tanto para que "o dar o melhor de mim mesma" fosse feito. Você é um exemplo de sucesso. Obrigada Zezé!**

**Ao professor Francisco Javier Enguita, que me proporcionou a exploração de um mundo novo na investigação dos microRNAs.**

**Ao professor Mario Sergio Palma, por abrir as portas do seu laboratório e acreditar em nosso trabalho!**

**Ao professor Alessandro Varani, pela sua disponibilidade em colaborar com o desenvolvimento deste trabalho dominando as ferramentas de bioinformática!**

**A técnica do laboratório, Rosângela, por toda ajuda e por compartilhar sua infinita experiência comigo. Hoje acredito que ela conhece cada fungo como ninguém e é sempre muito bom contar com o conhecimento dela. Muito obrigada Rô!**

**A Rosemira pelo seu querer bem com o coração mais puro e verdadeiro.**

**A Junya de Lacorte, por quem tenho admiração pela sua dedicação ao trabalho de forma séria e comprometida. Aquela que me ensinou com tanta paciência. Obrigada pela nossa parceria!**

**A todos os companheiros desta vida acadêmica desafiadora, que em algum momento certamente me ajudaram nesta caminhada científica: Lili, Mari, Priscila, Carol Tatoo, Mônica, Rodrigo, Haroldo, Aline, Laranja, Panta, Fer Sangalli, Carol Mineira, Regina, Jaque, Warley, Ana Cerrejón, Suélen, Julhiany, Tati, Wanessa, Luana, Kayla, Fernando Rogério Pavan, Paula Carolina de Souza, Gabriela Guimarães Sousa Leite, Felipe Oliveira, Camila Fernandes, Bibiana, Letícia, Maysa, Rosana, Marina, Christiane Pienna, Alexandra Ivo de Medeiros, Rondinelli Herculano, Natan, Mateus, Bruna, Andrei Moroz, Marisinha, Iracilda Zeppone Carlos, Eliana, Maria Célia Bertolini, Iguatemy Lourenço Brunetti, Renata Pires, Eliana Gertrudes de Macedo Lemos e Rosely Maria Zancopé Oliveira.**

**A dedicação das funcionárias da secretaria de pós-graduação, fundamentais para o bom andamento das atividades acadêmicas. Obrigada Claudia, Daniela, Flávia e Joyce!**

**A minha madrinha e comadre Cynthia Silva, que tem acompanhado de perto todas as etapas mais importantes da minha vida e que torce verdadeiramente pelo meu sucesso.**

**As minhas amigas farmacêuticas, que estão sempre dispostas a ouvir e dividir qualquer dificuldade: Bruna, Carol, Dani, Gi Spósito, Tha Frezin e Thais Ferreira. E aquelas que sempre me acompanham na caminhada da vida: Tawana, Aila e Graciele.**

**A Coordenação de Aperfeiçoamento de Pessoal de Nível Superior - CAPES, ao Conselho Nacional de Desenvolvimento Científico e Tecnológico - CNPq e a Fundação de Amparo à Pesquisa do Estado de São Paulo - FAPESP, pelo suporte financeiro.**

**Enfim, a todos aqueles citados aqui e os que por ventura eu tenha me esquecido, que contribuíram direta ou indiretamente para minha travessia nesta etapa tão importante da minha carreira. Muito obrigada!**

# ÍNDICE DE FIGURAS

# ÍNDICE DE TABELAS

## LISTA DE ABREVIATURAS

ACN – acetonitrila

BCRJ – banco de células do Rio de Janeiro

BHI-broth – meio infusão cérebro-coração caldo

Cbp1 – Calcium binding protein

CBSI – *Candida* bloodstream infections

cDNA – DNA complementar

CFSE – 5(6)-Carboxyfluorescein diacetate N-succinimidyl Ester

CID – decomposição induzida por colisão

Ct – Cycle threshold

$DL_{50}$ – Dose Letal 50%

DMEM – Dulbecco's modified Eagle's medium

DNA – ácido desoxirribonucleico

EF-1α – elongation factor 1-alpha

EPB41 – Erythrocyte protein band 4.1

EthD-1 – homodímero de etídio

ESI – fonte de ionização "electrospray"

FI – intensidade de fluorescência

FR – Forward-reverse

GAPDH – Glyceraldehyde-3-phosphate dehydrogenase

GC/MS – cromatografia gasosa acoplada à espectrometria de massas

GDEs – Genes Diferencialmente Expressos

GO – gene ontology

HBF – high biofilm formers

HIV – Vírus da imunodeficiência humana

Hsp60 – Heat shock protein 60 kDa

IP-PGC-TOF/MS – cromatografia de pareamento iônico-coluna de carbono grafítico poroso acoplada a um sistema de espectrometria de massas do tipo tempo de voo

LC-ESI-MS – cromatografia líquida acoplada à espectrometria de massas por ionização electrospray

LC-MS – cromatografia líquida acoplada à espectrometria de massas

LC-MS/MS – cromatografia líquida acoplada à espectrometria de massas sequencial

LCMS-IT-TOF – espectrômetro de massas híbrido que combina as tecnologias Ion Trap e tempo de voo

LBF – low biofilm formers

LNA – Locked Nucleic Acid

MØ – macrófagos

MEC – matriz extracelular

miRNAs – microRNAs

MOI – multiplicidade de infecção (Multiplicity of infection)

ncRNAs – RNAs não-codificantes

NGS – Next Generation Sequencing

pb – pares de bases

PBS – phosphate-buffered saline

PCR – reação em cadeia pela polimerase

PEI – polissacarídeos extracelulares insolúveis

PES – polissacarídeos extracelulares solúveis

PI – polissacarídeos intracelulares

PMA – phorbol 12-myristate 13-acetate

PMSF – Phenylmethylsulfonyl fluoride

QS – quorum-sensing

RIN – RNA integrity number

RNA – ácido ribonucléico

RNAi – RNA de interferência

RNAm – RNA mensageiro

RNAr – RNA ribossomal

RNAt – RNA transportador

RP – HPLC – Reversed phase high-performance liquid chromatography

RPKM – reads per kilobase por million

RPMI – Roswell Park Memorial Institute

RQ – quantificação relative (Fold Change)

RT-qPCR – reverse transcription-quantitative PCR

SFB – soro fetal bovino

S/N – relação sinal-ruído

TCA – ácido tricloroacético

TFA – ácido trifluoroacético

UFLC – Ultra Fast Liquid Chromatograph

UV – ultravioleta

YPS3 – yeast-phase-specific

## RESUMO

*Histoplasma capsulatum* variedade *capsulatum* é um patógeno fúngico dimórfico causador de uma importante micose sistêmica, denominada histoplasmose. A patogenia da histoplasmose ocorre como resultado da inalação dos microconídios da fase miceliar, que afetam primariamente os pulmões onde ocorre a diferenciação em leveduras, que posteriormente, induzem uma infecção pulmonar e disseminação para outros órgãos, particularmente em indivíduos imunocomprometidos. Recentemente, foi estabelecida uma correlação entre o modo de infecção de *H. capsulatum* e a formação de biofilmes, estruturas caracterizadas como redes tridimensionais complexas que induzem, entre outros, a resistência antifúngica. Por esta razão, é emergente a identificação de um novo alvo e/ou biomarcador que possa ser selecionado, a fim de estabelecer um novo regime terapêutico e/ou ferramenta diagnóstica para a histoplasmose. Com base nisto, este trabalho tem como objetivo analisar a regulação transcricional codificante e metabólica diferencial entre as duas formas de crescimento de *H. capsulatum*, em biofilmes e em crescimento planctônico, bem como determinar o perfil de microRNAs (miRNAs) aberrantes em células hospedeiras em resposta à infecção com leveduras livres e biofilmes. O sequenciamento completo das regiões transcritas foi realizado utilizando a plataforma HiSeq da Illumina e a investigação do padrão de miRNAs em macrófagos (Mø) hospedeiros infectados foi conduzida empregando uma técnica de RT-qPCR (reverse transcription-quantitative PCR). Subsequentemente, a produção de polissacarídeos totais foi determinada em amostras de culturas planctônicas, biofilmes e sobrenadante dos biofilmes e, adicionalmente, a abundância dos metabólitos de natureza não proteica e pequenos peptídeos nestas formas de crescimento foi estabelecida por LC-MS/MS. Em resumo, os dados obtidos revelaram que a estruturação das leveduras em biofilmes induz uma regulação negativa nos processos transcricionais direta (genoma codificante – RNAm) e indiretamente (genoma não-codificante – miRNAs) e, nos processos metabólicos das leveduras, resultante da: a) expressão reprimida da maioria dos genes (≈80% down-regulated) quando as leveduras livres passam a organizarem-se em biofilmes; b) superexpressão de todos os miRNAs alterados na comparação de células infectadas com biofilmes vs. leveduras planctônicas; c) intensidade relativa reduzida (DOWN) da maioria dos metabólitos (57%) produzidos pelas células em biofilmes em relação à intensidade nas homólogas livres, considerando os metabólitos com a mesma massa molecular entre biofilmes e culturas planctônicas e; d) produção significativamente menor de metabólitos exclusivos pelas culturas em biofilmes (8%) vs. células planctônicas (18%). Por conseguinte, no presente estudo, através das abordagens desenvolvidas foram indicadas as moléculas (genes, miRNAs

e metabólitos) que constituem uma fonte potencial para delinear: a) um marcador de biofilmes na infecção às células hospedeiras; b) novos protótipos para a terapêutica da histoplasmose e; c) novos biomarcadores como ferramentas diagnósticas para a histoplasmose.

Palavras-chave: Transcriptômica. Metabolômica. MicroRNAs. *Histoplasma capsulatum*. Biofilmes.

**ABSTRACT**

*Histoplasma capsulatum* variety *capsulatum* is a dimorphic fungal pathogen that causes an important systemic mycosis, called histoplasmosis. The pathogenesis of histoplasmosis occurs as a result of the inhalation of mycelial microconidia, which primarily affect the lungs where differentiation occurs in yeast, which subsequently induce pulmonary infection and dissemination to other organs, particularly in immunocompromised individuals. Recently, a correlation was established between the mode of infection of *H. capsulatum* and the formation of biofilms, structures characterized as complex three-dimensional networks that induce, among others, antifungal resistance. For this reason, it is emerging the identification of a new target that can be selected in order to establish a new therapeutic strategy for histoplasmosis. Based on this, this work aims to analyze the differential transcriptional and coding transcriptional regulation between the two forms of growth of *H. capsulatum* in biofilms and planktonic growth, as well as to determine the profile of aberrant microRNAs (miRNAs) in host cells post-infection with free yeasts and biofilms. Complete sequencing of the transcribed regions was performed using the Illumina HiSeq platform and the investigation of the miRNA pattern in infected host macrophages (Mø) was conducted using a reverse transcription-quantitative PCR (RT-qPCR) technique. Subsequently, the production of total polysaccharides was determined in samples of planktonic cultures, biofilms and supernatant of the biofilms and, additionally, the abundance of non-protein metabolites and small peptides in these growth forms was established by LC-MS/MS. In summary, the data obtained showed that the structure of yeasts in biofilms induces a negative regulation in the direct (coding genome - mRNA) and indirectly (non-coding genome - miRNAs) transcriptional processes and in the yeasts metabolic processes, resulting from: a) suppressed expression of most genes (≈80% down-regulated) when the free yeasts are organized in biofilms; b) overexpression of all altered miRNAs in the comparison of cells infected with biofilms vs. planktonic yeasts; c) reduced relative intensity (DOWN) of most of the metabolites (57%) produced by cells in biofilms compared to the intensity in the free homologues, considering the metabolites with the same molecular mass between biofilms and planktonic cultures; d) significantly lower production of exclusive metabolites by cultures in biofilms (8%) vs. planktonic cells (18%). Accordingly, in the present study, the approaches performed indicated molecules (genes, miRNAs and metabolites) that are a potential source for delineating: a) a marker of biofilms in infection to host cells; b) new prototypes for histoplasmosis therapy and; c) new biomarkers as diagnostic tools for histoplasmosis.

Key words: Transcriptomic. Metabolomic. MicroRNAs. *Histoplasma capsulatum*. Biofilms.

# SUMÁRIO

# Capítulo 1 - Tese

## 1. INTRODUÇÃO

*Histoplasma capsulatum* variedade *capsulatum* é um patógeno fúngico dimórfico, que quando inalado na fase miceliar afeta primariamente os pulmões e, em geral, indivíduos imunocomprometidos, causando uma importante micose sistêmica denominada histoplasmose (Rodríguez-Cerdeira *et al.*, 2012).

As infecções fúngicas invasivas têm aumentado durante as duas últimas décadas na América Latina e no mundo inteiro e, o número de pacientes em risco tem crescido drasticamente (Sifuentes-Osornio, Corzo-León e Ponce-De-León, 2012). Estima-se que aproximadamente 1,2 bilhões de pessoas são acometidas mundialmente por algum tipo de doença fúngica e, este dado se torna ainda mais alarmante considerando o número de pessoas que morrem anualmente por uma doença fúngica, um número que supera as mortes causadas por malária e tuberculose, com uma estimativa de 1,5 a 2 milhões de pessoas (Denning e Bromley, 2015).

A histoplasmose é descrita como uma micose amplamente distribuída nas Américas, com uma particular endemia nos vales dos rios Ohio e Mississipi nos Estados Unidos, México, Brasil e algumas regiões das Guianas (*Guiana Shield*) (Damasceno *et al*., 2016). Além disso, microfocos são registrados no leste dos Estados Unidos, sul da Europa e sudeste da Ásia. Atualmente, tem sido descrito como um patógeno de ampla dispersão geográfica em vista das oito populações genéticas de *H. capsulatum* distribuídas mundialmente entre as latitudes 54° Norte e 38° Sul (Kasuga *et al*., 2003; Anderson *et al*., 2006, Calanni *et al*., 2013), de maneira que tais populações foram classificadas em clados, sendo: (i) clado Norte Americano classe 1; (ii) clado Norte Americano classe 2; (iii) clado Latino Americano grupo A; (iv) clado Latino Americano grupo B; (v) clado Australiano; (vi) clado Holandês; (vii) clado Euro-Asiático e; (viii) clado Africano (Kasuga *et al*., 2003).

No Brasil, micoses sistêmicas ocasionadas por *H. capsulatum* são relativamente comuns, sendo descritas em casos clínicos isolados ou na ocorrência de surtos (Brilhante *et al.*, 2012; Myint *et al.*, 2014). Neste contexto, Oliveira, Unis e Severo (2006) relataram 26 surtos de histoplasmose no Brasil desde 1958, envolvendo 184 pacientes, com o número de casos por surto variando de 2 – 13. No entanto, estes dados não são otimizados uma vez que a histoplasmose pulmonar aguda é pouco diagnosticada e muitas vezes confundida com a tuberculose ou a leishmaniose (Antinori *et al*., 2014).

De fato, surtos de histoplasmose aguda têm sido registrados em diversos Estados brasileiros, entre eles São Paulo, Rio de Janeiro, Espírito Santo, Mato Grosso, Minas Gerais,

Goiás, Amazonas e Rio Grande do Sul, nos quais os indivíduos são infectados após exposição aos propágulos fúngicos em ambientes contaminados, envolvendo também pacientes imunocompetentes (Ferreira e Borges, 2009; Faiolla *et al.*, 2013; Passos *et al*., 2014). Em áreas endêmicas, aproximadamente 10% dos indíviduos imunocompetentes desenvolvem os sintomas da doença (Damasceno *et al.*, 2016). Apesar disso, indivíduos HIV-positivos estão predispostos a infecções fúngicas em função das alterações significativas em sua resposta imune celular (Colombo *et al.*, 2012).

Tendo, portanto, uma distribuição mundial, *H. capsulatum* é encontrado preferencialmente em excrementos de morcegos e aves na sua fase miceliar, a qual se caracteriza como o morfotipo geofílico, sapróbio-infectivo deste fungo, sendo capaz de permanecer no ambiente por períodos prolongados, fator que favorece sua disseminação (Rodríguez-Cerdeira *et al.*, 2012).

Sendo assim, a patogenia da histoplasmose inicia-se quando *H. capsulatum* é adquirido pela inalação de microconídios infectivos ou fragmentos de hifas, que atingem os alvéolos pulmonares, onde ocorre a diferenciação de microconídios em leveduras, que por sua vez são fagocitadas por macrófagos (Mø). As leveduras se multiplicam dentro dos fagolisossomas e, nessa fase, em contraste a função usual dos Mø de eliminar os microrganismos nocivos, estas células propiciam um ambiente favorável e protetor para a sobrevivência e replicação da fase leveduriforme de *H. capsulatum*, a qual se caracteriza como o morfotipo parasitário-virulento deste fungo (Tagliari *et al*., 2012).

Após a infecção, as manifestações clínicas abrangem desde um quadro assintomático, estado que ocorre com grande parte dos hospedeiros imunocompetentes após baixa exposição ao inóculo, à infecção disseminada e rapidamente fatal em hospedeiros imunocomprometidos. O papel da imunidade celular na defesa contra *H. capsulatum* é bem estabelecido (Deepe, 2009; Antonello *et al.*, 2011; Kroetz e Deepe, 2012; Deepe e Buesing, 2012). De fato, a forma disseminada da histoplasmose é mais comumente associada à reativação de focos quiescentes em indivíduos imunocomprometidos, em particular em pacientes infectados com o HIV (Marques *et al*., 2015). Segundo Ferreira e Borges (2009), entre 107 casos de histoplasmose disseminada diagnosticados na enfermaria de Doenças Infecciosas do Hospital de Clínicas da Universidade Federal de Uberlândia, Brasil, apenas um dos casos foi associado a um paciente imunocompetente.

Adicionalmente, os fatores de virulência desenvolvidos pelo fungo são essenciais para o sucesso da infecção. Entre eles destacam-se: a) a transição micélio-levedura induzida pela temperatura, a qual se denomina dimorfismo térmico; b) os mecanismos para aquisição de

ferro; c) uma pequena proteína secretada que é capaz de se ligar ao $Ca^{2+}$ em baixas concentrações (Cbp1); d) uma proteína de choque térmico (Hsp60); e) uma proteína extracelular específica da fase leveduriforme (YPS3); f) um polissacarídeo da parede celular, denominado α-(1-3)-glucano; g) a produção de melanina e; h) a formação dos biofilmes de *H. capsulatum*, que constituem estruturas cruciais no desenvolvimento de infecções, uma vez que microrganismos estruturados em biofilmes exibem altos níveis de resistência aos antimicrobianos em função da baixa perfusão de drogas, favorecendo o desenvolvimento de fenótipos resistentes (Weaver, Sheehan e Keath, 1996; Nosanchuk *et al*., 2002; Rappleye, Engle e Goldman, 2004; Bohse e Woods, 2007; Pitangui *et al*., 2012; Sardi *et al*., 2014).

Um biofilme pode ser definido como uma comunidade séssil de microrganismos, individualizado por células aderentes a um substrato, interface ou adesão célula-célula, circundadas por uma matriz extracelular (MEC) de polissacarídeos e que diferem profundamente das células homólogas livres em relação ao crescimento, expressão gênica e tradução de proteínas (Costerton *et al*., 1995). De fato, nosso grupo tem explorado aspectos únicos e determinantes para a formação dos biofilmes de *H. capsulatum in vitro* e suas possíveis implicações na infecção às células hospedeiras. Da mesma forma, outros investigadores caracterizaram recentemente a susceptibilidade antifúngica reduzida de biofilmes de *H. capsulatum in vitro* frente aos agentes antifúngicos itraconazol e anfotericina B, bem como frente à farnesol sozinho e combinado com antifúngicos, indicando os biofilmes como os prováveis implicadores das infecções fúngicas recorrentes (Brilhante *et al*., 2015).

Diante deste contexto, a gravidade destas formações resistentes na patogênese da histoplasmose se torna ainda mais relevante em vista dos relatos recentes que descrevem clinicamente a identificação de infecções por *H. capsulatum* em indivíduos com dispositivos médicos ou implantes cirúrgicos e ainda, relatos de histoplasmose endovascular em pacientes com implantes vasculares (Carreto-Binaghi *et al*., 2015).

Neste sentido, estudos prévios publicados pelo nosso grupo estabeleceram uma correlação entre o modo de infecção de *H. capsulatum* e a formação dos biofilmes (Pitangui *et al*., 2012; Sardi *et al*., 2014; Pitangui *et al*., 2016). Diante desta problemática, é reafirmada a emergência da identificação de um novo alvo que possa ser selecionado, a fim de estabelecer um novo regime terapêutico para a histoplasmose. Neste contexto, atualmente as abordagens “Ômicas” constituem ferramentas extremamente promissoras para a investigação de alvos e/ou biomarcadores dos biofilmes microbianos, no que diz respeito à quantificação das mudanças globais na abundância de transcritos de RNA mensageiro (RNAm) (transcriptômica), proteínas (proteômica/secretômica) e outros componentes biomoleculares

(metabolômica) em diferentes condições as quais uma célula ou organismo estiver submetido (Ozsolak e Milos, 2011; Muszkieta *et al.*, 2013). Tais ferramentas tiveram início na chamada Era Pós-Genômica e foram desenvolvidas para solucionar as limitações que permeiam a genômica de um organismo em questão. O sequenciamento genômico reflete a informação genética através de técnicas que identificam a sequência de nucleotídeos no genoma do organismo. Assim, é fato que aspectos tais como sequência, número e sintenia dos genes contidos no núcleo de uma célula se mantêm estáticos durante o ciclo celular, no entanto existe um equilíbrio dinâmico entre: a) transcrição gênica, b) tradução proteica e, c) produção de subprodutos metabólicos de acordo com a condição biológica a qual a célula é sujeita, definindo então diferentes transcriptomas, proteomas e metabolomas para a mesma célula ao longo de sua diferenciação celular (De Hoog and Mann, 2004).

Dessa forma, as análises transcriptômica, proteômica e metabolômica podem ser empregadas para a obtenção das diferenças entre a assinatura transcricional, traducional e metabólica de um microrganismo em biofilmes e em crescimento planctônico. Este campo de pesquisa tem adquirido novos conceitos e neste contexto Azevedo *et al.* (2009) sugeriu uma nova tendência, a chamada "biofômica" (*biofomics*) – uma abordagem "Ômica" para o campo dos biofilmes. O objetivo desta abordagem é reunir em um banco de dados o grande conjunto de dados ômicos gerados a partir dos estudos da habilidade de um microrganismo aderir à superfícies, se comunicar com células vizinhas e formar biofilmes. Tais dados coletados seriam disponíveis à comunidade científica e identificariam uma única assinatura dos biofilmes incluindo informações importantes como, fatores ambientais, fisiológicos e mutacionais que afetam a capacidade de um microrganismo desenvolver biofilmes. Isto poderia então impactar positivamente na Biologia de Sistemas e consequentemente no desenvolvimento de uma nova ferramenta diagnóstica e/ou terapêutica para estas formações resistentes.

O transcriptoma total comparativo constitui uma abordagem estratégica para investigar fatores envolvidos na patogênese de *H. capsulatum*. Esta análise utiliza o sequenciamento do RNA em larga escala caracterizando o transcriptoma, que corresponde ao conjunto completo de regiões transcritas em um genoma de maneira significativamente mais sensível quando comparado às abordagens de hibridização *microarray* (Wang *et al.*, 2009a). Os dados obtidos utilizando sequenciamento de RNA também têm sido utilizados para identificar novos eventos de *splicing* e quantificar a expressão de genes a partir de células cultivadas em diferentes condições experimentais (Marioni *et al.*, 2008; Mortazavi *et al.*, 2008; Sultan *et al.*, 2008; Trapnell, Pachter e Salzberg, 2009).

Segundo Wang *et al*. (2009b), plataformas de RNA-Seq são extremamente sensíveis e, neste estudo, caracteriza-se como uma ferramenta útil para categorizar, de forma inédita, os genes que representam a assinatura transcricional de *H. caspulatum* em suas diferentes formas de crescimento (biofilmes e planctônico), de maneira que serão identificados genes candidatos potenciais que codificam proteínas chave e que podem ser amplamente estudados como putativos alvos terapêuticos e/ou biomarcadores durante a infecção às células hospedeiras.

Alguns estudos têm reportado alterações transcricionais nos biofilmes de espécies de bactérias, entre elas *Pseudomonas aeruginosa*, *Desulfovibrio vulgaris* e espécies de *Sulfolobus* (Manos *et al*., 2008; Koerdt *et al.*, 2011; Clark *et al.*, 2012) e patógenos fúngicos, como *Candida albicans* (De Cremer *et al*., 2016).

Neste contexto, muitas informações importantes têm sido obtidas a partir da utilização de métodos Ômicos empregados em estudos recentes e tais informações podem ser integradas para o desenvolvimento de uma nova terapia das infecções causadas por biofilmes fúngicos.

No âmbito das análises transcriptômicas, uma investigação recente destaca dados relevantes a cerca dos biofilmes de *C. albicans.* Tal espécie caracteriza-se como a mais prevalente e patogênica entre todas as espécies de *Candida* relacionadas às infecções sistêmicas (*Candida* bloodstream infections – CBSI) e, este fato, é decorrente da habilidade do patógeno de formar biofilmes robustos. De acordo com Rajendran *et al.* (2016), os isolados clínicos de candidemia podem ser estratificados em dois grupos, os quais podem ter: a) alto potencial de formação de biofilmes (high biofilm formers – HBF) e; b) baixo potencial de formação de biofilmes (low biofilm formers – LBF). Assim, há um fenótipo heterogêneo dos biofilmes, o qual, de acordo com a sua classificação, impacta diretamente nos resultados clínicos e na mortalidade. Os autores deste estudo constataram, por análise comparativa de RNA-Seq, que há uma expressão gênica diferencial significativa entre os isolados HBF e LBF de *C. albicans*. A partir dos resultados transcriptômicos obtidos foi possível destacar uma importância destacada para a via aspartato aminotransferase na formação dos biofilmes, a qual pode ser explorada como um potencial alvo em biofilmes fúngicos.

A abordagem metabolômica permite um melhor entendimento acerca dos fenômenos complexos que ocorrem em nível de metabólitos durante os estágios de desenvolvimento de um biofilme, identificando os metabólitos em diferentes vias celulares e os avaliando como alvos terapêuticos potenciais e/ou como marcadores do biofilme na infecção às células hospedeiras. Com esta finalidade, plataformas de cromatografia líquida acoplada à espectrometria de massas (LC-MS/MS) têm sido amplamente empregadas na identificação de biomarcadores (Hou *et al*., 2014; Li *et al*., 2014; Zhou *et al.*, 2014). Dessa forma, neste

trabalho foi desenvolvida a padronização de uma análise metabolômica não direcionada para detecção de diversos grupos de metabólitos como moléculas de baixa massa molecular não proteicas e pequenos peptídeos, a fim de se obter posteriormente, um perfil metabólico característico de *H. capsulatum* em suas diferentes formas de crescimento. Tendo em vista o estudo do metabolismo celular, é necessário destacar algumas descrições feitas por Lindon *et al*. (2006) a partir dos seguintes conceitos: a) o metaboloma de um sistema biológico compreende o conjunto de todos os compostos químicos (intra- e extracelulares) consumidos (substratos) e excretados (metabólitos); b) o perfil metabólico, também denominado metabolômica, é definido como a investigação quantitativa de uma classe ampla de substratos intracelulares e metabólitos e; c) fingerprinting metabólico, também denominado metabonômica, constitui uma investigação qualitativa de metabólitos selecionados necessários para classificar uma amostra.

Uma investigação conduzida por Zhu *et al.* (2013) revelou o perfil metabólico dos biofilmes de *C. albicans* por uma técnica de cromatografia gasosa acoplada à espectrometria de massas (GC/MS), a partir da qual foram identificados 31 metabólitos produzidos diferencialmente entre culturas de biofilmes e células planctônicas. Este estudo demonstrou ainda que a trealose é determinante para o desenvolvimento dos biofilmes de *C. albicans*, uma vez que a ausência deste metabólito resultou na formação anormal e no aumento da sensibilidade dos biofilmes aos agentes antifúngicos anfotericina B e miconazol. Adicionalmente, um estudo desenvolvido por Chen *et al*. (2014) detectou 16 metabólitos diferencialmente produzidos entre culturas planctônicas e biofilmes de *C. albicans*, dos quais a maioria foi identificada como aminoácidos ou compostos relacionados, através de um sistema de cromatografia de pareamento iônico-coluna de carbono grafítico poroso acoplada a um sistema de espectrometria de massas do tipo tempo de voo (IP-PGC-TOF/MS).

Então, em vista da complexidade e da variabilidade dos biofilmes de fungos patogênicos, a integração de diferentes dados "Ômicos" se faz necessária. A combinação dos métodos "Ômicos" constitui um campo que tem sido explorado por alguns grupos de pesquisa em função da complementariedade entre eles. Esta combinação é o principal desafio da biologia de sistemas em vista da grande quantidade de dados gerado pelos projetos "Ômicos", os quais, uma vez integrados permitem o mapeamento e a elucidação de informações peculiares, em termos quantitativos, a cerca do comportamento de uma célula, tecido ou organismo em uma determinada condição biológica a qual estiver submetido (Moreira, 2015). Muszkieta *et al.* (2013) integraram três diferentes métodos "Ômicos", *microarray*, RNA-seq e análise proteômica, para comparar as diferentes assinaturas transcriptômica e proteômica dos

biofilmes de *Aspergillus fumigatus.* De acordo com os autores, alguns genes foram, de fato, correspondentes às proteínas diferencialmente reguladas, no entanto, há muitos desafios que permeiam a correlação entre dados de transcriptoma e proteoma. Estes desafios referem-se ao fato de que os dados detectados do transcriptoma codificante (RNAm) não refletem todos os processos regulatórios de uma célula, tais como os processos pós-transcricionais e a regulação pós-traducional, reafirmando a necessidade de integrar as abordagens "Ômicas". Assim, a comparação e a integração de abordagens "Ômicas" em diferentes níveis tem um potencial promissor para fornecer novas informações, que se reúnem para caracterizar a assinatura dos biofilmes microbianos, no que diz respeito à habilidade de formação, atividade fisiológica e estrutura.

De maneira adicional, a identificação dos microRNAs (miRNAs) expressos por uma célula ou organismo em uma determinada condição caracteriza o miRNoma. Assim, a identificação dos miRNAs diferencialmente expressos após interação *H. capsulatum*-célula hospedeira também constitui uma abordagem de importância cada vez mais reconhecida a ser desenvolvida neste trabalho, em vista da ocorrência generalizada dos miRNAs e suas diversas funções como moléculas regulatórias (Law *et al.*, 2013).

De fato, RNAs não-codificantes (ncRNAs) ganharam a atenção de muitos pesquisadores em função de inúmeras investigações que destacam o seu papel em diversos processos biológicos e doenças, incluindo vários tipos de cânceres humanos, doenças cardiovasculares e doenças respiratórias alérgicas, principalmente por regularem a expressão de vários genes (Garofalo, Leva e Croce, 2014; Leung e Natarajan, 2014; Liu *et al*., 2014; Rebane e Akdis, 2014; Yao-Shu, Xiao-Lin e Yong, 2014). Entre os ncRNAs, destacam-se os miRNAs, pequenas moléculas de RNA que afetam a estabilidade dos RNAm e cujas funções regulatórias são bem estabelecidas (O'connell *et al.*, 2010).

Os miRNAs apresentam-se em cadeia simples com 19 a 23 nucleotídeos e, de forma geral, a biogênese dessas pequenas moléculas tem origem no núcleo celular chegando ao citoplasma onde reconhecem os RNAm alvos e reprimem os processos pós-transcricionais ou induzem a clivagem do RNAm (Chitwood e Timmermans, 2007; Costa, Leitão e Enguita, 2012). As proteínas Argonautas, presentes no citoplasma, estão envolvidas no processo de maturação do miRNA, permitindo sua ligação ao RNAm, para que então inicie a inibição dos processos trancricionais dos RNAm-alvo. Essa atividade regulatória que miRNAs apresentam é um processo complexo, uma vez que um único RNAm transcrito pode ser alvo de vários miRNAs, assim como um único miRNA pode regular diversos RNAm-alvo (Costa, Leitão e Enguita, 2012; Turchinovich *et al*., 2013).

De maneira detalhada, a biogênese dos miRNAs inicia-se no núcleo a partir de um locus específico do genoma onde há a formação de um miRNA primário (ou pri-miRNA). Este miRNA é processado pelo complexo DROSHA-DGCR8, o que resulta na formação de um miRNA precursor também chamado pré-miRNA, que por sua vez é transportado para o citoplasma através de poros nucleares pela Exportina 5. No citoplasma, os pré-miRNAs são reconhecidos pela enzima DICER, que é responsável pela clivagem do loop destes precursores, processo que culmina na obtenção de fragmentos de 19 a 23 pares de bases e que permanecem ligados a essa enzima. Este complexo, entre a DICER e o pequeno fragmento, recruta diversas proteínas da família Argonauta, que em conjunto formam o complexo RISC. Finalmente, este complexo agrupado com o miRNA maduro têm como alvo uma sequência complementar do RNAm atuando na regulação negativa da expressão gênica por induzirem a clivagem da cauda poli-A (deadenilação) através da ação de exonucleases ou por inibirem a ação dos ribossomos na tradução (Li e Rana, 2014).

Poucas investigações têm demonstrado a expressão anormal de miRNAs em células hospedeiras em resposta às infecções fúngicas. Neste contexto, são descritos os miRNAs com expressão significativamente aumentada ou diminuída em relação aos controles em células epiteliais respiratórias e Mø murinos infectados com *C. albicans* e, em monócitos humanos e células dendríticas infectadas com *A. fumigatus* (Monk *et al*., 2010; Das Gupta *et al*., 2014; Muhammad *et al*., 2015; Agustinho *et al*., 2017). Recentemente, um estudo descreveu ainda o perfil de miRNAs desregulados após a infecção por *C. albicans in vivo*, em modelo animal alternativo *Caenorhabditis elegans* e, identificaram 16 miRNAs superexpressos e 4 miRNAs reprimidos nos nematodos em resposta à infecção (Sun *et al*., 2016). Com base nisso, os resultados obtidos no presente estudo contemplam a identificação de miRNAs desregulados em Mø hospedeiros em resposta à infecção com leveduras de *H. capsulatum* empregando a tecnologia de RT-qPCR (reverse transcription-quantitative PCR), uma plataforma que determina a abundância relativa de miRNAs nas amostras biológicas selecionadas.

Neste contexto, a identificação dos miRNAs anormalmente regulados em uma célula infectada constitui uma abordagem promissora para o desenvolvimento de novas opções terapêuticas e ferramentas diagnósticas. Em vista das alternativas terapêuticas empregando miRNAs, atualmente destaca-se uma tecnologia baseada na administração de um RNA de interferência (RNAi) para regular ou mimetizar a função de um miRNA *in vivo*. Tal tecnologia fundamenta-se na utilização dos chamados antimiRs ou mimics. Os antimiRs caracterizam-se como oligonucleotídeos anti-sentido de cadeia simples utilizados para inibir a função de um miRNA. Embora o mecanismo de ação exato destas moléculas permaneça

desconhecido, esta ferramenta tem demonstrado eficácia *in vivo* ao atuar em um miRNA e impedir sua atividade de repressão gênica, por meio da complementariedade perfeita entre a sequência do oligonucleotídeo administrado e o miRNA-alvo (Van Rooij *et al.,* 2008). Com este intuito, a indústria farmacêutica Santaris Pharma desenvolveu uma droga experimental para o tratamento da hepatite C, nomeada Miravirsen (anteriormente conhecido como SPC3649), a qual atua como um antagonista de miR-122, um miRNA reconhecidamente importante para a replicação do vírus da hepatite C. Atualmente, a droga encontra-se em fase II de Ensaios Clínicos e, quando administrada por via intravenosa ou subcutânea em chimpanzés tem impedido a função do miR-122 resultando na redução da carga viral (Borgia *et al*., 2016). Por outro lado, as opções terapêuticas com o emprego de miRNAs também concentram-se no fornecimento sintético de um miRNA mimic. Os mimics são oligonucleotídeos curtos de fita-dupla que são reconhecidos e transportados até o complexo RISC no citoplasma celular, a partir do qual o oligonucleotídeo pode atuar como um miRNA endógeno aumentando o nível do miRNA de interesse e bloqueando potencialmente a expressão do(s) gene(s)-alvo (Van Rooij *et al.*, 2008).

Adicionalmente, no âmbito do diagnóstico, miRNAs têm sido propostos como biomarcadores estáveis de várias doenças e neste campo de pesquisa, a nova ferramenta miRview mets (Rosetta Genomics Ltd., Nova Jersey, EUA) representa o que há de mais atual e evoluído. Esta ferramenta caracteriza-se como um teste diagnóstico capaz de identificar o tecido de origem de um tumor metastático por meio da quantificação do nível de expressão de 48 miRNAs reconhecidos como biomarcadores tumorais. Assim, o teste tem a propriedade de designar o sítio primário para uma amostra de câncer com base na expressão de miRNAs do tecido tumoral (Meiri *et al*., 2012).

Então, em linhas gerais, os objetivos propostos e executados neste projeto concentraram-se na busca de um novo alvo (terapia) e/ou candidatos a marcadores moleculares (diagnóstico) da histoplasmose em hospedeiros eucarióticos, a fim de estabelecer com clareza as vias de sinalização alteradas nos sistemas de infecção estudados. Para tanto, as tecnologias “Ômicas”, entre elas, transcriptoma e metaboloma, e um screening de miRNAs foram as abordagens empregadas para investigar a regulação transcricional, metabólica, bem como o perfil de RNAs não codificantes (miRNAs) de células leveduriformes de *H. capsulatum* estruturadas em biofilmes e os resultados obtidos são fundamentais para a consolidação do estudo da virulência dos biofilmes de *H. capsulatum* destacando informações científicas inovadoras a respeito do tema na ciência.

## 2. OBJETIVOS

### 2.1. Objetivo Geral

Investigação de potenciais alvos terapêuticos e/ou biomarcadores a partir da identificação de transcritos, metabólitos de natureza não proteica e pequenos peptídeos em biofilmes e culturas planctônicas de *H. capsulatum* através da análise do transcriptoma e metaboloma, bem como investigação dos miRNAs desregulados em Mø hospedeiros após a infecção.

### 2.2. Objetivos específicos

• Obtenção dos RNAs de cepas de *H. capsulatum* e controle de qualidade das amostras;

• Sequenciamento Hi Seq (Illumina) do RNA extraído das amostras de *H. capsulatum*;

• Análise dos Genes Diferencialmente Expressos (GDEs) entre culturas planctônicas e biofilmes de *H. capsulatum* e entre cepas nacional e internacional;

• Identificação, categorização funcional e localização de domínios proteicos dos GDEs;

• Quantificação da porcentagem de infecção de diferentes cepas de *H. capsulatum* a Mø alveolares murinos (AMJ2-C11) e determinação da viabilidade celular após infecção;

• Quantificação da porcentagem de infecção de diferentes cepas de *H. capsulatum* a Mø humanos (THP-1) e ensaio de viabilidade de Mø THP-1 like infectados com *H. capsulatum*, para definição da Multiplicidade de Infecção (Multiplicity of Infection, MOI);

• Screening de miRNAs expressos em Mø hospedeiros (Mø THP-1 like) após interação com leveduras de *H. capsulatum*;

• Determinação de polissacarídeos totais em amostras de culturas planctônicas, biofilmes e sobrenadante dos biofilmes de *H. capsulatum*;

• Extração de metabólitos produzidos e/ou modificados por *H. capsulatum* em biofilmes e sob condições planctônicas;

• Análises metabolômicas de *H. capsulatum* em biofilmes e em crescimento planctônico.

### 2.3. Representação Esquemática

A Figura 1 organiza de forma esquemática as moléculas correspondentes a cada uma das tecnologias “Ômicas”, destacando as abordagens desenvolvidas neste estudo, entre elas o transcriptoma, com enfoque para o estudo dos RNAs codificantes (RNAm) e não-codificantes (miRNAs) e, o metaboloma intracelular, direcionado para a detecção de moléculas de baixa massa molecular não proteicas e pequenos peptídeos.

**Figura 1. Representação Esquemática das tecnologias "Ômicas" e suas moléculas.** Destaque para as abordagens desenvolvidas neste estudo, entre elas Transcriptoma codificante e não-codificante (alaranjado) e metaboloma intracelular (amarelo).

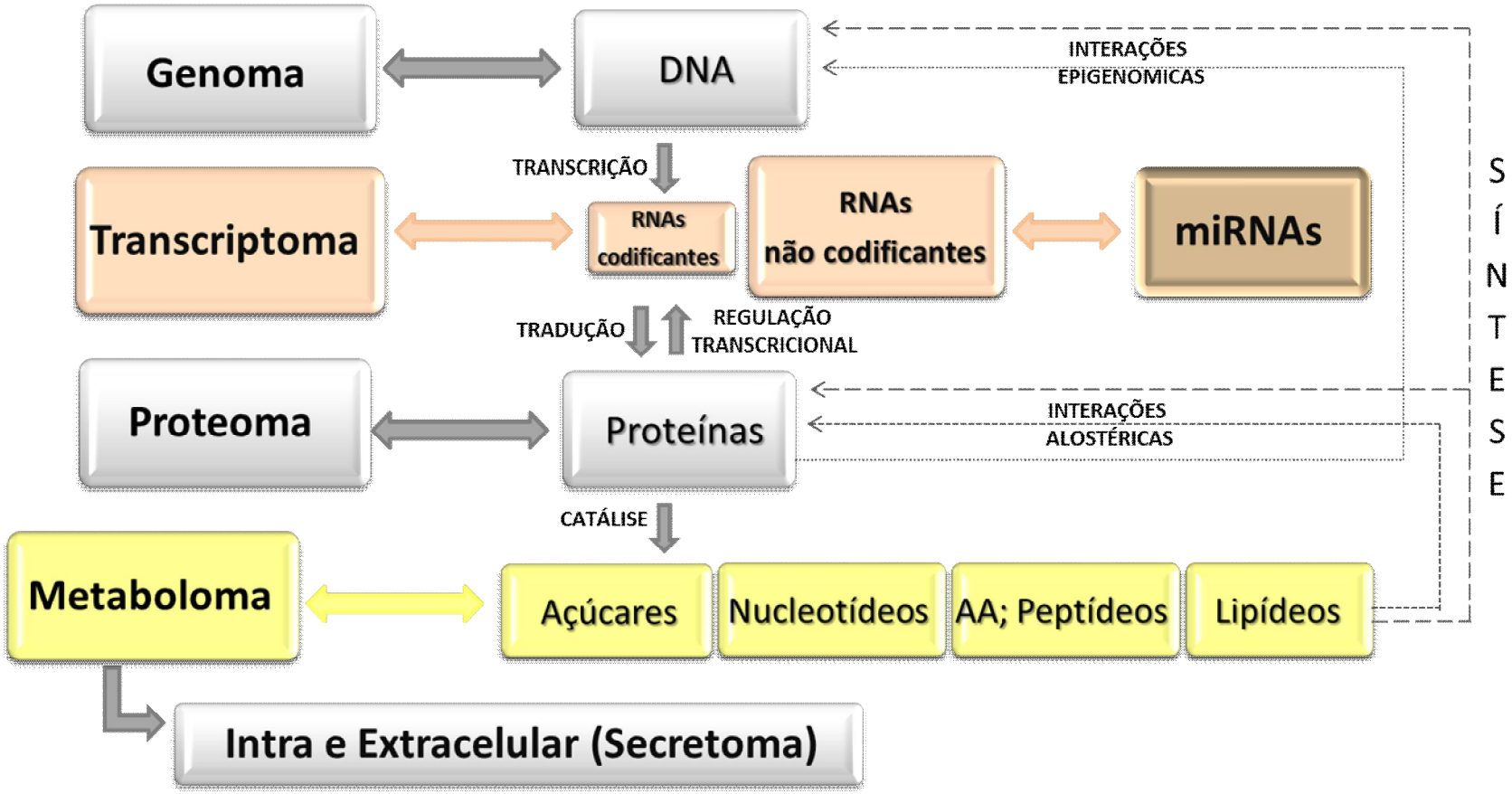

# 3. MATERIAIS E MÉTODOS

## 3.1. Microrganismos e condições de cultivo

Para a realização dos ensaios foram empregadas duas cepas de *H. capsulatum*, EH-315 e 60I. EH-315 foi isolada do intestino de um morcego infectado, espécie *Mormoops megalophylla*, capturado em uma caverna no estado de Guerrero, México, depositada na Coleção de Culturas de *H. capsulatum* do Laboratório de Imunologia de Fungos do Departamento de Microbiologia e Parasitologia da Faculdade de Medicina da Universidade Nacional Autônoma do México (UNAM) (www.histoplas-mex.unam.mx), México, registrada no banco de dados da Federação Mundial para Coleção de Culturas sob o número LIH-UNAM WDCM817. A cepa 60I foi isolada da boca de um paciente infectado, 49 anos, da cidade de Araraquara, São Paulo, Brasil e está depositada na Coleção do Laboratório de Micologia Clínica da Faculdade de Ciências Farmacêuticas da Universidade Estadual Paulista Júlio de Mesquita Filho (UNESP), Brasil.

Diante do exposto, as cepas empregadas neste estudo foram isoladas de diferentes fontes e ensaios previamente realizados demonstram que a cepa EH-315 exibe maior infectividade (Dose letal 50% - $DL_{50}$ – 3 x $10^5$ leveduras/mL) em relação à cepa 60I ($DL_{50}$ – 3 x $10^8$ leveduras/mL) sob condições experimentais empregando um ensaio de determinação da $DL_{50}$ em camundongos BALB/c machos (ML Taylor, comunicação pessoal).

Em uma investigação filogeográfica conduzida por Kasuga e colaboradores (2003), a cepa EH-315 é descrita como uma linhagem solitária, mas que se associa distancialmente ao clado Norte Americano classe 2. Tal classificação se deve ao fato de que a cepa EH-315 representou um genótipo único não pertencente a nenhum dos oito clados categorizados. Porém, segundo os autores, é importante ressaltar que a amostragem realizada, para a classificação mundial dos isolados, favoreceu isolados clínicos humanos e a cepa EH-315 se opõe a essa característica, uma vez que foi obtida a partir de um morcego silvestre. Então, é provável que estas linhagens, definidas como solitárias, representem populações maiores de fungos na natureza e, que não foram amostradas adequadamente pela investigação realizada.

Considerando a cepa 60I, sua categorização filogenética foi desenvolvida sob coordenação da Profa. Maria Lúcia Taylor no Laboratório de Imunologia de Fungos da Universidade Nacional Autonoma do México, de maneira que tal cepa é categorizada como pertencente ao clado Latino Americano grupo A (Taylor, M. L., 2017. Dados não publicados).

A fase leveduriforme de cada cepa foi mantida em meio infusão cérebro-coração caldo (BHI-broth) (Difco$^{TM}$) suplementado com 0,1% de cisteína e 1% de glicose, e incubada a 37°C durante 24 h sob agitação (100 rpm).

### 3.2. Culturas planctônicas e formação dos biofilmes de *H. capsulatum*

Para a formação dos biofilmes, os ensaios foram realizados conforme descrito por Peeters *et al.* (2008) com modificações descritas por Pitangui *et al.* (2012). Inicialmente, as leveduras foram suspensas em solução salina ou phosphate-buffered saline (PBS) 0,01M pH 7,2 e a suspensão ajustada à concentração de $5x10^6$ células/mL por contagem em hemocitômetro de Neubauer. Em seguida, 500 µL do inóculo foram adicionados às placas de poliestireno de 24 poços (TPP®, Trasadingen, Switzerland). As placas foram incubadas em agitador orbital a 80 rpm, 37°C, por 7 h para pré-adesão dos biofilmes. Posteriormente, 2.000 µL de BHI caldo suplementado com 0,1% de cisteína e 1% de glicose foram adicionados nos poços e as placas foram mantidas sob incubação por 72 h para a maturação dos biofilmes.

O crescimento planctônico, livre ou flutuante das leveduras de *H. capsulatum* foi realizado em erlenmeyer de 250 mL sob as mesmas condições de temperatura, nutrientes e período de incubação citadas anteriormente para a formação do biofilme maduro.

### 3.3. Análise transcriptômica

#### 3.3.1. Extração do RNA das cepas EH-315 e 60I de *H. capsulatum* para sequenciamento em larga escala (Illumina Hi Seq) utilizando o kit RNeasy Plant Mini Kit®

A extração do RNA das amostras foi realizada utilizando o kit RNeasy Plant mini kit® (Qiagen, Gaithersburg, MD) de acordo com as instruções do fabricante. Inicialmente, 100 mg de células leveduriformes (pellet celular), em biofilmes e em crescimento planctônico, foram rompidas com pérolas de vidro (3 mm) e congelamento em nitrogênio líquido. Em seguida, foram adicionados 450 µL do tampão RLC (fornecido) para um máximo de 100 mg de células, que foram vortexadas vigorosamente. Posteriormente, o lisado foi transferido para um pré-filtro acoplado a um tubo coletor de 2 mL (QIAshredder spin column – Lilás) e, então, centrifugado por 2 min a velocidade máxima (14.000 rpm). Em seguida, o pré-filtro foi descartado e o sobrenadante transferido para um novo tubo de microcentrifugação, cuidadosamente para não entrar em contato com os detritos do sedimento celular. Ao lisado limpo, foi adicionado etanol v/v (96 – 100%) e misturado imediatamente com o auxílio de uma pipeta. Então, a amostra foi transferida para um novo pré-filtro acoplado a um tubo coletor de 2 mL (RNeasy Mini spin column – Rosa). Novamente, a

amostra foi centrifugada por 15 s a 10.000 rpm e, após centrifugação, o líquido filtrado, presente no tubo coletor, foi descartado. O pré-filtro foi acoplado ao mesmo tubo coletor e ao pré-filtro foram adicionados 700 µL do tampão RW1, que foi novamente centrifugado por 15 s a 10.000 rpm, do qual o fluxo líquido foi novamente descartado. Em seguida, foram adicionados 500 µL do tampão RPE e centrifugado por 15 s a 10.000 rpm, a partir do qual o líquido foi novamente descartado do tubo coletor. Foi repetida a adição de 500 µL do tampão RPE e centrifugação por 2 min a 10.000 rpm, com posterior descarte do fluxo líquido. Uma etapa adicional foi realizada que consiste em acoplar a coluna de centrifugação (rosa) em um novo tubo de coleta e centrifugá-lo a velocidade máxima por 1 min para secar a membrana. Ao final, a coluna de centrifugação foi transferida para um novo tubo coletor de 1,5 mL, e à coluna foram adicionados 50 µL de água RNase-free. A amostra foi centrifugada por 1 min a 10.000 rpm para eluição do RNA total a partir da membrana. O RNA extraído foi recolhido em um único tubo.

### 3.3.2. Quantificação e avaliação da pureza e integridade do RNA das amostras

A quantificação das amostras após extração do RNA foi realizada em espectrofotômetro NanoVue Plus® (GE Healthcare), de forma a obter a concentração em ng/µL. Além disso, a pureza do RNA extraído foi analisada por espectrofotometria (NanoVue Plus, GE) com base na razão da absorbância $A_{260nm}/A_{280nm}$, sendo descrita como pureza ideal, o intervalo de 1,8 a 2,0. Posteriormente, a integridade do RNA das amostras foi avaliada, utilizando o equipamento Agilent 2100 Bioanalyzer® (Agilent Technologies) para análise do RNA extraído de eucariotos seguindo as recomendações do fabricante e, portanto, considerando o parâmetro RNA Integrity Number (RIN) como um valor maior ou igual a 8.

### 3.3.3. Construção das bibliotecas de DNA complementar (cDNA)

As bibliotecas de cDNA das cepas EH-315 e 60I de *H. capsulatum*, em crescimento planctônico e em biofilmes, foram preparadas segundo o protocolo TruSeq® RNA Sample Preparation v2 (Illumina Inc.; San Diego, CA, EUA) de acordo com as recomendações do fabricante com algumas adaptações descritas abaixo.

Inicialmente, o RNAm foi isolado, purificado e, em seguida foi realizada a fragmentação enzimática do RNAm e posterior ligação de random primers (oligonucleotídeos randômicos) para se proceder com a síntese da primeira fita de cDNA, utilizando-se para isto a enzima transcriptase reversa (SuperScript/Invitrogen). Após a síntese da primeira fita de cDNA, procedeu-se para a síntese da segunda fita, tendo ao final do processo um cDNA dupla fita. Então, esferas magnéticas (kit Ampure XP beads) foram adicionadas a fim de isolar o cDNA dupla fita do restante dos reagentes. Após este passo foi feita a reparação das

extremidades 3’ e 5’. Nesta etapa as extremidades 3’ e 5’ do cDNA fragmentado, que estão não-coesivas, foram reparadas usando o reagente End-Repair Mix da Illumina. O End-Repair Mix tem atividade exonuclease, que remove as pontas das extremidades 3’ e atividade polimerase que complementa as extremidades 5’ do cDNA fragmentado, de maneira que no final do processo foi obtido o cDNA fragmentado e com as extremidades coesivas.

Após a etapa de End-Repair um único nucleotídeo A (adenina) foi aderido à extremidade 3’ do cDNA fragmentado e reparado, a fim de prevenir que este fragmento de cDNA se ligue erroneamente a outro fragmento de cDNA durante a ligação dos adaptadores, já que a extremidade 3’ do adaptador apresenta um único nucleotídeo T (timina), que é complementar ao fragmento de cDNA que foi adenilado. Esta estratégia garante uma baixa formação de quimeras. Assim, os adaptadores, com barcodes específicos, foram ligados nas extremidades dos cDNAs fragmentados, preparando-os para a hibridização na lâmina de sequenciamento.

Posterior a ligação dos adaptadores foi feito o enriquecimento dos fragmentos de cDNA através de uma reação em cadeia pela polimerase (PCR) para enriquecer os fragmentos de cDNA que apresentam adaptadores ligados nas duas extremidades, 3’ e 5’. A PCR foi realizada utilizando-se primers que se anelam às extremidades dos adaptadores, garantindo que apenas os fragmentos de cDNA ligados aos adaptadores sejam amplificados. Para evitar distorções da representação da biblioteca, o número de ciclos utilizados na PCR foi o mínimo possível, em média 10 ciclos.

Ao final deste processo foi obtida a biblioteca que, posteriormente foi validada e quantificada antes do sequenciamento da mesma. A validação das bibliotecas de cDNA de ambas as cepas de *H. capsulatum*, em biofilmes e em crescimento planctônico, foi realizada através de eletroforese capilar no Agilent 2100 Bioanalyzer® (Agilent Technologies) com o chip específico para DNA (Agilent DNA-1000) e, para isto foi utilizado 1 µL da biblioteca e os procedimentos foram desenvolvidos conforme as recomendações do fabricante. A quantificação das bibliotecas foi feita através de uma quantificação absoluta qPCR, utilizando-se o aparelho 7500 Real Time PCR System (Applied Biosystems), de acordo com as recomendações do Guia Illumina Sequencing Library qPCR Quantification. A etapa seguinte consiste na normalização de todas as bibliotecas para uma concentração de 2 nM. Então, esta concentração foi validada utilizando o fluorímetro Qubit® 2.0 (Invitrogen) e os reagentes do Kit Qubit® dsDNA HS Assay (Life Technologies) e, finalmente as bibliotecas de cDNA foram ajustadas para uma concentração final de 18 pM.

### 3.3.4. Clusterização e sequenciamento dos transcritos das cepas EH-315 e 60I de *H. capsulatum* em biofilmes e em crescimento planctônico

O sequenciamento das bibliotecas de cDNA das cepas EH-315 e 60I de *H. capsulatum* nas duas formas de crescimento estudadas, foi realizado no Laboratório Multiusuário Centralizado ("Facility") para Sequenciamento de DNA em Larga Escala e Análise de Expressão Gênica da Faculdade de Ciências Agrárias e Veterinárias localizada no Campus da UNESP em Jaboticabal utilizando a plataforma HiScanSQ System (Illumina). Para isto foram utilizados dois kits. Inicialmente, foi utilizado o kit Paired-End Cluster Generation Kit v3 (Illumina), que se constitui por um conjunto de reagentes para geração de clusters paired-end no equipamento cBot utilizando a versão 3 de flow cell e que permite a estratégia de multiplex na plataforma HiSeq. Posteriormente, foi utilizado o kit TruSeq™ SBS Kit v3 - 200 Cycles (Illumina), constituído por reagentes que permitem até 209 ciclos de sequenciamento no sistema HiSeq e os procedimentos adotados seguiram as recomendações do fabricante. A técnica da Illumina baseia-se no sequenciamento por síntese, no qual bases únicas, que constituem os quatro nucleotídeos (ACGT), são incorporados à fita de DNA. Além disso, esta técnica inclui a utilização de um terminador reversível marcado fluorescentemente que gera uma fluorescência específica para cada base incorporada e então é clivado para permitir a incorporação da próxima base. Depois de cada etapa da síntese, os clusters são excitados por um laser emitindo a fluorescência da última base incorporada. Este sinal fluorescente é capturado por uma câmera, produzindo imagens da flow cell. Ao final deste processo, é feita a montagem das sequências específicas de cada uma das amostras.

### 3.3.5. Análise dos dados de sequenciamento

Os dados gerados pelo sequenciamento foram preparados e analisados de forma a obter o perfil de expressão gênica de cada amostra sequenciada, bem como a variação de expressão existente entre elas.

Inicialmente, foi realizada a trimagem das sequências utilizando o software Seqyclean 1.9.9 – Next Generation Sequencing Cleaning, adotando como parâmetros qualidade Phred 20, tamanho mínimo 50 pares de bases (pb) e exclusão das sequências de adaptadores de acordo com o preparo da biblioteca Truseq (Illumina). Então, uma montagem "de novo" foi realizada a partir dos dados do sequenciamento utilizando o software CLC Genomics Workbench 6.5.1 para alinhamento dos reads com a orientação da biblioteca no sentido Forward-Reverse (FR) com um comprimento otimizado de k-mer de 33.

Diferentes análises diferenciais considerando os GDEs foram realizadas comparando os perfis de expressão gênica entre culturas planctônicas da cepa EH-315 vs. biofilmes de

EH-315, culturas planctônicas de 60I vs. biofilmes de 60I, culturas planctônicas da cepa EH-315 vs. culturas planctônicas de 60I e, biofilmes de EH-315 vs. biofilmes de 60I. A partir dos dados normalizados, foi feito o cálculo do Fold Change e definido o valor P. O Fold Change indica a variação de expressão normalizada de fragmentos por transcrito entre duas amostras (biofilmes e culturas planctônicas, por exemplo), ou seja, o Fold Change é resultado da divisão do valor de expressão em RPKM (Reads Per Kilobase per Million) de um determinado transcrito na amostra biofilmes pelo valor de expressão do mesmo transcrito na amostra planctônica. Para as análises realizadas, comparações estatísticas foram conduzidas e valores de $P < 0,05$ foram considerados estatisticamente significantes.

Adicionalmente, correlações entre os GDEs foram realizadas e podem ser visualmente demonstradas por diagramas de Venn, que representam transcritos que foram expressos em ambas as condições e exclusivos (únicos) entre pares de amostras (Oliveros, 2007).

**3.3.6. Identificação, categorização funcional e localização de domínios proteicos**

A partir dos resultados obtidos através das análises descritas anteriormente, foi realizada a identificação e descrição funcional de dez transcritos induzidos e de dez reprimidos com os maiores valores de expressão diferencial entre as situações correlacionadas. Foram inseridos nesta análise os transcritos com anotação funcional disponível no software utilizado. Para tanto, uma análise foi conduzida utilizando o software Blast2GO (Conesa, Götz *et al*., 2005; http://www.blast2go.de/). Este software executa as análises integrando os sistemas Blastx do NCBI com os sistemas de categorização funcional do Gene Ontology Consortium e GO Slim Viewer. Esta análise possibilita a classificação funcional de cada transcrito em três domínios, sendo: a) processo biológico, que indica as operações ou os conjuntos de eventos moleculares com início e fim definidos em que o produto do gene estudado participa e que são fundamentais para o funcionamento de uma célula, tecido, órgãos ou organismo; b) função molecular, que indica as atividades elementares do produto do gene em nível molecular e; c) componente celular, que indica a parte da célula ou o ambiente extracelular em que o produto do gene desempenha sua função. Esta anotação de ontologias gênicas baseia-se na mineração de dados originados de sequências públicas com anotação disponível, com similaridade mínima de 60% entre as sequências.

**3.4. Determinação da viabilidade celular e porcentagem de infecção em Mø alveolares (AMJ2-C11) por diferentes cepas de *H. capsulatum***

**3.4.1. Cultura de células AMJ$_2$-C11**

Para estes ensaios foi utilizada a linhagem de Mø alveolares de camundongo ($AMJ_2$-C11), obtida do Banco de células do Rio de Janeiro (BCRJ). Estes foram cultivados em garrafas plásticas, em meio Dulbecco's modified Eagle's medium (DMEM, Sigma Chemical Co., St. Louis, MO, EUA) suplementado com soro fetal bovino (SFB, Cultilab, Brasil) 10% e antibióticos 1%, mantidos à temperatura de 36,5ºC e 5% de $CO_2$.

Decorridos 3 a 4 dias, as garrafas de células foram submetidas à tripsinização. Para isso, a monocamada formada foi lavada com PBS 0,05M, pH 7,2 estéril e, após lavagem, este foi desprezado para então acrescentar 2 mL de solução de Tripsina-EDTA (Gibco, Life Technologies, Carlsbad, CA, EUA). Seguidos 1-2 min, as células foram homogeneizadas com volumes variados do meio DMEM acrescido de SFB e antibióticos. O volume total da suspensão celular obtido foi transferido para outras garrafas, de modo a se obter uma concentração celular de $5 \times 10^5$ células/mL.

### 3.4.2. Determinação da viabilidade celular após infecção de células AMJ2-C11 utilizando o kit Live/Dead®

A fim de realizar em uma próxima etapa o transcriptoma da interação *H. capsulatum*-Mø hospedeiros foi determinada a viabilidade de células infectadas *in vitro* com diferentes cargas fúngicas. Este ensaio foi realizado utilizando o kit Live/Dead® (Life Technologies Inc.) que permite determinar a viabilidade celular com base na marcação fluorescente simultânea de células vivas e mortas, utilizando dois fluorocromos, a calceína AM e o homodímero de etídio (EthD-1). Este ensaio é aplicável às células eucarióticas, incluindo células aderentes ou de tecidos, mas não se aplica à marcação de fungos ou bactérias. As células vivas são distinguidas pela presença da atividade intracelular da esterase, responsável pela conversão enzimática do corante calceína AM não fluorescente para calceína intensamente fluorescente. O marcador polianiônico calceína é retido dentro das células viáveis, resultando em uma intensa e uniforme fluorescência verde. EthD-1 penetra nas células com membrana danificada e após a ligação aos ácidos nucleicos, produz uma fluorescência vermelha brilhante em células mortas, sendo que tal composto é excluído pelas células vivas, que apresentam membrana plasmática intacta.

Os ensaios foram realizados segundo as recomendações do fabricante. Inicialmente foi preparada uma solução adicionando 20 µL da solução estoque EthD-1 2 mM em 10 mL de PBS estéril. A essa solução foram adicionados 5 µL de uma solução de calceína AM 4 mM. A solução de trabalho preparada resultou aproximadamente, em uma solução de calcéina AM 2 µM (~494/517 nm) e EthD-1 4 µM (~528/617 nm) e então 100 µL desta foram adicionados diretamente às células após a formação da monocamada celular em placa

de poliestireno de 96 poços (TPP®, Trasadingen, Switzerland) e posterior infecção com leveduras de *H. capsulatum* em diferentes concentrações (5 x $10^6$, 5 x $10^5$, 5 x $10^4$ e 5 x $10^3$ leveduras/mL) por um período de 5 h a 37°C. Dessa forma, as células foram infectadas com a MOI em uma razão de 10 leveduras:1 Mø, 1:1, 1:10 e 1: 100, respectivamente. Em seguida, a placa foi incubada por 30 a 45 min em temperatura ambiente. As imagens foram adquiridas pelo equipamento IN Cell Analyzer 2000 (Ge Healthcare) e as análises foram realizadas utilizando o software Investigator 1000 Workstation (Ge Healthcare). Análises estatísticas foram realizadas utilizando o software GraphPad Prism versão 5.0. Os ensaios foram realizados em três replicatas biológicas e duas replicatas técnicas.

**3.4.3. Infecção por *H. capsulatum* às células AMJ2-C11 e determinação da porcentagem de infecção por citometria de fluxo**

Estes ensaios foram realizados para determinação da porcentagem de células hospedeiras infectadas com leveduras de *H. capsulatum* para posterior análise transcriptômica da infecção (fungo vs. célula hospedeira).

Após a formação da monocamada, as células foram lavadas três vezes com PBS estéril para então serem infectadas com as suspensões correspondentes de 5 x $10^6$ leveduras/mL das diferentes cepas de *H. capsulatum* (EH-315 e 60I). Dessa forma, Mø alveolares foram infectados em uma MOI de 10 leveduras:1 Mø. Para a preparação dos inóculos, as suspensões padronizadas de fungos em PBS (solução fisiológica tamponada com fosfatos 0,05 M, pH 7,2) foram então incubadas por 30 min à 37ºC com 5(6)-Carboxyfluorescein diacetate N-succinimidyl Ester (CFSE; Sigma Chemical Co., St. Louis, MO, EUA), lavadas em PBS e, novamente, após centrifugação os fungos foram ressuspendidos em PBS. A seguir foi realizada infecção na monocamada de celular em placas de poliestireno de 24 poços (TPP®, Trasadingen, Switzerland). Cada poço foi inoculado com 1 mL da suspensão de *H. capsulatum* em PBS marcada com CFSE e 1 mL de meio DMEM sem suplementos. A seguir, as células infectadas foram incubadas por 5 h a 37ºC e 5% de $CO_2$. Após período de incubação, as células foram então tripsinizadas, lavadas em meio com SFB para neutralização da tripsina e as suspensões foram recolhidas em eppendorfs e centrifugadas a 2.500 rpm à 4ºC. Os sobrenadantes foram descartados e a cada eppendorf foram adicionados 500 µL de FACSFlow para posterior contagem de células através de citometria de fluxo (FACSCanto™ Becton & Dickinson, San Diego, CA, EUA) de maneira a analisar os parâmetros relacionados ao tamanho (size forward scatter - FSC), granularidade (granularity side scatter - SSC) e fluorescência de 10.000 células por tubo. Os resultados

obtidos são representados pela intensidade de fluorescência (FI) de leveduras fluorescentemente marcadas com CFSE a partir dos dados analisados utilizando o software FACSDiva$^{TM}$ versão 6.1.3. Estes dados permitiram determinar a porcentagem de Mø alveolares infectados, diferenciando a capacidade de infecção das diferentes cepas de *H. capsulatum*. Os gráficos representativos da FI de CFSE foram divididos em dois quadrantes, à esquerda compreendendo células negativas não marcadas e, à direita compreendendo células positivas fluorescentemente marcadas (células infectadas). Mø alveolares AMJ2-C11 não infectados, bem como leveduras fluorescentemente marcadas e não marcadas foram utilizadas como controles do ensaio. Os ensaios foram realizados em três replicatas biológicas e duas replicatas técnicas e, os resultados descritos representam a média de todos os experimentos.

### 3.5. Screening de miRNAs expressos em células hospedeiras após interação com *H. capsulatum*

#### 3.5.1. Seleção de cepas e condições de cultivo

Para estes ensaios, Mø THP-1 like foram desafiados com as cepas EH-315 e 60I em crescimento planctônico, bem como pelos biofilmes da cepa EH-315. Mø sem infecção foram empregados como controle.

#### 3.5.2. Seleção da linhagem celular

Os ensaios referentes ao screening de miRNAs em células hospedeiras infectadas com *H. capsulatum* concentram-se na identificação de ncRNAs-alvos para o desenvolvimento de uma nova terapia e/ou ferramenta diagnóstica para a histoplasmose. Assim, tornou-se relevante empregar uma linhagem celular humana para avaliar o perfil de miRNAs expressos nesta linhagem em resposta à infecção e, reproduzir *in vitro*, a interação *H. capsulatum*-célula hospedeira humana. Por este fato, foi selecionada a linhagem THP-1 (ATCC® TIB-202™), caracterizada como monócitos obtidos do sangue periférico de *Homo sapiens*.

#### 3.5.3. Cultura de células THP-1

A linhagem celular de monócitos humanos THP-1 foi cultivada em meio Roswell Park Memorial Institute (RPMI-1640, Gibco, Life Technologies, Carlsbad, CA, EUA) contendo 10% de SFB, glicose 5 mM, L-glutamina 2 mM, gentamicina 50 mg/mL e 4-(2-Hydroxyethyl) piperazine-1-ethanesulfonic acid (HEPES, Sigma Chemical Co.) 20 mM a 37°C e 5% de $CO_2$. A linhagem madura, denominada Mø-like (M1) foi induzida pelo tratamento de células THP-1 com 30 ng/mL de phorbol 12-myristate 13-acetate (PMA, Sigma Chemical Co.) por 24 h em uma concentração de 5 x $10^5$ células/mL. Diferenciados,

Mø agora aderentes foram lavados com meio RPMI 1640 e incubados por 48 h com meio sem PMA.

### 3.5.4. Determinação da viabilidade celular após infecção de Mø THP-1 like utilizando o kit Live/Dead®

A fim de realizar o screening de miRNAs expressos após interação *H. capsulatum*-Mø hospedeiros foi determinada a viabilidade de células infectadas com diferentes cargas fúngicas utilizando o kit Live/Dead® (Life Technologies Inc.) que permite a marcação de células viáveis, emitindo uma fluorescência verde e, células mortas que emitem fluorescência vermelha. Os ensaios foram realizados segundo as recomendações do fabricante e a solução de Eth-D e calceína AM foi preparada e adicionada às placas após a infecção com leveduras de *H. capsulatum* em diferentes concentrações ($5 \times 10^6$, $5 \times 10^5$, $5 \times 10^4$ e $5 \times 10^3$ leveduras/mL) conforme detalhado no item 3.4.2. Dessa forma, as células foram infectadas com a MOI em uma razão de 10 leveduras:1 Mø, 1:1, 1:10 e 1:100, respectivamente, por 5 h. Posteriormente, a placa foi incubada por 30 a 45 min em temperatura ambiente. As imagens foram adquiridas pelo equipamento IN Cell Analyzer 2000 (Ge Healthcare) e as análises foram realizadas utilizando o software Investigator 1000 Worsktation (Ge Healthcare). Análises estatísticas foram realizadas utilizando o software GraphPad Prism versão 5.0. Os ensaios foram realizados em três replicatas biológicas e duas replicatas técnicas.

### 3.5.5. Ensaio de infecção de *H. capsulatum* em Mø THP-1 like e determinação da porcentagem de infecção por citometria de fluxo

Estes ensaios foram realizados para determinação da porcentagem de Mø infectados *in vitro* com leveduras de *H. capsulatum* para posterior screening de miRNAS expressos pelas células hospedeiras após infecção.

Após a diferenciação em Mø THP-1 like, a infecção foi realizada placas de poliestireno de 24 poços (TPP®, Trasadingen, Switzerland). A infecção celular, com diferentes cepas de *H. capsulatum* (EH-315 e 60I) em suas diferentes formas de crescimento, foi realizada com uma suspensão de leveduras padronizada de $5 \times 10^6$ células/mL previamente marcada com CFSE conforme descrito no item 3.4.3., considerando a razão da MOI para todas as amostras de 10 leveduras:1 Mø. As células infectadas foram incubadas a 37°C, na presença de 5% de $CO_2$ por 5 h. Após período de incubação o sobrenadante foi removido e as culturas foram tripsinizadas e lavadas com meio RPMI 1640 suplementado com SFB. A análise de células infectadas por citometria de fluxo (FACSCanto$^{TM}$ Becton & Dickinson, San Diego, CA, EUA) foi realizada conforme os parâmetros descritos no item 3.4.3. para determinação de Mø THP-1 like infectados. Três replicatas biológicas e duas

replicatas técnicas de cada amostra e do controle de células sem infecção foram realizadas e analisadas e, os resultados descritos representam a média de todos os experimentos.

**3.5.6. Obtenção do RNA total, quantificação e avaliação da integridade**

Para o screening de miRNAs diferencialmente expressos, as células infectadas e não infectadas foram lisadas com 2 mL de Trizol (Invitrogen, Carlsbad, CA, EUA) e armazenadas à -80ºC para posterior extração do RNA.

A extração de RNA celular foi realizada através da utilização do kit RNeasy Plant Mini kit® (50) (Qiagen Ltd), seguindo as instruções do fabricante. Após extração, os RNAs foram quantificados em NanoDrop® (Thermo Scientific) e analisados quanto a sua integridade utilizando o equipamento Agilent 2100 Bioanalyzer® (Agilent Technologies), considerando um valor de RIN maior ou igual a 8, segundo as recomendações do fabricante.

**3.5.7. Síntese de cDNA**

A síntese de cDNA foi realizada utilizando o kit Universal cDNA Synthesis kit II Exiqon. Esta reação foi conduzida em um termociclador com 1 ciclo de 60 min a 42ºC e 5 min a 95ºC e em seguida, os cDNA foram estocados à -20ºC.

**3.5.8. Quantificação dos miRNAs por PCR-Real Time**

Placas comerciais de 384-wells foram utilizadas para screening de 752 miRNAs humanos (Human miRNome Panel I and II, V4, Exiqon, Vedbaek, Dinamarca). O conteúdo dos painéis I e II é detalhado na Tabela 1. Reações foram preparadas contendo um mix de cDNA, Sybr®Green Master mix e água. Para cada amostra foi ensaiada em triplicata uma placa painel I e uma placa painel II, possibilitando o rastreamento dos principais miRNAs humanos conhecidos. Em seguida, foi realizada a reação de PCR Real Time utilizando o equipamento Viia7 (Applied Biosystems) no Laboratório de Farmacologia da Faculdade de Odontologia da Universidade de São Paulo (USP), Bauru, com 1 ciclo de 10 min a 95ºC, seguido por 45 ciclos de amplificação de 10 s a 95ºC e 1 min a 60ºC.

**Tabela 1.** Conteúdo das placas comerciais (Exiqon) Human miRNome, Painéis I e II, V4.

| Painel I | Painel II |
|---|---|
| 372 conjuntos de primers (LNA™*) para amplificação dos microRNAs humanos | 380 conjuntos de primers (LNA™*) para amplificação dos microRNAs humanos |
| 3 calibrantes inter-placa | 3 calibrantes inter-placa |
| 3 conjuntos de primers de genes de referência | 1 poço vazio |
| 5 conjuntos de primers controle RNA Spike-in | |
| 1 poço vazio | |

*LNA – *Locked Nucleic Acid*

### 3.5.9. Análise bioinformática dos miRNAs diferencialmente expressos

A partir dos dados encontrados, as análises foram realizadas através de ferramentas de bioinformática a fim de determinar os miRNAs diferencialmente expressos, bem como identificar suas funções e alvos. Diferentes análises comparativas foram realizadas entre Mø (THP-1) infectados com a cepa EH-315 vs. Mø sem infecção, Mø infectados com a cepa 60I vs. Mø sem infecção, Mø infectados com biofilmes da cepa EH-315 vs. Mø sem infecção, Mø infectados com biofilmes da cepa EH-315 vs. Mø infectados com a cepa EH-315 em crescimento planctônico e, Mø infectados com a cepa EH-315 vs. Mø infectados com a cepa 60I. Inicialmente, os dados foram processados pelo DataAssist™ Software v3.01 (Applied Biosystems), projetado para realizar quantificação relativa utilizando o método comparativo de Ct (ΔΔCt) (Ct – Cycle Threshold). Para tanto, os níveis de miRNAs foram normalizados aos níveis dos seguintes controles endógenos e exógenos e, calibradores: SNORD38B, SNORD49A, U6 snRNA, UniSp2, UniSp3 IPC, UniSp4, UniSp5, UniSp6, cel-miR-39-3p. De acordo com os dados obtidos, foram determinados os miRNAs diferencialmente expressos, considerando um valor de $P < 0,05$ como critério biológico. Adicionalmente, os miRNAs diferencialmente expressos foram caracterizados em superexpressos ou reprimidos em função do algoritmo Fold Change (RQ), que corresponde a quantificação relativa da expressão do miRNA na amostra teste em relação ao controle. Para calcular o Fold Change, o valor dos controles foi ajustado para 1. A partir da identificação dos miRNAs diferencialmente expressos, análises posteriores possibilitaram a determinação das vias celulares das quais participam e genes alvos que são regulados por tais miRNAs. Em vista disso, análises de vias foram realizadas utilizando os softwares miRPath 2.0 (http://diana.cslab.ece.ntua.gr/?sec=home; Vlachos *et al.*, 2012), uma ferramenta

computacional que identifica vias moleculares potencialmente alteradas pela expressão de um único ou vários miRNAs, e MIRSystem (http://mirsystem.cgm.ntu.edu.tw/; Lu *et al.*, 2012), uma ferramenta para prever os genes-alvo e suas vias associadas para muitos miRNAs simultaneamente. Posteriormente, análises dos genes-alvo validados, regulados pelos miRNAs diferencialmente expressos, foram realizadas utilizando o software miRWalk (http://www.umm.uni-heidelberg.de/apps/zmf/mirwalk/; Dweep *et al.*, 2015), um banco de dados completo que fornece informações sobre miRNAs de humanos, camundongos e ratos, bem como locais de ligação validados em seus genes-alvo. Finalmente, redes de associação dos miRNAs e seus genes-alvo foram construídas utilizando o software Navigator v2.2 (Network Analysis, Visualization, & Graphing TORonto).

### 3.6. Análise metabolômica

#### 3.6.1. Determinação de polissacarídeos totais em amostras de culturas planctônicas, biofilmes e sobrenadante dos biofilmes de *H. capsulatum*

Células leveduriformes de duas cepas clínicas (EH-315 e 60I) de *H. capsulatum* (5 x $10^6$ leveduras/mL) foram cultivadas em suas diferentes formas de crescimento, culturas planctônicas e biofilmes. Após preparo das amostras, pellets correspondentes foram centrifugados a 10.000 rpm por 5 min a 4°C. Após centrifugação, o sobrenadante, o qual contém os polissacarídeos extracelulares solúveis (PES), foi transferido para um tubo nomeado PES. Uma alíquota de NaOH 1 M foi adicionada ao pellet para extrair os polissacarídeos extracelulares insolúveis (PEI). O tubo foi agitado por 15 min, centrifugado e o sobrenadante foi tranferido para outro tubo nomeado PEI. Finalmente, uma alíquota de NaOH 1 M foi adicionada ao pellet residual para extrair os polissacarídeos intracelulares (PI). O tubo foi aquecido por 5 min a 100°C, centrifugado e, o sobrenadante foi transferido para outro tubo nomeado PI. Três volumes de Etanol gelado foram adicionados aos tubos contendo PES, PEI e PI.

Os tubos foram mantidos por 30 min a -20°C. Então, os tubos foram centrifugados e os pellets foram lavados duas vezes com Etanol 75% gelado. Os polissacarídeos precipitados foram ressuspensos em NaOH 1 M. Posteriormente, os carboidratos totais foram estimados pelo Método Fenol Sulfúrico (Dubois *et al.*, 1951). Em resumo, 100 µL de solução de Fenol 5 % e 500 µL de ácido Sulfúrico 95% foram adicionados a cada 100 µL das amostras. Então, o desenvolvimento da cor foi lida de maneira espectrofotômétrica a 490 nm. A quantificação de polissacarídeos totais foi realizada em biofilmes de *H. capsulatum*, no sobrenadante dos biofilmes e em culturas planctônicas das diferentes cepas.

### 3.6.2. Extração dos metabólitos

Os métodos utilizados nesta abordagem foram padronizados, a fim de otimizar a obtenção dos metabólitos (peptídeos e compostos de baixa massa molecular não proteicos).

De início, os pellets das duas amostras a serem estudadas (EH-315 em biofilmes e em crescimento planctônico), foram submetidos a um processo de extração proteica, para separação das proteínas e metabólitos. Para tanto, foram adicionados aos pellets 10 mL de Tris 10 mM, pH 8,8. Em seguida, foram adicionados inibidores de proteases, PMSF (Phenylmethylsulfonyl fluoride, Sigma Aldrich) 5 µL/mL. Então, foram adicionadas pérolas de vidro (3 mm), ocupando aproximadamente a metade do volume da suspensão de leveduras e Tris 10 mM. Para a extração das proteínas, as amostras foram submetidas a etapas alternadas de congelamento em nitrogênio líquido e agitação em vórtex, repetidas três vezes. Ao final deste procedimento, todo o conteúdo, em média 11-12 mL, foi transferido para um novo tubo falcon de 50 mL. As amostras foram, em seguida, centrifugadas a 4°C, 4.000 rpm, durante 45 min. Ao final da centrifugação, foi adicionado ao sobrenadante ácido Tricloroacético (TCA) 10% em Acetona 90% v/v. As amostras foram mantidas overnight na geladeira para precipitação proteica. Em seguida, os tubos foram centrifugados 4°C, 14.000 rpm durante 15 min e, após esse período o precipitado foi descartado e o sobrenadante das amostras coletado e transferido para tubos eppendorf de 2 mL. Posteriormente, o sobrenadante dos tubos foi conduzido à secagem em concentrador de amostras do tipo Speed Vac (Concentrator Plus Eppendorf) e estocadas a -20°C.

### 3.6.3. Análises cromatográficas

As amostras foram submetidas a duas etapas de purificação. Para a fase móvel foram utilizados dois solventes: solvente A [Água MilliQ ($H_2O$) contendo 0,1% TFA (ácido trifluoroacético) (v/v)] e solvente B [Acetonitrila (ACN) 100% contendo 0,1% TFA (v/v)]. Na primeira etapa de purificação, foram utilizados 200 µL de solução A para a ressuspensão das amostras que foram aplicadas em colunas sep-pak (Sep-Pak C18, 1 cc, Vac Cartridge, Waters Corp., Milford MA, EUA) e eluídos com 85% de solução B. Após eluição, as amostras foram submetidas à secagem e pesagem originando as amostras correspondentes ao crescimento da cepa EH-315 em culturas planctônicas (P85) e em biofilmes (B85).

Na segunda etapa de purificação, 200 µg de cada amostra foram ressuspensos e purificados utilizando um sistema RP-HPLC (Perkin-Elmer Flexar/Chromera). Neste sistema foi utilizado um gradiente de 5 a 95% de solução B, por 90 min, utilizando-se uma coluna XBrigde$^{TM}$ BEH300 C18 (2,1x100mm; 3,5 µm) (Waters), com fluxo de 0,2 mL/min. A

eluição das frações foi monitorada por medidas de absorção de luz ultravioleta em 214 nm. O controle de aquisição de dados foi feito através do software Chromera.

### 3.6.4. Análises de cromatografia líquida acoplada à espectrometria de massas (LC-MS/MS)

As análises de LC-MS/MS foram realizadas no Laboratório de Biologia Estrutural e Zooquímica do Departamento de Biologia do Instituto de Biociências da UNESP, Rio Claro, em colaboração com o Prof. Dr. Mario Sergio Palma.

As amostras em culturas planctônicas (P85) e em biofilmes (B85) foram submetidas à cromatografia líquida ultra-rápida e espectrometria de massas de alta resolução. As análises foram conduzidas em um sistema híbrido LCMS-IT-TOF (Shimadzu, Kyoto, Japão).

Foram aplicados 300 µg das amostras (B85 e P85) ressuspendidos em 100 µL de água e acidificados com ácido fórmico 1% (v/v), em um sistema Prominence UFLC (Ultra Fast Liquid Chromatograph – LC-20A Shimadzu) sob gradiente de ACN de 0 a 90% (v/v), contendo 0,1% (v/v) de TFA por 90 min, utilizando-se uma coluna XBrigdeTM BEH300 C18 (2,1x100mm; 3,5 µm) (Waters, Massachussetts, EUA). A eluição dos componentes foi monitorada por absorbância ultravioleta a 215 nm, com fluxo de 0,2 mL/min. A obtenção dos espectros de massas foi realizada em um espectrômetro de massas equipado com fonte de ionização “electrospray” (ESI), e analisador de massas híbrido formado pela combinação de sistemas “Ion Trap” e “Time-of-flight” (IT-ToF) (Shimadzu). As análises foram realizadas no modo positivo (ESI+) e contínuo, durante todo o experimento. Durante toda a análise a temperatura do CDL e da interface foi mantida a 200ºC, a voltagem na agulha a 4,5 kV e a voltagem no cone a 3,5 V. O fluxo de gás secante (Nitrogênio) foi de 100 L/h e o fluxo de gás nebulizador (Nitrogênio) de 1,5 L/min. A detecção no espectrômetro de massas foi realizada com varreduras feitas no intervalo de m/z 200 a 3000, com uma resolução de aproximadamente 15.000. As análises de espectrometria de massas sequenciais, ou seja, espectros de fragmentação peptídica em condições de decomposição induzida por colisão (CID) ($MS^2$) foram realizados utilizando-se os mesmos parâmetros dos experimentos de $MS^1$, exceto a varredura que foi feita num intervalo entre 50 e 2500 m/z. Foi utilizado argônio como gás de colisão, a uma pressão de 100 kPa. O software LCMS solution (Shimadzu) foi utilizado para controle de aquisição e análise de dados.

### 3.6.5. Análise dos dados de LC-MS/MS

Após aquisição dos dados pelo software LCMS solution foi empregado o comando “Mass Table”, para adquirir e transferir os espectros de massas para uma planilha do Excel (Microsoft Office 2010). Em seguida, foi realizada manualmente a deconvolução dos picos

de carga múltipla para os metabólitos detectados entre 200 e 2400 m/z. As análises foram conduzidas de maneira a considerar todos os picos de valores m/z que apresentaram relação sinal ruído (S/N) ≥ 10. Então, foi criada uma lista de massas e, todas as massas semelhantes foram checadas manualmente para confirmar a identificação e/ou distinguir os compostos isobáricos. No presente estudo, as moléculas que apresentaram uma diferença entre as massas reconstruídas ≤ 0,5 Da e tempo de retenção ≤ 1 min foram consideradas como moléculas idênticas. A análise de uma corrida em branco foi conduzida entre cada corrida cromatográfica. Os gráficos foram construídos utilizando o Microsoft Excel 2010.

## 4. RESULTADOS E DISCUSSÃO

### 4.1. Culturas planctônicas e formação dos biofilmes de *H. capsulatum*

A Figura 2 ilustra o crescimento das leveduras de *H. capsulatum* em culturas planctônicas (Figura 2A) e em biofilmes (Figuras 2B, 2C, 2D). Ensaios prévios demonstraram que a formação inicial dos biofilmes de *H. capsulatum* ocorre em um período de 7 h, no qual há adesão das leveduras à superfície abiótica estruturadas como arranjos em monocamada e, eventualmente como uma comunidade aderida. Posteriormente, os biofilmes consistentes são desenvolvidos em uma cinética de 24 h a 72 h, os quais são caracterizados por aumento da massa celular e produção de matriz extracelular. A cinética previamente realizada, referente à formação dos biofilmes pelas duas cepas (EH-315 e 60I), revela que a atividade metabólica exibida por ambas é semelhante (Pitangui *et al.*, 2012).

**Figura 2. Crescimento de leveduras de *H. capsulatum* em culturas planctônicas e biofilmes.** Crescimento planctônico das leveduras em erlenmeyer por um período de 72 h, sob agitação (100 rpm), à 37°C em meio de cultura BHI caldo suplementado com 0,1% de cisteína e 1% de glicose **(A)**. Início da formação dos biofilmes, após 7 h de pré-adesão, com adição de BHI caldo suplementado com 0,1% de cisteína e 1% de glicose **(B)**. Biofilme maduro de *H. capsulatum* formado após 72 h de incubação em BHI suplementado com 0,1% de cisteína e 1% de glicose **(C)** e, após a retirada do meio de cultura **(D)**.

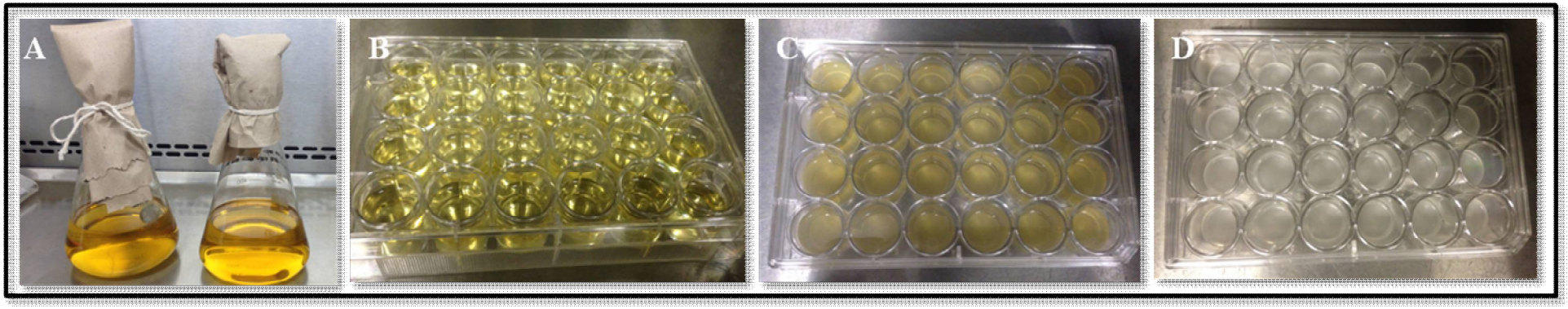


## 4.2. Análise transcriptômica

### 4.2.1. Quantificação e avaliação da pureza e integridade do RNA das amostras

A concentração de RNA obtida após extração das culturas de *H. capsulatum* e determinada por espectrofotometria é apresentada na Tabela 2. Em relação à razão $A_{260nm}/A_{280nm}$, os valores obtidos para o crescimento das cepas em biofilmes e em culturas planctônicas indicam pureza ideal do material extraído. Considerando a integridade do RNA das amostras, parâmetro avaliado através do equipamento Agilent 2100 Bioanalyzer® (Agilent Technologies), foi possível observar que o RNA obtido apresentava-se íntegro, portanto de boa qualidade, exibindo valores de RIN maior ou igual a 8. A Figura 3 ilustra os gráficos gerados pelo Bioanalyzer representando os picos correspondentes às moléculas de RNA ribossomal (RNAr) 18S e 28S, característicos do material extraído de organismos eucariotos.

**Tabela 2. Concentração de RNA obtido após extração utilizando o Kit RNeasy Plant Mini Kit®.** Extração da fase leveduriforme das cepas EH-315 e 60I de *H. capsulatum* em biofilmes e em culturas planctônicas e quantificação do material extraído utilizando espectrofotômetro (Nanovue®).

| Amostra | Concentração (ng/µL) | Pureza ($A_{260nm}/A_{280nm}$) |
|---|---|---|
| Biofilmes EH-315 | 954,4 | 2,01 |
| Culturas planctônicas EH-315 | 382,8 | 1,95 |
| Biofilmes 60I | 650,0 | 1,9 |
| Culturas planctônicas 60I | 500,0 | 2,03 |

**Figura 3. Eletroferograma da Integridade do RNA.** Integridade do RNA da cepa EH-315 e 60I de *H. capsulatum*, respectivamente, em culturas planctônicas **(A, C)** e em biofilmes **(B, D)** analisado por técnica de eletroforese capilar no equipamento Agilent 2100 Bioanalyzer® através do kit RNA 6000 Nano (GE Healthcare).

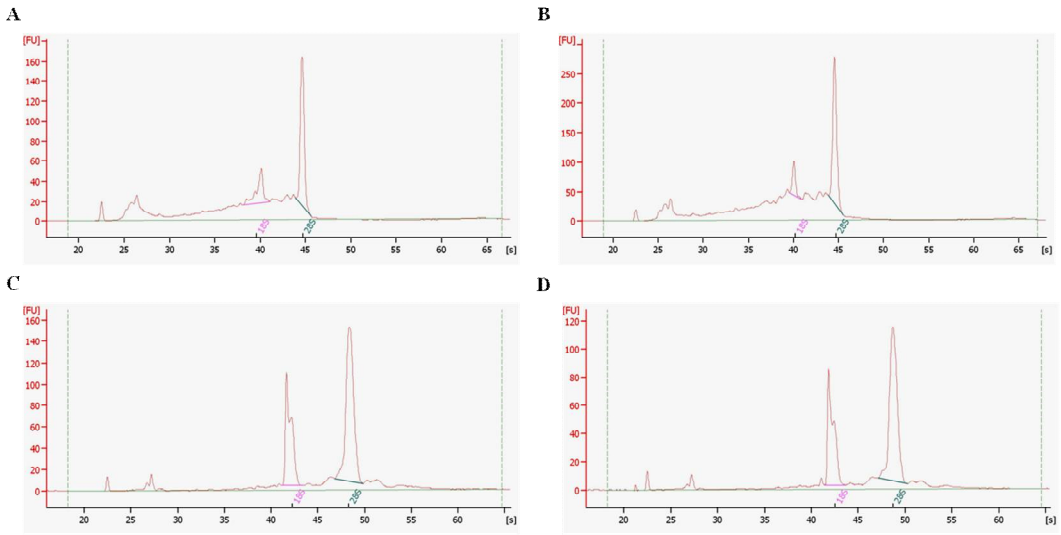


### 4.2.2. Construção das bibliotecas de cDNA

Após a quantificação e análise da pureza e integridade do RNA das amostras, foram construídas as bibliotecas de cDNA de ambas as cepas em biofilmes e culturas planctônicas. Posteriormente, as bibliotecas foram validadas através de análises realizadas no Agilent 2100 Bioanalyzer® (Agilent Technologies). A Figura 4 ilustra a validação das bibliotecas da cepa EH-315 em diferentes formas de cultura. Através dos gráficos gerados é possível verificar a pureza, bem como a dimensão das bibliotecas construídas, exibindo um pico de aproximadamente 260 pb. As bibliotecas geradas a partir do RNA da cepa 60I em culturas

planctônicas e biofilmes foram validadas conforme detalhado anteriormente e o produto final obtido exibiu pureza e dimensões semelhantes aos dados apresentados na Figura 4.

**Figura 4. Validação das bibliotecas de cDNA.** Gráficos representativos da pureza e dimensão das bibliotecas de cDNA construídas da cepa EH-315 em culturas planctônicas **(A)** e em biofilmes **(B)**, sendo o produto final obtido correspondente a uma banda de aproximadamente 260 pb.

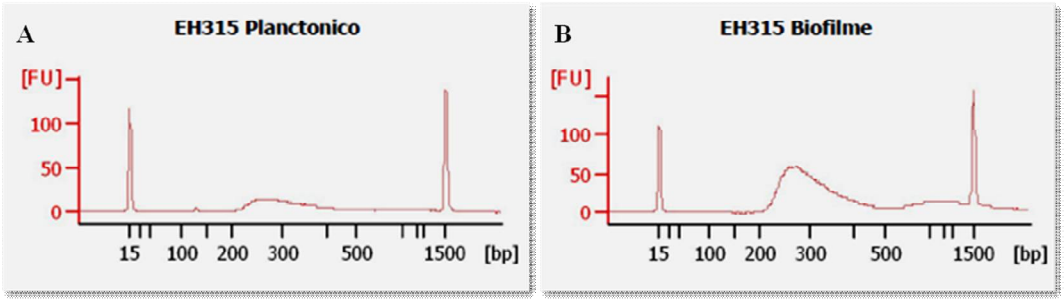


### 4.2.3. Sequenciamento dos transcritos de *H. capsulatum* em biofilmes e em crescimento planctônico

Após construção e validação das bibliotecas de cDNA foi realizada a clusterização e o sequenciamento dos transcritos de *H. capsulatum* utilizando a plataforma HiSeq Illumina, a partir da qual é realizada a leitura das bases por uma análise sequencial das imagens capturadas em cada ciclo de sequenciamento. Os dados gerados possibilitaram a obtenção do conjunto completo das regiões transcritas das cepas 60I e EH-315 nas distintas formas de crescimento estudadas por RNA-seq, método que utiliza Sequenciamento de nova geração (Next Generation Sequencing – NGS) para avaliar a diversidade do transcriptoma (Mortazavi *et al.*, 2008) e que tem recebido crescente importância para o diagnóstico, prognóstico e/ou para aplicações terapêuticas (Byron *et al.*, 2016). De acordo com o sequenciamento foi possível estabelecer análises comparativas entre as distintas cepas e formas de crescimento, estabelecendo os genes únicos e GDEs (induzidos ou reprimidos) entre as condições correlacionadas. Foram contrapostos os seguintes perfis transcriptômicos: EH-315 em biofilmes vs. EH-315 em crescimento planctônico; EH-315 em crescimento planctônico vs. 60I em crescimento planctônico; EH-315 em biofilmes vs. 60I em biofilmes; 60I em biofilmes vs. 60I em crescimento planctônico. Dessa forma, quatro comparações em pares foram realizadas a fim de gerar o maior número de informações possíveis e comparar as diferenças transcricionais dentro da mesma espécie (biofilmes vs. culturas planctônicas) e entre diferentes cepas (EH-315 vs. 60I). As análises comparativas referentes ao sequenciamento das leveduras de *H. capsulatum* estão descritas nas Tabelas 3, 4, 5 e 6, de

maneira a representar os 10 transcritos substancialmente induzidos e os 10 substancialmente reprimidos de cada uma das comparações realizadas. Assim, de uma forma geral, uma análise por RNA-Seq envolve etapas principais que culminam na: 1) preparação da biblioteca, na qual o RNA é convertido em pequenos fragmentos de cDNA; 2) NGS, na qual os fragmentos de DNA são sequenciados e 3) análise de bioinformática, na qual os fragmentos sequenciados são alinhados com um genoma de referência a fim de identificar as características biológicas relevantes (Davila *et al*., 2016). No presente estudo, o alinhamento das sequências obtidas foi realizado através de uma montagem "de novo" para criar um transcriptoma de referência das espécies fúngicas ensaiadas. De fato, a montagem "de novo", também denominada montagem independente de um genoma, é a única abordagem disponível para microrganismos que não dispõem de um genoma de referência. Por outro lado, para os microrganismos com genoma de referência, duas abordagens para a análise do transcriptoma podem ser conduzidas, sendo 1) montagem guiada por um genoma e/ou 2) montagem "de novo", embora a primeira abordagem seja preferencialmente empregada para estes microrganismos (Martin *et al*., 2011). Segundo Lu *et al*. (2013), o emprego de uma montagem "de novo" pode efetivamente complementar os resultados de uma montagem baseada em um genoma de referência, adotando desta forma uma abordagem integrativa.

No total, foram obtidas 41,3 e 108 milhões de leituras (reads) brutas das bibliotecas sequenciadas da cepa EH-315 em biofilmes e em culturas planctônicas, respectivamente. Para a cepa 60I, foram obtidas 24,5 milhões de leituras brutas a partir do sequenciamento das leveduras em biofilmes e 5,2 milhões de leituras brutas do sequenciamento das culturas planctônicas. Subsequentemente, após a remoção das sequências dos adaptadores, leituras ambíguas e leituras de baixa qualidade, foram geradas 32,8 e 29,2 leituras limpas de alta qualidade a partir do sequenciamento da cepa EH-315 em biofilmes e em condições planctônicas, respectivamente; em contrapartida, foram geradas 22,6 e 1,3 milhões de reads limpas de alta qualidade resultantes do sequenciamento da cepa 60I estruturada em biofilmes e em culturas planctônicas, respectivamente. Todas as leituras de alta qualidade foram montadas "de novo" pelo programa CLC Genomics Workbench.

**Tabela 3. GDEs pela cepa EH-315 em biofilmes e em crescimento planctônico.** Níveis de expressão de transcritos individuais foram comparados e estão representados os 10 transcritos induzidos e os 10 reprimidos nos biofilmes.

| Transcrito ID | Valores de expressão | | Valor de expressão diferencial | Valor de *P* |
|---|---|---|---|---|
| | EH-315 Biofilmes | EH-315 Crescimento Planctônico | | |
| **146** | 92,3 | 23,1 | **4,81** | 1,81521E-13 |
| **305** | 518,3 | 128,9 | **4,83** | 0 |
| **2908** | 105,7 | 26,1 | **4,86** | 2,77556E-15 |
| **493** | 41,2 | 9,9 | **5,0** | 6,17014E-07 |
| **137** | 131,0 | 30,6 | **5,143** | 0 |
| **1707** | 33,6 | 7,8 | **5,144** | 5,44759E-06 |
| **277** | 106,6 | 24,7 | **5,19** | 4,44089E-16 |
| **1198** | 46,5 | 5,4 | **10,2** | 3,61863E-10 |
| **465** | 98,5 | 2,0 | **56,4** | 0 |
| **61450** | 120,2 | 0,9 | **152,9** | 0 |
| **46597** | 4,0 | 130,9 | **-27,2** | 0 |
| **24398** | 1,4 | 41,0 | **-23,9** | 1,69078E-08 |
| **38853** | 9,9 | 272,2 | **-22,9** | 0 |
| **38839** | 18,4 | 410,3 | **-18,5** | 0 |
| **61888** | 2,1 | 45,9 | **-17,4** | 5,6363E-09 |
| **42322** | 3,3 | 61,4 | **-15,3** | 2,67337E-11 |
| **8470** | 6,5 | 101,6 | **-12,8** | 0 |
| **23857** | 3,8 | 54,1 | **-11,55** | 1,42935E-09 |
| **46990** | 2,3 | 32,8 | **-11,52** | 2,4039E-06 |
| **23310** | 6,4 | 85,4 | **-11,0** | 4,21885E-14 |

**Tabela 4. GDEs pelas cepas EH-315 e 60I em crescimento planctônico.** Níveis de expressão de transcritos individuais foram comparados e estão representados os 10 transcritos induzidos e os 10 reprimidos em culturas planctônicas da cepa EH-315, de maior infectividade.

| Transcrito ID | Valores de expressão | | Valor de expressão diferencial | Valor de *P* |
|---|---|---|---|---|
| | EH-315 Crescimento Planctônico | 60I Crescimento Planctônico | | |
| **420** | 47,0 | 2,1 | **15,5** | 7,60977E-09 |
| **13047** | 697,0 | 30,3 | **16,6** | 0 |
| **15558** | 304,6 | 12,5 | **17,6** | 0 |
| **21474** | 1200,4 | 48,2 | **17,9** | 0 |
| **344** | 77,2 | 2,9 | **19,0** | 4,88498E-14 |
| **44554** | 270,4 | 9,9 | **19,5** | 0 |
| **325** | 30,0 | 0,8 | **25,8** | 1,63844E-06 |
| **11** | 181,7 | 4,8 | **27,4** | 0 |
| **53197** | 589,8 | 11,0 | **38,8** | 0 |
| **38** | 397,3609 | 7,020689 | **40,7** | 0 |
| **3788** | 7,5 | 556,6 | **-102,0** | 0 |
| **20856** | 11,1 | 348,4 | **-43,2** | 0 |
| **56467** | 2,6 | 47,6 | **-24,6** | 1,38822E-12 |
| **2908** | 26,1 | 274,9 | **-14,5** | 0 |
| **3843** | 7,2 | 74,9 | **-14,4** | 0 |
| **2882** | 12,8 | 130,0 | **-14,0** | 0 |
| **26616** | 14,7 | 142,9 | **-13,4** | 0 |
| **1161** | 5,1 | 50,2 | **-13,3** | 4,97469E-12 |
| **6** | 104,0 | 987,7 | **-13,1** | 0 |
| **93** | 9,8 | 75,0 | **-10,5** | 4,44089E-16 |

**Tabela 5. GDEs pelas cepas EH-315 e 60I em biofilmes.** Níveis de expressão de transcritos individuais foram comparados e estão representados os 10 transcritos induzidos e os 10 reprimidos nos biofilmes da cepa EH-315, de maior infectividade.

| Transcrito ID | Valores de expressão | | Valor de expressão diferencial | Valor de *P* |
|---|---|---|---|---|
| | EH-315 Biofilmes | 60I Biofilmes | | |
| **5461** | 22,9 | 1,2 | **18,8** | 5,36305E-06 |
| **11714** | 32,1 | 1,7 | **19,0** | 7,01755E-08 |
| **15092** | 50,6 | 1,9 | **26,9** | 4,34475E-12 |
| **21254** | 63,0 | 2,3 | **27,9** | 9,54792E-15 |
| **8593** | 61,3 | 2,2 | **28,3** | 2,02061E-14 |
| **39888** | 20,5 | 0,5 | **36,3** | 7,69009E-06 |
| **1142** | 22,8 | 0,4 | **48,6** | 1,76989E-06 |
| **45906** | 205,8 | 0,8 | **243,4** | 0 |
| **63353** | 45,2 | 0,11 | **482,3** | 4,43046E-12 |
| **465** | 98,5 | 0,19 | **524,6** | 0 |
| **37** | 1,2 | 1814,1 | **-1421,3** | 0 |
| **8** | 3,8 | 840,7 | **-213,6** | 0 |
| **1373** | 65,2 | 10424,5 | **-155,3** | 0 |
| **148** | 4,8 | 387,5 | **-77,5** | 0 |
| **7** | 5,0 | 383,3 | **-73,5** | 0 |
| **4** | 95,1 | 6917,5 | **-70,6** | 0 |
| **1921** | 0,6 | 45,0 | **-70,5** | 1,86073E-10 |
| **49** | 12,0 | 725,5 | **-58,8** | 0 |
| **6** | 165,6 | 6682,5 | **-39,2** | 0 |
| **9** | 61,2 | 1169,4 | **-18,5** | 0 |

**Tabela 6. GDEs pela cepa 60I em biofilmes e em crescimento planctônico.** Níveis de expressão de transcritos individuais foram comparados e estão representados os 10 transcritos induzidos e os 10 reprimidos nos biofilmes.

| Transcrito ID | Valores de expressão | | Valor de expressão diferencial | Valor de *P* |
|---|---|---|---|---|
| | 60I Biofilmes | 60I Crescimento Planctônico | | |
| **325** | 38,2 | 0,8 | **38,9** | 1,20721E-08 |
| **196** | 243,2 | 5,2 | **39,1** | 0 |
| **4** | 6917,5 | 124,0 | **47,1** | 0 |
| **148** | 387,5 | 6,6 | **49,3** | 0 |
| **163** | 985,1 | 11,7 | **70,5** | 0 |
| **344** | 426,1 | 2,9 | **122,1** | 0 |
| **49** | 725,5 | 3,6 | **166,3** | 0 |
| **8** | 840,7 | 2,0 | **350,3** | 0 |
| **1373** | 10424,5 | 24,7 | **356,6** | 0 |
| **37** | 1814,1 | 2,0 | **756,0** | 0 |
| **56467** | 47,6 | 0,24 | **-261,6** | 6,35936E-13 |
| **407** | 33,5 | 0,22 | **-184,2** | 1,73886E-09 |
| **3788** | 556,6 | 7,4 | **-88,5** | 0 |
| **6709** | 29,2 | 0,54 | **-64,1** | 3,15179E-08 |
| **36293** | 20,7 | 0,45 | **-56,6** | 3,54529E-06 |
| **2882** | 130,0 | 2,7 | **-54,8** | 0 |
| **20856** | 348,4 | 7,5 | **-54,6** | 0 |
| **17339** | 21,9 | 0,9 | **-26,7** | 3,51931E-06 |
| **1720** | 103,0 | 5,9 | **-20,5** | 0 |
| **21254** | 26,4 | 2,3 | **-13,2** | 1,57865E-06 |

Os resultados demonstrados neste estudo foram obtidos considerando um valor ajustado de $P < 0,05$ como critério biológico para seleção de GDEs. Neste contexto, os genes que apresentaram uma expressão aumentada com valor de "Fold Change" $\geq 2$, foram considerados, neste trabalho, como genes induzidos (up-regulated ou superexpressos).

Enquanto que os genes que apresentaram uma expressão diminuída, com valor de “Fold Change” ≤ -2, foram considerados como genes reprimidos (down-regulated).

Diagramas de Venn dos genes correlacionados entre pares de amostras estão representados na Figura 5. Tais Diagramas representam graficamente o número de genes expressos em ambas as condições, bem como os genes expressos exclusivamente em cada amostra (genes únicos).

**Figura 5. Diagramas de Venn do transcriptoma de** *H. capsulatum.* Diagramas mostram o número de genes exclusivos de cada amostra e o número de genes expressos em ambas as condições. Correlações entre pares de amostras, sendo biofilmes de EH-315 vs. culturas planctônicas de EH-315 **(A)**, culturas planctônicas de EH-315 vs. culturas planctônicas de 60I **(B)**, biofilmes de EH-315 vs. biofilmes de 60I **(C)** e, biofilmes de 60I vs. culturas planctônicas de 60I **(D)**.

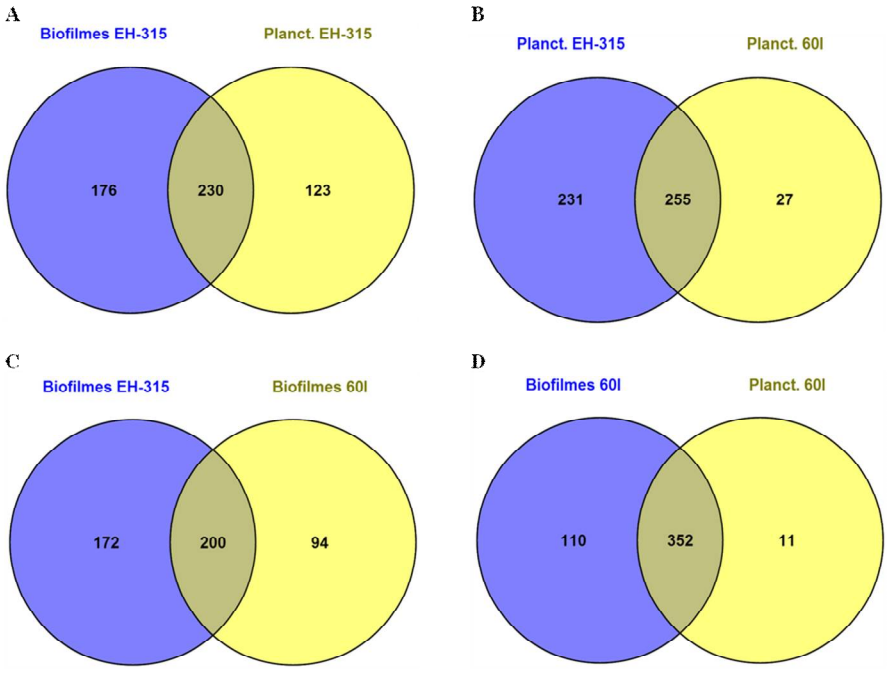


Adicionalmente, a Figura 6 ilustra análises comparativas do perfil transcriptômico diferencial entre os pares de amostras analisadas, considerando o número de GDEs, induzidos ou reprimidos.

**Figura 6. Perfil transcriptômico de** *H. capsulatum***.** Análises comparativas correspondentes ao perfil transcriptômico diferencial entre as amostras analisadas, considerando o número de transcritos induzidos (up-regulated) e reprimidos (down-regulated), obtidos por abordagem transcriptômica utilizando a plataforma Illumina e o equipamento HiscanSQ (Illumina). Perfil transcriptômico diferencial da cepa EH-315 em biofilmes e em crescimento planctônico **(A)**, das cepas EH-315 e 60I em crescimento planctônico **(B)**, das cepas EH-315 e 60I em biofilmes **(C)** e, da cepa 60I em biofilmes e em crescimento planctônico **(D)**.

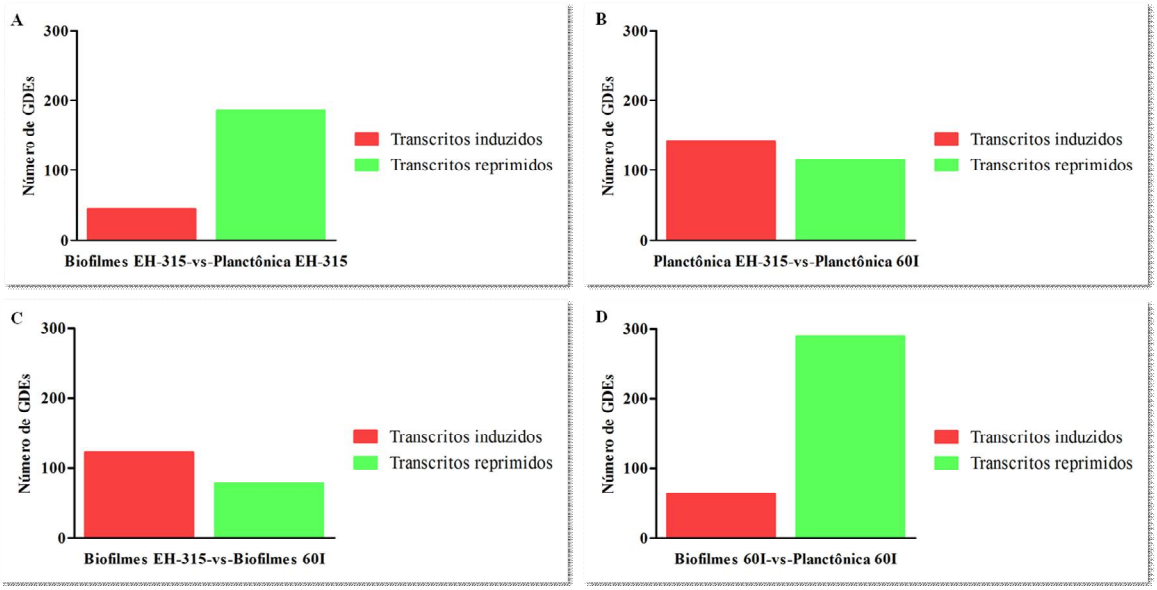


A análise dos dados de sequenciamento da cepa EH-315 em biofilmes e em crescimento planctônico, revela que 176 genes foram expressos unicamente (genes únicos) pela cepa EH-315 em biofilmes com um valor de expressão em RPKM variando entre 17 e 186. Por outro lado, 123 genes únicos foram expressos pela cepa EH-315 em crescimento planctônico com nível de expressão entre 22 e 82 RPKM (Figura 5A). Além disso, 44 genes foram induzidos por esta cepa de *H. capsulatum* em biofilmes, com um intervalo de expressão diferencial $\geq$ 2,0 e $\leq$ 152,9 em relação à segunda amostra analisada. Em contrapartida, 186 genes foram reprimidos pelo microrganismo em biofilmes e, com valores de expressão diferencial negativos entre 27,2 e 2,0 (Figura 6A).

Considerando a análise diferencial entre a cepa EH-315 e 60I em crescimento planctônico, os dados gerados revelam que foram expressos 231 genes únicos pela cepa EH-315 em crescimento planctônico, com nível de expressão variando entre 16 e 135 RPKM. Em relação à cepa 60I em crescimento planctônico, foram expressos apenas 27 genes únicos, com valor de expressão entre 22 e 272 RPKM (Figura 5B). Tendo em vista genes induzidos, a análise do transcriptoma da cepa EH-315 em crescimento planctônico revelou 141 genes up-regulated, com valores normalizados de "Fold Change" $\geq$ 2,0 e $\leq$ 40,7 comparado à expressão

dos mesmos genes pela cepa 60I em crescimento planctônico. Da mesma forma, a análise dos genes reprimidos pela cepa EH-315 em culturas planctônicas, revelou 114 genes down-regulated e, com “Fold Change” negativo entre 2,0 e 102,02 (Figura 6B).

Em relação ao perfil transcriptômico diferencial entre a cepa EH-315 e 60I em biofilmes, 172 genes únicos foram expressos exclusivamente pela cepa EH-315 em biofilmes, com nível de expressão entre 18 e 186 RPKM. Considerando a cepa 60I em biofilmes, foram expressos 94 genes únicos, com valores de expressão entre 21 e 985 RPKM (Figura 5C). Quanto aos genes induzidos, a cepa EH-315 em biofilmes exibiu 122, com um nível de expressão diferencial $\geq 2,0$ e $\leq 524,6$. Além disso, na análise da cepa EH-315 em biofilmes, 78 genes foram reprimidos com expressão diferencial negativa entre 2,0 e 1421,3 (Figura 6C).

Finalmente, foi realizada a análise transcriptômica diferencial da cepa 60I em biofilmes e culturas planctônicas e, neste caso, 11 genes únicos, com nível de expressão entre 17 e 135 RPKM, foram expressos pela cepa 60I em crescimento planctônico, livre ou flutuante. Em contrapartida, 110 genes únicos foram expressos pela mesma cepa em biofilmes, com nível de expressão variando entre 21 e 383 RPKM (Figura 5D). Na avaliação dos genes up-regulated, foi possível verificar que para a cepa 60I em biofilmes, 63 genes foram superexpressos e apresentaram valores de expressão diferencial $\geq 2,0$ e $\leq 756,03$. De maneira significativamente maior, 289 genes foram reprimidos pela mesma cepa em biofilmes, sendo que estes exibiram expressão diferencial negativa entre 2,0 e 261,64 (Figura 6D).

Diante do exposto, através da análise diferencial entre biofilmes e culturas planctônicas de ambas as cepas, é possível destacar que o microrganismo em biofilmes expressa um número significativamente maior de genes únicos quando comparado ao crescimento em condições planctônicas (Figuras 5A e 5D). Isso nos leva a concluir que quando estruturadas em biofilmes as leveduras de *H. capsulatum* exacerbam a expressão de genes únicos.

De maneira complementar, ambas as cepas estruturadas em biofilmes reprimem um número significativamente maior de genes em relação ao número de genes induzidos (Figuras 6A e 6D). Portanto, quando o microrganismo altera o seu estilo de vida de móvel para séssil, novos genes passam a ser expressos à medida que há, predominantemente, repressão na expressão de inúmeros genes.

Correlacionando as cepas EH-315 e 60I em crescimento planctônico, há muito genes ($n = 255$) que foram expressos em ambas, mas é nítido observar que a cepa EH-315, de maior

infectividade, expressa um número significativamente maior de genes únicos (n = 231) em relação à cepa 60I (n = 27), o que corresponde a um número, aproximadamente, 8,5 vezes menor (Figura 5B). Já em biofilmes, a razão entre o número de genes exclusivos expressos pela cepa EH-315 (n = 172) em relação à 60I (n = 94), reduz para um número, aproximadamente, 1,8 vezes menor (Figura 5C). Este fato sugere que em biofilmes, formações que conferem aumento da virulência e resistência dos microrganismos, cepas com infectividade divergente exibem elevado potencial de expressão de genes únicos. Portanto, a alta expressão de genes exclusivos em um biofilme não é dependente da infectividade de uma cepa.

Em contrapartida, o potencial de infecção das cepas pode estar associado a um aumento no número de genes induzidos. Este fato pode ser explicado uma vez que considerando a quantificação relativa dos GDEs induzidos e reprimidos entre as cepas, nota-se que a EH-315 superexpressa um número maior de genes do que o total de genes que são reprimidos em relação à expressão da cepa 60I nas duas formas de crescimento (Figuras 6B e 6C).

Assim, a plataforma de RNA-Seq empregada neste estudo permitiu uma caracterização robusta do perfil gênico que representam a assinatura transcricional dos biofilmes e de culturas planctônicas de cepas de infectividade divergente (EH-315 e 60I). Segundo Wang *et al.* (2009b), plataformas de RNA-Seq permitem quantificar precisamente o nível de expressão gênica, uma vez que o sequenciamento de cada transcrito é feito independentemente. Além disso, tais plataformas são extremamente sensíveis sendo capazes de identificar uma ampla faixa do nível de expressão, detectando níveis muito baixos ou muito altos.

Neste trabalho, conforme demonstrado anteriormente, entre os 230 GDEs correlacionando biofilmes vs. culturas planctônicas da cepa EH-315, 44 genes foram up-regulated e 186 foram down-regulated nos biofilmes. Subsequentemente, com base nestas análises prévias, foi determinada a anotação funcional referente à ontologia gênica (GO) do produto dos 20 transcritos com expressão diferencial significativa (10 up-regulated e 10 down-regulated) (Tabela 7). Tais proteínas merecem destaque e a Figura 7 exibe o Fold Change da expressão diferencial nos biofilmes da cepa EH-315 em relação à expressão em crescimento planctônico. Nesta condição diferencial, um transcrito cujo produto está associado à síntese de proteínas foi significativamente induzido (Fold Change 152,99), enquanto um gene que codifica um produto essencial para a via de processamento do DNA foi significativamente reprimido (Fold Change -9,10) nos biofilmes formados. Considerando

a categorização de um gene induzido significativamente cujo produto EF-1α (elongation factor 1-alpha) tem papel essencial na síntese proteica, segundo Merrick (1992), em eucariotos tal proteína é altamente conservada e dirige o RNA transportador (RNAt) carregado até o sítio aceptor do ribossomo em um transporte dependente de GTP. Estudos anteriores revelam ainda que EF-1α tem um papel importante na morfogênese do fungo dimórfico *Mucor racemosus* (Shearer, 1995). Concomitantemente, nota-se a repressão substancial de um transcrito codificante de um produto (issep1-like transposase) com papel fundamental em uma via de processamento do DNA. Atualmente, não existem estudos na literatura que descrevem a expressão de transposases em biofilmes fúngicos patogênicos. Em contrapartida, Duran-Pinedo *et al.* (2014) relataram superexpressão de um grande número de transposases putativas em biofilmes mistos de *Streptococcus mitis* com os patógenos periodontais *Porphyromonas gingivalis* e *Aggregatibacter actinomycetemcomitans*. De acordo com este estudo, a superexpressão das transposases não está associada apenas a um alto potencial para mobilidade genética (Mitchell *et al*., 2010), mas também a um processo de morte celular controlada nos biofilmes bacterianos.

**Tabela 7.** Categorização funcional dos genes com expressão significativamente alterada em biofilmes vs. culturas planctônicas da cepa EH-315 de *H. capsulatum* obtidos por RNA-Seq.

| Categoria ou Gene ID | Anotação Funcional | e-Value | Similaridade (média) | Fold-Change |
|---|---|---|---|---|
| **Genes Up-regulated** | | | | |
| contig_61450 | Elongation factor 1-alpha | 0 | 98,4% | 152,99 |
| contig_1198 | abc atp-binding protein | 4,3E-53 | 88,6% | 10,26 |
| contig_277 | Urease accessory protein | 4,5E-163 | 97,65% | 5,19 |
| contig_1707 | Lactoylglutathione lyase | 1,4E-65 | 98,8% | 5,14 |
| contig_137 | Pts system sucrose-specific iibc component | 0 | 98,85% | 5,14 |
| contig_493 | Replication protein | 4,6E-6 | 81,7% | 5,01 |
| contig_305 | lpxtg-motif cell wall anchor domain partial | 1,3E-136 | 75,1% | 4,83 |
| contig_146 | Lipoprotein | 7,6E-45 | 97,5% | 4,81 |
| contig_25 | Histidine kinase | 1,1E-80 | 98,65% | 4,77 |
| contig_297 | Nitrate transporter | 3,0E-62 | 99,6% | 4,38 |
| **Genes Down-regulated** | | | | |
| contig_34788 | Hypothetical protein BN871_FO_00160 | 2,5E-4 | 77% | -9,34 |
| contig_446 | Issep1-like transposase | 2,3E-43 | 100% | -9,10 |
| contig_3452 | Hypothetical protein BN871_FO_00160 | 8,4E-4 | 75% | -8,38 |
| contig_58 | Had tigr02254 family | 1,6E-156 | 96,75% | -6,38 |
| contig_18939 | Hypothetical protein BN871_FO_00160 | 5,5E-4 | 75% | -6,05 |
| contig_59844 | Hypothetical protein PaelaDRAFT_5811, partial | 7,8E-4 | 63% | -6,03 |
| contig_14036 | Two-component system sensor histidine kinase | 7,7E-37 | 98.5% | -5,81 |
| contig_8539 | Hypothetical protein BN871_FO_00160 | 8,4E-5 | 76% | -5,02 |
| contig_18657 | Hypothetical protein PaelaDRAFT_5811, partial | 7,6E-4 | 72% | -4,95 |
| contig_26924 | Hypothetical protein BN871_FO_00160 | 1,8E-4 | 72% | -4,58 |

**Figura 7. Fold Change Plot dos transcritos diferencialmente expressos em biofilmes vs. culturas planctônicas da cepa EH-315 de** *H. capsulatum*. Representação dos 20 transcritos com expressão diferencial significativa e anotação funcional (Gene Ontology – GO), sendo 10 superexpressos e 10 reprimidos pelos biofilmes.

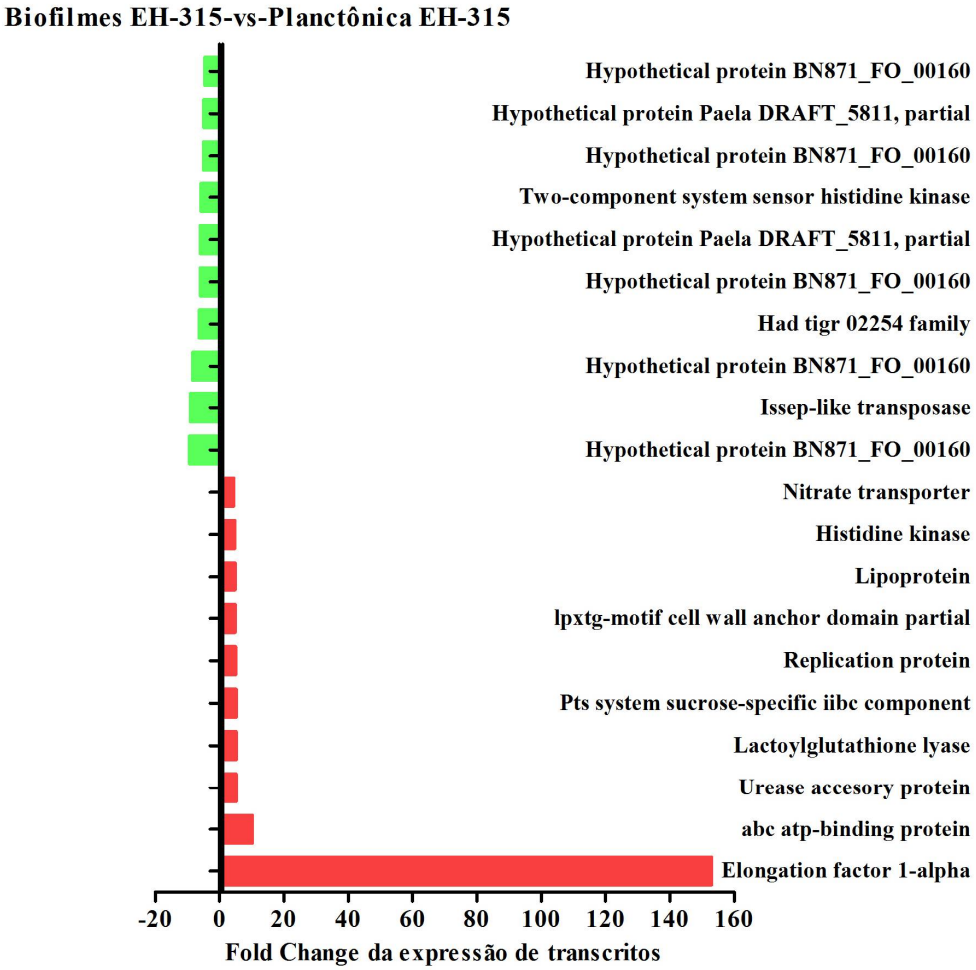


A análise transcriptômica diferencial entre culturas planctônicas de ambas as cepas (EH-315 e 60I) revelou que entre os 255 GDEs, 141 genes foram up-regulated e 114 foram down-regulated e a anotação funcional dos transcritos com expressão significativamente alterada destaca que um gene cujo produto (atpase involved in DNA repair) atua em uma via de reparo do DNA foi induzido significativamente (Fold Change 40,77). Diversas enzimas envolvidas em sistemas de reparo do DNA têm sido relacionadas à habilidade de alguns microrganismos para sobreviver em microambientes com peróxido de hidrogênio e pH ácido. Estes fatores propiciam estresse celular, tais como estresse oxidativo e ácido, uma vez que podem induzir danos ao DNA (Wen *et al.*, 2011). No mesmo momento, um transcrito codificante de uma proteína (Chk1 Checkpoint kinase 1-like partial) envolvida em vias

biológicas relacionadas ao controle do ciclo celular em resposta ao dano ao DNA foi reprimido substancialmente (Fold Change -102,02) (Tabela 8). De fato, o ciclo celular envolve sequencialmente a transição das fases G1, S e, G2 para a fase M, o que resulta na divisão e proliferação celular. Vias de checkpoint são responsáveis por um controle criterioso da transição entre estas fases, uma vez que tais vias são ativadas para garantir a finalização ideal da fase atual do ciclo celular, antes que a célula entre na próxima fase. Adicionalmente, a sinalização de checkpoint é crucial para promover a resposta a danos ao DNA e, nesta condição Chk1 induz a interrupção do ciclo celular e ativa o processo de reparo do DNA celular (Pabla *et al*., 2012). A Figura 8 exibe o Fold Change dos produtos dos 20 transcritos com expressão diferencial significativa em culturas planctônicas da cepa EH-315 em relação à expressão em crescimento planctônico da cepa 60I, com destaque para a superexpressão de uma proteína envolvida no reparo do DNA e para a repressão de uma proteína relacionada às vias de checkpoint.

**Tabela 8.** Categorização funcional dos genes com expressão significativamente alterada em culturas planctônicas da cepa EH-315 vs. culturas planctônicas da cepa 60I de *H. capsulatum* obtidos por RNA-Seq.

| Categoria ou Gene ID | Anotação Funcional | e-Value | Similaridade (média) | Fold-Change |
|---|---|---|---|---|
| **Genes Up-regulated** | | | | |
| contig_38 | atpase involved in dna repair | 5,1E-114 | 97,45% | 40,77 |
| contig_11 | Histidine decarboxylase | 0 | 84,9% | 27,48 |
| contig_344 | Membrane protein | 2,1E-28 | 93% | 19,02 |
| contig_460 | Replication initiation protein | 1,0E-169 | 92,75% | 13,31 |
| contig_34788 | Hypothetical protein BN871_FO_00160 | 2,7E-4 | 77% | 8,56 |
| contig_18939 | Hypothetical protein BN871_FO_00160 | 5,5E-4 | 75% | 7,76 |
| contig_1418 | mfs transporter | 1,4E-94 | 94,05% | 6,81 |
| contig_285 | Replication initiation protein | 0 | 96,4% | 5,88 |
| contig_305 | lpxtg-motif cell wall anchor domain partial | 1,5E-136 | 73,3% | 5,84 |
| contig_3403 | lpxtg-motif cell wall anchor domain partial | 3,2E-40 | 78,45% | 5,71 |
| **Genes Down-regulated** | | | | |
| contig_3788 | chk1 checkpoint-like partial | 1,2E-24 | 84,75% | -102,02 |
| contig_20856 | Proline dehydrogenase 1 | 0 | 99,1% | -43,24 |
| contig_56467 | Family transcriptional regulator | 2,4E-63 | 83,95% | -24,66 |
| contig_2882 | tpa: ac1147-like | 2,4E-28 | 80,9% | -14,09 |
| contig_1161 | s4 domain protein | 2,1E-46 | 99,3% | -13,31 |
| contig_1112 | 2-hydroxyacid dehydrogenase | 3,5E-140 | 99,4% | -10,16 |
| contig_5306 | Oligopeptide transport atp-binding protein | 1,4E-79 | 98,6% | -9,63 |
| contig_6087 | Oligopeptide abc atp-binding protein | 8,4E-76 | 97,2% | -9,54 |
| contig_94 | Carbon-nitrogen family | 0 | 98,7% | -8,84 |
| contig_4952 | Aldehyde dehydrogenase | 0 | 99,35% | -8,40 |

**Figura 8. Fold Change Plot dos transcritos diferencialmente expressos em culturas planctônicas da cepa EH-315 vs. culturas planctônicas da cepa 60I de** *H. capsulatum.* Representação dos 20 transcritos com expressão diferencial significativa e anotação funcional (Gene Ontology – GO), sendo 10 superexpressos e 10 reprimidos pelo crescimento planctônico da cepa EH-315.

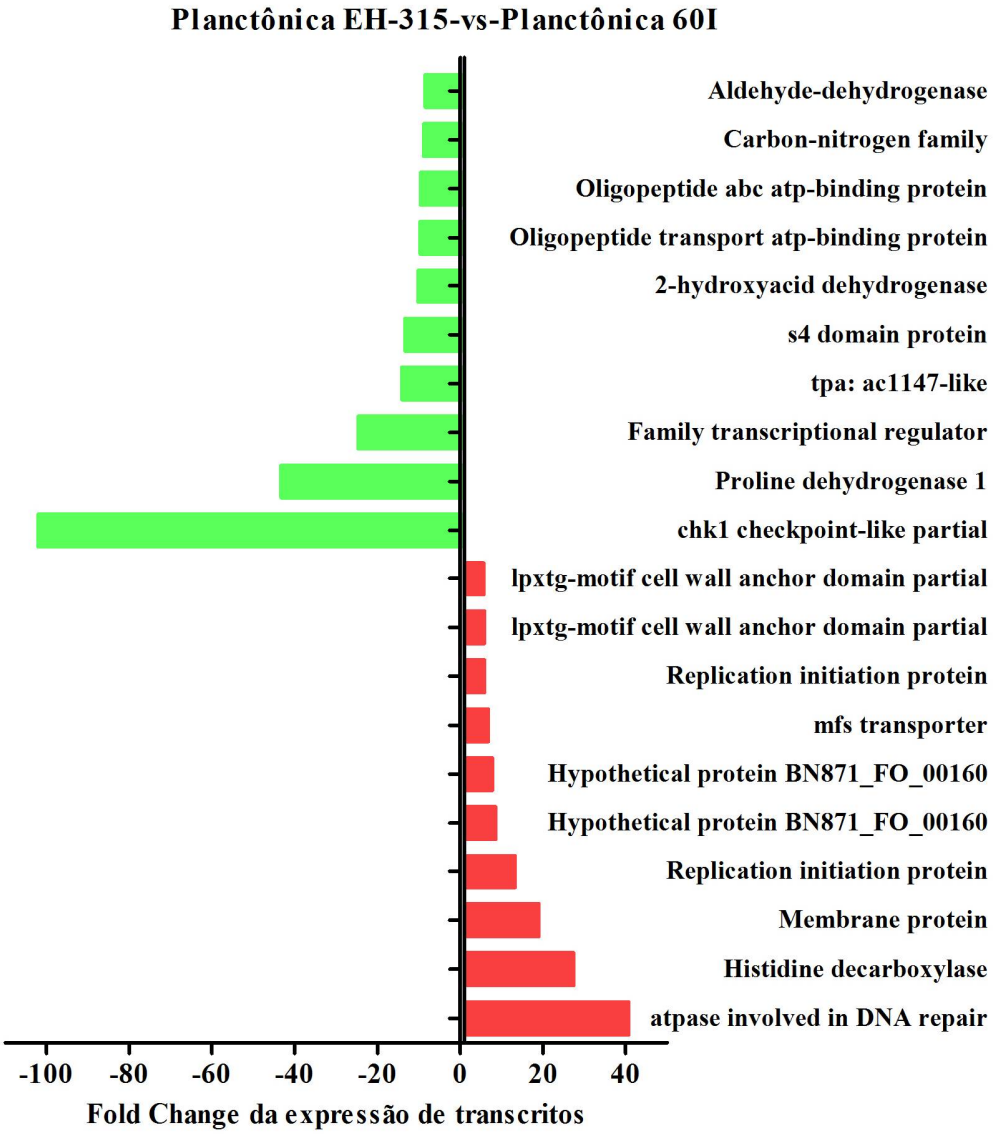


Adicionalmente, na assinatura transcricional dos biofilmes entre cepas de infectividade distinta, 200 genes foram expressos diferencialmente, sendo 122 genes up-regulated e 78 genes down-regulated nos biofilmes da cepa EH-315, de maior infectividade. O gene induzido com maior expressão diferencial (Fold Change 482,3) foi identificado como um gene codificador de GAPDH (Glyceraldehyde-3-phosphate dehydrogenase) (Tabela 9), bem conhecida como a sexta enzima da via glicolítica, mas também associada a eventos

nucleares, incluindo a transcrição, transporte de RNA, replicação de DNA e, ainda, a apoptose. Hara *et al*. (2005) descrevem que além das funções glicolíticas muito bem estabelecidas, GAPDH participa de um mecanismo molecular de citotoxicidade, no qual facilita a degradação de alvos nucleares promovendo a morte celular. Adicionalmente, outros papéis intracelulares de GAPDH têm sido descritos, incluindo indução da fusão de vesículas, atividade quinase e, ainda modulação do citoesqueleto. Neste contexto, GAPDH foi a primeira enzima glicolítica a ser encontrada em associação com a tubulina, uma relação complexa que pode estar envolvida na motilidade celular ou na organização intracelular espacial, incluindo a posição das organelas, bem como o transporte intracompartimental de elementos tubulares e vesiculares (Tisdale, 2002). Vallejo *et al*. (2012) descrevem GAPDH como uma proteína detectada microscopicamente na parede celular de *Paracoccidioides brasiliensis*, com função destacada na adesão aos componentes da MEC da célula hospedeira. Simultaneamente à indução de GAPDH, os biofilmes da cepa EH-315 exibiram uma repressão substancial (Fold Change -213,63) de um transcrito que tem como produto uma hidrolase associada à parede celular (Cell wall-associated hydrolase) (Tabela 9). Tal proteína é requerida como um importante fator de virulência dos fungos patogênicos e é reconhecida pelo seu importante papel na invasão dos tecidos do hospedeiro (Ghannoum, 2000). Da mesma forma, outras enzimas hidrolíticas, como a fosfolipase, apresentaram expressão diminuída em biofilmes de *C. albicans* e *P. brasiliensis* (Nailis *et al*., 2010; Sardi *et al*., 2015). Com isso, os dados obtidos neste estudo demonstram que os biofilmes da cepa 60I secretam uma maior quantidade de enzimas hidrolíticas, o que confere aumento da capacidade invasiva. A Figura 9 corresponde a uma representação esquemática do Fold Change de cada uma das 20 proteínas correspondentes aos transcritos que apresentaram expressão diferencial significativa nos biofilmes da cepa EH-315 em relação à expressão nos biofilmes da cepa 60I.

**Tabela 9.** Categorização funcional dos genes com expressão significativamente alterada nos biofilmes da cepa EH-315 vs. biofilmes da cepa 60I de *H. capsulatum* obtidos por RNA-Seq.

| Categoria ou Gene ID | Anotação Funcional | e-Value | Similaridade (média) | Fold-Change |
|---|---|---|---|---|
| **Genes Up-regulated** | | | | |
| contig_63353 | Glyceraldehyde-3-phosphate dehydrogenase | 0 | 94,4% | 482,30 |
| contig_8593 | Cytochrome p450 liketbp | 3,4E-20 | 73,9% | 28,39 |
| contig_15092 | Glycosyl transferase (glycosyl transferase family 2) | 1,7E-25 | 64,2% | 26,92 |
| contig_25144 | Protein tar1 | 4,7E-32 | 76,6% | 17,73 |
| contig_14320 | Signal peptide | 1,4E-11 | 100% | 13,21 |
| contig_3403 | Lpxtg-motif cell wall anchor domain partial | 3,0E-40 | 77,65% | 12,41 |
| contig_3495 | rRna intron-encoded homing partial | 2,5E-22 | 81,4% | 10,63 |
| contig_3841 | Uncharacterised protein | 8,9E-26 | 85.9% | 6,21 |
| contig_70 | 6-phospho-beta-galactosidase | 0 | 99,4% | 5,48 |
| contig_2468 | pf04134 family protein | 2,3E-55 | 92,5% | 5,47 |
| **Genes Down-regulated** | | | | |
| contig_8 | Cell wall-associated hydrolase | 5,0E-92 | 87,05% | -213,63 |
| contig_148 | Is1 transposase partial | 3,5E-43 | 90,2% | -77,52 |
| contig_7 | Hypothetical protein APECO1_1785 | 1,7E-64 | 75,1% | -73,54 |
| contig_4 | Na+ h+ antiporter | 4,8E-140 | 98,2% | -70,69 |
| contig_1921 | 40s ribosomal protein s6 | 4,7E-150 | 99,85% | -70,53 |
| contig_49 | Putative uncharacterized protein | 2,7E-60 | 85,25% | -58,80 |
| contig_9 | Permease | 4,3E-92 | 99,15% | -18,57 |
| contig_196 | Metal ion metal ion (mn2+ fe2+) transporter family | 3,9E-56 | 98,6% | -14,47 |
| contig_94 | Carbon-nitrogen family | 0 | 98,7% | -14,28 |
| contig_131 | Recombinase | 7,0E-96 | 92,65% | -11,88 |

**Figura 9. Fold Change Plot dos transcritos diferencialmente expressos em biofilmes da cepa EH-315 vs. biofilmes da cepa 60I de** *H. capsulatum.* Representação dos 20 transcritos com expressão diferencial significativa e anotação funcional (Gene Ontology – GO), sendo 10 superexpressos e 10 reprimidos pelos biofilmes da cepa EH-315.

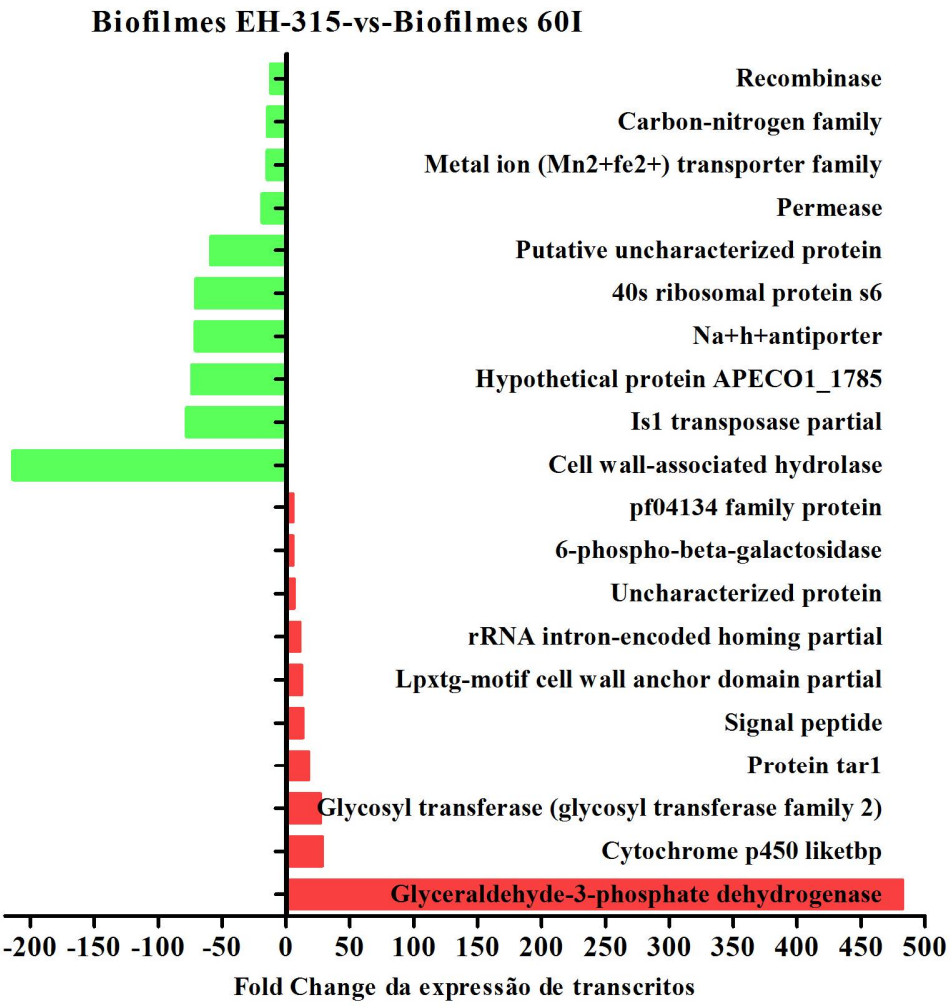


Por fim, a comparação transcricional da cepa 60I em biofilmes vs. culturas planctônicas revela que entre 352 GDEs, 63 foram up-regulated enquanto 289 genes foram down-regulated pelas leveduras em biofilmes. A Figura 10 ilustra o Fold Change das 20 proteínas com anotação funcional, identificadas como produtos dos 20 transcritos que apresentaram expressão diferencial significativa nos biofilmes da cepa 60I em relação à expressão nas culturas planctônicas desta cepa. A categorização funcional desta análise diferencial destaca uma superexpressão significativa (Fold Change -213,63) de um transcrito cujo produto (Cell wall-associated hydrolase) é descrito como uma hidrolase (Tabela 10). Conforme descrito anteriormente esta proteína tem papel pronunciado na invasão de tecidos.

Assim, conclui-se que a indução deste transcrito demonstra uma habilidade invasiva significativamente maior para as leveduras da cepa 60I em biofilmes do que as leveduras livres da mesma cepa. Ao mesmo tempo, houve repressão significativa (Fold Change -261,64) de um transcrito cujo produto atua como um regulador transcricional (Family transcriptional regulator). Neste contexto, Ryp1 constitui o regulador transcricional com funções regulatórias bem estabelecidas para *H. capsulatum*. Ryp1 governa aspectos relacionados à morfologia do fungo, sendo requerido para a transição micélio-levedura, a 37°C (Cain *et al*., 2012). De acordo com Webster e Sil (2008), Ryp1 é exigido para controlar praticamente todo o perfil de expressão da fase leveduriforme de *H. capsulatum*. Diante dos resultados da análise transcriptômica, nota-se que em biofilmes da cepa 60I a expressão de reguladores transcricionais é significativamente reprimida. No entanto, estudos posteriores podem ser designados a buscar de fato, os reguladores que estão envolvidos e o que isso implica na patogênese da histoplasmose.

Dessa forma, a tecnologia de sequenciamento da Illumina foi utilizada neste estudo para o sequenciamento e análise do transcriptoma de leveduras de *H. capsulatum*, caracterizando-se como uma abordagem eficiente para identificar genes críticos envolvidos na formação dos biofilmes de *H. capsulatum*. Assim, esta investigação possibilitou a identificação de genes candidatos potenciais que codificam proteínas chave. Tais genes podem ser amplamente estudados como putativos alvos terapêuticos e/ou biomarcadores durante a infecção às células hospedeiras.

**Tabela 10.** Categorização funcional dos genes com expressão significativamente alterada em biofilmes vs. culturas planctônicas da cepa 60I de *H. capsulatum* obtidos por RNA-Seq.

| Categoria ou Gene ID | Anotação Funcional | e-Value | Similaridade (média) | Fold-Change |
|---|---|---|---|---|
| **Genes Up-regulated** | | | | |
| contig_8 | Cell wall-associated hydrolase | 5,0E-92 | 87,5% | 350,37 |
| contig_49 | Putative uncharacterized protein | 2,7E-60 | 85,25% | 166,30 |
| contig_344 | Membrane protein | 2,0E-28 | 93% | 122,10 |
| contig_163 | Cell wall-associated hydrolase domain partial | 3,3E-20 | 83,1% | 70,56 |
| contig_148 | Is1 transposase partial | 3,5E-43 | 90,2% | 49,34 |
| contig_4 | Na+ h+ antiporter | 4,8E-140 | 98,2% | 47,15 |
| contig_196 | Metal ion metal ion (mn2+ fe2+) transporter family | 3,5E-56 | 98,6% | 39,12 |
| contig_9558 | BnaC09g26910D | 4,4E-18 | 74% | 35,25 |
| contig_11 | Histidine decarboxylase | 0 | 85,95% | 33,74 |
| contig_133 | Recombinase | 0 | 97,35% | 30,28 |
| **Genes Down-regulated** | | | | |
| contig_56467 | Family transcriptional regulator | 2,4E-63 | 84,35% | -261,64 |
| contig_407 | Restriction endonuclease | 1,4E-129 | 68,3% | -184,21 |
| contig_3788 | Chk1 checkpoint-like partial | 1,2E-24 | 84,75% | -88,52 |
| contig_6709 | Protein rep | 0 | 95,2% | -64,17 |
| contig_36293 | Sporulation lipoprotein domain protein | 1,8E-25 | 96,75% | -56,68 |
| contig_2882 | tpa: ac1147-like | 2,4E-28 | 80,9% | -54,88 |
| contig_20856 | Proline dehydrogenase 1 | 0 | 99,1% | -54,61 |
| contig_17339 | Dihydrolipoyllysine-residue e2 component of oxoglutarate dehydrogenase (succinyl-transferring) complex | 1,8E-55 | 100% | -26,76 |
| contig_1720 | Alpha-l1 nicotinic acetyl choline receptor | 1,3E-33 | 75,75% | -20,55 |
| contig_479 | Hth-type transcriptional regulator | 8,3E-29 | 99% | -13,05 |

**Figura 10. Fold Change Plot dos transcritos diferencialmente expressos em biofilmes vs. culturas planctônicas da cepa 60I de** *H. capsulatum.* Representação dos 20 transcritos com expressão diferencial significativa e anotação funcional (Gene Ontology – GO), sendo 10 superexpressos e 10 reprimidos pelos biofilmes.

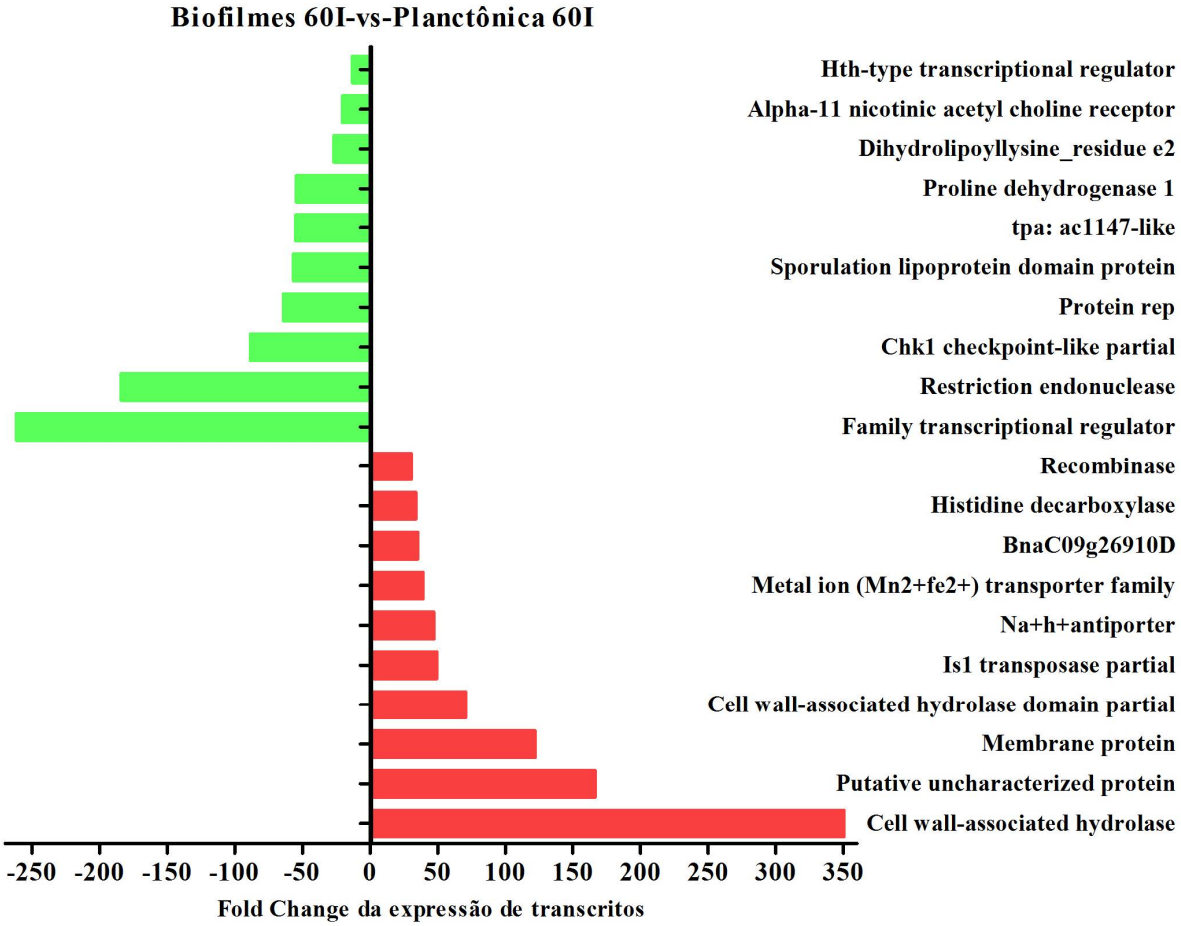


## 4.3. Determinação da viabilidade celular e porcentagem de infecção em Mø alveolares (AMJ2-C11) por diferentes cepas de *H. capsulatum*

### 4.3.1. Determinação da viabilidade celular após infecção de células AMJ2-C11 utilizando o kit Live/Dead®

Ensaios para determinação da viabilidade de células infectadas foram realizados previamente à obtenção do conjunto de transcritos da interação fungo-célula hospedeira. A Figura 11 demonstra os dados obtidos a partir da marcação com o kit Live/Dead® das células AMJ2-C11 desafiadas por diferentes concentrações de suspensão fúngica, compreendendo a MOI em uma razão de 10 leveduras:1 Mø, 1:1, 1:10 e 1:100. De acordo com as imagens obtidas através do IN Cell Analyzer as células podem ser vistas em sua maioria coradas de verde e com membrana íntegra para todas as MOIs, representando viabilidade uma vez que

há atividade de enzimas esterases (Figura 11A). Adicionalmente, os resultados obtidos a partir da análise de fluorescência pelo software Investigator 1000 Workstation confirmam estes dados, uma vez que em todas as concentrações fúngicas testadas, a viabilidade celular foi superior a 84%, não havendo diferença estatística entre as diferentes MOIs e o controle de células sem infecção (86,61%). Portanto, as MOIs empregadas não se demonstraram citotóxicas, uma vez que exibiram porcentagem de viabilidade celular semelhante ao controle de células sem infecção (Figura 11B).

**Figura 11. Ensaio de Viabilidade de Mø AMJ2-C11 infectados com leveduras de** *H. capsulatum* **após 5 h. (A)** Imagens adquiridas pelo IN Cell Analyzer caracterizando células verdes como viáveis marcadas pela Calceína AM e células vermelhas como mortas marcadas por homodímero de Etídio (EthD-1). **(B)** Valores correspondentes à viabilidade foram obtidos a partir da fluorescência das células marcadas utilizando o kit Live/Dead®. Análises conduzidas pelo software IN Cell Investigator 1000 Workstation. CN – Controle de células sem infecção.

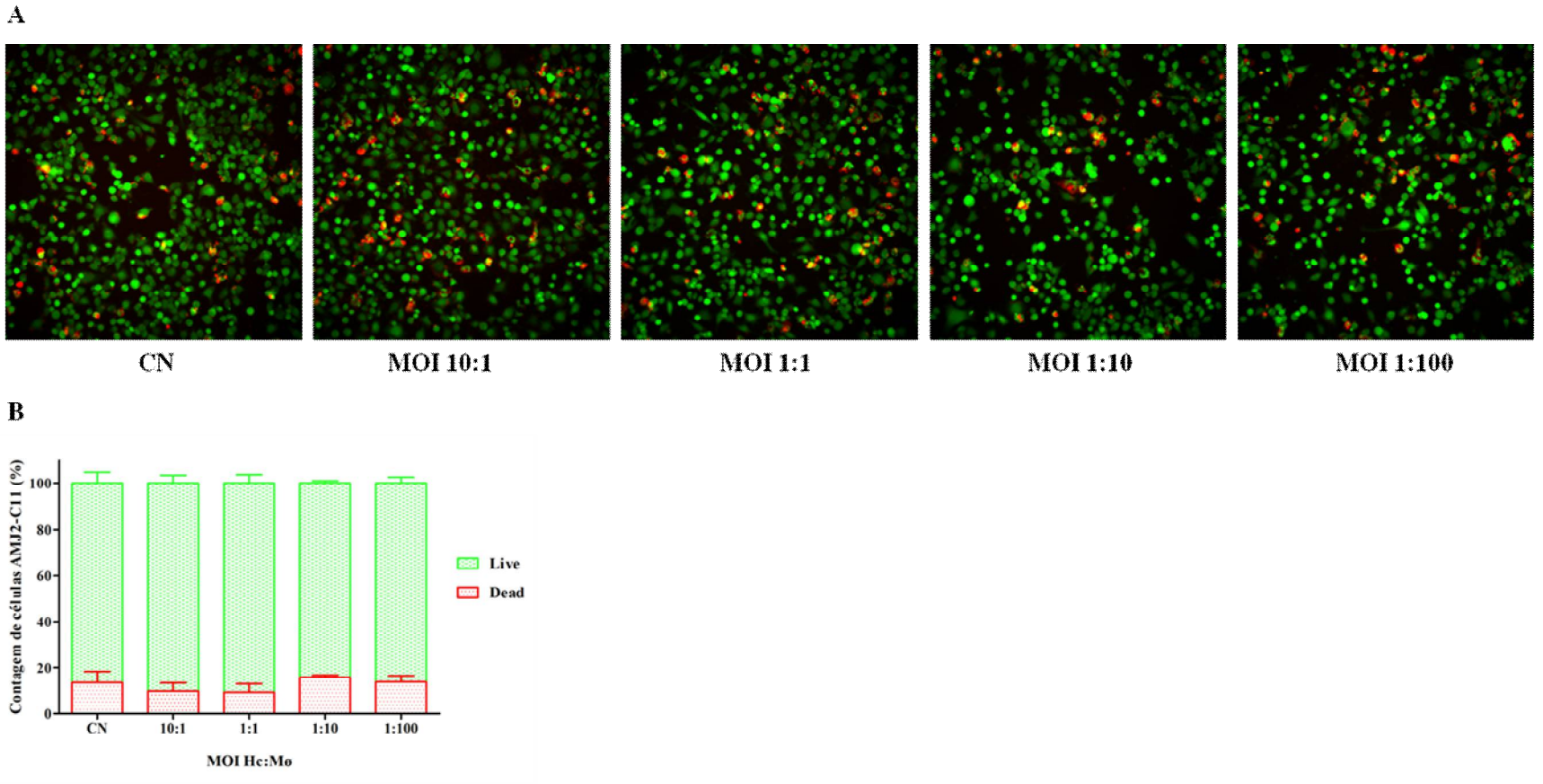

### 4.3.2. Determinação da porcentagem de infecção às células AMJ2-C11 por citometria de fluxo

Considerando o perfil de infecção de cepas de *H. capsulatum* em Mø alveolares, que são caracterizadas como as primeiras células efetoras que respondem ao fungo, é possível observar a capacidade de ambas as cepas em exibir porcentagens muito altas de infecção à Mø (Figuras 12D e 13D). Os resultados dos ensaios de infecção à Mø alveolares AMJ2-C11 com as diferentes cepas de *H. capsulatum* estão apresentados nas Figuras 12, 13 e 14. Os dados obtidos demonstram que as cepas EH-315 e 60I, de diferente infectividade, apresentam potencial de infecção semelhante, sendo capazes de infectar 98,34 ± 0,38% e 96,52 ± 3,14%, respectivamente, dos Mø alveolares murinos após 5 h de infecção (Figura 14). Estes resultados correspondem a FI de leveduras marcadas com CFSE através da análise da fluorescência de 10.000 células por tubo empregando como controle leveduras não marcadas, leveduras marcadas e células AMJ2-C11 sem infecção.

**Figura 12. Perfis de citometria ilustrando a intensidade de fluorescência (FI) de leveduras de** *H. capsulatum* **na infecção de células fagocíticas AMJ2-C11, analisadas por citômetro de fluxo FACSCanto™. (A)** Controle negativo de leveduras (cepa EH-315) não marcadas. **(B)** Controle positivo de leveduras (cepa EH-315) marcadas com CFSE. **(C)** Controle negativo de células AMJ2-C11 sem infecção. **(D)** FI da infecção de células AMJ2-C11 com leveduras de *H. capsulatum* (cepa EH-315), após 5 h. Dados obtidos pelo software FACSDiva™ e representativos da FI de 10.000 células por tubo.

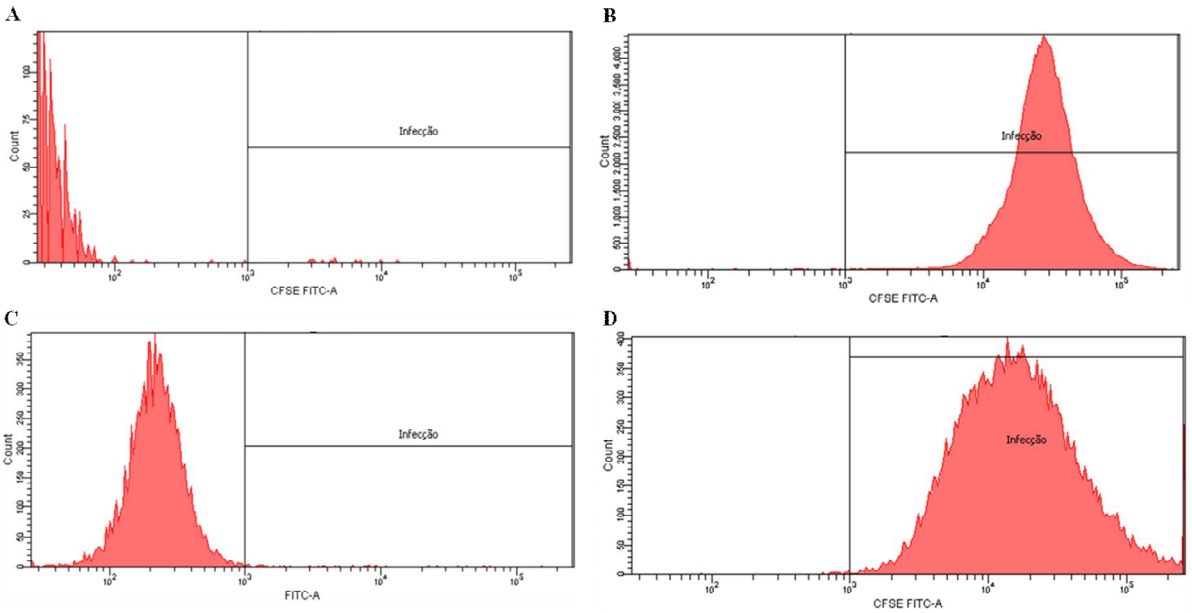

**Figura 13. Perfis de citometria ilustrando a intensidade de fluorescência (FI) de leveduras de *H. capsulatum* na infecção de células fagocíticas AMJ2-C11, analisadas por citômetro de fluxo FACSCanto™. (A)** Controle negativo de leveduras (cepa 60I) não marcadas. **(B)** Controle positivo de leveduras (cepa 60I) marcadas com CFSE. **(C)** Controle negativo de células AMJ2-C11 sem infecção. **(D)** FI da infecção de células AMJ2-C11 com leveduras de *H. capsulatum* (cepa 60I), após 5 h. Dados obtidos pelo software FACSDiva™ e representativos da FI de 10.000 células por tubo.

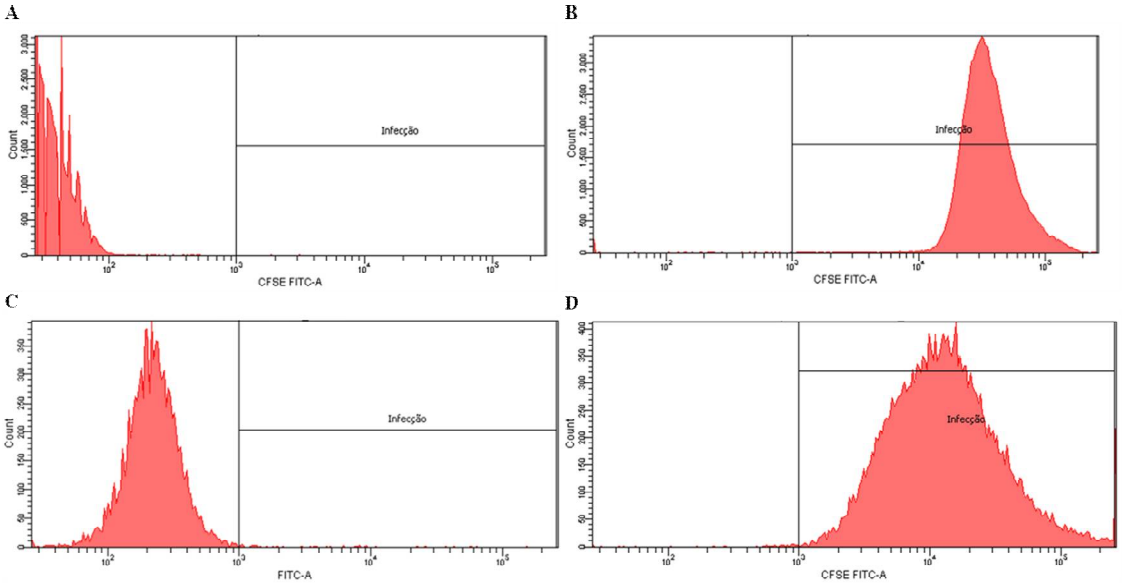


**Figura 14. Perfil de infecção de diferentes cepas de *H. capsulatum* à Mø alveolares murinos.** Valores obtidos a partir da FI de leveduras marcadas com CFSE após 5 h de infecção em células AMJ2-C11, através da análise de 10.000 células por tubo utilizando o software FACSDiva™.

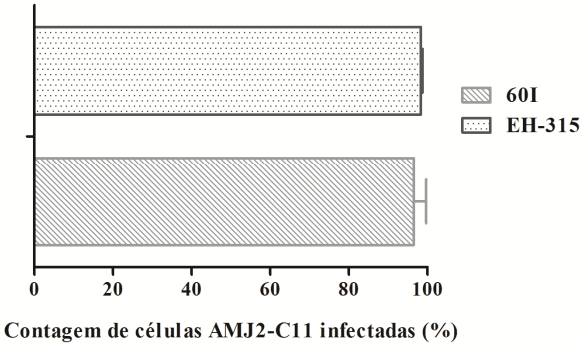


## 4.4. Screening de miRNAs expressos em células hospedeiras após interação com *H. capsulatum*

### 4.4.1. Determinação da viabilidade celular após infecção de Mø THP-1 like utilizando o kit Live/Dead®

Os ensaios para a determinação da viabilidade celular foram conduzidos previamente à realização do screening de miRNAs regulados na infecção fungo-Mø hospedeiros. A Figura 15 representa os dados obtidos a partir da marcação de Mø THP-1 like utilizando o kit Live/Dead® frente a diferentes concentrações da suspensão fúngica, com as MOIs nas seguintes razões, 10 leveduras:1 Mø, 1:1, 1:10 e 1:100. As imagens obtidas pelo IN Cell Analyzer possibilitam a visualização das células, que em sua maioria encontram-se coradas de verde em função da atividade de esterases intracelulares e com membrana íntegra para todas as MOIs, o que representa viabilidade (Figura 15A). Estes dados que aparentam alta viabilidade de células THP-1 frente à infecção podem se confirmados a partir da análise de fluorescência realizada pelo software Investigator 1000 Workstation, que demonstra em todas as concentrações fúngicas testadas uma viabilidade celular superior a 93,79%, não havendo diferença estatística entre as diferentes MOIs e o controle de células sem infecção (93,96%). Portanto, as MOIs empregadas não se demonstraram citotóxicas, uma vez que exibiram porcentagem de viabilidade celular semelhante ao controle de células sem infecção (Figura 15B). Tais resultados são de extrema importância, uma vez que a morte de Mø infectados poderia inviabilizar uma diferença significativa na expressão de miRNAs entre células infectadas e não infectadas.

**Figura 15. Ensaio de Viabilidade de Mø THP-1 like infectados com leveduras de** *H. capsulatum* **após 5 h. (A)** Imagens adquiridas pelo IN Cell Analyzer caracterizando células verdes como viáveis marcadas pela Calceína AM e células vermelhas como mortas marcadas por homodímero de Etídio (EthD-1). **(B)** Valores correspondentes à viabilidade foram obtidos a partir da fluorescência das células marcadas utilizando o kit Live/Dead®. Análises conduzidas pelo software IN Cell Investigator 1000 Workstation. CN – Controle de células sem infecção.

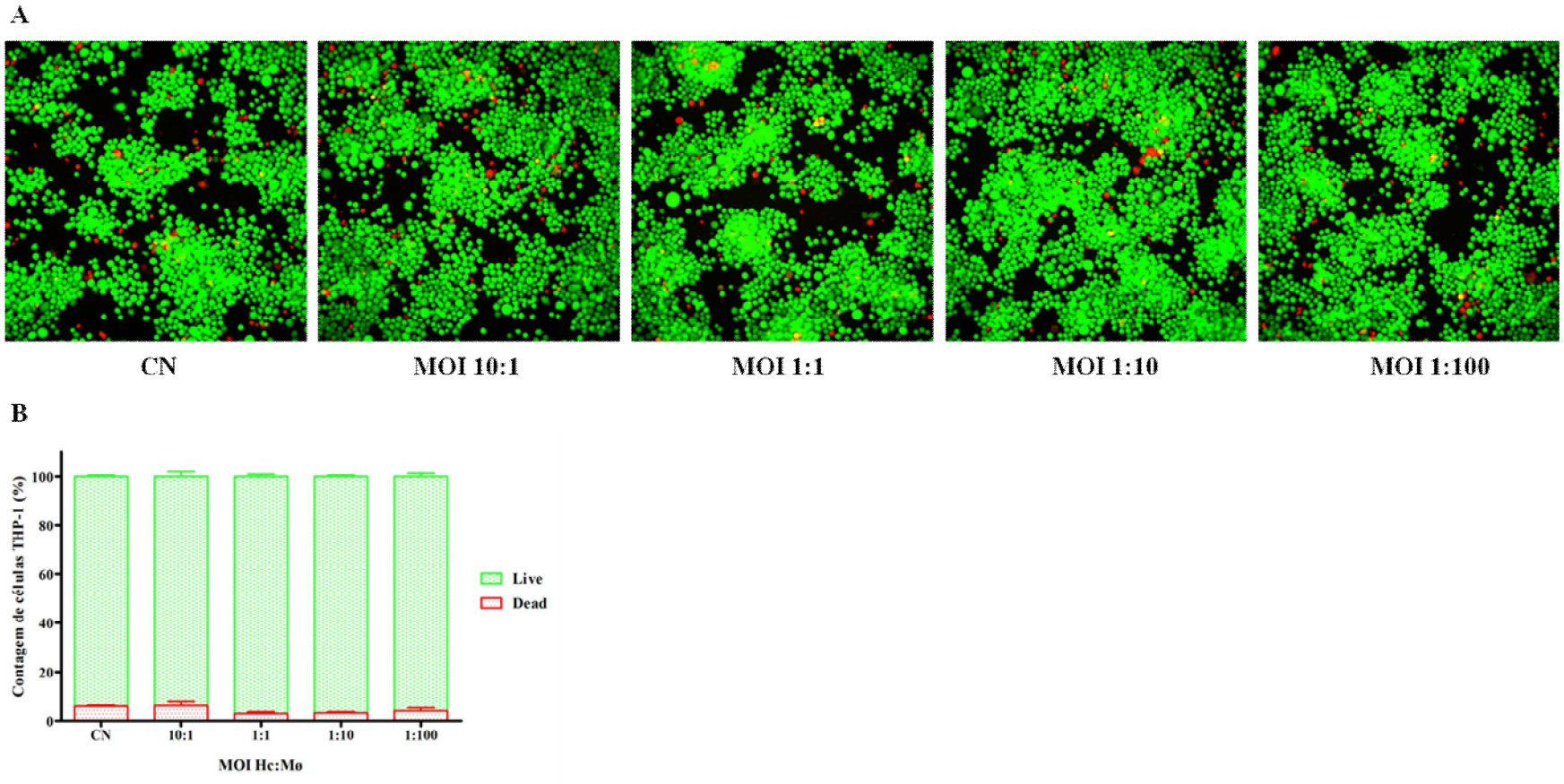

### 4.4.2. Determinação da porcentagem de infecção em Mø THP-1 like por citometria de fluxo

Análises de citometria de fluxo da infecção entre Mø THP-1 like e leveduras fluorescentemente marcadas com CFSE foram realizadas a fim de determinar a porcentagem de células infectadas e verificar se as cepas selecionadas infectam de fato Mø humanos. Para estes ensaios leveduras não marcadas, leveduras marcadas e células THP-1 sem infecção foram empregadas como controles. Os resultados foram obtidos através da análise de 10.000 células por tubo realizada pelo software FACSDiva™ (Becton & Dickinson, EUA) em consequência da FI emitida tanto por leveduras aderidas à membrana de Mø, bem como por leveduras intracelulares. As Figuras 16 e 17 representam os gráficos obtidos por citometria de fluxo compreendendo picos que, à esquerda representam células negativas não marcadas e, à direita, células positivas fluorescentemente marcadas, portanto infectadas. De acordo com os dados obtidos é possível verificar que ambas as cepas de *H. capsulatum* (EH-315 e 60I) exibem elevado potencial de interação com Mø THP-1 like, uma vez que altas porcentagens de células infectadas foram encontradas após 5 h de infecção, 93,36 ± 1,89% e 97,38 ± 0,90%, respectivamente (Figura 18).

**Figura 16. Perfis de citometria ilustrando a intensidade de fluorescência (FI) de leveduras de *H. capsulatum* na infecção de Mø THP-1 like e, analisadas por citômetro de fluxo FACSCanto™. (A)** Controle negativo de leveduras (cepa EH-315) não marcadas. **(B)** Controle positivo de leveduras (cepa EH-315) marcadas com CFSE. **(C)** Controle negativo de células THP-1 sem infecção. **(D)** FI da infecção de células THP-1 com leveduras de *H. capsulatum* (cepa EH-315), após 5 h. Dados obtidos pelo software FACSDiva™ e representativos da FI de 10.000 células por tubo.

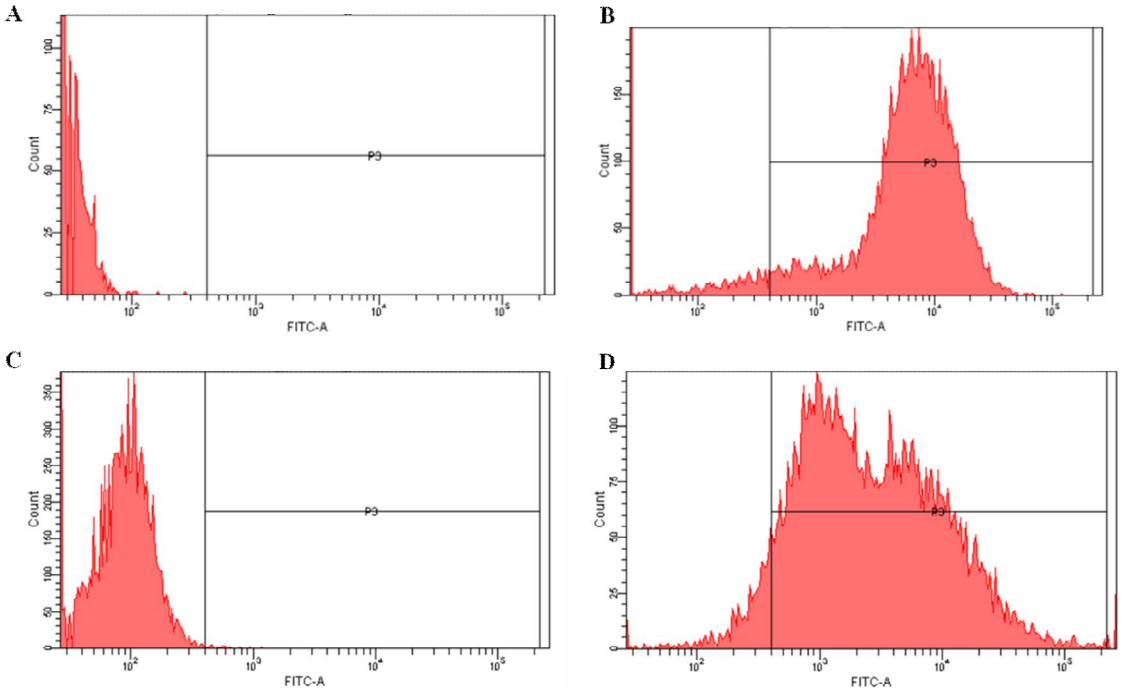

**Figura 17. Perfis de citometria ilustrando a intensidade de fluorescência (FI) de leveduras de *H. capsulatum* na infecção de Mø THP-1 like e, analisadas por citômetro de fluxo FACSCanto™. (A)** Controle negativo de leveduras (cepa 60I) não marcadas. **(B)** Controle positivo de leveduras (cepa 60I) marcadas com CFSE. **(C)** Controle negativo de células THP-1 sem infecção. **(D)** FI da infecção de células THP-1 com leveduras de *H. capsulatum* (cepa 60I), após 5 h. Dados obtidos pelo software FACSDiva™ e representativos da FI de 10.000 células por tubo.

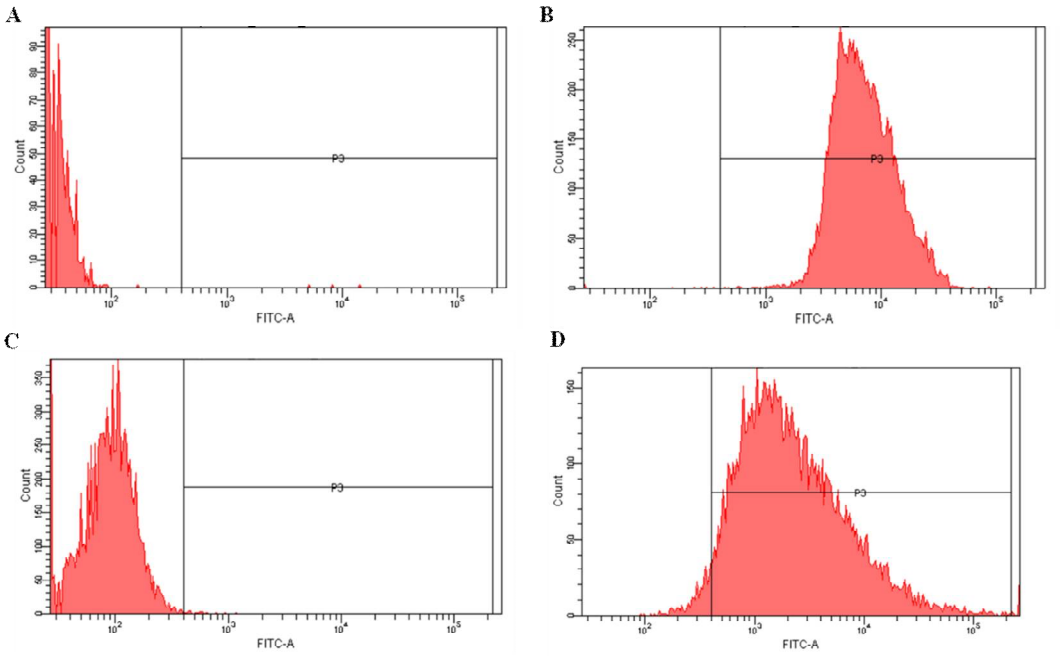


**Figura 18. Perfil de infecção de diferentes cepas de *H. capsulatum* à Mø humanos.** Valores obtidos a partir da FI de leveduras marcadas com CFSE após 5 h de infecção em células THP-1, através da análise de 10.000 células por tubo utilizando o software FACSDiva™.

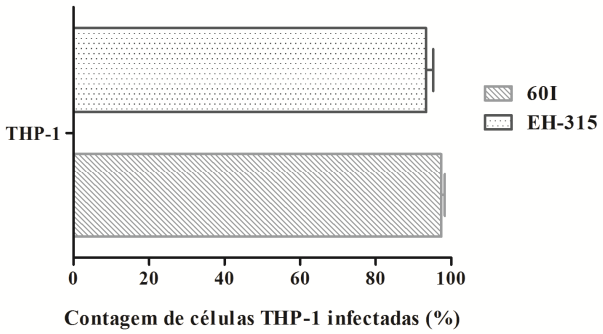


### 4.4.3. Quantificação e avaliação da pureza e integridade do RNA das amostras

Após verificar a viabilidade das células infectadas e a ocorrência da infecção, foi extraído o RNA total das amostras. As concentrações e purezas do RNA obtido estão demonstradas na Tabela 11. As análises por espectrofotometria indicam que altas concentrações de RNA das amostras foram obtidas e que o material extraído encontra-se em um grau de pureza ideal de acordo com os valores de referência (1,8 a 2,0). A partir destes dados, foi avaliada a integridade do RNA de cada amostra e os gráficos gerados pelo equipamento utilizado (Agilent 2100 Bioanalyzer®, Agilent Technologies) revelam que não há nenhum traço de degradação. Considerando o algoritmo RIN conclui-se que as amostras exibiram integridade ideal, com RIN maior ou igual a 8 (Figura 19).

**Tabela 11. Concentração de RNA obtido após extração utilizando o Kit RNeasy Plant Mini Kit®.** Extração da fase leveduriforme das cepas EH-315 e 60I de *H. capsulatum* em culturas planctônicas e das cepas EH-315 em biofilmes. Quantificação do material extraído utilizando espectrofotômetro (Nanovue®). *Unicata biológica; **Duplicata biológica; ***Triplicata biológica.

| Amostra | Concentração (ng/µL) | Pureza ($A_{260nm}/A_{280nm}$) |
|---|---|---|
| Mø vs. EH-315* | 1086,7 | 2,02 |
| Mø vs. EH-315** | 849,7 | 2,01 |
| Mø vs. EH-315*** | 942,7 | 2,03 |
| Mø vs. 60I* | 699,7 | 2,01 |
| Mø vs. 60I** | 1341,9 | 2,03 |
| Mø vs. 60I*** | 1087,7 | 2,02 |
| Mø vs. biofilmes EH-315* | 1340,9 | 2,02 |
| Mø vs. biofilmes EH-315** | 1931,5 | 2,03 |
| Mø vs. biofilmes EH-315*** | 1385,6 | 2,04 |
| Mø sem infecção* | 962,7 | 2,03 |
| Mø sem infecção** | 498,4 | 2,01 |
| Mø sem infecção*** | 1093,6 | 2,06 |

**Figura 19. Eletroferograma da Integridade do RNA de Mø THP-1 like.** Integridade do RNA de células THP-1 infectadas com as cepas EH-315 **(A, B, C)** e 60I **(D, E, F)** de *H. capsulatum* em culturas planctônicas e com a cepa EH-315 em biofilmes **(G, H, I)** em triplicata. Integridade do RNA do controle de células sem infecção **(J, K, L)** em triplicata. Análise realizada por técnica de eletroforese capilar no equipamento Agilent 2100 Bioanalyzer® através do kit RNA 6000 Nano (GE Healthcare). RIN – RNA Integrity Number.

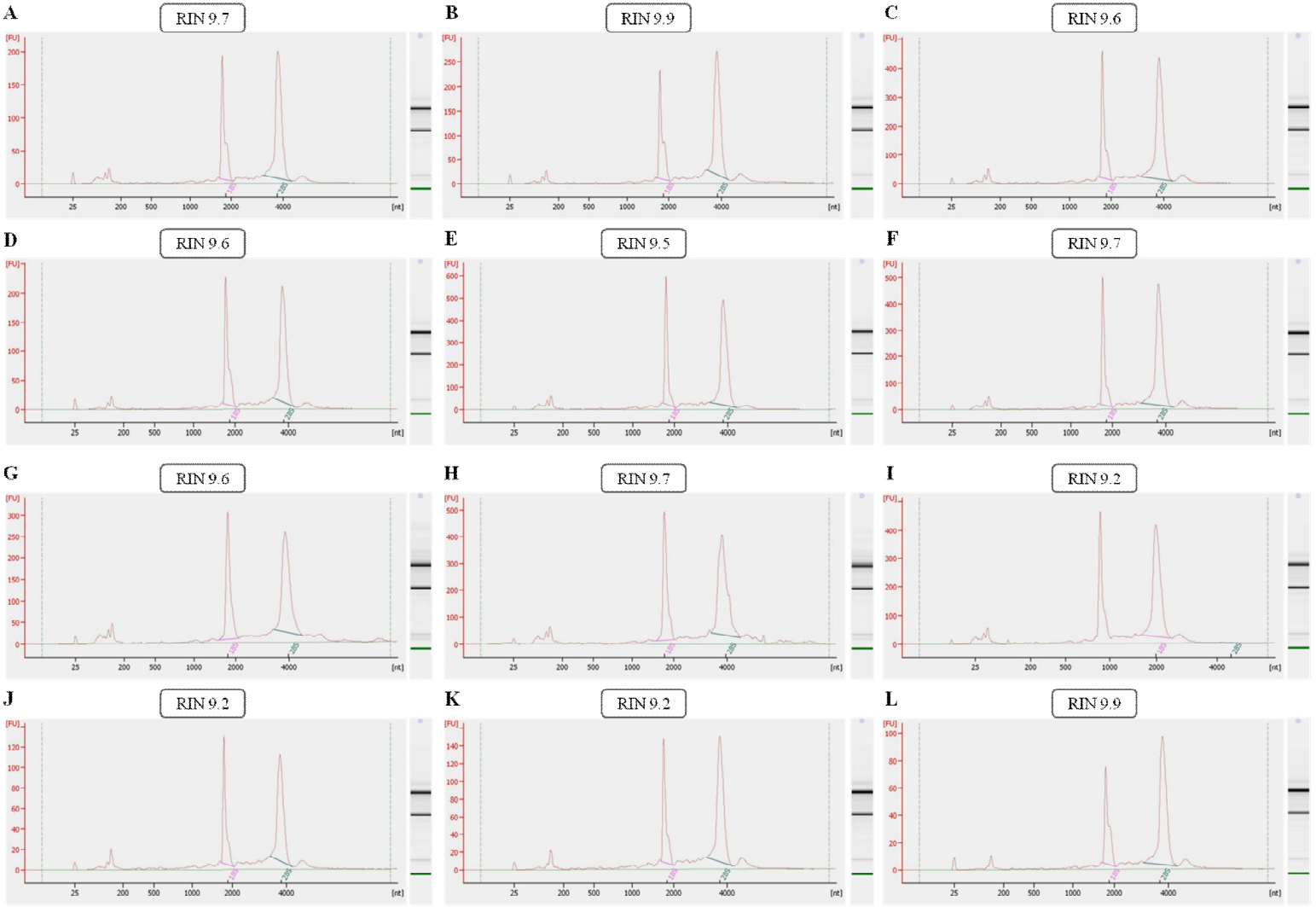

### 4.4.4. Análise da expressão de miRNAs em células THP-1 após infecção com leveduras de *H. capsulatum*

Após quantificação relativa, foram identificados miRNAs diferencialmente expressos utilizando o método comparativo de Ct (ΔΔCt). Foram contrapostos os miRNAs obtidos entre as seguintes condições: Mø THP-1 infectados com a cepa EH-315 vs. Mø THP-1 sem infecção (controle), Mø THP-1 infectados com a cepa 60I vs. Mø THP-1 sem infecção (controle), Mø THP-1 infectados com biofilmes da cepa EH-315 vs. Mø THP-1 sem infecção (controle), Mø THP-1 infectados com biofilmes da cepa EH-315 vs. Mø THP-1 infectados com a cepa EH-315 em crescimento planctônico (controle) e, Mø THP-1 infectados com a cepa EH-315 vs. Mø THP-1 infectados com a cepa 60I (controle). Sendo assim, cinco comparações em pares foram realizadas a fim de gerar o maior número de informações possíveis e comparar as diferenças entre os miRNAs superexpressos ou reprimidos dentro da mesma espécie (biofilmes vs. culturas planctônicas) e entre diferentes cepas (EH-315 vs. 60I).

Os resultados demonstrados nesta análise foram obtidos considerando um valor de $P \leq 0,05$ para seleção de miRNAs diferencialmente expressos. Considerando este cutoff, miRNAs que apresentaram uma expressão aumentada na amostra teste em relação ao controle com valor de $RQ \geq 2$, foram induzidos (up-regulated ou superexpressos). Enquanto que os miRNAs que apresentaram uma expressão diminuída na amostra em relação ao controle, com valor de $RQ < 1$, foram reprimidos (down-regulated). Em consequência, um Volcano Plot foi construído para detectar visualmente miRNAs diferencialmente expressos entre pares de amostras. A Figura 20 ilustra um Volcano Plot para cada análise diferencial realizada, com identificação para os miRNAs com expressão significativamente alterada ($P \leq 0,05$) nas amostras ensaiadas em relação aos seus respectivos controles.

**Figura 20. Volcano Plot dos perfis de miRNAs detectados em Mø infectados com leveduras de** *H. capsulatum***.** O eixo-X mostra o Fold Change (RQ) em log2 da expressão de miRNAs entre amostra teste e controle, enquanto o eixo-y mostra o valor de P em log10 ajustado para cada miRNA. Os pontos representados acima da linha cinza horizontal indicam significância estatística ($P \leq 0,05$). Pontos em verde indicam miRNAs reprimidos e em vermelho miRNAs superexpressos. Análises diferenciais entre **(A)** Mø THP-1 infectados com a cepa EH-315 vs. Mø THP-1 sem infecção; **(B)** Mø THP-1 infectados com a cepa 60I vs. Mø THP-1 sem infecção; **(C)** Mø THP-1 infectados com biofilmes da cepa EH-315 vs. Mø THP-1 sem infecção; **(D)** Mø THP-1 infectados com biofilmes da cepa EH-315 vs. Mø THP-1 infectados com a cepa EH-315 em crescimento planctônico e; **(E)** Mø THP-1 infectados com a cepa EH-315 vs. Mø THP-1 infectados com a cepa 60I.

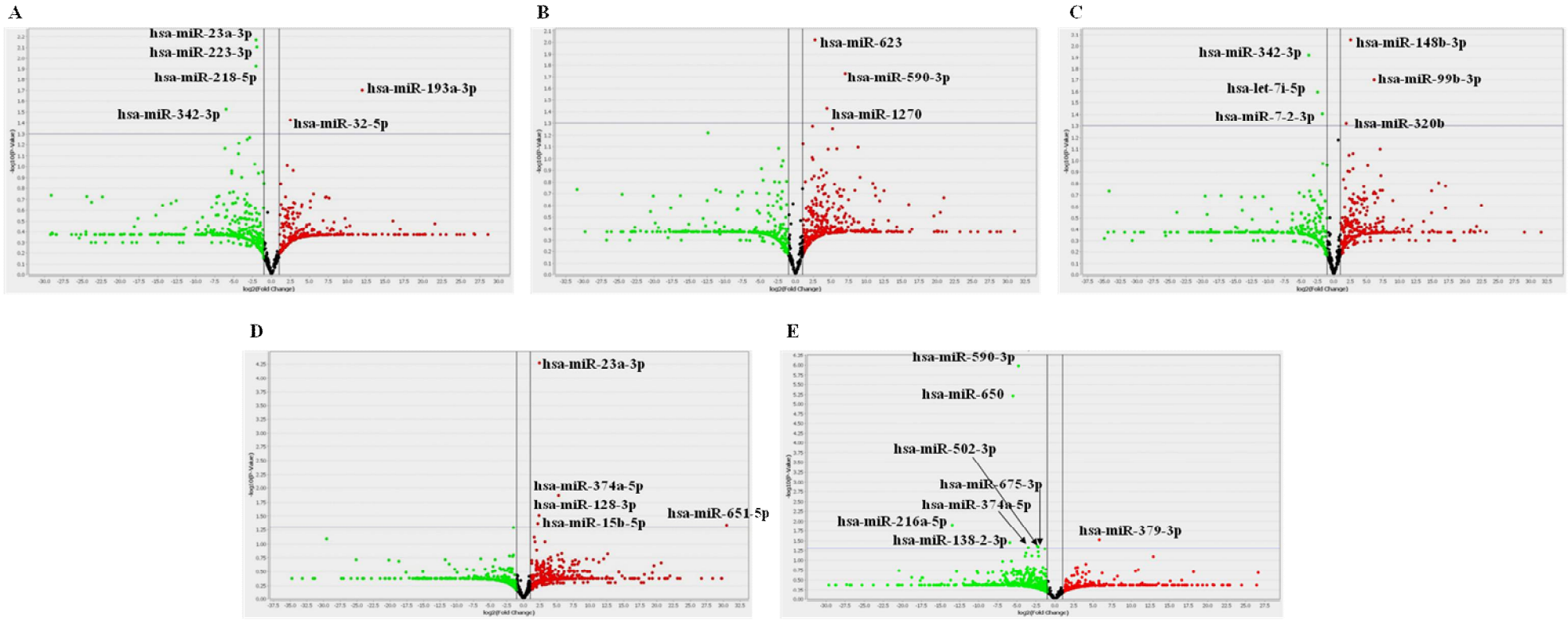

Diante destas análises, Mø THP-1 like infectados com diferentes cepas de *H. capsulatum* (EH-315 e 60I) e em diferentes formas de crescimento (biofilmes e culturas planctônicas) apresentaram perfis de expressão diferentes em relação ao controle sem infecção. Foram identificados um total de 6 miRNAs diferencialmente expressos pelas células THP-1 infectadas com a cepa EH-315 comparadas com o controle (sem infecção), dos quais 2 foram superexpressos (up-regulated) e 4 foram reprimidos (down-regulated) ($P \leq 0,05$). Considerando a infecção com a cepa 60I, células THP-1 superexpressam 3 miRNAs diferenciais em relação ao controle de célula sem infecção ($P \leq 0,05$). Adicionalmente, Mø THP-1 like infectados com biofilmes da cepa EH-315 exibiram 6 miRNAs diferencialmente expressos e, desses, 3 foram superexpressos e 3 foram reprimidos em comparação com a expressão em Mø sem infecção ($P \leq 0,05$). Posteriormente, as análises diferenciais dos perfis de expressão de miRNAs entre células THP-1 infectadas com biofilmes de EH-315 vs. infecção com leveduras planctônicas de EH-315 revelam uma superexpressão diferencial significativa ($P \leq 0,05$) de 5 miRNAs. Além disso, a comparação entre os perfis de expressão de miRNAs em Mø infectados com cepas de infectividade divergente, demonstra que 8 miRNAs tiveram uma expressão significativamente diferente ($P \leq 0,05$) na infecção pela cepa EH-315 em relação a infecção com a cepa 60I, dos quais 1 foi superexpresso e 7 foram reprimidos. Na Tabela 12 são representados todos os miRNAs diferencialmente expressos entre as comparações realizadas em pares, bem como o Fold Change (RQ) e os efeitos biológicos descritos para cada um deles. A Figura 21 exibe o Fold Change (log2) da expressão dos 28 miRNAs.

**Tabela 12. miRNAs diferencialmente expressos em Mø THP-1 não infectados e infectados com leveduras de *H. capsulatum*.** A quantificação relativa (RQ) dos miRNAs foi analisada pelo software DataAssist™ v3.01 (Applied Biosystems), em três replicatas, através do método comparativo de Ct (ΔΔCt) entre as amostras descritas. São apresentados miRNAs que tiveram expressão diferencial significativa (valor de $P \leq 0,05$). RQ dos miRNAs superexpressos em vermelho e dos miRNAs reprimidos em verde.

| miRNA ID | Fold Change (RQ) | Valor de *P* | Processos ou Categorias funcionais envolvidas | Referências |
|---|---|---|---|---|
| **Mø THP-1 infectados com a cepa EH-315 vs. Mø THP-1** | | | | |
| hsa-miR-193a-3p | **3961,50** | 0,01 | Inibe transformação celular | Iliopoulos et al., 2011; Wang et al., 2014 |
| hsa-miR-32-5p | **5,50** | 0,03 | Regulação da apoptose | Köpke et al., 2015 |
| hsa-miR-223-3p | **0,25** | 0,007 | Diferenciação monócitos-macrófagos; Proliferação celular; indução de apoptose | Cook et al., 2015; Xie et al., 2011 |
| hsa-miR-218-5p | **0,24** | 0,01 | Inibe proliferação do ciclo celular; Indução de apoptose | He et al., 2013 |
| hsa-miR-23a-3p | **0,24** | 0,006 | Sinalização de células T; Regulação da apoptose | Heikham e Shankar, 2010 |
| hsa-miR-342-3p | **0,01** | 0,02 | Inflamação; Sinalização de dor | Fourie et al., 2014 |
| **Mø THP-1 infectados com a cepa 60I vs. Mø THP-1** | | | | |
| hsa-miR-590-3p | **128,33** | 0,01 | Supressão de TGF-beta 1 | Tousi et al., 2015 |
| hsa-miR-1270 | **21,65** | 0,03 | Regulação de IFNα1 | Kimura et al., 2015 |
| hsa-miR-623 | **6,69** | 0,009 | Regulação da Endocitose mediada por receptor para desencadear a montagem de clatrina | http://www.bioinfo.mochsl.org.br/miriad/miRNA/hsa-mir-623/ |
| **Mø THP-1 infectados com biofilmes da cepa EH-315 vs. Mø THP-1** | | | | |
| hsa-miR-99b-3p | **69,97** | 0,02 | Proliferação celular | Kang et al., 2012 |
| hsa-miR-148b-3p | **5,78** | 0,008 | Regulação da resposta imune inata e regulação da apresentação de antigenos | Chen et al., 2013 |
| hsa-miR-320b | **3,65** | 0,04 | Proliferação e invasão celular | Zhou et al., 2015 |
| hsa-miR-7-2-3p | **0,29** | 0,03 | Super expressão inibe crescimento celular em linhagens pulmonares | Rai et al., 2011 |
| hsa-let-7i-5p | **0,18** | 0,02 | Induz sensibilidade a agentes antineoplásicos | Weng et al., 2014 |
| hsa-miR-342-3p | **0,07** | 0,01 | Inflamação; Sinalização de dor | Fourie et al., 2014 |

**Tabela 12. miRNAs diferencialmente expressos em Mø THP-1 não infectados e infectados com leveduras de *H. capsulatum*.** A quantificação relativa (RQ) dos miRNAs foi analisada pelo software DataAssist™ v3.01 (Applied Biosystems), em três replicatas, através do método comparativo de Ct (ΔΔCt) entre as amostras descritas. São apresentados miRNAs que tiveram expressão diferencial significativa (valor de $P \leq 0,05$). RQ dos miRNAs superexpressos em vermelho e dos miRNAs reprimidos em verde (continuação).

| miRNA ID | Fold Change (RQ) | Valor de *P* | Processos ou Categorias funcionais envolvidas | Referências |
|---|---|---|---|---|
| **Mø THP-1 infectados com biofilmes da cepa EH-315 vs. Mø THP-1 infectados com a cepa EH-315** | | | | |
| hsa-miR-651-5p | **1.483.361.248** | 0,04 | Ligação a actina; atividade carreadora de elétrons; contribuição na integridade estrutural da matriz extracelular | Algoritmos públicos TargetScan e miRanda |
| hsa-miR-374a-5p | **38,54** | 0,01 | Hipoxia; Redução da permeabilidade vascular do tecido pulmonar (reduz lesão pulmonar inflamatória induzida por exemplo, por LPS) | Adyshev et al., 2013; Adyshev et al., 2014; Looney et al., 2015 |
| hsa-miR-23a-3p | **5,32** | 0,0001 | Sinalização de células T; Regulação da apoptose | Heikham e Shankar, 2010 |
| hsa-miR-128-3p | **4,99** | 0,03 | Proliferação e invasão celular, apoptose | Yu et al., 2015 |
| hsa-miR-15b-5p | **4,46** | 0,04 | Regulação negativa dos níveis de TNFα e apoptose | Ye e Steinle et al., 2015 |
| **Mø THP-1 infectados com a cepa EH-315 vs. Mø THP-1 infectados com a cepa 601** | | | | |
| hsa-miR-379-3p | **903,56** | 0,02 | Regulação da adesão celular, resposta terapêutica e relação com perfis de resistência à drogas | Haenisch et al., 2011; Cazzoli et al., 2013 |
| hsa-miR-675-3p | **0,21** | 0,04 | Expressão reprimida está associada a migração e invasão celular | Lv et al., 2014 |
| hsa-miR-502-3p | **0,20** | 0,04 | Inibição de autofagia, do crescimento celular e da progressão do ciclo celular | Chen et al., 2015 |
| hsa-miR-374a-5p | **0,08** | 0,04 | Hipoxia; Redução da permeabilidade vascular do tecido pulmonar (reduz lesão pulmonar inflamatória induzida por exemplo, por LPS) | Adyshev et al., 2013; Adyshev et al., 2014; Looney et al., 2015 |
| hsa-miR-590-3p | **0,03** | 0 | Supressão de TGF-beta 1 | Tousi et al., 2015 |
| hsa-miR-650 | **0,02** | 0 | Inibe progressão do ciclo celular, influencia na proliferação de células B | Mraz et al., 2012 |
| hsa-miR-138-2-3p | **0,01** | 0,03 | Interação receptor-matriz extracelular | DIANA-microT-v3.0 (Maragkakis et al., 2009a; b) |
| hsa-miR-216a-5p | **0** | 0,01 | Expressão reprimida está associada com proliferação celular e supressão da apoptose | Wang et al., 2014 |

**Figura 21. Fold Change Plot dos miRNAs diferencialmente expressos em Mø THP-1 não infectados e infectados com leveduras de** *H. capsulatum***.** A quantificação relativa (RQ) dos miRNAs foi analisada pelo software DataAssist™ v3.01 (Applied Biosystems), em três replicatas, através do método comparativo de Ct (ΔΔCt) entre as amostras descritas. São apresentados os 28 miRNAs que tiveram expressão diferencial significativa (valor de $P \leq 0,05$). Análises diferenciais entre **(A)** Mø THP-1 infectados com a cepa EH-315 vs. Mø THP-1 sem infecção; **(B)** Mø THP-1 infectados com a cepa 60I vs. Mø THP-1 sem infecção; **(C)** Mø THP-1 infectados com biofilmes da cepa EH-315 vs. Mø THP-1 sem infecção; **(D)** Mø THP-1 infectados com biofilmes da cepa EH-315 vs. Mø THP-1 infectados com a cepa EH-315 em crescimento planctônico e; **(E)** Mø THP-1 infectados com a cepa EH-315 vs. Mø THP-1 infectados com a cepa 60I.

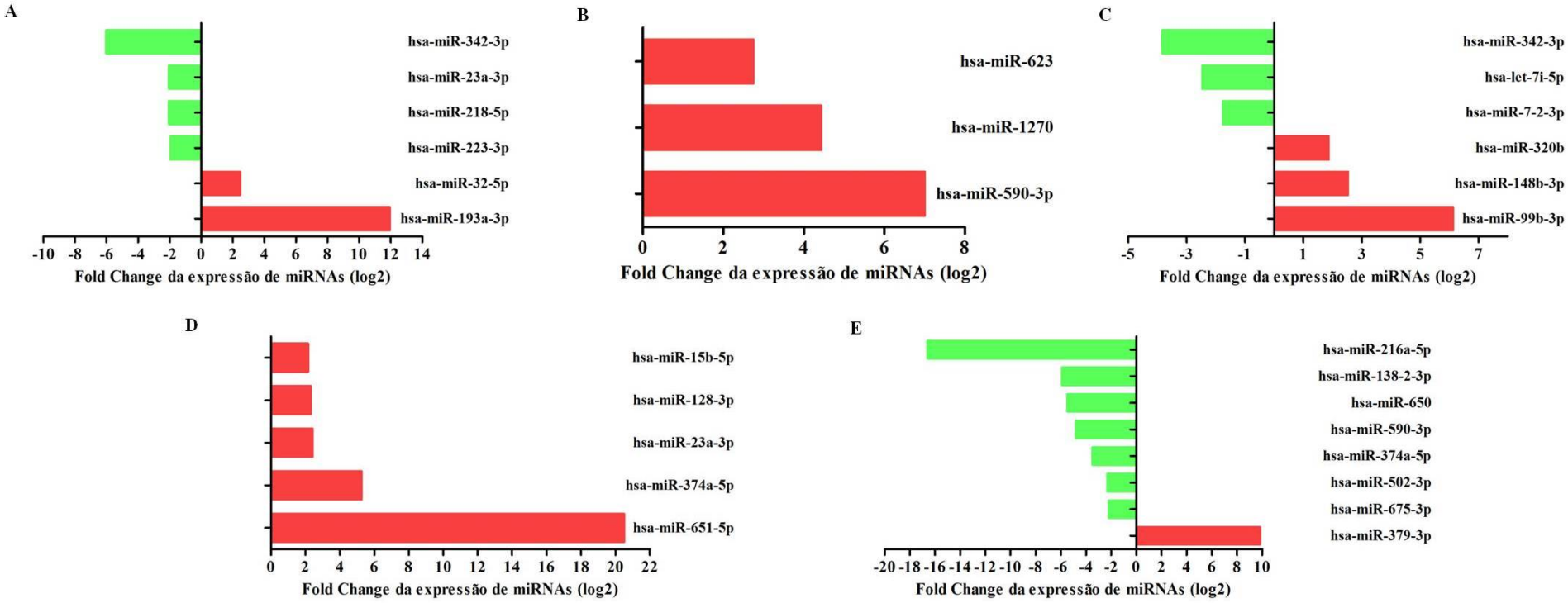

Adicionalmente, clusterizações hierárquicas são ilustradas por "Heat maps" que agrupam os perfis de miRNAs das replicatas de células THP-1 infectadas com leveduras de *H. capsulatum* e seus respectivos controles (Figura 22), isto é, os diagramas demonstram um agrupamento entre os miRNAs e as amostras triadas, de maneira que cada linha representa um miRNA e cada coluna, uma amostra. A árvore de clusterização dos miRNAs está representada em linhas hierárquicas à esquerda e acima. A escala de cores ilustra o nível relativo da expressão do miRNA em ΔCt (Ct amostra - Ct controle). Em uma reação de PCR em tempo real, uma reação positiva é detectada pelo acúmulo de um sinal fluorescente. O Ct é definido como o número de ciclos requeridos para que o sinal fluorescente ultrapasse o limiar (Threshold), ou seja, exceda o nível de background. Em vista disso, o nível de Ct é inversamente proporcional à quantidade do miRNA em uma amostra e, portanto, quanto menor o nível de Ct, maior é a quantidade do miRNA-alvo na amostra. Assim, na Figura 22 nota-se que a marcação em verde corresponde à expressão inferior do miRNA na amostra, enquanto em vermelho representa um nível de expressão do miRNA superior em uma amostra.

Notavelmente, células infectadas com leveduras de *H. capsulatum*, entre elas infecção com a cepa EH-315 em biofilmes e culturas planctônicas e com a cepa 60I, podem ser claramente distinguidas dos controles sem infecção (Figuras 22A, 22B e 22C). De acordo com a Figura 22A, torna-se necessário destacar o miRNA hsa-miR-193a-3p, que, de fato, em comparação com células sem infecção apresenta uma expressão superior significativa em células infectadas com a cepa EH-315. Por outro lado, na infecção com a cepa 60I, o diagrama de Heat map evidencia o miRNA hsa-miR-590-3p exibindo um nível de expressão muito maior na célula infectada em relação ao controle sem infecção (Figura 22B). Considerando a infecção com os biofilmes da cepa EH-315, destacam-se nitidamente dois miRNAs com expressão diferencial significativa em relação ao controle de células não infectadas, um deles com repressão substancial após a infecção (hsa-miR-342-3p) e, o segundo, com superexpressão substancial na célula infectada (hsa-miR-99b-3p) (Figura 22C). Na comparação entre Mø infectados com biofilmes de EH-315 vs. infecção com leveduras livres da mesma cepa, o perfil de expressão de miRNAs é claramente heterogêneo, com destaque para o miRNA hsa-miR-651-5p, significativamente superexpresso em resposta à infecção com os biofilmes (Figura 22D). Nota-se ainda um perfil de expressão distinto entre células infectadas com as leveduras planctônicas de EH-315 e células THP-1 infectadas com as leveduras livres de 60I, mas confirma-se a maior expressão diferencial do miRNA hsa-

miR-216a-5p, o qual foi substancialmente reprimido na célula infectada com a cepa de maior infectividade (EH-315) (Figura 22E).

**Figura 22. Análise de agrupamento hierárquico da expressão de miRNAs aberrantes em Mø infectados com leveduras de** *H. capsulatum***.** Esta figura ilustra "Heat maps" contendo cores (vermelho, verde e preto) que representam o nível de expressão dos miRNAs analisados pelo software DataAssist™ v3.01 (Applied Biosystems), em três replicatas. Análises diferenciais entre **(A)** Mø THP-1 infectados com a cepa EH-315 vs. Mø THP-1 sem infecção; **(B)** Mø THP-1 infectados com a cepa 60I vs. Mø THP-1 sem infecção; **(C)** Mø THP-1 infectados com biofilmes da cepa EH-315 vs. Mø THP-1 sem infecção; **(D)** Mø THP-1 infectados com biofilmes da cepa EH-315 vs. Mø THP-1 infectados com a cepa EH-315 em crescimento planctônico e; **(E)** Mø THP-1 infectados com a cepa EH-315 vs. Mø THP-1 infectados com a cepa 60I.

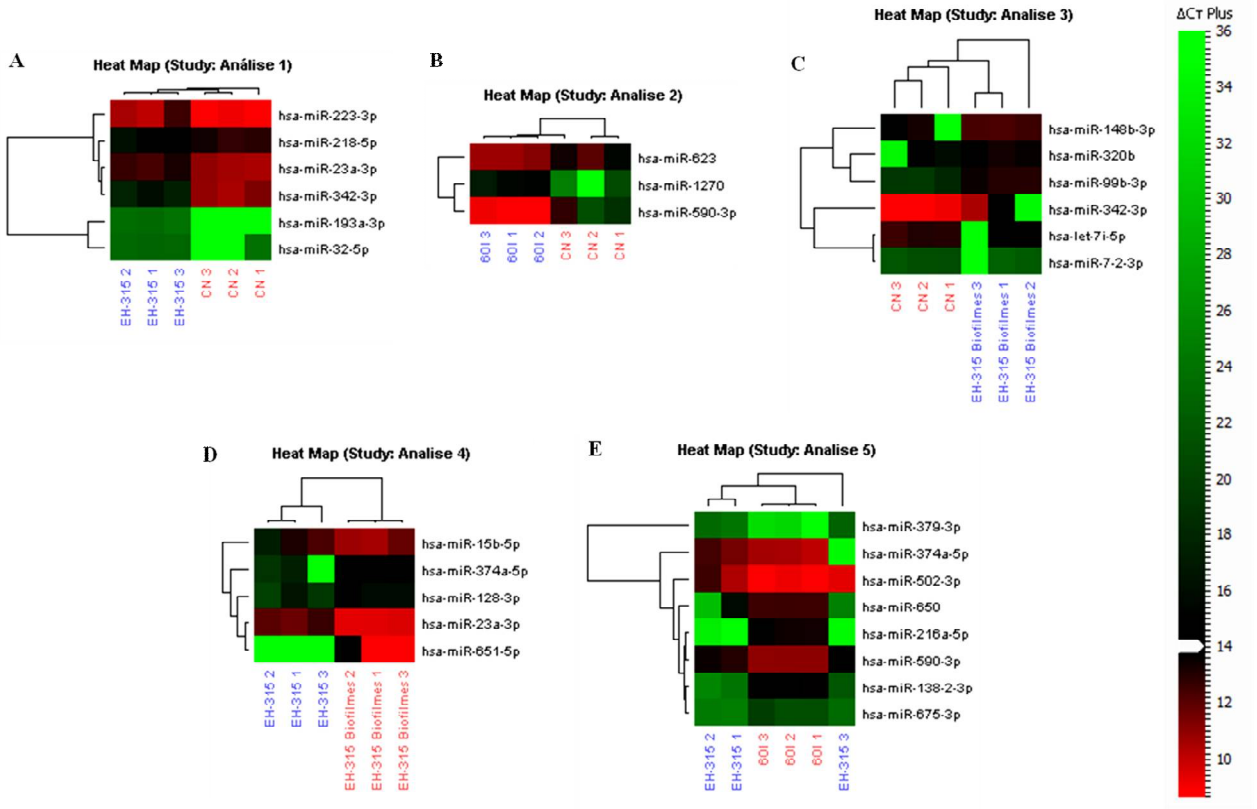

A partir destas análises, miRNAs diferencialmente expressos foram integrados com genes-alvo validados para identificar as relações regulatórias desempenhadas entre miRNAs e RNAm. Assim, genes-alvo validados regulados pelos miRNAs diferencialmente expressos foram identificados através de análises combinatórias realizadas pelo software miRWalk. Então, redes de interação miRNA-RNAm foram construídas utilizando o software Navigator v2.2. A Figura 23 exibe tais redes de interação, de maneira que os miRNAs estão representados em quadrados e estão nomeados conforme a nomenclatura preconizada para miRNAs (como exemplo: hsa-miR-342-3p – hsa, da espécie *Homo sapiens*; miR, abreviatura de miRNA; 342, identificação do miRNA em números; 3p, localização da cadeia do miRNA na extremidade 3'). Adicionalmente, os genes-alvo no RNAm são representados em círculos e são marcados com uma cor específica conforme a quantidade de miRNAs que os regula, de forma que os círculos em vermelho representam genes que são alvos de um único miRNA (Figura 23); nas Figuras 23A e 23D, os círculos em roxo representam genes no RNAm que são alvos de dois miRNAs distintos; e na Figura 23C os círculos em verde ilustram os genes que são regulados por dois miRNAs simultaneamente e o círculo em roxo representa um gene-alvo de três miRNAs. Além disso, nas redes de interação construídas as linhas em cinza interligam um miRNA ao seu gene-alvo no RNAm.

Assim, conforme demonstrado nas redes regulatórias construídas (Figura 23), a maioria dos genes-alvo são regulados negativamente por um único miRNA. No entanto, outros genes, em menor número, são down-regulados por dois ou três miRNAs distintos. Na análise diferencial entre Mø infectados com a cepa EH-315 vs. Mø sem infecção, 8 genes (DST, FOXN2, HBS1L, HIVEP1, NUFIP2, PTPN1-1, TUT1 e ZFC3H1) são regulados simultaneamente por 2 miRNAs distintos (Figura 23A). Na comparação entre Mø infectados com biofilmes da cepa EH-315 e Mø não infectados, 9 genes (ACTG1, DNMT1, EEF2, LPHN2, RFX3, RPL27A, TACC1, TNS3 e TOMM7OA) são down-regulados por dois miRNAs, enquanto 1 gene (EPB41) é regulado negativamente por 3 miRNAs diferentes (Figura 23C). Considerando a comparação entre células infectadas com biofilmes da cepa EH-315 vs. células infectadas com leveduras planctônicas da mesma cepa, 10 genes (B4GALT1, CNOT1, DDX5, JAK1, KDM3B, KMT2C, PIK3C2B, SEPT2, SERBP1 e STT3B) são regulados negativamente por 2 distintos miRNAs (Figura 23D). Segundo Broderick *et al*. (2011), o mesmo RNAm pode ser alvo de mais do que um miRNA, promovendo dessa forma uma regulação mais eficiente e mais específica.

**Figura 23. Redes de interação miRNA-RNAm.** Redes de interação construídas pelo software Navigator v2.2 resultante da análise de três replicatas. Os miRNAs são representados em quadrados. A maioria dos genes são alvos de um único miRNA específico (círculos em vermelho) e, os demais genes são regulados por dois ou três miRNAs distintos (círculos em verde e roxo). Análises diferenciais entre **(A)** Mø THP-1 infectados com a cepa EH-315 vs. Mø THP-1 sem infecção; **(B)** Mø THP-1 infectados com a cepa 60I vs. Mø THP-1 sem infecção; **(C)** Mø THP-1 infectados com biofilmes da cepa EH-315 vs. Mø THP-1 sem infecção; **(D)** Mø THP-1 infectados com biofilmes da cepa EH-315 vs. Mø THP-1 infectados com a cepa EH-315 em crescimento planctônico e; **(E)** Mø THP-1 infectados com a cepa EH-315 vs. Mø THP-1 infectados com a cepa 60I.

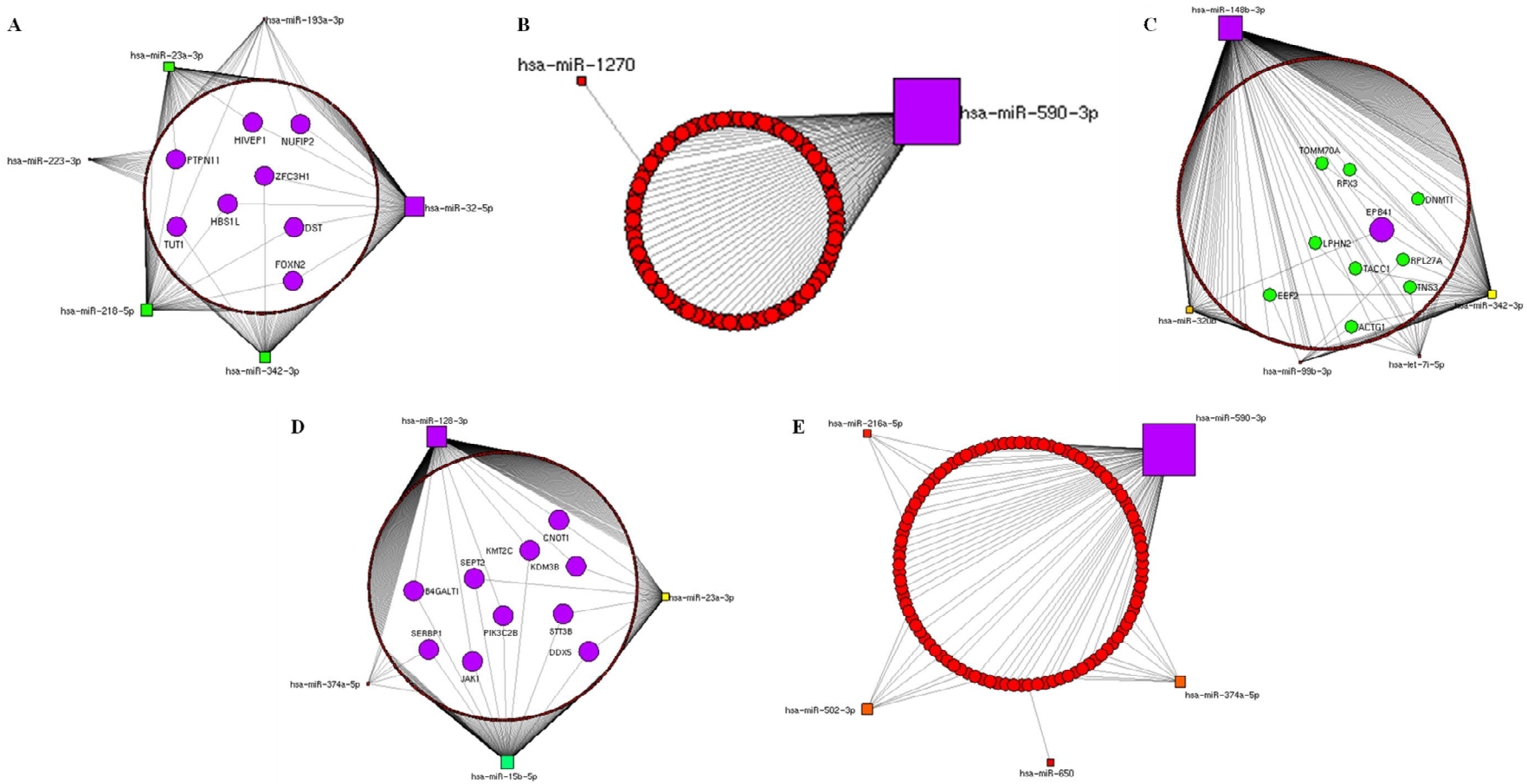

Para identificar as vias celulares potencialmente afetadas pelos miRNAs diferencialmente expressos, os softwares miRPath e MIRSystem foram empregados. Normalmente, os efeitos regulatórios dos miRNAs nos processos biológicos são exercidos por grupos destes ncRNAs que atuam de maneira coordenada. Assim, as vias de sinalização efetivamente desreguladas em Mø infectados com *H. capsulatum* como resultado da expressão de múltiplos miRNAs são demonstradas na Tabela 13. De acordo com os dados, em Mø infectados com a cepa EH-315, as vias mais relevantes afetadas pelos miRNAs, incluem vias relacionadas ao controle da adesão fungo-célula hospedeira (interação receptor-MEC, adesão focal), à biossíntese de polissacarídeos (biossíntese de glicosaminoglicanos), à regulação da estrutura e motilidade celular (regulação do citoesqueleto de actina), à degradação de proteínas (proteólise mediada por ubiquitina), à resposta a estímulos proinflamatórios (sinalização de MAPK) e à regulação da homeostase celular (apoptose, junções comunicantes).

Considerando Mø infectados com a cepa 60I, os miRNAs superexpressos afetam vias celulares associadas ao controle da adesão fungo-célula hospedeira (interação receptor-MEC), à biossíntese de polissacarídeos (biossíntese de glicosaminoglicanos), ao metabolismo de aminoácidos (degradação de lisina) e outros efeitos funcionais que regulam proliferação, apoptose, diferenciação e migração celular (sinalização de TGF-Beta).

Na infecção com biofilmes da cepa EH-315, inúmeras vias foram potencialmente desreguladas nos Mø infectados. Tais vias incluem controle da adesão fungo-célula hospedeira e interação célula-célula (interação receptor-MEC, adesão focal, junções aderentes), biossíntese de polissacarídeos (biossíntese de glicosaminoglicanos, biossíntese de N-glicanos), metabolismo de aminoácidos (degradação de lisina), efeitos celulares funcionais que regulam proliferação, apoptose, diferenciação e migração celular (sinalização de TGF-Beta), regulação da homeostase celular (apoptose, junções comunicantes, sinalização de Wnt, sinalização de p53) e resposta a estímulos proinflamatórios (sinalização de MAPK). De fato, uma grande diversidade de vias celulares foi desregulada em Mø após infecção com biofilmes de *H. capsulatum*, destacando assim a relevância destas formações no microambiente intracelular para a progressão da histoplasmose.

Este fato se torna ainda mais consolidado na comparação entre vias alteradas pelos miRNAs expressos por Mø infectados com biofilmes de *H. capsulatum* (EH-315) vs. miRNAs expressos após infecção com leveduras planctônicas desta cepa. Neste caso, miRNAs diferenciais dos biofilmes afetam vias associadas a biossíntese de polissacarídeos (biossíntese de glicosaminoglicanos), efeitos funcionais que regulam proliferação, apoptose,

diferenciação e migração celular (sinalização de TGF-Beta), regulação da homeostase celular (sinalização de Wnt, sinalização de p53), controle da adesão fungo-célula hospedeira (adesão focal), resposta a estímulos proinflamatórios (sinalização de MAPK), degradação de proteínas (proteólise mediada por ubiquitina) e, ainda regulação da resposta imunológica (sinalização do receptor de linfócitos T).

Finalmente, foram contrapostos os perfis de expressão de miRNAs entre Mø infectados com diferentes cepas (EH-315 vs. 60I). Os dados indicam que os miRNAs diferenciais da infecção com a cepa EH-315 regulam potencialmente vias relacionadas a adesão fungo-célula hospedeira (interação receptor-MEC), controle da proliferação, apoptose, diferenciação e migração celular (sinalização de TGF-Beta), biossíntese de polissacarídeos (biossíntese de glicosaminoglicanos), metabolismo de lipídeos (biossíntese de ácidos graxos insaturados), metabolismo de aminoácidos (degradação de lisina, valina, leucina e isoleucina) e degradação de proteínas (proteólise mediada por ubiquitina).

De forma geral, a partir das vias celulares potencialmente afetadas em Mø hospedeiros em resposta à infecção com leveduras de *H. capsulatum*, torna-se importante destacar que tal interação promove desregulação de aspectos determinantes nestas células fagocíticas, sugerindo características importantes da patogênese fúngica, uma vez que se relacionam aos aspectos inerentes à adesão às células hospedeiras, bem como à resposta inflamatória e ainda, à morte celular.

**Tabela 13. Vias associadas aos genes-alvo regulados pelos miRNAs diferencialmente expressos por Mø infectados com** *H. capsulatum.* Dados resultantes das análises realizadas pelos softwares miRPath 2.0 e MIRSystem utilizando o banco de dados KEGG (Kyoto Encyclopedia of Genes and Genomes).

| Vias KEGG | Número de genes | Valor de P |
|---|---|---|
| **Mø THP-1 infectados com a cepa EH-315 vs. Mø THP-1** | | |
| Interação receptor-Matriz extracelular (MEC) | 14 | 1,1e-06 |
| Biossíntese de glicosaminoglicanos | 6 | 1,7e-12 |
| Proteólise mediada por Ubiquitina | 26 | 0,01 |
| Adesão focal | 32 | 0,01 |
| Sinalização de MAPK (mitogen-activated protein kinase) | 35 | 0,02 |
| Apoptose | 12 | 0,04 |
| Junções comunicantes (GAP) | 17 | 0,04 |
| Regulação do citoesqueleto de actina | 29 | 0,04 |
| **Mø THP-1 infectados com a cepa 60I vs. Mø THP-1** | | |
| Biossíntese de glicosaminoglicanos | 7 | 1,9e-11 |
| Interação receptor-Matriz extracelular (MEC) | 21 | 7,9e-11 |
| Degradação de Lisina | 14 | 2,6e-05 |
| Sinalização de TGF-Beta | 21 | 0,0004 |
| **Mø THP-1 infectados com biofilmes da cepa EH-315 vs. Mø THP-1** | | |
| Biossíntese de glicosaminoglicanos | 7 | 2,1e-15 |
| Interação receptor-Matriz extracelular (MEC) | 19 | 1,8e-10 |
| Degradação de Lisina | 14 | 1,2e-06 |
| Sinalização de TGF-Beta | 26 | 2,1e-05 |
| Adesão focal | 49 | 0,001 |
| Sinalização de Wnt | 39 | 0,0002 |
| Junções comunicantes (GAP) | 19 | 0,009 |
| Junções aderentes | 17 | 0,01 |
| Sinalização de MAPK | 56 | 0,01 |
| Apoptose | 18 | 0,01 |
| Biossíntese de N-glicanos | 10 | 0,04 |
| Sinalização de p53 | 18 | 0,04 |

**Tabela 13. Vias associadas aos genes-alvo regulados pelos miRNAs diferencialmente expressos por Mø infectados com** *H. capsulatum.* Dados resultantes das análises realizadas pelos softwares miRPath 2.0 e MIRSystem utilizando o banco de dados KEGG (Continuação).

| Vias KEGG | Número de genes | Valor de P |
|---|---|---|
| **Mo THP-1 infectados com biofilmes da cepa EH-315 vs. Mo THP-1 infectados com a cepa EH-315** | | |
| Biossíntese de glicosaminoglicanos | 6 | 5,1e-41 |
| Sinalização de TGF-Beta | 26 | 3,4e-07 |
| Sinalização de p53 | 22 | 0,0001 |
| Sinalização de Wnt | 38 | 0,0008 |
| Adesão focal | 46 | 0,001 |
| Sinalização de MAPK | 56 | 0,002 |
| Proteólise mediada por Ubiquitina | 32 | 0,01 |
| Sinalização do receptor de células T | 25 | 0,02 |
| **Mo THP-1 infectados com a cepa EH-315 vs. Mo THP-1 infectados com a cepa 60I** | | |
| Interação receptor-Matriz extracelular (MEC) | 26 | 2,6e-09 |
| Sinalização de TGF-Beta | 35 | 1,2e-08 |
| Biossíntese de glicosaminoglicanos | 7 | 1,5e-05 |
| Biossíntese de ácidos graxos insaturados | 7 | 4,05e-05 |
| Degradação de Lisina | 14 | 0,006 |
| Proteólise mediada por Ubiquitina | 41 | 0,01 |
| Degradação de Valina, Leucina e Isoleucina | 12 | 0,03 |

Posteriormente, a fim de obter alvos regulados simultaneamente na infecção com diferentes cepas de *H. capsulatum* e em diferentes formas de crescimento, foi construída uma rede de interação miRNA-RNAm considerando genes-alvo validados regulados por todos os miRNAs com expressão diferencial significativa nas células infectadas com a cepa EH-315, com a cepa 60I e com os biofilmes da cepa EH-315 em relação às células controle sem infecção. Esta análise possibilitou um melhor direcionamento dos dados a fim de identificar um alvo comum e relevante na patogênese da histoplasmose. Na rede construída (Figura 24) os miRNAs são representados em quadrados e se localizam externamente aos círculos, ao passo que os genes-alvo são representados em círculos. Em vermelho, destacam-se os genes que são regulados por um único miRNAm, os quais constituem a maioria dos genes-alvo. Os círculos representados em roxo ilustram os genes que são alvos de dois miRNAs distintos e os círculos em azul representam genes-alvo de três miRNAs simultaneamente.

Diante do exposto, é possível observar que a rede regulatória construída (Figura 24) demonstra que 2 genes-alvo regulados por 3 miRNAs distintos entre as amostras integradas merecem destaque. O primeiro deles nomeia-se EPB41 (erythrocyte protein band 4.1) que codifica as proteínas 4.1 caracterizadas como componentes do citoesqueleto cortical subjacente à membrana celular. Tais proteínas estão envolvidas na organização da polaridade, bem como adesão e motilidade celular. Também atuam no transporte transmembrana e na resposta aos fatores de crescimento. Estas funções são desempenhadas por estas proteínas uma vez que elas conectam componentes do citoesqueleto cortical, entre eles, actina e proteínas de adesão transmembrana com receptores e transportadores (Schulz *et al*., 2010). Assim, a infecção com leveduras de *H. capsulatum* induz em Mø infectados a expressão dos miRNAs hsa-miR-148b-3p, hsa-miR-320b e hsa-miR-342-3p, que promovem de forma eficiente e específica a regulação do gene EPB41. Notavelmente, este gene contribui para a reorganização do citoesqueleto, bem como a adesão à membrana celular e componentes da matriz extracelular, características fundamentais para a patogênese da histoplasmose.

A infecção com leveduras de *H. capsulatum* orquestra ainda a regulação do gene NUFIP2 pela expressão dos miRNAs hsa-miR-32-5p, hsa-miR-590-3p e hsa-miR-193a-3p. Tal gene codifica a proteína nuclear fragile X mental retardation-interacting protein 2. Segundo Bish *et al*. (2015), NUFIP2 localiza-se em grânulos de estresse no citosol celular após exposição ao estresse, sugerindo uma função na repressão da tradução em resposta ao estresse celular. Grânulos de estresse são densas agregações ribonucleoproteicas compostas por RNAm traducionalmente paralisados, subunidades ribossomais e proteínas. Estes grânulos são formados em decorrência de diferentes formas de estresse celular incluindo estresse oxidativo, choque térmico ou privação de nutrientes e regulam a estabilidade ou tradução do RNAm (Bütepage *et al*., 2015). Atualmente, não há dados na literatura que descrevem uma correlação entre a formação de grânulos de estresse e a infecção por fungos patogênicos, como *H. capsulatum.* Assim, esta interação pode ser um importante alvo de estudo no futuro em vista da influência direta da formação destes grânulos na regulação da tradução em resposta à infecção.

**Figura 24. Redes de interação miRNA-RNAm.** Redes de interação construídas pelo software Navigator v2.2 resultante da análise de três replicatas. Análise dos genes-alvo regulados pelos miRNAs diferenciais entre Mø THP-1 infectados com a cepa EH-315, Mø THP-1 infectados com a cepa 60I e Mø THP-1 infectados com biofilmes da cepa EH-315 vs. Mø THP-1 sem infecção. Os miRNAs são representados em quadrados. A maioria dos genes são alvos de um único miRNA específico (círculos em vermelho) e, os demais genes são regulados por dois (círculos em roxo) ou três miRNAs distintos (círculos em azul).

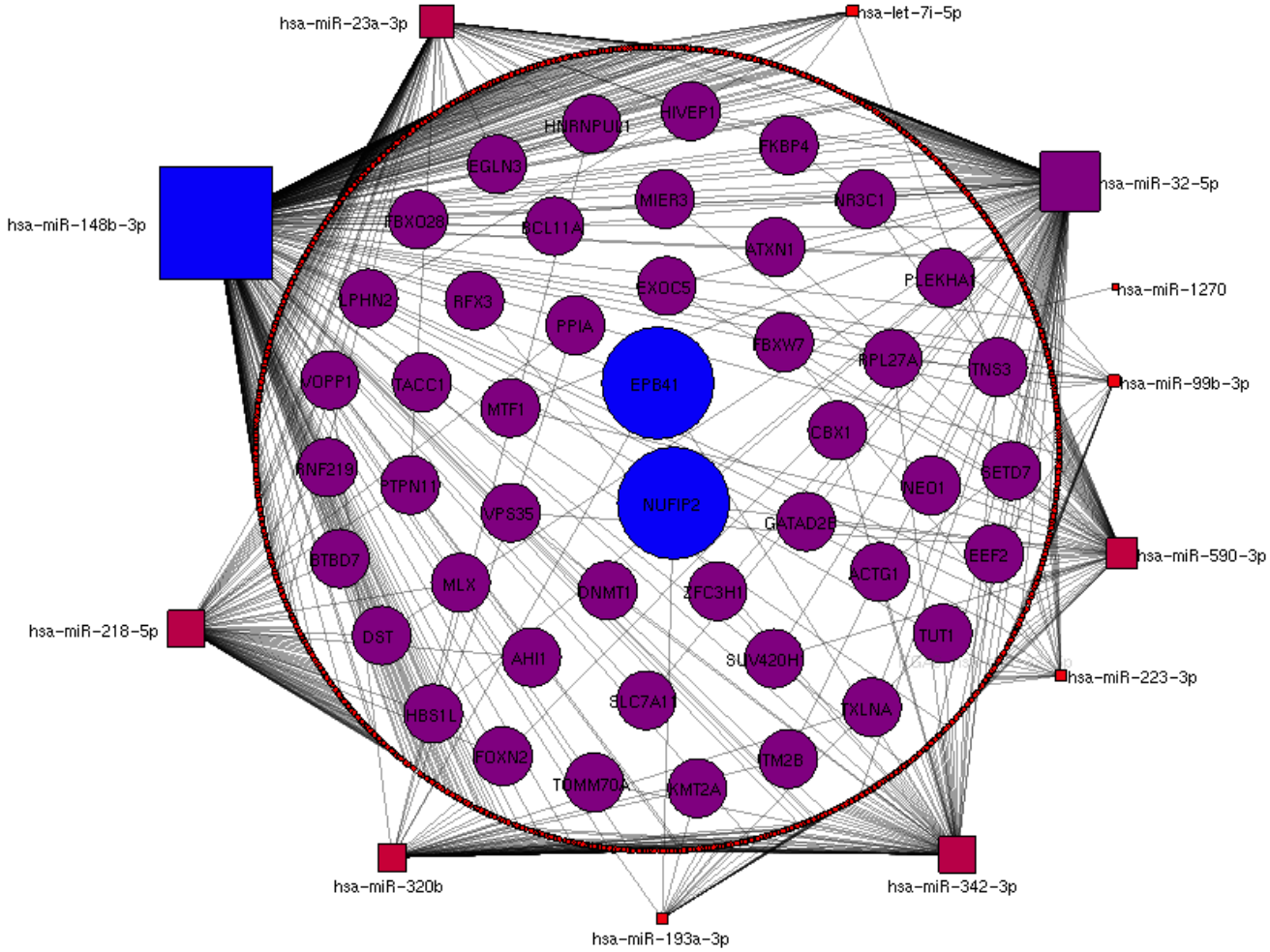

Em resumo, miRNAs determinam o destino das células, uma vez que controlam os níveis de expressão de fatores de sinalização e transcrição e reguladores do ciclo e morte celular. Assim, a expressão de miRNAs pode representar um mecanismo adotado pelo fungo para modular as funções da célula hospedeira. Neste sentido, as relações miRNA-RNAm que foram desreguladas após infecção com *H. capsulatum* foram estabelecidas e a partir disso novas estratégias terapêuticas podem ser projetadas a fim de restabelecer esta relação através do fornecimento sintético de miRNAs reprimidos (mimics) ou antagonizando a atividade de miRNAs superexpressos (antagomiRs, antimiRs ou blockmiRs).

### 4.5. Análise metabolômica

#### 4.5.1. Produção de polissacarídeos totais em amostras de culturas planctônicas, biofilmes e sobrenadante dos biofilmes de *H. capsulatum*

As análises bioquímicas foram realizadas neste ensaio para quantificar a produção de polissacarídeos totais em cada amostra analisada. Esta quantificação é de extrema importância para o estudo de biofilmes, uma vez que ela reflete diretamente a quantidade de MEC presente nestas estruturas. A MEC é alvo de diversos estudos, visto sua importância na manutenção da arquitetura tridimensional dos biofilmes, atuando como uma barreira física que mantém a integridade destas formações e sua resistência aos agentes antifúngicos (Seneviratne, Jin e Samaranayake, 2008). De acordo com os resultados obtidos, a quantificação de PES foi semelhante entre todas as amostras, não havendo diferença estatística. Considerando os PEI, os biofilmes das cepas EH-315 e 60I mostraram a maior produção, com diferença estatística para a produção de PEI pelas culturas planctônicas ($P$<0,001). Os níveis mais altos de PI, que representam reserva energética, também foram produzidos pelos biofilmes de EH-315 e 60I, com diferença estatística em relação aos PI quantificados nas condições planctônicas das cepas ($P$<0,001) (Figura 25).

Em contrapartida, a quantificação de polissacarídeos nos sobrenadantes dos biofilmes revelam os níveis mais baixos de produção de PES, PEI e PI. Este fato pode ser explicado pela presença de moléculas de Quorum-sensing (QS) de outra natureza química no meio extracelular. QS é caracterizado como um sistema de comunicação a partir do qual um microrganismo “conversa” com outro. Esta comunicação baseia-se na síntese e percepção dos chamados autoindutores, moléculas químicas que atuam como sinais e acumulam-se no ambiente extracelular (Kalia *et al.*, 2015). Tais moléculas têm natureza química variada, incluindo ácidos graxos, aminoácidos, peptídeos, polissacarídeos, entre outros e isto pode

explicar a produção reduzida de polissacarídeos pelo sobrenadante dos biofilmes de ambas as cepas (Figura 25).

**Figura 25. Produção de polissacarídeos totais por** *H. capsulatum.* Quantificação de Polissacarídeos Extracelulares Solúveis (PES), Polissacarídeos Extracelulares Insolúveis (PEI) e Polissacarídeos Intracelulares (PI) pelo método Fenol Sulfúrico em biofilmes, culturas planctônicas e sobrenadante dos biofilmes das cepas EH-315 e 60I de *H. capsulatum*. Valores dados pela média ± D.P. são resultados de uma análise two-way ANOVA. **P* <0,001, planctônica EH-315 vs. biofilmes EH-315, #*P* <0,001, planctônica 60I vs. biofilmes 60I.

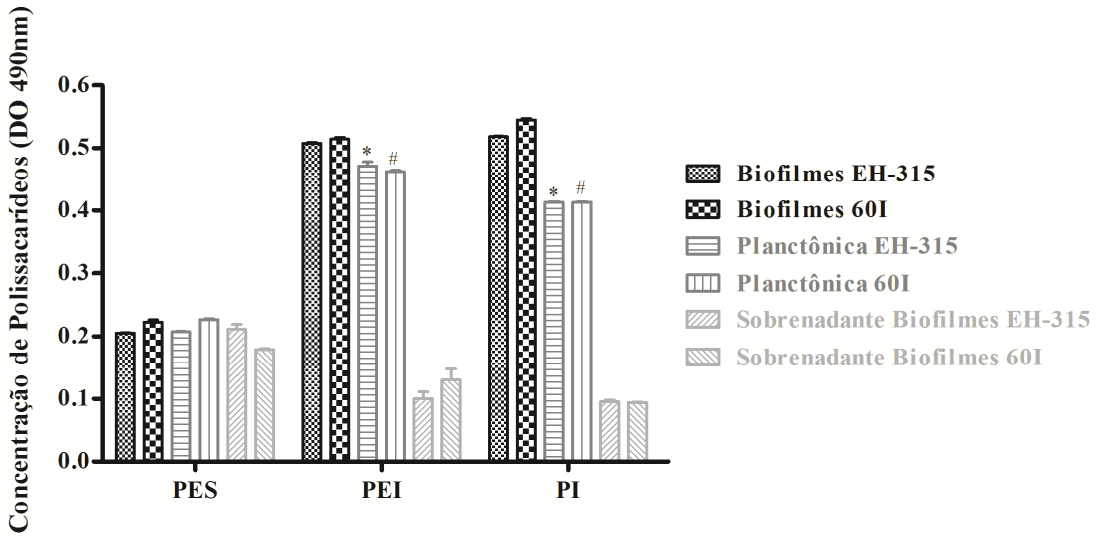


### 4.5.2. Análises cromatográficas

A Figura 26 apresenta os cromatogramas obtidos dos fracionamentos das amostras P85 (planctônica) e B85 (biofilmes). As amostras apresentaram perfis cromatográficos bastante distintos, visto que a amostra P85 apresentou 8 picos mais evidentes, numerados de 1 a 8, nos tempos de retenção de 6,5; 25,3; 34,5; 40,7; 52,5; 58,4; 67,0 e 79,2 min, respectivamente (Figura 26A), enquanto a amostra B85 apresentou apenas 3 picos mais evidentes, numerados de 1 a 3, nos tempos de retenção de 6,5; 32,7 e 46,3 min, respectivamente (Figura 26B). Na sobreposição dos cromatogramas (Figura 26C) é possível observar um pico no tempo de retenção de 6,5 min em comum para ambas as amostras, porém, com uma intensidade muito mais elevada para B85. Dentre os outros picos exclusivos de P85, é possível observar um pico mais intenso no tempo de 40,7 min.

**Figura 26. Perfil cromatográfico dos metabólitos de leveduras de** *H. capsulatum*. **(A)** Cromatograma dos metabólitos da cepa EH-315 em crescimento planctônico (P85). **(B)** Cromatograma dos metabólitos da cepa EH-315 em biofilmes (B85). **(C)** Sobreposição dos cromatogramas dos metabólitos da cepa EH-315: B85 em azul; P85 em vermelho. Gradiente de ACN contendo 0,1% TFA (v/v) de 5 a 95% (v/v) por 90 min; coluna XBrigdeTM BEH300 C18 (2,1x100mm; 3,5 µm); eluição monitorada por absorbância UV 214 nm; fluxo 0,2 mL/min. Sistema RP-HPLC (Perkin-Elmer Flexar/Chromera).

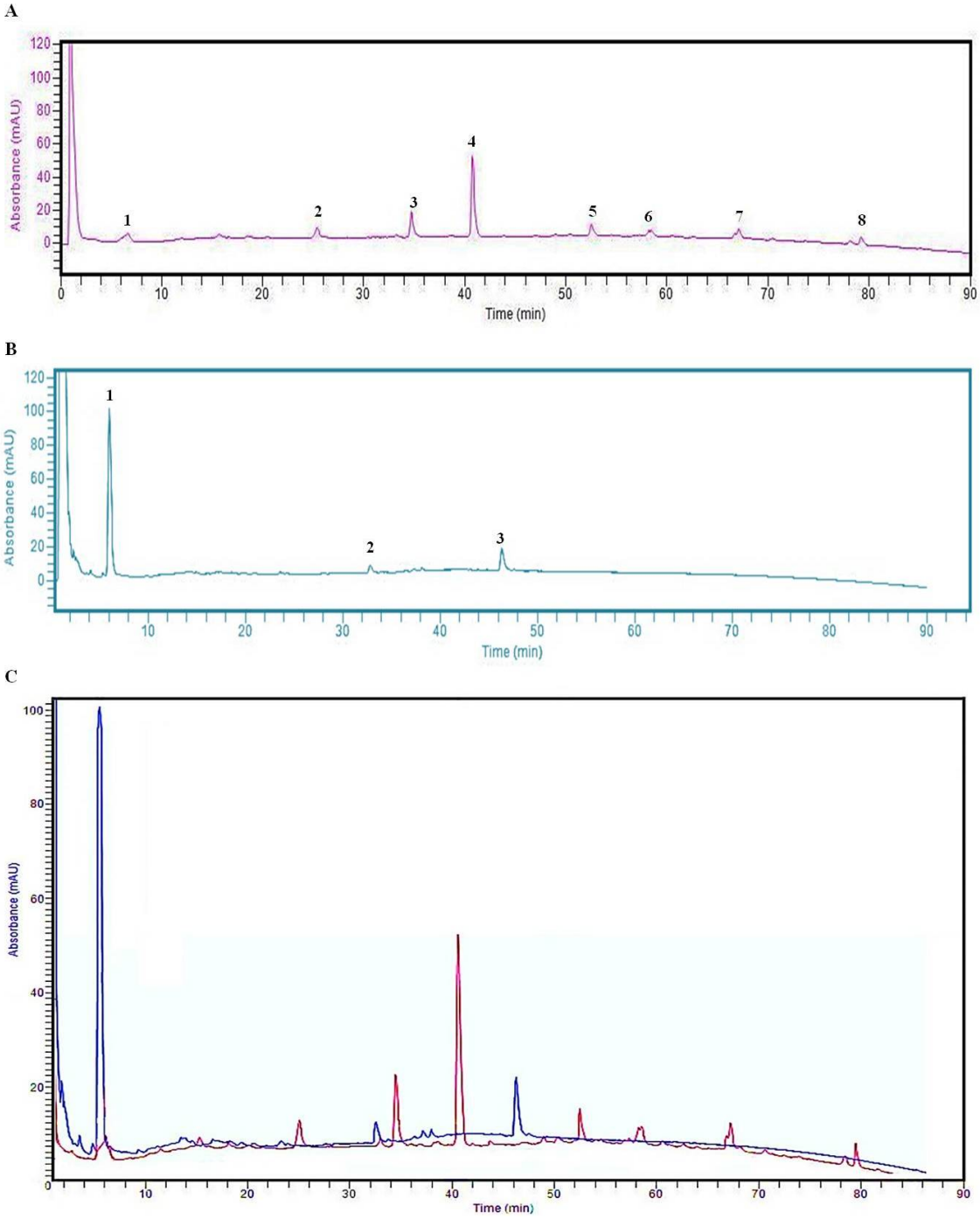

### 4.5.3. Análises de cromatografia líquida acoplada à espectrometria de massas (LC-MS/MS)

#### 4.5.3.1. Fracionamento das amostras

O fracionamento das amostras B85 e P85 revelou um perfil cromatográfico comparativo claramente distinto, a partir do qual é nítido observar um número reduzido de picos no perfil dos biofilmes em relação ao perfil das culturas planctônicas (Figura 27).

**Figura 27. Perfil cromatográfico dos metabólitos de leveduras de** *H. capsulatum*. **(A)** Cromatograma dos metabólitos da cepa EH-315 em crescimento planctônico (P85); **(B)** cromatograma dos metabólitos da cepa EH-315 em biofilmes (B85). Gradiente de ACN de 0 a 90% (v/v), contendo 0,1% (v/v) de TFA por 90 min; coluna XBrigdeTM BEH300 C18 (2,1x100mm; 3,5 µm; Waters); eluição monitorada por absorbância UV 215 nm; fluxo 0,2 mL/min. Sistema Prominence UFLC (Ultra Fast Liquid Chromatograph – Shimadzu).

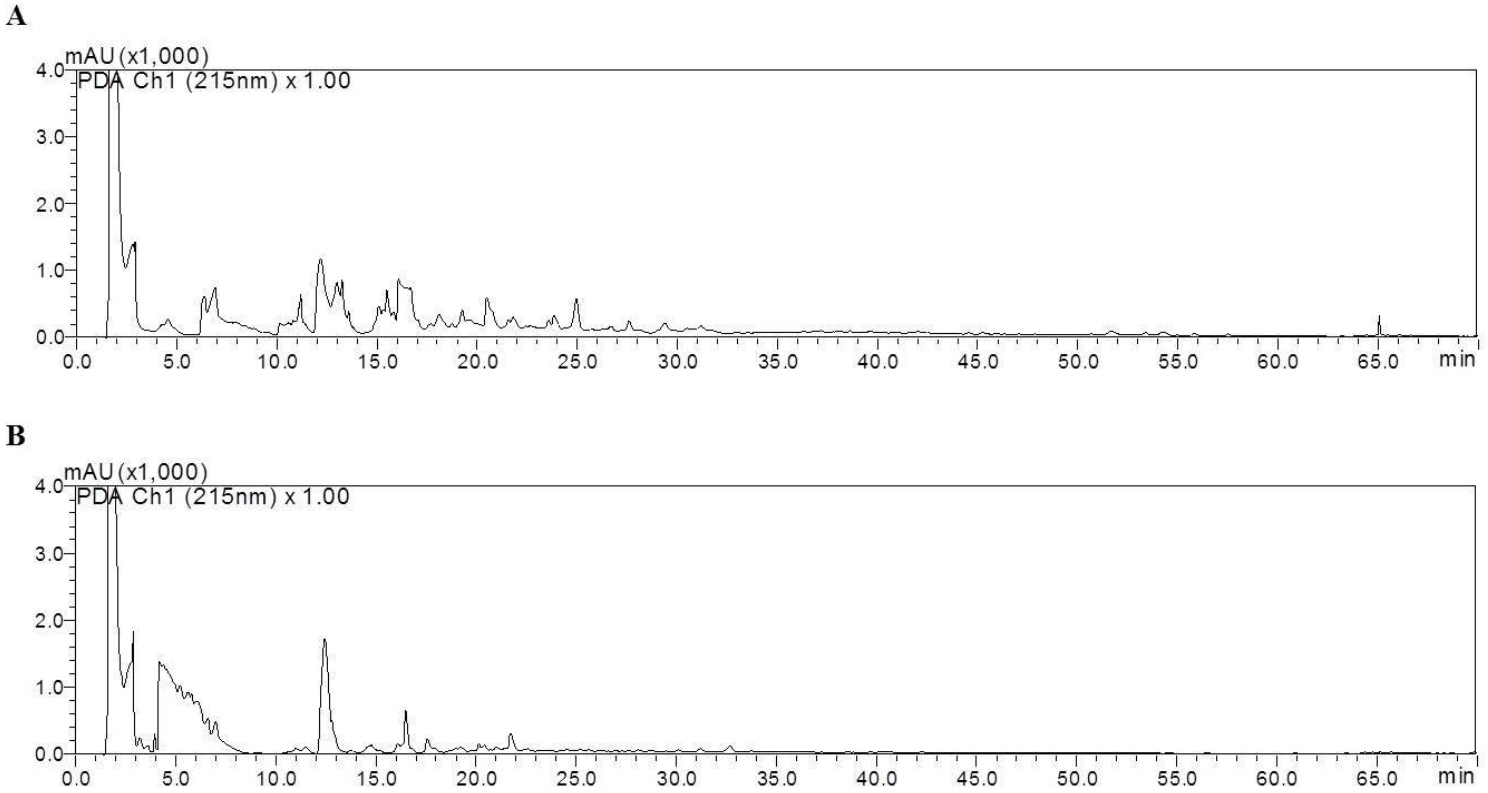

### 4.5.3.2. Abundância total de metabólitos dos biofilmes e das culturas planctônicas

Uma análise comparativa de abundância de massas foi realizada a partir dos espectros de massas obtidos e deconvoluídos dos metabólitos extraídos da cepa EH-315 em biofilmes vs. culturas planctônicas. Nas condições de análises utilizadas, os resultados indicaram que os componentes de ambas as amostras distribuíram-se em uma faixa de massa molecular de 200-2400 Da, de maneira que foram obtidos perfis diferentes para cada uma das amostras. De acordo com as massas moleculares dos componentes dos biofilmes vs. culturas planctônicas, foi possível selecionar um total de 630 moléculas, e a análise comparativa foi demonstrada em um diagrama de Venn (Figura 28A), sendo: a) 74% (467) dos compostos com a mesma massa entre as duas formas de crescimento do fungo; b) 18% dos componente com massas moleculares (112 compostos) exclusivas em culturas planctônicas e; c) 8% dos componentes com massas moleculares (51 compostos) exclusivas dos biofilmes. Diante do exposto, é necessário destacar que a grande maioria dos metabólitos (74%) tem massas moleculares comuns nos biofilmes e nas culturas planctônicas, no entanto, considerando as moléculas de massas exclusivas, em culturas planctôncias as células leveduriformes produzem um número significativamente maior de metabólitos (n = 112; 18%) do que o número produzido por células em biofilmes (n = 51; 8%).

**Figura 28. Diagramas comparativos dos metabólitos de biofilmes e culturas planctônicas de *H. capsulatum* por massas moleculares. (A)** Diagrama de Venn dos metabólitos da cepa EH-315 em biofilmes e culturas planctônicas evidenciando o número de compostos com massas moleculares comuns e distintas entre as amostras. **(B)** Gráfico representativo da porcentagem de metabólitos com massas moleculares coincidentes entre biofilmes e culturas planctônicas da cepa EH-315, massas exclusivas dos biofilmes e massas exclusivas das culturas planctônicas. Varreduras feitas no intervalo de m/z de 200 a 2400 Da.

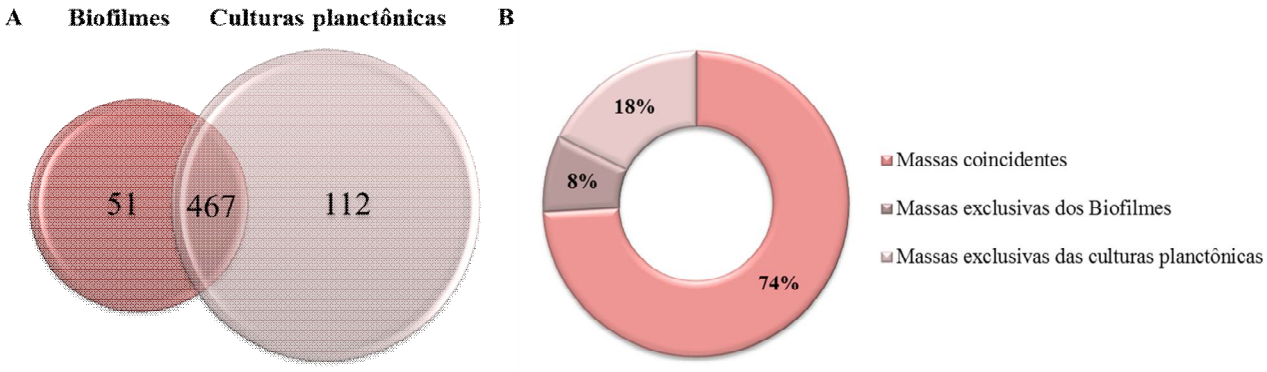

A Figura 29 demonstra a abundância total dos metabólitos (630) de acordo com as massas deconvoluídas de cada um deles, originados a partir das amostras de biofilmes (em vermelho) e culturas planctônicas (em azul), de maneira a sobrepor as massas moleculares dos componentes de acordo com sua intensidade relativa. Estes resultados confirmam as diferenças exibidas pelos perfis cromatográficos, uma vez que foi possível detectar inúmeros compostos com massas moleculares diferentes na correlação biofilme vs. planctônica.

**Figura 29. Sobreposição dos metabólitos totais detectados nas amostras de biofilmes e culturas planctônicas da cepa EH-315 de** *H. capsulatum* **por LC-MS/MS.** As amostras diferentes estão representadas em cores distintas; metabólitos dos biofilmes em vermelho e metabólitos das culturas planctônicas em azul.

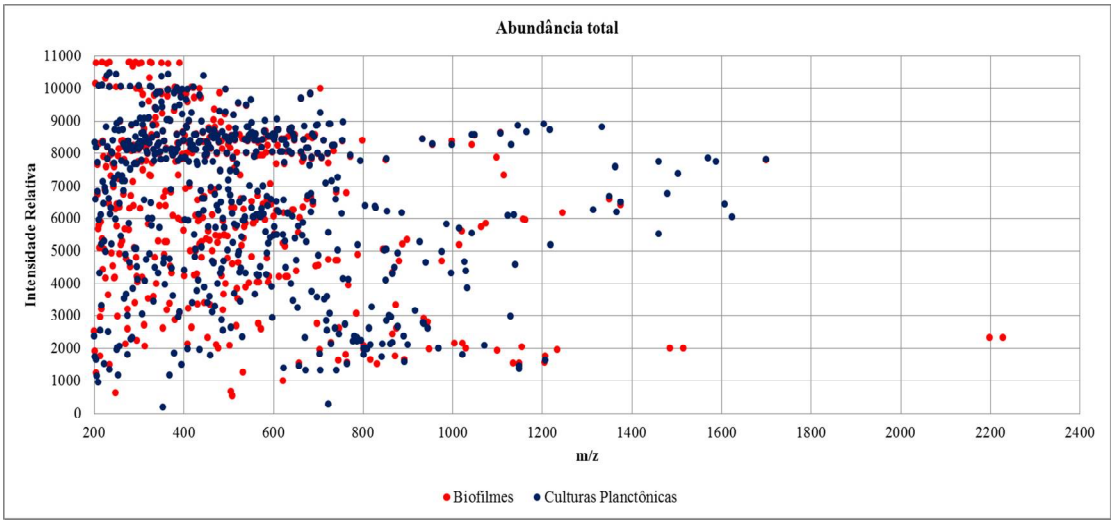


### 4.5.3.3. Abundância de metabólitos com massas moleculares comuns entre biofilmes e culturas planctônicas

#### 4.5.3.3.1. Abundância dos metabólitos por range de massas moleculares

Na análise posterior, foram consideradas as moléculas que apresentaram massas comuns entre biofilmes e culturas planctônicas (467) e, a distribuição destas moléculas por massas moleculares em relação à intensidade relativa está representada na Figura 30. Diante do exposto, verifica-se que considerando um range de massas entre 200 a 400 Da, há 197 moléculas (42%) que exibem a mesma massa molecular nas duas formas de crescimento; em uma faixa de 400 a 800 Da concentram-se a maioria das moléculas, faixa na qual foram detectados 245 metabólitos (53%); e em relação a um range de massas entre 800 a 1800 Da, uma pequena quantidade de metabólitos foi detectada, apenas 25 moléculas (5%). Assim, tendo em vista as moléculas detectadas com as mesmas massas moleculares nos biofilmes e

nas culturas planctônicas, sugere-se que há uma alta concentração de moléculas de massa molecular ≤ 800 Da nas duas condições de crescimento de *H. capsulatum* ao passo que há um número reduzido de compostos de massa ≥ 800 Da (possíveis peptídeos) nestas situações biológicas. Estes dados podem caracterizar a assinatura metabólica das leveduras de *H. capsulatum*, quer seja estruturadas em biofilmes ou em crescimento livre.

**Figura 30. Metabólitos de massas moleculares comuns entre biofilmes e culturas planctônicas da cepa EH-315 de *H. capsulatum* distribuídos em um range de 200-1800 Da. (A)** Metabólitos em um range de 200 a 400 Da, detecção de 197 moléculas de massas moleculares comuns; **(B)** metabólitos em um range de 400 a 800 Da, detecção de 245 moléculas de massas moleculares comuns e; **(C)** metabólitos em um range de 800 a 1800 Da, detecção de 25 moléculas de massas moleculares comuns.

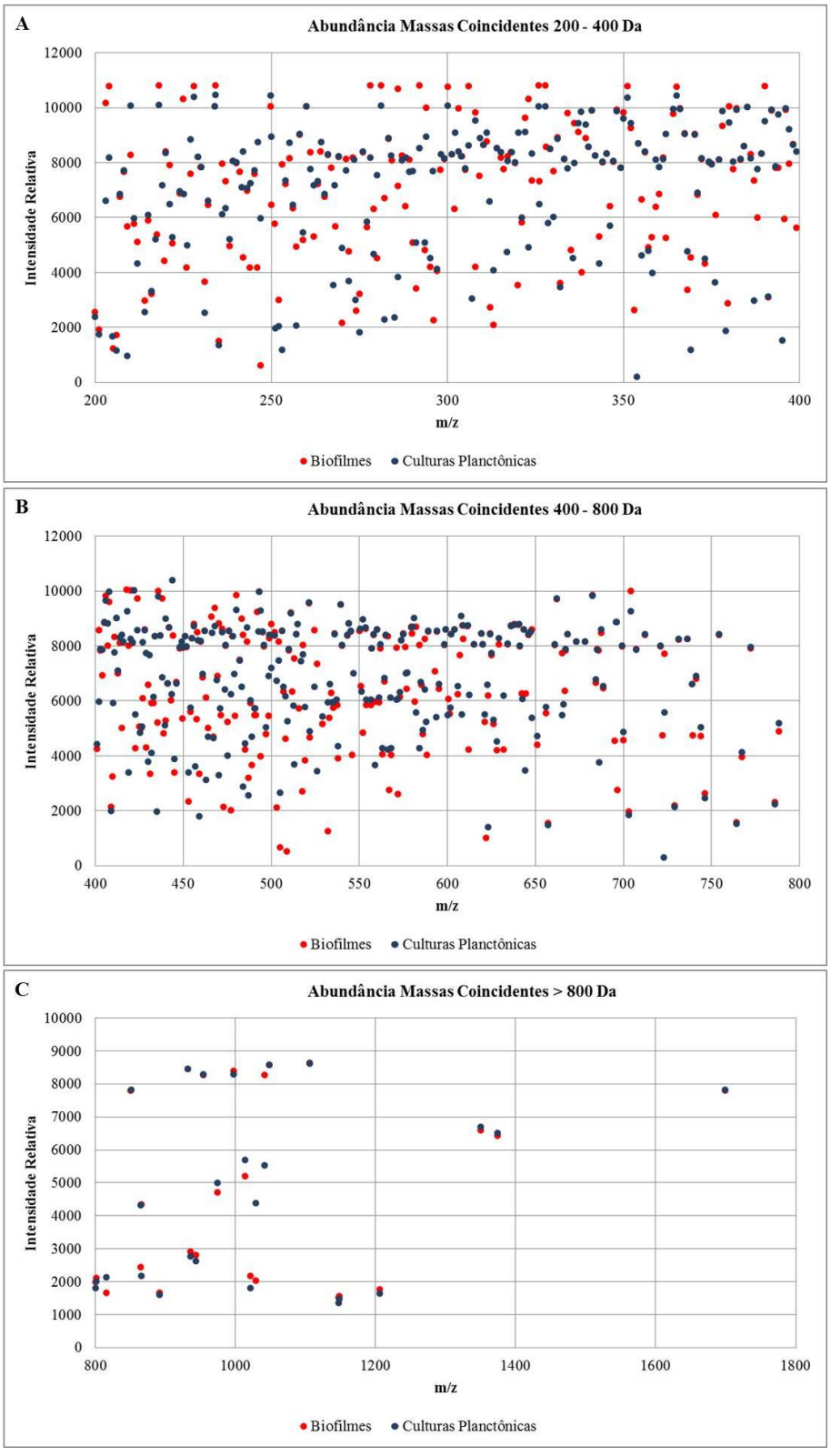

#### 4.5.3.3.2. Abundância dos metabólitos por intensidade relativa

Uma nova análise pôde ser conduzida a partir da intensidade relativa dos metabólitos de acordo com os dados obtidos por LC-MS/MS e considerando as moléculas que apresentaram a mesma massa molecular tanto nos biofilmes como em culturas planctônicas. Em vista disso, destacam-se as moléculas que exibiram intensidade aumentada nos biofilmes (UP) e aquelas com intensidade diminuída nos biofilmes (DOWN) em relação à intensidade das mesmas nas culturas planctônicas. Com a exploração destes dados, nota-se que apenas 1% das moléculas (6) manteve-se com a mesma intensidade entre biofilmes e culturas planctônicas. Por outro lado, a maioria das moléculas, o que corresponde a 57% (265) apresentaram a intensidade diminuída nos biofilmes em relação à sua intensidade em crescimento livre. Enquanto que 42% dos componentes (196) demonstraram intensidade aumentada em biofilmes comparada à intensidade das células planctônicas. Assim, estes resultados demonstram a heterogeneidade relativa ao perfil metabólico entre as células fúngicas móveis e sésseis, uma vez que 99% dos metabólitos detectados são produzidos em intensidades diferentes quando alteraram sua condição biológica de livres para estruturarem-se em biofilmes. As análises comparativas entre a intensidade relativa das moléculas que apresentaram a mesma massa molecular nos biofilmes e nas culturas planctônicas estão demonstradas na Figura 31, evidenciando metabólitos produzidos com intensidade aumentada e diminuída nos biofilmes em relação à intensidade nas leveduras planctônicas. De fato, salienta-se que a maioria (57%) dos metabólitos são produzidos em uma intensidade menor quando as células fúngicas organizam-se em biofilmes comparado à intensidade dos mesmos produzidos pelas células planctônicas.

**Figura 31. Diagramas comparativos dos metabólitos de biofilmes e culturas planctônicas de *H. capsulatum* por intensidade relativa.** Representação esquemática dos metabólitos com massas moleculares comuns entre as amostras. **(A)** Diagrama de Venn dos metabólitos da cepa EH-315 em biofilmes e culturas planctônicas evidenciando o número de compostos produzidos na mesma intensidade entre os diferentes cultivos, produzidos com intensidade aumentada nos biofilmes (UP) e produzidos com intensidade diminuída nos biofilmes (DOWN). **(B)** Gráfico representativo da intensidade dos metabólitos produzidos em biofilmes em relação à intensidade em culturas planctônicas da cepa EH-315. Varreduras feitas no intervalo de m/z de 200 a 1800 Da.

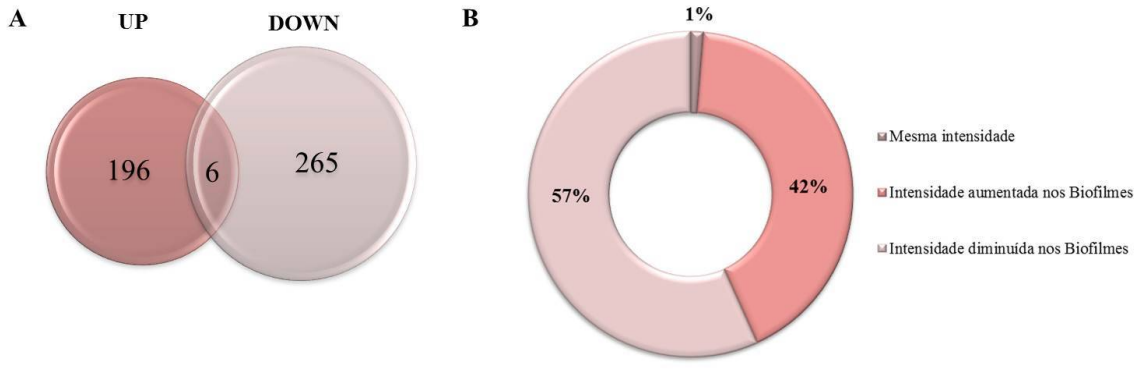

Adicionalmente, na Figura 32 é representado um panorama geral dos metabólitos produzidos com intensidade aumentada nos biofilmes em relação à intensidade nas células planctônicas (Figura 32A) e aqueles produzidos com intensidade diminuída nos biofilmes comparada à intensidade nas culturas planctônicas (Figura 32B). Os dados representados demonstram que tanto os metabólitos UP como os DOWN em biofilmes concentram-se em um range de massa molecular entre 200 a 800 Da. Os gráficos correlacionam a intensidade relativa dos metabólitos com sua relação m/z.

**Figura 32. Metabólitos de massas moleculares comuns entre biofilmes e culturas planctônicas da cepa EH-315 de *H. capsulatum* mas produzidos com intensidades diferentes. (A)** Metabólitos produzidos com intensidade aumentada nos biofilmes (UP – 196 moléculas); **(B)** Metabólitos produzidos com intensidade diminuída nos biofilmes (DOWN – 265 moléculas). Varreduras feitas no intervalo de m/z de 200 a 1800 Da.

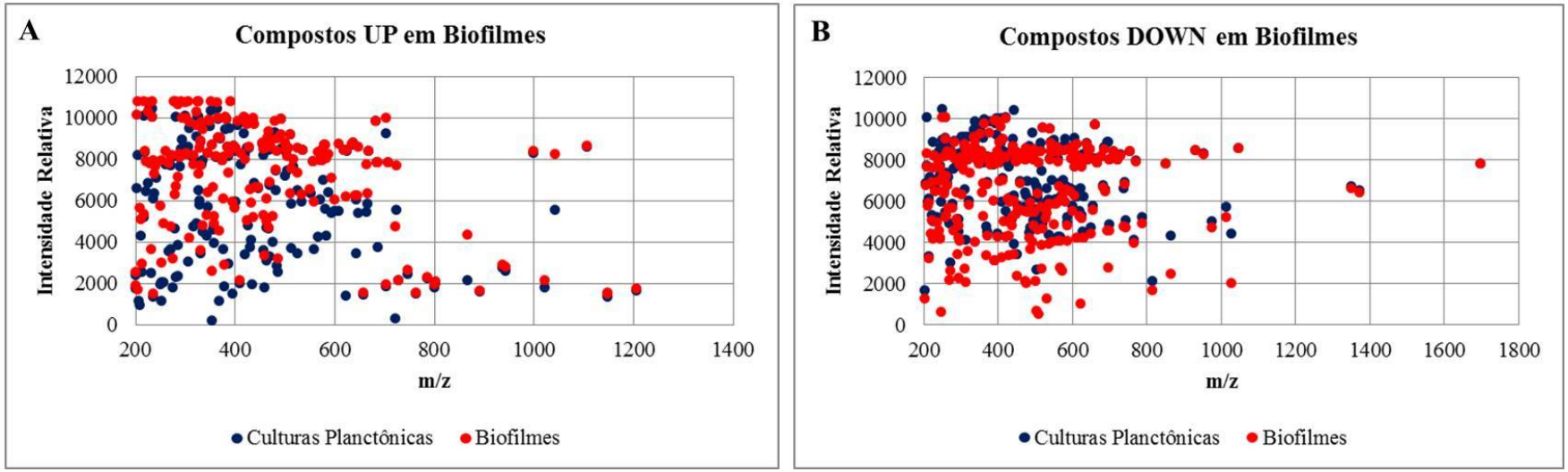

**4.5.3.4. Abundância de metabólitos com massas moleculares exclusivas dos biofilmes e das culturas planctônicas**

A partir dos dados obtidos por análise de LC-MS/MS é possível explorar ainda os metabólitos produzidos exclusivamente pelos biofilmes e aqueles produzidos unicamente pelas células planctônicas. A distribuição destas moléculas em ranges de massas moleculares em relação à intensidade relativa está demonstrada na Figura 33. Os gráficos evidenciam que considerando um range de massa molecular de 200 a 400 Da há a menor concentração de metabólitos produzidos, sendo 3 detectados unicamente nas células em biofilmes, enquanto que 2 são produzidos por culturas planctônicas; em uma faixa de massa molecular entre 400 a 800 Da foram detectados 20 moléculas produzidas somente pelos biofilmes e 55 produzidas pelas culturas planctônicas; e, então, o range de massa molecular entre 800 e 2400 Da concentra a maior parte dos metabólitos exclusivos de cada uma das condições biológicas, visto que nesta faixa há 28 metabólitos produzidos pelas leveduras em biofilmes e 55 produzidos pelas células livres. De fato, os dados aqui apresentados das moléculas de massas exclusivas são inversamente proporcionais aos resultados obtidos considerando as moléculas de massas moleculares comuns entre biofilmes e culturas planctônicas. Em relação aos metabólitos de massas exclusivas de uma ou outra forma de crescimento de *H. capsulatum*, eles concentram-se na faixa de massa molecular $\geq$ 800 Da e a menor concentração na produção destes ocorre em uma faixa $\leq$ 800 Da. De maneira inversa, a maioria dos metabólitos de massas moleculares comuns entre biofilmes e culturas planctônicas apresenta $\leq$800 Da, ao passo que a minoria concentra-se em uma faixa de massas $\geq$ 800 Da. Diante do exposto, sugere-se que os metabólitos que são produzidos de maneira exclusiva pelas leveduras de acordo com seu modo de crescimento (rede tridimensional ou livre) caracterizam-se como peptídeos em predomínio às moléculas de baixa massa molecular.

**Figura 33. Metabólitos de massas moleculares exclusivas dos biofilmes e das culturas planctônicas da cepa EH-315 de** *H. capsulatum* **distribuídos em um range de 200-2400 Da. (A)** Metabólitos em um range de 200 a 400 Da (Biofilmes - 3; Planctônica 2); **(B)** Metabólitos em um range de 400 a 800 Da (Biofilmes - 20; Planctônica - 55) e; **(C)** Metabólitos em um range de 800 a 1800 Da (Biofilmes - 28; Planctônica - 55).

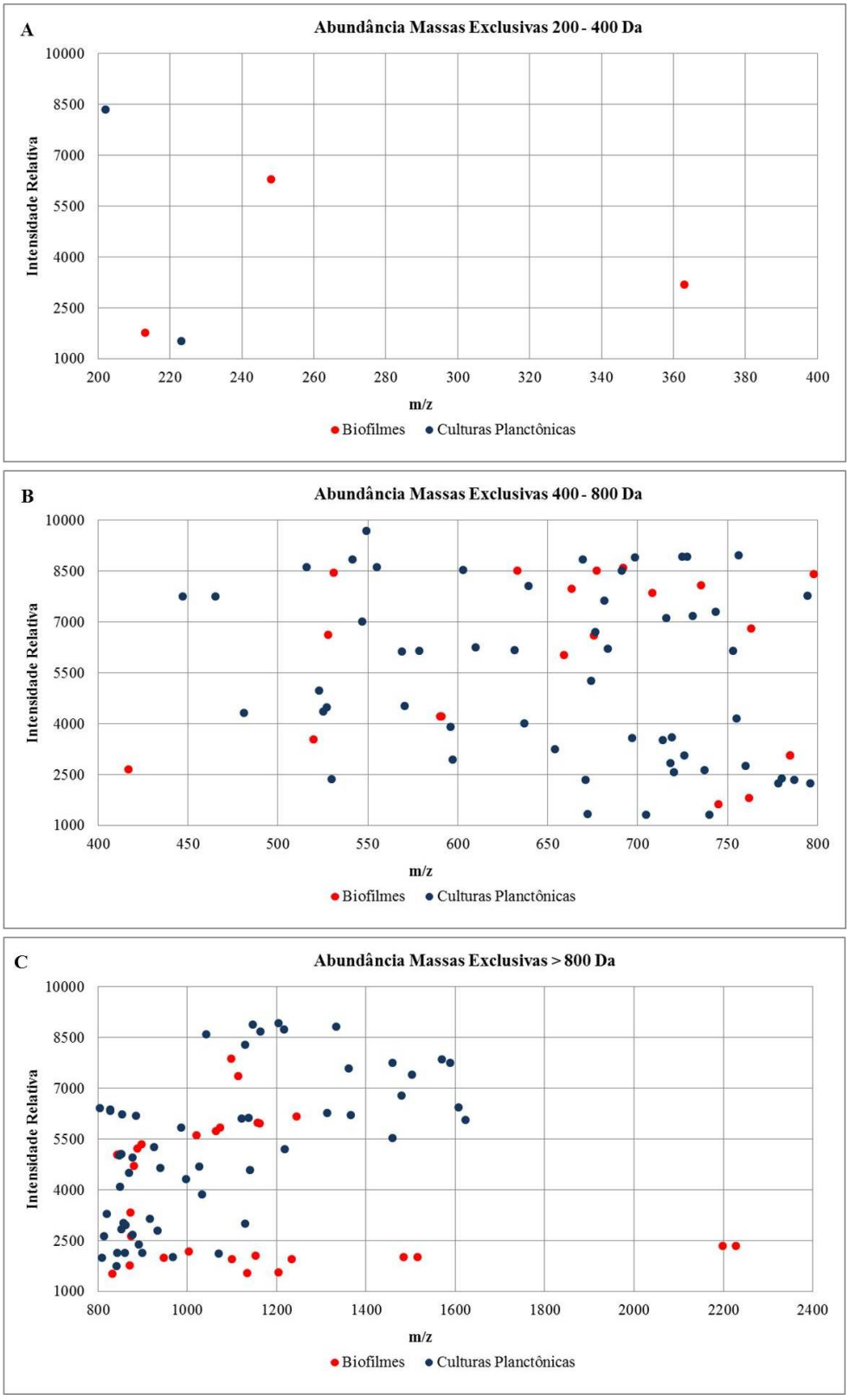

### 4.5.3.5. Representação esquemática do perfil metabólico de *H. capsulatum* em biofilmes e culturas planctônicas

**Figura 34. Representação esquemática do perfil metabólico de *H. capsulatum* em biofilmes e em culturas planctônicas.** P: cultivo das leveduras em condições planctônicas; B: cultivo das leveduras em biofilmes maduros. Massas moleculares em Dalton (Da). DOWN: metabólitos com intensidade diminuída nos biofilmes em relação à intensidade nas culturas planctônicas; UP: metabólitos com intensidade aumentada nos biofilmes em relação à intensidade nas culturas planctônicas.

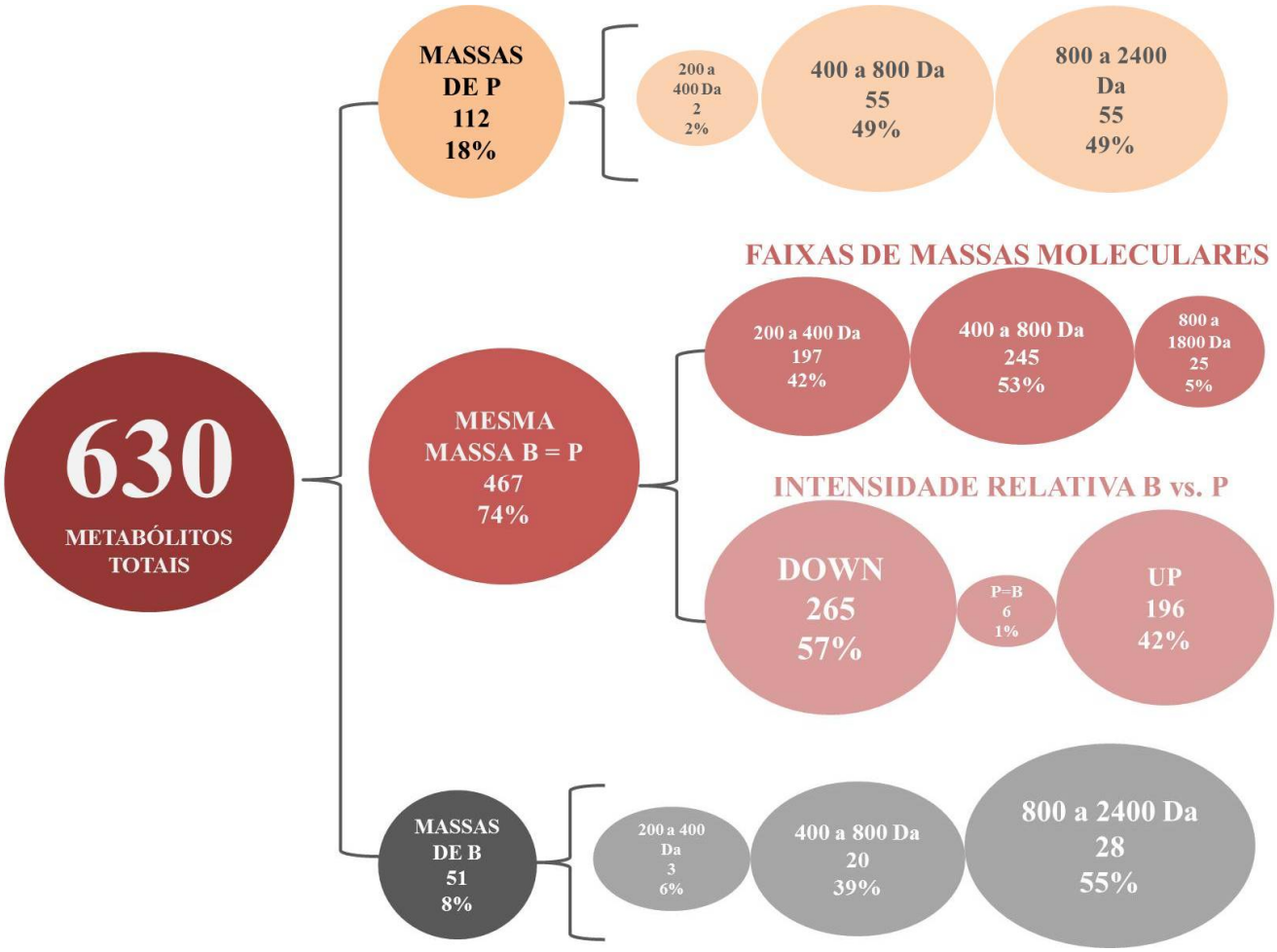


A Figura 34 representa esquematicamente e de forma resumida o perfil metabólico detectado por LC-MS/MS das amostras de biofilmes e culturas planctônicas das leveduras de *H. capsulatum*. Então, os dados anteriormente representados demonstram que: a) a maioria dos metabólitos produzidos por ambas as formas de crescimento (biofilmes e planctônicas)

possuem massas moleculares comuns (74%); b) considerando componentes de massas comuns, a maioria (95%) representa moléculas de massa molecular ≤ 800 Da; c) considerando a intensidade relativa dos componentes de massas comuns, em biofilmes a maioria dos metabólitos (57%) é produzida em intensidade menor (DOWN) do que o nível de produção detectado nas culturas planctônicas; d) considerando componentes de massas exclusivas, em biofilmes há uma menor produção de metabólitos em relação às culturas planctônicas (biofilmes vs. planctônica, 51 vs. 112) e; e) considerando componentes de massas exclusivas, em biofilmes a maioria (55%) representa compostos de massa molecular ≥ 800 Da.

A investigação do perfil metabólico dos biofilmes fúngicos patogênicos é atualmente uma abordagem pouco explorada. No presente estudo, foi estabelecido, de fato, que há uma alteração significativa na regulação metabólica à medida que as células leveduriformes de *H. capsulatum* deixam de ser livres para assumirem o formato de uma rede tridimensional extremamente organizada, a qual caracteriza os biofilmes. Os dados aqui apresentados foram explorados em termos de a) abundância total de metabólitos nas duas formas de crescimento; b) abundância relativa dos metabólitos que apresentaram as mesmas massas moleculares entre células em biofilmes e em culturas planctônicas mensurando-os em diferentes ranges de massa molecular; c) abundância relativa dos metabólitos que apresentaram as mesmas massas moleculares entre células em biofilmes e em culturas planctônicas classificando-os em UP ou DOWN de acordo com a intensidade, aumentada ou diminuída, respectivamente, em que foram produzidos nos biofilmes em relação à produção dos mesmos em células livres; e) abundância dos metabólitos produzidos unicamente pelas células em biofilmes e categorização das mesmas em diferentes ranges de massa molecular e; f) abundância dos metabólitos produzidos exclusivamente pelas células em culturas planctônicas e categorização das mesmas em diferentes ranges de massa molecular. Tais análises foram necessárias uma vez que não há dados na literatura que estabelecem o perfil metabólico dos biofilmes de *H. capsulatum* e, diante do exposto, salienta-se que há uma grande diversidade metabólica entre as distintas formas de crescimento do fungo, demonstrada pela assinatura da abundância dos metabólitos produzidos pelas leveduras de *H. capsulatum* (investigação intra-cultivo) e das distintas formas de crescimento (investigação inter-cultivos).

A técnica empregada neste estudo, cromatografia líquida acoplada à espectrometria de massas por ionização electrospray (LC-ESI-MS), caracteriza um método avançado que permite identificar e categorizar de forma altamente eficiente, rápida e sensitiva as proteínas e peptídeos de uma amostra, além de possibilitar a caracterização de componentes mais

abundantes, bem como dos constituintes raros (Calvete *et al.*, 2007). Outras investigações têm sido conduzidas à cerca da exploração da diversidade metabólica de amostras biológicas utilizando protocolos otimizados de LC-ESI-MS. Em um estudo conduzido por Dias *et al.* (2014) foram detectadas as variações referentes à diversidade peptídica do veneno da vespa social *Polybia paulista* coletada de um mesmo ninho em diferentes épocas do ano (estudo intra-ninho), bem como de diferentes ninhos na mesma estação (estudo inter-ninho). Tal investigação concentrou-se em uma análise diferencial de abundância metabólica, focada na quantificação peptídica dos venenos, bem como na distribuição dos peptídeos detectados por ranges de massas moleculares.

No que diz respeito aos biofilmes fúngicos patogênicos, como relatado anteriormente, os estudos relacionados à detecção da composição metabólica dos mesmos são limitados. Recentemente, o restrito número de abordagens desenvolvidas no contexto metabólico de biofilmes de *C. albicans* empregaram técnicas de GC/MS (Zhu *et al.* 2013; Chen *et al.*, 2014). Zhu e colaboradores (2013) identificaram as 31 pequenas moléculas metabólicas que foram diferencialmente produzidas durante o desenvolvimento dos biofilmes comparado à produção pelas células planctôncias de *C. albicans*. A partir disso, foi desenvolvida uma análise metabolômica direcionada e a trealose foi validada como um dissacarídeo imprescindível para a formação dos biofilmes maduros bem como para a resistência destas formações aos agentes antifúngicos (anfotericina B e miconazol). De fato, um estudo conduzido por Roessner *et al.* (2000) destacou um modelo de GC-MS como um método rápido, altamente sensível e quantitativo para verificar a diversidade de vários metabólitos indicativos do metabolismo do carbono e nitrogênio. Tal modelo pode ser empregado como um sistema para separação e detecção de metabólitos, uma vez que permite a análise simultânea de um grande número de compostos, tais como açúcares, álcoois de açúcar, aminas, aminoácidos e ácidos orgânicos.

Assim, a indicação do método a ser desenvolvido para análise metabolômica, quer seja por LC/MS ou GC/MS, está diretamente relacionada às características da amostra. De forma geral, os métodos de GC/MS são aplicados principalmente para a análise de compostos voláteis em amostras complexas, ao passo que os modelos de LC/MS podem ser aplicados especialmente para a análise de moléculas termicamente instáveis e não voláteis em amostras biológicas. De acordo com Lee *et al.* (2012) entre as vantagens do método de LC/MS destacam-se um tempo de análise significativamente mais curto e um preparo de amostra expressivamente mais simples comparado ao modelo de GC/MS, ambos desenvolvidos por estes autores para a análise de um agente intravenoso, o propofol, e seus metabólitos na urina.

Apesar disso, ambas as técnicas, GC/MS e LC/MS, proporcionam boa sensisibilidade e seletividade (Sumner *et al*., 2003).

Adicionalmente, é importante destacar que uma análise metabolômica é dividida em duas abordagens distintas, a metabolômica não direcionada e a direcionada. Por um lado a metabolômica não direcionada revela o perfil metabólico, focando na detecção do maior número possível de grupos de metabólitos para definir o padrão ou a impressão digital de uma condição biológica, sem necessariamente identificar ou quantificar um composto específico. Em contrapartida, a metabolômica direcionada caracteriza-se pelo monitoramento de metabólitos selecionados, focando na detecção de um grupo específico de metabólitos e, em muitos casos, requer a identificação e quantificação de vários metabólitos dentro de um grupo (Roberts *et al*., 2012). No presente estudo, foi conduzida uma análise metabolômica não direcionada, uma vez que tal estratégia abrange a análise de todos os analitos mensuráveis de uma amostra biológica, incluindo a detecção dos compostos quimicamente desconhecidos. De fato, existem desafios inerentes a esta abordagem, principalmente no que diz respeito à necessidade de desenvolver protocolos e o tempo demandado para processar a enorme quantidade de dados brutos gerados. Subsequentemente, a partir da obtenção dos dados, uma análise não direcionada requer a anotação dos sinais (metabólitos) detectados por intermédio de: a) bibliotecas *in silico* ou; b) uma investigação experimental e a identificação dos compostos utilizando quimíca analítica (Roberts *et al*., 2012). Diante do exposto, apesar dos desafios, a análise metabolômica não direcionada empregada neste estudo constitui uma ferramenta com potencial para a descoberta de um novo alvo e/ou um biomarcador e, para tanto, tendo estabelecido o perfil metabólico, as etapas posteriores concentram-se na caracterização estrutural dos metabólitos relevantes na análise diferencial biofilmes vs. culturas planctônicas que, posteriormente poderão ser validados com ensaios funcionais desenvolvidos para avaliar a atividade e função biológica do(s) novo(s) metabólito(s).

Os resultados alcançados no presente estudo contribuem significativamente para a compreensão de informações referentes ao genótipo e fenótipo das leveduras de *H. capsulatum* em biofilmes e o impacto destas formações na interação com o hospedeiro. Em resumo, é importante ressaltar que a estruturação das leveduras em biofilmes induz uma regulação negativa nos processos transcrionais de forma direta (genoma codificante – RNAm) e indireta (genoma não-codificante – miRNAs) e, nos processos metabólicos do fungo. Tal regulação negativa está associada a: a) repressão da maioria dos genes quando as leveduras livres passam a organizarem-se em biofilmes, visto que ≈80% dos genes são reprimidos pelo fungo nestas formações por ambas as cepas (EH-315 e 60I); b)

superexpressão de todos os miRNAs alterados na comparação de células infectadas com biofilmes vs. planctônicas; c) intensidade relativa reduzida (DOWN) da maioria dos metabólitos (57%) produzidos pelas células em biofilmes em relação à intensidade nas homólogas livres, considerando os metabólitos com a mesma massa molecular entre biofilmes e culturas planctônicas e; e) produção significativamente menor de metabólitos exclusivos pelas culturas em biofilmes (8%) vs. células planctônicas (18%).

Diante do exposto, faz-se necessário salientar que correlacionando o perfil de miRNAs de macrófagos infectados com os biofilmes da cepa EH-315 em relação ao perfil de infecção com leveduras livres, observa-se que após a infecção com os biofilmes há apenas a superexpressão de 5 miRNAs e, neste caso, nenhum miRNA anormalmente regulado teve sua expressão reprimida. De fato, como descrito anteriormente, os miRNAs regulam negativamente a expressão gênica e, portanto, estes resultados coincidem com os dados apresentados pela análise transcriptômica, uma vez que em biofilmes, há uma predominância de genes reprimidos pelas leveduras (81% de genes reprimidos pela cepa EH-315), ao passo que a minoria dos genes são induzidos nestas formações (19% de genes induzidos pela cepa EH-315). De outra forma, conclui-se que, quando estruturam-se em biofilmes, as células orquestram preferencialmente a repressão dos genes, fato comprovado na biologia do fungo (análise transcriptômica) e na interação fungo-célula hospedeira (screening de miRNAs), de maneira a avaliar diretamente a expressão gênica (sequenciamento do RNAm), bem como a análise da regulação indireta da expressão de genes (perfil dos miRNAs).

Neste sentido, é consenso que a adesão de um fungo a uma superfície biótica ou abiótica interfere no metabolismo celular e resulta na fisiologia diferencial das células em um biofilme em relação à população planctônica. Assim, a repressão de inúmeros genes, a superexpressão de miRNAs que regulam negativamente a expressão gênica e a produção reduzida de metabólitos, bem como a produção de muitos metabólitos com menor intensidade caracterizam processos fisiológicos de uma levedura de *H. capsulatum* em biofilmes que impactam da redução da atividade metabólica. Estes achados estão, provavelmente, relacionados ao arranjo arquitetônico dos biofilmes, uma vez que a atividade metabólica diminui com a profundidade das células (Lawrence *et al*., 1991; Harrison *et al*., 2004). A massa dos biofilmes se caracteriza como uma formação compacta de células entreligadas e intercaladas com uma rede amorfa de canais pelos quais os nutrientes e o oxigênio são difundidos e, segundo Bester *et al*. (2005), as taxas diferenciais de crescimento em biofilmes resultam em gradientes químicos que restringem o crescimento de um microrganismo dentro destas formações, em vista da difusão limitada de oxigênio e de nutrientes.

Efetivamente, integrar as abordagens conduzidas correlacionando ncRNAs, RNAm, proteínas e metabólitos é um grande e complexo desafio que exige futuras investigações e validações dos alvos terapêuticos e/ou alvos diagnósticos estabelecidos e demonstrados. Através da análise transcriptômica, alguns genes diferencialmente expressos entre biofilmes e células planctônicas foram apresentados e destacados como potenciais alvos. Adicionalmente, por intermédio da análise de ncRNAs, foram revelados os miRNAs-alvos anormalmente regulados em resposta à infecção fúngica, bem como os genes respectivos (RNAm) que sofrem regulação negativa. Finalmente, por meio da análise metabolômica, foram evidenciados inúmeros metabólitos diferenciais entre as distintas formas de cultivo de *H. capsulatum* que podem ser explorados como futuros alvos. O fato é que as moléculas destacadas (genes, miRNAs e metabólitos) constituem uma fonte potencial para delinear: a) um marcador de biofilmes na infecção às células hospedeiras, a fim de compreender a relação dos biofilmes como um fator de virulência; b) novos protótipos com mecanismos de ação direcionados para a terapêutica da histoplasmose e; c) novos biomarcadores como ferramentas diagnósticas da histoplasmose.

## 5. CONCLUSÕES

Os dados gerados pelo sequenciamento possibilitaram comparar as diferenças transcricionais dentro da mesma espécie (biofilmes vs. culturas planctônicas) e entre diferentes cepas (EH-315 vs. 60I). Sendo assim, a análise transcriptômica revelou genes-alvo que caracterizam a assinatura transcricional dos biofilmes e da infectividade de uma cepa e, em conclusão, destaca-se ainda que a maioria dos genes é reprimida (≈80% down-regulated) quando as leveduras livres passam a organizarem-se em biofilmes.

Conclui-se também que há um padrão de expressão anormal de miRNAs em Mø THP-1 em resposta à infecção com leveduras de *H. capsulatum* (cepa EH-315 em culturas planctônicas e biofilmes e cepa 60I em culturas planctônicas). Tais miRNAs identificados são responsáveis pelo destino das células infectadas, uma vez que atuam regulando negativamente a expressão de um gene (RNAm) alvo, interferindo em vias que determinam a patogênese da histoplasmose e que envolvem desde os aspectos inerentes à adesão às células hospedeiras, bem como à resposta inflamatória e ainda, à morte celular. Além disso, os resultados obtidos indicam que os genes-alvo EPB41 e NUFIP2 têm sua expressão potencialmente desregulada em células hospedeiras após a infecção com *H. capsulatum*. Assim, em vista da importância funcional reconhecida dos miRNAs identificados neste estudo, estes ncRNAs podem viabilizar uma estratégia terapêutica no futuro, a fim de reverter

a relação miRNA-RNAm à normalidade celular, por meio do fornecimento de um determinado miRNA (mimics) ou através do bloqueio de um miRNA expresso (antagomiRs). Destaca-se ainda que no screening diferencial biofilmes vs. culturas planctônicas todos os miRNAs alterados foram superexpressos na célula infectada, fato que demonstra a atuação de tais miRNAs convergindo para a regulação negativa da expressão gênica em resposta à infecção por biofilmes.

Adicionalmente, a análise metabolômica diferencial demonstra que em biofilmes há um aumento substancial de PEI e PI comparado ao crescimento de ambas as cepas (EH-315 e 60I) em culturas planctônicas, constatando a produção de matriz extracelular, bem como maior reserva energética indispensável a estas formações. Subsequentemente, a análise de abundância dos metabólitos detectados por LC-MS/MS revelou três grupos de metabólitos, sendo a) a grande maioria de moléculas com massas moleculares comuns (74%) entre biofilmes e culturas planctônicas, das quais 95% apresentam massa molecular $\leq$ 800 Da e 57% têm uma intensidade relativa reduzida quando as leveduras passam a estruturarem-se em biofilmes (DOWN); b) 8% das moléculas produzidas exibiram massa exclusiva nos biofilmes, das quais a maioria (55%) apresentou massa molecular $\geq$ 800 Da e; c) 18% das moléculas produzidas exibiram massa exclusiva nas culturas planctônicas. Portanto, em biofilmes há uma produção significativamente menor de metabólitos exclusivos.

Em conclusão, a integração entre as abordagens desenvolvidas revela que a estruturação das leveduras em biofilmes induz uma regulação negativa que impacta nos processos transcricionais direta (genoma codificante – RNAm) e indiretamente (genoma não-codificante – miRNAs) e, nos processos metabólicos, sugerindo uma redução significativa da atividade metabólica evidenciada tanto na biologia do fungo em biofilme (regulação transcricional e metabólica), como na interação *in vitro* biofilmes-células hospedeiras (perfil de miRNAs).

Em conjunto, através das plataformas exploradas foram identificadas (genes e miRNAs) e detectadas (metabólitos) moléculas que constituem uma fonte potencial para delinear: a) um marcador de biofilmes na infecção às células hospedeiras; b) novos protótipos para a terapêutica da histoplasmose e; c) novos biomarcadores como ferramentas diagnósticas para a histoplasmose.

## 6. REFERÊNCIAS

AGUSTINHO, D. P. *et al*. Dectin-1 is required for miR155 upregulation in murine macrophages in response to *Candida albicans*. **Virulence,** v. 8, n. 1, p. 41-52, 2017.

ANDERSON, H. *et al*. Histoplasmosis cluster, golf course, Canada. **Emerg Infect Dis**, v. 12, n. 1, p. 163–165, 2006.

ANTINORI, S. *Histoplasma capsulatum*: more widespread than previously thought. **Am J Trop Med Hyg**, v. 90, n. 6, p. 982-983, 2014.

ANTONELLO, V. S. *et al*. Oropharyngeal histoplasmosis: report of eleven cases and review of the literature. **Rev Soc Bras Med Trop,** v. 44, n. 1, p. 26-29, 2011.

AZEVEDO, N. F.; LOPES, S. P.; KEEVIL, C. W.; PEREIRA, M. O.; VIEIRA, M. J. Time to "go large" on biofilm research: advantages of an omics approach. **Biotechnol Lett,** v. 31, n. 4, p. 477-485, 2009.

BESTER, E. *et al*. Planktonic-cell yield of a Pseudomonad biofilm. **Appl Environ Microbiol,** v. 71, n. 12, p. 7792-7798, 2005.

BISH, R. *et al*. Comprehensive Protein Interactome Analysis of a Key RNA Helicase: Detection of Novel Stress Granule Proteins. **Biomolecules**, v. 5, n. 3, p. 1441-1466, 2015.

BOHSE, M. L.; WOODS, J. P. Expression and interstrain variability of the YPS3 gene of *Histoplasma capsulatum*. **Eukaryot Cell,** v. 6, n. 4, p. 609-615, 2007.

BORGIA, G. *et al*. The therapeutic potential of new investigational hepatitis C virus translation inhibitors. **Expert Opin Investig Drugs,** v. 25, n. 10, p. 1209-1214, 2016.

BRILHANTE, R. S. *et al*. Evaluation of the genetic diversity of *Histoplasma capsulatum* var. *capsulatum* isolates from north-eastern Brazil. **J Med Microbiol,** v. 61, n. Pt 12, p. 1688-1695, 2012.

BRILHANTE, R.S.N. *et al*. *Histoplasma capsulatum* in planktonic and biofilm forms: *in vitro* susceptibility to amphotericin B, itraconazole and farnesol. **J Med Microbiol**, v. 64, p. 394-399, 2015.

BRODERICK, J. A.; SALOMON, W. E.; RYDER, S. P.; ARONIN, N.; ZAMORE, P. D. Argonaute protein identity and pairing geometry determine cooperativity in mammalian RNA silencing. **RNA**, v. 17, n. 10, p. 1858–1869, 2011.

BÜTEPAGE, M.; ECKEI, L.; VERHEUGD, P.; LÜSCHER, B. Intracellular Mono-ADP-Ribosylation in Signaling and Disease. **Cells**, v. 4, n. 4, p. 569-595, 2015.

BYRON, S. A. *et al*. Translating RNA sequencing into clinical diagnostics: opportunities and challenges. **Nat Rev Genet,** v. 17, n. 5, p. 257-271, 2016.

CAIN, C. W., LOHSE, M. B., HOMANN, O. R., SIL, A., JOHNSON, A. D. A conserved transcriptional regulator governs fungal morphology in widely diverged species. **Genetics**, v. 190, n. 2, p. 511-521, 2012.

CALANNI, L. M. *et al*. Brote de histoplasmosis en la provincia de Neuquen, Patagonia Argentina. **Rev Iberoam Micol**, v. 30, n. 3, p. 193–199, 2013.

CALVETE, J. J.; JUÁREZ, P.; SANZ, L. Snake venomics. Strategy and applications. **J Mass Spectrom,** v. 42, n. 11, p. 1405-1414, 2007.

CARRETO-BINAGHI, L. E. Could *Histoplasma capsulatum* Be Related to Healthcare-Associated Infections?. **BioMed Res Int**, v. 2015, p. 1-11, 2015.

CHEN, X. *et al*. Ion-pairing chromatography on a porous graphitic carbon column coupled with time-of-flight mass spectrometry for targeted and untargeted profiling of amino acid biomarkers involved in *Candida albicans* biofilm formation. **Mol Biosyst,** v. 10, n. 1, p. 74-85, 2014.

CHITWOOD, D. H.; TIMMERMANS, M. C. Target mimics modulate miRNAs. **Nat Genet**, v. 39, n. 8, p. 935-936, 2007.

CLARK, M. E. *et al.* Transcriptomic and proteomic analyses of *Desulfovibrio vulgaris* biofilms: carbon and energy flow contribute to the distinct biofilm growth state. **BMC Genomics,** v. 13, p. 138, 2012.

COLOMBO, T. E. *et al*. Identification of fungal diseases at necropsy. **Pathol Res Pract,** v. 208, n. 9, p. 549-552, 2012.

CONESA, A.; GÖTZ, S.; GARCÍA-GÓMEZ, J.M.; TEROL, J.; TALÓN, M.; ROBLES, M. Blast2GO: a universal tool for annotation, visualization and analysis in functional genomics research. **Bioinformatics**, v. 18, p. 3674-3676, 2005.

COSTA, M. C.; LEITÃO, A. L.; ENGUITA, F. J. Biogenesis and Mechanism of Action of Small Non-Coding RNAs: Insights from the Point of View of Structural Biology. **Int J Mol Sci**, v. 13, n. 8, p. 10268-10295, 2012.

COSTERTON, J. W. *et al*. Microbial biofilms. **Annu Rev Microbiol,** v. 49, p. 711-745, 1995.

DAMASCENO, L. S. *et al*. The use of genetic markers in the molecular epidemiology of histoplasmosis: a systematic review. **Eur J Clin Microbiol Infect Dis,** v. 35, n. 1, p. 19-27, 2016.

DAS GUPTA, M., FLIESSER, M., SPRINGER, J., BREITSCHOPF, T., SCHLOSSNAGEL, H., SCHMITT. A. L., KURZAI, O., HÜNNIGER, K., EINSELE, H., LÖFFLER, J. *Aspergillus fumigatus* induces microRNA-132 in human monocytes and dendritic cells. **Int J Med Microbiol**, v. 304, n. 5-6, p. 592-596, 2014.

DAVILA, J. I. *et al*. Impact of RNA degradation on fusion detection by RNA-seq. **BMC Genomics,** v. 17, n. 1, p. 814, 2016.

DE CREMER, K. *et al.* Stimulation of superoxide production increases fungicidal action of miconazole against *Candida albicans* biofilms. **Sci Rep,** v. 6, p. 27463, 2016.

DE HOOG, C. L.; MANN, M. Proteomics. **Annu Rev Genomics Hum Genet,** v. 5, p. 267-293, 2004.

DEEPE, G. S. J. *Histoplasma capsulatum*. In: MANDELL, G. L.;BENNET, J. E., *et al* (Ed.). **Principles and Practice of Infectious Diseases**. **Philadelphia: Churchill Livingstone**, (7th ed.), p. 3305-3318, 2009.

DEEPE, G. S.; BUESING, W. R. Deciphering the pathways of death of *Histoplasma capsulatum*-infected macrophages: implications for the immunopathogenesis of early infection. **J Immunol**, v. 188, p. 334-344, 2012.

DENNING, D. W.; BROMLEY M. J. Infectious Disease. How to bolster the antifungal pipeline. **Science**, v. 347, n. 6229, p. 1414-1416, 2015.

DIAS, N. B. *et al*. Peptide diversity in the venom of the social wasp *Polybia paulista* (Hymenoptera): a comparison of the intra- and inter-colony compositions. **Peptides,** v. 51, p. 122-130, 2014.

DUBOIS, M.; GILLES, K.; HAMILTON, J.K.; REBERS, P.A.; SMITH, F. A colorimetric method for the determination of sugars. **Nature**, v. 168, p. 167, 1951.

DURAN-PINEDO, A. E., BAKER, V. D., FRIAS-LOPEZ, J. The periodontal pathogen *Porphyromonas gingivalis* induces expression of transposases and cell death of *Streptococcus mitis* in a biofilm model. **Infect Immun**, v. 82, n. 8, p. 3374-3382, 2014.

DWEEP, H. *et al.* miRWalk2.0: a comprehensive atlas of microRNA-target interactions. **Nature Methods**, v. 12, n. 8, p. 697, 2015.

FAIOLLA, R. C. *et al*. Histoplasmosis in immunocompetent individuals living in an endemic area in the Brazilian Southeast. **Rev Soc Bras Med Trop,** v. 46, n. 4, p. 461-465, 2013.

FERREIRA, M. S.; BORGES, A. S. [Histoplasmosis]. **Rev Soc Bras Med Trop,** v. 42, n. 2, p. 192-198, 2009.

GAROFALO, M.; LEVA, G. D.; CROCE, C. M. MicroRNAs as Anti-Cancer Therapy. **Curr Pharm Des**, v. 20, n. 33, p. 5328-5335, 2014.

GHANNOUM, M. A. Potential role of phospholipases in virulence and fungal pathogenesis. **Clin Microbiol Rev**, v. 13, n. 1, p. 122-143, 2000.

HARA, M. R. *et al*. S-nitrosylated GAPDH initiates apoptotic cell death by nuclear translocation following Siah1 binding. **Nat Cell Biol**, v. 7, n. 7, p. 665-674, 2005.

HARRISON, J. J. *et al*. Differences in biofilm and planktonic cell mediated reduction of metalloid oxyanions. **FEMS Microbiol Lett,** v. 235, n. 2, p. 357-362, 2004.

HOU, Y. *et al.* A metabolomics approach for predicting the response to neoadjuvant chemotherapy in cervical cancer patients. **Mol Biosyst**, v. 10, n. 8, p. 2126-2133, 2014.

KALIA, M.; YADAV, V.K.; SINGH, P.K.; SHARMA, D.; PANDEY, H.; NARVI, S.S.; AGARWAL, V. Effect of Cinnamon Oil on Quorum Sensing-Controlled Virulence Factors and Biofilm Formation in *Pseudomonas aeruginosa*. **PLoS One**, v. 11, n. 10(8):e0135495, 2015.

KASUGA, T. *et al*. Phylogeography of the fungal pathogen *Histoplasma capsulatum*. **Mol Ecol**, v. 12, n. 12, p. 3383–3401, 2003.

KOERDT, A. *et al*. Macromolecular fingerprinting of *Sulfolobus* species in biofilm: a transcriptomic and proteomic approach combined with spectroscopic analysis. **J Proteome Res,** v. 10, n. 9, p. 4105-4119, 2011.

KROETZ, D. N.; DEEPE, G. S. The role of cytokines and chemokines in *Histoplasma capsulatum* infection. **Cytokine,** v. 58, n. 1, p. 112-117, 2012.

LAW, P. T .Y. *et al*. Deep sequencing of small RNA transcriptome reveals novel non-coding RNAs in hepatocellular carcinoma. **Journal of Hepatology,** v. 58, n. 6, p. 1165–1173, 2013.

LAWRENCE, J. R. *et al*. Optical sectioning of microbial biofilms. **J Bacteriol,** v. 173, n. 20, p. 6558-6567, 1991.

LEE, S. Y. *et al*. Comparison of GC/MS and LC/MS methods for the analysis of propofol and its metabolites in urine. **J Chromatogr B Analyt Technol Biomed Life Sci,** v. 900, p. 1-10, 2012.

LEUNG, A.; NATARAJAN, R. Noncoding RNAs in vascular disease. **Curr Opin Cardiol**, v. 29, n. 3, p. 199-206, 2014.

LI, Y. *et al*. Serum metabolic profiling study of lung cancer using ultra high performance liquid chromatography/quadrupole time-of-flight mass spectrometry. **J Chromatogr B Analyt Technol Biomed Life Sci**, v. 966, p. 147-153, 2014.

LI, Z.; RANA, T. M. Therapeutic targeting of microRNAs: current status and future challenges. **Nat Rev Drug Discov,** v. 13, n. 8, p. 622-638, 2014.

LINDON, J. N., J.; HOLMES, E. **The Handbook of Metabonomics and Metabolomics**. 1st. Amsterdam, Holanda, 572 p. 2006.

LIU, A. M. *et al*. miR-122 targets pyruvate kinase M2 and affects metabolism of hepatocellular carcinoma. **PLoS One**, v. 9, n. 1, e86872, 2014.

LU, T. *et al*. miRSystem: An Integrated System for Characterizing Enriched Functions and Pathways of MicroRNA Targets. **PLoS One**, v. 7, n. (8), e42390, 2012.

LU, B.; ZENG, Z.; SHI, T. Comparative study of de novo assembly and genome-guided assembly strategies for transcriptome reconstruction based on RNA-Seq. **Sci China Life Sci,** v. 56, n. 2, p. 143-155, 2013.

MANOS, J. *et al*. Transcriptome analyses and biofilm-forming characteristics of a clonal *Pseudomonas aeruginosa* from the cystic fibrosis lung. **J Med Microbiol,** v. 57, n. Pt 12, p. 1454-1465, 2008.

MARIONI, J. C. *et al*. RNA-seq: an assessment of technical reproducibility and comparison with gene expression arrays. **Genome Res,** v. 18, n. 9, p. 1509-1517, 2008.

MARQUES, S. A.; HORTENSE, J.; REQUENA, C. B.; DE CAMARGO, R. M.; MARQUES, M. E. Disseminated cutaneous histoplasmosis in elderly patients. An uncommon presentation. **Rev Iberoam Micol**, v. 32, n. 2, p. 131-132, 2015.

MARTIN, J. A.; WANG, Z. Next-generation transcriptome assembly. **Nat Rev Genet,** v. 12, n. 10, p. 671-682, 2011.

MEIRI, E. *et al*. A second-generation microRNA-based assay for diagnosing tumor tissue origin. **Oncologist,** v. 17, n. 6, p. 801-812, 2012.

MERRICK, W. C. Mechanism and regulation of eukaryotic protein synthesis. **Microb Rev,** v. 56, 291-315, 1992.

MITCHELL, H. L., DASHPER, S. G., CATMULL, D. V., PAOLINI, R. A., CLEAL, S. M., SLAKESKI, N., TAN, K. H., REYNOLDS, E. C. *Treponema denticola* biofilm-induced expression of a bacteriophage, toxin-antitoxin systems and transposases. **Microbiology**, v. 156, n. 3, p. 774 –788, 2010.

MONK, C. E., HUTVAGNER, G., ARTHUR, J. S. Regulation of miRNA transcription in macrophages in response to *Candida albicans*. **PLoS One**, v. 5, n. 10, e13669, 2010.

MOREIRA, L. M. **Ciências genômicas: fundamentos e aplicações**. Ribeirão Preto: Sociedade Brasileira de Genética. 403 p. 2015.

MORTAZAVI, A. *et al*. Mapping and quantifying mammalian transcriptomes by RNA-Seq. **Nat Methods,** v. 5, n. 7, p. 621-628, 2008.

MUHAMMAD, S. A., FATIMA, N., SYED, N. I., WU, X., YANG, X. F., CHEN, J.Y. MicroRNA Expression Profiling of Human Respiratory Epithelium Affected by Invasive *Candida* Infection. **PLoS One**, v. 10, n. 8, e0136454, 2015.

MUSZKIETA, L.; BEAUVAIS, A.; PÄHTZ, V.; GIBBONS, J. G.; ANTON LEBERRE, V.; BEAU, R.; SHIBUYA, K.; ROKAS, A.; FRANCOIS, J. M.; KNIEMEYER, O.; BRAKHAGE, A. A.; LATGÉ, J. P. Investigation of *Aspergillus fumigatus* biofilm formation by various "omics" approaches. **Front Microbiol,** v. 4, p. 13, 2013.

MYINT, T. *et al*. Histoplasmosis in Patients With Human Immunodeficiency Virus/Acquired Immunodeficiency Syndrome (HIV/AIDS): Multicenter Study of Outcomes and Factors Associated With Relapse. **Medicine (Baltimore),** v. 93, n. 1, p. 11-18, 2014.

NAILIS, H. *et al*. Real-time PCR expression profiling of genes encoding potential virulence factors in *Candida albicans* biofilms: identification of model-dependent and -independent gene expression. **BMC Microbiol**, v. 10, p. 114, 2010.

NOSANCHUK, J. D., GÓMEZ, B. L., YOUNGCHIM, S., DÍEZ, S., AISEN, P., ZANCOPÉ-OLIVEIRA, R. M., RESTREPO, A., CASADEVALL, A., HAMILTON, A. J. *Histoplasma capsulatum* synthesizes melanin-like pigments *in vitro* and during mammalian infection. **Infect Immun**, v. 70, n. 9, p. 5124-5131, 2002.

O'CONNELL, R. M. *et al*. Physiological and pathological roles for microRNAs in the immune system. **Nat Rev Immunol**, v. 10, n. 2, p. 111-122, 2010.

OLIVEIRA, F. E. M.; UNIS, G.; SEVERO, L. C. An outbreak of histoplasmosis in the city of Blumenau, Santa Catarina. **J Bras Pneumol,** v. 32, n. 4, p. 375-378, 2006.

OLIVEROS, J.C. VENNY. An interactive tool for comparing lists with Venn Diagrams. Disponível em: http://bioinfogp.cnb.csic.es/tools/venny/index.html, 2007. Acesso em 20 de agosto de 2015.

OZSOLAK, F.; MILOS, P. M. RNA sequencing: advances, chalenges and opportunities. **Nat Rev Genet**, v. 12, p. 87–98, 2011.

PABLA, N., BHATT, K., DONG, Z. Checkpoint kinase 1 (Chk1)-short is a splice variant and endogenous inhibitor of Chk1 that regulates cell cycle and DNA damage checkpoints. **Proc Natl Acad Sci U S A**, v. 109, n. 1, p. 197-202, 2012.

PASSOS, A. N. *et al.* Immunological assays employed for the elucidation of an histoplasmosis outbreak in São Paulo, SP. **Braz J Microbiol,** v. 45, n. 4, p. 1357-1361, 2014.

PEETERS, E.; NELIS, H. J.; COENYE, T. Comparison of multiple methods for quantification of microbial biofilms grown in microtiter plates. **J Microbiol Methods,** v. 72, n. 2, p. 157-165, 2008.

PITANGUI, N. S. *et al*. Adhesion of *Histoplasma capsulatum* to pneumocytes and biofilm formation on an abiotic surface. **Biofouling,** v. 28, n. 7, p. 711-718, 2012.

PITANGUI, N. D. S. *et al*. An Intracellular Arrangement of *Histoplasma capsulatum* Yeast-Aggregates Generates Nuclear Damage to the Cultured Murine Alveolar Macrophages. **Frontiers in Microbiology,** v. 6, 1526, 2016.

RAJENDRAN, R. *et al.* Integrating *Candida albicans* metabolism with biofilm heterogeneity by transcriptome mapping. **Sci Rep,** v. 6, p. 35436, 2016.

RAPPLEYE, C. A.; ENGLE, J. T.; GOLDMAN, W. E. RNA interference in *Histoplasma capsulatum* demonstrates a role for alpha-(1,3)-glucan in virulence. **Mol Microbiol,** v. 53, n. 1, p. 153-165, 2004.

REBANE, A.; AKDIS, C. A. MicroRNAs in Allergy and Asthma. **Curr Allergy Asthma Rep**, v. 14, n. 4, p. 424, 2014.

ROBERTS, L. D. *et al.* Targeted metabolomics. **Curr Protoc Mol Biol,** v. Chapter 30, Unit 30.2. p. 1-24, 2012.

RODRÍGUEZ-CERDEIRA, C. *et al*. Systemic Fungal Infections in Patients with human inmunodeficiency virus. **Actas Dermosifiliogr**, 2012.

ROESSNER, U. *et al*. Technical advance: simultaneous analysis of metabolites in potato tuber by gas chromatography-mass spectrometry. **Plant J,** v. 23, n. 1, p. 131-142, 2000.

SARDI, J. C. O. *et al.* Highlights in pathogenic fungal biofilms. **Rev Iberoam Micol**, v. 31, n. 1, p. 22–29, 2014.

SARDI, J. C. *et al*. *In vitro Paracoccidioides brasiliensis* biofilm and gene expression of adhesins and hydrolytic enzymes. **Virulence**, v, 6, n. 6, p. 663-672, 2015.

SENEVIRATNE, C. J.; JIN, L.; SAMARANAYAKE, L. P. Biofilm lifestyle of *Candida*: a mini review. **Oral Dis,** v. 14, p. 582–590, 2008.

SCHULZ, W. A.; INGENWERTH, M.; DJUIDJE, C.E.; HADER, C.; RAHNENFÜHRER, J.; ENGERS, R. Changes in cortical cytoskeletal and extracellular matrix gene expression in prostate cancer are related to oncogenic ERG deregulation. **BMC Cancer**, v. 10, n. 505, p. 1-9, 2010.

SHEARER, G. Jr. Cloning and analysis of cDNA encoding an elongation factor 1 alpha from the dimorphic fungus *Histoplasma capsulatum*. **Gene**, v. 161, n. 1, p. 119-123, 1995.

SIFUENTES-OSORNIO, J.; CORZO-LEÓN, D. E.; PONCE-DE-LEÓN, L. A. Epidemiology of Invasive Fungal Infections in Latin America. **Curr Fungal Infect Rep,** v. 6, n. 1, p. 23-34, 2012.

SULTAN, M. *et al.* A global view of gene activity and alternative splicing by deep sequencing of the human transcriptome. **Science,** v. 321, n. 5891, p. 956-960, 2008.

SUMNER, L. W.; MENDES, P.; DIXON, R. A. Plant metabolomics: large-scale phytochemistry in the functional genomics era. **Phytochemistry,** v. 62, n. 6, p. 817-36, 2003.

SUN, L. *et al*. microRNAs Involved in the Control of Innate Immunity in *Candida* Infected *Caenorhabditis elegans*. **Sci Rep,** v. 6, 36036, 2016.

TAGLIARI, L.; TOLEDO, M. S.; LACERDA, T. G.; SUZUKI, E.; STRAUS, A.H.; TAKAHASHI, H. K. Membrane microdomain components of *Histoplasma capsulatum* yeast forms, and their role in alveolar macrophage infectivity. **Biochim Biophys Acta**, v. 1818, n. 3, p. 458-466, 2012.

TISDALE, E. J. Glyceraldehyde-3-phosphate dehydrogenase is phosphorylated by protein kinase Ciota /lambda and plays a role in microtubule dynamics in the early secretory pathway. **J Biol Chem**, v. 277, n. 5, p. 3334-3341, 2002.

TRAPNELL, C.; PACHTER, L.; SALZBERG, S. L. TopHat: discovering splice junctions with RNA-Seq. **Bioinformatics,** v. 25, n. 9, p. 1105-11, 2009.

TURCHINOVICH, A. *et al*. Circulating miRNAs: cell-cell communication function? **Front Genet**, v. 4, p. 119, 2013.

VALLEJO, M. C. *et al.* Vesicle and vesicle-free extracellular proteome of *Paracoccidioides brasiliensis*: comparative analysis with other pathogenic fungi. **J Proteome Res**, v. 11, n. 3, p. 1676-1685, 2012.

VAN ROOIJ, E.; MARSHALL, W. S.; OLSON, E. N. Toward microRNA-based therapeutics for heart disease: the sense in antisense. **Circ Res,** v. 103, n. 9, p. 919-928, 2008.

VLACHOS, I. S. *et al*. DIANA miRPath v.2.0: investigating the combinatorial effect of microRNAs in pathways. **Nucleic Acids Res**, 40 (Web Server issue): W498-504, 2012.

WANG, D. *et al.* Detection of multiple gene mutations in non-small-cell lung cancer by suspension *microarray*. **Zhonghua Yi Xue Za Zhi,** v. 89, n. 48, p. 3393-3396, 2009a.

WANG, Z.; GERSTEIN, M.; SNYDER, M. RNA-Seq: a revolutionary tool for transcriptomics. **Nat Rev Genet**, v. 10, n. 1, p. 57–63, 2009b.

WEAVER, C. H.; SHEEHAN, K. C.; KEATH, E. J. Localization of a yeast-phase-specific gene product to the cell wall in *Histoplasma capsulatum*. **Infect Immun,** v. 64, n. 8, p. 3048-3054, 1996.

WEBSTER, R. H., SIL, A. Conserved factors Ryp2 and Ryp3 control cell morphology and infectious spore formation in the fungal pathogen *Histoplasma capsulatum*. **Proc Natl Acad Sci U S A**, v. 105, n. 38, p. 14573-14578, 2008.

WEN, Z. T., NGUYEN, A. H., BITOUN, J. P., ABRANCHES, J., BAKER, H. V., BURNE, R. A. Transcriptome analysis of LuxS-deficient *Streptococcus mutans* grown in biofilms. **Mol Oral Microbiol**, v. 26, n. 1, p. 2-18, 2011.

YAO-SHU, T.; XIAO-LIN, C.; YONG, L. Roles of microRNAs in Allergic Airway Diseases. **Zhongguo Yi Xue Ke Xue Yuan Xue Bao**, v. 36, n. 1, p. 114-118, 2014.

ZHOU, Q. Y. *et al.* Metabolomics investigation of cutaneous T cell lymphoma based on UHPLC-QTOF/MS. **Asian Pac J Cancer Prev**, v. 15, n. 13, p. 5417-5421, 2014.

ZHU, Z. *et al*. Time course analysis of *Candida albicans* metabolites during biofilm development. **J Proteome Res,** v. 12, n. 6, p. 2375-2385, 2013.

# Capítulo 2 - Artigos

Clinical Microbiology: Open Access

Sardi et al., Clin Microbial 2013, 2:1
http://dx.doi.org/10.4172/2327-5073.1000103

Research Article Open Access

# *In vitro* Antifungal Susceptibility of *Candida albicans* Isolates from Patients with Chronic Periodontitis and Diabetes

**SARDI JCO*, GULLO FP, PITANGUI NS, FUSCO-ALMEIDA AM and MENDES-GIANNINI MJS**

*Department of Clinical Analysis, UNESP – Univ Estadual Paulista, Araraquara, Brazil*

## Abstract

Alterations that lead to deficiency of the immune system, such as diabetes mellitus, may promote proliferation of *Candida albicans* and selection of strains which have greater ability to adhere and to penetrate the host tissues. Recent studies indicate an increase of the antifungal resistance of *C. albicans* isolates in periodontal pockets, suggesting that the oral cavity could be a reservoir of resistant yeast to antifungal agents. Moreover, oral cavity can act as a reservoir of certain pathogens that may cause systemic infections. The periodontal pocket is an ecological niche suitable to host microorganisms that could act as opportunistic pathogens. The aim of this study is to contribute to the understanding of resistance to conventional antifungal against *C. albicans* isolates from patients with periodontitis and diabetes. The determination of the minimal inhibitory concentrations (MIC) was evaluated according to M27S3 of the CLSI (2008), with modifications. The results showed that 48.8% of the studied strains were resistant to one or more antifungals and 6.6% were resistant to fluconazole and voriconazole. These results suggest an increasing resistance to conventional antifungal agents among *Candida* species, suggesting that the oral cavity could host pathogen fungi.

**Keywords:** *Candida albicans*; Diabetes; antifungal; Minimal inhibitory concentrations (MIC); Resistance

## Introduction

A large proportion of healthy adult population holds yeast *Candida* genus in the oral cavity [1]. The mucosa is considered the main reservoir, but studies have shown that *Candida* species can be co-aggregated with bacteria in biofilm and that may be an important factor for manifestations of candidiasis and for colonization of cavities of caries and periodontal pockets [2]. According to some authors, the presence of yeast in subgingival regions may contribute to the pathogenesis of periodontal disease or increase the probability of candidemia, especially in cases of immunocompromised patients [3-5]. Periodontal disease is mainly caused by Gram negative anaerobic species, but has been reported in the literature that the proportion of yeast in the periodontal pockets is similar to some of periodontal bacteria [6], thus suggesting the possible role of *Candida* sp. in disease pathogenesis [2,4,7,8], but it is not clear, in the literature, whether this would continue after periodontal therapeutic antibacterial successive. Moreover, its permanence in these sites can be characterized as potential sources of dissemination, especially in immune compromised individuals [9]. Sardi et al. [10] found a higher prevalence of *C. albicans* in periodontal pockets of diabetic patients compared with non diabetic. Super infection by *Candida* can be refractory to conventional periodontal treatments in specific situations, such as in immune compromised patients. In these cases, the systemic therapy with antifungal drugs could be indicated. Few studies have reported the use of antifungals in *Candida* isolates in periodontal pockets. The presence of *Candida* in periodontal pockets has been investigated a little time and very little is known about the importance of this fungus in this pathology. Oral candidiasis used to be treated with polyenes amphotericin B or nistatin and the discovery of antifungal activity of azolic compounds represented an important advance in the treatment of superficial and systemic fungal infections Moreover, they inhibit germ tube formation, reducing the adherence to oral epithelial cells and acrylic surfaces in dentistry [11]. Caspofungin, an echinocandin, which has demonstrated activity against *Candida* species both *in vitro* and *in vivo* for systemic infections [12,13]. The aim of this study was to analyze antifungal susceptibility of *C. albicans* strains isolated from chronic periodontitis patients and diabetes.

## Methods

### Microorganisms

We used 45 clinical isolates of *Candida albicans* isolated from subgingival sites of patients with generalized chronic periodontitis and diabetes mellitus type II. These fungi were isolated from patients with age ranging between 31 to 68 years attending in clinic of Periodontics, Piracicaba Dental School, State University of Campinas (UNICAMP). Exclusion criteria were used: use of antibiotics and periodontal treatment during the previous 6 months. As control was used strain ATCC 90028 of *Candida albicans*. All microorganisms belong to the mycology collection of the Laboratory of Clinical Mycology, Department of Clinical Analysis, Faculty of Pharmaceutical Sciences, UNESP, Araraquara.

### Preparation of antifungal drugs

Conventional antifungal agents indicated for the treatment of candidiasis were used: amphotericin B, fluconazole, voriconazole and caspofungin. The preparation of the drugs was performed according to M27 S3 of the CLSI (Clinical and Laboratory Standards Institute)

***Corresponding author:** Janaina de Cassia Orlandi Sardi, Faculty of Pharmaceutical Sciences of Department of Clinical Analysis, Laboratory of Clinical Mycology, Univ Paulista (UNESP), Brazil, Tel: +55 16 3301 5716; E-mail: janaina-sardi@uol.com.br

**Received** January 28, 2013; **Accepted** March 02, 2013; **Published** March 08, 2013

**Citation:** SARDI JCO, GULLO FP, PITANGUI NS, FUSCO-ALMEIDA AM and MENDES-GIANNINI MJS (2013) *In vitro* Antifungal Susceptibility of *Candida albicans* Isolates from Patients with Chronic Periodontitis and Diabetes. Clin Microbial 2: 103. doi:10.4172/2327-5073.1000103

(2008). Amphotericin B (Sigma Chemical Company, St. Louis, MO, USA) and voriconazole (Sigma Chemical Company, St. Louis, MO, USA) are water-insoluble drugs, therefore, were solubilized in DMSO for the preparation the ten stock solutions with concentrations ranging from 0.0313 to 16 µg/mL. Fluconazole (Sigma Chemical Company, St. Louis, MO, USA) and caspofungin (Sigma Chemical Company, St. Louis, MO, USA) are water-soluble drugs therefore were solubilized in sterile water and ten stock solutions were prepared with a concentration range varying from 0125 to 64 µg/mL. All stock solutions were diluted in RPMI-1640 (Sigma-Aldrich, St. Louis, MO, USA) with L-glutamine, without sodium bicarbonate, supplemented with 2% glucose, and buffered to a pH of 7.0 using 0.165M 3-(N-Morpholino) (propanesulfonic acid) (MOPS), (Sigma-Aldrich, St. Louis, MO, USA) to preparation the working solutions. The range concentration for amphotericin B and voriconazole was 0.01565 to 8 µg/ml and for drugs fluconazole and caspofungin was 0.0625 to 32 µg/mL.

### Determination of minimum inhibitory concentration (MIC)

The sensibility of the clinical isolates to conventional antifungal agents was evaluated according to M27 S3 of the CLSI (2008), with modifications. From 24 hours cultivation of clinical isolates of *C. albicans* on Sabouraud dextrose, the inocula were prepared in RPMI-1640 to the final concentration of $1.0\times10^4$ CFU/mL and added in 96-well microplates (Difco, Detroit, USA) previously prepared with antifungal drugs. The plates were incubated in a shaker at 37°C/150 rpm for 24 hours. The reading of MIC was performed in a spectrophotometry at 490 nm. Through this test, the 45 clinical isolates were classified as sensitive (S), sensitive dose dependent (S-DD) and resistant (R), according with the breakpoints recommended by the CLSI (2008) (Table 1).

| | Fluconazole | Voriconazole | Anfotericin B | Caspofungin |
|---|---|---|---|---|
| **S*** | ≤ 8 µg/mL | ≤ 0,125 µg/mL | ≤ 1 µg/mL | ≤ 2 µg/mL |
| **S-DD*** | 16 – 32 µg/mL | 0,25 – 0,5 µg/mL | - | - |
| **R*** | ≥ 64 µg/mL | ≥ 1 µg/mL | ≥ 2 µg/mL | > 2 µg/mL |

S - sensitive / DD - dose dependent / R – resistant

**Table 1:**. Values of MIC for the classification of susceptibility to fluconazole, voriconazole, amphotericin B and Caspofungin in *Candida* species.

## Results

Through the determination of MIC was observed that from 45 clinical isolates of *C. albicans*, 48.8% were resistant to one or more antifungals. This percentage was determined by comparison between the MIC values of isolates with cutoff values found in the literature. Our results showed that 6.6% of clinical isolates were resistant to the azole class, being resistant to fluconazole as voriconazole. Figure 1 shows the percentage of clinical isolates sensitive, dose-dependent sensitive and resistant to azoles. Among the azoles, the fluconazole showed greater activity against clinical isolates with only five (11.2%) isolates resistant to this drug (Figure 1-A), differently from the voriconazole, in which 19 (42.2%) of the isolates were resistant (Figure 1-B).

We observed that a large percentage of clinical isolates were sensitive to amphotericin B, and only four (8.9%) classified as resistant (Figure 1-C). It was also observed that the antifungal caspofungin showed only two (4.4%) considered resistant isolates (Figure 1-D). Thus, the clinical isolates of *C. albicans* tested with these two drugs showed no fungal resistance, but showed significant resistance to azole antifungal class.

## Discussion

*Candida* species inhabit diverse ecosystems and are present in the genitourinary and gastrointestinal tracts, nail, skin, bronchus and oral cavity where they can establish themselves as regular commensal microbiota without causing harm to the host [14]. However, systemic diseases such as diabetes mellitus and AIDS, physiological conditions such as pregnancy, infancy or old age, nutritional factors, treatment with broad-spectrum antibiotics, immune suppressants and corticosteroids, in addition to local factors such as xerostomia and use of prosthetic devices are conditions that predispose to the development of *Candida* infections [2,10,15-19]. The use of broad-spectrum antimicrobial, such as tetracycline and metronidazole as an aid in periodontal treatment has also been an important factor for the development of super infections by resistant bacteria and *Candida* species, including patients

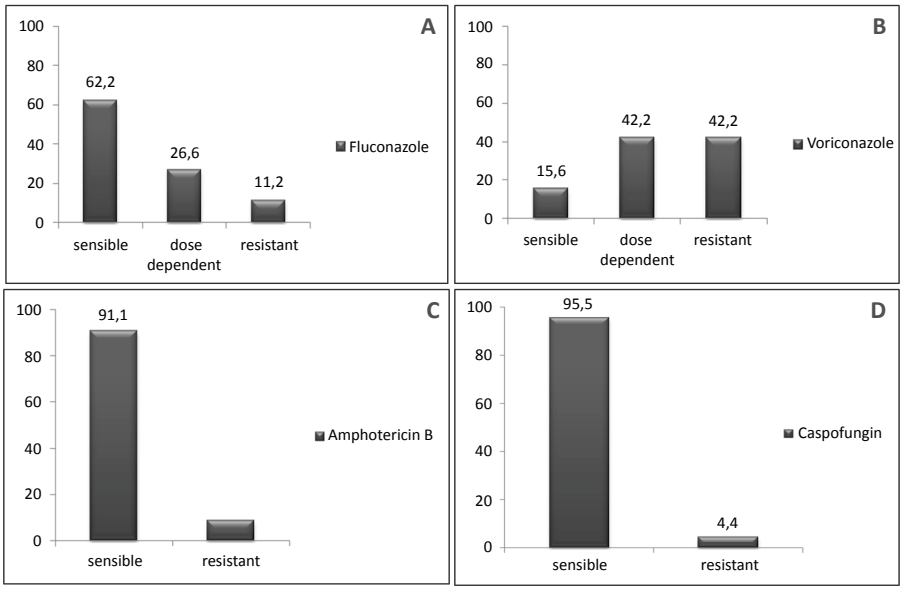


**Figure 1:** Relation of 45 clinical isolates of *Candida albicans* with antifungal fluconazole (A), voriconazole (B), amphotericin B (C) and Caspofungin (D).

with HIV [6,20]. Resistance to fluconazole has been reported by several authors [21-26]. In the present study, 62.2% of the *C. albicans* isolates tested were susceptible to fluconazole, 15.6% to voriconazole, 91.1% to amphotericin B and 95.5% to caspofungin. The intrinsic resistance of *Candida* species to fluconazole, an agent commonly used for treating antifungal and greater resistance to amphotericin B has been reported [27]. *Candida albicans* appears co-aggregate contributing to bacterial biofilm formation on this structural and impairing penetration of certain antimicrobial drugs [28]. Also, for these researchers *C. albicans* was found typically in the outer layers of the biofilm, and seemed to act, according to the authors, as a barrier that protected the microorganisms from the action of immune mechanismsby assisting the resistance of subgingival microbiota in the face of host defenses, and contributing to persistence of inflammation in the surrounding tissues.

Waltimo et al. [29] evaluated the antifungal susceptibility among isolates of *C. albicans* from periodontal pockets and showed that 100% of these isolates were sensitive to amphotericin B and 5 - flucytosine. However, susceptibility to azole antifungals proved variable cross-resistance occurring in relation to them. Dumitru et al. [30], studied isolates of *C. albicans* and found strains resistant to amphotericin B and four class azole antifungals. Furlletti et al. [31] showed that *C. albicans* isolated from periodontal pockets were resistant to amphotericin B and fluconazole-sensitive. Jewtuchowicz et al. [7] studied isolates of *C. dubliniensis* and *C. albicans* from periodontitis patients and healthy systematically and found that only one isolate was resistant to fluconazole and voriconazole. Junqueira et al. [32] demonstrated that isolates of *Candida* sp. oral cavity of HIV patients are resistant to fluconazole. In our study we found some isolates resistant to fluconazole (11.2%), voriconazole (42.2%), caspofungin (4.4%) and amphotericin B (8.9%), although the highest resistance occurred with the antifungal voriconazole. Some research has shown the presence of different species of *Candida* isolated from different anatomical sites resistant to voriconazole in diabetics patients [33-36]. Antifungal agents such as amphotericin B, 5-fluorocytosine, voriconazole and terbinafine are not usually used in the treatment of oral candidiasis, however, also deserve attention. Although such antifungals are only available for systemic use and are recommended for the treatment of disseminated infections, determination of minimum inhibitory concentration relative to oral cavity isolates obtained from patients with immune suppression, especially in cases of periodontitis is important to obtain epidemiological data and the possibility of this site being the original focus of disseminated fungal infections [37,38]. The results of this study suggest that clinical isolates of diabetic patients have a certain resistance to azoles, perhaps because these patients have already contacted and antifungal therapy with azoles may no longer be as effective in treating periodontal *Candida* super infections that are refractory to conventional treatments. Furthermore, studies on the correlation between clinical results and *in vitro* are needed to establish a better antifungal.

## References

1. Sardi JC, Scorzoni L, Bernardi T, Fusco-Almeida AM, Mendes Giannini MJ (2013) Candida species: current epidemiology, pathogenicity, biofilm formation, natural antifungal products and new therapeutic options. J Med Microbiol 62(1):10-24.
2. Sardi JC, Duque C, Mariano FS, Peixoto IT, Höfling JF, et al. (2010) Candida spp. in periodontal disease: a brief review. J Oral Sci 52: 177-185.
3. Reynaud AH, Nygaard-Østby B, Bøygard GK, Eribe ER, Olsen I, et al. (2001) Yeasts in periodontal pockets. J Clin Periodontol 28: 860-864.
4. Barros LM, Boriollo MF, Alves AC, Klein MI, Gonçalves RB, et al. (2008) Genetic diversity and exoenzyme activities of Candida albicans and Candida dubliniensis isolated from the oral cavity of Brazilian periodontal patients. Arch Oral Biol 53: 1172-1178.
5. Cuesta AI, Jewtuchowicz V, Brusca MI, Nastri ML, Rosa AC (2010) Prevalence of Staphylococcus spp and Candida spp in the oral cavity and periodontal pockets of periodontal disease patients. Acta Odontol Latinoam 23: 20-26.
6. Dahlén G, Wikström M (1995) Occurrence of enteric rods, staphylococci and Candida in subgingival samples. Oral Microbiol Immunol 10: 42-46.
7. Jewtuchowicz VM, Mujica MT, Brusca MI, Sordelli N, Malzone MC, et al. (2008) Phenotypic and genotypic identification of Candida dubliniensis from subgingival sites in immunocompetent subjects in Argentina. Oral Microbiol Immunol 23: 505-509.
8. Urzúa B, Hermosilla G, Gamonal J, Morales-Bozo I, Canals M, et al. (2008) Yeast diversity in the oral microbiota of subjects with periodontitis: Candida albicans and Candida dubliniensis colonize the periodontal pockets. Med Mycol 46: 783-793.
9. Ito CY, de Paiva Martins CA, Loberto JC, dos Santos SS, Jorge AO (2004) In vitro antifungal susceptibility of Candida spp. isolates from patients with chronic periodontitis and from control patients. Braz Oral Res 18: 80-84.
10. Sardi JC, Duque C, Camargo GA, Hofling JF, Gonçalves RB (2011) Periodontal conditions and prevalence of putative periodontopathogens and Candida spp. in insulin-dependent type 2 diabetic and non-diabetic patients with chronic periodontitis--a pilot study. Arch Oral Biol 56: 1098-1105.
11. Ellepola AN, Samaranayake LP (1998) The effect of limited exposure to antifungal agents on the germ tube formation of oral Candida albicans. J Oral Pathol Med 27: 213-219.
12. Fidel PL Jr, Vazquez JA, Sobel JD (1999) Candida glabrata: review of epidemiology, pathogenesis, and clinical disease with comparison to C. albicans. Clin Microbiol Rev 12: 80-96.
13. Danby CS, Boikov D, Rautemaa-Richardson R, Sobel JD (2012) Effect of pH on in vitro susceptibility of Candida glabrata and Candida albicans to 11 antifungal agents and implications for clinical use. Antimicrob Agents Chemother 56: 1403-1406.
14. Kleinegger CL, Lockhart SR, Vargas K, Soll DR (1996) Frequency, intensity, species, and strains of oral Candida vary as a function of host age. J Clin Microbiol 34: 2246-2254.
15. Tekeli A, Dolapci I, Emral R, Cesur S (2004) Candida carriage and Candida dubliniensis in oropharyngeal samples of type-1 diabetes mellitus patients. Mycoses 47: 315-318.
16. Pires-Gonçalves RH, Sartori FG, Montanari LB, Zaia JE, Melhem MS, et al. (2008) Occurrence of fungi in water used at a haemodialysis centre. Lett Appl Microbiol 46: 542-547.
17. Motta-Silva AC, Aleva NA, Chavasco JK, Armond MC, França JP, et al. (2010) Erythematous oral candidiasis in patients with controlled type II diabetes mellitus and complete dentures. Mycopathologia 169: 215-223.
18. Machado FC, de Souza IP, Portela MB, de Araújo Soares RM, Freitas-Fernandes LB, et al. (2011) Use of chlorhexidine gel (0.2%) to control gingivitis and candida species colonization in human immunodeficiency virus-infected children: a pilot study. Pediatr Dent 33: 153-157.
19. Brissaud O, Guichoux J, Harambat J, Tandonnet O, Zaoutis T (2012) Invasive fungal disease in PICU: epidemiology and risk factors. Ann Intensive Care 2: 6.
20. Odden K, Schenck K, Koppang H, Hurlen B (1994) Candidal infection of the gingiva in HIV-infected persons. J Oral Pathol Med 23: 178-183.
21. Gallè F, Sanguinetti M, Colella G, Di Onofrio V, Torelli R, et al. (2011) Oral candidosis: characterization of a sample of recurrent infections and study of resistance determinants. New Microbiol 34: 379-389.
22. Jiang C, Dong D, Yu B, Cai G, Wang X, et al. (2012) Mechanisms of azole resistance in 52 clinical isolates of Candida tropicalis in China. J Antimicrob Chemother .
23. Jung SI, Shin JH, Choi HJ, Ju MY, Kim SH, et al. (2012) Antifungal susceptibility to amphotericin B, fluconazole, voriconazole, and flucytosine in Candida bloodstream isolates from 15 tertiary hospitals in Korea. Ann Lab Med 32: 426-428.
24. Marchaim D, Lemanek L, Bheemreddy S, Kaye KS, Sobel JD (2012) Fluconazole-resistant Candida albicans vulvovaginitis. Obstet Gynecol 120: 1407-1414.
25. Moris DV, Melhem MS, Martins MA, Souza LR, Kacew S, et al. (2012) Prevalence and antifungal susceptibility of Candida parapsilosis complex

isolates collected from oral cavities of HIV-infected individuals. J Med Microbiol 61: 1758-1765.

26. Castelo-Branco DS, Brilhante RS, Paiva MA, Teixeira CE, Caetano EP, et al. (2013) Azole-resistant Candida albicans from a wild Brazilian porcupine (Coendou prehensilis): a sign of an environmental imbalance? Med Mycol .

27. Ghannoum MA, Herbert J, Isham N (2011) Repeated exposure of Candida spp. to miconazole demonstrates no development of resistance. Mycoses 54: e175-177.

28. Järvensivu A, Hietanen J, Rautemaa R, Sorsa T, Richardson M (2004) Candida yeasts in chronic periodontitis tissues and subgingival microbial biofilms in vivo. Oral Dis 10: 106-112.

29. Waltimo TM, Ørstavik D, Meurman JH, Samaranayake LP, Haapasalo MP (2000) In vitro susceptibility of Candida albicans isolates from apical and marginal periodontitis to common antifungal agents. Oral Microbiol Immunol 15: 245-248.

30. Dumitru R, Hornby JM, Nickerson KW (2004) Defined anaerobic growth medium for studying Candida albicans basic biology and resistance to eight antifungal drugs. Antimicrob Agents Chemother 48: 2350-2354.

31. Furlletti V, Mardegan R, Obando-Pereda G, Aníbal P, Duarte M, et al. (2008) Susceptibility of Candida spp. oral isolates for azolic antifungals and amphotericin B Braz J Oral Sci [Internet]7:1543-1549.

32. Junqueira JC, Vilela SF, Rossoni RD, Barbosa JO, Costa AC, et al. (2012) Oral colonization by yeasts in HIV-positive patients in Brazil. Rev Inst Med Trop Sao Paulo 54: 17-24.

33. Ahmad S, Khan Z, Mokaddas E, Khan ZU (2004) Isolation and molecular identification of Candida dubliniensis from non-human immunodeficiency virus-infected patients in Kuwait. J Med Microbiol 53: 633-637.

34. Ruan SY, Huang YT, Chu CC, Yu CJ, Hsueh PR (2009) Candida glabrata fungaemia in a tertiary centre in Taiwan: antifungal susceptibility and outcomes. Int J Antimicrob Agents 34: 236-239.

35. Chellan G, Shivaprakash S, Karimassery Ramaiyar S, Varma AK, Varma N, et al. (2010) Spectrum and prevalence of fungi infecting deep tissues of lower-limb wounds in patients with type 2 diabetes. J Clin Microbiol 48: 2097-2102.

36. Lockhart SR, Wagner D, Iqbal N, Pappas PG, Andes DR, et al. (2011) Comparison of in vitro susceptibility characteristics of Candida species from cases of invasive candidiasis in solid organ and stem cell transplant recipients: Transplant-Associated Infections Surveillance Network (TRANSNET), 2001 to 2006. J Clin Microbiol 49: 2404-2410.

37. Baccaglini L, Atkinson JC, Patton LL, Glick M, Ficarra G, et al. (2007) Management of oral lesions in HIV-positive patients. Oral Surg Oral Med Oral Pathol Oral Radiol Endod 103 Suppl: S50.

38. Cross LJ, Williams DW, Sweeney CP, Jackson MS, Lewis MA, et al. (2004) Evaluation of the recurrence of denture stomatitis and Candida colonization in a small group of patients who received itraconazole. Oral Surg Oral Med Oral Pathol Oral Radiol Endod 97: 351-358.

**Citation:** SARDI JCO, GULLO FP, PITANGUI NS, FUSCO-ALMEIDA AM and MENDES-GIANNINI MJS (2013) *In vitro* Antifungal Susceptibility of *Candida albicans* Isolates from Patients with Chronic Periodontitis and Diabetes. Clin Microbial 2: 103. doi:10.4172/2327-5073.1000103

Brazilian Journal of Microbiology 44, 4, 1035-1041 (2013)
ISSN 1678-4405


Review

# Anti dermatophytic therapy - Prospects for the discovery of new drugs from natural products

Luciana Arantes Soares, Janaína de Cássia Orlandi Sardi, Fernanda Patrícia Gullo, Nayla de Souza Pitangui, Liliana Scorzoni, Fernanda Sangalli Leite, Maria José Soares Mendes Giannini, Ana Marisa Fusco Almeida

Departamento de Análises Clínicas, Faculdade de Ciências Farmacêuticas, Universidade Estadual Paulista "Júlio Mesquita Filho", Araraquara, SP, Brazil.

Submitted: May 15, 2012; Approved: April 4, 2013.

## Abstract

Millions of people and animals suffer from superficial infections caused by a group of highly specialized filamentous fungi, the dermatophytes, which only infect keratinized structures. With the appearance of AIDS, the incidence of dermatophytosis has increased. Current drug therapy used for these infections is often toxic, long-term, and expensive and has limited effectiveness; therefore, the discovery of new anti dermatophytic compounds is a necessity. Natural products have been the most productive source for new drug development. This paper provides a brief review of the current literature regarding the presence of dermatophytes in immunocompromised patients, drug resistance to conventional treatments and new anti dermatophytic treatments.

**Key words:** dermatophytes, filamentous fungi, natural products, synthetic product.

## Dermatophytosis

Millions of people and animals suffer from superficial infections caused by a group of highly specialized filamentous fungi, the dermatophytes, which only infect keratinized structures (Burmester *et al.*, 2011). The American Academy of Dermatology estimates that 10-20% of the population is affected by dermatophytes (Pfaller and Sutton, 2006). Dermatophytes are a group of parasitic fungi that live at the expense of the keratin in the skin, nails and hair. These microorganisms fall into the genera *Trichophyton*, *Microsporum* and *Epidermophyton*, as characterized according to the formation and morphology of their conidia (Weitzman and Summerbell, 1995; White *et al.*, 2008 Peres *et al.*, 2010). In general, dermatophytes are confined to the stratum corneum of the epidermis and skin appendages, especially in the moist areas of the body, such as the regions between the toes, groin and below the breasts (Chuang *et al.*, 2007). Although dermatophyte infections are restricted to areas of the epidermis, they can be invasive and cause serious widespread infections in immunocompromised patients, with the development of granulomas (Peres *et al.*, 2010). In such cases, the disease no longer is superficial and reaches deeper layers of dermis, causing granulomatous lesions.

Dermatophytes produce proteolytic enzymes, keratinases, which are able to hydrolyze keratin, the main protein constituent of hair, nails and skin. The infection can be mild to severe, depending on the host immune response (Akcaglar *et al.*, 2011). The keratin, collagen and elastin constitute 25% of the mass of mammals. The enzyme required to hydrolyze these macromolecules is found in infected tissues and is therefore considered essential to the virulence of dermatophytes (Simpanya, 2000). Colonization by a dermatophyte, and its ability to cause an infection in the host, depends on several factors, among which are the "escape" mechanisms of the host resistance, including dry skin, a slightly acidic pH, the continuous regeneration skin, the fungicidal effect of fatty acids, the state of the keratinized layer and other factors, such as competition with the normal skin microbiota (Erbagci *et al.*, 2004). The establishment of the infection is initiated by the inoculation of arthrospores deposited on the skin, favored by a pre - exist-

Send correspondence to A.M.F. Almeida. Departamento de Análises Clínicas, Faculdade de Ciências Farmacêuticas, Universidade Estadual Paulista "Júlio Mesquita Filho", R. Expedicionários do Brasil 1621, 14801-902Araraquara, SP, Brazil. E-mail: almeidaf@fcfar.unesp.br.

ing skin lesion or abrasion (Sidrim and Rocha, 2004) and the microorganism's remarkable enzymatic ability to degrade keratin (Simpanya, 2000; Abdel-Rahman, 2001; Macêdo *et al.*, 2005) . It also can infect several animal species, creating generally dry, rounded and usually non-pruritic lesions, distributed focally on the skin without causing a general inconvenience to the affected animals (Pereira and Meireles, 2001; Sobestiansky, 2001) . The animals serve as reservoirs of zoophilic dermatophytes and their zoonotic infections have considerable importance (Cabañes, 2000; Baranova *et al.*, 2003) . Anthropophilic species are not part of the normal microbiota of humans nor are these microorganisms opportunistic, but true pathogens that infect keratinized tissues, nails or hair of healthy individuals (Baeza *et al.*, 2007; Monod, 2008). Dermatophytes digest keratin and have the ability to invade living tissues and cause certain injuries (Simpanya, 2000), with the severity of the infection being related to, in part, the reaction of the host to the invading organism, and other factors, such as species or virulence of the infecting strain, the host reaction to the metabolic products produced by the fungus, anatomic site of infection, and local environmental factors.

## Treatment of Mycosis

Forsuccessful of infection by dermatophytes, the pathogen required to overcome the defense mechanisms of the host. A important mechanism of host defense against these pathogens is the keratinization which is the process of epithelial desquamation leading to removal of the fungus (Peres *et al.*, 2010). For treating the fungal infections of skin, topical medications are appropriate only for early or mild infections, especially those caused by *T. rubrum*, the main cause of *Tinea pedis*. In nail infections (onychomycosis) and infections caused by zoophilic dermatophytes, mainly leading to the development of *Tinea capitis* and corporis, the usual therapy is systemic (Tani *et al.*, 2007; White *et al.*, 2008). Terbinafine inhibits the growth of dermatophytes of all genera and is the main drug of choice for the treatment of dermatophytoses, especially with chronic conditions. The naftifin and terbinafine represent the group of drugs synthetic, the allylamine, which were described as drugs in clinical treatment of superficial mycoses (Balfour and Faulds, 1992). It has shown fungicidal activity against a wide range of dermatophytes, molds and certain fungi dimorphic, and fungistatic activity against *Candida albicans* being that terbinafine has been the drug of first choice for dermatophytes (Abdel-Rahman and Nahata, 1997; McClellan *et al.*, 1999). Its mechanism of action relies on blocking the biosynthesis of ergosterol, an essential component of fungal cell membranes, through inhibition of fungal squalene epoxidase (Abdel-Rahman and Nahata, 1997). The tolerability of these drugs is generally high after topical administration or oral. In comparative studies, the incidence of adverse effects associated with use of terbinafine orally, was lower than that observed with griseofulvin and similar to itraconazole (Abdel-Rahman and Nahata, 1997). Terbinafine has emerged as a new therapeutic option for dermatophytoses in both humans and animals (Mancianti *et al.*, 1999). Griseofulvin is used exclusively to control the development of keratinized tissue infection by presenting only fungistatic and not fungicidal action. This drug is orally administered and treatment varies according to the clinical form of mycosis (Gupta *et al.*, 2001). In severe infections, the treatment must be prolonged (Deacon, 1998). The mechanism of action of this drug is associated with interfering with the polymerization of microtubules causing abnormalities in cell division due to achromatic spindle formation and abnormal growth, probably due to disruption of intracellular transport associated with microtubules (Odds, 2003). Currently, imidazole derivatives represent a major advance in oral and topical treatment of superficial mycoses, with dermatophytosis specifically, clotrimazole (topical), ketoconazole, itraconazole and fluconazole are commonly used because they are absorbed through the gastrointestinal tract and maintain an effective activity (Katzung *et al.*, 1998), with fluconazole being effective against other types of fungal infections (Follador *et al.*, 2001; Oliveira *et al.*, 2002). In therapy, there are two groups of antifungal azoles are used in the clinic: the imidazoles (ketoconazole, miconazole, clotrimazole and econazole) and triazoles (fluconazole, itraconazole, voriconazole and posaconazole). The use of imidazoles is limited to the treatment of superficial mycoses. Triazoles have a larger application in these therapies. In dermatology, chronic infection is treated with severe drugs such as terbinafine, itraconazole and fluconazole, which are the most used (Abdel-Rahman *et al.*, 1998; Fernández-Torres *et al.*, 2001; Fernández-Torres *et al.*, 2003). In an attempt to increase the cure rate of drug treatments, combined topical and oral anti-inflammatory drugs have been used. There have recently been cases of treating onychomycosis using topical amorolfine and ciclopirox (Gupta *et al.*, 2001).

## Resistance to Drugs

There is a large arsenal of antifungal drugs, however, their cellular targets are limited because of the similarity that exists between fungi and host cells. Drugs that are commonly used are directed against the biosynthetic pathway (Martinez-Rossi *et al.*, 2008). The reports of recurrences are usually associated with the discontinuation of therapy, although clinical resistance to the antifungal drug terbinafine has been described in the literature (Mukherjee *et al.*, 2003) described a case of clinical resistance to this drug. The strain studied was taken from a patient with onychomycosis was that treated with oral terbinafine, which was not effective with the microorganism presenting cross-resistance to several other drugs, including naftina, butenafine, and tonoftato tolciclato, suggesting a target-specific resistance mechanism. The report regarding their resistance

to terbinafine has been discussed and refers to the squalene epoxidase gene mutation leading to the substitution of amino acid L393F (Osborne *et al.*, 2006). Terbinafine resistance in mutants of the *Aspergillus* species was also mentioned, and this indicated that there was a mutation in the gene encoding squalene epoxidase enzine (ErgA), resulting in high resistance to this antifungal (Rocha *et al.*, 2006; Espinel-Ingroff, 2008). In studies on the mechanisms of resistance to the fungus *T. rubrum*, two ABC-type transporters, TruMDR1 and TruMDR2, were important in the process of resistance (Fachin *et al.*, 2006; Maranhão *et al.*, 2009). The clinical resistance to griseofulvin, or relapses after treatment, is common in dermatophytosis. In a study conducted by Zomorodian, *et al.* (2007), a decreased expression of the gene encoding beta-tubulin was observed for the fungus *T. rubrum* during drug administration, with the decrease being concentration dependent. This information contributed to a better understanding of the mechanism of action and therefore can assist in more rational use of pharmacological therapy. The *in vitro* resistance of an isolate can be classified as either intrinsic or acquired. Intrinsic resistance allows all normal members of a species to tolerate a particular drug. Acquired resistance is a term used when a resistant strain emerges from a population that was previously drug-sensitive (Kamai *et al.*, 2004) . The biochemical mechanisms may contribute to the phenotype of drug resistance in fungus involve a decrease in drug uptake, structural alterations in the target site and an increase in drug efflux or in intracellular target levels, gene amplification, gene transfer, gene deletion, point mutations, loss of cis - and trans-acting regulatory elements and transcriptional activation (Kamai *et al.*, 2004) . Few studies have reported mechanisms of drug resistance in dermatophytes, although more studies are required to determine the mechanisms by which resistance occurs for these pathogens.

## Natural and Synthetic Products

The search for plants with healing powers for various diseases dates back many years. From prehistory to the present day, thousands of plants have been used by people of all continents, either in the form of poultices, infusions, decoctions, and others. In the 90's, approximately ? of the American population had already made use of at least one type of unconventional therapy (Eisenberg *et al.*, 1993). In this context, interest in plants with therapeutic properties including those with antimicrobial activity has grown, not just form themselves into an alternative therapeutic approach, but also because the prospect of isolating substances with significant efficacy and a lower index of disadvantage (Queiroz *et al.*, 2009). Plants have been used in medicine for a long time, having been extensively used in folk medicine because they represent an economical alternative, are easy to obtain and are applicable to various pathologies (Rojas *et al.*, 2006). Plants are an important source of biologically active compounds, many of which are models for the synthesis of a large number of drugs (Yunes and Calixto, 2001; Simões *et al.*, 2003). Special attention has been directed to natural derivatives, based on the knowledge of antifungal compound production in nature (Wojtaszek, 1997; Gurgel *et al.*, 2005).

Natural products have served as a research resource for most drugs, providing a basis for chemical research and discovery of new drugs (Chin *et al.*, 2006). Several reasons have been offered to explain the success of natural products, among them is their great chemical diversity, the effects of evolutionary pressure in creating biologically active molecules, the structural similarity of protein targets in different species, among others (Harvey, 2007). Natural products are a source of numerous agents of therapeutic value. They also inspired, at various levels, the development and manufacture of synthetic agents of therapeutic importance. These agents are synthesized by manipulating the natural product, demonstrating that the synthesis of molecules can be used to discover and develop novel therapeutic agents (Wilson and Danishefsky, 2006). An ideal antifungal drug should have a broad spectrum of fungicidal activity and not cause toxicity to the host (Carrillo-Muñoz *et al.*, 2006). A large number of antifungal drugs have some connection with natural products. The class of polyenes and griseofulvin are natural products, whereas echinocandins are semisynthetic derivatives of natural products (Butler, 2005). Currently, antibiotics and antifungals represent a small group of drugs which plays an important role in fungal disease control, however, some of these antifungals have serious drawbacks such as toxicity, fungistatic activity, limited spectrum of action or resistance (García-Sosa *et al.*, 2011). The great importance of natural products in developing new therapeutic tools is evident. In this aspect, medicinal plants and their derivatives are important for pharmacological research and drug development. These natural products can be used directly as therapeutic agents, as well as a source of raw materials for synthesis, or can serve as prototypes for new pharmacologically active models (Brazil, 2006).

*Fructus Psoraleae* and *Folium Eucalypti Globuli* have long been used as Chinese medicines to treat dermatomycosis. Both pure compounds effectively inhibit the *in vitro* growth of *T. mentagrophytes* and *T. rubrum* (Lau *et al.*, 2010). In the study of Eisenberg *et al.* (1993) a volatile extract of *Eryngium duriaei subsp. juresianum*, presents an antifungal activity (Minimal inhibitory concentration (MIC) values = 0.16-0.32 µL.mL (-1)) against several dermatophyte species (*T. mentagrophytes, T. rubrum, E. floccosum; T. verrucosum, T. mentagrophytes var. interdigitale, M. canis* and *M. gypseum*) (Eisenberg *et al.*, 2010). Machado *et al.* (2009) evaluated the antifungal activity of *Eugenia umbelliflora Berg.* against some dermatophytes (*E. floccosum, M. canis, M. gypseum, T. rubrum, T. mentagrophytes*) and obtained good results, with MIC values between 200 and 1000 microg/mL, and in-

terestingly, inhibited 4/5 species with MIC values of < or = 500 microg/mL. Koroishi *et al.* (2008) studied the *Piper regnelli* extract, with the results indicating that this plant had strong activity against *T. mentagrophytes, T. rubrum*, *M. canis and M. gypseum*. Park *et al.* (2011) found good results against various pathogenic fungi (species dermatophytes) with the polyphenol Epigallocatechin 3 - O-Gallate (Table 1). The antifungal activities of the essential oils (EOs) of *Acantholippia seriphioides*, *Artemisia mendozana*, *Gymnophyton polycephalum*, *Satureja parvifolia*, *Tagetes mendocina*, and *Lippia integrifolia*, collected in the Central Andes area, province of San Juan, Argentina, were investigated against *M. gypseum*, *T. mentagrophytes,* and *T. rubrum* and were inhibited by the EOs of *G. polycephalum*, *L. integrifolia*, and *S. parvifolia*, with minimum inhibitory concentrations (MICs) between 31.2 and 1000 μg/ml. This study shows that these Andean species might be used to treat superficial fungal infections (Lima *et al.*, 2011). Ponnusamy *et al.*, 2010 investigated the medicinal plant *Wrightia tinctoria* activity against dermatophytic and non-dermatophytic fungi. Leaf chloroform extract showed activity at 0.5 mg/mL against *T. rubrum*, *E. floccosum*, *Aspergillus niger* and *Scopulariopsis brevicaulis*. The major compound, identified as indirubin, exhibited activity against dermatophytes such as *E. floccosum* (MIC = 6.25 μg/mL); *T. rubrum* and *T. tonsurans* (MIC = 25 μg/mL); *T. mentagrophytes* and *T. simii* (MIC = 50 μg/mL). It was also active against non-dermatophytes (*Aspergillus niger*, *Candida albicans* and *Cryptococcus* sp.) within a MIC range of 0.75-25 μg/mL. All of the new chemical entities approved as drugs between 1981-2006 total almost 1,184 products, with 5% as natural products, 47% as semi-synthetic derivatives of natural products, mimicking natural products and products synthesized with pharmacological groups based on natural products, 18% as by-products and vaccines and 30% as fully synthetic products (Newman and Cragg, 2007). The originality of many structures of natural products attracts attention to their use as a starting point for semi-synthesis and total synthesis (Butler, 2005). Soares *et al.* (2010) used semi-synthetic esters of protocatechuic acid isolated from *Cupania oblongifolia* against *T. rubrum* and *T. mentagrophytes,* demonstrating an antifungal activity with MIC values lower than 31.25 ug/mL. The modification of natural products by semi-synthesis has led to different types of drug combinations. The development of chemotherapeutic agents of synthetic origin and the discovery of powerful new antimicrobians isolated from natural sources account for invaluable contributions in the fight against bacterial and fungal resistance (Silveira *et al.*, 2006). Pisseri *et al.* (2009) conducted a randomized open clinical trial on 60 thorough breeding horses affected by equine ringworm using Tea Tree Oil (TTO). The animals were randomly divided into 2 groups of 30 subjects. Diagnostic criteria were the presence of clinical signs and positive *Trichophyton equinum* culture. Specificity control using TTO mixture in 5 not dermatophyte affected animals was achieved also. The antimycotic activity against *T. equinum* of a mixture containing 25% TTO in sweet almond oil, was evaluated in vivo treating 30 subjects, the others were administered enilconazole 2% solution. The animals of both groups were topically treated twice a day for 15 days with a 25% mixture of TTO diluted in sweet almond oil and every 3 days, four times with enilconazole rinses, respectively. All the treated animals showed complete clinical and a etiological healing. Part of control subjects also, showed an improvement and none of them exacerbate the lesions. The authors believe this TTO an alternative for practitioners interested in herbal medicines, contributing to fulfill the gap existing between

**Table 1** - Antifungal activity of natural products against a variety dermatophytes.

| Natural Products | Microorganisms | Reference |
|---|---|---|
| *Citrus bergamia (Rutaceae)* | *T. rubrum, T. mentagrophytes T. tonsurans, M canis, M. gypseum E. floccosum* | Sanguinetti *et al*., 2007 |
| *Brazilian Copaíba Oil (Fabaceae)* | *T. rubrum, M. Canis* | Santos *et al*., 2008 |
| *Piper regnellii (Piperaceae)* | *M. canis, M. gypseum, T. rubrum, T. mentagrophytes* | Koroishi *et al*., 2008 |
| *Syzygium aromaticum (Myrtaceae)* | *M. canis, M. gypseum, T. rubrum, T. mentagrophytes, E. floccusum* | Pinto *et al*., 2009 |
| *Eugenia umbelliflora Berg. (Myrtaceae)* | *M. canis, M.gypseum, T.rubrum, T.mentagrophytes, E.floccusum.* | Machado *et al*., 2009 |
| *Fructus Psoraleae (Leguminosae)* | *T.rubrum, T. mentagrophytes* | Lau *et al*., 2010 |
| *Protocatechuic acid (Cupania oblongifolia) (Sapindaceae)* | *T.rubrum, T. mentagrophytes* | Soares *et al*., 2010 |
| *Folium Eucalypti Globuli (Leptospermaceae)* | *T.rubrum, T. mentagrophytes* | Lau *et al*., 2010 |
| *Eryngium duriaei subsp. Juresianum (Umbelliferae)* | *T. mentagrophytes, T. rubrum, E. floccosum, T. verrucosum, T. mentagrophytes var interdigitale, M. canis and M. Gypseum* | Cavaleiro *et al*., 2011 |
| *Xanthones (Clusiaceae)* | *M. canis, M. gypseum, T. rubrum, T. mentagrophytes, E. floccusum* | Pinto *et al*., 2011 |
| *Epigallocatechin 3 – O- Gallate (green tea) (Theaceae)* | *M. canis, T.rubrum, T.mentagrophytes* | Park *et al*., 2011 |

in vitro and clinical studies. The extracts obtained from plants, such *Euphorbia prostata, Salvia Texana, Colubrina greggii, Clematis drummondii*, among others, have shown promising results for stimulating the search for new potential antifungal plant sources (Alanís-Garza *et al.*, 2007). Most antifungal drugs have a connection to natural products, it can be seen the potential antimicrobial plant products, and consequently, the real possibility of application of these products in the prevention and treatment of infectious diseases of fungal origin. However, it is necessary to mention the need for toxicological studies and clinical and security support for the use of these products as drugs.

## Conclusion

Millions of people and animals suffer from superficial infections caused by a group of highly specialized filamentous fungi, the dermatophytes. Interest in medicinal plants has increased, especially in Brazil, due to the fact of the vast diversity of plants with therapeutic potential. It is necessary to search for new drugs because of the increase of resistant isolates. More studies are needed to develop drugs for dermatophytosis, since the conventional drugs used for this pathology, while being cytotoxic, often lead to clinical resistance.

## References


Abdel-Rahman SM (2001) Polymorphic exocellular protease expression in clinical isolates of *Trichophyton tonsurans*. Mycopathologia. 150:117-120.

Abdel-Rahman SM, Nahata MC (1997) Oral terbinafine: a new antifungal agent. Ann Pharmacother 31: 445-456.

Abdel-Rahman SM, Powell DA, Nahata MC (1998) Efficacy of itraconazole in children with *Trichophyton tonsurans* tinea capitis. J Am Acad Dermatol 38:443-446.

Akcaglar S, Ener B, Toker SC, Ediz B, Tunali S, Tore O (2011) A comparative study of dermatophyte infections in Bursa, Turkey. Med Mycol 49:602-607.

Alanís-Garza BA, González-González GM, Salazar-Aranda R, Waksman de Torres N, Rivas-Galindo VM (2007) Screening of antifungal activity of plants from the northeast of Mexico. J Ethnopharmacol 114:468-471.

Baeza LC, Bailão AM, Borges CL, Pereira M, Soares CM, Mendes-Giannini MJ (2007) cDNA representational difference analysis used in the identification of genes expressed by *Trichophyton rubrum* during contact with keratin. Microbes Infect 9:1415-1421.

Balfour JA, Faulds D (1992) Terbinafine A review of its pharmacodynamic and pharmacokinetic properties, and therapeutic potential in superficial mycoses. Drugs 43:259-284.

Baranova Z, Kozak M, Bilek J (2003) Zoophilic dermatomycosis in a family caused by *Trichophyton mentagrophytes* var. *quincheanum* - A case report. Acta Vet Brno 72:311-314.

Brazil (2006) Ministry of Health SdC, Tecnology and Estrategic Inputs. National policy of medicinal plants and herbal medicine. In: Pharmaceuticals DDA editor, Brasilia.

Burmester A, Shelest E, Glöckner G, Heddergott C, Schindler S, Staib P, Heidel A, Felder M, Petzold A, Szafranski K, Feuermann M, Pedruzzi I, Priebe S, Groth M, Winkler R, Li W, Kniemeyer O, Schroeckh V, Hertweck C, Hube B, White TC, Platzer M, Guthke R, Heitman J, Wöstemeyer J, Zipfel PF, Monod M, Brakhage AA (2011) Comparative and functional genomics provide insights into the pathogenicity of dermatophytic fungi. Genome Biol 12:R7.

Butler MS (2005) Natural products to drugs: natural product derived compounds in clinical trials. Nat Prod Rep 22:162-195.

Butler MS (2005) Natural products to drugs: natural product derived compounds in clinical trials. Nat Prod Rep 22:162-195.

Cabañes FJ (2000) Emerging mycotoxins: introduction. Rev. Iberoam. Micol 17:S61-S62.

Carrillo-Muñoz AJ, Giusiano G, Ezkurra PA, Quindós G (2006) Antifungal agents: mode of action in yeast cells. Rev Esp Quimioter 19:130-139.

Cavaleiro C, Gonçalves MJ, Serra D, Santoro G, Tomi F, Bighelli A, Salgueiro L, Casanova J (2011) Composition of a volatile extract of *Eryngium duriaei* subsp. *juresianum* (M. Laínz) M. Laínz, signalised by the antifungal activity. J Pharm Biomed Anal 54:619-622.

Chin YW, Balunas MJ, Chai HB, Kinghorn AD (2006) Drug discovery from natural sources. AAPS Journal 8:E239-253.

Chuang PH, Lee CW, Chou JY, Murugan M, Shieh BJ, Chen HM (2007) Anti-fungal activity of crude extracts and essential oil of *Moringa oleifera* Lam. Bioresour Technol 98:232-236.

Deacon JW (1998) Introduction to modern mycology. 3ª ed. Blackwell, Oxford.

Eisenberg DM, Kessier RC, Foster C, Norlock FE, Calkins DR, Delbanco TL (1993) Unconventional Medicine in the United States - Prevalence, Costs, and Patterns of Use. N Engl J Med 328:246-252.

Eisenberg DM, Kessier RC, Foster C, Norlock FE, Calkins DR, Delbanco TL (1993) Unconventional Medicine in the United States - Prevalence, Costs, and Patterns of Use. N Engl J Med 328:246-252.

Erbagci Z (2004) Topical therapy for dermatophytoses: should corticosteroids be included? Am J Clin Dermatol 5:375-384.

Espinel-Ingroff A (2008) Mechanisms of resistance to antifungal agents: yeasts and filamentous fungi. Rev Iberoam Micol 25:101-106.

Fachin AL, Ferreira-Nozawa MS, Maccheroni W, Martinez-Rossi NM (2006) Role of the ABC transporter TruMDR2 in terbinafine, 4-nitroquinoline N-oxide and ethidium bromide susceptibility in *Trichophyton rubrum*. J Med Microbiol 55:1093-1099.

Fernández-Torres B, Carrillo AJ, Martín E, Del Palacio A, Moore MK, Valverde A, Serrano M, Guarro J (2001) In vitro activities of 10 antifungal drugs against 508 dermatophyte strains. Antimicrob Agents Chemother 45:2524-2528.

Fernández-Torres B, Inza I, Guarro J (2003) In vitro activities of the new antifungal drug eberconazole and three other topical agents against 200 strains of dermatophytes. J Clin Microbiol 41:5209-5211.

Follador I, Bittencourt A, Duran F, das Graças Araújo MG (2001) Cutaneous protothecosis: report of the second Brazilian case. Rev Inst Med Trop São Paulo 43:287-290.

García-Sosa K, Sánchez-Medina A, Álvarez SL, Zacchino S, Veitch NC, Simá-Polanco P, Peña-Rodriguez LM (2011)

Antifungal activity of sakurasosaponin from the root extract of *Jacquinia flammea*. Nat Prod Res 25:1185-1189.

Gupta AK, Adam P, Dlova N, Lynde CW, Hofstader S, Morar N, Aboobaker J, Summerbell RC (2001) Therapeutic options for the treatment of tinea capitis caused by Trichophyton species: griseofulvin *vs.* the new oral antifungal agents, terbinafine, itraconazole, and fluconazole. Pediatr Dermatol 18:433-438.

Gupta AK, Adam P, Dlova N, Lynde CW, Hofstader S, Morar N, Aboobaker J, Summerbell RC (2001) Therapeutic options for the treatment of tinea capitis caused by Trichophyton species: griseofulvin *vs.* the new oral antifungal agents, terbinafine, itraconazole, and fluconazole. Pediatr Dermatol 18:433- 438.

Gurgel LA, Sidrim JJ, Martins DT, Cechinel Filho V, Rao VS (2005) In vitro antifungal activity of dragon's blood from *Croton urucurana* against dermatophytes. J Ethnopharmacol 97:409-412.

Harvey AL (2007) Natural products as a screening resource. Curr Opin Chem Biol 11:480-484.

Kamai Y, Maebashi K, Kudoh M, Makimura K, Naka W, Uchida K, Yamaguchi H (2004) Characterization of mechanisms of fluconazole Characterization of mechanisms of fluconazole resistance in a *Candida albicans* isolate from a Japanese patient with chronic mucocutaneous candidiasis. Microbiol Immunol 48:937-943.

Katzung GB, Silva P, Mundim FD, Vooeux PJ (1998). Basic and clinical pharmacology. Editora Guanabara Koogan, Rio de Janeiro, Brazil.

Koroishi AM, Foss SR, Cortez DA, Ueda-Nakamura T, Nakamura CV, Dias Filho BP (2008) In vitro antifungal activity of extracts and neolignans from *Piper regnellii* against dermatophytes. J Ethnopharmacol 117:270-277.

Lau KM, Fu LH, Cheng L, Wong CW, Wong YL, Lau CP, Han SQ, Chan PK, Fung KP, Lau CB, Hui M, Leung PC (2010) Two antifungal components isolated from *Fructus Psoraleae* and *Folium Eucalypti* Globuli by bioassay-guided purification. Am J Chin Med 38:1005-1014.

Lima B, López S, Luna L, Agüero MB, Aragón L, Tapia A, Zacchino S, López ML, Zygadlo J, Feresin GE (2011). Essential oils of medicinal plants from the central andes of Argentina: chemical composition, and antifungal, antibacterial, and insect-repellent activities. Chem Biodivers 8:924-936.

Macêdo DP, Neves RP, Neves RP, Magalhães MC, Souza-Motta CM., Queiroz LA (2005) Pathogenic aspects of *Epidermophyton floccosum* Langeron et Milochevich as a possible a ethiologial agent of *Tinea capitis*. Braz J Microbiol 36:36-37.

Machado KE, Cechinel-Filho V, Cruz RC, Meyre-Silva C, Cruz AB (2009) Antifungal activity of *Eugenia umbelliflora* against dermatophytes. Nat Prod Commun 4:1181-1184.

Mancianti F, Pedonese F, Millanta F, Guarnieri L (1999) Efficacy of oral terbinafine in feline dermatophytosis due to *Microsporum canis*. J Feline Med Surg 1:37-41.

Maranhão FC, Paião FG, Fachin AL, Martinez-Rossi NM (2009) Membrane transporter proteins are involved in *Trichophyton rubrum* pathogenesis. J Med Microbiol 58:163-168.

Martinez-Rossi NM, Peres NT, Rossi A (2008) Antifungal resistance mechanisms in dermatophytes. Mycopathologia 166:369-383.

McClellan KJ, Wiseman LR, Markham A (1999) Terbinafine. An update of its use in superficial mycoses. Drugs 58:179-202.

Monod M (2008) Secreted proteases from dermatophytes. Mycopathologia 166:285-294.

Mukherjee PK, Leidich SD, Isham N, Leitner I, Ryder NS, Ghannoum MA (2003) Clinical *Trichophyton rubrum* strain exhibiting primary resistance to terbinafine. Antimicrob Agents Chemother 47:82-86.

Newman DJ, Cragg, GM (2007) Natural products as sources of new drugs over the last 25 years. J Nat Prod 70:461-477.

Odds CF (2003) Antifungal agents: Their diversity and increasing sophistication. Mycologist 17:51-55.

Oliveira JS, Kerbauy FR, Colombo AL, Bahia DM, Pinheiro GS, Silva MR, Ribeiro MS, Raineri G, Kerbauy J (2002) Fungal infections in marrow transplant recipients under antifungal prophylaxis with fluconazole. Braz J Med Biol Res 35:789-798.

Osborne CS, Leitner I, Hofbauer B, Fielding CA, Favre B, Ryder NS (2006) Biological, biochemical, and molecular characterization of a new clinical *Trichophyton rubrum* isolate resistant to terbinafine. Antimicrob Agents Chemother 50:2234-2236.

Park BJ, Taguchi H, Kamei K, Matsuzawa T, Hyon SH, Park JC (2011) In vitro antifungal activity of epigallocatechin 3-O-gallate against clinical isolates of dermatophytes. Yonsei Med J 52:535-538.

Pereira DB, Meireles MCA (2001) Diseases caused by fungi and Oomycetes. Diseases of ruminants and horses 4:367-383.

Peres NT, Maranhão FC, Rossi A, Martinez-Rossi NM (2010) Dermatophytes: host-pathogen interaction and antifungal resistance. An Bras Dermatol 85:657-667.

Pfaller MA, Sutton DA (2006) Review of in vitro activity of sertaconazole nitrate in the treatment of superficial fungal infections. Diagn Microbiol Infect Dis 56:147-152.

Pinto E, Afonso C, Duarte S, Vale-Silva L, Costa E, Sousa E, Pinto M (2011) Antifungal activity of xanthones: evaluation of their effect on ergosterol biosynthesis by high-performance liquid chromatography. Chem Biol Drug Des 77:212-222.

Pinto E, Vale-Silva L, Cavaleiro C, Salgueiro L (2009) Antifungal activity of the clove essential oil from *Syzygium aromaticum* on *Candida*, *Aspergillus* and dermatophyte species. J Med Microbiol 58:1454-1462.

Pisseri F, Bertoli A, Nardoni S, Pinto L, Pistelli L, Guidi G, Mancianti F (2009) Antifungal activity of tea tree oil from *Melaleuca alternifolia* against *Trichophyton equinum*: an in vivo assay. Phytomedicine 16:1056-1058.

Ponnusamy K, Petchiammal C, Mohankumar R, Hopper W (2010) In vitro antifungal activity of indirubin isolated from a South Indian ethnomedicinal plant *Wrightia tinctoria* R. Br J Ethnopharmacol 132:349-354.

Queiroz EF, Wolfender JL, Hostettmann K (2009) Modern approaches in the search for new lead antiparasitic compounds from higher plants. Current Drugs 10:202-211.

Rocha EM, Gardiner RE, Park S, Martinez-Rossi NM, Perlin DS (2006) A Phe389Leu substitution in ergA confers terbinafine resistance in *Aspergillus fumigatus*. Antimicrob Agents Chemother 50:2533-2536.

Rojas JJ, Ochoa VJ, Ocampo AS, Muñoz JF (2006) Screening for antimicrobial activity of ten medicinal plants used in Colombian folkloric medicine: a possible alternative in the

treatment of non-nosocomial infections. BMC Complement Altern Med 17:2.

Sanguinetti M, Posteraro B, Romano L, Battaglia F, Lopizzo T, De Carolis E, Fadda G (2007) In vitro activity of *Citrus bergamia* (bergamot) oil against clinical isolates of dermatophytes. J Antimicrob Chemother 59:305-308.

Santos AO, Ueda-Nakamura T, Dias Filho BP, Veiga Junior VF. Pinto AC, Nakamura CV (2008) Antimicrobial activity of Brazilian copaiba oils obtained from different species of the *Copaifera* genus. Mem Inst Oswaldo Cruz 103:277-281.

Sidrim JJC, Rocha MFG (2004) Medical Mycology light of authors contemporâneos. Guanabara Koogan. Rio de Janeiro, Brasil.

Silveira GP, Nome F, Gesser JC, Sá MM, Terenzi T (2006) The strategies used to combat bacterial resistence. Química Nova 29:844-855.

Simões CMO, Schenkel EP, Gosmann MG, Mello JCP, Ments LA, Petrovick PR (2003) *Pharmacognosy: The medicinal plant - products of plant origin and development of drugs*. 5ª ed. p. 291-320.

Simpanya MF (2000) Dermatophytes: Their taxonomy, ecology and pathogenicity. Rev Iberoam Micol 17:1-12.

Soares LA(2011) *Estudy of the activity antidermatiphytic of protocatechuate against T. rubrum and T. interdigitale*. Araraquara, São Paulo, Brazil, 85 p. (M.Sc. Dissertation Faculty of Pharmaceutical Sciences: University Estadual Paulista Júlio Júlio Mesquita Filho – UNESP).

Sobestiansky J (2001) Clinical and Swine Pathology e Patologia Suína. Goiania: Gráfica Art3. 2ed. p. 463.

Tani K, Adachi M, Nakamura Y, Kano R, Makimura K, Hasegawa A, Kanda N, Watanabe S (2007) The effect of dermatophytes on cytokine production by human keratinocytes. Arch Dermatol Res 299:381-387.

Weitzman I, Summerbell RC (1995) The dermatophytes. Clin Microbiol Rev 8:240-259.

White TC, Oliver BG, Gräser Y, Henn MR (2008) Generating and testing molecular hypotheses in the dermatophytes. Eukaryot Cell 7:1238-1245.

Wilson RM, Danishefsky SJ (2006) Small molecule natural products in the discovery of therapeutic agents: the synthesis connection. J Org Chem 71:8329-8351.

Wojtaszek P (1997) Oxidative burst: an early plant response to pathogen infection. Biochem J 322:681-692.

Yunes RA, Calixto JB (2001) *Plantas medicinais sob óptica da química medicinal moderna.* 2001. Moderna – Chapecó: Argos.

Zomorodian K, Uthman U, Tarazooie B, Rezaie S (2007) The effect of griseofulvin on the gene regulation of beta-tubulin in the dermatophyte pathogen *Trichophyton rubrum*. J Infect Chemother 13:373-379.

EC
Journals.ASM.org

# Frequency and Genetic Diversity of the *MAT1* Locus of *Histoplasma capsulatum* Isolates in Mexico and Brazil

**Gabriela Rodríguez-Arellanes,[a] Carolina Nascimento de Sousa,[b] Mauro de Medeiros-Muniz,[b] José A. Ramírez,[a] Cláudia V. Pizzini,[b] Marcos de Abreu-Almeida,[b] Manoel M. Evangelista de Oliveira,[b] Ana-Marisa Fusco-Almeida,[c] Tania Vite-Garín,[a] Nayla S. Pitangui,[c] Daniel A. Estrada-Bárcenas,[d] Antonio E. González-González,[a] María José Soares Mendes-Giannini,[c] Rosely M. Zancopé-Oliveira,[b] Maria-Lucia Taylor[a]**

Departamento de Microbiología-Parasitología, Facultad de Medicina, Universidad Nacional Autónoma de México (UNAM), México DF, Mexico[a]; Instituto de Pesquisa Clínica Evandro Chagas, Fundação Oswaldo Cruz, Rio de Janeiro, Brazil[b]; Faculdade de Ciências Farmacêuticas, Universidade Estadual Paulista, Araraquara, São Paulo, Brazil[c]; Colección Nacional de Cultivos Microbianos, Centro de Investigación y de Estudios Avanzados, Instituto Politécnico Nacional, México DF, Mexico[d]

**The *MAT1-1* and *MAT1-2* idiomorphs associated with the *MAT1* locus of *Histoplasma capsulatum* were identified by PCR. A total of 28 fungal isolates, 6 isolates from human clinical samples and 22 isolates from environmental (infected bat and contaminated soil) samples, were studied. Among the 14 isolates from Mexico, 71.4% (95% confidence interval [95% CI], 48.3% to 94.5%) were of the *MAT1-2* genotype, whereas 100% of the isolates from Brazil were of the *MAT1-1* genotype. Each *MAT1* idiomorphic region was sequenced and aligned, using the sequences of the G-217B (+ mating type) and G-186AR (− mating type) strains as references. BLASTn analyses of the *MAT1-1* and *MAT1-2* sequences studied correlated with their respective + and − mating type genotypes. Trees were generated by the maximum likelihood (ML) method to search for similarity among isolates of each *MAT1* idiomorph. All *MAT1-1* isolates originated from Brazilian bats formed a well-defined group; three isolates from Mexico, the G-217B strain, and a subgroup encompassing all soil-derived isolates and two clinical isolates from Brazil formed a second group; last, one isolate (EH-696P) from a migratory bat captured in Mexico formed a third group of the *MAT1-1* genotype. The *MAT1-2* idiomorph formed two groups, one of which included two *H. capsulatum* isolates from infected bats that were closely related to the G-186AR strain. The other group was formed by two human isolates and six isolates from infected bats. Concatenated ML trees, with internal transcribed spacer 1 (ITS1) -5.8S-ITS2 and *MAT1-1* or *MAT1-2* sequences, support the relatedness of *MAT1-1* or *MAT1-2* isolates. *H. capsulatum* mating types were associated with the geographical origin of the isolates, and all isolates from Brazil correlated with their environmental sources.**

*Histoplasma capsulatum* is a heterothallic ascomycete that has an anamorphic or asexual stage with two types of sexual compatibility, + and −, represented at the mating locus (*MAT1*) by the idiomorphic regions *MAT1-1* and *MAT1-2*, respectively. The teleomorphic (sexual) stage that results from + and − mating was first described as *Emmonsiella capsulata* by Kwon-Chung (1–4). Nowadays it is known as *Ajellomyces capsulatus*, which temporarily exhibits the dikaryotic and diploid phases that form haploid ascospores after two meiotic reductions. Thus, the species *H. capsulatum* and *A. capsulatus* constitute the same holomorphic organism. The classical studies of sexual compatibility in *H. capsulatum* were performed by mating fungal specimens in culture plates. However, this procedure is difficult because *H. capsulatum* isolates rapidly lose the ability to mate *in vitro* (5); therefore, molecular methods were developed to identify the mating type in this microorganism (6–8).

To date, there have been a few relevant studies in the United States about the use of genetic tools to determine sexual compatibility in *H. capsulatum*, in which the − mating type predominates (6–8). Recent findings have involved the product of the Velvet A gene (VeA), which belongs to the proteins of the Velvet family, in mating structure formation (cleistothecial) and virulence of *H. capsulatum* (9). *H. capsulatum* isolates exhibit a wide distribution and an important genetic diversity, as has been documented in Latin America (10–16). However, the frequency and genetic diversity of the + and − mating types are not well documented in most countries where *H. capsulatum* is found, and data reported in the United States are not necessarily representative of other geographical areas.

In the present work, we studied indigenous *H. capsulatum* isolates from Mexico (North America) and Brazil (South America) to determine the frequency and genetic diversity of the sexual compatibility types of *H. capsulatum* in these two distant geographical areas. Most of the isolates studied were obtained from naturally infected bats and contaminated soils, although some isolates from human clinical cases were also analyzed. PCR was used to identify and to perform genetic analyses of the *MAT1-1* and *MAT1-2* idiomorphs. The internal transcribed spacer 1 (ITS1)-5.8S-ITS2 region of the *H. capsulatum* isolates of each *MAT1* idiomorph was used for concatenated phylogenetic analyses of both genomic regions to increase the genetic relatedness of *H. capsulatum* isolates from different mating types. Therefore, our contribution is original, mainly for its frequency data and because it is the first one to use the *MAT1* locus as a geographical marker for *H. capsulatum*.

**Received** 17 January 2013 **Accepted** 17 May 2013
**Published ahead of print** 24 May 2013
Address correspondence to Maria-Lucia Taylor, emello@unam.mx.

doi:10.1128/EC.00012-13

**TABLE 1** General data and sexual compatibility of the *H. capsulatum* isolates studied

| Isolate | Associated clinical form[a] | Source[b] | Geographical origin[c] | Mating type[d] |
|---|---|---|---|---|
| EH-46 | D | Human (liver) | GR-Mexico | − |
| EH-53 | D | Human (blood) | HG-Mexico | − |
| EH-317 | D/HIV+ | Human (blood) | MS-Mexico | + |
| EH-315 | NA | *Mormoops megalophylla* (gut) | GR-Mexico | + |
| EH-373 | NA | *Artibeus hirsutus* (lung) | MS-Mexico | − |
| EH-374 | NA | *Artibeus hirsutus* (spleen) | MS-Mexico | − |
| EH-376 | NA | *Artibeus hirsutus* (lung) | MS-Mexico | − |
| EH-378 | NA | *Artibeus hirsutus* (lung) | MS-Mexico | − |
| EH-391 | NA | *Leptonycteris nivalis* (liver) | MS-Mexico | − |
| EH-405 | NA | *Leptonycteris nivalis* (lung) | PL-Mexico | − |
| EH-449B | NA | *Leptonycteris nivalis* (spleen) | MS-Mexico | − |
| EH-521 | NA | *Artibeus hirsutus* (lung) | MS-Mexico | + |
| EH-672H | NA | *Tadarida brasiliensis* (liver) | HG-Mexico | − |
| EH-696P | NA | *Tadarida brasiliensis* (lung) | NL-Mexico | + |
| 18H | D/HIV+ | Human (blood) | RJ-Brazil | + |
| 37307 | D/HIV+ | Human (bone marrow) | RJ-Brazil | + |
| 247BL | ND | Human (ND) | MS-Brazil | + |
| M396/08 | NA | *Molossus molossus* (NR) | SP-Brazil | + |
| M1084/08 | NA | *Molossus molossus* (NR) | SP-Brazil | + |
| M487/08 | NA | *Molossus molossus* (NR) | SP-Brazil | + |
| M975/08 | NA | *Molossus molossus* (NR) | SP-Brazil | + |
| AC05 | NA | Soil | RJ-Brazil | + |
| TI01 | NA | Soil | RJ-Brazil | + |
| IGS19 | NA | Soil | RJ-Brazil | + |
| RPS51 | NA | Soil | RJ-Brazil | + |
| CO2 | NA | Soil | RJ-Brazil | + |
| CO4 | NA | Soil | RJ-Brazil | + |
| IgS4/5 | NA | Soil | RJ-Brazil | + |

[a] Abbreviations: D, Disseminated histoplasmosis; HIV+, human immunodeficiency virus positive; NA, not applicable; ND, not determined.
[b] ND, not determined; NR, not registered.
[c] The state and country are shown. The country is shown after the hyphen, and the state is shown before the hyphen as follows: in Mexico, GR, Guerrero; HG, Hidalgo; MS-Mexico, Morelos, Mexico; PL, Puebla; NL, Nuevo León; in Brazil, RJ, Rio de Janeiro; MS-Brazil, Mato Grosso do Sul, Brazil; SP, São Paulo.
[d] The + mating type has the *MAT1-1* idiomorphic region, and the − mating type has the *MAT1-2* idiomorphic region.

**TABLE 2** Database accession numbers of *H. capsulatum MAT1* sequences analyzed

| Isolate | GenBank accession no. |
|---|---|
| *MAT1-1* isolates | |
| EH-696P | KC282441 |
| EH-315 | KC282442 |
| EH-317 | KC282443 |
| EH-521 | KC282444 |
| 37307 | KC282445 |
| 18H | KC282446 |
| RPS51 | KC282447 |
| IGS19 | KC282448 |
| AC05 | KC282449 |
| IgS4/5 | KC282450 |
| TI01 | KC282451 |
| CO2 | KC282452 |
| CO4 | KC282453 |
| 247BL | KC282454 |
| M396/08 | KC282455 |
| M975/08 | KC282456 |
| M487/08 | KC282457 |
| M1084/08 | KC282458 |
| *MAT1-2* isolates | |
| EH-46 | KC282431 |
| EH-53 | KC282432 |
| EH-373 | KC282433 |
| EH-374 | KC282434 |
| EH-376 | KC282435 |
| EH-378 | KC282436 |
| EH-672H | KC282437 |
| EH-391 | KC282438 |
| EH-449B | KC282439 |
| EH-405 | KC282440 |

## MATERIALS AND METHODS

***Histoplasma capsulatum.*** We studied 28 *Histoplasma capsulatum* isolates (14 from Mexico and 14 from Brazil) obtained from different infectious sources (Table 1). The isolates were maintained in the yeast phase by culture at 37°C in brain heart infusion broth (Bioxon; Becton, Dickinson, Mexico City, Mexico) supplemented with 0.1% L-cysteine and 1% glucose.

**Identification of sexual compatibility types.** We followed the protocols for yeast DNA extraction and the processing of PCR products of Bubnick and Smulian (6) with minor modifications. We used two sets of primers designed for the *MAT1* locus: (i) for the *MAT1-1* sequence, MAT1-1S (5′-CGTGGTTAGTTACGGAGGCA-3′) and MAT1-1AS (5′-TGAGGATGCGAGTGATGGGA-3′), which generated an amplicon of 440 bp; and (ii) for the *MAT1-2* sequence, MAT1-2S (5′-ACACAGTAG CCCAACCTCTC-3′) and MAT1-2AS (5′-TCGACAATCCCATCCAAT ACCG-3′), which generated an amplicon of 528 bp. The PCR was performed in a 25-μl reaction mixture, containing 200 μM each deoxynucleoside triphosphate (dNTP) (Applied Biosystems Inc., Foster City, CA, USA), 1.5 mM $MgCl_2$, 50 ng/μl of each primer, 2.5 U *Taq* DNA polymerase (New England BioLabs Inc., MA, USA), 1× *Taq* commercial buffer, and 75 ng/μl of each DNA sample.

PCR assays were performed in a Thermal iCycler (Bio-Rad Laboratories Inc., Hercules, CA, USA) programmed as follows: (i) 3 min at 95°C; (ii) 35 cycles, consisting of 30 s at 95°C, 30 s at 58°C, and 1 min 30 s at 72°C; and (iii) 10 min at 72°C. The PCR products were resolved by 1.5% agarose gel electrophoresis under the same conditions described by Bubnick and Smulian (6). The 100-bp DNA ladder was used as a molecular marker.

**ITS1-5.8S-ITS2 PCR.** The PCR assay was performed by the method of Muniz et al. (13), using the following primers: ITS4 (5′-TCCTCCGCTT ATTGATATGC-3′) and ITS5 (5′-GGAAGTAAAAGTCGTAACAAGG-3′), which generated an amplicon of 607 bp.

**Sequencing.** The resolved PCR products were purified using the Montage PCR centrifugal filter devices kit (Millipore Corporation, Bedford, MA, USA). The purified products were sent to the Molecular Biology Unit of the Cellular Physiology Institute, Universidad Nacional Autónoma de México (UNAM)-Mexico, for sequencing in an ABI automated apparatus (Applied Biosystems). Sequencing was performed for both DNA strands. The generated consensus *MAT1-1* and *MAT1-2* or ITS1-5.8S-ITS2 sequences for each isolate are deposited in GenBank or in the Fungi Barcode of Life Database (Bold System) and their available accession numbers are shown in Tables 2 and 3.

**Genetic analyses.** Sequences were aligned with Clustal-W in MEGA version 5.0 (MEGA-5) (http://www.megasoftware.net) and edited manually.

The sequences of the *MAT1-1* and *MAT1-2* idiomorphs from all the *H. capsulatum* isolates studied were compared by searching the GenBank database for homologous nucleotide sequences with the BLASTn algorithm. The sequence of the G-217B strain from Louisiana-United States, ATCC 22636 (GenBank accession number EF433757), was used as a reference for the *MAT1-1* idiomorphic region. The sequence of the G-186AR strain from Panama, ATCC 22635 (GenBank accession number EF433756), was used as a reference for the *MAT1-2* idiomorphic region.

The aligned sequences were submitted to evolutionary analyses to assume the similarity or divergence among isolates of each mating type, using the maximum likelihood (ML) method. Concatenated ML trees, with ITS1-5.8S-ITS2 and *MAT1-1* or *MAT1-2* sequences, were processed to provide more-robust phylogenetic data. Unrooted ML trees were constructed in MEGA-5, based on the Hasegawa-Kishino-Yano (HKY) model (17) for *MAT1* idiomorphs and Tamura-Nei (TrN) model for con-

**TABLE 3** Database accession numbers of *H. capsulatum* ITS1-5.8S-ITS2 sequences analyzed

| Isolate | Accession no.[a] |
|---|---|
| Mexican isolates | |
| EH-46 | HIST019-13 |
| EH-53 | HIST001-13 |
| EH-315 | HIST002-13 |
| EH-317 | HIST003-13 |
| EH-373 | HIST004-13 |
| EH-374 | HIST020-13 |
| EH-376 | HIST021-13 |
| EH-378 | HIST022-13 |
| EH-391 | HIST006-13 |
| EH-449B | HIST025-13 |
| EH-521 | HIST026-13 |
| EH-672H | HIST029-13 |
| EH-696P | HIST018-13 |
| Brazilian isolates | |
| IgS4/5 | GU320945.1 |
| TI01 | GU320964.1 |
| CO2 | KF114466 |
| CO4 | KF114465 |
| 37307 | KF114464 |
| 247BL | KF114463 |
| 18H | KF114471 |
| M396/08 | KF114467 |
| RPS51 | GU320962.1 |
| M975/08 | KF114469 |
| IGS19 | GU320944.1 |
| M487/08 | KF114468 |
| AC05 | GU320980.1 |
| M1084/08 | KF114470 |

[a] The Mexican isolates were deposited in the Fungi Barcode of Life Database (Bold System), and the Brazilian isolates were deposited in GenBank.

**TABLE 4** Variable sites within the *MAT1-1* idiomorph sequences of *H. capsulatum*

| Variable site in the *MAT1-1* idiomorph sequence |
|---|
| Noninformative sites common to all *MAT1-1* isolates |
| Transitions |
| Guanine to adenine at nt 807, 813, and 822 |
| Cytosine to thymine at nt 856 |
| Informative sites for nine isolates from RJ, Brazil[a] |
| Transitions |
| Cytosine to thymine at nt 782 and 1127 |
| Thymine to cytosine at nt 865 |
| Guanine to adenine at nt 1023 |
| Informative sites for five isolates (four from SP, Brazil, and one from MS, Brazil)[a] |
| Transition |
| Guanine to adenine at nt 1000 |

[a] RJ, Rio de Janeiro; SP, São Paulo; MS, Mato Grosso do Sul.

catenated analyses (18). Gaps and missing data were eliminated. A bootstrapping algorithm was implemented on the data set for 1,000 replicates. The highest bootstrap values were registered in each node of each ML tree.

**Statistics.** The *MAT1-1* and *MAT1-2* idiomorph frequencies were estimated in relation to each mating genotype, taking into account all *H. capsulatum* isolates from Mexico or Brazil studied. In regard to frequency data, the 95% confidence interval (95% CI) was calculated by normal distribution.

## RESULTS AND DISCUSSION

Previous studies of the clinical and environmental *H. capsulatum* strains in the United States using conventional mating tests with the fungal mycelial phase reported a higher frequency of the − mating type in clinical strains than in strains isolated from soil samples (5, 19). However, the predominance of the − genotype in clinical strains in the United States, even if supported by a large number of *H. capsulatum* samples from different sources as indicated by Kwon-Chung et al. (5, 19), is not necessarily true in other geographical areas. Although the above-published data have emphasized interesting findings about the disequilibrium of the − and + mating types in human clinical isolates associated with the clinical form of the disease (5, 6, 19), these findings may not apply to clinical isolates from other geographical areas, since *H. capsulatum* isolates exhibit a wide distribution and a significant genetic diversity as has been documented in Latin America (11). On the basis of our present results, it was impossible to infer a disequilibrium of − and + mating types due to the small number of human clinical isolates studied, and in regard to the environmental isolates, we did not find any evidence of disequilibrium.

Currently, DNA-based mating studies have been used to evaluate the distribution of the sexual compatibility types of *Ophiostoma quercus* in different geographical areas (20). According to this antecedent, in the present paper, by PCR of the *MAT1* locus, we determined the mating types of 6 autochthonous clinical isolates and 22 native environmental isolates (infected bats and contaminated soil) of *H. capsulatum* from two distant regions within the Americas (Mexico and Brazil) (Table 1). The *MAT1-2* genotype was predominant in Mexico, representing 71.4% (95% CI, 48.3 to 94.5%) of the isolates, whereas 100% of the isolates originating in Brazil were of the *MAT1-1* genotype.

Hence, the frequencies of *H. capsulatum* mating types were mainly associated with the geographical origin of the isolates and most likely correlate with their environmental sources.

Given that the − mating type is more widely distributed in the *H. capsulatum* isolates from the United States and Mexico (North America) and the + mating type is more frequent in Brazil (South America), as revealed by the present results, we suggest that the different mating types of *H. capsulatum* are distinctively spread across the American continent. In addition, the presence of two sexual compatibility types in the same geographical region, albeit unequally distributed, suggest that genetic dispersion of the *MAT1* locus in the environment could be associated with natural reservoirs of *H. capsulatum*.

For the *MAT1-1* idiomorph, 18 sequences from nucleotide (nt) 778 to 1171 were analyzed, whereas 10 sequences from nt 3038 to 3,584 were analyzed for the *MAT1-2* idiomorph. The sequences obtained for each idiomorph were aligned with the matching sequences of the *H. capsulatum* reference strains obtained from GenBank, G-217B (*MAT1-1*) or G-186AR (*MAT1-2*).

Based on the known sequence of reference strain G-217B, the sequences of the *MAT1-1* idiomorph region (14 from Brazilian *H. capsulatum* isolates and four from Mexican *H. capsulatum* isolates) were aligned by using MEGA-5, showing four noninformative sites common to all isolates (Table 4). In the *MAT1-1* genotype, four informative sites stand out, these sites were shared by nine isolates (seven isolates from soil samples and two isolates

**TABLE 5** Variable sites within the *MAT1-2* idiomorph sequences of *H. capsulatum*

| Variable site in the *MAT1-2* idiomorph sequence |
|---|
| Noninformative sites common to all *MAT1-2* isolates |
| Transitions |
| Cytosine to thymine at nt 3098 and 3248 |
| Adenine to guanine at nt 3125 and 3285 |
| Thymine to cytosine at nt 3200 |
| Transversion |
| Thymine to adenine at nt 3068 |
| Informative sites for eight isolates from MS, Mexico[a] |
| Transitions |
| Thymine to cytosine at nt 3156 |
| Guanine to adenine at nt 3284 |
| Adenine to guanine at nt 3449 |
| Transversions |
| Thymine to adenine at nt 3130 and 3212 |
| Cytosine to adenine at nt 3163 and 3188 |

[a] MS, Morelos.

from human clinical samples) from Rio de Janeiro, Brazil. In addition, one informative site was shared by four isolates recovered from *Molossus molossus* bats from São Paulo State and one human isolate from Mato Grosso do Sul State, Brazil (Table 4).

Two isolates from Mexico (EH-317 from a clinical case and EH-315 from an infected bat) with the *MAT1-1* genotype exhibited the same mutations, a transition (cytosine to thymine at nt 940) and a transversion (guanine to thymine at nt 955). The Mexican *H. capsulatum* isolate EH-521 was the most similar to reference strain G-217B, whereas the *H. capsulatum* isolate EH-696P, from the migratory *Tadarida brasiliensis* bat captured in Mexico, was the most divergent from all *MAT1-1 H. capsulatum* isolates studied (data not shown).

The *MAT1-2* sequences of the 10 Mexican isolates were compared to the *MAT1-2* sequence of reference strain G-186AR (GenBank) using MEGA-5, showing six noninformative sites common to all isolates (Table 5). In addition, eight isolates from Morelos State, Mexico, shared three transitions and four transversions (Table 5). However, four out of these eight *H. capsulatum* isolates, which were recovered from bats captured in the same cave of Morelos, diverge from this group by the absence of mutations between nt 3510 and 3513 (data not shown).

Two informative sites (both transversions, adenine to thymine at nt 3052 and guanine to thymine at nt 3480) were found only in isolates EH-374 and EH-672H (data not shown).

Alignment analysis showed that isolate EH-696P from Mexico, which had been recovered from a bat captured at the northeastern Mexican border, exhibited the greatest number of point mutations in its *MAT1-1* sequence, whereas the EH-374 and EH-672H isolates showed fewer mutations among the *MAT1-2* sequences (data not shown).

BLASTn analysis of nucleotide sequences of the *MAT1-1* idiomorph region of 18 *H. capsulatum* isolates demonstrated that five of the Brazilian isolates exhibited 99% similarity to the sequence of reference strain G-217B. The fact that these isolates came from a circumscribed geographical region in Brazil, that four of the isolates (M396/08, M487/08, M975/08, and M1084/08) were recovered from *M. molossus* bats from São Paulo and one isolate (247BL) came from a human clinical sample from Mato Grosso do Sul State, which borders São Paulo State, suggest that an unusual *MAT1-1* genotype is prevalent in this particular region. Likewise, nine Brazilian isolates from Rio de Janeiro (seven isolates from soil, isolates AC05, CO2, CO4, IgS4/5, IGS19, RPS51, and TI01, and two isolates from human samples, isolates 18H and 37307) exhibited 98% similarity. Three Mexican isolates (EH-315, EH-317, and EH-521) showed 98% similarity and the Mexican EH-696P isolate from the migratory bat *T. brasiliensis* was detected to have 96% similarity to the G-217B reference strain. The BLASTn algorithm search for similarities among sequences of the *MAT1-1* genotype revealed only a very low similarity of 6.8% with the gene sequence of a hypothetical protein of the ascomycete *Pyrenophora teres* f. sp. *teres*, which supports the close relationship of all *MAT1-1 H. capsulatum* isolates studied.

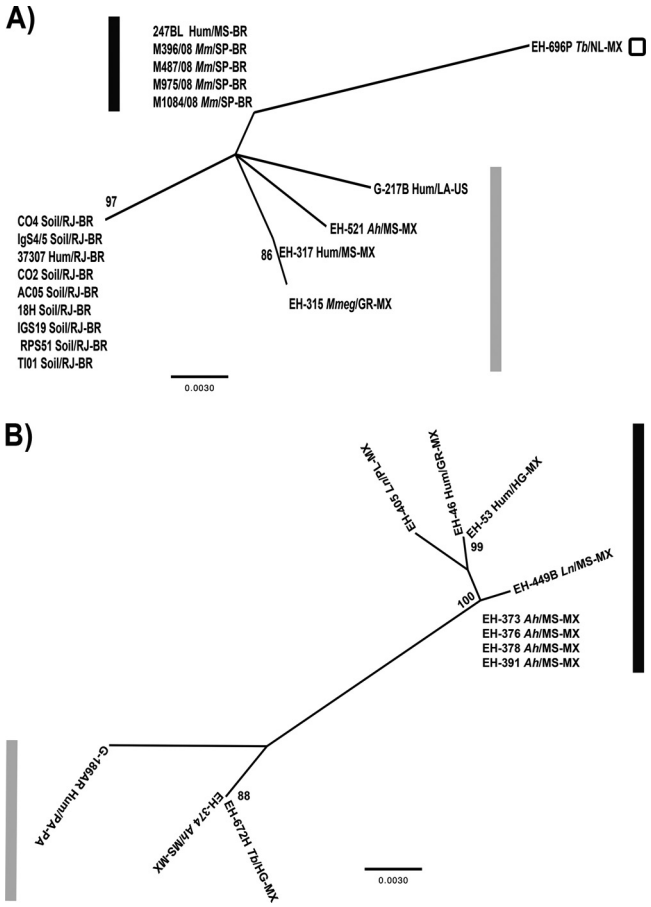


**FIG 1** Maximum likelihood trees for the *MAT1* locus of the *H. capsulatum* isolates studied. (A) *MAT1-1* tree. (B) *MAT1-2* tree. The ML analysis was based on the HKY model. The trees were generated by 1,000 replications, as outlined in Materials and Methods. The bootstrap values that were ≥70% are shown at the nodes. The G-217B (*MAT1-1*) and G-186AR (*MAT1-2*) sequences were obtained from the GenBank database and were used as reference strains. The black and gray bars indicate the different isolate groups. The isolates are named by their biological and geographical sources. The source (soil or biological) of the isolate is shown before the slash as follows: Hum, human; *Ah*, *Artibeus hirsutus*; *Ln*, *Leptonycteris nivalis*; *Mm*, *Molossus molossus*; *Mmeg*, *Mormoops megalophylla*; *Tb*, *Tadarida brasiliensis*. The geographical source of the isolate is shown after the slash. The state is shown after the slash and before the hyphen as follows: GR, Guerrero; HG, Hidalgo; LA, Louisiana; MS, Morelos (Mexico); MS, Mato Grosso do Sul (Brazil); NL, Nuevo León; PL, Puebla; PA, Panama; RJ, Rio de Janeiro; SP, São Paulo. The country is shown after the hyphen (Brazil [BR], Mexico [MX], United States [US]).

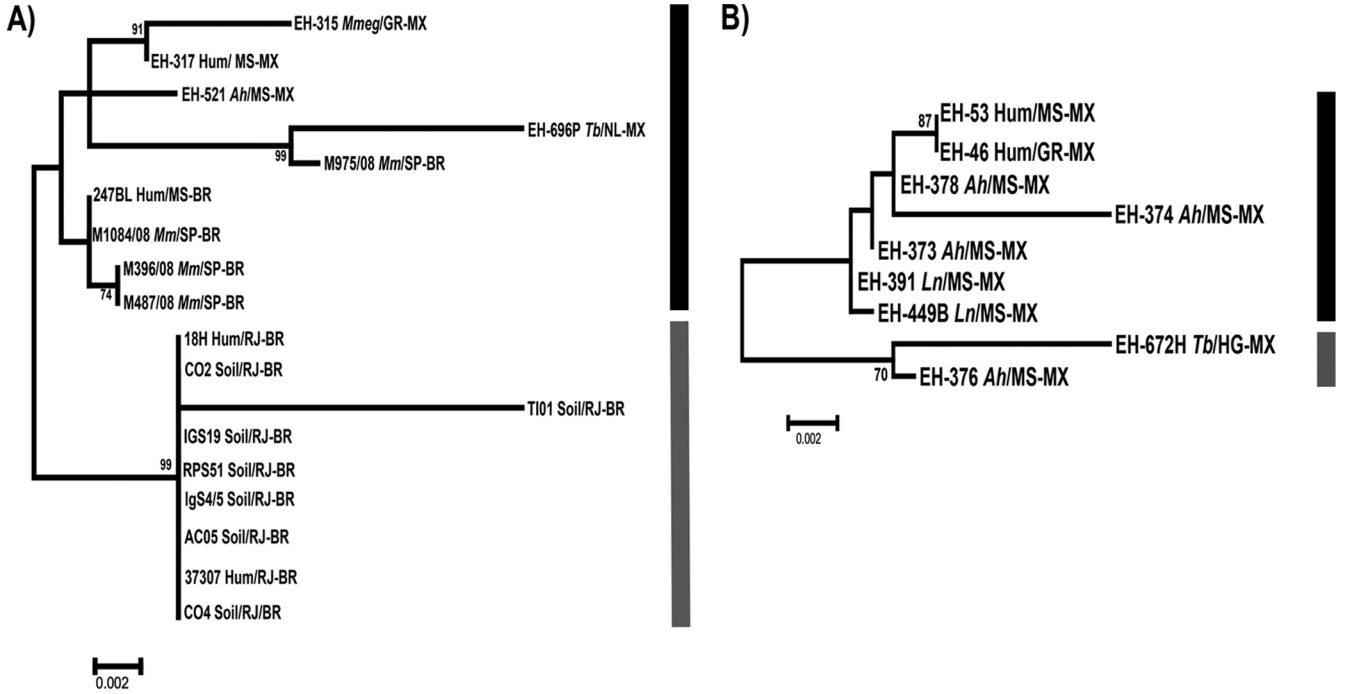


**FIG 2** Concatenated maximum likelihood trees for the ITS1-5.8S-ITS2 region and each *MAT1* locus of the *H. capsulatum* isolates studied. (A) ITS1-5.8S-ITS2 and *MAT1-1* concatenated tree. (B) ITS1-5.8S-ITS2 and *MAT1-2* concatenated tree. The ML analysis was based on the TrN model. The trees were generated by 1,000 replications, as outlined in Materials and Methods. The bootstrap values that were ≥70% are shown at the nodes. The black and dark gray bars indicate the different isolate groups. For abbreviations, see the legend to Fig. 1.

BLASTn analysis of 10 sequences from Mexican *H. capsulatum* isolates of the *MAT1-2* idiomorph region revealed their high similarity with the sequence of reference strain G-186AR. This reference sequence shared 98% similarity with sequences of two isolates from different bat species (EH-374 and EH-672H). The other eight Mexican isolates from the central zone of the country (EH-46 and EH-53 from human clinical samples; EH-373, EH-376, EH-378, EH-391, EH-405, and EH-449B from different bat species) showed 97% similarity with the sequence of the G-186AR reference strain. The BLASTn algorithm search for similarities among *MAT1-2* genotype sequences showed 49.1% similarity with the gene sequence of a predicted protein, with a high-mobility-group (HMG) DNA binding domain, of the fungal pathogen *Paracoccidioides brasiliensis* (clone 60855 isolate C4-PS3) and 44.4% similarity with the gene sequence of a protein, with an HMG DNA binding domain, of *Ajellomyces dermatitidis* (strain SLH14081). These data also confirm the relationship among all *MAT1-2 H. capsulatum* isolates studied.

The ML analysis of the sequences of the *MAT1-1* idiomorph demonstrated that our Brazilian isolates from infected bats captured in São Paulo State (Table 1) and the human clinical isolate from Mato Grosso do Sul, Brazil, constitute a well-defined group, representing a probable clonal population of *H. capsulatum*. In addition, seven *H. capsulatum* isolates from contaminated soil and two clinical isolates, all from Rio de Janeiro, Brazil (Table 1), formed a distinct subgroup that shared a probably clonal *MAT1-1* genotype, which is in agreement with previous data using different molecular markers published by Muniz et al. (12, 13). This subgroup clustered with three *MAT1-1* isolates from Mexico and the G-217B reference strain. The EH-696P isolate from a migratory bat captured in Mexico constituted a third group of the *MAT1-1* genotype and showed the largest genetic distance to all the *H. capsulatum* isolates with the *MAT1-1* genotype studied (Fig. 1A).

In contrast, ML analysis of the *MAT1-2* idiomorph, which included most sequences from Mexican isolates, demonstrated that these sequences could be categorized into two major groups. The first group was formed by two isolates from bats (EH-374 and EH-672H) and the G-186AR reference strain (Fig. 1B). The other group was formed by two human clinical isolates and six isolates from infected bats, four of which (EH-373, EH-376, EH-378, and EH-391) belong to a probably clonal population of *H. capsulatum*, as reported by Kasuga et al. (11).

Our results reveal a preferential distribution of *H. capsulatum* isolates with respect to the sequences of the idiomorphic regions of the *MAT1* locus, encompassing two distant geographical areas of the Americas, Mexico and Brazil. Moreover, our findings demonstrated a close relationship between the fungal isolation source and geographical origin within Brazil and also in the central states of Mexico (Guerrero, Morelos, Puebla, and Hidalgo), where most of the Mexican samples were isolated.

Regarding the population structure of the *H. capsulatum* isolates studied, some of the Mexican isolates classified by Kasuga et al. (11) were characterized as possibly recombinant, and others, such as environmental isolates from the Morelos State of Mexico, were characterized as a clonal population (11, 14–16).

Undoubtedly, understanding the *H. capsulatum* mating type distribution in areas of the Americas with a high prevalence of histoplasmosis would contribute to our knowledge of the *H. capsulatum* genetic plasticity generated by sexual recombination

events, which could eventually occur under environmental conditions.

Results of concatenated analyses, using ITS1-5.8S-ITS2 region and each *MAT1* idiomorph, support the relatedness of *MAT1-1* or *MAT1-2* isolates with robust data (Fig. 2A and B, respectively). In addition, ML concatenated analyses generated similar tree topologies as Fig. 1A and B, despite the fact that only two major groups were found. In these analyses, G-217B and G-186AR reference strains were not included because their ITS1-5.8S-ITS2 sequences were not available in different databases. The ITS1-5.8S-ITS2 sequence of the Mexican EH-405 isolate was not obtained due to the loss of this isolate and its DNA.

In conclusion, knowledge regarding the distribution of the *MAT1* locus in *H. capsulatum* and its genetic diversity should contribute to a better understanding of the biology of this fungus and the actual impact of its sexual compatibility genes distributed in natural conditions. We emphasize that in this paper we incorporated two completely new aspects. (i) We studied isolates from two very distant geographical areas to use the *MAT1* locus as a geographical marker. (ii) Most of the *H. capsulatum* isolates studied came from natural sources (wild infected bats), which makes our contribution unique as a result of its geographical frequency data.

## ACKNOWLEDGMENTS

This study was funded by the PAPIIT-DGAPA project from UNAM (IN204210), the Bilateral Collaboration Agreement between CONACYT-Mexico (B330/099/11) and CNPq-Brazil (490110/2009-6), the Bilateral Collaboration Agreement between UNAM-Mexico (15090-563-24-V-04) and UNESP-Brazil (000528/04/01/2005), and the FAPERJ E-26/111.532/2010. R.M.Z.-O. is supported in part by CNPq 350338/2000-0. C.N.D.S. is supported by INOVATEC FIOCRUZ/FAPERJ. T.V.-G. thanks CONACYT for scholarship 231985.

M.-L.T. thanks Ingrid Mascher for editorial assistance.

Rosely M. Zancopé-Oliveira and Maria-Lucia Taylor participated in the design and coordination of the study.

## REFERENCES

1. **Kwon-Chung KJ.** 1972. Sexual stage of *Histoplasma capsulatum*. Science **175:**326.
2. **Kwon-Chung KJ.** 1972. *Emmonsiella capsulata*: perfect state of *Histoplasma capsulatum*. Science **177:**368–369.
3. **Kwon-Chung KJ.** 1973. Studies on *Emmonsiella capsulata*. I. Heterothallism and development of the ascocarp. Mycologia **65:**109–121.
4. **Kwon-Chung KJ, Bennett JE.** 1992. Medical mycology. Lea and Febiger, Philadelphia, PA.
5. **Kwon-Chung KJ, Weeks RJ, Larsh HW.** 1974. Studies on *Emmonsiella capsulata* (*Histoplasma capsulatum*). II. Distribution of the two mating types in 13 endemic states of the United States. Am. J. Epidemiol. **99:**44–49.
6. **Bubnick M, Smulian AG.** 2007. The *MAT1* locus of *Histoplasma capsulatum* is responsive in a mating type-specific manner. Eukaryot. Cell **6:**616–621.
7. **Fraser JA, Stajich JE, Tarcha EJ, Cole GT, Inglis DO, Sil A, Heitman J.** 2007. Evolution of the mating type locus: insights gained from the dimorphic primary fungal pathogens *Histoplasma capsulatum*, *Coccidioides immitis*, and *Coccidioides posadasii*. Eukaryot. Cell **6:**622–629.
8. **Laskowski MC, Smulian AG.** 2010. Insertional mutagenesis enables cleistothecial formation in a non-mating strain of *Histoplasma capsulatum*. BMC Microbiol. **10:**49–64. doi:10.1186/1471-2180-10-49.
9. **Laskowski-Peak MC, Calvo AM, Rohrssen J, Smulian AG.** 2012. VEA1 is required for cleistothecial formation and virulence in *Histoplasma capsulatum*. Fungal Genet. Biol. **49:**838–846.
10. **Kasuga T, Taylor JW, White TJ.** 1999. Phylogenetic relationships of varieties and geographical groups of the human pathogenic fungus *Histoplasma capsulatum* Darling. J. Clin. Microbiol. **37:**653–663.
11. **Kasuga T, White TJ, Koenig G, McEwen J, Restrepo A, Castañeda E, Da Silva-Lacaz C, Heins-Vaccari EM, De Freitas RS, Zancopé-Oliveira RM, Qin Z, Negroni R, Carter DA, Mikami Y, Tamura M, Taylor ML, Miller GF, Poonwan N, Taylor JW.** 2003. Phylogeography of the fungal pathogen *Histoplasma capsulatum*. Mol. Ecol. **12:**3383–3401.
12. **Muniz MM, Pizzini CV, Peralta JM, Reiss E, Zancope-Oliveira RM.** 2001. Genetic diversity of *Histoplasma capsulatum* strains isolated from soil, animals, and clinical specimens in Rio de Janeiro State, Brazil, by a PCR-based random amplified polymorphic DNA assay. J. Clin. Microbiol. **39:**4487–4494.
13. **Muniz MM, Morais e Silva Tavares P, Meyer W, Nosanchuk JD, Zancope-Oliveira RM.** 2010. Comparison of different DNA-based methods for molecular typing of *Histoplasma capsulatum*. Appl. Environ. Microbiol. **76:**4438–4447.
14. **Taylor ML, Chávez-Tapia CB, Reyes-Montes MR.** 2000. Molecular typing of *Histoplasma capsulatum* isolated from infected bats, captured in Mexico. Fungal Genet. Biol. **30:**207–212.
15. **Taylor ML, Chávez-Tapia CB, Rojas-Martínez A, Reyes-Montes MR, Bobadilla del Valle M, Zuñiga G.** 2005. Geographical distribution of genetic polymorphism of the pathogen *Histoplasma capsulatum* isolated from infected bats, captured in a central zone of Mexico. FEMS Immunol. Med. Microbiol. **45:**451–458.
16. **Taylor ML, Hernández-García L, Estrada-Bárcenas D, Salas-Lizana R, Zancopé-Oliveira RM, García de La Cruz S, Galvão-Dias MA, Curiel-Quesada E, Canteros CE, Bojórquez-Torres G, Bogard-Fuentes CA, Zamora-Tehozol E.** 2012. Genetic diversity of *Histoplasma capsulatum* isolated from infected bats randomly captured in Mexico, Brazil and Argentina, using the polymorphism of $(GA)_n$ microsatellite and its flanking regions. Fungal Biol. **116:**308–317.
17. **Hasegawa M, Kishino H, Yano T.** 1985. Dating of the human-ape splitting by a molecular clock of mitochondrial DNA. J. Mol. Evol. **22:**160–174.
18. **Tamura K, Nei M.** 1993. Estimation of the number of nucleotide substitutions in the control region of mitochondrial DNA in humans and chimpanzees. Mol. Biol. Evol. **10:**512–526.
19. **Kwon-Chung KJ, Bartlett MS, Wheat LJ.** 1984. Distribution of the two mating types among *Histoplasma capsulatum* isolates obtained from an urban histoplasmosis outbreak. Sabouraudia **22:**155–157.
20. **Wilken PM, Steenkamp ET, Hall TA, De Beer ZW, Wingfield MJ, Wingfield BD.** 2012. Both mating types in the heterothallic fungus *Ophiostoma quercus* contain MAT1-1 and MAT1-2 genes. Fungal Biol. **116:**427–437.

Tropical Medicine & Surgery

Mini Review Open Access

# A Mini Review of *Candida* Species in Hospital Infection: Epidemiology, Virulence Factor and Drugs Resistance and Prophylaxis

**Janaina de Cássia Orlandi Sardi*, Nayla de Souza Pitangui, Fernanda Patrícia Gullo and Ana Marisa Fusco Almeida e Maria José Soares Mendes Giannini**

*Department of Clinical Analysis, Clinical Mycology Laboratory, Faculty of Pharmaceutical Sciences, UNESP - Univ Estadual Paulista, Araraquara, SP 14801- 902, Brazil*

## Abstract

The introduction of more efficient diagnostic methods, new techniques in surgery and transplantation, antibiotics and chemotherapeutics more potent and novel materials for prostheses, catheters and probes significantly increased the life expectancy and quality of life of critically ill patients, on the other hand, hospital-acquired infections emerged as important iatrogenic complications. Invasive infections are a growing problem in public health hospitals in Brazil and worldwide. Among the various etiological agents found in the hospital environment, the genus *Candida* has been the third most frequently isolated pathogen. In general, invasive fungal infections are associated with high morbidity and mortality, difficulties in diagnosis, antimicrobial resistance, length of hospital stay and increased hospital costs. This mini review of the literature describes about epidemiology of hospital infection of *Candida* species, as well as its virulence factors and drugs resistance.

**Keywords:** *Candida* spp.; Epidemiology; Neutropenia; Nosocomial infection; Drug resistance; Virulence factors

## Introduction

Nosocomial infections, also called "hospital-acquired infections", are infections acquired during hospital care which is not present or incubating at admission. Infections occurring more than 48 hours after admission are usually considered nosocomial [1,2]. The transformation of the commensal yeast in important agent of infections in hospital due results of the very progress of medicine as: the emergence of a large number of invasive procedures, breaking barriers of natural protection, intensive use of broad-spectrum antibiotics and the ability to sustain life of people very weak and susceptible to opportunistic microorganisms [3]. Although increasing the number of commercially available antifungal agents in recent years, they are still at a disadvantage when compared to antibacterial drugs. Resistance to antifungal agents has represented a major challenge for the clinic and a major public health problem. Faced with the observed difficulties in the treatment of mycoses in some groups of patients it is recommended, where possible the isolation of the agent responsible for the infection and the determination of minimum inhibitory concentration (MIC) of drugs [4]. The literature on the presence of *Candida* species in hospital infection, their current epidemiology, virulence factors and drug resistance are reviewed in the present report.

## Epidemiology

Infections caused by *Candida* species are termed candidiasis or candidosis. Its spectrum is quite extensive, ranging from the colonization of tissues and mucosal, up to the systemic organ invasion, thus expressing the variety of relations that occur between the host and commensal microorganisms. Candidemia corresponds to the most important opportunistic mycosis in the world, besides being among the leading causes of nosocomial infections. The main risk factors are patients in ICUs, neutropenia related to cancer, major surgery and preterm infants [5]. Nosocomial infections constitute a serious public health problem, and are among the major causes of morbidity and mortality in humans, leading to increased hospitalization time and, consequently, generating high costs for patient treatment [6]. The epidemiological surveillance program in the United States has shown that 5-10% of patients who go into hospitals acquire nosocomial infection [7]. In the United States, the prevalence of fungal infections increased from 6% in 1980 to 10.4% in 1990, according to the National Nosocomial Infections Surveillance of that country. Of these, about 80% were caused by *Candida* species. Moreover, this same surveillance system reported that in the period 1989 to 1999 there were significant increases in the prevalence of infections caused by *C. albicans* and *C. glabrata* [8]. *C. albicans* is the sixth cause of most common nosocomial infection according to studies by CDC [9].

*C. tropicalis* has a high prevalence in cases of candidemia in Brazil and worldwide. Its transmission mechanism is essentially endogenous [10]. It is considered that 50 to 60% of patients colonized with this species develop systemic infections [11], frequently observed in neutropenic patients suffering from diseases such as cancer and hematological disorders or bone marrow recipients [12,13]. However, *C. glabrata* constitutes the fourth leading cause of nosocomial infection fungal yeast in Brazil, although it is reported less frequently in our country than in Europe or the United States and Canada [14-16]. This species is associated with both the cases of candidemia in elderly patients as in the case of candiduria. Moreover, this kind of infection is associated to intrinsic resistance to fluconazole [11].

The clinical manifestations of nosocomial fungal infections may present in various forms: bloodstream infections (fungaemia), Urinary Tract Infection (UTI), surgical wound infections, skin abscesses related to insertion of the catheter, infection of the heart muscle and other

***Corresponding author:** Janaina de Cassia Orlandi Sardi, Faculty of Pharmaceutical Sciences of Department of Clinical Analysis, Laboratory of Clinical Mycology, Univ Paulista (UNESP), Brazil, Tel: +55 16 3301 5716; E-mail: janaina-sardi@uol.com.br

**Received** June 20, 2013; **Accepted** August 26, 2013; **Published** September 01, 2013

**Citation:** de Cássia Orlandi Sardi J, de Souza Pitangui N, Gullo FP, e Maria José Soares Mendes Giannini AMFA (2013) A Mini Review of *Candida* Species in Hospital Infection: Epidemiology, Virulence Factor and Drugs Resistance and Prophylaxis. Trop Med Surg 1: 141. doi: 10.4172/2329-9088.1000141

[17]. The state of immunosuppression occurs when the integrity of the defense system of the host is broken [18,19]. Polymorphonuclear cell phagocytic system, immunity mediated by T lymphocytes and physico-chemical barriers of the skin and mucous membranes are the primary defenses against fungal infections [20]. Several factors (Intensive Care Unit [ICU], vascular access, transplantation and neutropenia) can produce interference in these defense mechanisms and predispose individuals to mycotic processes [21]. However, the risk of infection is determined by the interaction between epidemiological factors, degree of immunosuppression, and exposure to potentially pathogenic fungi in the hospital environment [22]. The epidemiological pattern of infection observed in the ICU is the result of a combination of factors related to the condition of medical-surgical patients and the degree of iatrogenic intervention [23,24]. Intensive care units represent a point of interface between the more severe patients who receive multiple therapies and aggressive and more resistant pathogens, which are selected by prolonged antimicrobial therapy [25,26]. In the hospital environment, patients in intensive care units are the most vulnerable because they are exactly those whose management is done from intravascular catheters, probes bladder and mechanical ventilation, and other invasive methods, which increases the risk of opportunistic infection [23,27]. Invasive fungal infections are important complications or disseminated in immunocompromised and non-immunocompromised receiving special care in intensive care units [28,29]. The increased incidence of invasive mycosis in ICU patients is associated, in general, with antineoplastic chemotherapy, immunosuppressive therapy, broad-spectrum antibiotics, use of access devices and prostheses, orthopedic and abdominal surgeries complex, extensive burns, degenerative metabolic diseases, prematurity and environmental exposure and length of stay in the unit [30,31].

Catheterization is one of the most important aspects of modern medical practice, especially in the case of patients with neoplasms, surgical patients and transplant recipients and other ICU critical patients that require fluids, blood products, multiple drugs, nutritional support and monitoring [32]. However, such devices expose patients to local, systemic or metastatic infectious complications [33,34]. These infections can result in increased rates of mortality, longer hospital stays and higher medical costs [35-37]. The incidence of catheter-related infection varies considerably with the material composition and device type, length of stay, frequency of manipulation, ability to adhere to the catheter and virulence factors of pathogens and clinical condition of the patients [32,33]. The most serious infections are associated with central venous catheters [38]. These devices are a major source of infection in hospitals, accounting for over 90% of all bloodstream infections [39,40]. The central venous access may be needed for extended periods of time and the catheter can be manipulated several times a day for administration of substances, hemodynamic and to obtain samples for laboratory analysis, thus increasing the possibility of infectious events occur [32,41]. Although showing comparatively lower incidence of infection and more related to the occurrence of phlebitis, peripheral venous catheters have considerable morbidity due to their widespread use [33,42]. Urinary catheter to monitor urine output is also important causes of nosocomial infection, showing percentage of morbidity and significant mortality and hospital costs [25,43]. Colombo and Guimaraes [44] conducted a study involving cases of candiduria as epidemiology, diagnosis and therapy. This infection is an important cause of nosocomial infection, since 20% of hospitalized patients may present candiduria during hospitalization. Among isolates of *Candida* found in urinary infections, the species *C. albicans* is still the most prevalent (50 to 70% of cases), followed by *C. glabrata* (5 to 33%) and other non-*albicans* species such as *C. tropicalis*, *C. parapsilosis, C. krusei, C. lusitaniae and C. guillermondi*. The Table 1 adapted Colombo and Guimaraes [44] show an increased incidence of infections by non-*albicans* species in brazilian studies. In this table we can see the highlighted *C. tropicalis* (4.6 to 52.5%) and *C. glabrata* (7 to 8.8%). The Table 1 shows the significant incidence of non-albicans species in patients with candiduria in U.S. and Brazil hospitals, highlighting the species *C. glabrata* (16% of cases) and *C. tropicalis* (8%).

*Candida* spp. has been isolated in 8% of cases of nosocomial infection of the bloodstream and nearly half of the isolates are *Candida* non-albicans, including *C. glabrata* and *C. krusei* [32,45]. This finding, the emergence of strains resistant to antifungal drugs has been a trend [46-48]. Occasionally, the transplanted organ itself can be a source of infection [49,50]. Although bacterial and viral processes occur more frequently, those caused by fungi are associated with a high mortality rate [51]. The fungal species and the type of infection differ with the transplanted organ and geographic area. However, *Candida* spp. and *Aspergillus* spp. are responsible for over 80% of cases [41,52].

The cytotoxic chemotherapeutic affect the tissues with high replication, including hair, gonads, bone marrow and the epithelial cells of the gastro-intestinal and genito-urinary tract [53]. Mucositis and ulcerative lesions of the oropharynx, esophagus and intestines induced by cytostatic therapy have been related to the pathogenesis of opportunistic fungal infections in patients with oncohematologic colonizing processes [54-56]. It is well established that the use of broad spectrum antibiotics for prevention and treatment of bacterial complications, particularly those acting at high concentrations in the gastro-intestinal tract and which exhibit good activity against gram negative anaerobic bacteria results in a substantial increase in the population endogenous *Candida* spp. [57,58]. This increase, combined with the destruction of the epithelial barrier following antineoplastic chemotherapy has been considered an important factor for the development of endogenous acquisition of candidemia [37,59].

Chang et al. [60] evaluated 152 isolates of candidemia in Medicine Hospital of China in Taiwan, from October 2004 to December 2006. In this study 95% of the isolates belong to the four main species of *Candida*: *C. albicans* (52.6%), *C. glabrata* (8.6%), *C. parapsilosis* (14.5%) and *C. tropicalis* (19.7%). There is a considerable increase of candidemia by non-albicans species. The authors show a high prevalence of *C. parapsilosis* in candidemia in children, but non-albicans species with higher isolation rate in this study was *C. tropicalis,* as described in another study conducted in Brazil [61]. In Brazil, a study evaluating the

| | Etiological Agent | No de isolates | Percentage |
|---|---|---|---|
| **Hospital U.S.** | *Candida albicans* | 446 | 52,0% |
| | *Candida glabrata* | 134 | 16,0% |
| | *Candida tropicalis* | 68 | 8,0% |
| | *Candida parapsilosis* | 35 | 4,0% |
| | *Candida krusei* | 9 | 1,0% |
| | Others | 162 | 19,0% |
| **Hospital Brazil** | *Candida albicans* | 24 | 48,3% |
| | *Candida glabrata* | 5 | 7,9% |
| | *Candida tropicalis* | 19 | 30,7% |
| | *Candida parapsilosis* | 4 | 6,2% |
| | *Candida krusei* | 2 | 4,4% |
| | Others | 1,4 | 2,5% |

Adapted from Colombo and Guimarães [44]

**Table 1:** Etiology of 861 episodes of candiduria sample of hospitals in the U.S. and in hospitals in Brazil (2001-2006).

frequency and distribution of *Candida* species infections in hospitals, showed that *C. albicans* remains the species most important, accounting for 44% of clinical isolates obtained, but the non-*albicans* species have high significance between infections highlighting *C. tropicalis* 21.7% of the isolates, *C. parapsilosis* (14.4%), *C. glabrata* (11.2%) and *C. krusei* (3.5%). The authors show a significant increase in the incidence of *C. glabrata* reaching 23.5% and this increase may be related to risk factors and high prevalence of infection by this species in patients with malignant diseases [61]. Another study conducted in a rural tertiary hospital in India, showed a high incidence of *Candida* spp isolated in different hospital departments. The largest number of positive isolates of *Candida* was in ICU (32.69%), followed by surgical units (25%), department of medicine (19.23%), department of obstetrics (17.31%), department of pediatrics (3.85%) and orthopedic department (1.92%). The isolates were identified as 53.85% *Candida* non-*albicans*, 25% of which were identified as *C. glabrata, C. tropicalis* (21.43%), *C. kefyr* (21.43%) and *C. krusei* (17.58%). A greater awareness of the risk factors and transmission of fungal infections by health care workers helps to prevent nosocomial outbreaks caused by *Candida* spp infections [62].

A review of opportunistic fungal infections in Latin America, was conducted by Nucci et al. [5], reporting significantly the high incidence of *Candida* species infections in hospitals in Brazil, Argentina, Chile, Costa Rica and Mexico. In most studies of the epidemiology of candidemia, the primary agent is *C. albicans*, but two surveys in Argentina in neonates and a survey in Porto Alegre, Brazil, showed a higher incidence of infection with *C. parapsilosis*. The Brazilian Network Candidemia Study, has shown in recent studies that *C. albicans* accounts for 40.9% of all cases of candidemia, followed *C. tropicalis* (20.9%), *C. parapsilosis* (20.5%) and *C. glabrata* (3.5%). The candidemia caused by *C. tropicalis* is associated with cancer, especially in patients with leukemia and neutropenia [5].

Other species such as *C. rugosa* and *C. guilliermondii* are relatively uncommon in the development of candidemia, but Medeiros et al. [62,63] found an outbreak by *C. guillermondii* in a hospital in Brazil, which is very troubling, since these two species have low sensitivity to fluconazole and itraconazole and they are considered resistant.

## Virulence Factors Relevant for Nosocomial Candidemia

Virulence factors are genetically determined, but expressed by microorganisms when subjected to certain conditions [64]. Virulence attributes specialized and developed by *Candida* spp. are directly involved in adhesion and invasion of host tissues, biofilm formation and evasion of the immune system, factors that determine infection [65]. Hematogenous infections caused by *Candida* spp are preceded by colonization of yeast in the patient and in general these are responsible for yeast infection. The main risk factors that lead to candidemia include yeast colonization in catheters and hands of health professionals [66]. A study conducted at a hospital in Paraná, Brazil, evaluated the potential virulence of yeasts isolated from catheters and the hands of professionals in relation to adherence and hydrophobicity. The results indicate that yeasts isolated from catheters exhibited greater virulence potential, since they were more adherent and hydrophobic when compared to yeasts isolated from hands of workers [64]. Moreover, it is clear that numerous *Candida* species secrete proteins to survive in different environments of the host. Recent studies highlight the analysis of the secretome of *C. albicans* as an approach that has enabled a deeper understanding of virulence mechanisms adopted by the fungus to cause infection. It is predicted that the secretome of *C. albicans* includes more than 200 proteins involved in pathways that act in host tissue penetration, nutrient acquisition, tissue destruction, formation of the extracellular matrix of the cell wall remodeling, cell separation and thus biofilm formation [65]. Punctuating potential virulence factors, there is the production of proteases and phospholipases, which correlate directly to the ability of the microorganism to adhere to host cells, a fact that determines the success of colonization and infection. This adhesion is facilitated, since the production of proteases and phospholipases are capable of inducing a dysfunction or even rupture of membranes in host cells [67]. The secretion of these hydrolytic enzymes is a process that requires attention especially in ICU patients with candidemia associated with the use of catheters De Luca et al. [68,69] investigated the activity of proteases and phospholipases in 59 episodes of candidemia documented in the Clinical Institute Humanitas, Milan, Italy, and the results indicate that all strains of C. albicans exhibited phospholipase activity and 48% had proteinase activity. Moreover, the secretion of protease was identified in only one strain of *C. parapsilosis*. In *C. glabrata* no enzyme was detected. Therefore, in systemic infections, C. albicans has higher proteinase activity compared to the species Candida non-albicans. In addition, Candida species interact directly with host cells and this property is associated with the interactive surface adhesins. Regarding membership, physical integration between the yeast cells and the host is a process fully mediated structural integrity of the fungal cell wall and by virtue of its location, and this interaction can occur between proteins and proteins or between proteins and sugars. In general, the adhesins described have so far been identified by far-Western blotting, immunoprecipitation and affinity chromatography [70] and a group that has received considerable attention includes Als family proteins that have been identified as adhesins wall fungal cells that interact with multiple ligands of the host cell [71]. In this context, biofilm formation also involves surface interactions. Some studies have shown that als genes are up-regulated during biofilm formation of *C. albicans* [72-74]. Biofilms directly affect the quality of life and survival of patients with candidemia, since when installed in intravascular catheters, peritoneal dialysis catheters and other implanted devices serve as a reservoir of infectious particles, which then break off from an initial structure and spread occupying niches not previously colonized, creating a metastatic infection in other organs [75].

Two important aspects related to biofilms complicate therapy in systemic infections caused by *Candida* species. Initially, it is important to note that much of the clinical manifestations of candidiasis are uniquely associated with biofilm formation and, in a second aspect, the cells found in the structure of the biofilm exhibit high levels of resistance to most clinically used antifungals [76,77]. In this regard, several studies have focused on the investigation of biofilms of *Candida* species with the goal of finding new therapeutic targets. The latest innovation described in this context involves a study conducted by Srinivasan et al. [76] who developed a device named *C. albicans* biofilm chip (CaBChip), a high-density robotic microarray that consists of *C. albicans* nano-biofilms used to print yeast cells onto a solid substrate. The main advantages of CaBChip include automation, miniaturization, and cost savings in amount of reagents, qualities that make this device ideal for drug discovery using the real high-throughput screening.

## Drugs Resistance

The antifungal drugs may interfere with the synthesis of nucleic acids (pyrimidines), microtubules (griseofulvin), synthesis of ergosterol (azoles, allylamines, thiocarbamates, morpholines), cell membrane integrity (polyene), cell wall synthesis (echinocandins, nicomicinas) and protein synthesis (sodarinas) and other cellular sites [78-80].

The clinical use of systemic antifungal drugs are the most common amphotericin B and its lipid preparations, itraconazole, fluconazole, triazoles (voriconazole, posaconazole and ravuconazole) and derivatives of echinocandins (caspofungin, micafungin and anidulafungin) [81-83]. However, available in Brazilian public hospitals, are only derived polyene (amphotericin B) and azoles (itraconazole and fluconazole) [84]. The resistance can be defined in terms of clinical and microbiological [85,86]. The concept of microbiological resistance includes the resistance primary (or intrinsic) which is present in an organism that without prior exposure to secondary resistance and antifungal drugs (or acquired) which is one developed in response to exposure to these substances [87]. Typically, the secondary resistance is due to phenotypic changes and/or genotypic character stable or transitory [88,89]. In turn, the strength has been defined as clinical progression or persistence of an infection, despite the establishment of appropriate antimicrobial therapy [90]. The occurrence of clinical resistance is associated with host factors, pharmacological factors, iatrogenic factors and fungal factors [91]. Inside of invasive fungal infections, the clinical resistance typically manifests in patients with profound, prolonged neutropenia, patients undergoing multiple therapies and patients with prostheses and catheters [31,92]. The primary resistance to amphotericin B has a limited occurrence. Some emerging pathogens such as *Aspergillus* spp., *C. glabrata*, *C. guilliermondii, C. krusei, C. lusitaniae, Fusarium* spp., *Scedosporium* spp., *Scopulariopsis* spp. and *Trichosporon beigelii*, however, have shown some degree of primary resistance in vitro [93,94]. Likewise, the secondary resistance to polyene drug is hardly prevalent among fungal species. However, some cases of disseminated infection by strains of *C. glabrata, C. krusei* and *C. albicans* that have developed resistance to amphotericin B during the antifungal treatment have been described [90]. A polyene resistance is primarily related to qualitative and quantitative changes of the fungal cell membrane lipids [93]. The biochemical mechanisms of resistance include reduction of ergosterol content without concomitant change in its composition, replacement of sterols with greater affinity for polyene and reorientation of existing sterols, making the connection with the polyene and sterically less favorable thermodynamics [95,96]. Other sources of resistance are increased cell catalase activity that acts minimizing oxidative destruction produced by polyene drugs and decreased content of β-1,3-glucan that stabilizes the fungal cell wall, influencing access of macromolecules, such as amphotericin B the plasma membrane [87,97]. Different molecular mechanisms of resistance to azoles are possible [87,91]. The secondary resistance to these drugs is best described in yeasts [98]. In *Candida* spp. resistance may result from overexpression of pumps that enables elimination, regulating the transport and / or intracellular accumulation of azoles. ABC transporters and carriers MSF are the two major efflux pumps found in these fungi. Overexpression of ABC transporters in *C. albicans* genes coding for CDR1 and CDR2, and mdr1 gene encoding the MSF carriers determine decreased susceptibility to most clinical use and the fluconazole and azole respectively [85,99]. Different molecular mechanisms of resistance to azoles are possible [86,87]. A resistance mechanism is directly related to the structural change of the enzyme lanosterol 14-demethylase (ERG11p) which is the cell site and the azole derivatives key enzyme in the synthesis of ergosterol. Increased expression of the ERG11 gene also appears to contribute to resistance to azole derivatives [100]. The change in the ergosterol biosynthetic pathway is another mechanism associated with resistance. This toxic methylated sterol is formed by blocking ERG11p, being a consequence of the activity of azole drugs on the fungal cell. Erg3 gene mutation removes the toxic effect and is considered a mechanism of resistance [92,99].

Chang et al. [60] studied the susceptibility of 52 isolates of *C. guilliermondii* antifungal caspofungin, anidulafungin and micafungin and the results showed that these antifungals used exhibited good activity (98%) *in vitro* against this species of *Candida*. Studies performed in Korea for Jang et al. [99,101] to determine the fluconazole and voriconazole susceptibility of *Candida* bloodstream isolates (BSIs) using both the CLSI and EUCAST methods, demonstrated of the 341 BSIs of 3 common *Candida* species (i.e., *C. albicans, C. tropicalis*, and *C. parapsilosis*), presented 0.3% to 1.5% of isolates categorized as fluconazole and voriconazole resistant according to the CLSI and EUCAST.

Antifungal resistance of *Candida* species is a clinical problem in the management of diseases caused by these pathogens. Studies performed for Eddouzi et al. [100,102] identified from a collection of 423 clinical samples taken from Tunisian hospitals two clinical Candida species (*Candida albicans* JEY355 and *Candida tropicalis* JEY162) with decreased susceptibility to azoles and polyenes. For JEY355, the fluconazole (FLC) MIC was 8 μg/ml. Azole resistances in *C. albicans* JEY355 was mainly caused by overexpression of a multidrug efflux pump of the major facilitator superfamily, Mdr1. The regulator of Mdr1, MRR1, contained a yet-unknown gain-of-function mutation (V877F) causing MDR1 overexpression. *C. tropicalis* JEY162 isolate demonstrated cross-resistance between FLC (MIC>128 μg/ml), voriconazole (MIC>16 μg/ml), and amphotericin B (MIC>32 μg/ml). Sterol analysis using gas chromatography-mass spectrometry revealed that ergosterol was undetectable in JEY162 and that it accumulated 14α-methyl fecosterol, thus indicating a perturbation in the function of at least two main ergosterol biosynthesis proteins (Erg11 and Erg3). Sequence analyses of *C. tropicalis* ERG11 (CtERG11) and CtERG3 from JEY162 revealed a deletion of 132 nucleotides and a single amino acid substitution (S258F), respectively. The authors conclusion, in addition to identify to identifying a novel MRR1 mutation in *C. albicans,* constitutes the first report on a clinical *C. tropicalis* with defective activity of sterol 14α-demethylase and sterol α-(5,6)-desaturase leading to azole-polyene cross-resistance. Table 2 shows the mechanisms of resistance of clinical isolates of *Candida albicans* from HIV-positive patients to fluconazole and itraconazole. In this work, Cataldo and Petrosillo [103], which describe a review of antifungal susceptibility testing of *Candida* and their clinical break points.

## Prophylaxis in Nosocomial Infection

Health professionals can act as vectors of disease, disseminating new infections among patients if professionals do not use preventive strategies to reduce rates of disease transmission [103]. It is important to underscore that, beyond prophylaxis with antifungal agents, standard measures to prevent nosocomial infections should always be applied both for their efficacy and for their low cost. Because transmission of *Candida* could occur via the hands of health care workers, especially during the care of catheters, all hospitals need to improve their adherence to hand hygiene. Also, extremely important is adherence

| N° isolates (*Candida albicans*) | Molecular change |
|---|---|
| 1 | None (WT) |
| 3 | Increase in MDR1 mRNA |
| 4 | Mutation *ERG11* gene, loss of hetezygosity in *ERG11*, increase in *ERG11* mRNA |
| 2 | Increase in CDR mRNA |

Adapted from Pfaller and Diekema [103]

**Table 2:** Azoles resistance mechanisms in isolates of Candida albicans from an HIV-infected patient with recurrent oropharyngeal candidiasis.

to current recommendations for placement and care of central venous catheters. Finally, the correct use of antibiotics is another important component of candidemia prevention that would lead to a decrease in economic and ecological costs.

## Conclusion

Several studies have shown increased resistance of isolates of species *Candida*, as well as increased morbidity and mortality caused by this pathogen in hospitalized individuals, thus it is necessary to prevent infection with this pathogen.

### References

1. Garner JS, Jarvis WR, Emori TG, Horan TC, Hughes JM (1988) CDC definitions for nosocomial infections, 1988. Am J Infect Control 16: 128-140.
2. Ducel G, Fabry J, Nicolle L (2002) World Health Organization Prevention of hospital-acquired infections A PRACTICAL GUIDE (2ndedn).
3. Edwards JE Jr (1991) Invasive candida infections--evolution of a fungal pathogen. N Engl J Med 324: 1060-1062.
4. Batista JM, Birman EG, Cury AE (1999) Susceptibility to antifungal drugs of Candida albicans strains isolated from patients with denture stomatitis. Rev Odontol Univ São Paulo13: 343-348.
5. Nucci M, Queiroz-Telles F, Tobón AM, Restrepo A, Colombo AL (2010) Epidemiology of opportunistic fungal infections in Latin America. Clin Infect Dis 51: 561-570.
6. Barchiesi F, Caggiano G, Falconi Di Francesco L, Montagna MT, Barbuti S, et al. (2004) Outbreak of fungemia due to Candida parapsilosis in a pediatric oncology unit. Diagn Microbiol Infect Dis 49: 269-271.
7. Lacaz CS, Porto E, Martins JEC, Heins-Vaccari E, Melo NT (2002) Tratado de Micologia Médica – Lacaz. Sarvier, São Paulo, SP, Brazil.
8. Trick WE, Fridkin SK, Edwards JR, Hajjeh RA, Gaynes RP; National Nosocomial Infections Surveillance System Hospitals (2002) Secular trend of hospital-acquired candidemia among intensive care unit patients in the United States during 1989-1999. Clin Infect Dis 35: 627-630.
9. Sheevani, Sharma P, Aggarwal A (2013) Nosocomial Candida infection in a rural tertiary care hospital. J Clin Diagn Res 7: 405-406.
10. Cantón E, Viudes A, Pemán J (2001) [Systemic nosocomial infection by yeasts]. Rev Iberoam Micol 18: 51-55.
11. Colombo AL, Guimarães T (2003) [Epidemiology of hematogenous infections due to Candida spp]. Rev Soc Bras Med Trop 36: 599-607.
12. Kontoyiannis DP, Vaziri I, Hanna HA, Boktour M, Thornby J, et al. (2001) Risk Factors for Candida tropicalis fungemia in patients with cancer. Clin Infect Dis 33: 1676-1681.
13. Leung AY, Chim CS, Ho PL, Cheng VC, Yuen KY, et al. (2002) Candida tropicalis fungaemia in adult patients with haematological malignancies: clinical features and risk factors. J Hosp Infect 50: 316-319.
14. Colombo AL, Nucci M, Salomão R, Branchini ML, Richtmann R, et al. (1999) High rate of non-albicans candidemia in Brazilian tertiary care hospitals. Diagn Microbiol Infect Dis 34: 281-286.
15. Fidel PL Jr, Vazquez JA, Sobel JD (1999) Candida glabrata: review of epidemiology, pathogenesis, and clinical disease with comparison to C. albicans. Clin Microbiol Rev 12: 80-96.
16. Antunes AG, Pasqualotto AC, Diaz MC, d'Azevedo PA, Severo LC (2004) Candidemia in a Brazilian tertiary care hospital: species distribution and antifungal susceptibility patterns. Rev Inst Med Trop Sao Paulo 46: 239-241.
17. Mavor AL, Thewes S, Hube B (2005) Systemic fungal infections caused by Candida species: epidemiology, infection process and virulence attributes. Curr Drug Targets 6: 863-874.
18. Pizzo PA (1999) Fever in immunocompromised patients. N Engl J Med 341: 893-900.
19. Carneiro-Sampaio M, Coutinho A (2007) Immunity to microbes: lessons from primary immunodeficiencies. Infect Immun 75: 1545-1555.
20. Del Favero A (2000) Management of fungal infections in neutropenic patients: more doubts than certainties? Int J Antimicrob Agents 16: 135-137.
21. Torres-Rodríguez JM (1996) [Current status of antifungal prophylaxis in opportunistic mycoses]. Enferm Infecc Microbiol Clin 14: 44-53.
22. Bow EJ (1998) Invasive fungal infections in patients receiving intensive cytotoxic therapy for cancer. Br J Haematol 101 Suppl 1: 1-4.
23. Petri MG, König J, Moecke HP, Gramm HJ, Barkow H, et al. (1997) Epidemiology of invasive mycosis in ICU patients: a prospective multicenter study in 435 non-neutropenic patients. Paul-Ehrlich Society for Chemotherapy, Divisions of Mycology and Pneumonia Research. Intensive Care Med 23: 317-325.
24. Richards M, Thursky K, Buising K (2003) Epidemiology, prevalence, and sites of infections in intensive care units. Semin Respir Crit Care Med 24: 3-22.
25. Leone M, Albanèse J, Antonini F, Michel-Nguyen A, Blanc-Bimar MC, et al. (2003) Long-term epidemiological survey of Candida species: comparison of isolates found in an intensive care unit and in conventional wards. J Hosp Infect 55: 169-174.
26. Meersseman W, Lagrou K, Maertens J, Van Wijngaerden E (2007) Invasive aspergillosis in the intensive care unit. Clin Infect Dis 45: 205-216.
27. Schelenz S (2008) Management of candidiasis in the intensive care unit. J Antimicrob Chemother 61 Suppl 1: i31-34.
28. Cornwell EE 3rd, Belzberg H, offne TV, Dougherty WR, Morales IR, et al. (1995) The pattern of fungal infections in critically ill surgical patients. Am Surg 61: 847-850.
29. Vincent JL, Anaissie E, Bruining H, Demajo W, el-Ebiary M, et al. (1998) Epidemiology, diagnosis and treatment of systemic Candida infection in surgical patients under intensive care. Intensive Care Med 24: 206-216.
30. Holzheimer RG, Dralle H (2002) Management of mycoses in surgical patients -- review of the literature. Eur J Med Res 7: 200-226.
31. Playford EG, Marriott D, Nguyen Q, Chen S, Ellis D, et al. (2008) Candidemia in nonneutropenic critically ill patients: risk factors for non-albicans Candida spp. Crit Care Med 36: 2034-2039.
32. O'grady NP, Alexander M, Dellinger EP, Gerberding JL, Heard SO, et al (2002) Guidelines for the prevention of intravascular catheter-related infections. Centers for Disease Control and Prevention. MMWR Recomm Rep 51: 1-29.
33. Greene JN (1996) The microbiology of colonization, including techniques for assessing and measuring colonization. Infect Control Hosp Epidemiol 17: 114-118.
34. Ramasethu J (2008) Complications of vascular catheters in the neonatal intensive care unit. Clin Perinatol 35: 199-222, x.
35. Moss HA, Elliot TSJ (1997) The cost of infections related to central venous catheters designed for long-term use. Br J Med Econ 11: 1-7.
36. Pittet D, Li N, Woolson RF, Wenzel RP (1997) Microbiological factors influencing the outcome of nosocomial bloodstream infections: a 6-year validated, population-based model. Clin Infect Dis 24: 1068-1078.
37. Cheng MF, Yang YL, Yao TJ, Lin CY, Liu JS, et al. (2005) Risk factors for fatal candidemia caused by Candida albicans and non-albicans Candida species. BMC Infect Dis 5: 22.
38. Tacconelli E, Tumbarello M, Pittiruti M, Leone F, Lucia MB, et al. (1997) Central venous catheter-related sepsis in a cohort of 366 hospitalised patients. Eur J Clin Microbiol Infect Dis 16: 203-209.
39. Gowardman JR, Montgomery C, Thirlwell S, Shewan J, Idema A, et al. (1998) Central venous catheter-related bloodstream infections: an analysis of incidence and risk factors in a cohort of 400 patients. Intensive Care Med 24: 1034-1039.
40. Calandra T, Cohen J; International Sepsis Forum Definition of Infection in the ICU Consensus Conference (2005) The international sepsis forum consensus conference on definitions of infection in the intensive care unit. Crit Care Med 33: 1538-1548.
41. Maki DG, Kluger DM, Crnich CJ (2006) The risk of bloodstream infection in adults with different intravascular devices: a systematic review of 200 published prospective studies. Mayo Clin Proc 81: 1159-1171.
42. Safdar N, Maki DG (2006) Lost in translation. Infect Control Hosp Epidemiol 27: 3-7.
43. Ha US, Cho YH (2006) Catheter-associated urinary tract infections: new

aspects of novel urinary catheters. Int J Antimicrob Agents 28: 485-490.

44. Colombo AL, Guimarães T (2007) [Candiduria: a clinical and therapeutic approach]. Rev Soc Bras Med Trop 40: 332-337.

45. Galbán B, Mariscal F (2006) [Epidemiology of candidemia in ICU]. Rev Iberoam Micol 23: 12-15.

46. Nguyen MH, Peacock JE Jr, Morris AJ, Tanner DC, Nguyen ML, et al. (1996) The changing face of candidemia: emergence of non-Candida albicans species and antifungal resistance. Am J Med 100: 617-623.

47. Pfaller MA, Jones RN, Messer SA, Edmond MB, Wenzel RP (1998) National surveillance of nosocomial blood stream infection due to species of Candida other than Candida albicans: frequency of occurrence and antifungal susceptibility in the SCOPE Program. SCOPE Participant Group. Surveillance and Control of Pathogens of Epidemiologic. Diagn Microbiol Infect Dis 30: 121-129.

48. Pfaller MA, Messer SA, Houston A, Rangel-Frausto MS, Wiblin T, et al. (1998) National epidemiology of mycoses survey: a multicenter study of strain variation and antifungal susceptibility among isolates of Candida species. Diagn Microbiol Infect Dis 31: 289-296.

49. Len O, Pahissa A (2007) [Donor-transmitted infections]. Enferm Infecc Microbiol Clin 25: 204-212.

50. Singer AL, Kucirka LM, Namuyinga R, Hanrahan C, Subramanian AK, et al. (2008) The high-risk donor: viral infections in solid organ transplantation. Curr Opin Organ Transplant 13: 400-404.

51. Silveira FP, Husain S (2007) Fungal infections in solid organ transplantation. Med Mycol 45: 305-320.

52. Manuel RJ, Kibbler CC (1998) The epidemiology and prevention of invasive aspergillosis. J Hosp Infect 39: 95-109.

53. Shaw MT, Spector MH, Ladman AJ (1979) Effects of cancer, radiotherapy and cytotoxic drugs on intestinal structure and function. Cancer Treat Rev 6: 141-151.

54. Bow EJ (2005) Long-term antifungal prophylaxis in high-risk hematopoietic stem cell transplant recipients. Med Mycol 43 Suppl 1: S277-287.

55. Clarkson JE, Worthington HV, Eden OB (2007) Interventions for preventing oral candidiasis for patients with cancer receiving treatment. Cochrane Database Syst Rev 1: 3807.

56. Volpato LE, Silva TC, Oliveira TM, Sakai VT, Machado MA (2007) Radiation therapy and chemotherapy-induced oral mucositis. Braz J Otorhinolaryngol 73: 562-568.

57. Anaissie E (1992) Opportunistic mycoses in the immunocompromised host: experience at a cancer center and review. Clin Infect Dis 14 Suppl 1: S43-53.

58. Segal BH, Freifeld AG (2007) Antibacterial prophylaxis in patients with neutropenia. J Natl Compr Canc Netw 5: 235-242.

59. Sims CR, Ostrosky-Zeichner L, Rex JH (2005) Invasive candidiasis in immunocompromised hospitalized patients. Arch Med Res 36: 660-671.

60. Chang TP, Ho MW, Yang YL, Lo PC, Lin PS, et al. (2013) Distribution and drug susceptibilities of Candida species causing candidemia from a medical center in central Taiwan. J Infect Chemother.

61. Moretti ML, Trabasso P, Lyra L, Fagnani R, Resende MR, et al. (2013) Is the incidence of candidemia caused by Candida glabrata increasing in Brazil? Five-year surveillance of Candida bloodstream infection in a university reference hospital in southeast Brazil. Med Mycol 51: 225-230.

62. Medeiros EA, Lott TJ, Colombo AL, Godoy P, Coutinho AP, et al. (2007) Evidence for a pseudo-outbreak of Candida guilliermondii fungemia in a university hospital in Brazil. J Clin Microbiol 45: 942-947.

63. Tamura NK, Negri MF, Bonassoli LA, Svidzinski TI (2007) [Virulence factors for Candida spp recovered from intravascular catheters and hospital workers hands]. Rev Soc Bras Med Trop 40: 91-93.

64. Sorgo AG, Heilmann CJ, Brul S, de Koster CG, Klis FM (2013) Beyond the wall: Candida albicans secret(e)s to survive. FEMS Microbiol Lett 338: 10-17.

65. Hota B (2004) Contamination, disinfection, and cross-colonization: are hospital surfaces reservoirs for nosocomial infection? Clin Infect Dis 39: 1182-1189.

66. Costa CR, Passos XS, e Souza LK, Lucena Pde A, Fernandes Ode F, et al. (2010) Differences in exoenzyme production and adherence ability of Candida spp. isolates from catheter, blood and oral cavity. Rev Inst Med Trop Sao Paulo 52: 139-143.

67. Mohan das V, Ballal M (2008) Proteinase and phospholipase activity as virulence factors in Candida species isolated from blood. Rev Iberoam Micol 25: 208-210.

68. De Luca C, Guglielminetti M, Ferrario A, Calabr M, Casari E (2012) Candidemia: species involved, virulence factors and antimycotic susceptibility. New Microbiol 35: 459-468.

69. Chaffin WL (2008) Candida albicans cell wall proteins. Microbiol Mol Biol Rev 72: 495-544.

70. Hoyer LL, Green CB, Oh SH, Zhao X (2008) Discovering the secrets of the Candida albicans agglutinin-like sequence (ALS) gene family--a sticky pursuit. Med Mycol 46: 1-15.

71. García-Sánchez S, Aubert S, Iraqui I, Janbon G, Ghigo JM, et al. (2004) Candida albicans biofilms: a developmental state associated with specific and stable gene expression patterns. Eukaryot Cell 3: 536-545.

72. Green CB, Cheng G, Chandra J, Mukherjee P, Ghannoum MA, et al. (2004) RT-PCR detection of Candida albicans ALS gene expression in the reconstituted human epithelium (RHE) model of oral candidiasis and in model biofilms. Microbiology 150: 267-275.

73. O'Connor L, Lahiff S, Casey F, Glennon M, Cormican M, et al. (2005) Quantification of ALS1 gene expression in Candida albicans biofilms by RT-PCR using hybridisation probes on the LightCycler. Mol Cell Probes 19: 153-162.

74. Uppuluri P, Chaturvedi AK, Srinivasan A, Banerjee M, Ramasubramaniam AK, et al. (2010) Dispersion as an important step in the Candida albicans biofilm developmental cycle. PLoS Pathog 6: e1000828.

75. Ramage G, Bachmann S, Patterson TF, Wickes BL, López-Ribot JL (2002) Investigation of multidrug efflux pumps in relation to fluconazole resistance in Candida albicans biofilms. J Antimicrob Chemother 49: 973-980.

76. Srinivasan A, Lopez-Ribot JL, Ramasubramanian AK (2012) Candida albicans biofilm chip (CaBChip) for high-throughput antifungal drug screening. J Vis Exp: e3845.

77. Vanden Bossche H (1997) Mechanisms of antifungal resistance. Rev Iberoam Micol 14: 44-49.

78. Georgopapadakou NH (1998) Antifungals: mechanism of action and resistance, established and novel drugs. Curr Opin Microbiol 1: 547-557.

79. Loo DS (2006) Systemic antifungal agents: an update of established and new therapies. Adv Dermatol 22: 101-124.

80. Anaissie EJ (2008) Diagnosis and therapy of fungal infection in patients with leukemia--new drugs and immunotherapy. Best Pract Res Clin Haematol 21: 683-690.

81. Mensa J, Pitart C, Marco F (2008) Treatment of critically ill patients with candidemia. Int J Antimicrob Agents 32 Suppl 2: S93-97.

82. Cornely OA, Böhme A, Buchheidt D, Einsele H, Heinz WJ, et al (2009) Primary prophylaxis of invasive fungal infections in patients with hematologic malignancies. Recommendations of the Infectious Diseases Working Party of the German Society for Haematology and Oncology. Haematologica 94: 113-122.

83. Salci TP, Gimenes M, dos Santos CA, Svidzinski TI, Caparroz-Assef SM (2013) Utilization of fluconazole in an intensive care unit at a university hospital in Brazil. Int J Clin Pharm 35: 176-180.

84. Mellado E, Cuenca-Estrella M, Rodríguez-Tudela JL (2002) [Clinical relevance of mechanisms of antifungal drug resistance in filamentous fungi]. Enferm Infecc Microbiol Clin 20: 523-529.

85. Espinel-Ingroff A (2008) Mechanisms of resistance to antifungal agents: yeasts and filamentous fungi. Rev Iberoam Micol 25: 101-106.

86. Loeffler J, Stevens DA (2003) Antifungal drug resistance. Clin Infect Dis 36: S31-41.

87. Kontoyiannis DP, Lewis RE (2002) Antifungal drug resistance of pathogenic fungi. Lancet 359: 1135-1144.

88. Perea S, Patterson TF (2002) Antifungal resistance in pathogenic fungi. Clin Infect Dis 35: 1073-1080.

89. Espinel-Ingroff A (2000) Clinical utility of in vitro antifungal susceptibility testing. Rev Esp Quimioter 13: 161-166.

90. White NJ (1998) Preventing antimalarial drug resistance through combinations. Drug Resist Updat 1: 3-9.

91. Masiá Canuto M, Gutiérrez Rodero F (2002) Antifungal drug resistance to azoles and polyenes. Lancet Infect Dis 2: 550-563.

92. Cuenca-Estrella M, Gomez-Lopez A, Mellado E, Buitrago MJ, Monzon A, et al. (2006) Head-to-head comparison of the activities of currently available antifungal agents against 3,378 Spanish clinical isolates of yeasts and filamentous fungi. Antimicrob Agents Chemother 50: 917-921.

93. Ghannoum MA, Rice LB (1999) Antifungal agents: mode of action, mechanisms of resistance, and correlation of these mechanisms with bacterial resistance. Clin Microbiol Rev 12: 501-517.

94. Barker KS, Rogers PD (2006) Recent insights into the mechanisms of antifungal resistance. Curr Infect Dis Rep 8: 449-456.

95. Sanglard D (2002) Resistance of human fungal pathogens to antifungal drugs. Curr Opin Microbiol 5: 379-385.

96. Sanglard D, Odds FC (2002) Resistance of Candida species to antifungal agents: molecular mechanisms and clinical consequences. Lancet Infect Dis 2: 73-85.

97. Mishra NN, Prasad T, Sharma N, Payasi A, Prasad R, et al. (2007) Pathogenicity and drug resistance in Candida albicans and other yeast species. A review. Acta Microbiol Immunol Hung 54: 201-235.

98. Klepser ME (2001) Antifungal resistance among Candida species. Pharmacotherapy 21: 124S-132S.

99. Jang MJ, Shin JH, Lee WG, Kim MN, Lee K, et al. (2013) In vitro fluconazole and voriconazole susceptibilities of Candida bloodstream isolates in Korea: use of the CLSI and EUCAST epidemiological cutoff values. Ann Lab Med 33: 167-173.

100. Eddouzi J, Parker JE, Vale-Silva LA, Coste A, Ischer F, et al. (2013) Molecular mechanisms of drug resistance in clinical Candida species isolated from Tunisian hospitals. Antimicrob Agents Chemother 57: 3182-3193.

101. Pfaller MA, Diekema DJ (2012) Progress in antifungal susceptibility testing of Candida spp. by use of Clinical and Laboratory Standards Institute broth microdilution methods, 2010 to 2012. J Clin Microbiol 50: 2846-2856.

102. Saloojee H, Steenhoff A (2001) The health professional's role in preventing nosocomial infections. Postgrad Med J 77: 16-19.

103. Cataldo MA, Petrosillo N (2011) Economic considerations of antifungal prophylaxis in patients undergoing surgical procedures. Ther Clin Risk Manag 7: 13-20.

**Citation:** de Cássia Orlandi Sardi J, de Souza Pitangui N, Gullo FP, e Maria José Soares Mendes Giannini AMFA (2013) A Mini Review of *Candida* Species in Hospital Infection: Epidemiology, Virulence Factor and Drugs Resistance and Prophylaxis. Trop Med Surg 1: 141. doi: 10.4172/2329-9088.1000141

Rev Iberoam Micol. 2014;31(1):22–29

Revista Iberoamericana de Micología

www.elsevier.es/reviberoammicol

Mycologic Forum

# Highlights in pathogenic fungal biofilms

Janaina De Cássia Orlandi Sardi[a,c], Nayla De Souza Pitangui[a,c], Gabriela Rodríguez-Arellanes[b], Maria Lucia Taylor[b], Ana Maria Fusco-Almeida[a,d], Maria José Soares Mendes-Giannini[a,*,d]

[a] Department of Clinical Analysis, Laboratory of Clinical Mycology, Faculty of Pharmaceutical Sciences, Universidade Estadual Paulista (UNESP), Araraquara, São Paulo, Brazil
[b] Fungal Immunology Laboratory, Department of Microbiology and Parasitology, School of Medicine, National Autonomous University of Mexico (UNAM), Mexico City, Mexico

ARTICLE INFO

*Article history:*
Received 19 August 2013
Accepted 27 September 2013
Available online 16 November 2013

*Keywords:*
Biofilm
Quorum sensing
Pathogenic fungi
Adhesins
Anti-biofilm therapy

ABSTRACT

A wide variety of fungi have demonstrated the ability to colonize surfaces and form biofilms. Most studies on fungal biofilms have focused on *Candida albicans* and more recently, several authors have reported the involvement of other genera of yeasts and *Candida* species, as well as of filamentous fungi in the formation of biofilms, including: *Cryptococcus neoformans*, *Cryptococcus gattii*, *Rhodotorula* species, *Aspergillus fumigatus*, *Malassezia pachydermatis*, *Histoplasma capsulatum*, *Paracoccidioides brasiliensis*, *Pneumocystis* species, *Coccidioides immitis*, *Fusarium* species, *Saccharomyces cerevisiae*, *Trichosporon asahii*, Mucorales and *Blastoschizomyces*. There is a current interest in describing the particular characteristics of the biofilm formation by of these fungi. A major concern is the control of biofilms, requiring knowledge of the biofilm mechanisms. However, our knowledge of these microbial communities is limited, due to the complexity of these systems and metabolic interactions that remain unknown. This mini-review aims to highlight recently discovered fungal biofilms and to compare them with the current knowledge on biofilms.

This manuscript is part of the series of works presented at the "V International Workshop: Molecular genetic approaches to the study of human pathogenic fungi" (Oaxaca, Mexico, 2012).



## Aspectos sobresalientes en la formación de biopelículas por hongos patógenos

*Palabras clave:*
Biopelículas
Quorum sensing
Patógenos fúngicos
Adhesinas
Tratamiento anti-biopelículas

RESUMEN

Una amplia variedad de hongos poseen la capacidad para colonizar superficies y formar biopelículas (biofilms). La mayoría de los estudios efectuados sobre biopelículas de hongos han prestado atención a *Candida albicans* y, más recientemente, varios autores han descrito la implicación de otros géneros de levaduras y especies de *Candida*, al igual que de hongos filamentosos, en la formación de biopelículas, incluidos *Cryptococcus neoformans*, *Cryptococcus gattii*, especies de *Rhodotorula*, *Aspergillus fumigatus*, *Malassezia pachydermatis*, *Histoplasma capsulatum*, *Paracoccidioides brasiliensis*, especies de *Pneumocystis*, *Coccidioides immitis*, especies de *Fusarium*, *Saccharomyces cerevisiae*, *Trichosporon asahii*, mucorales y *Blastoschizomyces*. En la actualidad suscita interés la descripción de las características particulares de la formación de biopelículas de estos hongos. Una preocupación importante es el control de las biopelículas, que requiere una comprensión de los mecanismos de su formación. Sin embargo, nuestros conocimientos sobre estas comunidades microbianas son limitados debido a la complejidad de estos sistemas y a las interacciones metabólicas que aún no conocemos. Esta revisión tiene como objetivo poner de relieve las biopelículas fúngicas descubiertas recientemente y compararlas con los conocimientos actuales disponibles sobre ellas.

Este artículo forma parte de una serie de estudios presentados en el «V International Workshop: Molecular genetic approaches to the study of human pathogenic fungi» (Oaxaca, México, 2012).



* Corresponding author.
*E-mail address:* gianninimj@gmail.com (M.J.S. Mendes-Giannini).
[c] Equal contribution to the development of the review.
[d] Supervisors.

1130-1406/$ – see front matter 
http://dx.doi.org/10.1016/j.riam.2013.09.014

It is estimated that 95% of the microorganisms found in nature are attached in biofilms. According to Costerton et al.,[21] a biofilm can be defined as a complex structured community of microorganisms, surrounded by an extracellular matrix of polysaccharides, adhered to each other at a surface or interface. This three-dimensional structure may become integrated naturally into any solid surface in contact with non-sterile water.[139] Hence, these structures started to have great importance in diverse human activities. McCoy et al.[80] were the first to describe the formation of biofilms in pipes. From this study, greater attention was given by researchers to this topic, after all the negative aspects of biofilm formation, and led the scientific community to seek alternatives to eliminate harmful biofilms that would cause damage to equipments through biocorrosion, product contamination,[59] and represent significant losses to industries globally. If on one hand the biofilms can cause serious damage, on the other side they can be used in numerous bioprocesses. Examples include production of vinegar,[10] citric acid,[114] pharmaceutical applications through the production of secondary metabolites,[96] and biological processes for extracting metals from ores.[109] Recognition of biofilms, from the 1980s on, contributed to recognize numerous persistent infectious diseases persistent as being caused by biofilms.[22] Some infections caused by the use of medical devices in hospital environments such as catheters, are also related to biofilms.[32] The extracellular polymers (EPS) matrix, which holds the biofilm cohesive, is also responsible for the persistence of biofilm-related infections,[20] and protects microorganisms from disinfectants. Besides, resistance to UV radiation and dehydration (EPS matrix hydrated) has been demonstrated.[14,139] This report aims to review the advances in fungal biofilms and in adhesins genes involved in biofilm formation, quorum sensing (QS), as well as to cover some new therapeutic strategies against fungal biofilms.

## Fungal biofilms

Infections associated with the formation of biofilms are recognized as a significant and growing clinical problem; therefore, research in mycology has been increasingly focused on in biofilm phenotyping.[57] Recent advances in molecular techniques and confocal microscopy have shown that the formation of biofilms is the natural and preferred form of fungal growth and a major cause of persistent human infections. Microorganisms in biofilms grow in multicellular communities and produce an extracellular matrix that provides protection against from host defense mechanisms and antifungal drugs.[22]

A wide variety of fungi have demonstrated the ability to colonize surfaces and form biofilms. Most studies on fungal biofilms have focused on *Candida albicans* and more recently, several authors have reported the involvement of other genera of yeasts and *Candida* species as well as of filamentous fungi in the formation of biofilms, including: *Cryptococcus neoformans*, *Cryptococcus gattii*, *Rhodotorula* species, *Aspergillus fumigatus*, *Malassezia pachydermatis*, *Histoplasma capsulatum*, *Paracoccidioides brasiliensis* (unpublished data), *Pneumocystis* species, *Coccidioides immitis*, *Fusarium* species, *Saccharomyces cerevisiae*, *Trichosporon asahii*, Mucorales, and *Blastoschizomyces*.[13,25,26,28,31,75,88,99,104,110,122,137]

There is growing interest in uncovering the true participation of fungal biofilms in human disease. These formations play an important role in the development of infections, since microorganisms that grow in biofilms exhibit unique phenotypic characteristics when compared to their planktonic counterparts.[104] These characteristics include increased resistance to host defense mechanisms and antibiotic therapy.[78]

The adherence of a biofilm to the host may trigger an acute fungemia and/or disseminated infection. This occurs when cell clusters are dispersed from the initial biofilm and occupy a niche not previously colonized.[106] A recent study developed by Uppuluri et al.[133] demonstrated that cells that detach from a biofilm have a greater association with mortality as compared to planktonic microorganisms. In fact, over 65% of human infections involve the formation of biofilms, which is related to the increasing use of biomaterials in medical practice and the increasing number of immunocompromised patients.[19,107] In addition, more than 500,000 deaths per year are caused by biofilm-associated infections.[89]

As a result, biofilms have important and, often, deleterious effects on human health. Fungal biofilm formation on catheters and prostheses contributes to the development of nosocomial infections.[135] According to Kojic et al.,[63] the persistence of fungal infections occurs due to the ability of a fungus to form biofilms on a wide variety of medical devices and because of persisting cells representing an important mechanism of resistance.[115] Once infected, the in vivo eradication of a biofilm usually requires the administration of toxic concentrations of antimicrobials, and the recommended treatment includes removal of the contaminated device; however, this is a difficult and costly procedure that can result in medical complications.[43] Therefore, fungal biofilms have become a major clinical and economic problem.

Multidrug tolerance is caused by a small subpopulation of microbial cells termed persisters that become a reservoir from which recurrence of infection may be developed. These cells are responsible for an important mechanism of resistance in chronic infections extensively studied in bacteria,[7,106,115] which have attracted some attention recently in the context of fungal biofilms.[9] In *C. albicans* biofilms, a small subset of yeast cells have been described that is highly resistant to amphotericin B, following adhesion, and this is independent of the upregulation of efflux pumps and cell membrane composition. *C. albicans* persisters were detected only in biofilms and not in diverse planktonic populations.[65] When a biofilm was killed with amphotericin B and reinoculated with cells that survived, a new biofilm was produced with a new subpopulation of persisters; this suggests that these cells were not mutants but phenotypic variants of the wild type. The basis of this drug resistance is not clear and involves different mechanisms, including the presence of a small number of persisters, which are cells that survive high doses of an antimicrobial agent. Unlike bacterial persisters, *C. albicans* persisters have so far been observed only in biofilms and not in planktonic populations. Identification of important cellular components that are responsible for the occurrence of persisters in fungal biofilms could open the way to the rational design of antibiofilm agents.[68,115]

Recent findings have reported the involvement of new fungal genera and species in the formation of pathogenic biofilms and it is important to look for the role they can play in infections. There is a current interest in describing the particular characteristics of biofilm formation of the species *Rhodotorula*, *A. fumigatus*, *M. pachydermatis* and the dimorphic fungi *H. capsulatum*, *Coccidioides* spp., and *Paracoccidioides* spp.[37,89,99,105,106]

It was also recently demonstrated that *Rhodotorula* species are able to form biofilms. The increase in invasive infections caused by emerging pathogens such as *Rhodotorula* is related to the increased occurrence of degenerative and malignant diseases in different populations, the growing number of patients who undergo organ transplantation therapies that include immunosuppression, broad-spectrum antibiotics and invasive medical procedures[131]; and the use of implantable medical devices, such as central venous catheters, which facilitate the formation of biofilms by these pathogens, causing fungemia followed by eye infections, peritonitis, and meningitis.[29,116,131,132] Nunes et al.[94] studied various isolates of *Rhodotorula* species and noted that this genus is able to form biofilms, which could play a role in the pathogenesis

of infections caused by these species. Canabarro et al.[12] isolated *Rhodotorula* sp. in association with *C. albicans* subgingival biofilms from patients with severe chronic periodontitis.

Recent reports describe the growth of biofilm structures for the filamentous fungus *A. fumigatus*.[60,106] This species is responsible for approximately 90% of cases of invasive aspergillosis, a severe infectious disease characterized by high mortality rates.[51,105] *Aspergillus* colonization and biofilm formation predominantly occurs in patients with genetic functional lung abnormalities, such as cystic fibrosis or chronic obstructive pulmonary disease.[52,86] Biofilms of *Aspergillus* can affect diverse biomaterials, such as catheters, prostheses, cardiac pacemakers, heart valves and breast implants.[35,61] In addition, a spherical mass of hyphae, called aspergilloma, can form in the respiratory tract[106] or the urinary tract.[67,79] All clinical antifungal drugs are significantly less effective under the biofilm or spherical hyphae conditions, suggesting that there is need for high dosages or antifungal combination therapy for better penetration of drugs in biofilms.[87]

Another pathogen that has received growing attention is the fungus *M. pachydermatis*, capable of forming in vitro biofilms on devices commonly used in the medical practice, including polystyrene microplates and polyurethane catheters.[13] *M. pachydermatis* is a commensal yeast found on the skin and mucosa of healthy dogs and cats,[11] but has become an important pathogen of human fungemia in intensive care units[5] and has been isolated from preterm neonates, children and adults. These infections are directly associated with the formation of biofilms on catheters in patients receiving parenteral nutrition with lipid formulations.[18,24]

Recently, an in vitro study demonstrated the efficiency of *H. capsulatum* to form biofilms on abiotic surfaces.[99] *H. capsulatum* is the causative agent of histoplasmosis, a systemic fungal disease that has become a major health problem in Latin America and worldwide.[93] High concentrations of this fungus are found in areas with bird and bat droppings, such as caves, chicken coops, or even urban buildings.[1,56,123] A study by Pitangui et al.[99] determined the pattern of infection of *H. capsulatum* in epithelial cells, characterized as a compact mass of yeast cells, which possibly leads to the formation of a complex three-dimensional architecture of biofilms and promotes the internalization of yeast into host cells. A previous study by Suarez-Alvarez et al.[124] described the profile of *H. capsulatum* yeast adhesion on different bat organs. That study also noted that the yeasts are found in clusters in the lung parenchyma, spleen, liver, and intestine. Recent advances in high-throughput methods for the investigation of biofilms opened the possibility of starting an "omics" approach to study these complex structures in the next decade. Additionally, in vivo studies are needed to define the true role and growth regulation of *H. capsulatum* biofilms.

Paracoccidioidomycosis is a systemic mycosis of great relevance in Latin America, especially in Brazil, which has the highest concentration of endemic areas, as more than 80% of the reported cases occurred in this country. The causative agents are the dimorphic fungi *P. brasiliensis* and *P. lutzii*.[4,72] These fungi have several virulence factors that can cause harm to the host. The adhesion, colonization and characteristics of these fungi enable them to withstand the hostile environments of the host and are correlated with the development of disease.[39,84] Adhesion is a widely distributed phenomenon that is shared by many microorganisms, enabling them to colonize in their habitats. Many fungi, especially pathogenic fungi, are able to adhere to host tissues, which is the first step in the process of biofilm formation. The present authors were able to demonstrate biofilm formation by *P. brasiliensis*. Those experiments were performed in vitro, with the fungus forming biofilms at low oxygen tensions (unpublished data).

Davis et al.[28] described recurrent coccidioidal meningitis and *C. immitis* biofilm was found on the tip of the ventricle-peritoneal shunt tubing despite the patient's taking an adequate dosage of fluconazole.

## Quorum sensing in fungal biofilms

The regulation of the expression of virulence genes is a crucial step in pathogenesis and in microorganism adaptation to host tissues.[2] QS is a mechanism of microbial communication dependent on cell density that can regulate several behaviors in bacteria such as secretion of virulence factors, biofilm formation, competence and bioluminescence.[2] It is a major mechanism of microbial communication and QS occurs by the continuous release and monitoring of hormone-like molecules called auto-inducers or QS molecules.[138] QS has been observed in many bacterial species regulating the most diverse processes, including secretion of virulence factors, biofilm formation, and antibiotic production; now, it is believed that the same occurs in fungi.[2,46,85] In pathogenic microbes, the coordinated expression of virulence factors during infection of a host probably constitutes a significant survival advantage by enhancing the chances of establishing infection and escaping the immune response.[138] Several molecules have been described as belonging to QS. Lipids, such as sphingolipids, farnesol and oxylipins are signaling molecules in pathogenic fungi.[121] Recently, aromatic alcohols phenylethanol and tryptophol molecules were identified as quorum-sensing in *S. cerevisiae*. These compounds, which are also produced by *C. albicans*, showed growth on *S. cerevisiae* pseudohyphae at relatively low concentrations.[16]

Farnesol and tyrosol are QS molecules in *C. albicans*. The primary mechanism of regulation of QS is the production of auto-inducers that are released into the external environment, where they accumulate and concomitant measurement of their concentration is achieved through its interaction with its receptor, which may be as much as being in intracellular cell surface.[48] In bacteria, these inducers have been widely studied and they are related to various cellular processes, such as antibiotic production, sporulation ability, and expression of virulence genes, DNA transfer and formation of biofilms.[50] Shirtliff et al.[120] have shown that 40 mM or 100 mM farnesol concentrations are able to induce high regulation of *C. albicans* protein involved in protection against oxidative stress. Sharma et al.[119] demonstrated that farnesol can modulate the action of drugs on planktonic cells of *C. albicans*. Ramage et al.[108] evaluated the effects of farnesol on biofilm development and observed that farnesol inhibits the formation of hyphae when added in the initial phase of biofilm formation and, hence, can compromise the structure. Other studies have shown detrimental effects of farnesol on many microorganisms, including fungi and bacteria, such as *Staphylococcus aureus*, *S. cerevisiae*, *Aspergillus* species, *P. brasiliensis* and *Mycobacterium smegmatis*.[58,117] The high density of microorganisms in biofilms led to speculate that detection of QS plays a specific and important role in the physiology of biofilms. In other bacteria, QS detection can function in the dispersion of individual organisms from biofilm.[98,103] It seems, therefore, that the morphogenesis in *C. albicans* is under control of antagonistic tyrosol and farnesol.[17] Both farnesol and tyrosol in biofilms have been studied to emphasize the morphological aspect. The same can happen with other fungi, potentially increasing the efficacy of drugs, leading to new strategies for the treatment of fungal infections.[30]

## Genes involved in the formation of fungal biofilms

It is clear that the current knowledge on fungal biofilms has increased significantly and much of that knowledge has been gained through in vitro and in vivo studies of *Candida* biofilms.[66] Through research focused on the biofilm of *C.*

*albicans*, the molecular characteristics of fungal biofilm development were elucidated.[40,107] The increased amount of studies on *Candida* biofilms is partly because this pathogen is associated with infections of several medical devices, leading to high mortality (approaching 40%).[41] Recently, the transcriptional network that governs the development of biofilms for *C. albicans* was identified. This network consists of six master transcription regulators (EFG1, TEC1, BCR1, NDT80, ROB1, and BRG1) and approximately 1000 target genes, whose expression is controlled by these regulators. The six master regulators were identified by screening a library of approximately 165 mutant transcripts during in vitro biofilm formation and observing that the mutants had changed during the event. Six deletion mutants that produced defects in biofilm formation were identified, three are new (ROB1, BRG1 and NDT80) and three were previously known to play a role in the development of biofilms (BCR1, TEC1 and EFG1). All six identified genes were associated with defects in both in vitro and in vivo biofilm formation.[41] Banerjee et al.[6] studied the role of UME6 and found it to be a regulator of hyphae in *C. albicans* biofilms. Another study, performed by Taff et al.,[126] demonstrated that three enzymes were related to the production of extracellular polysaccharides, encoded by genes BGL2, PHR1, and XOG1. It has been shown that these enzymes are essential for the delivery of β-1,3-glucan for the matrix of the biofilm biomass and accumulation of a mature, extracellular matrix. Through the construction of mutants, researchers have demonstrated an increased biofilm susceptibility to commonly used antifungals, such as fluconazole. These investigators have proposed that the discovery of inhibitors of these enzymes provide promising anti-biofilm effects. The use of molecular biology tools has helped to unravel the "mystery" of microbial biofilms. Much has been discovered; however, despite advances in technology and arrays to evaluate enzymes and proteins, a way to completely eliminate biofilms has yet to be discovered.

## Adhesins in fungal biofilm

Adherence is a precondition for colonization and an essential step in the establishment of infection. Adherence is mediated through a large number of differentially regulated cell wall-bound adhesins. Studies with *Candida* spp. and *P. brasiliensis* have shown that these fungi have great potential for adherence to epithelial cells.[8,83]

Among several groups of genes involved in biofilm formation, it was found that the family ALS (agglutinin-like sequence), present in *C. albicans*, *Candida tropicalis* and *Candida glabrata*, plays a key role in this process and encodes proteins having the characteristics of adhesin glycoproteins on the cell surface.[38] It has been shown that ALS genes exhibit increased expression during the formation of biofilm.[95] The family present in *C. albicans* ALS includes eight genes (ALS1–ALS7 and ALS9) encoding many surface glycoproteins.[23,53] Molecular studies on the expression of ALS genes showed that they are differentially expressed and regulated as a function of cell physiological processes, such as the growth stage and cell morphology, i.e., yeast or predominantly in the form of hypha and pseudo-hypha.[54,55] ALS1, encoding cell surface glycoproteins, exhibits high expression in *C. albicans* biofilm cells.[23] Gene ALS3 also showed high expression, however, it is apparently associated with the production of *C. albicans* hyphae.[23,55] Nailis et al.[90] compared gene expression of ALS1 and ALS3 among cells of *C. albicans* biofilm formed on the surface of silicone and on suspended cells (planktonic) and found a significant increase in the expression of ALS1 biofilm cells, and decreased expression of ALS3. Moreover, Nobile et al.[92] concluded, after several tests with mutants als1/als1 als3/als3 that ALS3 and ALS1 are essential for biofilm formation in vivo and reduced expression of these proteins entails the formation of a fragile biofilm, whereas their functions are compatible with biofilm structure and biochemical property. Zhao et al.[140] demonstrated that the decrease in ALS2 protein expression resulted in the reduction of biofilm biomass, suggesting that ALS2 contributes to the later stages of biofilm development and not to the adhesion stage. In an experimental model of catheter infection in vivo, ALS1 and AlS3 also had redundant functions, and other highly expressed genes of the family – ALS5, ALS6, ALS7, and ALS9 – were able to partially or completely replace the absence of ALS1 and/or ALS3, facilitating the development of biofilm in such an experimental model, whereas ALS2 and ALS4 were unable to do so, and all ALS genes could be replaced by ALS3 or ALS1 models in vivo and in vitro.

*C. albicans* adheres to epithelial cells in culture, mainly through EAP1 adhesion. EAP1 is a member of a family of up to 23 putative adhesin-encoding genes present in this yeast genome. EAP1 expression in vitro is controlled both positively and negatively; in addition, it presents high cell-to-cell heterogeneity, which depends on Sir-mediated silencing. EPA6 also encode functional adhesions in *C. glabrata*.[64]

Some molecules of *H. capsulatum* have been identified as ligands of extracellular matrix components. McMahon et al.[81] reported that a 50-kDa protein present in the fungus cell walls is able to bind to laminin, an extracellular matrix component of host lung cells. This protein is an essential step in the pathogenesis of the fungus, once in the alveolar macrophages yeasts inhibit the production of proinflammatory cytokines, facilitating infection.[127] There are no studies demonstrating *H. capsulatum* adhesins related to biofilm formation.

Pathogenic fungi such as *Paracoccidioides* spp., have multiple factors that can cause damage to the host and contribute to the virulence phenotype. Adhesion, colonization and characteristics of fungi enable them to resist the hostile environments of the host and are correlated to disease development.[3,27,33,49,82] Further, this protein has virulence potential with high affinity for laminin, thereby increasing the capacity of the fungi to invade and destroy tissues.[134] Adherence of *Paracoccidiodies* to epithelial cells is also greatly reduced in the presence of anti-gp43.[47] Gp43 also interacts with fibronectin, another component of the extracellular matrix.[82] Other adhesion molecules in *P. brasiliensis* have also been described, such as a 30-kDa adhesion molecule, with the ability to bind to laminin, and are expressed in *P. brasiliensis*, isolates with high adhesion capacity. Enolase is a cytoplasmic enzyme most abundantly expressed in many microorganisms.[97] Thus, for many years enolase was seen as a soluble glycolytic enzyme, present exclusively in the cytoplasm. In 2009, Donofrio et al.,[33] demonstrated that enolase from *P. brasiliensis* (*Pb*Eno) is a fibronectin-binding protein and genetic and proteomic evidences support its localization on the cell surface.[69,71] Studies conducted in the Clinical Mycology Laboratory, UNESP, Araraquara, Brazil, have shown an increase of some adhesins of *P. brasiliensis* in hypoxic conditions, precisely the condition that occurs in biofilm formation (unpublished data).

## Antibiofilm strategies

Fungal biofilm resistance mechanisms include extracellular matrix, efflux pump activity, persisters, cell density, overexpression of drug targets, stress responses, and the general physiology of the cell.[106] Thus, to increase the efficiency of new treatment strategies against bacterial and fungal infections, factors that lead to biofilm growth inhibition, biofilm disruption, or biofilm eradication are being sought. These factors could include enzymes, sodium salts, metal nanoparticles, antibiotics, acids, chitosan derivatives, or plant extracts. Biofilm formation almost always leads to a large increase in resistance to antimicrobial agents (up to 1000-fold decrease in susceptibility) in comparison with planktonic cultures

grown in conventional liquid media.[22] Many studies have focused on the search for natural or synthetic products for various fungal biofilms, but biofilms of *Candida* species are the most studied.

Studies performed by Pires et al.[100] showed the presence of biofilms in the fluid pathways of hemodialysis machines. The impacts of four biocides used for the disinfection of hemodialysis systems were tested against *Candida parapsilosis* and *Candida orthopsilosis* biofilms generated by isolates obtained from a hydraulic circuit, and collected in a hemodialysis unit. Acetic acid was shown to be the most effective agent against *Candida* biofilms. Strategies for effective disinfection procedures used for hemodialysis systems should also seek to kill and inhibit biofilms. On the other hand, some natural products have been tested against *C. orthopsilosis* and *C. parapsilosis* on planktonic and biofilm conditions and could be natural anticandidal agents that can be effectively utilized for the control of the yeasts.[101,102] In the Clinical Mycology Laboratory, UNESP, has been consolidating a platform for the development of antifungal and bioreagents. This platform is based on FAPESP programs, such as the Biota-FAPESP, the BIOPROSPECTA, and also in SISBIOTA – CNPq. Among natural substances evaluated that deserves highlighting lies maytenin with antifungal potential against several fungal species.[45]

Another promising strategy is the antifungal activity of silver nanoparticles. Silver (Ag) has been well known for its antimicrobial characteristics, and has a long history of applications in medicine with a well-tolerated tissue response.[91,115] In the hope of inhibiting biofilm formation, thereby reducing the chance of microbial infections and rejection, AgNP has been used for lining of medical implants with titanium.[42,70] Recently, Sun et al.[125] reported the antibiofilm activity of terpinen-4-ol-loaded lipid nanoparticles against *C. albicans* biofilms and this compound (10 μg/ml) eradicated formed biofilms.

Studies with antibodies have been performed by several authors to test their effects on diverse fungal and bacterial organisms. The latest therapeutic treatment of *Cryptococcus* biofilms suggests that monoclonal antibodies (MAbs) are potentially useful in clinical treatment.[77] Martinez et al.[74] demonstrated that alpha radiation, guided by MAb, effectively impairs fungal biofilm formation. Other authors have found that administering a prophylactic dose of antibodies specific to biofilms, immediately after insertion of a medical device, is effective in managing biofilm formation.[76]

Another important therapeutically promise is photodynamic therapy (PDT), widely used for species of *Candida* biofilms. Several authors have associated light emitting diode with other substances.[15,111] There are two major types of cellular damage: DNA damage and the destruction of cellular membranes and organelles. Recent studies have shown that the antimicrobial effect can be obtained with the use of photosensitizers belonging to different chemical groups. Junqueira et al.[62] assessed the PDT on biofilms of *Candida* spp., *Trichosporon mucoide*, and *Kodamaea ohmeri*.

Because the biofilm matrix is composed of DNA, proteins, and extracellular polysaccharides, recent studies have indicated that the disruption of the biofilm structure could be achieved via degradation of individual biofilm compounds by several enzymes such as DNAse, lactonases, α-amylases, and lyase.[128]

## Research methodology used recently in biofilms

Infections associated with biofilm formation are resistant to conventional antifungal therapy and due to the high morbidity and mortality caused by these formations there is an urgent need to use new technologies and innovative therapies for success in eradicating these infections.[113] In this sense, the ease of working with new models, in vivo approaches of "omics" techniques of molecular biology and nano science are innovative avenues of research that have paved the way for new lines of study in the search for antifungal targets.

In vitro biofilm models are needed to elucidate mechanisms of development of biofilms. Nevertheless, results of testing in vitro of biofilm formation by clinical isolates do not always agree with results in vivo.[112] In this context, invertebrate models become useful to visualize infection, determining the true role of biofilms in infectious processes and how these formations directly affect the health of the host.[113] A recent review published by Edwards and Kjellerup[34] highlights the advances in cell–cell interactions and the understanding how host immune system reacts to biofilm formation in five invertebrate models: *Lemna minor* (duckweed), *Arabidopsis thaliana* (thale cress), *Dictyostelium discoideum* (slime mold), *Drosophila melanogaster* (common fruit fly), and *Caenorhabditis elegans* (roundworm). These models were described and assessed for their relevance to infections associated with polymicrobial biofilm formation. According to the authors, it is possible to use each of these models to investigate the peculiar characteristics of such biofilm, however *C. elegans* is presented as the most complete model to elucidate virulence factors, host innate immune function and to visualize the infection. Some authors have adopted *C. elegans* as a model to determine the toxicity and antifungal activity of fungicidal compounds, aimed at the discovery of new targets for the treatment of biofilms of *C. albicans*.[36,130] Thus, the nematode *C. elegans* has given rise to promising perspectives for innovative human therapies.

Concomitantly, another important branch of research should be stressed, "omics" approaches have been widely exploited by pharmaceutical and biotechnology companies for the development of safer and more effective drugs. Currently, there is great interest in the search for effective drugs against novel targets and, in this context, we highlight proteins by proteomic analysis, since the identification of a target protein essential to cell survival can provide important information for the treatment of mycoses.[44,136] The proteome of *C. albicans* in planktonic and biofilm cultures is well documented by several authors.[73,118,129] In this sense, our group in Brazil has noted that there is a different pattern of proteins when comparing *H. capsulatum* in planktonic and biofilm cultures. Using mass spectrometry more than 40 proteins, belonging to different functional groups, were differentially expressed and identified between the biofilm and dispersed cells, and the three main functional groups include proteins involved in the metabolism of amino acids, nuclear proteins, and translation protein (unpublished data). Additionally, our group has been working on the standardization of methodologies that aim to characterize the differential transcriptional profile exhibited by fungi shaped biofilm and planktonic conditions through transcriptomics analysis. In addition, we aim at identifying the secreted molecules and metabolites, generated during biofilm formation, using secretomic and metabolomics analyses, respectively. These techniques should allow targeting cellular receptors for biofilm disruption in the interaction with host cells.

## Conclusions

Biofilms control is necessary and has been the subject of many investigations in the fields of biotechnology and public health, as biofilms are present in many situations, from human disease to industry. A major concern is the control of biofilms, for which knowledge of biofilm mechanisms is essential. However, information of microbial communities is scarce, due to the complexity of these systems and to metabolic interactions that remain unknown. For this reason, advances in high-throughput methods have allowed the interaction of systems, combining genomics, transcriptomics, proteomics, and metabolomics to elucidate the real function and ecology of these complex formations.

## Conflict of interest

None declared.

## Acknowledgements

The authors acknowledge receipt of grant from Brazilian organizations: FAPESP No. 2011/12734-3, 2012/01270-9, BIOTA-2003/02176-7, Bioprospecta-2004/07932-7, and CNPq-Sisbiota-563311/2010-0. This paper constitutes partial fulfillment of the Bilateral Collaboration Agreement between UNAM-Mexico (Ref: 15090-563-24-V-04) and UNESP-Brazil (Ref: 000528/04/01/2005), and of the project DGAPA-UNAM (PAPIIT IN204210).

## References

1. Aidé MA. Histoplasmosis. J Bras Pneumol. 2009;35:1145–51.
2. Albuquerque P, Casadevall A. Quorum sensing in fungi: a review. Med Mycol. 2012;50:337–45.
3. Andreotti PF, Monteiro da Silva JL, Bailão AM, Soares CM, Benard G, Soares CP, et al. Isolation and partial characterization of a 30 kDa adhesin from *Paracoccidioides brasiliensis*. Microbes Infect. 2005;7:875–81.
4. Arantes TD, Theodoro RC, Da Graça Macoris SA, Bagagli E. Detection of *Paracoccidioides* spp. in environmental aerosol samples. Med Mycol. 2013;51:83–92.
5. Ashbee HR, Leck AK, Puntis JW, Parsons WJ, Evans EG. Skin colonization by *Malassezia* in neonates and infants. Infect Control Hosp Epidemiol. 2002;23:212–6.
6. Banerjee M, Uppuluri P, Zhao XR, Carlisle PL, Vipulanandan G, Villar CC, et al. Expression of UME6, a key regulator of *Candida albicans* hyphal development, enhances biofilm formation via Hgc1- and Sun41-dependent mechanisms. Eukaryot Cell. 2013;12:224–32.
7. Behrends V, Ryall B, Zlosnik JE, Speert DP, Bundy JG, Williams HD. Metabolic adaptations of *Pseudomonas aeruginosa* during cystic fibrosis chronic lung infections. Environ Microbiol. 2013;15:398–408.
8. Biasoli MS, Tosello ME, Magaró HM. Adherence of *Candida* strains isolated from the human gastrointestinal tract. Mycoses. 2002;45:465–9.
9. Bink A, Vandenbosch D, Coenye T, Nelis H, Cammue BP, Thevissen K. Superoxide dismutases are involved in *Candida albicans* biofilm persistence against miconazole. Antimicrob Agents Chemother. 2011;55:4033–7.
10. Boletti FT. Manufactor of vinegar. Microbiology: a textbook on microorganisms general and applied. CE Marshall; 1921.
11. Cafarchia C, Otranto D. The pathogenesis of *Malassezia* yeasts. Parassitologia. 2008;50:65–7.
12. Canabarro A, Valle C, Farias MR, Santos FB, Lazera M, Wanke B. Association of subgingival colonization of *Candida albicans* and other yeasts with severity of chronic periodontitis. J Periodontal Res. 2012;48:428–32.
13. Cannizzo FT, Eraso E, Ezkurra PA, Villar-Vidal M, Bollo E, Castellá G, et al. Biofilm development by clinical isolates of *Malassezia pachydermatis*. Med Mycol. 2007;45:357–61.
14. Ceri H, Olson M, Morck D, Storey D, Read R, Buret A, et al. The MBEC Assay System: multiple equivalent biofilms for antibiotic and biocide susceptibility testing. Methods Enzymol. 2001;337:377–85.
15. Chen CM, Lee JA, Huang TC. Construction of a light-emitting diode fluorescence detector for high-performance liquid chromatography and its application to fluorometric determination of L-3-hydroxybutyrate. Biomed Chromatogr. 2012;26:256–60.
16. Chen H, Fink GR. Feedback control of morphogenesis in fungi by aromatic alcohols. Genes Dev. 2006;20:1150–61.
17. Chen H, Fujita M, Feng Q, Clardy J, Fink GR. Tyrosol is a quorum-sensing molecule in *Candida albicans*. Proc Natl Acad Sci U S A. 2004;101:5048–52.
18. Chryssanthou E, Broberger U, Petrini B. *Malassezia pachydermatis* fungaemia in a neonatal intensive care unit. Acta Paediatr. 2001;90:323–7.
19. Cos P, Toté K, Horemans T, Maes L. Biofilms: an extra hurdle for effective antimicrobial therapy. Curr Pharm Des. 2010;16:2279–95.
20. Costerton JW, Geesey GG, Cheng KJ. How bacteria stick. Sci Am. 1978;238:86–95.
21. Costerton JW, Lewandowski Z, Caldwell DE, Korber DR, Lappin-Scott HM. Microbial biofilms. Annu Rev Microbiol. 1995;49:711–45.
22. Costerton JW, Stewart PS, Greenberg EP. Bacterial biofilms: a common cause of persistent infections. Science. 1999;284:1318–22.
23. Cuéllar-Cruz M, López-Romero E, Villagómez-Castro JC, Ruiz-Baca E. *Candida* species: new insights into biofilm formation. Future Microbiol. 2012;7:755–71.
24. Curvale-Fauchet N, Botterel F, Legrand P, Guillot J, Bretagne S. Frequency of intravascular catheter colonization by *Malassezia* spp. in adult patients. Mycoses. 2004;47:491–4.
25. Cushion MT, Collins MS, Linke MJ. Biofilm formation by *Pneumocystis* spp. Eukaryot Cell. 2009;8:197–206.
26. D'Antonio D, Parruti G, Pontieri E, Di Bonaventura G, Manzoli L, Sferra R, et al. Slime production by clinical isolates of *Blastoschizomyces capitatus* from patients with hematological malignancies and catheter-related fungemia. Eur J Clin Microbiol Infect Dis. 2004;23:787–9.
27. da Silva Neto BR, de Fátima da Silva J, Mendes-Giannini MJ, Lenzi HL, de Almeida Soares CM, Pereira M. The malate synthase of *Paracoccidioides brasiliensis* is a linked surface protein that behaves as an anchorless adhesin. BMC Microbiol. 2009;9:272.
28. Davis LE, Cook G, Costerton JW. Biofilm on ventriculo-peritoneal shunt tubing as a cause of treatment failure in coccidioidal meningitis. Emerg Infect Dis. 2002;8:376–9.
29. De Almeida GM, Costa SF, Melhem M, Motta AL, Szeszs MW, Miyashita F, et al. *Rhodotorula* spp. isolated from blood cultures: clinical and microbiological aspects. Med Mycol. 2008;46:547–56.
30. Derengowski LS, De-Souza-Silva C, Braz SV, Mello-De-Sousa TM, Báo SN, Kyaw CM, et al. Antimicrobial effect of farnesol, a *Candida albicans* quorum sensing molecule, on *Paracoccidioides brasiliensis* growth and morphogenesis. Ann Clin Microbiol Antimicrob. 2009;8:13.
31. Di Bonaventura G, Pompilio A, Picciani C, Iezzi M, D'Antonio D, Piccolomini R. Biofilm formation by the emerging fungal pathogen *Trichosporon asahii*: development, architecture, and antifungal resistance. Antimicrob Agents Chemother. 2006;50:3269–76.
32. Donlan RM. Biofilms and device-associated infections. Emerg Infect Dis. 2001;7:277–81.
33. Donofrio FC, Calil AC, Miranda ET, Almeida AM, Benard G, Soares CP, et al. Enolase from *Paracoccidioides brasiliensis*: isolation and identification as a fibronectin-binding protein. J Med Microbiol. 2009;58:706–13.
34. Edwards S, Kjellerup BV. Exploring the applications of invertebrate host-pathogen models for in vivo biofilm infections. FEMS Immunol Med Microbiol. 2012;65:205–14.
35. Escande W, Fayad G, Modine T, Verbrugge E, Koussa M, Senneville E, et al. Culture of a prosthetic valve excised for streptococcal endocarditis positive for *Aspergillus fumigatus* 20 years after previous A fumigatus endocarditis. Ann Thorac Surg. 2011;91:e92–3.
36. Ewbank JJ, Zugasti O. *C. elegans*: model host and tool for antimicrobial drug discovery. Dis Model Mech. 2011;4:300–4.
37. Figueredo LA, Cafarchia C, Desantis S, Otranto D. Biofilm formation of *Malassezia pachydermatis* from dogs. Vet Microbiol. 2012;160:126–31.
38. Filler SG. *Candida*–host cell receptor–ligand interactions. Curr Opin Microbiol. 2006;9:333–9.
39. Filler SG, Sheppard DC. Fungal invasion of normally non-phagocytic host cells. PLoS Pathog. 2006;2:e129.
40. Finkel JS, Mitchell AP. Genetic control of *Candida albicans* biofilm development. Nat Rev Microbiol. 2011;9:109–18.
41. Fox EP, Nobile CJ. A sticky situation: untangling the transcriptional network controlling biofilm development in *Candida albicans*. Transcription. 2012;3:315–22.
42. García-Contreras R, Argueta-Figueroa L, Mejía-Rubalcava C, Jiménez-Martínez R, Cuevas-Guajardo S, Sánchez-Reyna PA, et al. Perspectives for the use of silver nanoparticles in dental practice. Int Dent J. 2011;61:297–301.
43. Garsin DA, Willems RJ. Insights into the biofilm lifestyle of enterococci. Virulence. 2010;1:219–21.
44. Gomase VS, Kale KV, Tagore S, Hatture SR. Proteomics: technologies for protein analysis. Curr Drug Metab. 2008;9:213–20.
45. Gullo FP, Sardi JC, Santos VA, Sangalli-Leite F, Pitangui NS, Rossi SA, et al. Antifungal activity of maytenin and pristimerin. Evid Based Complement Alternat Med. 2012;2012:3407–87.
46. Gupta RK, Chhibber S, Harjai K. Quorum sensing signal molecules cause renal tissue inflammation through local cytokine responses in experimental UTI caused by *Pseudomonas aeruginosa*. Immunobiology. 2013;218:181–5.
47. Hanna SA, Monteiro da Silva JL, Giannini MJ. Adherence and intracellular parasitism of *Paracoccidioides brasiliensis* in Vero cells. Microbes Infect. 2000;2:877–84.
48. Hense BA, Kuttler C, Müller J, Rothballer M, Hartmann A, Kreft JU. Does efficiency sensing unify diffusion and quorum sensing? Nat Rev Microbiol. 2007;5:230–9.
49. Hernández O, Almeida AJ, Tamayo D, Torres I, Garcia AM, López A, et al. The hydrolase PbHAD32 participates in the adherence of *Paracoccidioides brasiliensis* conidia to epithelial lung cells. Med Mycol. 2012;50:533–7.
50. Hogan DA. Talking to themselves: autoregulation and quorum sensing in fungi. Eukaryot Cell. 2006;5:613–9.
51. Hogan LH, Klein BS, Levitz SM. Virulence factors of medically important fungi. Clin Microbiol Rev. 1996;9:469–88.
52. Horré R, Symoens F, Delhaes L, Bouchara JP. Fungal respiratory infections in cystic fibrosis: a growing problem. Med Mycol. 2010;48:S1–3.
53. Hoyer LL, Green CB, Oh SH, Zhao X. Discovering the secrets of the *Candida albicans* agglutinin-like sequence (ALS) gene family—a sticky pursuit. Med Mycol. 2008;46:1–15.
54. Hoyer LL, Payne TL, Hecht JE. Identification of *Candida albicans* ALS2 and ALS4 and localization of als proteins to the fungal cell surface. J Bacteriol. 1998;180:5334–43.
55. Hoyer LL, Scherer S, Shatzman AR, Livi GP. *Candida albicans* ALS1: domains related to a *Saccharomyces cerevisiae* sexual agglutinin separated by a repeating motif. Mol Microbiol. 1995;15:39–54.
56. Huhn GD, Austin C, Carr M, Heyer D, Boudreau P, Gilbert G, et al. Two outbreaks of occupationally acquired histoplasmosis: more than workers at risk. Environ Health Perspect. 2005;113:585–9.
57. Jabra-Rizk MA, Falkler WA, Meiller TF. Fungal biofilms and drug resistance. Emerg Infect Dis. 2004;10:14–9.

58. Jabra-Rizk MA, Shirtliff M, James C, Meiller T. Effect of farnesol on *Candida dubliniensis* biofilm formation and fluconazole resistance. FEMS Yeast Res. 2006;6:1063–73.
59. Jass J, O'Neill JG, Walker JT. Direct biofilm monitoring by a capacitance measurement probe in continuous culture chemostats. Methods Enzymol. 2001;337:63–70.
60. Jayshree RS, Shafiulla M, George J, David JK, Bapsy PP, Chakrabarti A. Microscopic, cultural and molecular evidence of disseminated invasive aspergillosis involving the lungs and the gastrointestinal tract. J Med Microbiol. 2006;55:961–4.
61. Jeloka TK, Shrividya S, Wagholikar G. Catheter outflow obstruction due to an aspergilloma. Perit Dial Int. 2011;31:211–2.
62. Junqueira JC, Jorge AO, Barbosa JO, Rossoni RD, Vilela SF, Costa AC, et al. Photodynamic inactivation of biofilms formed by *Candida* spp., *Trichosporon mucoides*, and *Kodamaea ohmeri* by cationic nanoemulsion of zinc 2,9,16,23-tetrakis(phenylthio)-29H, 31H-phthalocyanine (ZnPc). Lasers Med Sci. 2012;27:1205–12.
63. Kojic EM, Darouiche RO. *Candida* infections of medical devices. Clin Microbiol Rev. 2004;17:255–67.
64. Kucharíková S, Tournu H, Lagrou K, Van Dijck P, Bujdáková H. Detailed comparison of *Candida albicans* and *Candida glabrata* biofilms under different conditions and their susceptibility to caspofungin and anidulafungin. J Med Microbiol. 2011;60:1261–9.
65. LaFleur MD, Kumamoto CA, Lewis K. *Candida albicans* biofilms produce antifungal-tolerant persister cells. Antimicrob Agents Chemother. 2006;50:3839–46.
66. Lebeaux D, Ghigo JM. Management of biofilm-associated infections: what can we expect from recent research on biofilm lifestyles? Med Sci (Paris). 2012;28:727–39.
67. Lee SW. An aspergilloma mistaken for a pelviureteral stone on nonenhanced CT: a fungal bezoar causing ureteral obstruction. Korean J Urol. 2010;51:216–8.
68. Lewis K. Persister cells: molecular mechanisms related to antibiotic tolerance. Handb Exp Pharmacol. 2012;211:121–33.
69. López-Villar E, Monteoliva L, Larsen MR, Sachon E, Shabaz M, Pardo M, et al. Genetic and proteomic evidences support the localization of yeast enolase in the cell surface. Proteomics. 2006;6:S107–18.
70. Lu X, Zhang B, Wang Y, Zhou X, Weng J, Qu S, et al. Nano-Ag-loaded hydroxyapatite coatings on titanium surfaces by electrochemical deposition. J R Soc Interface. 2011;8:529–39.
71. Marcos CM, de Fátima da Silva J, de Oliveira HC, Moraes da Silva RA, Mendes-Giannini MJ, Fusco-Almeida AM. Surface-expressed enolase contributes to the adhesion of *Paracoccidioides brasiliensis* to host cells. FEMS Yeast Res. 2012;12:557–70.
72. Marques-da-Silva SH, Rodrigues AM, de Hoog GS, Silveira-Gomes F, Camargo ZP. Occurrence of *Paracoccidioides lutzii* in the Amazon region: description of two cases. Am J Trop Med Hyg. 2012;87:710–4.
73. Martínez-Gomariz M, Perumal P, Mekala S, Nombela C, Chaffin WL, Gil C. Proteomic analysis of cytoplasmic and surface proteins from yeast cells, hyphae, and biofilms of *Candida albicans*. Proteomics. 2009;9:2230–52.
74. Martinez LR, Bryan RA, Apostolidis C, Morgenstern A, Casadevall A, Dadachova E. Antibody-guided alpha radiation effectively damages fungal biofilms. Antimicrob Agents Chemother. 2006;50:2132–6.
75. Martinez LR, Casadevall A. *Cryptococcus neoformans* biofilm formation depends on surface support and carbon source and reduces fungal cell susceptibility to heat, cold, and UV light. Appl Environ Microbiol. 2007;73:4592–601.
76. Martinez LR, Casadevall A. Specific antibody can prevent fungal biofilm formation and this effect correlates with protective efficacy. Infect Immun. 2005;73:6350–62.
77. Martinez LR, Christaki E, Casadevall A. Specific antibody to *Cryptococcus neoformans* glucuronoxylomannan antagonizes antifungal drug action against cryptococcal biofilms in vitro. J Infect Dis. 2006;194:261–6.
78. Martinez LR, Fries BC. Fungal biofilms: relevance in the setting of human disease. Curr Fungal Infect Rep. 2010;4:266–75.
79. Martinez-Pajares JD, Martinez-Ferriz MC, Moreno-Perez D, Garcia-Ramirez M, Martin-Carballido S, Blanch-Iribarne P. Management of obstructive renal failure caused by bilateral renal aspergilloma in an immunocompetent newborn. J Med Microbiol. 2010;59:367–9.
80. McCoy WF, Bryers JD, Robbins J, Costerton JW. Observations of fouling biofilm formation. Can J Microbiol. 1981;27:910–7.
81. McMahon JP, Wheat J, Sobel ME, Pasula R, Downing JF, Martin WJ. Murine laminin binds to *Histoplasma capsulatum*. A possible mechanism of dissemination. J Clin Invest. 1995;96:1010–7.
82. Mendes-Giannini MJ, Andreotti PF, Vincenzi LR, da Silva JL, Lenzi HL, Benard G, et al. Binding of extracellular matrix proteins to *Paracoccidioides brasiliensis*. Microbes Infect. 2006;8:1550–9.
83. Mendes-Giannini MJ, Monteiro da Silva JL, de Fátima da Silva J, Donofrio FC, Miranda ET, Andreotti PF, et al. Interactions of *Paracoccidioides brasiliensis* with host cells: recent advances. Mycopathologia. 2008;165:237–48.
84. Mendes-Giannini MJ, Soares CP, da Silva JL, Andreotti PF. Interaction of pathogenic fungi with host cells: molecular and cellular approaches. FEMS Immunol Med Microbiol. 2005;45:383–94.
85. Miller MB, Bassler BL. Quorum sensing in bacteria. Annu Rev Microbiol. 2001;55:165–99.
86. Moss RB. Allergic bronchopulmonary aspergillosis and *Aspergillus* infection in cystic fibrosis. Curr Opin Pulm Med. 2010;16:598–603.
87. Mowat E, Butcher J, Lang S, Williams C, Ramage G. Development of a simple model for studying the effects of antifungal agents on multicellular communities of *Aspergillus fumigatus*. J Med Microbiol. 2007;56:1205–12.
88. Mowat E, Williams C, Jones B, McChlery S, Ramage G. The characteristics of *Aspergillus fumigatus* mycetoma development: is this a biofilm? Med Mycol. 2009;47:S120–6.
89. Müller FM, Seidler M, Beauvais A. *Aspergillus fumigatus* biofilms in the clinical setting. Med Mycol. 2011;49:S96–100.
90. Nailis H, Coenye T, Van Nieuwerburgh F, Deforce D, Nelis HJ. Development and evaluation of different normalization strategies for gene expression studies in *Candida albicans* biofilms by real-time PCR. BMC Mol Biol. 2006;7:25.
91. Nam KY. In vitro antimicrobial effect of the tissue conditioner containing silver nanoparticles. J Adv Prosthodont. 2011;3:20–4.
92. Nobile CJ, Schneider HA, Nett JE, Sheppard DC, Filler SG, Andes DR, et al. Complementary adhesin function in *C. albicans* biofilm formation. Curr Biol. 2008;18:1017–24.
93. Nosanchuk JD, Zancopé-Oliveira RM, Hamilton AJ, Guimarães AJ. Antibody therapy for histoplasmosis. Front Microbiol. 2012;3. http://dx.doi.org/10.3389/fmicb.2012.00021.
94. Nunes JM, Bizerra FC, Ferreira RC, Colombo AL. Molecular identification, antifungal susceptibility profile, and biofilm formation of clinical and environmental *Rhodotorula* species isolates. Antimicrob Agents Chemother. 2013;57:382–9.
95. O'Connor L, Lahiff S, Casey F, Glennon M, Cormican M, Maher M. Quantification of ALS1 gene expression in *Candida albicans* biofilms by RT-PCR using hybridisation probes on the LightCycler. Mol Cell Probes. 2005;19:153–62.
96. Okita WB, Kirwan DJ. Simulation of secondary metabolite production by immobilized living cells: penicillin production. Biotechnol Prog. 1986;2:83–90.
97. Pancholi V. Multifunctional alpha-enolase: its role in diseases. Cell Mol Life Sci. 2001;58:902–20.
98. Parsek MR, Fuqua C. Biofilms 2003: emerging themes and challenges in studies of surface-associated microbial life. J Bacteriol. 2004;186:4427–40.
99. Pitangui NS, Sardi JC, Silva JF, Benaducci T, Moraes da Silva RA, Rodríguez-Arellanes G, et al. Adhesion of *Histoplasma capsulatum* to pneumocytes and biofilm formation on an abiotic surface. Biofouling. 2012;28:711–8.
100. Pires RH, da Silva JD, Martins CH, Fusco Almeida AM, Soares CP, Mendes-Giannini MJ. Effectiveness of disinfectants used in hemodialysis against both *Candida orthopsilosis* and *C. parapsilosis* sensu stricto biofilms. Antimicrob Agents Chemother. 2013;57:2417–21.
101. Pires RH, Lucarini R, Mendes-Giannini MJ. Effect of usnic acid on *Candida orthopsilosis* and *C. parapsilosis*. Antimicrob Agents Chemother. 2012;56:595–7.
102. Pires RH, Montanari LB, Martins CH, Zaia JE, Almeida AM, Matsumoto MT, et al. Anticandidal efficacy of cinnamon oil against planktonic and biofilm cultures of *Candida parapsilosis* and *Candida orthopsilosis*. Mycopathologia. 2011;172:453–64.
103. Puskas A, Greenberg EP, Kaplan S, Schaefer AL. A quorum-sensing system in the free-living photosynthetic bacterium *Rhodobacter sphaeroides*. J Bacteriol. 1997;179:7530–7.
104. Ramage G, Mowat E, Jones B, Williams C, Lopez-Ribot J. Our current understanding of fungal biofilms. Crit Rev Microbiol. 2009;35:340–55.
105. Ramage G, Rajendran R, Gutierrez-Correa M, Jones B, Williams C. *Aspergillus* biofilms: clinical and industrial significance. FEMS Microbiol Lett. 2011;324:89–97.
106. Ramage G, Rajendran R, Sherry L, Williams C. Fungal biofilm resistance. Int J Microbiol. 2012. http://dx.doi.org/10.1155/2012/528521.
107. Ramage G, Saville SP, Thomas DP, López-Ribot JL. *Candida* biofilms: an update. Eukaryot Cell. 2005;4:633–8.
108. Ramage G, Saville SP, Wickes BL, López-Ribot JL. Inhibition of *Candida albicans* biofilm formation by farnesol, a quorum-sensing molecule. Appl Environ Microbiol. 2002;68:5459–63.
109. Rawlings DE, Dew D, du Plessis C. Biomineralization of metal-containing ores and concentrates. Trends Biotechnol. 2003;21:38–44.
110. Reynolds TB, Fink GR. Bakers' yeast, a model for fungal biofilm formation. Science. 2001;291:878–81.
111. Ribeiro DS, Frigerio C, Santos JL, Prior JA. Photoactivation by visible light of CdTe quantum dots for inline generation of reactive oxygen species in an automated multipumping flow system. Anal Chim Acta. 2012;735:69–75.
112. Rohde H, Frankenberger S, Zähringer U, Mack D. Structure, function and contribution of polysaccharide intercellular adhesin (PIA) to *Staphylococcus epidermidis* biofilm formation and pathogenesis of biomaterial-associated infections. Eur J Cell Biol. 2010;89:103–11.
113. Römling U, Balsalobre C. Biofilm infections, their resilience to therapy and innovative treatment strategies. J Intern Med. 2012;272:541–61.
114. Sakurai A, Imai H, Takenaka Y, Sakakibara M. Simulation of citric acid production by rotating disk contactor. Biotechnol Bioeng. 1997;56:689–96.
115. Sardi JC, Scorzoni L, Bernardi T, Fusco-Almeida AM, Mendes Giannini MJ. *Candida* species: current epidemiology, pathogenicity, biofilm formation, natural antifungal products and new therapeutic options. J Med Microbiol. 2013;62:10–24.
116. Savini V, Sozio F, Catavitello C, Talia M, Manna A, Febbo F, et al. Femoral prosthesis infection by *Rhodotorula mucilaginosa*. J Clin Microbiol. 2008;46:3544–5.
117. Semighini CP, Hornby JM, Dumitru R, Nickerson KW, Harris SD. Farnesol-induced apoptosis in *Aspergillus nidulans* reveals a possible mechanism for antagonistic interactions between fungi. Mol Microbiol. 2006;59:753–64.

118. Seneviratne CJ, Wang Y, Jin L, Abiko Y, Samaranayake LP. *Candida albicans* biofilm formation is associated with increased anti-oxidative capacities. Proteomics. 2008;8:2936–47.
119. Sharma M, Prasad R. The quorum-sensing molecule farnesol is a modulator of drug efflux mediated by ABC multidrug transporters and synergizes with drugs in *Candida albicans*. Antimicrob Agents Chemother. 2011;55:4834–43.
120. Shirtliff ME, Krom BP, Meijering RA, Peters BM, Zhu J, Scheper MA, et al. Farnesol-induced apoptosis in *Candida albicans*. Antimicrob Agents Chemother. 2009;53:2392–401.
121. Singh A, Del Poeta M. Lipid signalling in pathogenic fungi. Cell Microbiol. 2011;13:177–85.
122. Singh R, Shivaprakash MR, Chakrabarti A. Biofilm formation by zygomycetes: quantification, structure and matrix composition. Microbiology. 2011;157:2611–8.
123. Smith JA, Kauffman CA. Pulmonary fungal infections. Respirology. 2012;17:913–26.
124. Suárez-Alvarez RO, Pérez-Torres A, Taylor ML. Adherence patterns of *Histoplasma capsulatum* yeasts to bat tissue sections. Mycopathologia. 2010;170:79–87.
125. Sun LM, Zhang CL, Li P. Characterization, antibiofilm, and mechanism of action of novel PEG-stabilized lipid nanoparticles loaded with terpinen-4-ol. J Agric Food Chem. 2012;60:6150–6.
126. Taff HT, Nett JE, Zarnowski R, Ross KM, Sanchez H, Cain MT, et al. A *Candida* biofilm-induced pathway for matrix glucan delivery: implications for drug resistance. PLoS Pathog. 2012;8:e1002848.
127. Tagliari L, Toledo MS, Lacerda TG, Suzuki E, Straus AH, Takahashi HK. Membrane microdomain components of *Histoplasma capsulatum* yeast forms, and their role in alveolar macrophage infectivity. Biochim Biophys Acta. 2012;1818:458–66.
128. Taraszkiewicz A, Fila G, Grinholc M, Nakonieczna J. Innovative strategies to overcome biofilm resistance. BioMed Res Int. 2013;2013:1–13. http://dx.doi.org/10.1155/2013/150653.
129. Thomas DP, Bachmann SP, Lopez-Ribot JL. Proteomics for the analysis of the *Candida albicans* biofilm lifestyle. Proteomics. 2006;6:5795–804.
130. Thevissen K, Pellens K, De Brucker K, François IE, Chow KK, Meert EM, et al. Novel fungicidal benzylsulfanyl-phenylguanidines. Bioorg Med Chem Lett. 2011;21:3686–92.
131. Tuon FF, Costa SF. *Rhodotorula* infection. A systematic review of 128 cases from literature. Rev Iberoam Micol. 2008;25:135–40.
132. Unal A, Koc AN, Sipahioglu MH, Kavuncuoglu F, Tokgoz B, Buldu HM, et al. CAPD-related peritonitis caused by *Rhodotorula mucilaginosa*. Perit Dial Int. 2009;29:581–2.
133. Uppuluri P, Chaturvedi AK, Srinivasan A, Banerjee M, Ramasubramaniam AK, Köhler JR, et al. Dispersion as an important step in the *Candida albicans* biofilm developmental cycle. PLoS Pathog. 2010;6:e1000828.
134. Vicentini AP, Gesztesi JL, Franco MF, de Souza W, de Moraes JZ, Travassos LR, et al. Binding of *Paracoccidioides brasiliensis* to laminin through surface glycoprotein gp43 leads to enhancement of fungal pathogenesis. Infect Immun. 1994;62:1465–9.
135. Vlamakis H. The world of biofilms. Virulence. 2011;2:431–4.
136. Walgren JL, Thompson DC. Application of proteomic technologies in the drug development process. Toxicol Lett. 2004;149:377–85.
137. Walsh TJ, Schlegel R, Moody MM, Costerton JW, Salcman M. Ventriculoatrial shunt infection due to *Cryptococcus neoformans*: an ultrastructural and quantitative microbiological study. Neurosurgery. 1986;18:373–5.
138. Williams P. Quorum sensing, communication and cross-kingdom signalling in the bacterial world. Microbiology. 2007;153:3923–38.
139. Xavier JB, Picioreanu C, Rani SA, van Loosdrecht MC, Stewart PS. Biofilm-control strategies based on enzymic disruption of the extracellular polymeric substance matrix—a modelling study. Microbiology. 2005;151:3817–32.
140. Zhao X, Oh SH, Yeater KM, Hoyer LL. Analysis of the *Candida albicans* Als2p and Als4p adhesins suggests the potential for compensatory function within the Als family. Microbiology. 2005;151:1619–30.

International Journal of Medical and Health Sciences Research

journal homepage: http://www.pakinsight.com/?ic=journal&journal=9

# GENETIC EVALUATION AND ACTIVITY OF ANTIFUNGAL AGAINST CLINICAL ISOLATES *CANDIDA ALBICANS* BIOFILMS

**Jaqueline Derissi Braz**

*Department of Clinical Analysis, Laboratory of Clinical Mycology, Faculty of Pharmaceutical Sciences, UNESP, Araraquara, Brazil*

**Nayla De Souza Pitangui**

*Department of Clinical Analysis, Laboratory of Clinical Mycology, Faculty of Pharmaceutical Sciences, UNESP, Araraquara, Brazil*

**Caetano Toshiro Yamashita**

*Department of Clinical Analysis, Laboratory of Clinical Mycology, Faculty of Pharmaceutical Sciences, UNESP, Araraquara, Brazil*

**Ana Marisa Fusco-Almeida**

*Department of Clinical Analysis, Laboratory of Clinical Mycology, Faculty of Pharmaceutical Sciences, UNESP, Araraquara, Brazil*

**Maria José Soares Mendes-Giannini**

*Department of Clinical Analysis, Laboratory of Clinical Mycology, Faculty of Pharmaceutical Sciences, UNESP, Araraquara, Brazil*

**Janaina De Cássia Orlandi Sardi**

*Department of Clinical Analysis, Laboratory of Clinical Mycology, Faculty of Pharmaceutical Sciences, UNESP, Araraquara, Brazil*

## ABSTRACT

*Candida yeasts are common in the oral cavity and can cause candidosis in the presence of predisposing factors, especially diabetes. The manifestation of the disease is related to this set of local factors such as the presence of dental prostheses, salivary pH, salivary flow and tobacco and the ability to form biofilms. Biofilms are specific and organized communities of cells under the control of signaling molecules rather than random accumulations of cells resulting from cell division and frequently are drugs resistance. Aim: The objectives of this study were to determine the genetic patterns of these C. albicans isolates and to evaluate the in vitro activity amphotericin B and caspofungin against C. albicans biofilms. Methods: Microbial samples were collected from subgingival sites and seeded in CHROMagar for subsequent identification of C. albicans by PCR. Genotypes were defined based on the identification of the transposable introns in the 25S rDNA by PCR. Results: In this study, 6 strains were identified as C. albicans and of these, 3 strains were*

*genotype A and 3 were genotype B. The results showed that both amphotericin B and caspofungin exhibited strong antifungal activities against C. albicans biofilm formation and inhibiting the biofilm formation ranging from 70.8 – 95.3% and 77.7 - 88.7%, respectively. The antifungals studied had low inhibitory effect on preformed biofims, ranging from 39.5 - 50.8% for amphotericin B and from 23.1 - 36.9% for caspofungin at the same concentration. The activity of the two drugs was most effective in inhibit biofilm formation.*



**Keywords:** *C. albicans*, Identification, Biofilm, Caspofungin, Amphotericin B, Resistance.

**Contribution/ Originality**

This study contributes in existent in literature, demonstrating that clinical isolates that deserve special attention in connection with the difficulty of treatment.

## 1. INTRODUCTION

*Candida* yeasts inhabit various ecosystems, including the oral cavity and participate as normal commensal microbiota without harming the host [1, 2]. However, systemic diseases like diabetes and AIDS, physiological conditions such as pregnancy, infancy or old age, nutritional factors, treatment with broad-spectrum antibiotics, immunosuppressive corticosteroids, in addition to local factors such use of prosthetic devices are conditions that predispose to the development of infections by *Candida* sp. [3] The mucosa is considered the main reservoir, but studies have shown that *C. albicans* aggregate seems to be contributing to bacterial biofilms in the formation of these structure and hindering the penetration of certain antimicrobial drugs. This fact may be an important factor in the manifestations of candidiasis and the colonization process periodontal pockets [4]. The ability to form biofilm is considered a potent virulence factor and various models have been proposed for understanding the mechanism of formation of these structures [5]. One of the most important consequences of the biofilm mode of growth is the marked resistance to many antifungal agents [6]. Caspofungin act as inhibitors of β-(1,3)-glucan synthesis in the fungal cell wall and have a favorable pharmacological profile. This study evaluated if amphotericin B and caspofungin are effective in the prevention and treatment of *C. albicans* biofilm isolated from patients with periodontitis and diabetes.

## 2. MATERIAL AND METHODS

This research was approved by the ethical committee for research of the Piracicaba Dental School, State University of Campinas, SP, Brazil.

### 2.1. Fungal Isolate

A total of 6 *Candida* spp. isolates were obtained from the subgingival biofilm of patients with chronic periodontitis and controlled insulin-dependent type 2 diabetes mellitus from the Faculty Clinic. Pooled biofilms from each site were separated in Eppendorf® microtubes containing 1mL of reduced transport fluid (RTF). Immediately after collecting, the samples from each site were diluted and plated onto a Sabouraud Dextrose Agar (SDA) with Chloramphenicol and chromogenic

medium (CHROMagar Candida®, Biomerieux, Paris, France) and incubated at 37°C for 48 h in aerobic condition. The green colonies grown on the agar plate were randomly selected and cultures were stored in glycerol stock at -20°C for later identification by PCR.

### 2.2. PCR (Polymerase Chain Reaction)

DNA from the *Candida* isolates was extracted using a protocol described by Nascimento, et al. [7] and quantified in a spectrophotometer at 260 nm (Genesys 10UV, Rochester, NY, USA) to obtain a standard concentration of 100 ng/mL and was stored at – 20°C for subsequent PCR reactions. DNA samples were identified by PCR using specific primers for the portion corresponding to the gene AAT1a (ID 3643468) (F: 5'ACT GCT CAA ACC ATC TCT GG -3' and R: 5' CAC AAG GCA AAT GAA GGA AT – 3' with fragment size of 472bp) of *C. albicans.* Sardi, et al. [8]. Purified DNA from *C. albicans* (ATCC 90028) was used as a positive control. This primer was designed specifically for *C. albicans*. The molecular mass ladder (100 bp DNA ladder, Gibco, Grand Island, NY, USA) was included for running in the agarose gel. PCR amplification was performed with a GeneAmp PCR system 2400 (Perkin-Elmer-Applied Biosystems) under the following thermal conditions: 72° C for 5 min, 38 cycles of 95° C for 30 s, 55°C for 45s and 72° C for 30 s and extension at 72°C for 5 min. The PCR products were separated by electrophoresis in 2% agarose gels and Tris-borate-EDTA running buffer (pH.8.0). The DNA was stained with 0.5ug ethidium bromide/mL and visualized under UV illumination (Pharmacia LKB-MacroVue, San Gabriel, CA, USA).

### 2.3. Genotyping

Ribosomal sequences are extensively used for genotyping of many fungal pathogens. The method developed by McCullough, et al. [9] uses a pair of primers designed to span the region that includes the site of the 1 intron transposable group of the 25S rRNA gene (rDNA), to classify *C. albicans* strains into three genotypes, according to the size of the PCR products: genotype A (approximately 450 bp), genotype B (approximately 840 bp), and genotype C (two products: approximately 450 and 840 bp). DNA of the yeasts previously extracted and spectrophotometrically quantified (100 ng/mL) was submitted to PCR reactions. PCR was performed using the primers CA-INT-L (5' ATA AAG GGA AGT CGG CAA ATA GAT CCG TAA – 3') and CA – INT- R (5' CCT TGG CTG TGG TTT CGC TAG ATA GTA GAT – 3'). The products were analyzed by electrophoresis through 3% (wt/vol) agarose gel. Bands were visualized by UV transllumination after ethidium bromide staining.

### 2.4. Biofilm Tests and Determination of Antifungal Activity on the Inhibition of Biofilms and On Pre-Formed Biofilms

The biofilm assays were performed according to Pierce, et al. [10] with some modifications. Yeasts were incubated in 20 ml of YPD medium at 30°C for 18 hours. Then we proceeded to wash the cells in phosphate buffered saline - (PBS). Subsequently, the cells were adjusted at a concentration of 1 x $10^7$/mL in RPMI. They were then dispensed 100 µL of this suspension in the wells of 96 microtiter wells. The plates were incubated in a bacteriological incubator, shaking at

37°C for 24 hours. Subsequently, the medium was aspirated and the supernatant plate was gently washed with PBS. The quantification of the biofilm assay was performed using the colorimetric method 2, 3-bis (2-methoxy-4-nitro-5-sulfo-phenyl)-2H-tetrazolium-5-carboxanilide (XTT) to see if there was the formation of biofilm. To determine the antifungal activity of caspofungin and amphotericin B, after the formation of biofilms were placed antifungal solutions (100 µL solution of antifungal agent) in serial dilution incubated at 37°C for 24 hours. The tests were performed in duplicate. After the incubation time, aspired to the drug and each well was washed three times with sterile PBS. Subsequently, placed in each well 100 µL of the dye XTT cell viability and the plates were incubated for 4 hours at 37 ° C. The reading was performed and quantified by ELISA (Enzyme-linked immunosorbent assay) to 490nm. The concentration of caspofungin ranged from 64 µg/mL to 0.0625 µg/mL and amphotericin B 16 µg/mL to 0.0312 µg/mL. For the inhibition of biofilm, the drug was placed with the inoculum and after 24 hours, the reading was performed. The diluition of the drugs was carried out in accordance with the microdilution method described according to the M27-S3 of the CLSI 2008, with modifications.

## 3. RESULTS

### 3.1. Identification of *C. albicans* by PCR

In this current study, 6 *Candida* spp. strains were obtained from the subgingival biofilm of patients with chronic periodontitis and controlled insulin-dependent type 2 diabetes mellitus, and isolated in CHROMagar. All were identified as *Candida albicans* by PCR.

### 3.2. Genotyping

A total of 6 strains isolated from patients with chronic periodontitis diabetics were submitted to molecular typing by the method described above. 50% were genotype A and 50% were genotype B. Genotype C was not found in this present study.

### 3.3. Biofilm Tests and Determination of Antifungal Activity on the Inhibition of Biofilms and On Pre-Formed Biofilms

All isolates were able to form biofilm. The results showed that both amphotericin B and caspofungin exhibited strong antifungal activities against *C. albicans* biofilm formation and inhibiting the biofilm formation ranging from 70.8 – 95.3% and 77.7 – 88.7%, respectively at concentration of 2µg/mL, as showed in Figure 2A and B. The antifungals studied had low inhibitory effect on preformed biofilms, ranging from 39.5 - 50.8% for amphotericin B and from 23.1 - 36.9% for caspofungin at the same concentration, as showed in Figure 2C and D.

## 4. DISCUSSION

In this current study, 6 *Candida* spp. strains were obtained from the subgingival biofilm of patients with chronic periodontitis and controlled insulin-dependent type 2 diabetes mellitus, and isolated in CHROMagar and were identified as *Candida albicans* by PCR. This isolates were submitted to molecular typing by the method described above. 50% were genotype A and 50% were genotype B. Genotype C was not found in this present study. The ability of *C. albicans* to

form biofilm is well established in literature [10, 11]. In our study, all isolates were able to form biofilm. In relation the action of the antifungal agents in biofilms, many studies have shown that biofilm formation impairs the action of conventional antifungals [5]. Our results showed that both amphotericin B and caspofungin exhibited strong antifungal activities against *C. albicans* biofilm formation and inhibiting the biofilm formation ranging from 70.8 – 95.3% and 77.7 – 88.7% respectively at concentration of 2µg/mL (Figure 2 A and B). The antifungals studied had low inhibitory effect on preformed biofilms, ranging from 39.5 to 50.8% for amphotericin B and from 23.1 to 36.9% for caspofungin at the same concentration (Figure 2C and D). There was no difference between the MICs of genotypes A and B. Tobudic, et al. [12] studied amphotericin B, and caspofungin in biofilms obtained MIC (minimum inhibitory concentration) of 4 µg/ml for both antifungals. The ability of *Candida* spp. to form drug-resistant biofilms is an important factor in its contribution to human disease. Like the vast majority of microbial biofilms [13], sessile cells within a *C. albicans* biofilm are less susceptible to antimicrobial agents than are planktonic cells [14, 15]. The formation of biofilms causes clinical problems of concern because they increase resistance to antifungal therapies; the mechanism of biofilm resistance to antimicrobial agents is not fully known. One hypothesis that can explain this resistance is the presence of the matrix, which restricts the penetration of drugs through the formation of a diffusion barrier [16] and only the most superficial layers are in contact with lethal doses of antibiotics. Cateau, et al. [17] found that micafungin has activity inhibitory excellent adhesion of *C. albicans* to catheters silicone prevents the development of biofilms on this substrate and eradicates the biofilm developed on 12 h, keeping this effect for 48 h, allowing the utility to consider potential for sealing intravascular catheters. Antibiofilm activity of echinocandins has also been check in various animal models or cellular [18], without found significant advantages in this activity with the combination caspofungin with other antifungals such as voriconazole [19, 20].

Jain, et al. [21] who found that biofilms of isolates obtained from urinary catheters showed a resistance to caspofungin and fluconazole, although they were inhibited by MIC50 < 1 ug/ml amphotericin B.

In this study, the activity of the two drugs was most effective in inhibited biofilm formation because it shows that the selected isolates have different contents of lipids and glucans in biofilm formation, probably showing that caspofungin in the case of the glucan synthase may be a key to the structure of biofilms.

## 5. CONCLUSION

In conclusion, our results showed that both antifungal agents can inhibit biofilm formation however in preformed biofilms of the same action is lower.

## REFERENCES

[1] P. Eggimann, J. Garbino, and D. Pittet, "Epidemiology of Candida species infections in critically ill non-immunosuppressed patients," *Lancet Infect Dis.*, vol. 3, pp. 685-702, 2003.

[2] L. C. Shao, C. Q. Sheng, and W. N. Zhang, "Recent advances in the study of antifungal lead compounds with new chemical scaffolds," *Yao Xue Xue Bao.*, vol. 42, pp. 1129-1136, 2007.

[3] CLSI, "Reference method for broth dilution antifungal susceptibility testing of filamentous fungi; approved standard-second edition. CLSI document M38-A2," *Clinica and Laboratory Standards Institute (formely NCCLS), 940 West Valley Road, Wayne, Pa*, 2008.

[4] J. Sardi, C. Duque, J. Höfling, and R. Gonçalves, "Genetic and phenotypic evaluation of Candida albicans strains isolated from subgingival biofilm of diabetic patients with chronic periodontitis," *Med Mycol.*, vol. 50, pp. 467-75, 2012.

[5] J. Chandra, D. Kuhn, P. Mukherjee, L. Hoyer, T. McCormick, and M. Ghannoum, "Biofilm formation by the fungal pathogen Candida albicans: Development, architecture, and drug resistance," *J Bacteriol. Sep.*, vol. 183, pp. 5385-94, 2001.

[6] F. Růzicka, V. Holá, M. Votava, and R. Tejkalová, "Importance of biofilm in Candida parapsilosis and evaluation of its susceptibility to antifungal agents by colorimetric method," *Folia Microbiol (Praha)*, vol. 52, pp. 209-14, 2007.

[7] E. Nascimento, R. Martinez, and A. Lopes, "Detection and selection of microsatellites in the genome of paracoccidioides brasiliensis as molecular markers for clinical and epidemiological studies," *J Clin Microbiol.*, vol. 42, pp. 5007-5014, 2004.

[8] J. Sardi, A. Fusco-Almeida, and M. Mendes-Giannini, "New antimicrobial therapies used against fungi present in subgingival sites – A brief review," *Arch Oral Biol.*, vol. 56, pp. 951-9, 2011.

[9] M. McCullough, K. Clemons, and D. Stevens, "Molecular and phenotypic characterization of genotypic Candida albicans subgroups and comparison with Candida dubliniensis and Candida stellatoidea," *J Clin Microbiol.*, vol. 37, pp. 417-421, 1999.

[10] C. Pierce, P. Uppuluri, A. Tristan, F. J. Wormley, E. Mowat, G. Ramage, and J. Lopez-Ribot, "A simple and reproducible 96-well plate-based method for the formation of fungal biofilms and its application to antifungal susceptibility testing," *Nat Protoc.*, vol. 3, pp. 1494-500, 2008.

[11] G. Ramage, E. Mowat, B. Jones, C. Williams, and J. Lopez-Ribot, "Our current understanding of fungal biofilms," *Crit Rev Microbiol.*, vol. 35, pp. 340-55, 2009.

[12] S. Tobudic, C. Kratzer, A. Lassnigg, W. Graninger, and E. Presterl, "In vitro activity of antifungal combinations against Candida albicans biofilms," *J Antimicrob Chemother., Feb). Epub 2009 Dec 8. PubMed PMID: 19996142*, vol. 65, pp. 271-4, 2010.

[13] R. Rajendran, D. P. Robertson, P. J. Hodge, D. F. Lappin, and G. Ramage, "Hydrolytic enzyme production is associated with Candida albicans biofilm formation from patients with type 1 diabetes," *Mycopathologia*, vol. 170, pp. 229-235, 2010.

[14] D. M. Kuhn and M. A. Ghannoum, "Candida biofilms: Antifungal resistance and emerging therapeutic options," *Curr Opin Investig Drugs*, vol. 5, pp. 186-197, 2004.

[15] R. Rautemaa and G. Ramage, "Oral candidosis--clinical challenges of a biofilm disease," *Crit Rev Microbiol.*, vol. 37, pp. 328-36, 2011.

[16] P. Gilbert, D. G. Allison, and A. J. McBain, "Biofilms in vitro and in Vivo: Do singular mechanisms imply cross-resistance?," *Symp Ser Soc Appl Microbiol.*, vol. 31, pp. 98-110, 2002.

[17] E. Cateau, M. Rodier, and C. Imbert, "In vitro efficacies of caspofungin or micafungin catheter lock solutions on Candida albicans biofilm growth," *J Antimicrob Chemother*, vol. 62, pp. 153-155, 2008.

[18] J. Shuford, K. Piper, J. Steckelberg, and R. Patel, "In vitro biofilm characterization and activity of antifungal agents alone and in combination against sessile and planktonic clinical Candida albicans isolates," *Diagn Microbiol Infect Dis.*, vol. 57, pp. 277-281, 2007.

[19] J. Shuford, M. Rouse, K. Piper, J. Steckelberg, and R. Patel, "Evaluation of caspofungin and amphotericin B deoxycholate against Candida albicans biofilms in an experimental intravascular catheter infection model," *J Infect Dis.*, vol. 194, pp. 710- 713, 2006.

[20] Q. Guillermo, y. María Villar-Vidal, and E. Elena, "Actividad de la micafungina contra las biopelículas de Candida," *Rev Iberoam Micol.*, vol. 26, pp. 49-55, 2009.

[21] N. Jain, R. Kohli, E. Cook, P. Gialanella, T. Chang, and B. Fries, "Biofilm formation by and antifungal susceptibility of Candida isolates from urine," *Appl Environ Microbiol.*, vol. 73, pp. 1697-1703, 2007.

**Figure-1.** *C. albicans* biofilms observed in optical microscope 40x.

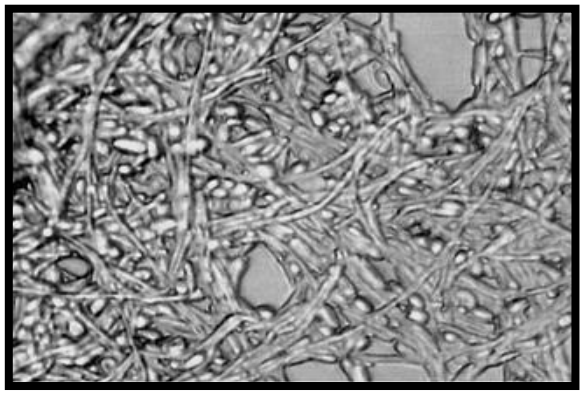

**Figure-2.** Activity of antifungal against clinical isolates *C. albicans* biofilms. Activity of amphotericin B **(A)** and caspofungin **(B)** in inhibiting the biofilm formation quantified by XTT. Activity of amphotericin B **(C)** and caspofungin **(D)** in preformed biofilm quantified by XTT.

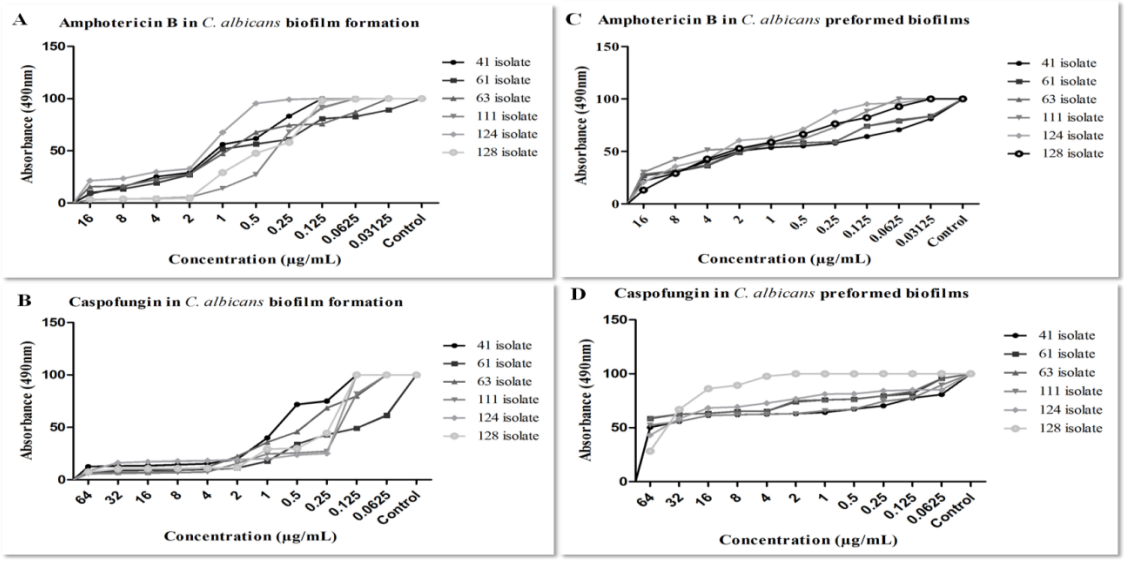

Hindawi Publishing Corporation
Evidence-Based Complementary and Alternative Medicine
Volume 2014, Article ID 957860, 9 pages
http://dx.doi.org/10.1155/2014/957860

*Research Article*

# Anti-*Trichophyton* Activity of Protocatechuates and Their Synergism with Fluconazole

**Luciana Arantes Soares,[1] Fernanda Patrícia Gullo,[1] Janaina de Cássia Orlandi Sardi,[1] Nayla de Souza Pitangui,[1] Caroline Barcelos Costa-Orlandi,[1] Fernanda Sangalli-Leite,[1] Liliana Scorzoni,[1] Luis Octávio Regasini,[2] Maicon Segalla Petrônio,[2] Patrícia Fernanda Souza,[2] Dulce Helena Siqueira Silva,[2] Maria José Soares Mendes-Giannini,[1] and Ana Marisa Fusco-Almeida[1,3]**

[1] *Laboratory of Clinical Mycology, Department of Clinical Analysis, Faculty of Pharmaceutical Sciences, UNESP, Rodovia Araraquara-Jaú, Km 1, 14801-902 Araraquara, SP, Brazil*
[2] *Institute of Chemistry, UNESP, Rua Professor Francisco Degni 55, 14800-900 Araraquara, SP, Brazil*
[3] *Department of Clinical Mycology, Faculty of Pharmaceutical Sciences, Universidade Estadual Paulista (UNESP), Rodovia Araraquara-Jaú, Km 1, 14801-902 Araraquara, SP, Brazil*

Correspondence should be addressed to Ana Marisa Fusco-Almeida; ana.marisa@uol.com.br

Received 17 February 2014; Revised 23 May 2014; Accepted 1 June 2014; Published 18 June 2014

Academic Editor: Mohd Roslan Sulaiman



Dermatophytosis and superficial mycosis are a major global public health problem that affects 20–25% of the world's population. The increase in fungal resistance to the commercially available antifungal agents, in conjunction with the limited spectrum of action of such drugs, emphasises the need to develop new antifungal agents. Natural products are attractive prototypes for antifungal agents due to their broad spectrum of biological activities. This study aimed to verify the antifungal activity of protocatechuic acid, 3,4-diacetoxybenzoic, and fourteen alkyl protocatechuates (3,4-dihydroxybenzoates) against *Trichophyton rubrum* and *Trichophyton mentagrophytes* and to further assess their activities when combined with fluconazole. Susceptibility and synergism assays were conducted as described in M38-A2 (CLSI), with modifications. Three strains of *Trichophyton rubrum* and three strains of *Trichophyton mentagrophytes* were used in this work. The pentyl, hexyl, heptyl, octyl, nonyl, and decyl protocatechuates showed great fungicidal effects, with minimum inhibitory concentration (MIC) values ranging from 0.97 to 7.8 mg/L. Heptyl showed a synergistic activity (FIC index = 0.49), reducing the MIC of fluconazole by fourfold. All substances tested were safe, especially the hexyl, heptyl, octyl, and nonyl compounds, all of which showed a high selectivity index, particularly in combination with fluconazole. These ester associations with fluconazole may represent a promising source of prototypes in the search for anti-*Trichophyton* therapeutic agents.

## 1. Introduction

Superficial fungal infections are a major global public health problem that affects 20–25% of the population worldwide [1]. Among these diseases, dermatophytosis, or tinea, is one of the most frequent fungal infections. This infection is caused by dermatophyte species that belong to the *Trichophyton, Microsporum,* or *Epidermophyton* genera [2]. These dermatophytes commonly invade different keratinophilic regions of the body, causing tinea corporis, tinea cruris, tinea pedis, tinea manus, tinea capitis, tinea barbae, and tinea unguium [3]. Dermatophyte infections can lead to either mild or severe symptoms, depending on the immunological response of the host [4]. Several patient groups also seem to be especially at risk of infection, including individuals with uncontrolled diabetes, AIDS, renal diseases, psoriasis, and types of immunosuppression, such as transplant recipients and patients on long-term corticosteroid therapy [5].

There is an urgent need to find new sources of substances with antidermatophytic activity because the treatment of

dermatophytosis is long and expensive, particularly in the case of onychomycosis. Furthermore, the spectrum of the available drugs is limited, such drugs may induce adverse effects, and several reports of antifungal resistance have been published [6–9]. For this reason, various antifungal agents have been introduced into clinical practice, among them, amorolfine, ciclopirox, griseofulvin, terbinafine, itraconazole, fluconazole, and more recently, voriconazole [10, 11]. However, efforts should be concentrated on the discovery and development of novel, safer, and effective antidermatophytic agents.

Protocatechuic acid (3,4-dihydroxybenzoic) is a phenolic compound produced by the secondary metabolism of plants. It is naturally present in almost all plant materials, including food, fruits, and vegetables [12–14]. Together with its natural and synthetic derivatives, it has been associated with a broad spectrum of biological actions and is known to have antioxidant, proapoptotic [15], anti-inflammatory, antiglycative [16], and antimelanogenic [17] functions. However, the major interest in protocatechuic acid and its derivatives is due to its antimicrobial properties. It has been reported that protocatechuic acids have activity against susceptible and antibiotic-resistant *Campylobacter* spp. and *Helicobacter pylori* [18, 19]. Furthermore, it has been shown that *n*-octyl 3,4-dihydroxybenzoate has fungicidal activity against *Saccharomyces cerevisiae* [20].

Thus, considering the broad spectrum of protocatechuates and the need for the discovery of new antifungal agents, this study aimed to investigate the antifungal activity of a synthetic homologous series of *n*-alkyl protocatechuates against *Trichophyton rubrum* and *Trichophyton mentagrophytes*. This study also aimed to investigate the chemical characteristics of the compounds responsible for the biological activity of dermatophytes, including the importance of free hydroxyl radicals and the size of the carbon side chain.

## 2. Methods

*2.1. Compounds Synthesis.* Synthetic compounds of protocatechuic acid were prepared as described by de Faria et al. [21], with minor modifications. Briefly, a 3 mL solution of *N*, *N*-dicyclohexylcarbodiimide (DCC, 1 mmol) in *p*-dioxane was added to a cooled (5°C) solution of 0.2 mmol protocatechuic acid (**1**) (Sigma-Aldrich, St. Louis, MO, USA) and 20 mmol of *n*-alkyl alcohols in 6 mL of *p*-dioxane. The solution was stirred for 48 h and the solvent was removed under reduced pressure. The residue was partitioned 3 times with EtOAc and filtered. The filtrate was washed successively with a saturated aqueous citric acid solution (3 times) and saturated aqueous $NaHCO_3$ (3 times), dried over anhydrous $MgSO_4$, and evaporated under reduced pressure. The crude products were purified over a silica gel column (0.06–0.20 mm, ACROS Organics, USA) and eluted isocratically with $CHCl_3$/MeOH (98 : 2) to produce esters **2**–**15**. Their structures were then established by $^1H$ and $^{13}C$ NMR spectral analysis. For the synthesis of compound **16**, protocatechuic acid (20 mmol) was dissolved in dried pyridine (5.0 mL) and anhydride acetic (5.0 mL) under a hydrogen atmosphere. The mixture was then stirred for 48 h at room temperature, dried under reduced pressure, and purified by column chromatography with a mixture of $CHCl_3$/MeOH (85 : 15) to produce product **16**. The NMR spectroscopic data for compound **16** were compatible with it being 3,4-diacetoxybenzoic acid.

*2.2. Microorganisms.* To evaluate its antifungal activity, six species of dermatophytes were tested: two clinical strains of *Trichophyton rubrum* (Tr1 and Tr2), *Trichophyton rubrum* ATCC MYA 3108, two clinical strains of *Trichophyton mentagrophytes* (Tm1 and Tm2), and *Trichophyton mentagrophytes* ATCC 40131 (Tm3). The microorganisms were obtained from the collection of the Clinical Mycology Laboratory of the Department of Clinical Analyses at the School of Pharmaceutical Sciences of Universidade Estadual Paulista (UNESP). The strains were cultivated on Sabouraud dextrose agar (Difco, BD Biosciences) and incubated at 28°C for 7–15 days. For all experiments, the strains were cultivated on Potato Dextrose Agar (Difco, BD Biosciences) and incubated at 28°C as described above or until sporulation.

*2.3. Dilution of Test Substances.* The dilution of the synthetic compounds was performed with DMSO (Synth, Diadema, Sao Paulo, Brazil) as described by Scorzoni et al. [22]. The concentrations of the compounds on 96-well plates (TPP, Trasadigen, Switzerland) ranged from 500 mg/L to 0.97 mg/L. The antifungal drugs were diluted according to the CLSI M38-A2 document [23]. Stock solutions of Fluconazole (Sigma-Aldrich, St. Louis, MO, USA) were prepared, considering its power. Serial twofold dilutions were prepared according to the recommendations of Zhang and collaborators [24], with some modifications.

*2.4. Minimum Inhibitory Concentration (MIC).* The antifungal activity tests were performed using the broth microdilution method as described in M38-A2, a document produced by the Clinical and Laboratory Standards Institute (CLSI, 2008) [23], with modifications. The medium used was RPMI 1640 with L-glutamine (Sigma-Aldrich, St. Louis, MO, USA) buffered to pH 7.0 with 0.165 M morpholinepropanesulfonic acid (MOPS) (Sigma-Aldrich, St. Louis, MO, USA), supplemented with 2% glucose. The cell suspension was prepared in a 0.85% saline solution. The suspension of conidia was then transferred to small sterile test tubes where they remained for 40 minutes to separate the microconidia, which were lighter and therefore present in the supernatant. The separated microconidia were then counted with a hematocytometer, and their concentration was adjusted to obtain a final concentration ranging from $2.5 \times 10^3$ to $5 \times 10^3$ CFU/mL. These suspensions were diluted in RPMI 1640 (Sigma-Aldrich, St. Louis, MO, USA) and inoculated on 96-well plates (TPP, Trasadigen, Switzerland) that had been previously prepared with the compounds diluted at concentrations from 250 to 0.48 mg/L. Positive (100 $\mu$L of RPMI medium with 100 $\mu$L of inoculum) and negative (200 $\mu$L of RPMI) controls were included in all experiments. The plates were incubated with agitation at 35°C for 7 days. The MIC reading was performed by spectrophotometry at 490 nm. For fluconazole, the MIC

was defined as the concentration that produced a 50% inhibition of fungal growth.

*2.5. Minimum Fungicide Concentration (MFC).* A qualitative analysis of the fungal viability was performed by transferring a portion of the wells to a plate with Sabouraud (Difco, BD Biosciences) medium and incubating it at 35°C for the time determined for each fungal agent. The MFC was defined as the lowest extract concentration that did not allow the growth of any fungal colonies on the solid medium after the incubation period [25]. A visual reading was performed to confirm the death or growth inhibition provided by fluconazole and the sixteen semisynthetic substances derived from protocatechuic acid.

*2.6. Synergistic Activity.* The drug activity was assessed using a checkerboard method derived from a standardised procedure established by the National Committee for Clinical Laboratory Standards (M38-A2) [23]. Briefly, the test was performed on the same medium used for susceptibility testing. Volumes of 50 $\mu$L of each drug in a concentration four times the final concentration were dispensed in 96-well plates (TPP, Trasadigen, Switzerland). To each well, 100 $\mu$L of the fungal suspension was added to produce a final concentration of $5.0 \times 10^3$ CFU/mL.

As a negative control, we used 200 $\mu$L of RPMI, while as a positive control, we used 100 $\mu$L of RPMI medium with 100 $\mu$L of inoculum. The plates were incubated at 35°C, and the reading was completed after 168 hours. We conducted visual and spectrophotometric readings at 490 nm. To determine the effect of combinatorial fractions, we calculated the fractional inhibitory concentration (FIC). The FIC was calculated by taking the MIC of the substance in combination/MIC of the substance alone. The sum of the fractional inhibitory concentration (FIC) of each substance consists of the fractional inhibitory concentration index: (the MIC of drug A in combination/the MIC of drug A alone) + (the MIC of drug B in combination/the MIC of drug B alone). A synergistic relationship was defined as FIC index $\leq 0.5$, an additive relationship was defined as $0.5 <$ FIC index $\leq 1.0$, an indifferent relationship was defined as $1.0 <$ FIC index $\leq 4.0$, and an antagonistic relationship was defined as FIC index $>4.0$ [26–28].

*2.7. Cytotoxicity Assay.* The cytotoxicity of sixteen semisynthetic compounds derived from protocatechuic acid was assessed using a sulphorhodamine B assay in NOK (oral human keratinocyte) cell lines obtained from the American Type Culture Collection (Manassas, VA, USA). The strains were maintained in bottles appropriate for cell culture with keratinocyte serum free medium (Gibco, Life Technologies) and incubated in standard conditions of 37°C and 5% $CO_2$. Cell concentrations ranging from 2.5 to $5.0 \times 10^4$ cells/mL were used for the formation of cell monolayers. The concentrations of pure substances were kept in contact with the cells for 24 hours. After the incubation period, the cells were treated with the sulphorhodamine B reagent (Sigma-Aldrich, St. Louis, MO, USA) as previously described by Skehan et al. [29], with some modifications.

*2.8. Statistical Analysis.* All experiments were performed in triplicate. Statistical analysis was performed with a *t*-test or one-way ANOVA with GraphPad Prism 5 software (Version 5, USA). $P$ values $< 0.05$ were considered statistically significant.

## 3. Results

*3.1. Antidermatophytic Activity.* Protocatechuic acid, 3.4 diacetoxibenzoic acid, and fourteen-alkyl protocatechuate (3,4-dihydroxybenzoate) derivatives were evaluated against 6 strains of *Trichophyton rubrum* and *Trichophyton mentagrophytes*. The minimum inhibitory concentration (MIC) ranged from ≥250 to 1.95 mg/L. Pentyl, hexyl, heptyl, octyl, nonyl, and decyl protocatechuate compounds showed the best MIC values, ranging from 1.95 to 7.8 mg/L for both species, with MFC values ranging from 1.95 to 15.6 mg/L and 0.97 to 15.6 mg/L, for *Trichophyton rubrum* and *Trichophyton mentagrophytes,* respectively (Table 1). In contrast, protocatechuic acid and acid 3.4 diacetoxybenzoate showed the highest values of MIC and MFC, from 125 to >250 mg/L, for both species and were thus considered to have low antidermatophytic activity. The potentiation of antifungal activity was observed with an increase of methylation in the structure of protocatechuic acid. However, the addition of nine methyl groups [$(CH_2)$ $9CH_3$] led to a progressive reduction in the MIC values. The addition of methyl groups produced a reduction in the MIC and MFC values for strains of both species. The addition of a methyl group ($CH_3$) produced a range of MIC and MFC values of 31.25 to 62.50 mg/L for the isolates of *Trichophyton rubrum* and *Trichophyton mentagrophytes*. The only exception was for Tm1 because despite its MIC of 62.50 mg/L, its MFC remained at 250 mg/L. Ethyl and propyl showed MIC and MFC values ranging from 15.62 to 62.50 mg/L for both species of dermatophytes. The addition of four methyl groupings (pentyl protocatechuate) produced a strong antifungal activity, as the MIC values were low, ranging from 3.90 to 7.80 mg/L, while the MFC ranged from 3.90 to 15.60 mg/L. Therefore, dodecyl, tetradecyl, hexadecyl, and octadecyl showed low activities, with their MIC and MFC values ranging from 125 to >250 mg/L for *Trichophyton rubrum* strains and from 31.25 and >250 mg/L for *Trichophyton mentagrophytes* strains.

*3.2. Synergistic Activity.* The activity of the combination of fluconazole with pentyl, hexyl, heptyl, octyl, and nonyl protocatechuates was evaluated and classified as antagonistic, indifferent, additive, and synergistic based on the FIC index, as shown in Table 2. The FIC index was calculated based on the results of the checkerboard test.

The combinations were tested in clinical isolates of *Trichophyton rubrum* (Tr1) and *Trichophyton mentagrophytes* (Tm1) and in the reference strain *Trichophyton mentagrophytes* ATCC 40131 (Tm3).

Table 1: MIC and MFC values (mg/L) and quantitative analysis of fungal cellular viability of protocatechuic acid derivates against *Trichophyton* spp.

| | R | Tr1 MIC (MFC) | Tr2 MIC (MFC) | Tr3 MIC (MFC) | Tm1 MIC (MFC) | Tm2 MIC (MFC) | Tm3 MIC (MFC) |
|---|---|---|---|---|---|---|---|
| Acid protocatechuic | H | 250 (250) | 250 (250) | 250 (250) | 250 (>250) | 250 (>250) | 125 (125) |
| Acid 3.4 diacetoxybenzoic | — | 250 (250) | >250 (>250) | >250 (>250) | 250 (250) | >250 (>250) | 250 (250) |
| Protocatechuate methyl | $CH_3$ | 62.5 (62.5) | 31.2 (31.2) | 31.2 (62.5) | 62.5 (250) | 62.5 (62.5) | 31.2 (62.5) |
| Protocatechuate ethyl | $CH_2CH_3$ | 31.2 (31.2) | 31.2 (31.2) | 31.2 (31.2) | 31.2 (62.5) | 31.2 (31.2) | 31.2 (125) |
| Protocatechuate propyl | $(CH_2)2CH_3$ | 15.6 (15.6) | 31.2 (31.2) | 31.2 (31.2) | 15.6 (62.5) | 62.5 (62.5) | 15.6 (31.2) |
| Protocatechuate butyl | $(CH_2)3CH_3$ | 15.6 (15.6) | 7.80 (7.80) | 7.80 (7.80) | 7.80 (62.5) | 15.6 (15.6) | 15.6 (15.6) |
| Protocatechuate pentyl | $(CH_2)4CH_3$ | **7.80 (7.80)** | **7.80 (7.80)** | **7.80 (7.80)** | **3.90 (15.6)** | **7.80 (7.80)** | **7.80 (7.80)** |
| Protocatechuate hexyl | $(CH_2)5CH_3$ | **3.90 (3.90)** | **1.95 (3.90)** | **3.90 (3.90)** | **1.95 (3.90)** | **3.90 (3.90)** | **3.90 (7.80)** |
| Protocatechuate heptyl | $(CH_2)6CH_3$ | **1.95 (1.95)** | **1.95 (1.95)** | **1.95 (1.95)** | **3.90 (3.90)** | **0.97 (0.97)** | **3.90 (3.90)** |
| Protocatechuate octyl | $(CH_2)7CH_3$ | **1.95 (1.95)** | **7.80 (7.80)** | **0.97 (1.95)** | **1.95 (3.90)** | **1.95 (1.95)** | **3.90 (3.90)** |
| Protocatechuate nonyl | $(CH_2)8CH_3$ | **1.95 (1.95)** | **3.90 (3.90)** | **1.95 (3.90)** | **3.90 (3.90)** | **3.90 (3.90)** | **3.90 (3.90)** |
| Protocatechuate decyl | $(CH_2)9CH_3$ | **3.90 (3.90)** | **3.90 (3.90)** | **3.90 (7.8)** | **7.80 (7.80)** | **3.90 (3.90)** | **3.90 (15.6)** |
| Protocatechuate dodecyl | $(CH_2)11CH_3$ | >250 (>250) | 125 (125) | >250 (250) | 250 (250) | 62.5 (62.5) | 31.2 (62.5) |
| Protocatechuate tetradecyl | $(CH_2)13CH_3$ | >250 (>250) | 125 (125) | >250 (>250) | >250 (>250) | 125 (250) | >250 (>250) |
| Protocatechuate hexadecyl | $(CH_2)15CH_3$ | >250 (>250) | >250 (>250) | >250 (>250) | >250 (>250) | >250 (>250) | >250 (>250) |
| Protocatechuate octadecyl | $(CH_2)17CH_3$ | >250 (>250) | >250 (>250) | >250 (>250) | >250 (>250) | >250 (>250) | >250 (>250) |

MIC: minimal inhibitory concentration; MFC: minimal fungicidal concentration; Tr1 and Tr2: *T. rubrum* clinical isolates; Tr3: *T. rubrum* ATCC MYA 3108; Tm1 and Tm2: *T. interdigitale* clinical isolates; and Tm3: *T. mentagrophytes* ATCC 40131.

Table 2: Activity of fluconazole combined with pentyl, hexyl, heptyl, octyl, and nonyl protocatechuates against *T. rubrum* and *T. mentagrophytes* (mg/L).

| | MIC (mg/L) | | | | | | | | | | | FIC index (association type) | | | | |
|---|---|---|---|---|---|---|---|---|---|---|---|---|---|---|---|---|
| | Substances alone | | | | | | Substances combined | | | | | | | | | |
| | FLU | **7** | **8** | **9** | **10** | **11** | FLU + **7** | FLU + **8** | FLU + **9** | FLU + **10** | FLU + **11** | FLU + **7** | FLU + **8** | FLU + **9** | FLU + **10** | FLU + **11** |
| Tr1 | 2.0 | 7.8 | 3.9 | 1.9 | 1.9 | 1.9 | 0.12$^{*}$—7.80 | 2.00—0.48$^{*}$ | 0.12$^{*}$—1.9 | 2.00—0.06$^{**}$ | 2.00—0.03$^{**}$ | 1.0 (A) | 1.1 (I) | 1.0 (A) | 1.0 (A) | 1.0 (A) |
| Tm1 | 1.0 | 3.9 | 1.9 | 3.9 | 1.9 | 3.9 | 1.00—0.03$^{**}$ | 1.00—0.03$^{**}$ | 1.00—0.03$^{**}$ | 1.00—0.03$^{**}$ | 1.00—0.03$^{**}$ | 1.0 (A) | 1.0 (A) | 1.0 (A) | 1.0 (A) | 1.0 (A) |
| Tm3 | 0.5 | 7.8 | 3.9 | 3.9 | 3.9 | 3.9 | 0.50—0.03 | 0.12—1.9$^{*}$ | 0.12—0.97$^{*}$ | 0.12—1.9$^{*}$ | 0.50—0.03 | 1.0 (A) | 0.72 (A) | 0.48 (S) | 0.72 (A) | 1.0 (A) |

MIC: minimal inhibitory concentration; FIC: fractional inhibitory concentration; S: synergistic effect; A: additive effect; I: indifferent effect Tr1: clinical strain of *T. rubrum*; Tm1: clinical strain of *T. mentagrophytes*; and Tm3: *T. mentagrophytes* ATCC 40131. $^{*}P < 0.05$; $^{**}P < 0.01$.

Table 3: Evaluation of $IC_{50}$ and selectivity index of pentyl, hexyl, heptyl, octyl, and nonyl in NOK cells.

| | Substances | Cytotoxicity $IC_{50}$ (mg/L) | SI ($IC_{50}$/MFC) | | | | | |
|---|---|---|---|---|---|---|---|---|
| | | | Tr1 | Tr2 | Tr3 | Tm1 | Tm2 | Tm3 |
| **7** | Pentyl | 57.0 | 7.3 | 7.3 | 7.3 | 3.7 | 7.3 | 7.3 |
| **8** | Hexyl | 66.5 | **17.0** | **17.0** | **17.0** | **17.0** | **17.0** | 8.5 |
| **9** | Heptyl | 78.1 | **40.0** | **40.0** | **40.0** | **20.0** | **80.5** | **20.0** |
| **10** | Octyl | 54.0 | **27.7** | 7.0 | **27.7** | **13.8** | **27.7** | **13.8** |
| **11** | Nonyl | 52.1 | **26.7** | **13.2** | **13.2** | **13.2** | **13.2** | **13.2** |

For the clinical isolates of *Trichophyton rubrum* (Tr1), the MIC value of fluconazole was 2.0 mg/L. When associated with the protocatechuate pentyl (compound **7**), a reduction in the MIC of fluconazole of 16.66 times (0.12 mg/L) ($P < 0.05$) and a conservation of the MIC of compound **7** (7.8 mg/L) were observed. The same occurred when fluconazole was associated with protocatechuate heptyl (substance **9**) ($P < 0.05$). Thus, both associations were classified as additive, with an FIC index of 1.0. The other acids tested showed a conservation of the fluconazole MIC (2.0 mg/L) ($P > 0.05$) and a reduction in the MIC value of protocatechuates. Compound **8** (hexyl protocatechuate) reduced the MIC value by a factor of 8.125 (0.48 mg/L) ($P < 0.05$). Compound **10** (octyl protocatechuate) reduced the MIC by a factor of 31.66 (0.06 mg/L) ($P < 0.01$), and compound **11** (nonyl protocatechuate) reduced the MIC by 63.33 times (0.03 mg/L) ($P < 0.01$). Thus, these combinations were classified as additive, with an FIC index of 1.0. The only exception was compound **8**, which had an FIC index of 1.1 and was thus classified as indifferent.

In the clinical isolate Tm1, the combination of fluconazole and all protocatechuates acids tested showed a conservation of the fluconazole MIC (1.0 mg/L) ($P > 0.05$) and a 130-fold reduction in the MIC values of the protocatechuates for substances **7**, **9,** and **11** (0.03 mg/L) ($P < 0.01$) and in 63.33 times for compound **8** and **10** (0.03 mg/L) ($P < 0.01$). All combinations were classified as additive for Tm1, with an FIC index value of 1.0. However, for the strain ATCC 40131 (Tm3), a conservation in the fluconazole MIC (0.5 mg/L) was observed when combined with compounds **7** and **11** ($P > 0.05$). The combination of the activity between these compounds was classified as additive, with an FIC index equal to 1.0. A reduction in the MIC values of two-, four-, and twofold, respectively, for substances **8**, **9,** and **10** ($P < 0.05$) was observed when combined with fluconazole. A fourfold reduction (0.12 mg/L) in the MIC value was observed when associated with these compounds ($P < 0.05$). The associations between fluconazole and compounds 8 and 10 were classified as additive and had an FIC index equal to 0.72, whereas the association with compound **9** instead had a synergistic activity, with an FIC index equal to 0.48.

*3.3. Cytotoxicity Assay.* The compounds pentyl (**7**), hexyl (**8**), heptyl (**9**), octyl (**10**), and nonyl (**11**) were evaluated in a cytotoxicity assay in NOK cells. These substances showed high values for $IC_{50}$ after reaching the necessary concentration to produce 50% lethality of 57 mg/L for cells treated with compound **7**, 66.5 mg/L for cells treated with compound **8**, 78.1 mg/L for cells treated with compound **9**, 54 mg/L for cells treated with compound **10,** and 52.1 mg/L for cells treated with compound **11**. These results showed that these compounds had a low toxicity in human oral keratinocytes (Table 3). The selectivity index (SI) was calculated for all six strains of *Trichophyton rubrum* and *Trichophyton mentagrophytes*. A selectivity index greater than 10 indicates a substance with a higher selectivity for fungi. Considering all six strains, compounds **9** and **11** had SI values greater than 10. The SI values for compounds **9** and **11** ranged from 20.0 to 80.5 and 13.2 to 26.7, respectively.

## 4. Discussion

It is estimated that superficial mycoses affect approximately 25% of the world's population [30]. Due to the high rate of recurrence of superficial fungal infections and the increasing problem of antifungal resistance, especially against the azole family of drugs, new treatment alternatives with fungicidal activity are sorely needed [31–33]. In this context, the anti-*Trichophyton* spp. activity of protocatechuic acid, 3,4-diacetoxibenzoic acid, and fourteen alkyl protocatechuates (3,4-dihydroxybenzoates) were evaluated on their own or in combination with fluconazole. In the sixteen compounds studied, significant antifungal activity was found. Remarkable results were observed in six compounds against the two species with pentyl, hexyl, heptyl, octyl, nonyl, and decyl compounds. These results showed that increasing the length of the side chain by up to 9 carbons enhanced both the hydrophobicity and thus the antifungal activity of the compounds. However, the addition of more than 9 carbons leads to a reduction in the antifungal activity. The same protocatechuic acid esters were used by de Faria et al. [21]. However, in their work, the antioxidant activity of those compounds was evaluated. They also reported that the alkylation process increased the hydrophobicity of these compounds, resulting in an increased inhibition of the oxidative process. Nihei and collaborators [20] evaluated the series of alkyl 3,4-dihydroxybenzoates (protocatechuates) and their fungicidal activity against the yeast *Saccharomyces cerevisiae*. Nonyl and octyl, 3,4-dihydroxybenzoates obtained the lowest values of MIC. In addition, the anti-*Saccharomyces* activity was also correlated with the hydrophobicity of the carbon chain. Thus, by analysing the structure-activity relationship of these compounds, we can conclude that the carbon chain has a key role not only in antioxidant activity, as described by de

Faria and collaborators [21], but also in the antifungal activity against *Trichophyton* spp.

Due to the lack of new classes of drugs or different molecular targets, drug combinations can be considered a strategy for therapy [34]. Several studies have proposed the use of natural compounds in combination with drugs to establish a new strategy for the treatment and prevention of certain diseases [35–38]. Different combinations of statins and some antifungal drugs were tested against four dermatophyte species (*Trichophyton mentagrophytes*, *Trichophyton rubrum*, *Microsporum canis*, and *Microsporum gypseum*). Most of the synergistic activity was found with the combination of statins with terbinafine and the different azoles [39]. Our results showed additive and synergistic activity of the protocatechuic acid derivatives with fluconazole against *Trichophyton rubrum* and *Trichophyton mentagrophytes*. We observed a synergistic activity of fluconazole associated with the heptyl derivative (**9**) when tested against Tm3, with a reduction in the MIC value of fluconazole and heptyl by four- and eightfold, respectively; an additive activity was observed for Tm1 and Tm3 with this combination. For the isolate Tr1, we observed additive activity with the association of pentyl, heptyl, octyl, and nonyl with fluconazole. For this isolate, the combination of a hexyl derivative (**8**) with this azole was found to not produce a change in its antifungal activity, such that this association was considered indifferent. All other combinations produced additive activity against the isolates tested. The great advantage of using phenolic compounds in combination with conventional therapies is that they can increase the susceptibly of microorganisms compared to the usual drugs and therefore are associated with reduced toxicity [38].

Palafox-Carlos and collaborators [40] reported an antioxidative synergistic effect between phenolic acids present in mango (*Mangifera indica* L.) and protocatechuic acid, gallic acid, vanillic acid, and chlorogenic acid. The authors found that the association showed a synergistic effect and that the gallic and protocatechuic acids presented higher antioxidative capacities. Jayaraman and collaborators [38] studied the combination of seven antibiotics and six phytochemical compounds, including protocatechuic acid, against isolates of *Pseudomonas aeruginosa* and found that the combination of protocatechuic acid and sulfamethoxazol showed synergistic activity against all bacterial isolates, with a fractional inhibitory concentration index of 0.25 to 0.5.

The efficacy of fluconazole can be improved using combination therapy [34]. Aala and collaborators [41] found good activity between allicin in combination with ketoconazole or fluconazole demonstrating a synergistic or additive interaction against dermatophytes. Galgóczy and coauthors [42] evaluated the *in vitro* antifungal activity against strains of dermatophytes, combining the protein (PAF) of *Penicillium chrysogenum* with fluconazole (FCZ). PAF and FCZ acted synergistically and/or additively on all of the tested fungi except *Microsporum gypseum*, for which no interactions were detected [42].

When the cytotoxicity of the substances was evaluated, high $IC_{50}$ values were found. The $IC_{50}$ indicates the concentration of the compound that is necessary to kill 50% of the cell line. The selective index was also calculated using the ratio of the $IC_{50}$ and MFC. For all of the isolates of the two species tested, most IS values of the substances were higher than 10, and the best results were found for the heptyl and nonyl derivatives. The IS values indicate that the concentrations tested caused injury to the fungal cells but no toxicity to the human cells [43–45].

Compounds not recognised as antifungal agents may cause potent inhibition of growth when used in combination with fluconazole. Our results suggest that the combination of substances can act with synergistic or additive activity in the treatment of dermatomycosis. More studies related to these combinations should be performed to identify a possible mechanism of action and to provide a verification of their *in vivo* activity. The evaluation of drug combinations defines a strategy for the discovery of new therapies, leading to a future clinical evaluation. In addition to the potent antidermatophytic capabilities, the protocatechuate derivatives presented a low toxicity to keratinocytes, demonstrating that the topical use of these novel compounds may represent a promising new option for the treatment of superficial mycoses.

## 5. Conclusion

In summary, new therapeutic trials are important to unravel biological data and thus result in the discovery of new combination drug. Overall, our results may contribute to a database of information on test susceptibility and synergism of dermatophytes *in vitro*, targeting the development and optimization of antifungal drugs. In the present work the esters of protocatechuic acid as well as their associations with commercial drug could be a promising therapeutic approach. More studies are needed to determine the mechanism of action of these substances providing the molecular basis of understanding.

## Conflict of Interests

The authors report no conflict of interests regarding the publication of this paper.

## Acknowledgments

The authors thank CAPES (Coordination for the Improvement of Higher Level) and PADC (Support Program for Scientific, Faculty of Pharmaceutical Sciences, UNESP) for their financial support.

## References

[1] S. Asticcioli, A. di Silverio, L. Sacco, I. Fusi, L. Vincenti, and E. Romero, "Dermatophyte infections in patients attending a tertiary care hospital in Northern Italy," *New Microbiologica*, vol. 31, no. 4, pp. 543–548, 2008.

[2] M. A. Yehia, T. S. El-Ammawi, K. M. Al-Mazidi, M. A. Abu El-Ela, and H. S. Al-Ajmi, "The spectrum of fungal infections with a special reference to dermatophytoses in the capital area of Kuwait during 2000–2005: a retrospective analysis," *Mycopathologia*, vol. 169, no. 4, pp. 241–246, 2010.

[3] H. Degreef, "Clinical forms of dermatophytosis (ringworm infection)," *Mycopathologia*, vol. 166, no. 5-6, pp. 257–265, 2008.

[4] S. R. Almeida, "Immunology of dermatophytosis," *Mycopathologia*, vol. 166, no. 5-6, pp. 277–283, 2008.

[5] G. Piérard, "Onychomycosis and other superficial fungal infections of the foot in the elderly: a pan-European survey," *Dermatology*, vol. 202, no. 3, pp. 220–224, 2001.

[6] A. K. Gupta, C. W. Lynde, G. J. Lauzon et al., "Cutaneous adverse effects associated with terbinafine therapy: 10 case reports and a review of the literature," *The British Journal of Dermatology*, vol. 138, no. 3, pp. 529–532, 1998.

[7] J. L. S. Carazo, L. O. Losada, and V. P. Sanjuan, "Current treatment of superficial mycosis," *Revista Iberoamericana de Micologia*, vol. 16, no. 1, pp. S26–S30, 1999.

[8] N. M. Martinez-Rossi, N. T. Peres, and A. Rossi, "Antifungal resistance mechanisms in dermatophytes," *Mycopathologia*, vol. 166, no. 5-6, pp. 369–383, 2008.

[9] D. A. Santos and J. S. Hamdan, "*In vitro* activities of four antifungal drugs against *Trichophyton rubrum* isolates exhibiting resistance to fluconazole," *Mycoses*, vol. 50, no. 4, pp. 286–289, 2007.

[10] C. B. Costa-Orlandi, G. M. Magalhães, M. B. Oliveira, E. L. S. Taylor, C. R. S. Marques, and M. A. de Resende-Stoianoff, "Prevalence of dermatomycosis in a Brazilian tertiary care hospital," *Mycopathologia*, vol. 174, no. 5-6, pp. 489–497, 2012.

[11] G. S. Njateng, D. Gatsing, R. S. Mouokeu, P. K. Lunga, and J. Kuiate, "*In vitro* and *in vivo* antidermatophytic activity of the dichloromethane-methanol (1:1 v/v) extract from the stem bark of *Polyscias fulva* Hiern (Araliaceae)," *BMC Complementary and Alternative Medicine*, vol. 13, article 95, 2013.

[12] A. Kanaujia, R. Duggar, S. T. Pannakal et al., "Insulinomimetic activity of two new gallotannins from the fruits of *Capparis moonii*," *Bioorganic and Medicinal Chemistry*, vol. 18, no. 11, pp. 3940–3945, 2010.

[13] R. Masella, C. Santangelo, M. D'Archivio, G. LiVolti, C. Giovannini, and F. Galvano, "Protocatechuic acid and human disease prevention: biological activities and molecular mechanisms," *Current Medicinal Chemistry*, vol. 19, no. 18, pp. 2901–2917, 2012.

[14] R. Merkl, I. Hrádková, V. Filip, and J. Šmidrkal, "Antimicrobial and antioxidant properties of phenolic acids alkyl esters," *Czech Journal of Food Sciences*, vol. 28, no. 4, pp. 275–279, 2010.

[15] M. C. Yin, C. C. Lin, H. C. Wu, S. M. Tsao, and C. K. Hsu, "Apoptotic effects of protocatechuic acid in human breast, lung, liver, cervix, and prostate cancer cells: potential mechanisms of action," *Journal of Agricultural and Food Chemistry*, vol. 57, no. 14, pp. 6468–6473, 2009.

[16] C. Y. Lin, C. S. Huang, C. Y. Huang, and M. C. Yin, "Anticoagulatory, antiinflammatory, and antioxidative effects of protocatechuic acid in diabetic mice," *Journal of Agricultural and Food Chemistry*, vol. 57, no. 15, pp. 6661–6667, 2009.

[17] T. H. Chou, H. Y. Ding, R. J. Lin, J. Y. Liang, and C. H. Liang, "Inhibition of melanogenesis and oxidation by protocatechuic acid from *Origanum vulgare* (oregano)," *Journal of Natural Products*, vol. 73, no. 11, pp. 1767–1774, 2010.

[18] M. C. Yin and C. Y. Chao, "Anti-*Campylobacter*, anti-aerobic, and anti-oxidative effects of roselle calyx extract and protocatechuic acid in ground beef," *International Journal of Food Microbiology*, vol. 127, no. 1-2, pp. 73–77, 2008.

[19] W. H. Liu, C. C. Hsu, and M. C. Yin, "*In vitro* anti-*Helicobacter pylori* activity of diallyl sulphides and protocatechuic acid," *Phytotherapy Research*, vol. 22, no. 1, pp. 53–57, 2008.

[20] K. Nihei, A. Nihei, and I. Kubo, "Rational design of antimicrobial agents: antifungal activity of alk(en)yl dihydroxybenzoates and dihydroxyphenyl alkanoates," *Bioorganic and Medicinal Chemistry Letters*, vol. 13, no. 22, pp. 3993–3996, 2003.

[21] C. M. de Faria, A. C. Nazaré, M. S. Petrônio et al., "Protocatechuic acid alkyl esters: hydrophobicity as a determinant factor for inhibition of NADPH oxidase," *Current Medicinal Chemistry*, vol. 19, no. 28, pp. 4885–4893, 2012.

[22] L. Scorzoni, T. Benaducci, A. M. Fusco-Almeida, D. H. S. Silva, V. da Silva BolzaniI, and M. J. S. M. Gianinni, "The use of standard methodology for determination of antifungal activity of natural products against medical yeasts *Candida* sp and *Cryptococcus* sp.," *Brazilian Journal of Microbiology*, vol. 38, no. 3, pp. 391–397, 2007.

[23] CLSI, *Reference Method for Broth Dilution Antifungal Susceptibility Testing of Filamentous Fungi, Approved Standard*, CLSI document M38-A2, Clinical and Laboratory Standards Institute, Wayne, Pa, USA, 2nd edition, 2008.

[24] J. Zhang, J. Chen, H. Q. Huang et al., "Comparison of a glucose consumption based method with the CLSI M38-A method for testing antifungal susceptibility of *Trichophyton rubrum* and *Trichophyton mentagrophytes*," *Chinese Medical Journal*, vol. 123, no. 14, pp. 1909–1914, 2010.

[25] F. Barchiesi, C. Silvestri, D. Arzeni et al., "*In vitro* susceptibility of dermatophytes to conventional and alternative antifungal agents," *Medical Mycology*, vol. 47, no. 3, pp. 321–326, 2009.

[26] G. M. Eliopoulos and C. T. Eliopoulos, "Abtibiotic combinations: should they be tested?" *Clinical Microbiology Reviews*, vol. 1, no. 2, pp. 139–156, 1988.

[27] R. L. White, D. S. Burgess, M. Manduru, and J. A. Bosso, "Comparison of three different *in vitro* methods of detecting synergy: time-kill, checkerboard, and E test," *Antimicrobial Agents and Chemotherapy*, vol. 40, no. 8, pp. 1914–1918, 1996.

[28] M. D. Johnson, C. MacDougall, L. Ostrosky-Zeichner, J. R. Perfect, and J. H. Rex, "Combination antifungal therapy," *Antimicrobial Agents and Chemotherapy*, vol. 48, no. 3, pp. 693–715, 2004.

[29] P. Skehan, R. Storeng, D. Scudiero et al., "New colorimetric cytotoxicity assay for anticancer-drug screening," *Journal of the National Cancer Institute*, vol. 82, no. 13, pp. 1107–1112, 1990.

[30] B. Havlickova, V. A. Czaika, and M. Friedrich, "Epidemiological trends in skin mycoses worldwide," *Mycoses*, vol. 51, supplement 4, pp. 2–15, 2008.

[31] G. Tchernev, P. K. Penev, P. Nenoff et al., "Onychomycosis: modern diagnostic and treatment approaches," *Wiener Medizinische Wochenschrift*, vol. 163, no. 1-2, pp. 1–12, 2013.

[32] A. K. Gupta and Y. Kohli, "Evaluation of *in vitro* resistance in patients with onychomycosis who fail antifungal therapy," *Dermatology*, vol. 207, no. 4, pp. 375–380, 2003.

[33] M. Ghannoum, N. Isham, A. Verma, S. Plaum, A. Fleischer Jr., and B. Hardas, "*In vitro* antifungal activity of naftifine hydrochloride against dermatophytes," *Antimicrobial Agents and Chemotherapy*, vol. 57, no. 9, pp. 4369–4372, 2013.

[34] E. H. Endo, D. A. Garcia Cortez, T. Ueda-Nakamura, C. V. Nakamura, and B. P. Dias Filho, "Potent antifungal activity of extracts and pure compound isolated from pomegranate peels and synergism with fluconazole against *Candida albicans*," *Research in Microbiology*, vol. 161, no. 7, pp. 534–540, 2010.

[35] D. F. Coutinho, I. H. Pashkuleva, C. M. Alves, A. P. Marques, N. M. Neves, and R. L. Reis, "The effect of chitosan on the *in vitro* biological performance of chitosan-poly (butylene succinate) blends," *Biomacromolecules*, vol. 9, no. 4, pp. 1139–1145, 2008.

[36] H. D. Coutinho, J. G. Costa, E. O. Lima, V. S. Falcão-Silva, and J. P. Siqueira, "Herbal therapy associated with antibiotic therapy: potentiation of the antibiotic activity against methicillin—resistant *Staphylococcus aureus* by *Turnera ulmifolia* L," *BMC Complementary and Alternative Medicine*, vol. 9, article 13, 2009.

[37] H. Coutinho, E. Matias, K. Santos et al., "Enhancement of the norfloxacin antibiotic activity by gaseous contact with the essential oil of *Croton zehntneri*," *Journal of Young Pharmacists*, vol. 2, no. 4, pp. 362–364, 2010.

[38] P. Jayaraman, M. K. Sakharkar, C. S. Lim, T. H. Tang, and K. R. Sakharkar, "Activity and interactions of antibiotic and phytochemical combinations against *Pseudomonas aeruginosa in vitro*," *International Journal of Biological Sciences*, vol. 6, no. 6, pp. 556–568, 2010.

[39] I. Nyilasi, S. Kocsub, K. Krizsan et al., "Susceptibility of clinically important dermatophytes against statins and different statin-antifungal combinations," *Medical Mycology*, vol. 52, no. 2, pp. 140–148, 2014.

[40] H. Palafox-Carlos, J. Gil-Chávez, R. R. Sotelo-Mundo, J. Namiesnik, S. Gorinstein, and G. A. González-Aguilar, "Antioxidant interactions between major phenolic compounds found in "Ataulfo" mango pulp: chlorogenic, gallic, protocatechuic and vanillic acids," *Molecules*, vol. 17, no. 11, pp. 12657–12664, 2012.

[41] F. Aala, U. Yusuf, A. Khodavandi, and F. Jamal, "*In vitro* antifungal activity of allicin alone and in combination with two medications against six dermatophytic fungi," *African Journal of Microbiology Research*, vol. 4, no. 5, pp. 380–385, 2010.

[42] L. Galgóczy, T. Papp, I. Pócsi, N. Hegedűs, and C. Vágvölgyi, "*In vitro* activity of *Penicillium chrysogenum* antifungal protein (PAF) and its combination with fluconazole against different dermatophytes," *Antonie van Leeuwenhoek*, vol. 94, no. 3, pp. 463–470, 2008.

[43] C. Bézivin, S. Tomasi, F. D. Lohezic-Le, and J. Boustie, "Cytotoxic activity of some lichen extracts on murine and human cancer cell lines," *Phytomedicine*, vol. 10, no. 6-7, pp. 499–503, 2003.

[44] M. Protopopova, C. Hanrahan, B. Nikonenko et al., "Identification of a new antitubercular drug candidate, SQ109, from a combinatorial library of 1,2-ethylenediamines," *Journal of Antimicrobial Chemotherapy*, vol. 56, no. 5, pp. 968–974, 2005.

[45] F. P. Gullo, J. C. O. Sardi, V. A. F. F. M. Santos et al., "Antifungal activity of maytenin and pristimerin," *Evidence-Based Complementary and Alternative Medicine*, vol. 2012, Article ID 340787, 6 pages, 2012.

Hindawi Publishing Corporation
Evidence-Based Complementary and Alternative Medicine
Volume 2014, Article ID 506273, 8 pages
http://dx.doi.org/10.1155/2014/506273

*Research Article*

# Antifungal Activity of Decyl Gallate against Several Species of Pathogenic Fungi

**Ana Carolina Alves de Paula e Silva,[1] Caroline Barcelos Costa-Orlandi,[1] Fernanda Patrícia Gullo,[1] Fernanda Sangalli-Leite,[1] Haroldo Cesar de Oliveira,[1] Julhiany de Fátima da Silva,[1] Liliana Scorzoni,[1] Nayla de Souza Pitangui,[1] Suélen Andrea Rossi,[1] Tatiane Benaducci,[1] Vanessa Gonçalves Wolf,[1] Luis Octávio Regasini,[2] Maicon Segalla Petrônio,[2] Dulce Helena Siqueira Silva,[2] Vanderlan S. Bolzani,[2] Ana Marisa Fusco-Almeida,[1] and Maria José Soares Mendes-Giannini[1]**

[1] *Departamento de Análises Clínicas, Faculdade de Ciências Farmacêuticas, Universidade Estadual Paulista Júlio Mesquita Filho (UNESP), Rodovia Araraquara-Jaú, km 1, 14 800 901 Araraquara, SP, Brazil*
[2] *Departamento de Química Orgânica, Instituto de Química, Universidade Estadual Paulista Júlio Mesquita Filho (UNESP), Rua Professor Francisco Degni, 55, Bairro Quitandinha, 14800-060 Araraquara, SP, Brazil*

Correspondence should be addressed to Ana Carolina Alves de Paula e Silva; ana_alpasi@hotmail.com and Maria José Soares Mendes-Giannini; gianninimj@gmail.com

Received 11 June 2014; Revised 13 October 2014; Accepted 28 October 2014; Published 20 November 2014

Academic Editor: José L. Ríos



This work aims to demonstrate that the gallic acid structure modification to the decyl gallate (G14) compound contributed to increase the antifungal activity against several species of pathogenic fungi, mainly, *Candida* spp., *Cryptococcus* spp., *Paracoccidioides* spp., and *Histoplasma capsulatum*, according to standardized microdilution method described by Clinical Laboratory Standard Institute (CLSI) documents. Moreover this compound has a particularly good selectivity index value, which makes it an excellent candidate for broad-spectrum antifungal prototype and encourages the continuation of subsequent studies for the discovery of its mechanism of action.

## 1. Introduction

In the last two decades, there has been a rapid increase in the incidence of invasive fungal infections (IFIs) caused by fungal pathogens with diminished susceptibility or resistance to many standard antifungal agents. The early treatment of IFIs is essential for optimal clinical outcomes. The effectiveness of standard antifungal drugs (polyenes, azoles, and echinocandins) is not predictable against some emerging fungi and may cause undesirable side effects. Furthermore, the use of antifungals is often inappropriate, exposing patients to adverse effects, drug interactions, and the development of resistance to and super infections by other fungi, reducing their effectiveness and resulting in significant health expenditures. All of these factors are particularly problematic for immunocompromised (IC) or hospitalized patients with serious underlying diseases [1–5]. Considering that the diagnosis of these diseases remains challenging and that treatment is suboptimal, it is difficult to identify and implement the correct therapies.

The use of modified substances from natural compounds as prototypes of molecules for the treatment of diseases has increased abundantly in recent years. However, many of these products have no proven efficacy and safety. The aim of this study was adding new results about the antifungal activity *in vitro* of 14 alkyl gallates against important pathogenic

fungi, mainly, *Candida parapsilosis*, *C. krusei*, *Cryptococcus gattii*, *Histoplasma capsulatum*, and *Paracoccidioides* spp. The literature presents several data about a wide range of biological activities, and its chemical structures have correlation with the antifungal activity and the cytotoxicity [6, 7]. Kubo et al. [8] made an important observation about the length and hydrophobicity of alkyl groups; to a large extent, these factors are associated with their antifungal activity. Because of the wide range of properties and commercial applications, alkyl gallates are compounds of great interest to both pharmaceutical and chemical industries [9]. Besides, we highlighted the decyl gallate role as a promising broad-spectrum antifungal.

## 2. Materials and Methods

*2.1. Microorganisms.* *C. albicans* ATCC 90028 (Ca), *C. krusei* ATCC 6258 (Ck), *C. parapsilosis* ATCC 22019 (Cp), *C. neoformans* ATCC 90012 (Cn), and *C. gattii* ATCC 56990 (Cg) were selected for the study. Four filamentous species were also used, including *T. mentagrophytes* ATCC 11481 (Tm), *T. rubrum* ATCC 28189 (Tr), *A. fumigatus* ATCC 7100 (Af), and *A. niger* ATCC 16404 (An). All species were obtained from the collection of Clinical Mycology Laboratory, School of Pharmaceutical Sciences, UNESP, Araraquara, São Paulo, Brazil. This study also included the dimorphic fungi *H. capsulatum* var. *capsulatum* EH-315 strain (Hc); *P. brasiliensis* isolates 18, D03, and 339 (belonging to the S1 phylogenetic species), isolate 02 (PS2 phylogenetic species), and isolate Epm83 (PS3 phylogenetic species); and *P. lutzii* strain 01 (ATCC MYA-826) and two isolates, EE and 8334MMT (origin is described in Acknowledgments).

*2.2. Susceptibility Tests.* The minimum inhibitory concentration (MIC; mg $L^{-1}$) was determined by the antifungal susceptibility test for all species, following the reference broth microdilution method, as outlined in the CLSI. The M27-A3 document [10] was used for yeast and dimorphic fungi species. For dimorphic fungi microdilution test was performed according to de Paula e Silva et al. [11]. The M38-A2 document [12] was used for filamentous species. The determination of the minimum fungicidal concentration (MFC; mg $L^{-1}$), which is the lowest concentration that did not allow the growth of any fungal colony on the solid medium after the incubation period, was performed as was done by Regasini et al. [13] and Gullo et al. [14]. For this an aliquot from the wells was transferred to a plate with Sabouraud medium (Sigma-Aldrich, St. Louis, MO, USA) and incubated at 37°C for the time determined for each species. All the tests were performed in triplicate and in three independents assays. The strain *C. krusei* ATCC 6258 was used also as a quality control for both tests.

The following antifungal drugs were used as controls: amphotericin B (AMB), itraconazole (ITZ), fluconazole (FLZ), terbinafine (TERB), and griseofulvin (GRIS; Sigma-Aldrich, St. Louis, MO, USA). All antifungal drugs were diluted according to the instructions of each CLSI document. The final dilutions and inoculum were in RPMI 1640 medium with L-glutamine without bicarbonate (Gibco; Grand Island, NT, USA) buffered to pH 7.0 with 0.165 M 3-*N*-morpholinopropanesulfonic acid (Sigma-Aldrich, St. Louis, MO, USA) with 2% glucose.

Table 1: Molecular structure of gallic acid (G1) and alkyl gallates (G2–G17).

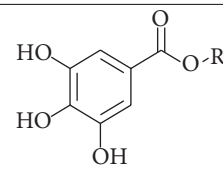


| | | | |
|---|---|---|---|
| R | G1 | Gallic acid | H |
| | G2 | Methyl gallate | $CH_3$ |
| | G3 | Ethyl gallate | $CH_2CH_3$ |
| | G4 | Propyl gallate | $(CH_2)_2CH_3$ |
| | G5 | Isopropyl gallate | $CH(CH_3)_2$ |
| | G6 | Butyl gallate | $(CH_2)_3CH_3$ |
| | G7 | Pentyl gallate | $(CH_2)_4CH_3$ |
| | G9 | Isobutyl gallate | $CH_2CH(CH_3)_2$ |
| | G10 | Hexyl gallate | $(CH_2)_5CH_3$ |
| | G11 | Heptyl gallate | $(CH_2)_6CH_3$ |
| | G12 | Octyl gallate | $(CH_2)_7CH_3$ |
| | G14 | Decyl gallate | $(CH_2)_9CH_3$ |
| | G15 | Undecyl gallate | $(CH_2)_{10}CH_3$ |
| | G16 | Dodecyl gallate | $(CH_2)_{11}CH_3$ |
| | G17 | Tetradecyl gallate | $(CH_2)_{13}CH_3$ |

*2.3. Preparation of Alkyl Gallates.* Alkyl gallates (Table 1) were synthesized as previously described by Morais et al. [15]. Five milligrams of each dried substance was diluted and solubilized aseptically in appropriate quantities of dimethylsulfoxide (DMSO; Sigma-Aldrich, St. Louis, MO, USA). The amount of DMSO used was previously tested and did not affect the fungal viability (data not shown). For the experiments, the concentration of each substance was calculated for a range of concentrations from 62.5 to 0.002 mg $L^{-1}$ by dilutions in RPMI 1640 medium in a microdilution plate; then the test was performed in accordance with the M27-A3 and M38-A2 documents.

*2.4. Cytotoxicity Tests.* The cellular cytotoxicity of the alkyl gallates was evaluated against lung tumor cells (A549) and normal fibroblast pulmonary cells (MRC-5), which were obtained from the American Type Culture Collection (Manassas, VA, USA). The cytotoxicity test was performed by MTT [16] using 3-(4,5-dimethyl-2-thiazolyl)-2,5-diphenyl-2*H*-tetrazolium bromide (Sigma-Aldrich, St. Louis, MO, USA) at 5 mg $mL^{-1}$. Spectrophotometric readings were taken from microplates in an ELISA reader (Bio-Rad model 3550) at a wavelength of 540 nm. Untreated cells constituted the positive control (viable cells), and cells treated with hydrogen peroxide (Sigma-Aldrich, St. Louis, MO, USA) constituted the negative control (death cells). All the tests were performed

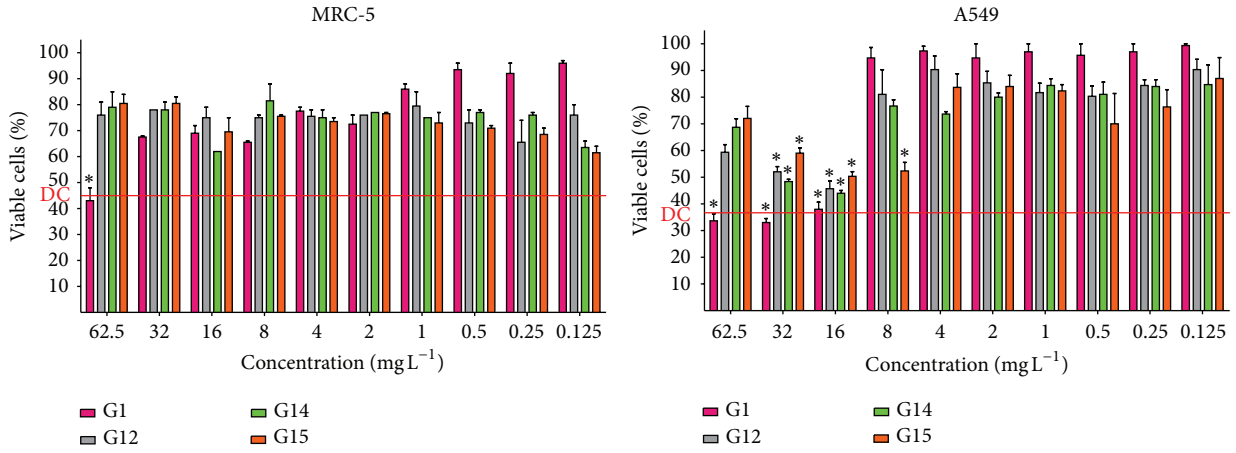


Figure 1: Cell viability tested in MRC-5 and A549 after treatment with different concentrations of gallic acid (G1), octyl gallate (G12), decyl gallate (G14), and undecyl gallate (G15). ∗ Indicates that there was no difference statistic ($P > 0.05$) in relation death control (red line represents the mean percentage of viable cells in the death control (DC)).

in triplicate in three independents assays. A test was performed on plates without cells to verify that the reaction cannot occur between alkyl gallates and the reagent to avoid false-positive results (data not shown). Statistical analysis was performed using 2-way ANOVA with Bonferroni post-test using GraphPAd Prism 5 software. $P$ values > 0.05 were considered statistically not significant in relation to the death control.

The $IC_{50}$ values of both cell lines were calculated in relation to G1 molecule and the best antifungal activity of alkyl gallate is the G14. This value represents the concentration required for 50% cell death (i.e., the concentration of each alkyl gallate that results in 50% absorbance reduction compared with untreated cells, termed the $IC_{50}$) [17]. The selective index (SI) was calculated to both cells lines, which is defined as the ratio of the measured $IC_{50}$ in the two cell lines to the MIC of the tested alkyl gallate (i.e., SI = $IC_{50}$/MIC). The SI was considered significant when >10 [18, 19].

## 3. Results

Table 2 shows the MICs of gallic acid (G1) and the alkyl gallates. These molecules correspond to esters with a different number of carbon chains (G2 to G17, as shown in Table 1). Depending on the fungi, the G1 MIC value varied from 4 to 62.5 mg L$^{-1}$ and the same results were observed for G2 to G11. In general, from the alkyl gallates G12 to G15, there was a decrease in the MIC, ranging from 2 to 16 mg L$^{-1}$, to the majority of fungal species, except to *Aspergillus sp.* and *C. krusei,* which presented value of 31 and >62.5 mg L$^{-1}$. There was an increase in the MIC value to the alkyl gallates G16 and G17. For the genus *Paracoccidioides*, G12 to G15 presented the lowest MICs for the majority of isolates (0.004 to 0.5 mg L$^{-1}$), and the G16 showed low MIC values (0.015 to 0.125 mg L$^{-1}$). The MIC value to *H. capsulatum* was 2 mg L$^{-1}$ for the G12 to G15 alkyl gallates.

Some of the best MICs of the alkyl gallates were similar to or lower than the MICs found for current therapeutic antifungal agents. *C. krusei* and *T. rubrum* are FLZ resistant strains with MIC of 64 mg L$^{-1}$ to these agents, and the G12 and G14 presented MICs of 4–8 mg L$^{-1}$. Most of the alkyl gallates showed MFC values similar to the MIC values. Nevertheless, G14 had the best MIC when it was evaluated against most fungal species.

*The cytotoxicity of gallic acid and the alkyl gallates* were *evaluated in respiratory* epithelial cells showing high cell viability to MRC5 and A549 cells line, revealing the low cytotoxicity of these compounds to both cell lines. Figure 1 shows the results of the cytotoxicity test when the cell lines were treated with G1 and the alkyl gallates G12, G14, and G15, that is, those that had the best antifungal activity against most fungi species tested in this study, and we could observe that these selected alkyl gallates showed low cytotoxicity to both cell lines. In this test, the viability percentage is considered satisfactory when it is above the mean percentage of death control. In Supplementary Material we present the results of the cytotoxicity test to all alkyl gallates used in this study (see Supplementary Material available online at http://dx.doi.org/10.1155/2014/506273).

Table 3 presents the $IC_{50}$ values of A549 and MRC-5 cell lines for G1 and G14. These alkyl gallates showed $IC_{50}$ values above the MICs and MFCs determined for the different fungi. The SI was also demonstrated in Table 3, and we could observe that G14 showed the greatest antifungal activity against the majority of fungal species and had higher SI values for both the MRC-5 and A549 cell lines.

## 4. Discussion

Gallic acid (GA) or 3,4,5-trihydroxybenzoic acid is a natural plant triphenol and it can be produced by acid hydrolysis of tannic acid. The substitution of the GA acid portion allows the obtainment of analogues esters with distinct physicochemical characteristics, especially lipophilicity that is evaluated by

Table 2: MICs/MFCs of gallic acid and alkyl gallates against different fungal species.

| | Ca | Ck | Cp | Cn | Cg | Tm | Tr | Afu | Ani | Hc | EE | 8334MMT | 01 | 18 | D03 | 339 | 02 | Emp83 |
|---|---|---|---|---|---|---|---|---|---|---|---|---|---|---|---|---|---|---|
| G1 | 62.5/# | 31/# | 31/# | 31/>62.5 | 31/>62.5 | 31/# | 16/# | >62.5/# | >62.5/# | 1/# | 8/# | >62.5/# | 4/# | 16/# | >62.5/# | 31/# | 4/# | 4/# |
| G2 | >62.5/# | >62.5/# | >62.5/# | >62.5/# | 16/>62.5 | 62.5/# | 62.5/# | >62.5/# | >62.5/# | 31/# | 4/# | 16/# | 2/# | 16/# | 16/# | 16/# | 16/# | 1/# |
| G3 | >62.5/# | >62.5/# | >62.5/# | >62.5/# | 16/>62.5 | 62.5/# | 62.5/# | >62.5/# | >62.5/# | 62.5/# | 8/# | 16/# | 1/# | 8/# | 4/# | 8/# | 16/# | 1/# |
| G4 | >62.5/# | >62.5/# | >62.5/# | >62.5/# | 16/>62.5 | 62.5/# | 31/# | >62.5/# | >62.5/# | 31/# | 2/# | 8/# | 1/# | 8/# | 2/# | 4/# | 4/# | 0.25/# |
| G5 | >62.5/# | >62.5/# | >62.5/# | 62.5/>62.5 | 16/>62.5 | 62.5/# | 31/# | >62.5/# | >62.5/# | 16/# | 2/# | 4/# | 2/# | 16/# | 2/# | 4/# | 4/# | 0.015/# |
| G6 | >62.5/# | >62.5/# | >62.5/# | 16/>62.5 | 8/>62.5 | 31/# | 16/# | >62.5/# | >62.5/# | 16/# | 2/# | 8/# | 2/# | 2/# | 2/# | 4/# | 4/# | 0.015/# |
| G7 | >62.5/# | >62.5/# | >62.5/# | 8/>62.5 | 4/>62.5 | 16/# | 16/# | >62.5/# | >62.5/# | 4/# | 0.5/# | 2/# | 0.25/# | 0.5/# | 0.25/# | 1/# | 1/# | 0.015/# |
| G9 | >62.5/# | >62.5/# | >62.5/# | 16/>62.5 | 4/>62.5 | 31/# | 31/# | * | * | 8/# | 4/# | 8/# | 1/# | 2/# | 1/# | 4/# | 2/# | 0.25/# |
| G10 | 62.5/# | 31/>62.5 | 31/# | 8/31 | 2/31 | 16/# | 8/# | >62.5/# | >62.5/# | 4/# | 0.5/# | 2/# | 0.25/# | 0.25/# | 0.25/# | 0.5/# | 2/# | 1/# |
| G11 | 16/31 | 31/# | 31/# | 2/16 | 1/16 | 4/# | 8/# | 62.5/# | 31/# | 2/# | 0.125/# | 0.25/# | 0.125/# | 0.125/# | 0.125/# | 0.03/# | 0.5/# | 0.25/# |
| G12 | 8/# | 8/# | 8/# | 2/8 | 1/8 | 8/# | 8/# | 31/# | 31/# | 2/# | 0.125/# | 0.25/# | 0.125/# | 0.015/# | 0.125/# | 0.015/# | 0.25/# | 0.015/# |
| G14 | 4/# | 4/31 | 4/# | 1/4 | 1/2 | 4/# | 8/# | 31/# | 8/# | 2/# | 0.03/# | 0.125/# | 0.125/# | 0.004/# | 0.125/# | 0.004/# | 0.004/# | 0.008/# |
| G15 | 2/# | 4/>62.5 | 2/4 | 1/4 | 0.5/4 | 4/# | 4/# | >62.5/# | >62.5/# | 2/# | 0.03/# | 0.03/# | 0.125/# | 0.015/# | 0.125/# | 0.008/# | 0.03/# | 0.015/# |
| G16 | 2/62.5 | 4/>62.5 | 4/16 | 1/4 | 1/4 | 4/# | 4/# | >62.5/# | >62.5/# | 4/# | 0.03/# | 0.03/# | 0.125/# | 0.125/# | 0.125/# | 0.06/# | 0.015/# | 0.5/# |
| G17 | 4/>62.5 | 4/>62.5 | 31/# | 1/16 | 0.5/4 | 4/# | >62.5/# | >62.5/# | >62.5/# | >62.5/# | 0.125/# | 0.25/# | 0.125/# | 0.25/# | 0.125/# | 0.125/# | 0.03/# | 0.06/# |
| **AMB** | **1** | **2** | **0.5** | **0.25** | **0.5** | * | * | **8** | **4** | **0.03** | **0.25** | **0.25** | **0.06** | **0.125** | **0.008** | **0.06** | **0.125** | **0.06** |
| **ITZ** | **0.5** | **0.5** | **0.25** | * | * | * | * | **>16** | **>16** | **0.03** | **0.008** | **0.03** | **0.008** | **0.015** | **0.015** | **0.015** | **0.008** | **0.015** |
| **FLZ** | **1** | **64** | **2** | **4** | **4** | **1** | **64** | * | * | **0.125** | * | * | * | * | * | * | * | * |
| **TERB** | * | * | * | * | * | **0.008** | **0.03** | * | * | * | * | * | * | * | * | * | * | * |
| **GRIS** | * | * | * | * | * | **0.5** | **1** | * | * | * | * | * | * | * | * | * | * | * |

#MFC = MIC, *compound not tested for this species.

Table 3: The $IC_{50}$ and SI values for both cell lines and all fungi species against gallic acid (G1) and decyl gallate (G14).

| | SI | | | |
|---|---|---|---|---|
| | G1 | | G14 | |
| | MRC-5 | A549 | MRC-5 | A549 |
| Ca | 0 | 0 | >10 | 2 |
| Ck | 0 | 0 | 2 | >10 |
| Cp | 0 | 0 | >10 | >10 |
| Cn | 0 | 0 | >10 | >10 |
| Cg | 0 | 0 | >10 | >10 |
| Tm | 0 | 0 | >10 | >10 |
| Tr | 0 | 0 | 6 | 9 |
| Af | 0 | 0 | 2 | 2 |
| An | 0 | 0 | 6 | 9 |
| Hc | 3 | 2 | >10 | >10 |
| EE | 0 | 0 | >10 | >10 |
| 8334MMT | 0 | 0 | >10 | >10 |
| 1 | 1 | 1 | >10 | >10 |
| 18 | 0 | 0 | >10 | >10 |
| D03 | 0 | 0 | >10 | >10 |
| 339 | 0 | 0 | >10 | >10 |
| 2 | 1 | 1 | >10 | >10 |
| Epm83 | 1 | 1 | >10 | >10 |
| $IC_{50}$ (mg $L^{-1}$) | 73 | 93 | 50 | 71 |

the partition coefficient, called alkyl gallates, according to the atom carbon number in the side chain [6, 7]. GA acts as an antiapoptotic agent and protects human cells against oxidative damage, as it has the ability to scavenge and reduce reactive oxygen species (ROS) formation [20]. The alkyl gallates, like methyl, propyl, octyl, and dodecyl gallates, have a wide range of biological activities, used in food manufacturing as antioxidants, as well as in the pharmaceutical and cosmetic industries, as well as antifungal [6, 21], antibacterial [22], antiviral [23], antitumoral [7], and antihemolytic activities [24]. Because of these several interesting properties and commercial applications, alkyl gallates are compounds of great interest to both pharmaceutical and chemical industries.

Our group showed MIC values equivalent to the values found by Leal et al. [6], which confirm the reproducibility of antifungal activity of the alkyl gallates, and brings new results with other important pathogenic fungi, as *C. parapsilosis*, *C. krusei*, *C. gattii*, *H. capsulatum*, and *Paracoccidioides* spp. Current increases of antifungal drug resistance in *Candida* spp. and clinical treatment failures are of concern, as invasive candidiasis is a significant cause of mortality in intensive care units [25]. Cryptococcosis is an important globally infectious disease. The majority of illness is among patients with defective cell-mediated immunity. The most common clinical presentation is *Cryptococci* meningitis, with over 1 million cases and 600,000 deaths per year [26]. Between the most commonly endemic mycoses described are paracoccidioidomycosis and histoplasmosis; both are difficult to diagnose, because of limiting factors as isolation conditions and sensitivity and specificity of microscopic examination of fluids and tissues which does not lead to immediate diagnosis, hindering successful subsequent treatments [27]. These difficulties constitute serious problems and underscore the need for a better understanding of the pathophysiology of different fungal infections, which could help to identify new targets of drug therapy and lead to the development of new antifungal agents [2, 3].

Then, to evaluate the susceptibility to gallic acid and alkyl gallates, 18 fungi species were assayed. G1 showed high MIC value for most isolates and the same results were observed for G2 to G11, suggesting that the esterification process in the original G1 molecule did not improve the antifungal activity. However, the esterification process for the formation of G12 to G15 showed MICs values significantly different; in other words, chains with eight to eleven carbons enhanced the antifungal activity. These findings indicate that this modification contributed positively to improvement of the antifungal activity of the compound. However, this pattern was not observed in G16 and G17 against most isolates. Instead, higher MICs values were recorded, suggesting a cutoff limit for the chain size.

There was not a change in the susceptibility among the alkyl gallates that presented antifungal activity and the species of same genus, but the MIC value found was considered low. This pattern was observed for *Candida* and *Cryptococcus* species, important yeasts more frequently in the last years in critically ill patients [25, 26]. These results confirm the hypothesis that these compounds can be better studied to find the unique compound against the majority of clinical importance fungi.

*Histoplasma capsulatum* showed constant MIC values to G12 to G15, which indicate that the chains with eight to eleven carbons have the same effect on this fungus, and the *Paracoccidioides* genus is more susceptible to alkyl gallates than the other fungal species tested. These results show that these compounds can be effective in cases of therapies with difficult diagnosis of specific species or genus. High susceptibility between the species *P. lutzii* and *P. brasiliensis* was observed suggesting the necessity of more studies about the mechanism action involved.

We agree with the conclusion presented by Leal et al. [6] that the activity can vary with the fungi tested, mainly between groups of fungi, and that the antifungal activity of alkyl gallates appears to be dependent on the presence of a catechol moiety along with a hydrophobic alkyl chain, similar to the activity of alkanols described by Kubo et al. [28].

Several studies suggest the mechanism of action involves these compounds. Fujita and Kubo [29] suggested by glucose-induced medium acidification method [30] that an alkyl gallate with nine carbons in the chain side causes damage in the cellular membrane including the plasma membrane, because this compound has three hydrophilic hydroxyl groups in the head of gallate acids and the hydrophobic alkyl chain in the tail, disturbing the stable structure of lipid membrane bilayers. The probable explanation is that hydroxyl groups would interact with hydrophilic groups thrusting on the membrane to form hydrogen binds. The nonpolar carbon chains are folded into the membrane bilayers, resulting in

a change of the membrane fluidity. This injury probably resulted in the leakage of potassium ions from fungi cells. This study also suggested that this alkyl gallate might achieve inner membrane of mitochondria, influencing mitochondrial functions related to ROS generation.

The development of an antifungal agent is considered challenging because potential targets can be shared by yeast and mammalian cells; both are eukaryotes and have some homologous metabolic pathways. The optimal antifungal agent should have a wide activity spectrum, have a fungicidal action rather than fungistatic action, be available for oral and parenteral use, be safe in the efficacious dose, have a great cost-effectiveness, and be stable to microbial resistance. Considering all these points, novel and selective molecular targets for the development of new antifungal agents with the goal of minimizing toxicity are of great importance.

In this sense, *in vitro* cytotoxicity assays are the first step to assess whether a compound with potential antifungal activity is promising to become a future antifungal agent. In this study, two lung cell lines were used for the cytotoxicity by MTT assay, since the majority of fungi tested are bound to the respiratory tract. Then, the cell viability for both lines remained greater than 50% at most of concentrations of G14 and the other two alkyl gallates, G12 and G15, considered with good antifungal activity, by the MTT assay.

MTT assay detects the decrease of viable cells number by the reduction of tetrazolium salt to formazan into living cells that occurs mainly through electron transfer at the mitochondrial level [16, 31]. There are in the literature several reports about the cytotoxicity of alkyl gallates. Locatelli et al. [7] described in a review that alkyl gallates are not cytotoxic against rat liver slices and/or nontumoral cell line (monkey kidney fibroblasts, VERO cells), normal mouse brain endothelial cells, human lymphocytes, or when administered in rats or mice.

Another factor to consider is the detachable selectivity index. The SI is an indication of the relative safety of a compound, where higher SI values reflect greater safety, once that this value is defined as the ratio of the $IC_{50}$ for the MIC value. In other words, the necessary concentration of the alkyl gallate to kill 50% of the health mammalians cells is higher than the concentration considered fungicide. Then SI will be greater than 10 because the values are inversely related. The ratio between the safety and potency of a compound is a very important parameter to consider in the development of therapeutic products [17, 32, 33]. Accordingly, the alkyl gallate G14 had better MIC values and presented an SI above 10 against most fungi, revealing that this alkyl gallate is safe. These data suggest the importance of more studies about the difference of action mechanism between the fungal and mammalian cells, searching for the explanation of the fact that an alkyl gallate with a ten-carbon chain had better activity than the others, with one carbon to more or less.

A point that should be emphasized in favor of this compound is that most of MIC values were similar to or lower than the values of standard antifungal agents, indicating the importance of these substances as promising antifungal agents. One of the major obstacles to antifungal therapy is toxicity, the associated high cost, the development of intrinsic resistance, or a reduced susceptibility to available antifungal agents.

Amphotericin B is considered the "gold standard" to mainstay of antifungal therapy because of its broad-spectrum activity and few cases of mycological resistance. However, it is associated with frequent and potentially serious adverse effects. The serious adverse effects led to the development of AmB formulations, which presented lower rates of nephrotoxicity, but the cost of these agents is substantial, and access is limited in resource-limited settings [34, 35]. On the other hand, the recent increases in *Candida* spp. resistance to echinocandins and azoles have led to clinical failures. This is a matter of concern because of the limited number of drug classes targeting different fungal components and because the number of patients at risk receiving treatment is continually growing, thus further increasing antifungal drug pressure [25]. In this sense, besides of the possibility of a treatment isolate with this alkyl gallate, a combinatory therapy of the alkyl gallate with the available antifungals agents can be an option that can lead to reduce the dose or improving the action of both antifungal agents.

In conclusion, in this preliminary study, among a series of 14 alkyl gallates, our group selected the decyl gallate that was considered to have the best antifungal activity for a wide variety of pathogenic fungi with clinical importance. These suggest how important the structure activity relationship is to obtain the best antifungal performance. It is a promising compound for further studies once the cytotoxicity tests were compatible with those already described in the literature, and the fungicide action mechanism is not prejudice to mammals cells, showing a SI that guarantees the safety required in this initial step.

## Conflict of Interests

The authors declare that there is no conflict of interests regarding the publication of this paper.

## Acknowledgments

This work was financially supported by the Brazilian organizations FAPESP, Conselho Nacional de Desenvolvimento Científico e Tecnológico (CNPq), and PADCFCF-UNESP. A. C. A. de Paula e Silva has a fellowship from CAPES. The authors are very grateful to Eduardo Bagagli from the Biosciences Institute of Botucatu, Universidade Estadual Paulista (UNESP), for kindly providing the *Paracoccidioides* isolates and to Maria Lucia Taylor from the Fungal Immunology Laboratory of the Department of Microbiology and Parasitology, School of Medicine, National Autonomous University of Mexico (UNAM), for kindly providing the *H. capsulatum* strain used in this study.

## References

[1] L. Ostrosky-Zeichner, "Invasive mycoses: diagnostic challenges," *American Journal of Medicine*, vol. 125, no. 1, pp. S14–S24, 2012.

[2] M. A. Pfaller and D. J. Diekema, "Epidemiology of invasive mycoses in North America," *Critical Reviews in Microbiology*, vol. 36, no. 1, pp. 1–53, 2010.

[3] M. H. Miceli, J. A. Díaz, and S. A. Lee, "Emerging opportunistic yeast infections," *The Lancet Infectious Diseases*, vol. 11, no. 2, pp. 142–151, 2011.

[4] A. Martín-Peña, M. Aguilar-Guisado, and J. M. Cisneros, "Does the current treatment of invasive fungal infection need to be reviewed?" *Enfermedades Infecciosas y Microbiología Clínica*, vol. 32, no. 8, pp. 523–528, 2014.

[5] S. C. A. Chen, E. G. Playford, and T. C. Sorrell, "Antifungal therapy in invasive fungal infections," *Current Opinion in Pharmacology*, vol. 10, no. 5, pp. 522–530, 2010.

[6] P. C. Leal, A. Mascarello, M. Derita et al., "Relation between lipophilicity of alkyl gallates and antifungal activity against yeasts and filamentous fungi," *Bioorganic & Medicinal Chemistry Letters*, vol. 19, no. 6, pp. 1793–1796, 2009.

[7] C. Locatelli, F. B. Filippin-Monteiro, and T. B. Creczynski-Pasa, "Alkyl esters of gallic acid as anticancer agents: a review," *European Journal of Medicinal Chemistry*, vol. 60, pp. 233–239, 2013.

[8] I. Kubo, P. Xiao, K.-I. Nihei, K.-I. Fujita, Y. Yamagiwa, and T. Kamikawa, "Molecular design of antifungal agents," *Journal of Agricultural and Food Chemistry*, vol. 50, no. 14, pp. 3992–3998, 2002.

[9] I. Kubo, N. Masuoka, T. J. Ha, K. Shimizu, and K.-I. Nihei, "Multifunctional antioxidant activities of alkyl gallates," *The Open Bioactive Compounds Journal*, vol. 3, pp. 1–11, 2010.

[10] M27-A3, *Reference Method for Broth Dilution Antifungal Susceptibility Testing of Yeast; Approved Standard*, Clinical and Laboratory Standards Intitute, Wayne, Pa, USA, 3rd edition, 2008.

[11] A. C. de Paula e Silva, H. C. Oliveira, J. F. Silva et al., "Microplate alamarblue assay for paracoccidioides susceptibility testing," *Journal of Clinical Microbiology*, vol. 51, no. 4, pp. 1250–1252, 2013.

[12] M38-A2, "Reference method for broth dilution antifungal susceptibility testing of filamentous fungi; approved standard-second edition," in *Clinical and Laboratory Standards Institute (CLSI)*, Clinical and Laboratory Standards Intitute, Wayne, Pa, USA, 2008.

[13] L. O. Regasini, M. Pivatto, L. Scorzoni et al., "Antimicrobial activity of *Pterogyne nitens* Tul., Fabaceae, against opportunistic fungi," *Revista Brasileira De Farmacognosia-Brazilian Journal of Pharmacognosy*, vol. 20, no. 5, pp. 706–711, 2010.

[14] F. P. Gullo, J. C. O. Sardi, V. A. F. F. M. Santos et al., "Antifungal activity of maytenin and pristimerin," *Evidence-Based Complementary and Alternative Medicine*, vol. 2012, Article ID 340787, 6 pages, 2012.

[15] M. C. C. Morais, S. Luqman, T. P. Kondratyuk et al., "Suppression of TNF-$\alpha$ induced NF$\kappa$B activity by gallic acid and its semi-synthetic esters: possible role in cancer chemoprevention," *Natural Product Research*, vol. 24, no. 18, pp. 1758–1765, 2010.

[16] T. Mosmann, "Rapid colorimetric assay for cellular growth and survival: application to proliferation and cytotoxicity assays," *Journal of Immunological Methods*, vol. 65, no. 1-2, pp. 55–63, 1983.

[17] M. Adamu, V. Naidoo, and J. N. Eloff, "Some Southern African plant species used to treat helminth infections in ethnoveterinary medicine have excellent antifungal activities," *BMC Complementary and Alternative Medicine*, vol. 12, article 213, 2012.

[18] R. Villar, E. Vicente, B. Solano et al., "In vitro and in vivo antimycobacterial activities of ketone and amide derivatives of quinoxaline 1,4-di-N-oxide," *Journal of Antimicrobial Chemotherapy*, vol. 62, no. 3, pp. 547–554, 2008.

[19] E. Vicente, S. Pérez-Silanes, L. M. Lima et al., "Selective activity against Mycobacterium tuberculosis of new quinoxaline 1,4-di-N-oxides," *Bioorganic and Medicinal Chemistry*, vol. 17, no. 1, pp. 385–389, 2009.

[20] L. A. Savi, P. C. Leal, T. O. Vieira et al., "Evaluation of anti-herpetic and antioxidant activities, and cytotoxic and genotoxic effects of synthetic alkyl-esters of gallic acid," *Arzneimittel-Forschung*, vol. 55, no. 1, pp. 66–75, 2005.

[21] S. Ito, Y. Nakagawa, S. Yazawa, Y. Sasaki, and S. Yajima, "Antifungal activity of alkyl gallates against plant pathogenic fungi," *Bioorganic and Medicinal Chemistry Letters*, vol. 24, no. 7, pp. 1812–1814, 2014.

[22] I. C. Silva, L. O. Regasini, M. S. Petrãnio et al., "Antibacterial activity of alkyl gallates against *Xanthomonas citri* subsp. *citri*," *Journal of Bacteriology*, vol. 195, no. 1, pp. 85–94, 2013.

[23] O. A. Flausino Jr., L. Dufau, L. O. Regasini et al., "Alkyl hydroxybenzoic acid derivatives that inhibit HIV-1 protease dimerization," *Current Medicinal Chemistry*, vol. 19, no. 26, pp. 4534–4540, 2012.

[24] V. F. Ximenes, M. G. Lopes, M. S. Petrônio, L. O. Regasini, D. H. Siqueira Silva, and L. M. da Fonseca, "Inhibitory effect of gallic acid and its esters on 2,2′-azobis(2- amidinopropane)hydrochloride (AAPH)-induced hemolysis and depletion of intracellular glutathione in erythrocytes," *Journal of Agricultural and Food Chemistry*, vol. 58, no. 9, pp. 5355–5362, 2010.

[25] D. Maubon, C. Garnaud, T. Calandra, D. Sanglard, and M. Cornet, "Resistance of *Candida* spp. to antifungal drugs in the ICU: where are we now?" *Intensive Care Medicine*, vol. 40, no. 9, pp. 1241–1255, 2014.

[26] D. J. Sloan and V. Parris, "*Cryptococcal meningitis*: epidemiology and therapeutic options," *Clinical Epidemiology*, vol. 6, no. 1, pp. 169–182, 2014.

[27] M. J. Buitrago, L. Bernal-Martínez, M. V. Castelli, J. L. Rodríguez-Tudela, and M. Cuenca-Estrella, "Histoplasmosis and paracoccidioidomycosis in a non-endemic area: a review of cases and diagnosis," *Journal of Travel Medicine*, vol. 18, no. 1, pp. 26–33, 2011.

[28] I. Kubo, H. Muroi, and A. Kubo, "Structural functions of antimicrobial long-chain alcohols and phenols," *Bioorganic & Medicinal Chemistry*, vol. 3, no. 7, pp. 873–880, 1995.

[29] K. Fujita and I. Kubo, "Plasma membrane injury induced by nonyl gallate in *Saccharomyces cerevisiae*," *Journal of Applied Microbiology*, vol. 92, no. 6, pp. 1035–1042, 2002.

[30] R. S. Haworth, E. J. Cragoe Jr., and L. Fliegel, "Amiloride and 5-(N-ethyl-N-isopropyl)amiloride inhibit medium acidification and glucose metabolism by the fission yeast *Schizosaccharomyces pombe*," *Biochimica et Biophysica Acta*, vol. 1145, no. 2, pp. 266–272, 1993.

[31] F. Sangalli-Leite, L. Scorzoni, A. C. Mesa-Arango et al., "Amphotericin B mediates killing in Cryptococcus neoformans through the induction of a strong oxidative burst," *Microbes and Infection*, vol. 13, no. 5, pp. 457–467, 2011.

[32] L. C. Albernaz, J. E. de Paula, G. A. S. Romero et al., "Investigation of plant extracts in traditional medicine of the Brazilian Cerrado against protozoans and yeasts," *Journal of Ethnopharmacology*, vol. 131, no. 1, pp. 116–121, 2010.

[33] T. F. F. Magalhães, C. M. da Silva, Â. de Fátima et al., "Hydroxyaldimines as potent in vitro anticryptococcal agents," *Letters in Applied Microbiology*, vol. 57, no. 2, pp. 137–143, 2013.

[34] S. Mistro, I. D. M. MacIel, R. G. de Menezes, Z. P. Maia, R. T. Schooley, and R. Badaró, "Does lipid emulsion reduce amphotericin B nephrotoxicity? A systematic review and meta-analysis," *Clinical Infectious Diseases*, vol. 54, no. 12, pp. 1774–1777, 2012.

[35] D. Ellis, "Amphotericin B: spectrum and resistance," *Journal of Antimicrobial Chemotherapy*, vol. 49, 1, pp. 7–10, 2002.

Hindawi Publishing Corporation
BioMed Research International
Volume 2015, Article ID 982429, 11 pages
http://dx.doi.org/10.1155/2015/982429

*Review Article*

# Could *Histoplasma capsulatum* Be Related to Healthcare-Associated Infections?

**Laura Elena Carreto-Binaghi,[1] Lisandra Serra Damasceno,[2] Nayla de Souza Pitangui,[3] Ana Marisa Fusco-Almeida,[3] Maria José Soares Mendes-Giannini,[3] Rosely Maria Zancopé-Oliveira,[2] and Maria Lucia Taylor[1]**

[1]*Departamento de Microbiología-Parasitología, Facultad de Medicina, Universidad Nacional Autónoma de México (UNAM), Circuito Interior, Ciudad Universitaria, Avenida Universidad 3000, 04510 México, DF, Mexico*
[2]*Instituto Nacional de Infectologia Evandro Chagas, Fundação Oswaldo Cruz (FIOCRUZ), Avenida Brasil 4365, Manguinhos, 21040-360 Rio de Janeiro, RJ, Brazil*
[3]*Departamento de Análises Clínicas, Faculdade de Ciências Farmacêuticas, Universidade Estadual Paulista (UNESP), Rodovia Araraquara-Jaú Km 1, 14801-902 Araraquara, SP, Brazil*

Correspondence should be addressed to Maria Lucia Taylor; luciataylor@yahoo.com.mx

Received 30 October 2014; Revised 12 May 2015; Accepted 12 May 2015

Academic Editor: Kurt G. Naber



Healthcare-associated infections (HAI) are described in diverse settings. The main etiologic agents of HAI are bacteria (85%) and fungi (13%). Some factors increase the risk for HAI, particularly the use of medical devices; patients with severe cuts, wounds, and burns; stays in the intensive care unit, surgery, and hospital reconstruction works. Several fungal HAI are caused by *Candida* spp., usually from an endogenous source; however, cross-transmission via the hands of healthcare workers or contaminated devices can occur. Although other medically important fungi, such as *Blastomyces dermatitidis*, *Paracoccidioides brasiliensis*, and *Histoplasma capsulatum*, have never been considered nosocomial pathogens, there are some factors that point out the pros and cons for this possibility. Among these fungi, *H. capsulatum* infection has been linked to different medical devices and surgery implants. The filamentous form of *H. capsulatum* may be present in hospital settings, as this fungus adapts to different types of climates and has great dispersion ability. Although conventional pathogen identification techniques have never identified *H. capsulatum* in the hospital environment, molecular biology procedures could be useful in this setting. More research on *H. capsulatum* as a HAI etiologic agent is needed, since it causes a severe and often fatal disease in immunocompromised patients.

## 1. Introduction

The term healthcare-associated infection (HAI) refers to infections associated with healthcare delivery in any setting (e.g., hospitals, long-term care facilities, ambulatory settings, and home care). This term reflects the inability to determine with certainty where the pathogen is acquired since patients may be colonized or exposed to potential pathogens outside the healthcare setting, before receiving healthcare or during healthcare delivery [1, 2].

In recent years, there has been an overall increase in HAI, which is likely a consequence of the advances in medical and surgical procedures related to specific therapies, in addition to the large number of immunocompromised patients who are hospitalized [3]. It is estimated that every day one out of 25 hospital patients has, at least, one HAI. In 2011, there were 722,000 HAI in the United States' hospitals and about 75,000 hospital patients with HAI died during their hospitalization. More than half of all HAI occurred outside the intensive care unit [4].

HAI commonly occur by direct transmission from individual to individual or through fomites manipulated by healthcare workers, as well as through surfaces and devices contaminated by biofilms (surgical instruments, catheters,

mechanical ventilation systems, and others) [5, 6]. Other mechanisms of transmission are aerial dispersion of opportunistic or environmental microorganisms and endogenous dissemination of commensal or opportunistic pathogens [7–9].

Although the role of the inanimate hospital environment in the spread of HAI has been controversial, nowadays molecular biology methodologies are being used to identify pathogens, measure the quality of environmental and hand hygiene over time, and establish a link between outbreaks and cross-transmission events, according to geographic and temporal variables [8].

Currently, changes in morbidity and mortality patterns due to aging of the world population, treatments with immunosuppressive drugs, and the use of invasive devices (particularly long-term ones) have led to a rise in the need of healthcare facilities for patients who are more susceptible to opportunistic infections [10]. Environmental disturbances associated with construction activities near health institutions pose additional airborne and waterborne disease threats for those patients who are at risk for healthcare-associated fungal infections [2]. Particularly, hospitalized patients could be exposed to infective fungal propagules such as microconidia and small hyphal fragments of *Histoplasma capsulatum* that thrive in bat and bird droppings, deposited in the surrounding hospital recreational areas.

Thus, the aims of this paper were to review the reported cases of *H. capsulatum* infections in healthcare settings, in order to propose the different factors that could be related to healthcare-associated histoplasmosis and discuss the features that could favor the presence of this fungus in the hospital environment.

## 2. Etiologic Agents of HAI

The etiologic agents of HAI are mainly bacteria (85%) and fungi (13%), in contrast to viruses and parasites that are rarely reported. Some environmental factors have been identified to increase the risk for fungal HAI, particularly the use of medical devices, like central venous and urinary catheters; the presence of severe cuts, wounds, and burns; stays in the intensive care unit, surgery, and hospital reconstruction works [4].

Host factors, such as extremes of age and underlying diseases, human immunodeficiency virus/acquired immune deficiency syndrome (HIV/AIDS), malignancy, and transplants, can increase susceptibility to infection, as well as a variety of medications that alter the normal flora, like antimicrobial agents, gastric acid suppressants, steroids, antirejection drugs, antineoplastic agents, and immunosuppressive drugs [2].

Most HAI associated with fungi are caused by *Candida* spp. These infections usually come from an endogenous source. However, cross-transmission via the hands of healthcare workers or contaminated devices can occur [11]. HAI outbreaks by other yeasts, such as *Malassezia* spp., *Saccharomyces* spp., and *Trichosporon* spp., have also been identified in newborns, patients with hematologic malignancies, and transplant recipients [12–18]. Mechanical ventilation, duration of hospital stay, prolonged use of intravascular catheters, parenteral lipid formulations, and prior exposure to broad spectrum antibiotics (including antifungal therapy) are important predisposing conditions identified in these outbreaks [13, 14, 16–18].

The occurrence of invasive fungal infections (IFIs) depends on several factors like the time of exposure to an infectious agent, the patient's immune status, the pathogen's virulence factors, and the host-pathogen interaction [19]. IFI associated with healthcare is mainly caused by opportunistic fungi, from endogenous or environmental sources, which form biofilms in fomites and abiotic surfaces [9].

Species of filamentous fungi, such as *Aspergillus* spp. [20, 21], *Rhizopus* spp. [22], *Rhizomucor* spp. [22, 23], *Absidia corymbifera* [22, 24], *Fusarium* spp. [25–27], *Paecilomyces* spp. [28, 29], *Curvularia* spp. [30], *Phialemonium* spp. [31–34], and *Scedosporium* spp. [35–37], have been particularly associated with HAI in patients with hematologic diseases. The most common sources reported in the above-mentioned filamentous fungal infections were contamination of medical supplies, like intravenous solutions, contact lens solutions [38, 39], bandages [24], pressure cuffs, and invasive devices (endotracheal tubes) [11, 21–23, 40]. Besides, other species of fungi such as *Aureobasidium* spp. [41], *Trichosporon* spp. [42, 43], *Rhodotorula* spp. [44–46], and *Phaeoacremonium parasiticum* [47] have been implicated in nosocomial pseudooutbreaks through contamination of endoscopes.

A very important opportunistic fungus, *Pneumocystis jirovecii*, has also been associated with HAI by person-to-person airborne transmission [48–58]. Infection by *P. jirovecii* presents as an interstitial pneumonia in immunocompromised hosts, particularly HIV patients; in this group, pneumocystosis is considered an AIDS-definitory condition, when CD4+ T lymphocytes are below 200 cells/$\mu$L [59]. Currently, an increase of pneumocystosis in non-HIV patients is being observed, especially in patients with transplants, individuals with autoimmune disorders or malignancies, and those using immunosuppressive treatments, like steroids and immunobiological drugs [50, 55, 60–62]. Molecular biology techniques have detected a high prevalence of colonization (10–55%) in immunocompromised patients and in the general population. Individuals colonized by *P. jirovecii* can be considered reservoirs and therefore contribute to the transmission of this pathogen among immunosuppressed patients in the hospital environment [62].

Other important respiratory pathogens, such as *Blastomyces dermatitidis*, *Paracoccidioides brasiliensis*, and *H. capsulatum*, have never been associated with infections in the hospital environment; however, *B. dermatitidis* has been found in pseudooutbreaks associated with contaminated bronchoscopes [63].

## 3. *H. capsulatum* Infection

*H. capsulatum* is a dimorphic fungus with a mycelial saprobe-geophilic morphotype (infective M-phase), usually found in bat and bird guano, and a yeast morphotype (parasitic and virulent Y-phase) preferentially located within phagocytes. Infection occurs through inhalation of aerosolized M-phase

propagules, mainly microconidia and hyphal fragments, accumulated in confined spaces usually inhabited by bats or birds [64].

There are eight genetic populations of *H. capsulatum* distributed worldwide [65], between the latitudes 54° North [66] and 38° South [67], suggesting a broad geographic dispersion of the pathogen. *H. capsulatum* has been found in ecological niches with special conditions: air and soil temperatures (18–28°C), humidity (>60%), and darkness (fosters sporulation). Particularly, this fungus needs the presence of high concentrations of nitrogen and phosphorus for the M-phase growth, in addition to other micronutrients, which are plentiful in bat or bird guano [64, 68–70]. Besides, this fungus' ubiquitous distribution in nature (soil, treetops, yards, and public parks, among others) makes it feasible to find the M-phase in open spaces, either in rural or urban areas around hospitals [64, 70]. In a large outbreak that occurred in Acapulco, Mexico, the presence of the fungus was revealed in ornamental potted plants, containing organic material known as compost supplemented with bat guano that is used as fertilizer [70].

Histoplasmosis is a systemic mycosis preferentially distributed in endemic areas of the Americas. Most *H. capsulatum* infections are asymptomatic. A low number of individuals develop pneumonia, which is the main clinical form in immunocompetent patients (primary pulmonary histoplasmosis) with distinctive histopathological features, like chronic granulomatous infiltrate [69]. Epidemic outbreaks of histoplasmosis are related to occupational exposure or recreational activities and affect individuals worldwide [66, 71–73]. However, this disease is one of the most common opportunistic infections among HIV/AIDS patients with CD4+ T lymphocytes below 150 cells/$\mu$L (known as AIDS-definitory condition), who may develop severe and fatal disseminated histoplasmosis [59]; approximately 30% of these patients die from this infection [74–76]. *H. capsulatum* infections have also been described in patients with transplants [77, 78], invasive devices, and/or surgical implants [79–81].

*H. capsulatum* shares some features with the etiologic agents of HAI, bacteria or fungi, which support the nosocomial involvement of *H. capsulatum* infection: worldwide distribution (facilitated by flying reservoirs), its ubiquity, production of aerosolized infective propagules that spread the fungus in the environment and favor the infection by the respiratory pathway, development of biofilm and quorum-sensing (QS) events, and opportunistic behavior in immunosuppressed hosts.

## 4. Biofilm Formation

It is estimated that 95% of the microorganisms found in nature are attached in biofilms [82]. Over 60–65% human infections involve the formation of biofilms by normal commensal flora or nosocomial pathogens [83–89]. A biofilm is a complex structured community of microorganisms, surrounded by an extracellular matrix of polysaccharides, adhering to each other over a surface or interface [82]; sometimes protein-like adhesins of the pathogen are also involved in biofilm formation [90]. Biofilms constitute a potential source of chronic, recurrent infections and cross-contamination events [7, 89]. Microorganisms in biofilms are protected from the host's immune system and may be 1,000-fold more resistant to antibiotics than planktonic cells [91], due to poor penetration of drugs, low growth rate, and development of the microorganism's resistant phenotypes within biofilms [84, 92].

Fungal biofilms have been found not only in wild soil and water, but also in urban environments, like piping systems, water reservoirs, and constructions, and in healthcare equipments [8, 85, 93–96]. Among the fungal biofilms found on these surfaces, the medically important fungi, such as *Candida* spp., *Aspergillus* spp., *Cryptococcus* spp., *Rhodotorula* spp., *Penicillium* spp., *Sporothrix* spp., *Acremonium* spp., and *Paecilomyces* spp., must be highlighted [8, 90, 93–98].

In medical devices, *Candida* spp. is the most common fungi associated with biofilm formation, usually with endovascular and urinary catheter-related infections in intensive care units, resulting in invasive candidiasis with high mortality [99–101]. The distribution of *Candida* species is variable and in recent years non-*albicans Candida* species have been frequently found in patients with hemodialysis catheter-related candidemia [102].

The presence of biofilms has also been described in ventriculoperitoneal (VP) shunts in patients with *Candida* spp., *Cryptococcus neoformans,* and *Coccidioides immitis* meningoencephalitis. These biofilms were associated with recurrent peritonitis and meningitis [88, 103]. Various fungi have been able to form biofilms on abiotic surfaces in experimental models, such as *A. fumigatus* [104], *M. pachydermatis* [105], *Blastoschizomyces capitatus* [106], *Candida* spp. [107], *Pneumocystis* spp. [108], *Rhodotorula* spp. [109, 110], *C. neoformans* [111], *S. cerevisiae* [112], *Fusarium* spp. [113], *T. asahii* [114], and zygomycetes [115].

Epidemiological surveillance definitions of HAI include surgical site infections associated with surgical implants or medical indwelling devices, when they occur within 30–90 days after the surgical procedure [4]. Clinically, *H. capsulatum* infections have been identified in individuals with invasive devices or surgical implants, and some authors have described endovascular histoplasmosis in patients with vascular prosthetic or synthetic implants [80, 81, 116–119]. Usually, the diagnosis is made by isolation of the fungus in vegetation or over synthetic materials. In addition, histopathological observation has revealed fibrin, large aggregates of yeast cells, mild chronic inflammatory cell infiltrates (predominantly macrophages) [80, 116, 118], and *H. capsulatum* hyphae (M-phase) in a few cases [117]. Furthermore, *H. capsulatum* endocarditis has also been described in native heart valves [118–120]. The aforementioned factors suggest the ability of *H. capsulatum* Y-phase to form biofilms in vivo (human solid organs and medical devices). Recently, it was described that *H. capsulatum* is able to form biofilms on abiotic surfaces [121]. Besides, *H. capsulatum* yeasts have been found clustered in the cells of bats' spleen, lung, and liver and in the lamina propria of intestine villi [122].

There are some reports of *H. capsulatum* peritonitis associated with infected catheters in patients with end-stage renal disease under continuous ambulatory peritoneal dialysis [123–128]. All of these peritoneal histoplasmosis'

cases occurred in residents from an endemic area, in a period longer than 90 days, in contrast with the epidemiological definition of HAI. Thus, continuous exposure to the fungus' infective M-phase propagules appears to be an important risk factor, since no other epidemiological feature could be associated with these cases.

Veeravagu et al. [129] reported a case of *H. capsulatum* meningitis associated with a VP shunt that was diagnosed two days after surgery. It is noteworthy that the patient did not come from an endemic area. Furthermore, *H. capsulatum* was isolated from the VP shunt tip and the surgical instruments, so this could be considered a nosocomial histoplasmosis.

Currently, it is unknown if *H. capsulatum* is able to form biofilms in its filamentous form, which could contaminate hospital environments, medical devices, and supplies, facilitating the direct inoculation of the infective form through cross-contamination. However, it is not a farfetched idea, because biofilms have been described in filamentous fungi, such as *Aspergillus* spp. [104] and zygomycetes [115].

## 5. Quorum Sensing (QS)

QS is a mechanism of microbial communication dependent on cell density that can regulate several behaviors in bacteria, such as secretion of virulence factors, biofilm formation, survival, and bioluminescence. Fungal QS systems were first described in the pathogenic fungus *C. albicans*, with important signaling molecules, called farnesol and tyrosol (alcohols derived from aromatic amino acids), which control fungal growth, morphogenesis, and biofilm formation, inducing detrimental effects on host cells and other microbes. The concentration of these alcohols increases proportionally to the microbial population and, after reaching a critical threshold, a regulatory response is triggered leading to the coordinated expression or repression of QS-dependent target genes in the entire microbial population [130].

QS activities have also been described in other fungi, such as *H. capsulatum* [131], *Ceratocystis ulmi* [132], and *Neurospora crassa* [133]; however, the molecules responsible for such activities have not yet been purified. In *H. capsulatum*, regulation of $\alpha$-(1,3)-glucan synthesis in the Y-phase cell wall has been shown to occur in response to cell density [134].

Albuquerque and Casadevall [130] proposed that fungal QS molecules are not only a product of fungal catabolism, but they should have some characteristics: to accumulate in the extracellular environment during fungal growth at a concentration proportional to the population cell density restricted to a specific stage of growth, to induce a coordinated response in the entire population once a threshold concentration is reached, and to reproduce the QS phenotype when added exogenously to the fungal culture. More research about these molecules is needed to elucidate the QS mechanisms in each fungus model, involving different pathogenic events, including biofilm formation.

## 6. *H. capsulatum* Infection in Drug-Induced Immunocompromised Individuals

IFIs related to immunosuppression caused by drugs in patients with transplant occur because cellular immunity is modified, usually within the first six months posttransplant. During this period, the IFI acquired an opportunistic nature and emerged as HAI [135–137]. After six months posttransplant, patients usually remain stable and continue receiving immunosuppressive drugs at low doses. Thus, they are susceptible to common infections acquired in the community [79, 135–137].

*H. capsulatum* infections have been identified in solid organ transplant (SOT) recipients [138, 139]. However, a low frequency of histoplasmosis related to HAI has been observed in the first six months posttransplant. Freifeld et al. [138] identified nine cases of pulmonary histoplasmosis in SOT recipients in a period of 30 months, but only four patients developed the disease in the first six months posttransplant. In a 10-year cohort study, Cuellar-Rodriguez et al. [140] found only three cases of histoplasmosis in SOT recipients in the first six months posttransplant; however, eleven cases were identified after the first year posttransplant.

Other authors evaluated the incidence of IFIs in SOT recipients, in a 5-year cohort study [141, 142]. Of the 1,208 cases of IFI, histoplasmosis was diagnosed in 48 patients, where 18 cases (37.5%) occurred in the first six months posttransplant, particularly in kidney, liver, and kidney-pancreas transplants [141]. In general, these patients were receiving immunosuppressive drugs, like tacrolimus, sirolimus, mycophenolate mofetil, and steroids [138, 140, 142].

A more recent study about IFIs identified an increase in the number of histoplasmosis cases in SOT recipients [142]. Among the 70 cases of IFIs reported, 52 (80%) were diagnosed as histoplasmosis, in a 5-year period. The median time from transplant to the diagnosis of this fungal disease was one year. Five SOT recipients developed histoplasmosis within 30 days of transplant; two patients acquired the infection from their donated organs, and three patients developed pulmonary histoplasmosis irrespectively of the transplanted organs [142]. In rare cases, histoplasmosis has also been diagnosed in patients treated with immunobiological molecules, like different monoclonal antibodies [143, 144].

## 7. Fungal Respiratory Infections in the Hospital Environment

Inadvertent exposure to opportunistic environmental and airborne pathogens can result in infections with significant morbidity and mortality [9]. Fungal infections can range from mild to life-threatening; they vary among mild skin rashes, fungal pneumonia, meningitis, and IFIs. In the hospital, the most common fungal HAI are caused by *Candida* spp. and *Aspergillus* spp. [19].

Airborne infections in susceptible hosts may result from exposure to environmental microorganisms that are ubiquitous in nature, growing in soil, water, dust, or organic matter [2, 9]. Spores or hyphal fragments of fungi usually lie scattered in the environment, especially near decomposing organic matter. *Aspergillus fumigatus* is the species most often associated with pulmonary IFIs [3]. Infection occurs after inhalation of conidia stirred up from construction or renovation works in the hospital. The main risk factor for this HAI is the concentration of *Aspergillus* conidia in the

air [2, 145–149], and the most susceptible individuals are hematopoietic stem cell transplant recipients, neutropenic patients, and those with hematologic malignancies [136, 145, 150–153].

Infections due to *C. neoformans*, *H. capsulatum*, or *C. immitis* can occur in healthcare settings if the nearby ground is disturbed and a malfunction of the facility's air-intake components allows these pathogens to enter the hospital ventilation system [9]. Several outbreaks of histoplasmosis have been associated with disruption of the environment [67, 72, 154]. *H. capsulatum* contaminated environments related to bat and bird colonies living in abandoned buildings and on treetops could disperse the fungus around the hospital. Under this statement, the dispersion of *H. capsulatum* infective propagules could represent a potential risk factor for hospital-acquired histoplasmosis, especially in individuals hospitalized in units lacking adequate air quality control. *H. capsulatum* has never been identified in air quality studies from hospital settings [152]. This could be explained by the difficulties in this fungus' isolation, including prolonged culture growth in laboratory conditions, special nutritional needs, and culture inhibition by the presence of other fast-growing fungi [64, 68].

## 8. Molecular Biology as a Diagnostic Tool in HAI

Hospital-acquired pneumonia represents one of the most difficult treatment challenges in infectious diseases. Many studies suggest that the timely administration of appropriate pathogen-directed therapy could be lifesaving. However, results of bacterial cultures and antimicrobial susceptibility testing can take 48 hours or longer, but some fungi may not even be able to grow in the first week after culturing.

Nowadays, physicians rely on clinical and epidemiological factors to choose an initial empiric therapy for HAI. A number of rapid molecular tests have been developed to identify pathogens and the bases for most molecular assays are polymerase chain reaction and nucleic-acid-sequence-based amplification. These methodologies offer the promise of dramatically improving the ability to identify pathogens in respiratory tract specimens with high sensitivity and specificity. Data from such applications can also be electronically integrated into shared molecular databases, where clinicians and epidemiologists could ascertain local, regional, national, and international trends [155].

Molecular identification of fungi in hospitals has been scarcely described [156–158]. Lo Passo et al. [156] reported transmission of *Trichosporon asahii* by an endoscopic procedure, when isolated from an esophageal ulcer. *T. asahii* isolates were genotyped by restriction fragment length polymorphism and random amplification of polymorphic DNA, confirming the endoscopic device as the source of transmission.

Notwithstanding, there are some undefined issues regarding the use of these molecular biology tools.

(i) Molecular assays have been used mainly for bacteria and viruses, leaving aside the importance of other microorganisms, such as pathogenic fungi; however, there are specific markers for almost every fungal pathogen, which have recently improved the molecular diagnostic bundle for HAI [157].

(ii) The significance of finding a pathogen's DNA in respiratory tract specimens, in the absence of a positive culture, will show different airway ecology from what it is known, and it exposes the inability to distinguish between infecting and colonizing organisms [155].

(iii) The complexities of the pulmonary microbiome and its metagenomic diversity represent a great challenge with many unanswered questions remaining [155].

(iv) New procedures combining molecular biology techniques and environmental sampling of air have revealed some fungal pathogens living in the hospital surroundings [158], which may be relevant for the acquisition of respiratory HAI.

## 9. Conclusions

*H. capsulatum* infection associated with healthcare has been linked to medical devices and surgical implants. The M-phase of *H. capsulatum* may be present in hospital settings, as this fungus adapts to different types of climates and has great dispersion ability. Although conventional pathogen identification techniques have never identified *H. capsulatum* in the hospital environment, histoplasmosis HAI cases have been reported in the last decades. Molecular biology procedures could be useful in this fungus' identification in the air of hospitals and in the diagnosis of this mycosis. More research is needed about *H. capsulatum* involvement in HAI, since it causes a severe and often fatal disease in immunocompromised individuals.

## Conflict of Interests

The authors declare that there is no conflict of interests among them and with any financial organization regarding the material discussed in the present paper.

## Authors' Contribution

Maria Lucia Taylor, Laura Elena Carreto-Binaghi, and Lisandra Serra Damasceno contributed equally to the design of this study. Laura Elena Carreto-Binaghi and Lisandra Serra Damasceno contributed equally to draft the paper. Nayla de Souza Pitangui, Ana Marisa Fusco-Almeida, and Maria José Soares Mendes-Giannini contributed with their critical opinion to improve the paper. Rosely Maria Zancopé-Oliveira and Maria Lucia Taylor were supervisors of this study. All of the authors read and approved the final version of the paper. Laura Elena Carreto-Binaghi and Lisandra Serra Damasceno contributed equally to the development of the review.

## Acknowledgments

Laura Elena Carreto-Binaghi thanks the "Programa de Doctorado en Ciencias Biomédicas" of the UNAM and the

Scholarship no. 329884 provided by the "Consejo Nacional de Ciencia y Tecnología (CONACyT)," Mexico. Lisandra Serra Damasceno thanks the "Programa de Pós-graduação Stricto Sensu em Pesquisa Clínica em Doenças Infecciosas do Instituto Nacional de Infectologia Evandro Chagas," FIOCRUZ, and the Scholarship no. 99999.002336/2014-06 provided by the "Programa Institucional de Bolsas de Doutorado Sanduíche no Exterior" from the "CAPES Foundation, Ministry of Education of Brazil," Brazil. The authors from UNESP acknowledge receipt of grant from Brazilian organizations: FAPESP-2013705853-1 and CNPq-480316/2012-0. This paper constitutes partial fulfillment of the Bilateral Collaboration Agreement between UNAM-FIOCRUZ and UNAM-UNESP. The authors thank I. Mascher for editorial assistance.

## References

[1] L. McKibben, T. Horan, J. I. Tokars et al., "Guidance on public reporting of healthcare-associated infections: recommendations of the Healthcare Infection Control Practices Advisory Committee," *American Journal of Infection Control*, vol. 33, no. 4, pp. 217–226, 2005.

[2] J. D. Siegel, E. Rhinehart, M. Jackson, and L. Chiarello, "2007 Guideline for isolation precautions: preventing transmission of infectious agents in health care settings," *The American Journal of Infection Control*, vol. 35, no. 10, pp. S65–S164, 2007.

[3] G. J. Alangaden, "Nosocomial fungal infections: epidemiology, infection control, and prevention," *Infectious Disease Clinics of North America*, vol. 25, no. 1, pp. 201–225, 2011.

[4] Centers for Disease Control and Prevention, "Healthcare-associated infections (HAIs)," http://www.cdc.gov/HAI/surveillance/index.html.

[5] S. Khodavaisy, M. Nabili, B. Davari, and M. Vahedi, "Evaluation of bacterial and fungal contamination in the health care workers' hands and rings in the intensive care unit," *Journal of Preventive Medicine and Hygiene*, vol. 52, no. 4, pp. 215–218, 2011.

[6] D. J. Weber, D. Anderson, and W. A. Rutala, "The role of the surface environment in healthcare-associated infections," *Current Opinion in Infectious Diseases*, vol. 26, no. 4, pp. 338–344, 2013.

[7] M. Abdallah, C. Benoliel, D. Drider, P. Dhulster, and N.-E. Chihib, "Biofilm formation and persistence on abiotic surfaces in the context of food and medical environments," *Archives of Microbiology*, vol. 196, no. 7, pp. 453–472, 2014.

[8] B. Hota, "Contamination, disinfection, and cross-colonization: are hospital surfaces reservoirs for nosocomial infection?" *Clinical Infectious Diseases*, vol. 39, no. 8, pp. 1182–1189, 2004.

[9] L. Sehulster and R. Y. W. Chinn, "Guidelines for environmental infection control in health-care facilities. Recommendations of CDC and the Healthcare Infection Control Practices Advisory Committee (HICPAC)," *Morbidity and Mortality Weekly Report Recommendations and Reports*, vol. 52, no. 10, pp. 1–42, 2003.

[10] M. Serrano, F. Barcenilla, and E. Limón, "Infección nosocomial en centros sanitarios de cuidados prolongados," *Enfermedades Infecciosas y Microbiología Clínica*, vol. 32, no. 3, pp. 191–198, 2014.

[11] S. K. Fridkin, D. Kaufman, J. R. Edwards, S. Shetty, and T. Horan, "Changing incidence of *Candida* bloodstream infections among NICU patients in the United States: 1995-2004," *Pediatrics*, vol. 117, no. 5, pp. 1680–1687, 2006.

[12] C. Girmenia, L. Pagano, B. Martino et al., "Invasive infections caused by *Trichosporon* species and *Geotrichum capitatum* in patients with hematological malignancies: a retrospective multicenter study from Italy and review of the literature," *Journal of Clinical Microbiology*, vol. 43, no. 4, pp. 1818–1828, 2005.

[13] D. P. Kontoyiannis, H. A. Torres, M. Chagua et al., "Trichosporonosis in a tertiary care cancer center: risk factors, changing spectrum and determinants of outcome," *Scandinavian Journal of Infectious Diseases*, vol. 36, no. 8, pp. 564–569, 2004.

[14] V. Krcmery Jr., F. Mateička, A. Kunová et al., "Hematogenous trichosporonosis in cancer patients: report of 12 cases including 5 during prophylaxis with itraconazol," *Supportive Care in Cancer*, vol. 7, no. 1, pp. 39–43, 1999.

[15] E. C. Repetto, C. G. Giacomazzi, and F. Castelli, "Hospital-related outbreaks due to rare fungal pathogens: a review of the literature from 1990 to June 2011," *European Journal of Clinical Microbiology & Infectious Diseases*, vol. 31, no. 11, pp. 2897–2904, 2012.

[16] G. R. Barber, A. E. Brown, T. E. Kiehn, F. F. Edwards, and D. Armstrong, "Catheter-related *Malassezia furfur* fungemia in immunocompromised patients," *The American Journal of Medicine*, vol. 95, no. 4, pp. 365–370, 1993.

[17] E. Chryssanthou, U. Broberger, and B. Petrini, "*Malassezia pachydermatis* fungaemia in a neonatal intensive care unit," *Acta Paediatrica*, vol. 90, no. 3, pp. 323–327, 2001.

[18] S.-Y. Ruan, J.-Y. Chien, and P.-R. Hsueh, "Invasive trichosporonosis caused by *Trichosporon asahii* and other unusual *Trichosporon* species at a medical center in Taiwan," *Clinical Infectious Diseases*, vol. 49, no. 1, pp. e11–e17, 2009.

[19] J. Pemán and M. Salavert, "Epidemiología y prevención de las infecciones nosocomiales causadas por especies de hongos filamentosos y levaduras," *Enfermedades Infecciosas y Microbiología Clínica*, vol. 31, no. 5, pp. 328–341, 2013.

[20] K. A. Marr, R. A. Carter, M. Boeckh, P. Martin, and L. Corey, "Invasive aspergillosis in allogeneic stem cell transplant recipients: changes in epidemiology and risk factors," *Blood*, vol. 100, no. 13, pp. 4358–4366, 2002.

[21] K. A. Marr, R. A. Carter, F. Crippa, A. Wald, and L. Corey, "Epidemiology and outcome of mould infections in hematopoietic stem cell transplant recipients," *Clinical Infectious Diseases*, vol. 34, no. 7, pp. 909–917, 2002.

[22] A. Antoniadou, "Outbreaks of zygomycosis in hospitals," *Clinical Microbiology and Infection*, vol. 15, supplement 5, pp. 55–59, 2009.

[23] D. Garner and K. Machin, "Investigation and management of an outbreak of mucormycosis in a paediatric oncology unit," *The Journal of Hospital Infection*, vol. 70, no. 1, pp. 53–59, 2008.

[24] G. Christiaens, M. P. Hayette, D. Jacquemin, P. Melin, J. Mutsers, and P. de Mol, "An outbreak of *Absidia corymbifera* infection associated with bandage contamination in a burns unit," *The Journal of Hospital Infection*, vol. 61, no. 1, pp. 88–89, 2005.

[25] E. J. Anaissie, R. T. Kuchar, J. H. Rex et al., "Fusariosis associated with pathogenic *Fusarium* species colonization of a hospital water system: A new paradigm for the epidemiology of opportunistic mold infections," *Clinical Infectious Diseases*, vol. 33, no. 11, pp. 1871–1878, 2001.

[26] M. Nucci, K. A. Marr, F. Queiroz-Telles et al., "*Fusarium* infection in hematopoietic stem cell transplant recipients," *Clinical Infectious Diseases*, vol. 38, no. 9, pp. 1237–1242, 2004.

[27] P. Sampathkumar and C. V. Paya, "*Fusarium* infection after solid-organ transplantation," *Clinical Infectious Diseases*, vol. 32, no. 8, pp. 1237–1240, 2001.

[28] B. Orth, R. Frei, P. H. Itin et al., "Outbreak of invasive mycoses caused by *Paecilomyces lilacinus* from a contaminated skin lotion," *Annals of Internal Medicine*, vol. 125, no. 10, pp. 799–806, 1996.

[29] A. Tarkkanen, V. Raivio, V.-J. Anttila et al., "Fungal endophthalmitis caused by *Paecilomyces variotii* following cataract surgery: a presumed operating room air-conditioning system contamination," *Acta Ophthalmologica Scandinavica*, vol. 82, no. 2, pp. 232–235, 2004.

[30] M. A. Kainer, H. Keshavarz, B. J. Jensen et al., "Saline-filled breast implant contamination with *Curvularia* species among women who underwent cosmetic breast augmentation," *The Journal of Infectious Diseases*, vol. 192, no. 1, pp. 170–177, 2005.

[31] T. Clark, G. D. Huhn, C. Conover et al., "Outbreak of bloodstream infection with the mold *Phialemonium* among patients receiving dialysis at a hemodialysis unit," *Infection Control and Hospital Epidemiology*, vol. 27, no. 11, pp. 1164–1170, 2006.

[32] L. A. Proia, M. K. Hayden, P. L. Kammeyer et al., "*Phialemonium*: an emerging mold pathogen that caused 4 cases of hemodialysis-associated endovascular infection," *Clinical Infectious Diseases*, vol. 39, no. 3, pp. 373–379, 2004.

[33] C. Y. Rao, C. Pachucki, S. Cali et al., "Contaminated product water as the source of *Phialemonium curvatum* bloodstream infection among patients undergoing hemodialysis," *Infection Control and Hospital Epidemiology*, vol. 30, no. 9, pp. 840–847, 2009.

[34] J. Strahilevitz, G. Rahav, H.-J. Schroers et al., "An outbreak of *Phialemonium* infective endocarditis linked to intracavernous penile injections for the treatment of impotence," *Clinical Infectious Diseases*, vol. 40, no. 6, pp. 781–786, 2005.

[35] M. Alvarez, B. L. Ponga, C. Rayon et al., "Nosocomial outbreak caused by *Scedosporium prolificans* (*inflatum*): four fatal cases in leukemic patients," *Journal of Clinical Microbiology*, vol. 33, no. 12, pp. 3290–3295, 1995.

[36] A. Guerrero, P. Torres, M. T. Duran, B. Ruiz-Díez, M. Rosales, and J. L. Rodriguez-Tudela, "Airborne outbreak of nosocomial *Scedosporium prolificans* infection," *The Lancet*, vol. 357, no. 9264, pp. 1267–1268, 2001.

[37] B. Ruiz-Díez, F. Martín-Díez, J. L. Rodríguez-Tudela, M. Alvárez, and J. V. Martínez-Suárez, "Use of random amplification of polymorphic DNA (RAPD) and PCR-fingerprinting for genotyping a *Scedosporium prolificans* (*inflatum*) outbreak in four leukemic patients," *Current Microbiology*, vol. 35, no. 3, pp. 186–190, 1997.

[38] D. C. Chang, G. B. Grant, K. O'Donnell et al., "Multistate outbreak of *Fusarium* keratitis associated with use of a contact lens solution," *The Journal of the American Medical Association*, vol. 296, no. 8, pp. 953–963, 2006.

[39] S.-M. Saw, P.-L. Ooi, D. T. H. Tan et al., "Risk factors for contact lens-related *Fusarium* keratitis: a case-control study in Singapore," *Archives of Ophthalmology*, vol. 125, no. 5, pp. 611–617, 2007.

[40] M. J. Abzug, S. Gardner, M. P. Glode, M. Cymanski, M. H. Roe, and L. F. Odom, "Heliport-associated nosocomial mucormycoses," *Infection Control and Hospital Epidemiology*, vol. 13, no. 6, pp. 325–326, 1992.

[41] S. J. Wilson, R. J. Everts, K. B. Kirkland, and D. J. Sexton, "A pseudo-outbreak of *Aureobasidium* species lower respiratory tract infections caused by reuse of single-use stopcocks during bronchoscopy," *Infection Control and Hospital Epidemiology*, vol. 21, no. 7, pp. 470–472, 2000.

[42] N. Singh, O. Belen, M.-M. Léger, and J. M. Campos, "Cluster of *Trichosporon mucoides* in children associated with a faulty bronchoscope," *The Pediatric Infectious Disease Journal*, vol. 22, no. 7, pp. 609–612, 2003.

[43] S. Singh, N. Singh, R. Kochhar, S. K. Mehta, and P. Talwar, "Contamination of an endoscope due to *Trichosporon beigelli*," *The Journal of Hospital Infection*, vol. 14, no. 1, pp. 49–53, 1989.

[44] M. E. Hagan, S. A. Klotz, W. Bartholomew, L. Potter, and M. Nelson, "A pseudoepidemic of *Rhodotorula rubra*: a marker for microbial contamination of the bronchoscope," *Infection Control and Hospital Epidemiology*, vol. 16, no. 12, pp. 727–728, 1995.

[45] K. K. Hoffmann, D. J. Weber, and W. A. Rutala, "Pseudoepidemic of *Rhodotorula rubra* in patients undergoing fiberoptic bronchoscopy," *Infection Control and Hospital Epidemiology*, vol. 10, no. 11, pp. 511–514, 1989.

[46] W. L. Whitlock, R. A. Dietrich, E. H. Steimke, and M. F. Tenholder, "*Rhodotorula rubra* contamination in fiberoptic bronchoscopy," *Chest*, vol. 102, no. 5, pp. 1516–1519, 1992.

[47] M. Blake, J. M. Embil, E. Trepman, H. Adam, R. Myers, and P. Mutcher, "Pseudo-outbreak of *Phaeoacremonium parasiticum* from a hospital ice dispenser," *Infection Control and Hospital Epidemiology*, vol. 35, no. 8, pp. 1063–1065, 2014.

[48] M. Chabé, I. Durand-Joly, and E. dei-Cas, "La transmisson des infections à *Pneumocystis*," *Médecine Sciences*, vol. 28, no. 6-7, pp. 599–604, 2012.

[49] M. G. J. De Boer, L. E. S. B. van Coppenraet, A. Gaasbeek et al., "An outbreak of *Pneumocystis jiroveci* pneumonia with 1 predominant genotype among renal transplant recipients: interhuman transmission or a common environmental source?" *Clinical Infectious Diseases*, vol. 44, no. 9, pp. 1143–1149, 2007.

[50] S. Gianella, L. Haeberli, B. Joos et al., "Molecular evidence of interhuman transmission in an outbreak of *Pneumocystis jirovecii* pneumonia among renal transplant recipients," *Transplant Infectious Disease*, vol. 12, no. 1, pp. 1–10, 2010.

[51] F. Gigliotti and T. W. Wright, "*Pneumocystis*: where does it live?" *PLoS Pathogens*, vol. 8, no. 11, Article ID e1003025, 2012.

[52] B. Höcker, C. Wendt, A. Nahimana, B. Tönshoff, and P. M. Hauser, "Molecular evidence of *Pneumocystis* transmission in pediatric transplant unit," *Emerging Infectious Diseases*, vol. 11, no. 2, pp. 330–332, 2005.

[53] R. F. Miller, H. E. Ambrose, V. Novelli, and A. E. Wakefield, "Probable mother-to-infant transmission of *Pneumocystis carinii* f. sp. *hominis* Infection," *Journal of Clinical Microbiology*, vol. 40, no. 4, pp. 1555–1557, 2002.

[54] A. Morris and K. A. Norris, "Colonization by *Pneumocystis jirovecii* and its role in disease," *Clinical Microbiology Reviews*, vol. 25, no. 2, pp. 297–317, 2012.

[55] L. M. Phipps, S. C.-A. Chen, K. Kable et al., "Nosocomial *Pneumocystis jirovecii* pneumonia: lessons from a cluster in kidney transplant recipients," *Transplantation*, vol. 92, no. 12, pp. 1327–1334, 2011.

[56] S. Schmoldt, R. Schuhegger, T. Wendler et al., "Molecular evidence of nosocomial *Pneumocystis jirovecii* transmission among 16 patients after kidney transplantation," *Journal of Clinical Microbiology*, vol. 46, no. 3, pp. 966–971, 2008.

[57] S. L. Vargas, C. A. Ponce, F. Gigliotti et al., "Transmission of *Pneumocystis carinii* DNA from a patient with *P. carinii*

pneumonia to immunocompetent contact health care workers," *Journal of Clinical Microbiology*, vol. 38, no. 4, pp. 1536–1538, 2000.

[58] A. E. Wakefield, A. R. Lindley, H. E. Ambrose, C.-M. Denis, and R. F. Miller, "Limited asymptomatic carriage of *Pneumocystis jiroveci* in Human Immunodeficiency Virus-Infected patients," *The Journal of Infectious Diseases*, vol. 187, no. 6, pp. 901–908, 2003.

[59] J. E. Kaplan, C. Benson, K. K. Holmes, J. T. Brooks, A. Pau, and H. Masur, "Guidelines for prevention and treatment of opportunistic infections in HIV-infected adults and adolescents: recommendations from CDC, the National Institutes of Health, and the HIV Medicine Association of the Infectious Diseases Society of America," *Morbidity and Mortality Weekly Report: Recommendations and Reports*, vol. 58, no. 4, pp. 1–207, 2009.

[60] C. Damiani, F. Choukri, S. le Gal et al., "Possible nosocomial transmission of *Pneumocystis jirovecii*," *Emerging Infectious Diseases*, vol. 18, no. 5, pp. 877–878, 2012.

[61] A. A. Rostved, M. Sassi, J. A. L. Kurtzhals et al., "Outbreak of *Pneumocystis* pneumonia in renal and liver transplant patients caused by genotypically distinct strains of *Pneumocystis jirovecii*," *Transplantation*, vol. 96, no. 9, pp. 834–842, 2013.

[62] S. le Gal, C. Damiani, A. Rouillé et al., "A cluster of pneumocystis infections among renal transplant recipients: molecular evidence of colonized patients as potential infectious sources of *Pneumocystis jirovecii*," *Clinical Infectious Diseases*, vol. 54, no. 7, pp. e62–e71, 2012.

[63] L. E. Nicolle, J. McLeod, L. Romance, S. Parker, and M. Paraskevas, "Pseudo-outbreak of blastomycosis associated with contaminated bronchoscopes," *Infection Control and Hospital Epidemiology*, vol. 13, no. 6, p. 324, 1992.

[64] M. L. Taylor, M. R. Reyes-Montes, C. B. Chávez-Tapia et al., "Ecology and molecular epidemiology findings of *Histoplasma capsulatum*, in Mexico," in *Research Advances in Microbiology*, R. M. Mojan and M. Benedik, Eds., pp. 29–35, Global Research Network, Kerala, India, 2000.

[65] T. Kasuga, T. J. White, G. Koenig et al., "Phylogeography of the fungal pathogen *Histoplasma capsulatum*," *Molecular Ecology*, vol. 12, no. 12, pp. 3383–3401, 2003.

[66] H. Anderson, L. Honish, G. Taylor et al., "Histoplasmosis cluster, golf course, Canada," *Emerging Infectious Diseases*, vol. 12, no. 1, pp. 163–165, 2006.

[67] L. M. Calanni, R. A. Pérez, S. Brasili et al., "Brote de histoplasmosis en la provincia de Neuquén, Patagonia Argentina," *Revista Iberoamericana de Micología*, vol. 30, no. 3, pp. 193–199, 2013.

[68] M. L. Taylor, C. B. Chávez-Tapia, R. Vargas-Yañez et al., "Environmental conditions favoring bat infection with *Histoplasma capsulatum* in Mexican shelters," *American Journal of Tropical Medicine and Hygiene*, vol. 61, no. 6, pp. 914–919, 1999.

[69] R. Tewari, L. J. Wheat, and L. Ajello, "Agents of histoplasmosis," in *Medical Mycology, Topley & Wilson's Microbiology and Microbial Infections*, L. Ajello and R. J. Hay, Eds., pp. 373–407, Arnold and Oxoford University Press, New York, NY, USA, 1998.

[70] M. L. Taylor, G. M. Ruíz-Palacios, M. D. R. Reyes-Montes et al., "Identification of the infectious source of an unusual outbreak of histoplasmosis, in a hotel in Acapulco, state of Guerrero, Mexico," *FEMS Immunology and Medical Microbiology*, vol. 45, no. 3, pp. 435–441, 2005.

[71] Centers for Disease Control and Prevention, "Histoplasmosis outbreak among day camp attendees—Nebraska, June 2012," *Morbidity and Mortality Weekly Report*, vol. 61, no. 37, pp. 747–748, 2012.

[72] D. T. Haselow, H. Safi, D. Holcomb et al., "Histoplasmosis associated with a bamboo bonfire—arkansas, October 2011," *Morbidity and Mortality Weekly Report*, vol. 63, no. 8, pp. 165–168, 2014.

[73] J. Morgan, M. V. Cano, D. R. Feikin et al., "A large outbreak of histoplasmosis among American travelers associated with a hotel in Acapulco, Mexico, spring 2001," *The American Journal of Tropical Medicine and Hygiene*, vol. 69, no. 6, pp. 663–669, 2003.

[74] L. S. Dasmasceno, A. R. Novaes Jr., C. H. M. Alencar et al., "Disseminated histoplasmosis and aids: relapse and late mortality in endemic area in North-Eastern Brazil," *Mycoses*, vol. 56, no. 5, pp. 520–526, 2013.

[75] L. S. Damasceno, A. N. Ramos, C. H. Alencar et al., "Disseminated histoplasmosis in HIV-infected patients: determinants of relapse and mortality in a north-eastern area of Brazil," *Mycoses*, vol. 57, no. 7, pp. 406–413, 2014.

[76] P. Couppié, C. Aznar, B. Carme, and M. Nacher, "American histoplasmosis in developing countries with a special focus on patients with HIV: diagnosis, treatment, and prognosis," *Current Opinion in Infectious Diseases*, vol. 19, no. 5, pp. 443–449, 2006.

[77] M. M. Lo, J. Q. Mo, B. P. Dixon, and K. A. Czech, "Disseminated histoplasmosis associated with hemophagocytic lymphohistiocytosis in kidney transplant recipients," *American Journal of Transplantation*, vol. 10, no. 3, pp. 687–691, 2010.

[78] H. Trimarchi, M. Forrester, F. Lombi et al., "Histoplasmosis diseminada en un paciente trasplantado renal," *Nefrología*, vol. 28, no. 5, pp. 571–572, 2008.

[79] P. A. Isotalo, K. L. Chan, F. Rubens, D. S. Beanlands, F. Auclair, and J. P. Veinot, "Prosthetic valve fungal endocarditis due to histoplasmosis," *The Canadian Journal of Cardiology*, vol. 17, no. 3, pp. 297–303, 2001.

[80] S. Jinno, B. M. Gripshover, T. L. Lemonovich, J. M. Anderson, and M. R. Jacobs, "*Histoplasma capsulatum* prosthetic valve endocarditis with negative fungal blood cultures and negative Histoplasma antigen assay in an immunocompetent patient," *Journal of Clinical Microbiology*, vol. 48, no. 12, pp. 4664–4666, 2010.

[81] N. Lorchirachonkul, S. Foongladda, R. Ruangchira-Urai, and M. Chayakulkeeree, "Prosthetic valve endocarditis caused by *Histoplasma capsulatum*: the first case report in Thailand," *Journal of the Medical Association of Thailand*, vol. 96, supplement 2, pp. S262–S265, 2013.

[82] J. W. Costerton, Z. Lewandowski, D. E. Caldwell, D. R. Korber, and H. M. Lappin-Scott, "Microbial biofilms," *Annual Review of Microbiology*, vol. 49, pp. 711–745, 1995.

[83] L. E. Davis, G. Cook, and J. William Costerton, "Biofilm on ventriculoperitoneal shunt tubing as a cause of treatment failure in coccidioidal meningitis," *Emerging Infectious Diseases*, vol. 8, no. 4, pp. 376–379, 2002.

[84] S. P. Bachmann, K. VandeWalle, G. Ramage et al., "*In vitro* activity of caspofungin against *Candida albicans* biofilms," *Antimicrobial Agents and Chemotherapy*, vol. 46, no. 11, pp. 3591–3596, 2002.

[85] W. Costerton, R. Veeh, M. Shirtliff, M. Pasmore, C. Post, and G. Ehrlich, "The application of biofilm science to the study and control of chronic bacterial infections," *The Journal of Clinical Investigation*, vol. 112, no. 10, pp. 1466–1477, 2003.

[86] R. M. Donlan and J. W. Costerton, "Biofilms: survival mechanisms of clinically relevant microorganisms," *Clinical Microbiology Reviews*, vol. 15, no. 2, pp. 167–193, 2002.

[87] K. Lewis, "Riddle of biofilm resistance," *Antimicrobial Agents and Chemotherapy*, vol. 45, no. 4, pp. 999–1007, 2001.

[88] A. S. Lynch and G. T. Robertson, "Bacterial and fungal biofilm infections," *Annual Review of Medicine*, vol. 59, pp. 415–428, 2008.

[89] B. Adam, G. S. Baillie, and L. J. Douglas, "Mixed species biofilms of *Candida albicans* and *Staphylococcus epidermidis*," *Journal of Medical Microbiology*, vol. 51, no. 4, pp. 344–349, 2002.

[90] J. C. O. Sardi, N. S. Pitangui, G. Rodríguez-Arellanes, M. L. Taylor, A. M. Fusco-Almeida, and M. J. S. Mendes-Giannini, "Highlights in pathogenic fungal biofilms," *Revista Iberoamericana de Micología*, vol. 31, no. 1, pp. 22–29, 2014.

[91] B. W. Trautner and R. O. Darouiche, "Catheter-associated infections: pathogenesis affects prevention," *Archives of Internal Medicine*, vol. 164, no. 8, pp. 842–850, 2004.

[92] R. Patel, "Biofilms and antimicrobial resistance," *Clinical Orthopaedics and Related Research*, no. 437, pp. 41–47, 2005.

[93] M. S. Doggett, "Characterization of fungal biofilms within a municipal water distribution system," *Applied and Environmental Microbiology*, vol. 66, no. 3, pp. 1249–1251, 2000.

[94] W. F. McCoy, J. D. Bryers, J. Robbins, and J. W. Costerton, "Observations of fouling biofilm formation," *Canadian Journal of Microbiology*, vol. 27, no. 9, pp. 910–917, 1981.

[95] T. Takuma, K. Okada, A. Yamagata, N. Shimono, and Y. Niki, "Mold colonization of fiberglass insulation of the air distribution system: effects on patients with hematological malignancies," *Medical Mycology*, vol. 49, no. 2, pp. 150–156, 2011.

[96] P. W. J. J. van der Wielen and D. van der Kooij, "Nontuberculous mycobacteria, fungi, and opportunistic pathogens in unchlorinated drinking water in the Netherlands," *Applied and Environmental Microbiology*, vol. 79, no. 3, pp. 825–834, 2013.

[97] L. A. Nagy and B. H. Olson, "The occurrence of filamentous fungi in drinking water distribution systems," *Canadian Journal of Microbiology*, vol. 28, no. 6, pp. 667–671, 1982.

[98] M. E. Davey and G. A. O'Toole, "Microbial biofilms: from ecology to molecular genetics," *Microbiology and Molecular Biology Reviews*, vol. 64, no. 4, pp. 847–867, 2000.

[99] R. Cauda, "Candidaemia in patients with an inserted medical device," *Drugs*, vol. 69, supplement 1, pp. 33–38, 2009.

[100] E. M. Kojic and R. O. Darouiche, "*Candida* infections of medical devices," *Clinical Microbiology Reviews*, vol. 17, no. 2, pp. 255–267, 2004.

[101] G. Ramage, S. P. Saville, D. P. Thomas, and J. L. López-Ribot, "*Candida* biofilms: an update," *Eukaryotic Cell*, vol. 4, no. 4, pp. 633–638, 2005.

[102] D. Sychev, I. D. Maya, and M. Allon, "Clinical outcomes of dialysis catheter-related candidemia in hemodialysis patients," *Clinical Journal of the American Society of Nephrology*, vol. 4, no. 6, pp. 1102–1105, 2009.

[103] C. C. Chiou, T. T. Wong, H. H. Lin et al., "Fungal infection of ventriculoperitoneal shunts in children," *Clinical Infectious Diseases*, vol. 19, no. 6, pp. 1049–1053, 1994.

[104] E. Mowat, C. Williams, B. Jones, S. McChlery, and G. Ramage, "The characteristics of *Aspergillus fumigatus* mycetoma development: is this a biofilm?" *Medical Mycology*, vol. 47, supplement 1, pp. S120–S126, 2009.

[105] F. T. Cannizzo, E. Eraso, P. A. Ezkurra et al., "Biofilm development by clinical isolates of *Malassezia pachydermatis*," *Medical Mycology*, vol. 45, no. 4, pp. 357–361, 2007.

[106] D. D'Antonio, G. Parruti, E. Pontieri et al., "Slime production by clinical isolates of *Blastoschizomyces capitatus* from patients with hematological malignancies and catheter-related fungemia," *European Journal of Clinical Microbiology & Infectious Diseases*, vol. 23, no. 10, pp. 787–789, 2004.

[107] J. C. O. Sardi, L. Scorzoni, T. Bernardi, A. M. Fusco-Almeida, and M. J. S. Mendes-Giannini, "*Candida* species: current epidemiology, pathogenicity, biofilm formation, natural antifungal products and new therapeutic options," *Journal of Medical Microbiology*, vol. 62, part 1, pp. 10–24, 2013.

[108] M. T. Cushion, M. S. Collins, and M. J. Linke, "Biofilm formation by *Pneumocystis* spp," *Eukaryotic Cell*, vol. 8, no. 2, pp. 197–206, 2009.

[109] J. Gattlen, M. Zinn, S. Guimond, E. Körner, C. Amberg, and L. Mauclaire, "Biofilm formation by the yeast *Rhodotorula mucilaginosa*: process, repeatability and cell attachment in a continuous biofilm reactor," *Biofouling*, vol. 27, no. 9, pp. 979–991, 2011.

[110] J. M. Nunes, F. C. Bizerra, R. C. Ferreira, and A. L. Colombo, "Molecular identification, antifungal susceptibility profile, and biofilm formation of clinical and environmental *Rhodotorula* species isolates," *Antimicrobial Agents and Chemotherapy*, vol. 57, no. 1, pp. 382–389, 2013.

[111] L. R. Martinez and A. Casadevall, "*Cryptococcus neoformans* biofilm formation depends on surface support and carbon source and reduces fungal cell susceptibility to heat, cold, and UV light," *Applied and Environmental Microbiology*, vol. 73, no. 14, pp. 4592–4601, 2007.

[112] T. B. Reynolds and G. R. Fink, "Bakers' yeast, a model for fungal biofilm formation," *Science*, vol. 291, no. 5505, pp. 878–881, 2001.

[113] M. Dyavaiah, R. Ramani, D. S. Chu et al., "Molecular characterization, biofilm analysis and experimental biofouling study of *Fusarium isolates* from recent cases of fungal keratitis in New York State," *BMC Ophthalmology*, vol. 7, article 1, 2007.

[114] G. Di Bonaventura, A. Pompilio, C. Picciani, M. Iezzi, D. D'Antonio, and R. Piccolomini, "Biofilm formation by the emerging fungal pathogen *Trichosporon asahii*: development, architecture, and antifungal resistance," *Antimicrobial Agents and Chemotherapy*, vol. 50, no. 10, pp. 3269–3276, 2006.

[115] R. Singh, M. R. Shivaprakash, and A. Chakrabarti, "Biofilm formation by zygomycetes: quantification, structure and matrix composition," *Microbiology*, vol. 157, no. 9, pp. 2611–2618, 2011.

[116] S. J. Head, T. M. Dewey, and M. J. MacK, "Fungal endocarditis after transfemoral aortic valve implantation," *Catheterization and Cardiovascular Interventions*, vol. 78, no. 7, pp. 1017–1019, 2011.

[117] C. Ledtke, S. J. Rehm, T. G. Fraser et al., "Endovascular infections caused by *Histoplasma capsulatum*: a case series and review of the literature," *Archives of Pathology & Laboratory Medicine*, vol. 136, no. 6, pp. 640–645, 2012.

[118] P. T. Wilmshurst, G. E. Venn, and S. J. Eykyn, "*Histoplasma* endocarditis on a stenosed aortic valve presenting as dysphagia and weight loss," *British Heart Journal*, vol. 70, no. 6, pp. 565–567, 1993.

[119] N. Patel and M. S. Bronze, "*Histoplasma* infection of aortofemoral bypass graft," *American Journal of the Medical Sciences*, vol. 347, no. 5, pp. 421–424, 2014.

[120] S. Bhatti, L. Vilenski, R. Tight, and R. A. Smego Jr., "*Histoplasma* endocarditis: clinical and mycologic features and outcomes," *Journal of Infection*, vol. 51, no. 1, pp. 2–9, 2005.

[121] N. S. Pitangui, J. C. O. Sardi, J. F. Silva et al., "Adhesion of *Histoplasma capsulatum* to pneumocytes and biofilm formation on an abiotic surface," *Biofouling*, vol. 28, no. 7, pp. 711–718, 2012.

[122] R. O. Suárez-Alvarez, A. Pérez-Torres, and M. L. Taylor, "Adherence patterns of *Histoplasma capsulatum* yeasts to bat tissue sections," *Mycopathologia*, vol. 170, no. 2, pp. 79–87, 2010.

[123] A. Ijaz and D. Choudhury, "A case of rare, fungal peritonitis caused by *Histoplasma capsulatum* in a patient on CAPD," *Nature Reviews Nephrology*, vol. 6, no. 7, pp. 435–439, 2010.

[124] M. Jain and S. G. Revankar, "A case of peritoneal histoplasmosis in a patient receiving chronic ambulatory peritoneal dialysis," *Mycoses*, vol. 55, no. 1, pp. 99–100, 2012.

[125] W. Lim, S. P. Chau, P. C. K. Chan, and I. K. P. Cheng, "*Histoplasma capsulatum* infection associated with continuous ambulatory peritoneal dialysis," *Journal of Infection*, vol. 22, no. 2, pp. 179–182, 1991.

[126] J. O. Lopes, S. H. Alves, J. P. Benevenga, O. R. Regio, and A. Calil, "*Histoplasma capsulatum* peritonitis associated with continuous ambulatory peritoneal dialysis," *Mycopathologia*, vol. 122, no. 2, pp. 101–102, 1993.

[127] J. O. Lopes, S. H. Alves, J. P. Benevenga, and A. C. Rose, "The second case of peritonitis due to *Histoplasma capsulatum* during continuous ambulatory peritoneal dialysis in Brazil," *Mycoses*, vol. 37, no. 5-6, pp. 161–163, 1994.

[128] S. M. Marcic, P. L. Kammeyer, C. Aneziokoro, L. Bartnicki, S. Yong, and D. J. Leehey, "'Culture-negative' peritonitis due to *Histoplasma capsulatum*," *Nephrology, Dialysis, Transplantation*, vol. 21, no. 10, p. 3002, 2006.

[129] A. Veeravagu, C. Ludwig, J. Q. Camara-Quintana, B. Jiang, N. Lad, and L. Shuer, "Fungal infection of a ventriculoperitoneal shunt: histoplasmosis diagnosis and treatment," *World Neurosurgery*, vol. 80, no. 1-2, pp. 222.e5–222.e13, 2013.

[130] P. Albuquerque and A. Casadevall, "Quorum sensing in fungi—a review," *Medical Mycology*, vol. 50, no. 4, pp. 337–345, 2012.

[131] S. Kügler, T. S. Sebghati, L. G. Eissenberg, and W. E. Goldman, "Phenotypic variation and intracellular parasitism by *Histoplasma capsulatum*," *Proceedings of the National Academy of Sciences of the United States of America*, vol. 97, no. 16, pp. 8794–8798, 2000.

[132] J. M. Hornby, S. M. Jacobitz-Kizzier, D. J. McNeel, E. C. Jensen, D. S. Treves, and K. W. Nickerson, "Inoculum size effect in dimorphic fungi: extracellular control of yeast-mycelium dimorphism in *Ceratocystis ulmi*," *Applied and Environmental Microbiology*, vol. 70, no. 3, pp. 1356–1359, 2004.

[133] M. G. Roca, J. Arlt, C. E. Jeffree, and N. D. Read, "Cell biology of conidial anastomosis tubes in *Neurospora crassa*," *Eukaryotic Cell*, vol. 4, no. 5, pp. 911–919, 2005.

[134] K. R. Klimpel and W. E. Goldman, "Cell walls from avirulent variants of *Histoplasma capsulatum* lack $\alpha$-(1,3)-glucan," *Infection and Immunity*, vol. 56, no. 11, pp. 2997–3000, 1988.

[135] D. L. Paterson and N. Singh, "Invasive aspergillosis in transplant recipients," *Medicine*, vol. 78, no. 2, pp. 123–138, 1999.

[136] J. A. Fishman, "Overview: fungal infections in the transplant patient," *Transplant Infectious Disease*, vol. 4, supplement 3, pp. 3–11, 2002.

[137] M. Assi, S. Martin, L. J. Wheat et al., "Histoplasmosis after solid organ transplant," *Clinical Infectious Diseases*, vol. 57, no. 11, pp. 1542–1549, 2013.

[138] A. G. Freifeld, P. C. Iwen, B. L. Lesiak, R. K. Gilroy, R. B. Stevens, and A. C. Kalil, "Histoplasmosis in solid organ transplant recipients at a large Midwestern university transplant center," *Transplant Infectious Disease*, vol. 7, no. 3-4, pp. 109–115, 2005.

[139] K. Y. Ibrahim, N. B. Carvalho, E. V. Mimicos, H. Yeh-Li, M. N. Sotto, and F. O. França, "Cutaneous and bone marrow histoplasmosis after 18 years of renal allograft transplant," *Mycopathologia*, vol. 178, no. 3-4, pp. 273–278, 2014.

[140] J. Cuellar-Rodriguez, R. K. Avery, M. Lard et al., "Histoplasmosis in solid organ transplant recipients: 10 years of experience at a large transplant center in an endemic area," *Clinical Infectious Diseases*, vol. 49, no. 5, pp. 710–716, 2009.

[141] P. G. Pappas, B. D. Alexander, D. R. Andes et al., "Invasive fungal infections among organ transplant recipients: results of the Transplant-Associated Infection Surveillance Network (Transnet)," *Clinical Infectious Diseases*, vol. 50, no. 8, pp. 1101–1111, 2010.

[142] C. A. Kauffman, A. G. Freifeld, D. R. Andes et al., "Endemic fungal infections in solid organ and hematopoietic cell transplant recipients enrolled in the Transplant-Associated Infection Surveillance Network (TRANSNET)," *Transplant Infectious Disease*, vol. 16, no. 2, pp. 213–224, 2014.

[143] N. Lan, D. T. Patil, and B. Shen, "*Histoplasma capsulatum* infection in refractory Crohn's disease of the pouch on anti-TNF biological therapy," *The American Journal of Gastroenterology*, vol. 108, no. 2, pp. 281–283, 2013.

[144] B. J. van Welzen, K. J. van Erpecum, P.-J. A. Haas, F. J. ten Kate, and T. Mudrikova, "Severe cholestasis due to disseminated histoplasmosis under adalimumab-containing immunosuppressive therapy," *Clinics and Research in Hepatology and Gastroenterology*, vol. 37, no. 4, pp. e105–e107, 2013.

[145] D. W. Denning, A. Marinus, J. Cohen et al., "An EORTC multicentre prospective survey of invasive aspergillosis in haematological patients: diagnosis and therapeutic outcome. EORTC Invasive Fungal Infections Cooperative Group," *The Journal of Infection*, vol. 37, no. 2, pp. 173–180, 1998.

[146] S. K. Fridkin and W. R. Jarvis, "Epidemiology of nosocomial fungal infections," *Clinical Microbiology Reviews*, vol. 9, no. 4, pp. 499–511, 1996.

[147] S. Heinemann, F. Symoens, B. Gordts, H. Jannes, and N. Nolard, "Environmental investigations and molecular typing of *Aspergillus flavus* during an outbreak of postoperative infections," *The Journal of Hospital Infection*, vol. 57, no. 2, pp. 149–155, 2004.

[148] S. Krishnan, E. K. Manavathu, and P. H. Chandrasekar, "*Aspergillus flavus*: an emerging non-fumigatus *Aspergillus* species of significance," *Mycoses*, vol. 52, no. 3, pp. 206–222, 2009.

[149] C. F. Pegues, E. S. Daar, and A. R. Murthy, "The epidemiology of invasive pulmonary aspergillosis at a large teaching hospital," *Infection Control and Hospital Epidemiology*, vol. 22, no. 6, pp. 370–374, 2001.

[150] P. D. Barnes and K. A. Marr, "Risks, diagnosis and outcomes of invasive fungal infections in haematopoietic stem cell transplant recipients," *British Journal of Haematology*, vol. 139, no. 4, pp. 519–531, 2007.

[151] O. Lortholary, S. Ascioglu, P. Moreau et al., "Invasive aspergillosis as an opportunistic infection in nonallografted patients with multiple myeloma: a European Organization for Research and Treatment of Cancer," *Clinical Infectious Diseases*, vol. 30, no. 1, pp. 41–46, 2000.

[152] S. Niaré-Doumbo, A. C. Normand, Y. L. Diallo et al., "Preliminary study of the fungal ecology at the haematology and medical-oncology ward in Bamako, Mali," *Mycopathologia*, vol. 178, no. 1-2, pp. 103–109, 2014.

[153] E. C. M. Williamson, M. R. Millar, C. G. Steward et al., "Infections in adults undergoing unrelated donor bone marrow transplantation," *British Journal of Haematology*, vol. 104, no. 3, pp. 560–568, 1999.

[154] A. Allard, D. Décarie, J.-L. Grenier, M.-C. Lacombe, and F. Levac, "Histoplasmosis outbreak associated with the renovation of an old house—Quebec, Canada, 2013," *Morbidity and Mortality Weekly Report*, vol. 62, no. 51-52, pp. 1041–1044, 2013.

[155] A. Endimiani, K. M. Hujer, A. M. Hujer et al., "Are we ready for novel detection methods to treat respiratory pathogens in hospital-acquired pneumonia?" *Clinical Infectious Diseases*, vol. 52, supplement 4, pp. S373–S383, 2011.

[156] C. Lo Passo, I. Pernice, A. Celeste, G. Perdichizzi, and F. Todaro-Luck, "Transmission of *Trichosporon asahii* oesophagitis by a contaminated endoscope," *Mycoses*, vol. 44, no. 1-2, pp. 13–21, 2001.

[157] B. L. Gómez, "Molecular diagnosis of endemic and invasive mycoses: advances and challenges," *Revista Iberoamericana de Micología*, vol. 31, no. 1, pp. 35–41, 2014.

[158] N. Refojo, E. Duarte-Escalante, M. C. Dignani et al., "Genotipificación de aislamientos clínicos de *Aspergillus flavus* y su relación con aislamientos ambientales de un centro oncohematológico," *Revista Iberoamericana de Micología*, vol. 30, no. 1, pp. 25–30, 2013.

RESEARCH PAPER

Virulence 6:6, 642–651; August/September 2015; © 2015 Taylor & Francis Group, LLC

# *In vitro Paracoccidioides brasiliensis* biofilm and gene expression of adhesins and hydrolytic enzymes

Janaina de Cássia Orlandi Sardi[1], Nayla de Souza Pitangui[1], Aline Raquel Voltan[1], Jaqueline Derissi Braz[1], Marcelo Pelajo Machado[2], Ana Marisa Fusco Almeida[1], and Maria Jose Soares Mendes Giannini[1,*]

[1]Departamento de Análises Clínicas; Laboratório de Micologia Clínica; Faculdade de Ciências Farmacêuticas; University Estadual Paulista; Araraquara, Brasil; [2]Departamento de Patologia; Instituto Oswaldo Cruz; Rio de Janeiro, Brasil

**Keywords:** adhesins, biofilms, gene expression, *Paracoccidioides brasiliensis*, real-time PCR, virulence factors

*Paracoccidioides* species are dimorphic fungi that initially infect the lungs but can also spread throughout the body. The spreading infection is most likely due to the formation of a biofilm that makes it difficult for the host to eliminate the infection. Biofilm formation is crucial for the development of infections and confines the pathogen to an extracellular matrix. Its presence is associated with antimicrobial resistance and avoidance of host defenses. This current study provides the first description of biofilm formation by *Paracoccidioides brasiliensis* (Pb18) and an analysis of gene expression, using real-time PCR, associated with 3 adhesins and 2 hydrolytic enzymes that could be associated with the virulence profile. Biofilm formation was analyzed using fluorescence microscopy, scanning electron microscopy (SEM) and confocal laser scanning microscopy (CLSM). Metabolic activity was determined using the XTT reduction assay. *P. brasiliensis* was able to form mature biofilm in 144 h with a thickness of 100 μm. The presence of a biofilm was found to be associated with an increase in the expression of adhesins and enzymes. GP43, enolase, GAPDH and aspartyl proteinase genes were over-expressed, whereas phospholipase was down-regulated in biofilm. The characterization of biofilm formed by *P. brasiliensis* may contribute to a better understanding of the pathogenesis of paracoccidioidomycosis as well as the search for new therapeutic alternatives; while improving the effectiveness of treatment.

## Introduction

The incidence of systemic fungal diseases has been growing worldwide in recent years, highlighting fungal diseases as an important topic in the field of medicine. Paracoccidioidomycosis (PCM) is a systemic mycosis with higher incidence in Latin America. The majority of cases occur in Brazil, which has the highest concentration of endemic areas, with more than 80% of the reported cases occurring in Brazil. The etiological agent of PCM is *Paracoccidioides* spp.[1,2] This genus is composed of 2 species, *Paracoccidioides lutzii* and *P. brasiliensis*; the latter is subclassified into 3 different phylogenetic groups.[1,2]

An occupational predisposing factor for acquiring PCM is a work environment that exposes the population to soil, e.g., work on plantations in rural areas.[3] In such an environment, propagules from the mycelial form have access to the lungs.

The ability of microorganisms to adapt to environmental changes is of fundamental importance, as this ability enables pathogens to survive and cause disease. Tissue necrosis generates hypoxic conditions, and both host and pathogens adapt to survive. The adaptations of fungi to hostile environments with low oxygen levels are underexplored, especially because granulomas appear to have a hypoxic environment.[4]

Pathogenic fungi, such as *Paracoccidioides* spp, have multiple virulence factors that can damage the host. A necessary step in colonization and the development of disease involves the ability of microorganisms to adhere to host surfaces. Adherence is a widely distributed biological phenomenon, which enables microorganisms to colonize their particular habitats. Many fungi, especially pathogenic fungi, are able to adhere to host tissue, the first step in the process of biofilm formation.[5,6] One important event during infection by *Paracoccidioides* spp. is adherence to pulmonary epithelial cells. Several proteins of this fungus (adhesins) have been shown to be ligands of the extracellular matrix in studies performed primarily with lung epithelial cells.[7–10] Various molecules have been described as adhesins in *Paracoccidioides* spp The 43-kDa glycoprotein is involved in *Paracoccidioides* adhesion,[11] as are the 30-, 32- and 54-kDa forms.[8,12] The glycoprotein gp43 and the 30-kDa protein are able to bind laminin.[11,13] Enolase is a fibronectin-binding protein in *Paracoccidioides* spp. that is also present in the cytoplasm and the cell wall, but at a higher levels in the cell wall, suggesting that it performs

*Correspondence to: Maria José Soares Mendes Giannini; Email: giannini@fcfar.unesp.br; gianninimj@gmail.com
Submitted: 05/12/2014; Revised: 03/02/2015; Accepted: 03/15/2015
http://dx.doi.org/10.1080/21505594.2015.1031437

additional functions related to the glycolytic pathway.[8,12] *In vitro* studies have shown that the glyceraldehyde-3-phosphate-dehydrogenase (GAPDH) adhesin may be involved in the pathogenesis of the fungus because this molecule is capable of mediating the ability of the fungus to enter the cell.[14,15]

Additionally, certain hydrolytic enzymes, such as phospholipase, are used by various microorganisms to invade host tissues.[16] These molecules have been described in *P. brasiliensis* and may play an important role in invasion by this fungus.[16–18] *P. brasiliensis* is also known to produce a variety of proteinases.[19,20] The aspartyl proteinases, also known as acid proteases, constitute one of the 4 superfamilies of proteolytic enzymes. They are generally similar to pepsin and show specificity for preferential cleavage at peptide bonds between hydrophobic amino acid residues.[19]

Biofilms are a form of natural microbial growth that is important in the development of infections. They serve as niches for pathogens and are associated with high levels of resistance to antimicrobial agents.[21] The growth and antibiotic resistance of microorganisms differ based on whether they are located in biofilms or in planktonic form.

Fungi of many types have demonstrated the ability to colonize surfaces and form biofilms (Cryptococcus neoformans, Rhodotorula espécies, Aspergillus fumigatus, Malassezia pachydermatis, Histoplasma capsulatum, Pneumocystis species, Coccidioides immitis, Fusarium species, Saccharomyces cerevisiae, Trichosporon asahii, Zygomycetes, Blastoschizomyces and more recently Trichophyton rubrum and Trichophyton mentagrophytes). Most of the previous studies have focused on biofilms of Candida albicans, but other species of Candida, other yeasts and filamentous fungi are known to form biofilms.[22–25] Most importantly, fungal biofilms are of clinical importance, particularly in the context of chronic diseases.[26] For biofilms to successfully form in a host, microorganisms must first adhere to target tissues and concurrently obtain essential nutrients for growth and development. Recently, an in vitro study demonstrated the efficiency with which Histoplasma capsulatum var. capsulatum forms biofilms on abiotic surfaces.[23] Biofilm formation has been associated with the expression of various adhesins.[27] Therefore, the current study aimed to verify the ability of P. brasiliensis to form a biofilm and to investigate the gene expression of several adhesins that could be associated with the biofilm formation of this pathogen.

## Results

### Infection of pneumocytes and alveolar macrophages by *P. brasiliensis*

The notion that *P. brasiliensis* can form biofilms is based on experiments showing that the fungus can appear in clumps that strongly resemble the formation of a fungal mass, which is highly characteristic of biofilms. Infections of *P. brasiliensis* (Pb18) yeast cells in pneumocytes and macrophages were evaluated by confocal laser microscopy and In Cell Analyzer 2000. Pb18 was able to adhere to pneumocytes, as fungal masses were attached to several areas of these cells (**Fig. 1B**). The same pattern of interaction occurred with phagocytic cells, in which an agglomeration of fungal cells was observed around the alveolar macrophage (**Fig. 1D**). **Figure 1A and C** show uninfected macrophages and A549 cells, respectively.

### Kinetics of biofilm formation by *P. brasiliensis*

All biofilm standardization was performed with *P. brasiliensis* (Pb18), the strain used in virulence studies. The kinetics of biofilm formation by *P. brasiliensis* was measured on polystyrene microtiter plates using the XTT reduction assay to determine the amount of metabolic activity. The formation of a biofilm was consistent after 144 h of incubation at 37°C in a $CO_2$ incubator. The initial formation of a biofilm was observed after 7 h. This initial period included pre-adhesion, during which *P. brasiliensis* (Pb18) became attached to the plastic surface in a monolayer arrangement. Over a period of 48 – 120 h, an increase in the biofilm was observed, and the metabolic activity of the biofilm, measured using the XTT reduction assay, increased over time as the cellular mass increased. During the maturation stage (48 – 144 h), the architecture of the *P. brasiliensis* biofilm became more complex (**Fig. 2**).

### Biofilm morphology of *P. brasiliensis*

The morphology of the *P. brasiliensis* biofilm was evaluated using calcofluor white fluorescence microscopy, SEM and CLMS. The *P. brasiliensis* biofilm showed an intense blue coloration, derived from the binding of fluorochrome to the fungal cell wall (**Fig. 3**). SEM revealed a highly organized network of fungal cells in the form of a biofilm and an extracellular matrix (**Fig. 4**). The Pb18 biofilm consisted of a dense network of yeast; an orthogonal image was analyzed to determine the thickness and architecture of the biofilm. The sections of the 3-dimensional image (**Fig. 5B and D**) showed that the *P. brasiliensis* biofilm had a thickness of approximately 100 μm, as observed by CLMS.

### Gene expression analysis using real-time PCR (qRT-PCR)

The gene expression of certain adhesins and enzymes of *P. brasiliensis* was compared between the biofilm and planktonic conditions. The expression of GP43, GAPDH and aspartyl proteinase was significantly higher in the biofilm when compared to the planktonic condition (**Fig. 6**). The expressions of aspartyl proteinase, GAPDH, GP43 and enolase were 10, 9, 2.5 and 1.5 times greater in the biofilm, respectively, than in the planktonic form. The expression of phospholipase was less in the biofilm when compared to the planktonic form.

## Discussion

Biofilm formation has been described for various fungi, including *Candida* species, *C. neoformans*, *C. immitis*, *A. fumigatus*, *Fusarium solani* and, more recently, *H. capsulatum*.[21,23–25] Adhesion is a biological process that allows various organisms to colonize their habitats. The organisms that form biofilms may grow differently in the planktonic and biofilm forms. The aim of the present research was to investigate the ability of *P. brasiliensis*

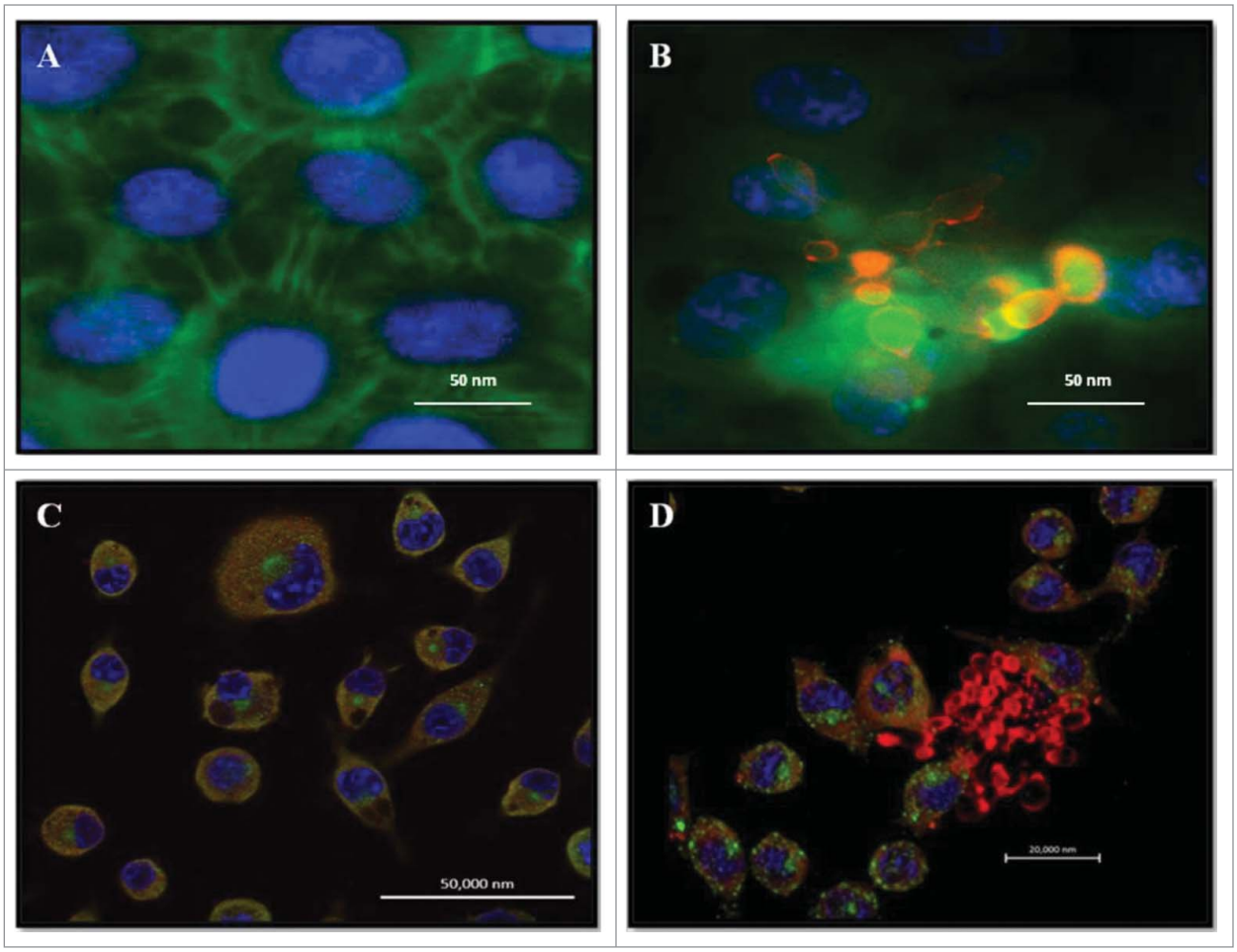


**Figure 1.** Double Immunofluorescence for epithelial cell line A549 and alveolar macrophages murine AMJ2-C11. (**A**) Uninfected A549 cells. (**B**) A549 cells infected with *P. brasiliensis*. A549 cells were labeled with FITC-phalloidin (green), *P. brasiliensis* stained with anti-cell free antibody and Alexa Fluor® 594 conjugate and nucleus was labeled with DAPI (blue). (**C**) Uninfected macrophages. (**D**) Macrophages infected with *P. brasiliensis*. Macrophages were immunolabeled with the primary antibodies anti- cytoplasmic protein and secondary conjugated Alexa Fluor R 488 (green), and *P. brasiliensis* immunolabeled with anti-cell-free antibody (red) and secondary conjugated Alexa Fluor ® 594, and nucleus was labeled with DAPI (blue) (Zeiss LSM 510 Meta Confocal Microscope).

to form a biofilm and to analyze the expression of genes encoding adhesins and hydrolytic enzymes that could be associated with biofilm formation.

In our study, *P. brasiliensis* was able to form a biofilm *in vitro* under hypoxic conditions. Studies by Bonhomme et al.[40] and Stichternoth & Ernst,[41] have indicated that hypoxia is required for *C. albicans* to form biofilms.

The kinetics of biofilm formation by the Pb18 strain showed that the biofilm initially formed before 7 h had elapsed, which included the adhesion period. Mature biofilms were produced from 120 to 144 h. *P. brasiliensis* is a slowly growing fungus. In terms of the time required for formation, Pb18 shows a longer delay and slower growth when compared with other fungi. In contrast, growth is more rapid in the dimorphic fungus, *H. capsulatum* (72 h), and in *C. albicans* (24 h).[23,42] The thickness of the mature biofilm was approximately 100 μm, which is greater than that found for other fungi, such as *C. neoformans,* which exhibited a biofilm thickness of 76 μm, as demonstrated by Martinez et al.[43] The metabolic activity of the biofilm increased over time as the cellular mass increased.

The Pb18 fungal cells may also form an agglomeration resembling a biofilm. However, this structure occurs in *ex vivo* cells, shown in **Figure 1B and D**. Pb18 formed fungal masses in epithelial cells (**Fig. 1B**) and in phagocytic cells (**Fig. 1D**). It was thought that this fungus has the ability to form biofilm, since histopathological findings found fungal mass granulomas. This aspect may be similar to that observed in histopathological observations of organized granulomas, with compact aggregates of macrophages, epithelial cells and masses of yeasts.[44] The same pattern was observed for *H. capsulatum*, which formed a ring of fungal cells in phagocytic cells. This structure may result from a particular type of interaction of this fungus with the tissue. Biofilm formation may contribute to a chronic state of this disease.[23]

The up-regulation of selected genes was demonstrated using qRT-PCR. The results allowed the identification of a potential adhesin of *P. brasiliensis*. Adhesins have an important role in

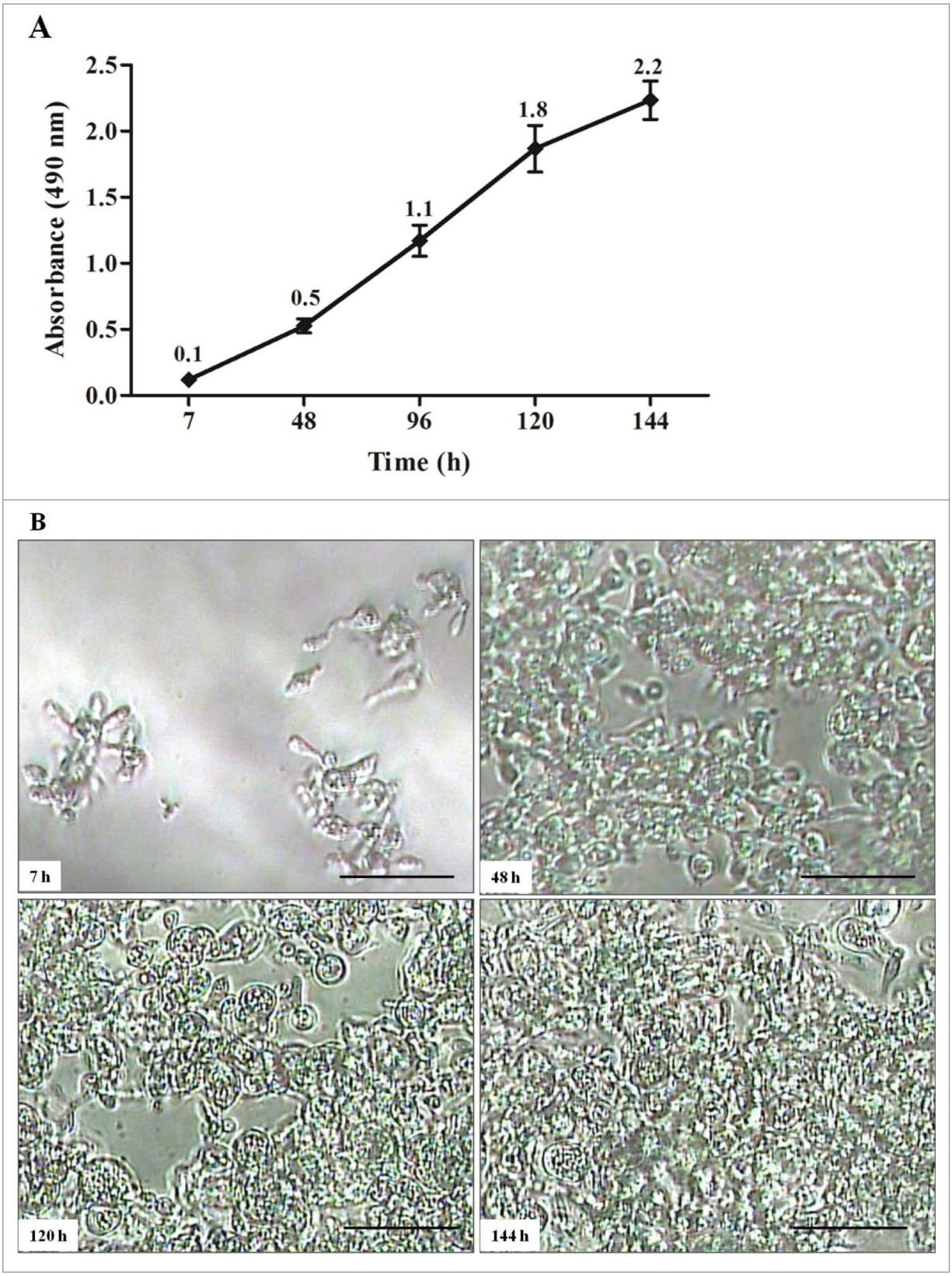


**Figure 2.** Kinetics of biofilm formation by *P. brasiliensis* in microdilution plates. (**A**) Measurements determined by the XTT reduction assay. Each point represents the mean of 3 measurements of absorbance at 490nm on a microtiter reader (iMarkTM Microplate Reader; BIO-RAD). (**B**) Kinetics monitored by Microphotograph taken using a camera attached to an inverted microscope. Bars = 30 nm for all panels.

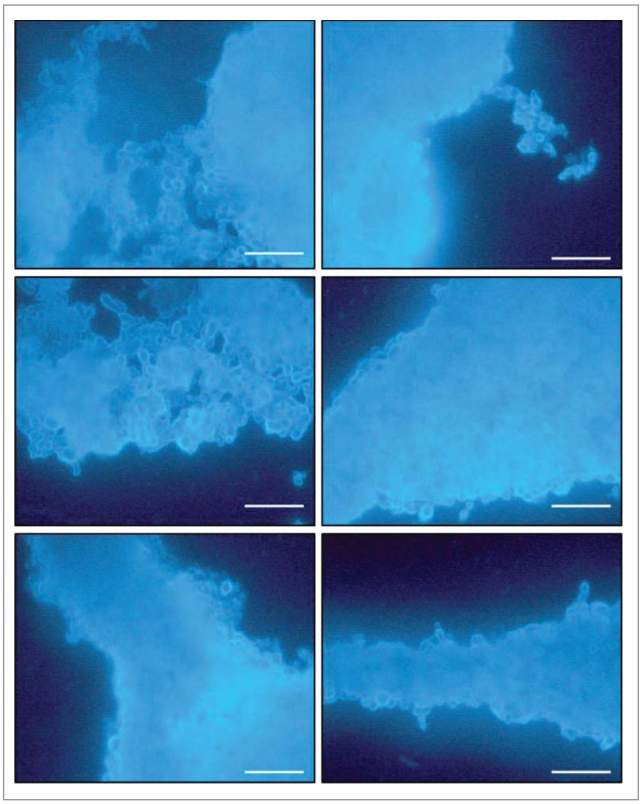

**Figure 3.** Images of mature biofilms of *P. brasiliensis* (Pb 18), formed after incubation for 144 h at 37°C 40× magnification. Images were acquired by Fluorescence microscopy and the fungi biofilms were stained by Calcofluor White Stain reagent (Fluka ®). All scale bars are 125 μm.

biofilm formation, as demonstrated by *C. albicans*, in which ALS genes exhibited increased expression during the formation of biofilms.[45] The real-time PCR performed in the current study detected the expression of GP43, GAPDH, aspartyl proteinase and phospholipase in both planktonic form and biofilm growth, but at different levels. The GP43, GAPDH and aspartyl proteinase genes were significantly ($P \leq 0.05$) overexpressed in the biofilm, whereas phospholipase was downregulated. These results are consistent with data demonstrating an increased expression of adhesins in *Candida* biofilms,[46] the most studied fungal biofilm, as well as in bacterial studies.[47]

Various studies have indicated that the 43-kDa glycoprotein is involved in *Paracoccidioides* adhesion.[11,29] In the present study, GP43 was up-regulated in biofilm formation, demonstrating that this glycoprotein could be involved in adhesion and biofilm formation ($P < 0.05$).

A remarkable level of expression of the GAPDH adhesin was observed; almost 10-fold greater in the biofilm form when compared to the planktonic form ($P < 0.05$). Studies performed by Bailão and collaborators,[14] demonstrated that this adhesin was also upregulated in the yeast form based on recovery of the compound from infected mice.

Verstrepen and Klis,[48] also emphasized the remarkable ability of fungi to express adhesins and form biofilms. This characteristic is of great medical importance, because the presence of a mature biofilm hinders the action of antifungal agents, and biofilms can become a reservoir of cells that show resistance to certain drugs. Therefore, there is a considerable interest in the persistence of infection due to biofilms in infectious diseases.

Aspartyl proteinase and phospholipase were up-regulated and down-regulated, respectively, in the *P. brasiliensis* biofilm when compared with the planktonic form. The results of the present study are consistent with previous research by Ramage et al.[27] and Nailis et al.,[46] in which an increased expression of aspartyl proteinase and a decreased expression of phospholipase were demonstrated in a *C. albicans* biofilm. Ramage et al.[27] reported that the production of proteinase by *C. albicans* aided and established adhesion, invasion and tissue destruction and may be related to the severity of disease because the expression of this enzyme was significantly higher in mature biofilms.

Proteinases produced by *P. brasiliensis*, *A. fumigatus*, *T. rubrum*, and *C. neoformans* have been described in previous studies and are of great importance because they may split the major components of the basement membrane *in vitro* and are, therefore, potentially relevant for the spread of this fungus.[19,49,50] Additionally, these proteins are hydrolytic enzymes capable of either hydrolyzing large substrates into small units for transportation into the cell to serve as a nutrient or for degrading tissue and facilitating colonization or invasion, serving as a virulence factor for the pathogen.

The current paper is the first study of *P. brasiliensis* biofilms. Additional studies are required to determine the role of these biofilms *in vivo* in association with pathogenesis.

## Materials and Methods

### Microorganism

Experiments were performed using a clinical isolate of *P. brasiliensis* (Pb18). The strain was cultivated in Fava-Netto at 37°C for 5 d in an atmosphere with a reduced level of oxygen (5% $CO_2$). This strain was isolated from a case of paracoccidioidomycosis (PMC) and then maintained at the Faculty of Medicine, University of São Paulo, Brazil. This strain is considered a highly virulent isolate (Pb18 isolate), as described in the intraperitoneal infection of susceptible, genetically homogeneous B10A mice.[28] Pb18 also presents a high level of adhesion.[29]

### Preparation of inoculum

A suspension of *P. brasiliensis* (Pb18) was prepared in PBS and was adjusted to $10^8$ cells/ml for the infection assay based on observations performed with a Neubauer counting chamber.

### Antisera and reagents

A cell-free antigen was obtained using Pb18 and was prepared as described elsewhere.[30] Approximately 300 mg of the fungus was added to 1 ml of sterile PBS. This mixture was vortexed for 30 seconds and centrifuged at 400 g for 1 minute. The supernatant (cell-free antigen) was collected, aliquoted and stored at

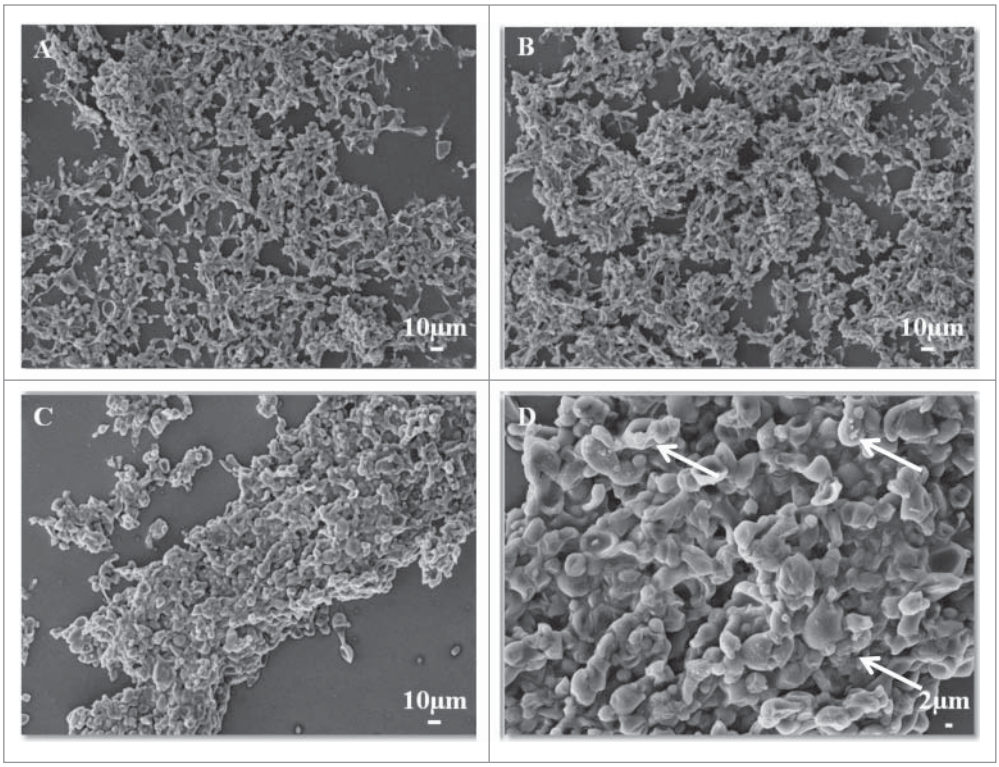


**Figure 4.** SEM images of mature biofilms of *P. brasiliensis* (Pb 18), in different dimensions, formed after incubation for 144 h at 37°C (**A–D**). In the arrows in **Figure 4D** showing the presence of extracellular matrix.

−20°C. The Bradford method (BioRad, São Paulo,SP, Brazil) was used to quantify the protein concentration and the samples were analyzed using the SDS-PAGE method. A polyclonal antibody produced against *P. brasiliensis* cell-free antigen was prepared as described in Mendes-Giannini et al.[5] Rabbits were inoculated with injections of 1.0 ml of antigen mixed with 1.0 ml of complete Freund´s adjuvant. After 3 months of injections of antigen, the rabbits were bled, and the fractions of antisera were separated by precipitation with ammonium sulfate and stored at – 70°C.

The following antibodies were used in this current study: Alexa Fluor 488 goat anti-rabbit IgG (Molecular Probes, USA), Alexa Fluor® 594 goat anti-rabbit IgG (Molecular Probes, Invitrogen, USA) and Alexa Fluor® 488 goat anti-mouse IgG (Molecular Probes, USA). Fluorescein isothiocyanate (FITC)-labeled phalloidin and all other reagents were purchased from Sigma-Aldrich, USA.

**Macrophages and epithelial cell line A549 culture**

Macrophages, alveolar line AMJ2-C11 (ATCC CRL-2456), were cultivated overnight in Dulbecco's modified Eagle's medium (DMEM) (Sigma-Aldrich, Brazil), supplemented with 10% fetal calf serum (Cultilab, Brazil). Cultures of a human lung adenocarcinoma, cell line A549, were obtained from the American Type Culture Collection (ATCC-Rockville, MD). These cells were seeded in Ham's F-12 medium supplemented with 10% fetal calf serum.

**Infection assay**

Macrophages and continuous epithelial cell line A549 cells were cultured at 36.5°C in 24-well plates with the well bottoms covered with coverslips. The cultures were adjusted to $1 \times 10^5$ cells per well. A total of $1 \times 10^5$ Pb18 yeast-phase cells/ml were added to the cells to obtain a yeast/macrophage ratio of 1:1. After infection, these cover slips were fixed with 4% paraformaldehyde and submitted to immunofluorescence. The coverslips were permeabilized with a solution of Triton X-100, 0.5% in PBS, for 20 minutes. The coverslips were then washed, the "cell-free" antiserum was added, and the samples were incubated at room temperature for 1 hour, washed again, and conjugated anti-rabbit labeled with Alexa 594 (INVITROGEN) at a ratio of 1:300 was added. Phalloidin-FITC conjugate (SIGMA) at a ratio of 1:100 at 4°C was added and the specimens sat overnight. The specimens were again washed, 100 µl DAPI (4 '- 6 – diamidino – 2 – phenylindole) was added for 10 minutes to mark the cores, washed with PBS, mounted on slides with buffered glycerol, and examined using a confocal microscope (Zeiss LSM 510 Meta Confocal Microscope).

The cultures were then incubated for 7 h at 36.5°C to observe adhesion. The assay was analyzed using conventional fluorescence microscopy and scanning confocal laser microscopy (CLMS) (Zeiss LSM 510 Meta Confocal Microscope, Carl Zeiss, Jena, Göttingen).

**Biofilm assay**

The assay was performed as described by Silva et al.[31] with slight modifications. Initially, 500 µl of a culture of $1 \times 10^8$ cells/ml in saline was added to the wells of a 24-well plate (TPP, Trasadingen, Switzerland) and covered with coverslips. The plates were incubated at 37°C for 7 h in 5% $CO_2$ for biofilm pre-adhesion. After pre-adhesion for 7 h, the supernatant was removed from each well. Subsequently, 1000 µL of mFUM (Modified Fluid Universal Medium – Guggenheim et al.[32]) was added to each well and the plates were further incubated for 144 h. The culture medium was renewed every 48 hours. After biofilm formation for 144 h, the supernatant was again removed, and the wells were rinsed using 400 µl of PBS. Six wells were filled with a sterile medium as a control. All assays were repeated at least 3 times.. To characterize the biofilm, measurements of biofilm metabolic activity were made using XTT. At the structural level, *P. brasiliensis* biofilm formation was characterized

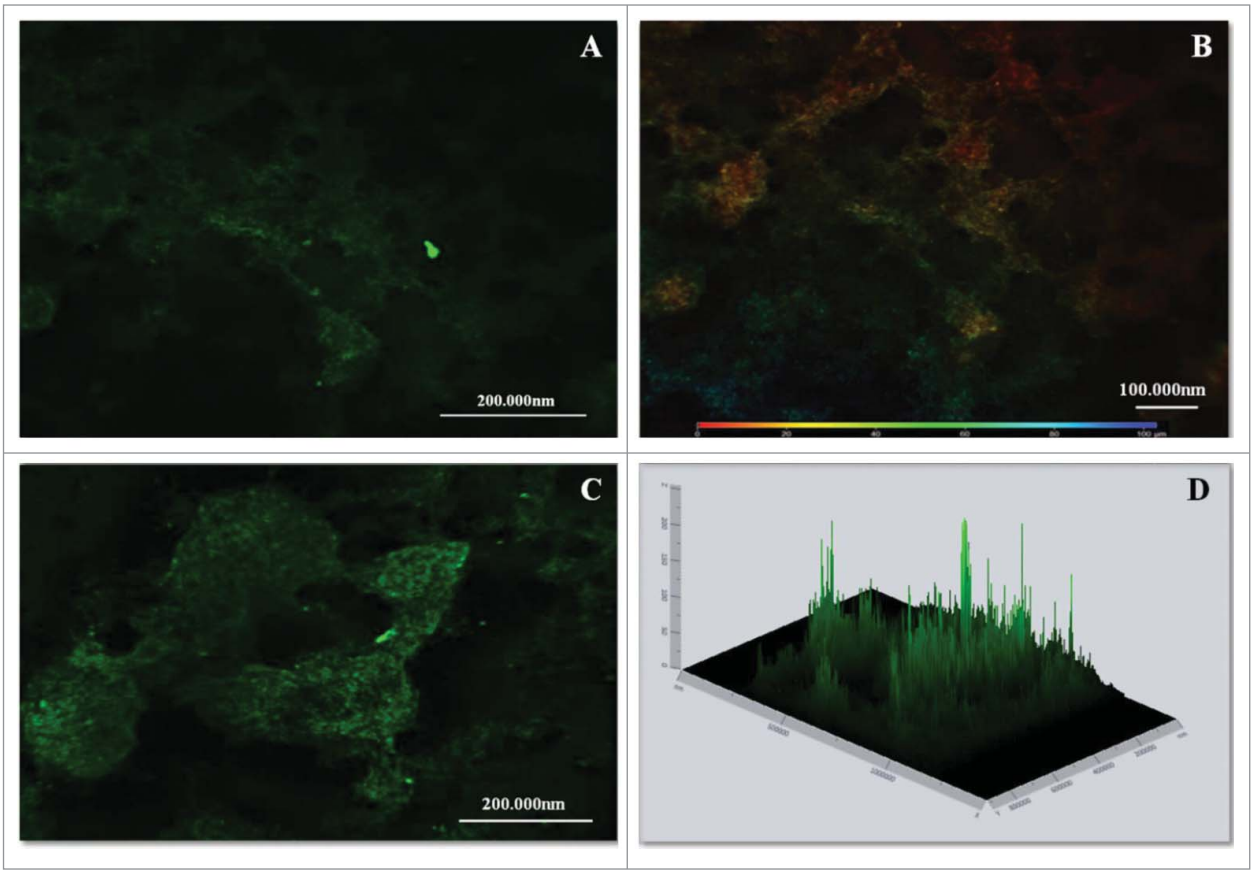


**Figure 5.** CLSM images of mature biofilms of *P. brasiliensis (144 h)*. Fluorescence labeling of *P. brasiliensis* biofilms. (**A and C**) Biofilm was immunolabeled with primary antibodies anti-cell-free and secondary conjugated Alexa Fluor ® 488. (**B**) Scale depth image A showing the thickness of the biofilm. (**D**) Projection of biofilm formation of *P. brasiliensis* 2.5D (Zeiss LSM 510 Meta Confocal Microscope).

using Calcofluor White Stain (Fluka®, São Paulo, SP., Brazil) and scanning electron microscopy (SEM), and biofilm measurements were performed using confocal laser scanning microscopy (CLSM).

**Measurement of biofilm metabolic activity**

A quantitative measurement of *P. brasiliensis* biofilm formation was obtained from the XTT reduction assay. For this measurement, 50 μL of XTT salt solution (1 mg $ml^{-1}$ in PBS) and 4 μl of menadione solution (1 mM in ethanol; Sigma-Aldrich, São Paulo, SP., Brazil) were added to each well of the microtiter plates and incubated at 37°C for 3 h, resulting in a colorimetric reaction that is correlated with cell viability. This reaction was measured using a microtiter reader (iMarkTM Microplate Reader; BIORAD, Brazil) at 490 nm. In all assays, culture media were included as negative controls.[31–33]

**Fluorescence microscopy**

For fluorescence microscopy, coverslips with biofilm were stained with Calcofluor White Stain reagent (1g/L – Fluka®). To prepare the coverslips, 50 μl of dye were added. The coverslips were carefully removed from each well and transferred to a slide for observation under a fluorescence microscope. Calcofluor is a non-specific fluorochrome that binds to cellulose and chitin in the fungal cell wall. This staining procedure provides a rapid method for the detection of yeasts and pathogenic fungi.[34] A range of wavelengths, from 300 to 440 nm, can be used for excitation. Emission occurred at a wavelength of 355 nm.

**Scanning electron microscopy**

Biofilms formed on coverslips were processed as described by Morris et al.[35] and modified by Ells and Truelstrup Hansen.[36] Briefly, the specimens were washed 3 times with PBS to remove planktonic cells and then fixed with 1% glutaraldehyde in 0.2 M sodium cacodylate buffer for 18 h at 4°C. After three PBS washes of 10 min each, the biofilms that still adhered to the coverslips were fixed with 1% osmium tetroxide for 2 h. The specimens were washed with PBS and dehydrated with an increasing gradient of ethanol, from 50% to 100% ethanol, at room temperature. The samples were dried using the critical point method in a Samdri 780A desiccator (Rockville, MD, USA) using $CO_2$. Topographic features of the biofilms were analyzed with a Zeiss-Leica/440 SEM at the Institute of Chemistry of Sao Carlos, University of Sao Paulo, using a voltage of 25 kV and a 10 mm working distance.

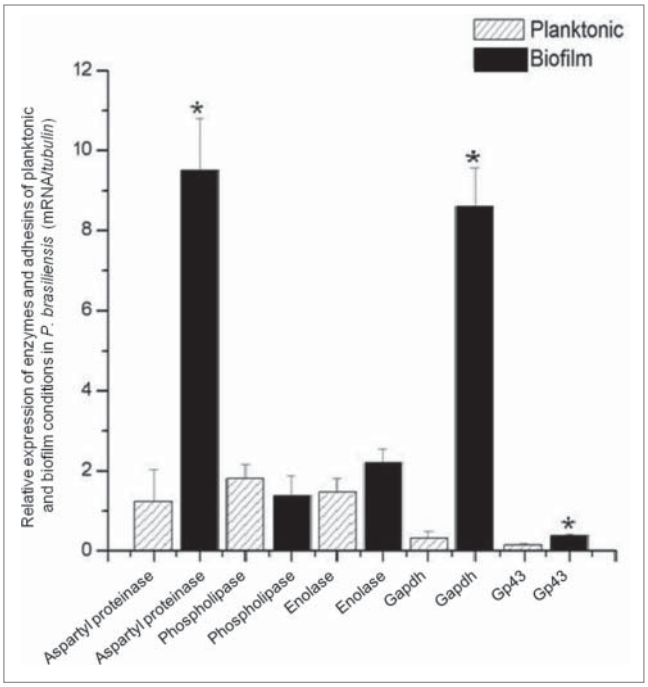


**Figure 6.** Relative expression of adhesins/ enzymes of *P. brasiliensis* during growth in biofilm and planktonic conditons, both in low oxygen tension using real-time PCR (qRT-PCR). Statistical analyzes were performed by Student's t-test, $P < 0.05$.

**Indirect immunofluorescence**

After biofilm formation, the biofilm was fixed with 4% paraformaldehyde, washed in PBS, and permeabilized in 0.5% Triton X-100 for 30 minutes. After permeabilization, anti-*P. brasiliensis* (cell-free) serum was added for 1 h, unbound antibodies were removed by washing with PBS, and Alexa Fluor®488 goat anti-rabbit IgG was then added for 1 h. The biofilm was then washed 3 times with PBS and analyzed under confocal laser scanning microscopy (LSM 510 – META, Zeiss). For the adhesion assay, the same procedure was used, but the secondary antibody was Alexa Fluor®594 goat anti-rabbit IgG, added for 1 h. FITC-labeled phalloidin was then added for 1 h and observed using confocal microscopy.

**RNA isolation and cDNA synthesis**

RNA extraction was performed from mature biofilms (144h) and planktonic cells (144h). Planktonic cells were cultured in mFUM in bottles. Every 48 hours, the cells in suspension were withdrawn and centrifuged, then placed in fresh medium in a new flask for a period of 144 hours. After 144 hours, the biofilm and planktonic cells were washed and centrifuged. The resulting pellet was stored in Ultra freezer for subsequent RNA extraction. Total RNA was obtained by the addition of TRIZOL® (Invitrogen, Carlsbad, CA, USA) after growing the Pb18 strain in both the biofilm and planktonic forms under 5% $CO_2$ conditions. Total RNA was treated with DNase I (Invitrogen, Carlsbad, CA, USA). RNA quality (i.e., the presence of discrete 18S and 28S rRNA peaks) was determined in 1.5% agarose gels in 1× TBE buffer for 2 h at 100 V. The gels were stained with GelRed and observed under UV light. Two independent RNA samples were prepared for use in the experiments. First-strand cDNA synthesis was performed using 1 μg/μl RNA and the enzyme Superscript III reverse transcriptase (Invitrogen, Carlsbad, CA, USA).[37]

**Table 1** Primers utilized in this study

| Gene | Primers |
|---|---|
| GP43 | Sense 5′-CTTGTCTGGGCCAAAAACTC-3′<br>Antisense 5′-GCCAGGGTTTGTTTGACTGT-3′ |
| Enolase | Sense 5′-TAGGCACCCTCACTGAATCC-3′<br>Antisense 5′-GCTCTCAATCCCACAACGAT-3′ |
| Phospholipase | Sense 5′-TGTTGGTGCGATCAAAAGAC-3<br>Antisense 5′-GGATACGACGTCGCCACTAT-3 |
| Aspartyl Proteinase | Sense 5′-AAAGGAAACACGGAAACACG-3<br>Antisense 5′-CGTTCCTGAGACGGTGGTAT-3 |
| GAPDH | Sense 5′-AAATGCTGTTGAGCACGATG-3′<br>Antisense 5′-CTGTGCTGGATATCGCCTTT-3′ |
| β-tubulin (Housekeeping gene) | Sense 5′-TGGCCACTTTCTCTGTCGTTC3′<br>Antisense 5′-CAGGGTGGCATTGTATGGCT3′ |

**Gene expression analysis for real-time PCR (qRT-PCR)**

The expression levels of 5 genes involved in various cellular functions of *P. brasiliensis* were measured and described during growth in biofilm and planktonic forms, both under low oxygen tension. Quantitative real-time PCR (qRT-PCR) was performed for genes using the primer constants shown in **Table 1**. The concentrations of primers used were adjusted to 0.5 μM for improved amplification efficiency. The quantity of cDNA used was 1 μl, and 12.5 μl of Maxima®SYBR Green (Fermentas, São Paulo, SP., Brazil) was added. The final volume was adjusted to 25 μl. PCR was performed with a starting temperature of 50°C for 2 minutes, followed by 10 minutes at 95°C, then 40 cycles at 95°C for 15 seconds, followed by annealing and synthesis at 60°C for 1 minute. The reactions were performed in triplicate using an Applied Biosystems 7500 thermal cycler. Variations in mRNA expression were calculated using the $2^{-\Delta CT}$ formula, where ΔCT is the difference between the targets and the housekeeping gene β-tubulin in accordance with previous studies performed by several authors. The data were analyzed using the $2^{-\Delta\Delta C_T}$ method.[38] The specific primers for qRT-PCR were designed using the Primer 3 software.[39]

**Statistical analysis**

The data were analyzed using the Origin 6.0 software (Origin Lab Corporation, Northampton, MA). A $P$ value $\leq 0.05$ was considered statistically significant.

**Disclosure of Potential Conflicts of Interest**

No potential conflicts of interest were disclosed.

**Funding**

The authors thank CNPq (National Council for Scientific and Technological Development) and PADC (Support Program for Scientific, Faculty of Pharmaceutical Sciences, UNESP) for their financial support.

## References


1. Marques-da-Silva SH, Rodrigues AM, de Hoog GS, Silveira-Gomes F, Camargo ZP. Occurrence of *Paracoccidioides lutzii* in the Amazon region: description of two cases. Am J Trop Med Hyg 2012; 87:710-4; PMID:22927496; http://dx.doi.org/10.4269/ajtmh.2012.12-0340
2. Arantes TD, Theodoro RC, Da Graça Macoris SA, Bagagli E. Detection of *Paracoccidioides* spp. in environmental aerosol samples. Med Mycol 2013; 51:83-92; PMID:22762209; http://dx.doi.org/10.3109/13693786.2012.698444
3. Franco M, Montenegro MR, Mendes RP, Marques SA, Dillon NL, Mota NG. Paracoccidioidomycosis: a recently proposed classification of its clinical forms. Rev Soc Bras Med Trop 1987; 20:129-32; PMID:3507739; http://dx.doi.org/10.1590/S0037-86821987000200012
4. Grahl N, Shepardson KM, Chung D, Cramer RA. Hypoxia and fungal pathogenesis: to air or not to air? Eukaryot Cell 2012; 11:560-70; PMID:22447924; http://dx.doi.org/10.1128/EC.00031-12
5. Mendes-Giannini MJ, Taylor ML, Bouchara JB, Burger E, Calich VL, Escalante ED, Hanna SA, Lenzi HL, Machado MP, Miyaji M, et al. Pathogenesis II: fungal responses to host responses: interaction of host cells with fungi. Med Mycol 2000; 38 (Suppl 1):113-23; PMID:11204137; http://dx.doi.org/10.1080/mmy.38.s1.113.123
6. Mendes-Giannini MJ, Soares CP, da Silva JL, Andreotti PF. Interaction of pathogenic fungi with host cells: Molecular and cellular approaches. FEMS Immunol Med Microbiol 2005; 45:383-94; PMID:16087326; http://dx.doi.org/10.1016/j.femsim.2005.05.014
7. Hernández O, Almeida AJ, Tamayo D, Torres I, Garcia AM, López A, Restrepo A, McEwen JG. The hydrolase PbHAD32 participates in the adherence of *Paracoccidioides brasiliensis* conidia to epithelial lung cells. Med Mycol 2012; 50:533-7; http://dx.doi.org/10.3109/13693786.2011.619583
8. Donofrio FC, Calil AC, Miranda ET, Almeida AM, Benard G, Soares CP, Veloso SN, Soares CM, Mendes Giannini MJ. Enolase from *Paracoccidioides brasiliensis*: isolation and identification as a fibronectin-binding protein. J Med Microbiol 2009; 58:706-13; PMID:19429745; http://dx.doi.org/10.1099/jmm.0.003830-0
9. Caro E, Gonzalez A, Muñoz C, Urán ME, Restrepo A, John Hamilton A, Elena Cano L. Recognition of laminin by *Paracoccidioides brasiliensis* conidia: a possible mechanism of adherence to human type II alveolar cells. Med Mycol 2008; 46:795-804; PMID:18608937; http://dx.doi.org/10.1080/13693780802073108
10. Mendes-Giannini MJ, Hanna SA, da Silva JL, Andreotti PF, Vincenzi LR, Benard G, Lenzi HL, Soares CP. Invasion of epithelial mammalian cells by *Paracoccidioides brasiliensis* leads to cytoskeletal rearrangement and apoptosis of the host cell. Microbes Infect 2004; 6:882-91; PMID:15310464; http://dx.doi.org/10.1016/j.micinf.2004.05.005
11. Vicentini AP, Gesztesi JL, Franco MF, de Souza W, de Moraes JZ, Travassos LR, Lopes JD. Binding of *Paracoccidioides brasiliensis* to laminin through surface glycoprotein gp43 leads to enhancement of fungal pathogenesis. Infect Immun 1994; 62:1465-9; PMID:8132354
12. Marcos CM, de Fátima da Silva J, de Oliveira HC, Moraes da Silva RA, Mendes-Giannini MJ, Fusco-Almeida AM. Surface-expressed enolase contributes to the adhesion of *Paracoccidioides brasiliensis* to host cells. FEMS Yeast Res 2012; 12:557-70; PMID:22443156; http://dx.doi.org/10.1111/j.1567-1364.2012.00806.x
13. Andreotti PF, Monteiro da Silva JL, Bailão AM, Soares CM, Benard G, Soares CP, Mendes-Giannini MJ. Isolation and partial characterization of a 30 kDa adhesin from *Paracoccidioides brasiliensis*. Microbes Infect 2005; 7:875-81; PMID:15862780; http://dx.doi.org/10.1016/j.micinf.2005.02.005
14. Bailão AM, Schrank A, Borges CL, Dutra V, Walquíria Inês Molinari-Madlum EE, Soares Felipe MS, Soares Mendes-Giannini MJ, Martins WS, Pereira M, Maria de Almeida Soares C. Differential gene expression by *Paracoccidioides brasiliensis* in host interaction conditions: representational difference analysis identifies candidate genes associated with fungal pathogenesis. Microbes Infect 2006; 8:2686-97; http://dx.doi.org/10.1016/j.micinf.2006.07.019
15. Barbosa MS, Báo SN, Andreotti PF, de Faria FP, Felipe MS, dos Santos Feitosa L, Mendes-Giannini MJ, Soares CM. Glyceraldehyde-3-phosphate dehydrogenase of *Paracoccidioides brasiliensis* is a cell surface protein involved in fungal adhesion to extracellular matrix proteins and interaction with cells. Infect Immun 2006; 74:382-9; PMID:16368993; http://dx.doi.org/10.1128/IAI.74.1.382-389.2006
16. Ghannoum MA. Potential role of phospholipases in virulence and fungal pathogenesis. Clin Microbiol Rev 2000; 13:122-43, table of contents; PMID:10627494; http://dx.doi.org/10.1128/CMR.13.1.122-143.2000
17. Parente JA, Salem-Izacc SM, Santana JM, Pereira M, Borges CL, Bailão AM, Soares CM. A secreted serine protease of *Paracoccidioides brasiliensis* and its interactions with fungal proteins. BMC Microbiol 2010; 10:292; PMID:21080956; http://dx.doi.org/10.1186/1471-2180-10-292
18. Maza PK, Oliveira P, Toledo MS, Paula DM, Takahashi HK, Straus AH, Suzuki E. *Paracoccidioides brasiliensis* induces secretion of IL-6 and IL-8 by lung epithelial cells. Modulation of host cytokine levels by fungal proteases. Microbes Infect 2012; 14:1077-85; PMID:22687715; http://dx.doi.org/10.1016/j.micinf.2012.05.016
19. Tacco BA, Parente JA, Barbosa MS, Báo SN, Gsóes Tde S, Pereira M, Soares CM. Characterization of a secreted aspartyl protease of the fungal pathogen *Paracoccidioides brasiliensis*. Med Mycol 2009; 47:845-54; PMID:20028235; http://dx.doi.org/10.3109/13693780802695512
20. Longo LV, Nakayasu ES, Matsuo AL, Peres da Silva R, Sobreira TJ, Vallejo MC, Ganiko L, Almeida IC, Puccia R. Identification of human plasma proteins associated with the cell wall of the pathogenic fungus *Paracoccidioides brasiliensis*. FEMS Microbiol Lett 2013; 341:87-95; PMID:23398536; http://dx.doi.org/10.1111/1574-6968.12097
21. Pierce GE. *Pseudomonas aeruginosa*, *Candida albicans*, and device-related nosocomial infections: implications, trends, and potential approaches for control. J Ind Microbiol Biotechnol 2005; 32:309-18; PMID:15868157; http://dx.doi.org/10.1007/s10295-005-0225-2
22. Sánchez-Vargas LO, Estrada-Barraza D, Pozos-Guillen AJ, Rivas-Caceres R. Biofilm formation by oral clinical isolates of *Candida* species. Arch Oral Biol 2013; 58:1318-26; http://dx.doi.org/10.1016/j.archoralbio.2013.06.006
23. Pitangui NS, Sardi JC, Silva JF, Benaducci T, Moraes da Silva RA, Rodríguez-Arellanes G, Taylor ML, Mendes-Giannini MJ, Fusco-Almeida AM. Adhesion of *Histoplasma capsulatum* to pneumocytes and biofilm formation on an abiotic surface. Biofouling 2012; 28:711-8; PMID:22784100; http://dx.doi.org/10.1080/08927014.2012.703659
24. Kaur S, Singh S. Biofilm formation by *Aspergillus fumigatus*. Med Mycol 2013; 52(1):2-9; PMID:23962172
25. Sengupta J, Saha S, Khetan A, Sarkar SK, Mandal SM. Effects of lactoferricin B against keratitis-associated fungal biofilms. J Infect Chemother 2012; 18:698-703; PMID:22410856; http://dx.doi.org/10.1007/s10156-012-0398-3
26. Bjarnsholt T, Alhede M, Alhede M, Eickhardt-Sørensen SR, Moser C, Kühl M, Jensen PØ, Høiby N. The in vivo biofilm. Trends Microbiol 2013; 21:466-74; PMID:23827084; http://dx.doi.org/10.1016/j.tim.2013.06.002
27. Ramage G, Coco B, Sherry L, Bagg J, Lappin DF. In vitro *Candida albicans* biofilm induced proteinase activity and SAP8 expression correlates with in vivo denture stomatitis severity. Mycopathologia 2012; 174:11-9; PMID:22302440; http://dx.doi.org/10.1007/s11046-012-9522-2
28. Singer-Vermes LM, Burger E, Franco MF, Di-Bacchi MM, Mendes-Giannini MJ, Calich VL. Evaluation of the pathogenicity and immunogenicity of seven *Paracoccidioides brasiliensis* isolates in susceptible inbred mice. J Med Vet Mycol 1989; 27:71-82; PMID:2746437; http://dx.doi.org/10.1080/02681218980000111
29. Hanna SA, Monteiro da Silva JL, Giannini MJ. Adherence and intracellular parasitism of *Paracoccidioides brasiliensis* in Vero cells. Microbes Infect 2000; 2:877-84; PMID:10962270; http://dx.doi.org/10.1016/S1286-4579(00)00390-7
30. Camargo ZP, Taborda CP, Rodrigues EG, Travassos LR. The use of cell-free antigens of *Paracoccidioides brasiliensis* in serological tests. J Med Vet Mycol 1991; 29:31-8; PMID:1905751; http://dx.doi.org/10.1080/02681219180000061
31. Silva S, Henriques M, Oliveira R, Williams D, Azeredo J. In vitro biofilm activity of non-*Candida albicans* *Candida* species. Curr Microbiol 2010; 61:534-40; PMID:20401483; http://dx.doi.org/10.1007/s00284-010-9649-7
32. Guggenheim B, Giertsen E, Schüpbach P, Shapiro S. Validation of an in vitro biofilm model of supragingival plaque. J Dent Res 2001; 80:363-70; PMID:11269730; http://dx.doi.org/10.1177/00220345010800011201
33. Martinez LR, Casadevall A. *Cryptococcus neoformans* biofilm formation depends on surface support and carbon source and reduces fungal cell susceptibility to heat, cold, and UV light. Appl Environ Microbiol 2007; 73:4592-601; PMID:17513597; http://dx.doi.org/10.1128/AEM.02506-06
34. Harrington BJ, Hageage GJ. Calcofluor white: a review of its uses and applications in clinical mycology and parasotology. Lab Med 2003; 34:361-7; http://dx.doi.org/10.1309/EPH2TDT8335GH0R3
35. Morris CE, Monier J, Jacques M. Methods for observing microbial biofilms directly on leaf surfaces and recovering them for isolation of culturable microorganisms. Appl Environ Microbiol 1997; 63:1570-6; PMID:16535579
36. Ells TC, Truelstrup Hansen L. Strain and growth temperature influence *Listeria* spp. attachment to intact and cut cabbage. Int J Food Microbiol 2006; 111:34-42; PMID:16824634; http://dx.doi.org/10.1016/j.ijfoodmicro.2006.04.033
37. Voltan AR, Sardi JeC, Soares CP, Pelajo Machado M, Fusco Almeida AM, Mendes-Giannini MJ. Early Endosome Antigen 1 (EEA1) decreases in macrophages infected with *Paracoccidioides brasiliensis*. Med Mycol 2013; 51:759-64; PMID:23566224; http://dx.doi.org/10.3109/13693786.2013.777859
38. Livak KJ, Schmittgen TD. Analysis of relative gene expression data using real-time quantitative PCR and the 2(-Delta Delta C(T)) Method. Methods 2001; 25:402-8; http://dx.doi.org/10.1006/meth.2001.1262
39. Rozen S, Skaletsky H. Primer3 on the WWW for general users and for biologist programmers. Methods Mol Biol 2000; 132:365-86; PMID:10547847
40. Bonhomme J, Chauvel M, Goyard S, Roux P, Rossignol T, d'Enfert C. Contribution of the glycolytic flux and hypoxia adaptation to efficient biofilm formation by *Candida albicans*. Mol Microbiol 2011; 80:995-1013; PMID:21414038; http://dx.doi.org/10.1111/j.1365-2958.2011.07626.x
41. Stichternoth C, Ernst JF. Hypoxic adaptation by Efg1 regulates biofilm formation by *Candida albicans*. Appl Environ Microbiol 2009; 75:3663-72;

PMID:19346360; http://dx.doi.org/10.1128/AEM.00098-09
42. Pierce CG, Uppuluri P, Tummala S, Lopez-Ribot JL. A 96 well microtiter plate-based method for monitoring formation and antifungal susceptibility testing of *Candida albicans* biofilms. J Vis Exp 2010; 21: 2287; http://dx.doi.org/10.3791/2287
43. Martinez LR, Casadevall A. Susceptibility of *Cryptococcus neoformans* biofilms to antifungal agents *in vitro*. Antimicrob Agents Chemother. 2006; 50:1021-1033; PMID:16495265; http://dx.doi.org/10.1128/AAC.50.3.1021-1033.2006
44. Da Silva FC, Svidzinski TI, Patussi EV, Cardoso CP, De Oliveira Dalalio MM, Hernandes L. Morphologic organization of pulmonary granulomas in mice infected with *Paracoccidioides brasiliensis*. Am J Trop Med Hyg 2009; 80:798-804; PMID:19407127
45. O'Connor L, Lahiff S, Casey F, Glennon M, Cormican M, Maher M. Quantification of ALS1 gene expression in *Candida albicans* biofilms by RT-PCR using hybridisation probes on the LightCycler. Mol Cell Probes 2005; 19:153-62; PMID:15797814; http://dx.doi.org/10.1016/j.mcp.2004.10.007
46. Nailis H, Kucharíková S, Ricicová M, Van Dijck P, Deforce D, Nelis H, Coenye T. Real-time PCR expression profiling of genes encoding potential virulence factors in *Candida albicans* biofilms: identification of model-dependent and -independent gene expression. BMC Microbiol 2010; 10:114; PMID:20398368; http://dx.doi.org/10.1186/1471-2180-10-114
47. Sanchez CJ, Shivshankar P, Stol K, Trakhtenbroit S, Sullam PM, Sauer K, Hermans PW, Orihuela CJ. The pneumococcal serine-rich repeat protein is an intra-species bacterial adhesin that promotes bacterial aggregation in vivo and in biofilms. PLoS Pathog 2010; 6:e1001044
48. Verstrepen KJ, Klis FM. Flocculation, adhesion and biofilm formation in yeasts. Mol Microbiol 2006; 60:5-15; PMID:16556216; http://dx.doi.org/10.1111/j.1365-2958.2006.05072.x
49. Leng WC, Wang LL, Wei CD, Yang J, Jin Q. Analysis of secreted proteases of *Trichophyton rubrum*. Wei Sheng Wu Xue Bao 2005; 45:601-5; PMID:16245880
50. Pinti M, Orsi CF, Gibellini L, Esposito R, Cossarizza A, Blasi E, Peppoloni S, Mussini C. Identification and characterization of an aspartyl protease from *Cryptococcus neoformans*. FEBS Lett 2007; 581:3882-6; PMID:17651737; http://dx.doi.org/10.1016/j.febslet.2007.07.006

frontiers in Microbiology

ORIGINAL RESEARCH
published: 11 January 2016
doi: 10.3389/fmicb.2015.01526

# An Intracellular Arrangement of *Histoplasma capsulatum* Yeast-Aggregates Generates Nuclear Damage to the Cultured Murine Alveolar Macrophages

*Nayla de Souza Pitangui[1], Janaina de Cássia Orlandi Sardi[1], Aline R. Voltan[1], Claudia T. dos Santos[1], Julhiany de Fátima da Silva[1], Rosangela A. M. da Silva[1], Felipe O. Souza[1], Christiane P. Soares[1], Gabriela Rodríguez-Arellanes[2], Maria Lucia Taylor[2], Maria J. S. Mendes-Giannini[1] and Ana M. Fusco-Almeida[1]**

[1] Faculdade de Ciências Farmacêuticas, UNESP – Univ Estadual Paulista, Campus Araraquara, Departamento de Análises Clínicas, Laboratório de Micologia Clínica, São Paulo, Brazil, [2] Departamento de Microbiologia y Parasitologia, Facultad de Medicina, Universidad Nacional Autónoma de México, México City, México

OPEN ACCESS

**Edited by:**
*Hector Mora Montes, Universidad de Guanajuato, Mexico*

**Reviewed by:**
*Leonardo Nimrichter, Federal University of Rio de Janeiro, Brazil*
*Erin E. McClelland, Middle Tennessee State University, USA*

***Correspondence:**
*Ana M. Fusco-Almeida*
*ana.marisa@uol.com.br*

**Specialty section:**
*This article was submitted to Fungi and Their Interactions, a section of the journal Frontiers in Microbiology*

**Received:** *09 January 2015*
**Accepted:** *18 December 2015*
**Published:** *11 January 2016*

**Citation:**
*Pitangui NdS, Sardi JdCO, Voltan AR, dos Santos CT, da Silva JdF, da Silva RAM, Souza FO, Soares CP, Rodríguez-Arellanes G, Taylor ML, Mendes-Giannini MJS and Fusco-Almeida AM (2016) An Intracellular Arrangement of Histoplasma capsulatum Yeast-Aggregates Generates Nuclear Damage to the Cultured Murine Alveolar Macrophages. Front. Microbiol. 6:1526. doi: 10.3389/fmicb.2015.01526*

*Histoplasma capsulatum* is responsible for a human systemic mycosis that primarily affects lung tissue. Macrophages are the major effector cells in humans that respond to the fungus, and the development of respiratory disease depends on the ability of *Histoplasma* yeast cells to survive and replicate within alveolar macrophages. Therefore, the interaction between macrophages and *H. capsulatum* is a decisive step in the yeast dissemination into host tissues. Although the role played by components of cell-mediated immunity in the host's defense system and the mechanisms used by the pathogen to evade the host immune response are well understood, knowledge regarding the effects induced by *H. capsulatum* in host cells at the nuclear level is limited. According to the present findings, *H. capsulatum* yeast cells display a unique architectural arrangement during the intracellular infection of cultured murine alveolar macrophages, characterized as a formation of aggregates that seem to surround the host cell nucleus, resembling a "crown." This extranuclear organization of yeast-aggregates generates damage on the nucleus of the host cell, producing DNA fragmentation and inducing apoptosis, even though the yeast cells are not located inside the nucleus and do not trigger changes in nuclear proteins. The current study highlights a singular intracellular arrangement of *H. capsulatum* yeast near to the nucleus of infected murine alveolar macrophages that may contribute to the yeast's persistence under intracellular conditions, since this fungal pathogen may display different strategies to prevent elimination by the host's phagocytic mechanisms.

**Keywords: *Histoplasma capsulatum*, host-pathogen interactions, intracellular arrangement, nucleus, alveolar macrophages**

## INTRODUCTION

Many studies have been performed to elucidate the interaction between the dimorphic fungus *Histoplasma capsulatum* and host macrophages, specifically to determine the role played by the components of the host's cell-mediated immunity and the evasion mechanisms used by the pathogen. In some conditions, in contrast to their usual function of eliminating deleterious microorganisms, macrophages give rise to a favorable environment for the survival and reproduction of the *H. capsulatum* yeast phase, which is the parasitic-virulent morphotype of this fungus (Medeiros et al., 2002; Tagliari et al., 2012). *H. capsulatum* has been described as a facultative intracellular pathogen, and it is almost exclusively found within host-parasitized cells (Wu-Hsieh et al., 1998; Hilty et al., 2008). Once the pathogen has been phagocytosed, several immunological factors can modulate the course of the infection (Allen and Deepe, 2005).

According to Newman et al. (2011), the destruction of alveolar macrophages and their subsequent ingestion by other immune cells are events that promote the propagation of the infection to different organs during the acute stage of primary histoplasmosis. Thus, it is clear that the interaction between the macrophage and *H. capsulatum* is a decisive step in the occurrence of yeast dissemination into host tissues.

Apoptosis of phagocytes in the initial stage of infection by *H. capsulatum* activates CD4+ and CD8+ T cells, both of which partially act as a defense mechanism for the host. Hsieh et al. (2011), described that apoptosis induced by the infection is an important immune function recognized by the antimicrobial host response mainly in the defense against phagosome-enclosed pathogens. Hence, inhibition of apoptosis modulates the inflammatory response and also interferes in the outcome of the infection process. According to Allen and Deepe (2005), IL-4 and IL-10 production are enhanced when apoptosis is inhibited, with the release of these cytokines exacerbating the fungal infection. This result occurs because the apoptosis of macrophages, which is induced early in a pulmonary infection by *H. capsulatum*, releases IL-10, which inhibits apoptosis of neighboring macrophages, enabling and delimiting the intracellular residence of *H. capsulatum* yeast (Deepe and Buesing, 2012).

Nuclear fragmentation is a morphological cellular alteration associated with apoptosis (Deepe and Buesing, 2012); thus, nuclear damage in host cells can be characterized as a cellular effect that contributes to the pathogenesis of histoplasmosis. Glukhov et al. (2008) reported that bacterial endotoxins induce nuclear DNA damage in human mononuclear cells, which is associated with the infectious process and disease manifestation. However, knowledge of the DNA fragmentation induced by microorganisms is limited. Hence, it is necessary to investigate the behavior of nuclear envelope proteins during infection.

Nuclear envelope proteins promote a functional link between support structures, cytoplasmic compartments, and nucleoplasmic compartments. These proteins have been identified as components of the LINC complex (nucleoskeleton and cytoskeleton linker), which are specific to the outer and inner nuclear membranes. The LINC complex is composed primarily of SUN nuclear proteins and by Nesprin, although other envelope proteins, such as Emerin, can also be identified. An illustration of the LINC complex organization can be found in Haque et al. (2010). These proteins play important roles in the positioning, migration and maintenance of nuclear architecture (Ostlund et al., 2009; Taranum et al., 2012). In addition, this complex is critically important because the blade and associated proteins play a role in modulating gene expression (Martins et al., 2012).

In general, Nesprin binds to actin and several other motor proteins of the microtubule network. In the inner nuclear membrane, SUN-domain proteins (SUN1, SUN2, and SUN3) bind to the blade in the nucleoplasm. Moreover, the Emerin protein characterized as a transmembrane protein may be associated with microtubules in the outer nuclear membrane, and can bind to the nuclear lamina when it is located in the inner nuclear membrane. Thus, the LINC complex passes through the perinuclear space and connects the components of the cytoskeleton with the nuclear lamina (Crisp et al., 2006; Martins et al., 2012). The labeling of nuclear envelope proteins in host cells could contribute to the characterization of the behavior of these proteins during the course of an *in vitro* infection.

The mechanisms by which *H. capsulatum* interacts with macrophages and evades host immune defenses have been well documented. However, this is the first report that attempts to characterize the interaction pattern and the nuclear damage of parasitized host cells after the internalization of *H. capsulatum* yeast in order to verify the correlation of these yeast cells with host cell integrity. Apoptosis assays were performed as well as the staining of nuclear envelope proteins in host cells infected with the fungus. Our study highlights the intracellular behavior and the effects induced by *H. capsulatum* at a nuclear level in cultured infected alveolar macrophages.

## MATERIALS AND METHODS

### Fungal Growth Conditions

*H. capsulatum* strains EH-315 and 60I were used. The EH-315 strain was isolated from a naturally infected bat and was deposited in the *H. capsulatum* Culture Collection of the Fungal Immunology Laboratory of the Department of Microbiology and Parasitology, from the School of Medicine, National Autonomous University of Mexico (UNAM) (www.histoplas-mex.unam.mx). This collection is registered in the database of the World Federation for Culture Collections under the number LIH-UNAM WDCM817 (www.wfcc.info/ccinfo/index.php/collection/by_id/817/). The 60I strain was isolated from a human clinical case and was deposited in the collection of the Clinical Mycology Laboratory of the Faculty of Pharmaceutical Sciences, UNESP, Brazil. Yeasts were grown in brain–heart infusion (BHI-broth) (Difco Laboratories, Detroit, MI, USA) and supplemented with 0.1% L-cysteine and 1% glucose, at 37°C, for 24 h, and with rotary agitation (100 rpm). Dispersed *H. capsulatum*

yeast cells were washed three times with phosphate-buffered saline (PBS), followed by low-speed centrifugation for 1 min at 600 × *g* to remove large yeast clumps. Suspensions of single yeast cells were separated for counting with a hematocytometer.

## Macrophage Cultures

Murine alveolar macrophages, AMJ2-C11 cell-line, were cultured overnight at 37°C on coverslips placed in the well-bottom of 24-well plates (TPP®, Trasadingen, Switzerland) using Dulbecco's modified Eagle's medium (DMEM) (Sigma-Aldrich, St Louis, MO, USA) supplemented with 10% heat-inactivated fetal calf serum (Cultilab, Campinas, SP, Brazil).

## Ethics Statement

Rabbits were used for antibody production. They were processed exactly as outlined in the experimental protocol recommended by the Ethics Committee on Animal Experiments of the Faculty of Pharmaceutical Sciences of Araraquara—UNESP (reference number: 10/2011/CEUA/FCF), which was approved for this study. All efforts were made to minimize suffering in all animal procedures.

## Immunoglobulin to Cell-Free Antigen of *H. capsulatum*

*H. capsulatum* cell-free antigen, a rich solution of cell wall associated antigens, was prepared as described previously by Sá-Nunes et al. (2005). Protein concentration was quantified using the Bradford method (BioRad Laboratories Inc., Hercules, CA, USA). To prepare a polyclonal antibody raised against cell-free antigen of *H. capsulatum,* rabbits were inoculated by intradermal injection of 1.0 mL of the cell-free antigen mixed with 1.0 mL of complete Freund's adjuvant. Subsequent injections of this antigen with incomplete Freund's adjuvant were given weekly for a period of 4 weeks, and thereafter monthly, for a period of 3 months. The rabbits were bled at the 7th day after the last dose. The immunoglobulin fraction of each rabbit anti-serum was separated by precipitation with ammonium sulfate and stored at −70°C.

## Infection Rate of *H. capsulatum* in Alveolar Macrophages Detected by Colony Forming Units (CFU)

For this assay, a reference strain from the American Type Culture Collection (ATCC), G-217B, was compared with strains EH-315 and 60I. The infection rate of each strain was estimated using the AMJ2-C11 alveolar macrophage cell-line (ATCC, CRL-2456). The assay was performed in 24-well plates (TPP®) containing $10^5$ AMJ2-C11 macrophages per well, as described by Sardi et al. (2012). Each cultured macrophage monolayer was infected with 500 μL of yeast inoculum ($1 \times 10^6$ yeasts/mL) and plates were incubated at 37°C for 0, 7, 15, 30, 60, 120, 180, and 300 min (5 h). After each incubation time, a macrophage monolayer was washed three times with sterile PBS to remove released yeast cells. Then, the AMJ2-C11 cells were detached at 37°C for 2 min using trypsin-EDTA (Gibco Life Technologies, Carlsbad, CA, USA) diluted in PBS. Subsequently, 100 μL of each infected macrophage suspension was plated on supplemented BHI-agar (Difco) and incubated at 37°C, for 24–72 h. After incubation, fungal colonies were counted and the CFU/mL was estimated for each strain tested, corresponding to the number of *H. capsulatum* yeast cells that was able to infect the alveolar macrophage monolayer at each incubation time. For each assay, a control for yeast cell viability was performed in which yeast cells were maintained with trypsin-EDTA for 2 min and Trypan blue solution was added afterward to detect viability. *H. capsulatum* infection rate curves were constructed based on the data of each strain incubated at the different times. Tests were set up in triplicate in two independent assays.

The interaction between alveolar macrophages and *H. capsulatum* yeast were also monitored by conventional Giemsa staining and indirect fluorescence.

## Indirect Immunofluorescence

Samples of infected macrophages were maintained under the optimal culture conditions for a 5 h incubation. The infected monolayers were fixed with 4% paraformaldehyde, washed in PBS, and permeabilized in 0.5% Triton X-100 for 30 min. Polyclonal anti–*H. capsulatum* antibody was added for a 1 h incubation at room temperature, and unbound antibodies were removed by washing with PBS. Alexa Fluor®594-conjugate goat anti-rabbit IgG (Invitrogen-Molecular Probes, Eugene, OR, USA) was added and incubated for 1 h at room temperature and, subsequently, fluorescein isothiocyanate (FITC)-labeled phalloidin (Sigma-Aldrich, St Louis, MO, USA) was added with 1 h of incubation at 37°C. All nuclei were stained using 4′,6-Diamino-2-phenylindole (DAPI) (Sigma-Aldrich, St Louis, MO, USA). The infected and non-infected macrophages were washed three times with PBS and analyzed under fluorescence microscopy. All the images were acquired by the IN Cell Analyzer 2000 System (GE Healthcare Bio-Sciences Corp., Piscataway, NJ, USA). Additionally, the percentage of the infected macrophage population and the number of yeast cells per macrophage were determined using Investigator IN Cell 1000 Workstation software (GE Healthcare Bio-Sciences Corp.). This software includes an accurate analysis module that allows reaching reliable results to measure the morphology and the fluorescence intensity of user-defined nuclear and cytoplasmic compartments. Thus, cells can be classified into subpopulations by applying one or more filters, according to one or two user-selectable fluorescence or morphological events. For the analysis, the AMJ2-C11 alveolar macrophages were counted as cells based on some parameters, such as cells fluorescence intensity, nuclei fluorescence intensity, cells area, and nuclei area. To measure yeast cells they were assumed as being "organelles," and the following parameters were considered, organelles mean area, organelles total area, organelles number per macrophages, organelles fluorescence intensity. The final results were automatically obtained in a worksheet detailing the measures by well, by field, and by cell, regarding the indicated parameters as numerical values. The assay was performed in duplicate.

## Infection Rate of *Histoplasma capsulatum* in Alveolar Macrophages Detected by Flow Cytometry

For this assay, AMJ2-C11 macrophage monolayers containing $10^5$ macrophages per well were formed in 24-well plates (TPP®). After, 500 μL ($1 \times 10^6$ yeasts/mL) of each inoculum of *H. capsulatum* was stained with 10 μM carboxyfluorescein diacetate succinimidyl ester (CFSE) (Invitrogen, Carlsbad, CA, USA) at 37°C for 30 min. Stained *H. capsulatum* strains were added to their respective macrophage monolayer, and the plates were incubated at 37°C, 5 h. After the incubation time, the monolayers were washed three times with sterile PBS, and macrophages were detached at 37°C for 2 min using trypsin-EDTA (Gibco Life Technologies) diluted in PBS. Macrophage suspensions were harvested in Eppendorf tubes and centrifuged at 600 × *g*, 4°C. Supernatants were removed and PBS was added to each Eppendorf tube before cell counting by flow cytometry (BD FACSCanto Becton Dickinson, San Diego, CA, USA). For the analyses, we considered parameters related to the size (size forward scatter—FSC), granularity (granularity side scatter—SSC) and fluorescence of 10,000 cells per tube. The results were determined through the fluorescence intensity (FI) of yeast cells labeled with CFSE as estimated by BD FACSDiva software. Gates of specific population were viewed and analyzed by dot-plot. These data allowed one to determine the percentage of infected alveolar macrophages and discriminate the infectivity of different strains of *H. capsulatum*. Non-infected AMJ2-C11 alveolar macrophages, fluorescein-labeled yeast, and unlabeled yeast were used as negative controls in the assay. Assays were performed in three biological replicates and two technical replicates.

## Comet Assay

AMJ2-C11 macrophages, in 24-well plates, were infected with *H. capsulatum* strains EH-315 or 60I using a standardized suspension of $1 \times 10^6$ yeasts/mL and incubated at 37°C for 5 h. Non-infected macrophages were used as a negative control. The alkaline version of the comet assay (single cell gel electrophoresis) was performed as described by Singh et al. (1988). Duplicate slides were prepared and stained with ethidium bromide. We screened 50 AMJ2-C11 macrophages per sample with a fluorescence microscope (Carl Zeiss GmbH, Oberkochen, Germany) equipped with a 515–560 nm excitation filter, a 590 nm barrier filter, and a 40× objective. The level of DNA damage was assessed by an image analysis system (TriTek CometScore, version 1.5; TriTek Corp., Sumerduck, VA, USA), and the DNA percentage in comet tail was obtained for each treatment. Additionally, the percentage of the macrophage population that showed DNA damage was determined.

## TUNEL Assay

DNA fragmentation in infected macrophages was evaluated using TUNEL (terminal deoxynucleotidyl transferase dUTP nick-end labeling) staining following the protocol recommended by the manufacturer (Roche Diagnostics, Penzberg, Germany), which has the feature of specific labeling of fragmented DNA sequences that occur during the process of apoptosis. Infection was performed with *H. capsulatum* strains EH-315 and 60I in AMJ2-C11 macrophages cultured in 96-well plates. The macrophages were incubated with a standardized suspension ($1 \times 10^6$ yeasts/mL) of *H. capsulatum* EH-315 or 60I and infection was allowed for 30 min, 2 h, and 5 h. Non-infected macrophages were used as a negative control. After each incubation time, macrophages were PBS washed and fixed in 4% paraformaldehyde for 1 h at room temperature. Samples were washed three times with cold PBS and incubated with 200 μL permeabilization solution (0.05 M Tris, 0.02 M CaCl2, and 2.5 mg/mL proteinase K) for 15 min at room temperature. After further washing with cold PBS, free reactive sites of the macrophage monolayer on the coverslips were blocked with 200 μL of a solution containing 3% bovine serum albumin and 20% fetal bovine serum in PBS at 37°C for 1 h. Then, the monolayers were washed three times with cold PBS and incubated with the components of the "TUNEL" mixture (dUTP solution containing the enzyme FITC-conjugated and "terminal deoxynucleotidyl transferase") at 37°C, for 1 h, in a moist chamber under darkness. During the incubation period, the 3′ ends of the apoptotic DNA fragments were incorporated into the FITC-labeled nucleotides. This reaction was catalyzed by terminal transferase. After incubation, three washes were performed with cold PBS, and 100 μL of 1% paraformaldehyde was added per well. Analysis of DNA fragmentation in macrophages was conducted to compare the EH-315 and 60I strains, using non-infected macrophages as a negative control. Images were captured using the IN Cell Analyzer 2000 System for light microscopy and were analyzed by Investigator IN Cell 1000 Workstation software (GE Healthcare Bio-Sciences Corp.). The results were evaluated using as parameter the fluorescence intensity emitted by the nucleus in each condition tested.

## Labeling of the Nuclear Envelope Proteins SUN2, Nesprin2, and Emerin

AMJ2-C11 macrophages, cultured in 24-well plates (TPP®), were infected with a standardized suspension of $1 \times 10^6$ yeasts/mL of *H. capsulatum* strains EH-315 or 60I at 37°C for 5 h. Nuclear envelope proteins were marked in either infected or non-infected AMJ2-C11 macrophages (negative control).

Initially, infected and non-infected macrophage samples were fixed with 4% paraformaldehyde, washed with PBS and permeabilized with 0.5% Triton X-100 for 30 min. Then, blocking was performed with 2.5% bovine serum albumin, 1% non-fat milk, and 8% fetal bovine serum. Primary anti-*H. capsulatum* antibody was added for 1 h. Unbound antibodies were removed by washing in PBS, then, Alexa Fluor®594-conjugate goat anti-rabbit IgG (secondary antibody) was added for 1 h. Afterward, in another staining series, anti-SUN2 antibody (Santa Cruz Biotechnology Inc., Heidelberg, Germany), anti-Nesprin2 antibody (Abcam, Cambridge, UK), or anti-Emerin antibody (Abcam) obtained in mice was added as a primary antibody, and macrophage samples were incubated overnight. Unbound antibodies were removed by PBS washing and a secondary Alexa Fluor®488-conjugate goat anti-mouse IgG

antibody was added for 1 h. All nuclei were DAPI stained. The infected and non-infected macrophages were then washed three times with PBS and analyzed under confocal laser scanning microscopy (Leica TCS SP5 Confocal Microscopy System). The assay was performed in duplicate.

## Statistical Analyses

Data were analyzed using Origin 7.0 (Origin Lab. Corporation, Northampton, MA, USA). ANOVA was used to compare groups in CFU and TUNEL assays with the Bonferroni post-test. $P$ was calculated by Student's $t$-test and $P \leq 0.001$ were considered statistically significant. For the comet assay, the infected and non-infected macrophages (control) were compared using the Kruskal–Wallis test and the associated Dunn post-test with $P \leq 0.05$ were considered as statistically significant.

# RESULTS

## Infection Rate of *Histoplasma capsulatum* in AMJ2-C11 Alveolar Macrophage Cell-Line Detected by CFU

The infection rate of *H. capsulatum* yeasts was assessed with the *H. capsulatum* reference strain G-217B and strains EH-315 and 60I. As seen in **Figure 1**, strains EH-315 and 60I developed higher infection rates than the G-217B reference strain. Additionally, the EH-315 strain always exhibited the highest AMJ2-C11 macrophage infection rate at all times studied. **Figure 1** shows the number of yeast cells that infected the alveolar macrophages through the CFU/mL counting with these three fungal strains. The results suggested that at 120 min of contact, between alveolar macrophages and strain EH-315, the number of yeast cells in the macrophages increased. At 180 min, the infection rate declined, and it increased again at 300 min. With regard to the strain 60I, the number of yeast cells was increased at 60 min and at 120–180 min, the infection rate declined. Similarly to strain EH-315, the infection rate of strain 60I increased again at 300 min.

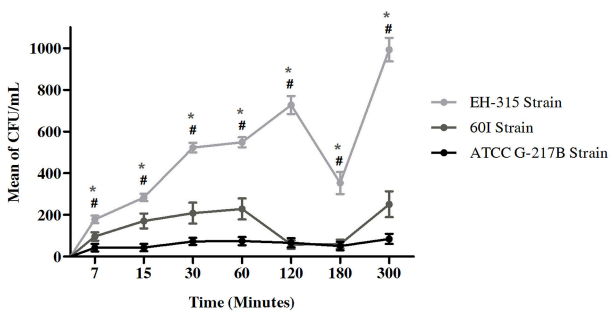


**FIGURE 1 | Infection rate assays of AMJ2-C11 alveolar macrophage with *H. capsulatum* strains G-217B, EH-315, and 60I.** Rates of *H. capsulatum* yeasts were considered using CFU/mL. Scores given are the mean ± S.D. and statistics were performed by Two-way ANOVA with the Bonferroni post-test. *$P < 0.001$ for EH-315 vs. 60I strain and #$P < 0.001$ for EH-315 vs. G-217B strain.

## Observation of *Histoplasma capsulatum* in AMJ2–C11 Macrophages

Infection of macrophages by *H. capsulatum* yeast (strains EH-315 and 60I) was also evaluated using Giemsa staining. This methodology was very useful for analyzing how yeasts interact with host macrophages (**Figure 2**). However, this staining did not provide accurate localization of yeast cells within phagocytes.

Indirect fluorescence microscopy, using images of the IN Cell Analyzer, revealed several intracellular yeasts in infected macrophages. An interesting finding was detected with this methodology, where intracellular *H. capsulatum* yeast cells aggregated in an architectural shape apparently surrounding the macrophage nucleus, resembling a "crown" (**Figure 3**). Moreover, additional analyses with Investigator IN Cell 1000 Workstation software showed that strain EH-315 infected 95% of the macrophage population with an infection multiplicity up to 30 cells per macrophage, whereas strain 60I infected 86% of macrophages with up to 24 yeast cells per macrophage.

## Flow Cytometry Assay

Results were expressed as FI of yeast labeled with CFSE and correspond to the fluorescence data of 10,000 cells per tube. To quantify the percentage of yeast cells bound to or within AMJ2-C11 macrophages, combination of two gates were applied to yeast cells and AMJ2-C11 cell-line (**Figure 4**). After using these combined gates, immediately the percentage of yeast cells interacting with AMJ2-C11 alveolar macrophages was

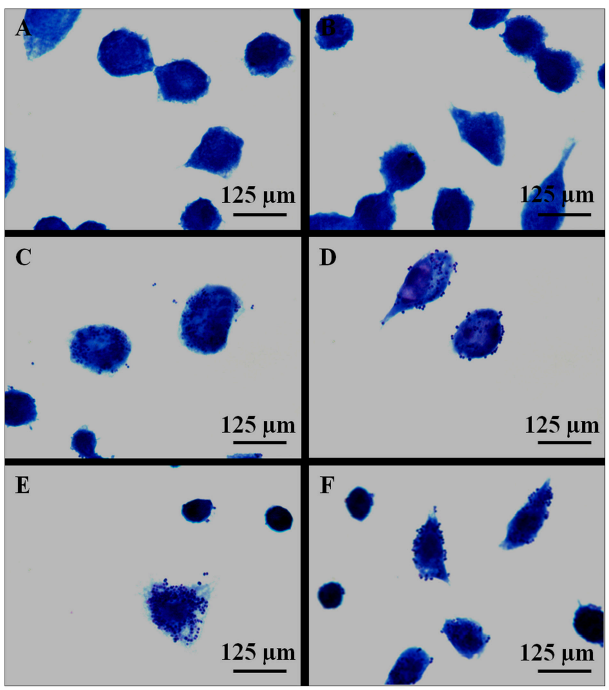


**FIGURE 2 | Giemsa staining of AMJ2-C11 macrophages after 5 h of *H. capsulatum* infection. (A,B)** Control of non-infected macrophages incubated with PBS. **(C,D)** Macrophages infected with *H. capsulatum* strain EH-315. **(E,F)** Macrophages infected with *H. capsulatum* strain 60I. The results are representative of two assays.

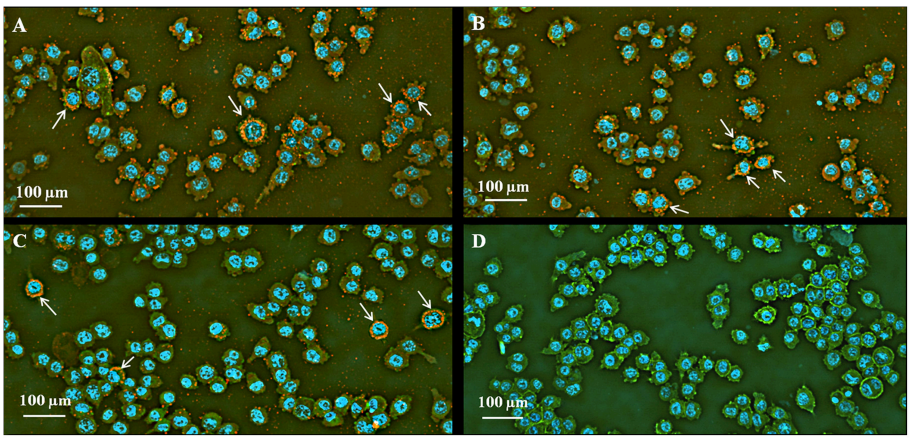


**FIGURE 3 | Effect of *H. capsulatum* yeast cells on the infection of AMJ2-C11 macrophages.** Macrophages infected with *H. capsulatum* yeast cells were incubated at 37°C for 5 h (see details in Section Materials and Methods). **(A,B)** AMJ2-C11 macrophages infected with the EH-315; **(C)** AMJ2-C11 macrophages infected with 60I; and **(D)** non-infected AMJ2-C11 macrophages. Indirect immunofluorescence: FITC-phalloidin in green showing the macrophage cytoplasm; Alexa Fluor®594 in red to yellow staining *H. capsulatum* yeast cells; DAPI in blue staining macrophages nucleus. Images were obtained using IN Cell Analyzer light microscopy. The results are representative of two assays. Arrows indicate the architectural arrangement of yeast-aggregates apparently surrounding the nuclei of the phagocytic cells.

determined. Regarding the profile of *H. capsulatum* infection in alveolar macrophages, strains EH-315 and 60I showed high infection rates in AMJ2–C11 macrophages. Moreover, both strains have a similar potential for infection because they are able to infect murine alveolar macrophages at rates of 98.34 and 96.52%, respectively, after 5 h of infection. The results represent the average of three independent assays set up in triplicate.

## Comet Assay

A similar pattern of DNA fragmentation was observed in infected AMJ2–C11 macrophages by comet assay, when *H. capsulatum* strains EH-315 and 60I were tested. Typical images of the comet assay showing DNA fragmentation in the tail are presented in **Figure 5A**. In the analysis of macrophage nuclear fragmentation by *H. capsulatum*, DNA damage corresponded to the percentage of DNA in the tail of the comet, and the results demonstrated that, for strains EH-315 and 60I, macrophage DNA damage was 10.67 ± 0.91% and 10.78 ± 1.31%, respectively; whereas 1.75 ± 0.18% of DNA damage was associated with the non-infected macrophages used as a negative control. Significant differences ($P < 0.05$) were found when macrophages infected with each strain were statistically compared with their respective negative controls (**Figure 5B**).

In addition, the comet assay data also revealed that 86.71% of the macrophage population infected with strain EH-315 showed DNA damage. Similarly, strain 60I induced DNA damage in 81.98% of infected alveolar macrophages. There was no statistically significant difference between the percentages of macrophages undergoing DNA damage induced by the EH-315 or 60I *H. capsulatum* strains. However, significant differences ($P < 0.05$) were found between each macrophage population infected with a fungal strain compared with its respective non-infected control, which revealed 34.41% of DNA damage (**Figure 5C**).

## TUNEL

**Figure 6A** shows images obtained by the IN Cell Analyzer for the TUNEL assay that was used to quantify macrophage apoptosis. The measurement of apoptotic nuclei was performed by the release of nuclear fluorescence intensity detected with the TUNEL method; thus, as the fluorescent labeling increases more damage is detected. DNA fragmentation was detected in AMJ2-C11 macrophages infected with *H. capsulatum* strain EH-315 or 60I at 30 min, 2 h and 5 h post-infection. The infection of macrophages with *H. capsulatum*, after 2 and 5 h, resulted in more apoptotic cells than the non-infected controls, and the number of apoptotic nuclei obtained from macrophages infected with each fungal strain was similar, as shown in **Figure 6B**.

## Labeling of the Nuclear Envelope Proteins SUN2, Nesprin2, and Emerin

Confocal microscopy was used to generate 3D images of infected macrophages labeled with anti-SUN2, anti-Nesprin2 and anti-Emerin antibodies. A diffuse distribution of these proteins was found outside on the nuclear envelope, with a similar pattern for non-infected macrophages, as shown in **Figure 7**. In addition, data from confocal microscopy also indicate that the nuclear fragmentation induced after infection, which was demonstrated by the comet and TUNEL assays, may occur as the result of the architectural conformation displayed by *H. capsulatum*, in which yeast cells appear to surround the macrophage nucleus after 5 h of infection (**Figure 7** and Videos S1–S6). Moreover, during infection the formation of large phagosomes within *H. capsulatum*-infected macrophages was noted (**Figure 7B**). These events were not found in non-infected macrophages.

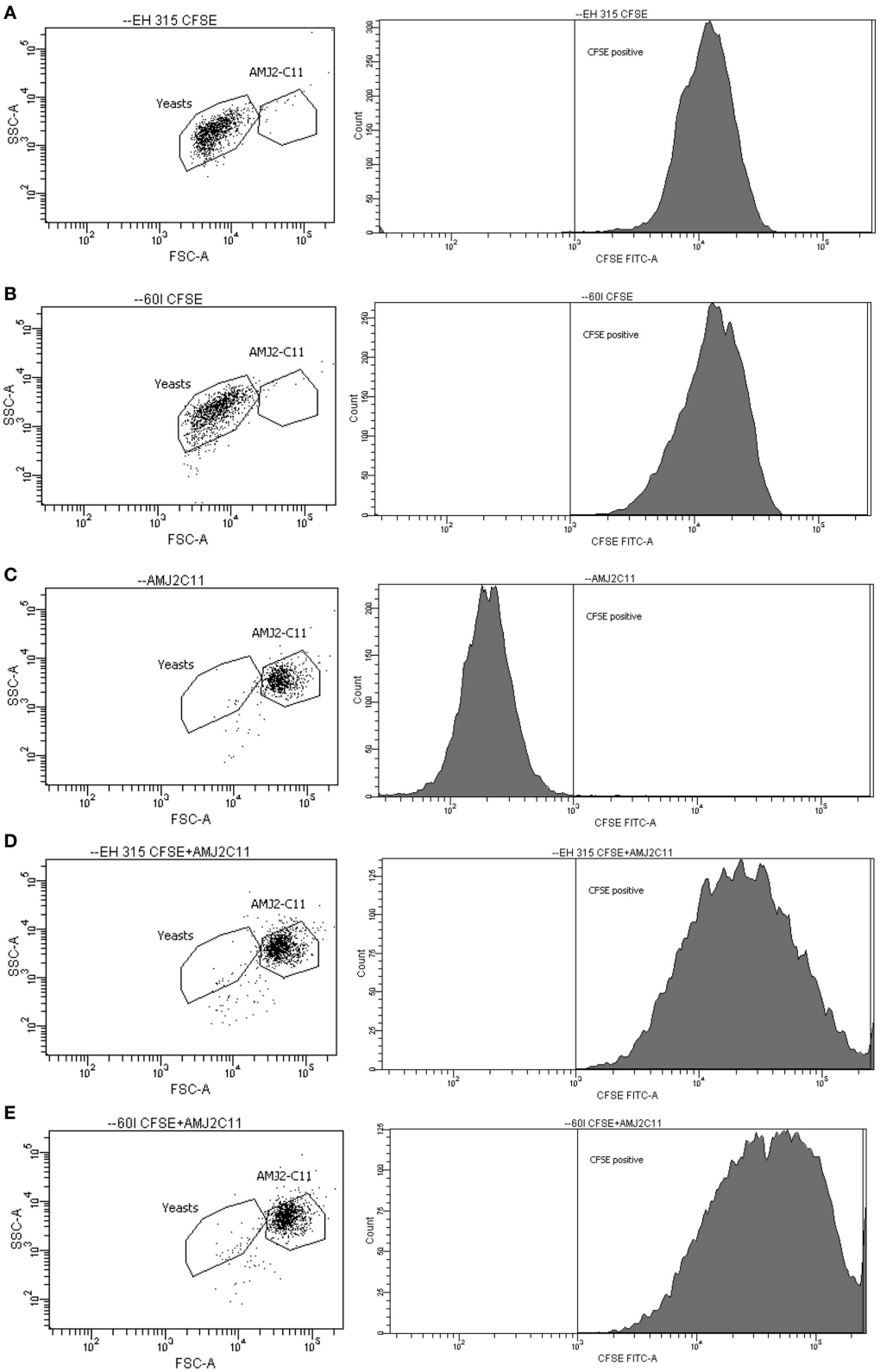


**FIGURE 4 | Dot-plot and histogram profiles of AMJ2-C11 alveolar macrophages and CFSE-labeled *H. capsulatum* yeast cells, at 5 h post-infection.** **(A,B)** Population of labeled yeast cells (EH-315 and 60I strain, respectively); **(C)** specific gate for AMJ2-C11 alveolar macrophages; and **(D,E)** Infected alveolar macrophages by EH-315 and 60I strain, respectively. The cells were analyzed by flow cytometer BD FACSCanto.

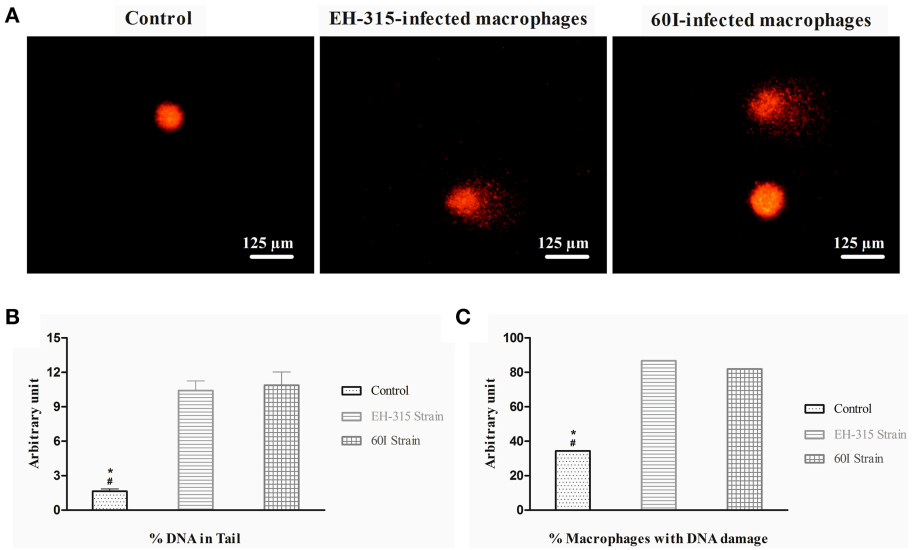


**FIGURE 5 | Comet assay data of AMJ2-C11 macrophages infected with *H. capsulatum* yeasts. (A)** Images were acquired using a fluorescence microscope equipped with a 515–560 nm excitation filter and a 590 nm barrier filter. **(B)** Evaluation of nuclear fragmentation in AMJ2-C11 macrophages infected with *H. capsulatum*. Control (non-infected macrophages). Values are representative of the percentage of fragmented DNA present in the comet's tail. **(C)** Percentage of macrophage population showing DNA damage in infected and non-infected (control) cells. Scores given are the mean ± SD. Data were analyzed by Kruskal-Wallis test with Dunn's post-test. *$P < 0.05$ when control vs. strain EH-315 was compared; #$P < 0.05$ when control vs. strain 60I was compared.

## DISCUSSION

Interactions of pathogenic fungi with host tissues are essential factors in the pathogenesis of mycoses (Tronchin et al., 2008). *H. capsulatum* infects different host cells, such as neutrophils, macrophages, dendritic cells, and epithelial cells.

The present study demonstrated particular characteristics of the interaction between *H. capsulatum* yeast cells and cultured murine alveolar macrophages. We compared two virulent *H. capsulatum* strains isolated from different sources, EH-315 and 60I, based on their behavior and potential infection for AMJ2-C11 alveolar macrophages. The EH-315 strain developed higher virulence (LD50 $3 \times 10^5$ yeasts/mL) when compared to the 60I strain (LD50 $3 \times 10^8$ yeasts/mL) under experimental conditions using an LD50 assay in male BALB/c mice (ML Taylor, personal communication).

We evaluated the ability of the EH-315 and 60I strains to infect alveolar macrophages when compared with the ATCC strain G-217B using CFU analysis of *H. capsulatum* yeast at 7–300 min (5 h) post-infection. The results demonstrated that the three strains of *H. capsulatum* have distinct efficiency for infecting alveolar macrophages. Strain EH-315 developed a better ability to infect macrophages than strains 60I and G-217B. However, regarding the efficacy of the CFU assay, other researchers have described the inconvenience and limitations of this method. According to Berkes et al. (2012), several factors contribute to non-optimize microorganisms plating that routinely reaches only 30% effectiveness for *H. capsulatum*, as the CFU number is generally lower than the number of viable yeasts plated.

Few studies have associated pathogen virulence with the ability to infect host cells or to adhere to abiotic surfaces. Thewes et al. (2008) performed phenotypic screening to compare the SC5314 strain of *Candida albicans*, which is invasive and highly virulent, with the strain ATCC 10231, which is non-invasive and less virulent. Their findings highlight that strain ATCC 10231 caused less damage to fibroblasts and epithelial cells when compared to SC5314. According to those authors, biological properties that influence adherence and invasion to host cells are critical attributes of *C. albicans* in colonization and disease progression, and the results of this study demonstrated that virulence had a direct influence on the ability of this fungus to colonize, damage, and invade host tissues. Furthermore, Sepúlveda et al. (2014) compared *H. capsulatum* strains with distinct genotype and virulence and noted that strain G-217B exhibited delayed response to the virulence effect, as in macrophage damage and cytokine production when compared to other strains. Likewise, Sahaza et al. (2015) highlighted that lung inflammatory responses, in regard to cytokine profile and lung-granuloma formation, varied in intensity and time when two different virulent *H. capsulatum* strains from distinct phylogenetic species, EH-46 (LAm A) and G-217B (NAm 2), were used. Our data corroborated those reported by Sepúlveda et al. (2014) and Sahaza et al. (2015), as strain G-217B showed delayed infection potential against host cells.

In the current study, the infection profile of *H. capsulatum* strains on alveolar macrophages over a period of 5 h was characterized by a variable behavior (increases and decreases) in the yeast infection rate of alveolar macrophages. We hypothesize

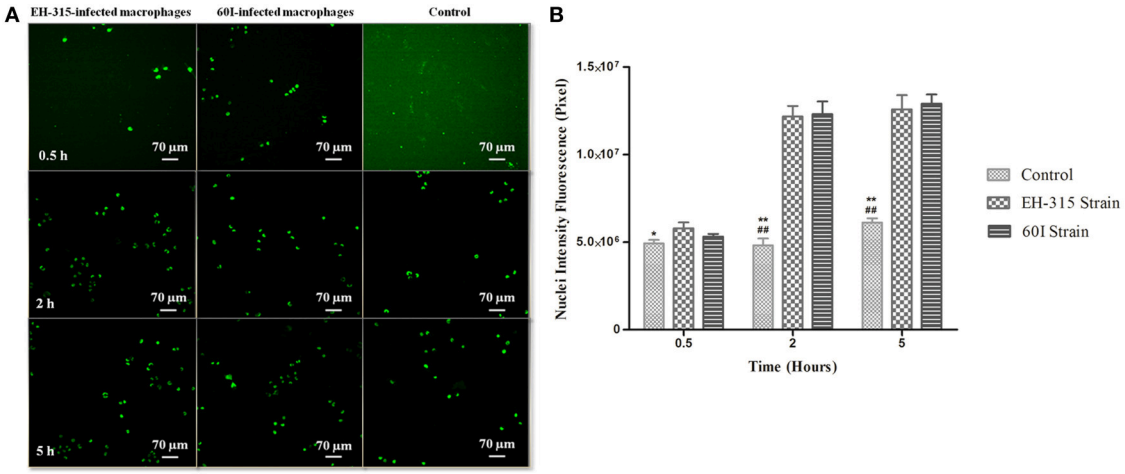


**FIGURE 6 | TUNEL staining of alveolar macrophages after *H. capsulatum* infection. (A)** DNA fragmentation in the nucleus of AMJ2-C11 macrophages infected with *H. capsulatum* yeasts. Images were obtained after 0.5, 2, and 5 h after infection of alveolar macrophages with *H. capsulatum* strains EH-315 or 60I. Infected alveolar macrophages were compared with non-infected macrophages incubated with PBS (control). Each photomicrograph was processed by IN Cell Analyzer light microscopy using a 20X power field. The results are representative of two assays. **(B)** Detection of nuclear fluorescence intensity derived from DNA fragmentation in AMJ2-C11 macrophages infected with *H. capsulatum* strain EH-315 or 60I and non-infected macrophages (control). TUNEL-positive macrophages are represented by the nuclear fluorescence intensity with values derived from analysis of images using Investigator IN Cell 1000 Workstation software. Scores given are the mean ± S.D and statistics were performed by Two-way ANOVA with the Bonferroni post-test. $^{*}P < 0.05$ and $^{**}P < 0.001$, control vs. strain EH-315, $\#\#P < 0.001$, control vs. strain 60I.

that this profile occurs as a result of the dynamic interactions between yeast and macrophage membrane receptors.

According to our results, macrophage infections were also monitored at 5 h by Giemsa staining and indirect fluorescence. As we mentioned before, Giemsa staining did not provide well-defined yeast localization within phagocytes, whereas quantification of the macrophage population that was effectively infected with *H. capsulatum* yeasts was successfully achieved by flow cytometric methodology. For these infection assays, the 5 h post-infection time was selected based on a previous kinetic study that showed the largest number of yeast cells interacting with alveolar macrophages at this time-point of infection. Once the CFSE-labeled yeasts had interacted with alveolar macrophages, the percentage of infected cells containing yeast cells was accurately quantified. It is important to note that flow cytometry has been employed to quantify several fungal infections (Chang et al., 1998; Berkes et al., 2012).

*H. capsulatum* is a pathogen that commonly survives within macrophages by developing several intracellular evasion mechanisms (Strasser et al., 1999; Sebghati et al., 2000). Microscopic images obtained by indirect immunofluorescence assays showed a singular pattern of *H. capsulatum* in the infected macrophages under *in vitro* conditions, which was similar for the two fungal strains tested. Interestingly, the yeast cells of both strains were able to form aggregates in the cytoplasm of the infected macrophages with an apparent distribution surrounding the macrophage nucleus after 5 h of infection. These findings could be related to a new strategy for fungal intracellular survival.

Based on the potential for infection displayed by both strains of *H. capsulatum* in alveolar macrophages, it became necessary to evaluate the genotoxic potential of this fungus in AMJ2-C11 macrophages to identify the ability of *H. capsulatum* to induce damage to DNA in host cells. According to Yang et al. (2011), genotoxic agents chemically interact with the genetic material and cause oxidative changes or disruptions in the DNA molecule.

The results of comet and TUNEL assays showed that the two strains of *H. capsulatum* (EH-315 and 60I) caused significant damage to the nuclear DNA of the AMJ2-C11 macrophages after 5 h of infection when compared to non-infected macrophages. Nuclear fragmentation is characterized as a cellular alteration associated with apoptosis (Deepe and Buesing, 2012). In this context, several studies have shown that *H. capsulatum* yeast cells induce apoptosis in different host cell-lines, including macrophages (Allen and Deepe, 2005; Lin et al., 2005; Deepe and Buesing, 2012). According to Das et al. (1999), apoptosis allows the host to develop an effective response against infectious diseases such as tuberculosis.

A study conducted by Del Vecchio et al. (2009) demonstrated the ability of a dimorphic fungus, *Paracoccidioides brasiliensis,* to induce apoptosis in A549 epithelial cells after 24 and 48 h of infection using the TUNEL assay to assess DNA fragmentation. Previous studies have reported that strains of *C. albicans* also induce apoptosis of macrophages after 30 min of infection under *in vitro* conditions. According to the authors, the ability of *C. albicans* to induce apoptosis may modulate a standard anti-inflammatory immune response in the host (Gasparoto et al., 2004). Moreover, polysaccharides of *Cryptococcus neoformans* also induce apoptosis in macrophages under *in vitro* and*in vivo* conditions, compromising the host immune response (Villena et al., 2008).

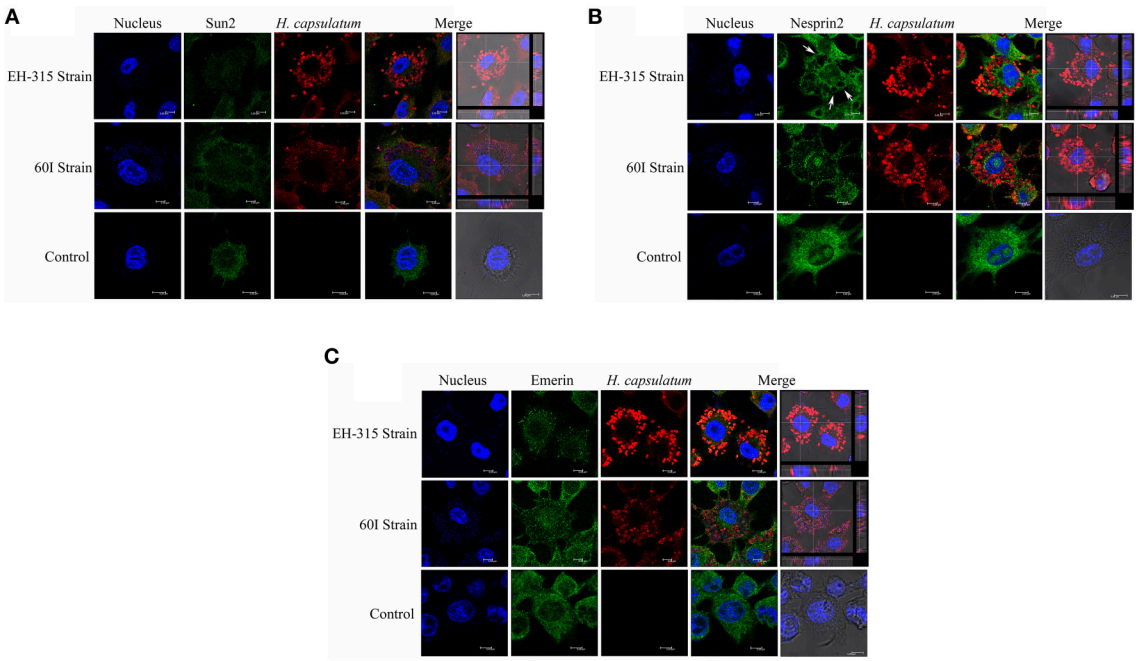


**FIGURE 7 | Labeling of nuclear envelope proteins SUN2, Nesprin2, and Emerin in *H. capsulatum* infected alveolar macrophages.** In Panels **(A–C)** show confocal scanning microscopy images of representative AMJ2-C11 macrophages infected with *H. capsulatum* strains EH-315 and 60I at 37°C for 5 h. Non-infected macrophages were processed as a control. **(A)** AMJ2-C11 stained for SUN2, **(B)** Nesprin2, and **(C)** Emerin as indicated in the figure. The arrows show phagosome formation where several yeast cells are present. DAPI was used for nuclear staining (blue). Alexa Fluor®488 and Alexa Fluor®594 conjugates were used as secondary antibodies to reveal nuclear proteins (green) and yeast cells (red), respectively. Bright field images were merged with Alexa Fluor®594 and DAPI stain with orthogonal z stack sections after 5 h of macrophage-yeast infection. The assay was performed twice.

According to our findings, the apoptosis of infected macrophages could be related to the formation of *H. capsulatum* aggregates that extend throughout the cytoplasm and display a conformational architecture that arrange themselves near to the macrophage nucleus. This conformational aggregation of yeast cells could form in the intracellular environment and remain within the macrophages, causing damage to the nucleus of the host cell and producing DNA fragmentation. This can be explained by the high percentage of infected macrophages with yeast-aggregates after 5 h of infection, which was similar to the percentage of macrophage suffering DNA damage induced by both strains. This new structural arrangement could be associated with the ability of *H. capsulatum* yeasts to prevent elimination by the immune system (Pitangui et al., 2012). The preference of *H. capsulatum* yeast cells to form intracellular aggregates became understandable when a high number of yeasts appeared as linked to each other, during infection of murine alveolar macrophages (**Figure 7** and Videos S1–S6).

Confocal microscopy images were used to determine if the effects on host cell nuclei induced by *H. capsulatum* aggregates could change the behavior of the nuclear membrane proteins SUN2, Nesprin2, and Emerin. The analyses revealed that infected macrophages with yeast-aggregates surrounding the macrophage nuclei did not show disruption in the organization of the nuclear lamina that underlies the nuclear envelope, given that the staining of nuclear proteins showed a very similar distribution to that seen in non-infected macrophages. Meinke et al. (2011) reported that disruption of SUN2 or Nesprin2 prevents nuclear movement. In the present study, it was possible to observe diffuse distribution of these proteins outside on the nuclear envelope in both infected and non-infected macrophages.

To date, a few studies have described Nesprin isoforms (Zhang et al., 2007; Morris and Randles, 2010; Randles et al., 2010) as a product generated by the alternative splicing of genes encoding Nesprin1 and Nesprin2. These isoforms vary in size, but they contain a common C-terminal region (Randles et al., 2010) and play important roles in cellular organization, especially in positioning the nucleus and other organelles. Nesprin isoforms appear in different subcellular fractions, including outer and inner nuclear membranes associated with organelles such as mitochondria, Golgi complex, sarcoplasmic reticulum and in the plasmatic membrane, where the isoforms form a network connecting these structures to the actin cytoskeleton (Zhang et al., 2007; Morris and Randles, 2010). Therefore, Nesprin can be found away from the nucleus (Gough et al., 2003), which is consistent with the results obtained in this study, where we observed diffuse presence of this protein in the cytoplasm of infected and non-infected macrophages. However, according to Randles et al. (2010), it is difficult to determine whether other isoforms are also present due to the absence of specific antibodies.

Emerin was also found to be diffuse throughout the cytoplasm of non-infected and *H. capsulatum* infected macrophages.

Conversely, a study using host cells infected with herpes simplex virus 1 found an irregular distribution of Emerin, as opposed to a uniform alignment on the nuclear membrane, which appeared like bubbles on the surface of the outer nuclear membrane (Leach et al., 2007). Recently, Ho et al. (2013) reported that Emerin regulates gene expression by modulating actin polymerization in the cytoplasm.

According to our results, it is necessary to emphasize that *H. capsulatum* yeast-aggregates were able to cause damage in the nuclear DNA and induce apoptosis in alveolar macrophages after 5 h of infection. This damage to the DNA of macrophages while the yeast cells are not located inside the core could be a fungus strategy for the facilitation of its persistence throughout the host infection. This finding has never been previously described. Hence, the intracellular arrangement and the occurrence of effects induced by *H. capsulatum* yeast-aggregates during the infection could promote the survival of the pathogen in the hostile conditions of the intracellular environment while also contributing to host tissue damage.

## AUTHOR CONTRIBUTIONS

NS, CS and AF conceived and designed the study. NS, JS, AV, CS, JS, RS and FS performed the experiments and analyzed the data. RS, FS and CS collaborated with reagents/materials/analysis tools. All authors read and approved the final manuscript. NS and AF wrote the paper with contributions from GR, MT and MM.

## ACKNOWLEDGMENTS

This work was supported by grants from the Brazilian institutions: Fundação de Amparo à Pesquisa do Estado de São Paulo (FAPESP 2013/05853-1 http://www.fapesp.br/), Conselho Nacional de Desenvolvimento Científico e Tecnológico (CNPq 480316/2012-0 http://www.cnpq.br/) and Programa de Apoio ao Desenvolvimento Científico (PADC) da Faculdade de Ciências Farmacêuticas, UNESP—Univ Estadual Paulista. Nayla de Souza Pitangui has a fellowship from Coordenação de Aperfeiçoamento de Pessoal de Nível Superior (CAPES http://www.capes.gov.br/). The funders had no role in study design, data collection and analysis, decision to publish or manuscript preparation.

## SUPPLEMENTARY MATERIAL

The Supplementary Material for this article can be found online at: http://journal.frontiersin.org/article/10.3389/fmicb.2015.01526

## REFERENCES

Allen, H. L., and Deepe, G. S. (2005). Apoptosis modulates protective immunity to the pathogenic fungus *Histoplasma capsulatum*. *J. Clin. Invest*. 115, 2875–2885. doi: 10.1172/JCI25365

Berkes, C. A., Chan, L. L., Wilkinson, A., and Paradis, B. (2012). Rapid quantification of pathogenic fungi by Cellometer image-based cytometry. *J. Microbiol. Methods* 91, 468–476. doi: 10.1016/j.mimet.2012.09.008

Chang, W. L., Van der Heyde, H. C., and Klein, B. S. (1998). Flow cytometric quantitation of yeast a novel technique for use in animal model work and *in vitro* immunologic assays. *J. Immunol. Methods* 211, 51–63. doi: 10.1016/S0022-1759(97)00191-9

Crisp, M., Liu, Q., Roux, K., Rattner, J. B., Shanahan, C., Burke, B., et al. (2006). Coupling of the nucleus and cytoplasm: role of the LINC complex. *J. Cell Biol*. 172, 41–53. doi: 10.1083/jcb.200509124

Das, G., Vohra, H., Saha, B., Agrewala, J. N., and Mishra, G. C. (1999). Apoptosis of Th1-like cells in experimental tuberculosis (TB). *Clin. Exp. Immunol*. 115, 324–328. doi: 10.1046/j.1365-2249.1999.00755.x

Deepe, G. S., and Buesing, W. R. (2012). Deciphering the pathways of death of *Histoplasma capsulatum*-infected macrophages: implications for the immunopathogenesis of early infection. *J. Immunol*. 188, 334–344. doi: 10.4049/jimmunol.1102175

Del Vecchio, A., Silva, J. F., Silva, J. L., Andreotti, P. F., Soares, C. P., Benard, G., et al. (2009). Induction of apoptosis in A549 pulmonary cells by two *Paracoccidioides brasiliensis* samples. *Mem. Inst. Oswaldo Cruz* 104, 749–754. doi: 10.1590/S0074-02762009000500015

Gasparoto, T. H., Gaziri, L. C., Burger, E., de Almeida, R. S., and Felipe, I. (2004). Apoptosis of phagocytic cells induced by *Candida albicans* and production of IL-10. *FEMS Immunol. Med. Microbiol*. 42, 219–224. doi: 10.1016/j.femsim.2004.05.006

Glukhov, I. L., Sirota, N. P., and Kuznetsova, E. A. (2008). DNA damage in human mononuclear cells induced by bacterial endotoxin. *Bull. Exp. Biol. Med*. 146, 301–303. doi: 10.1007/s10517-008-0275-3

Gough, L. L., Fan, J., Chu, S., Winnick, S., and Beck, K. A. (2003). Golgi localization of Syne-1. *Mol. Biol. Cell*. 14, 2410–2424. doi: 10.1091/mbc.E02-07-0446

Haque, F., Mazzeo, D., Patel, J. T., Smallwood, D. T., Ellis, J. A., Shanahan, C. M., et al. (2010). Mammalian SUN protein interaction networks at the inner nuclear membrane and their role in laminopathy disease processes. *J. Biol. Chem*. 285, 3487–3498. doi: 10.1074/jbc.M109.071910

Hilty, J., Smulian, A. G., and Newman, S. L. (2008). The *Histoplasma capsulatum* vacuolar ATPase is required for iron homeostasis, intracellular replication in macrophages and virulence in a murine model of histoplasmosis. *Mol. Microbiol*. 70, 127–139. doi: 10.1111/j.1365-2958.2008.06395.x

Ho, C. Y., Jaalouk, D. E., Vartiainen, M. K., and Lammerding, J. (2013). Lamin A/C and emerin regulate MKL1-SRF activity by modulating actin dynamics. *Nature* 497, 507–511. doi: 10.1038/nature12105

Hsieh, S. H., Lin, J. S., Huang, J. H., Wu, S. Y., Chu, C. L., Kung, J. T., et al. (2011). Immunization with apoptotic phagocytes containing *Histoplasma capsulatum* activates functional CD8(+) T cells to protect against histoplasmosis. *Infect. Immun*. 79, 4493–4502. doi: 10.1128/IAI.05350-11

Leach, N., Bjerke, S. L., Christensen, D. K., Bouchard, J. M., Mou, F., Park, R., et al. (2007). Emerin is hyperphosphorylated and redistributed in herpes simplex virus type 1-infected cells in a manner dependent on both UL34 and US3. *J. Virol*. 81, 10792–10803. doi: 10.1128/JVI.00196-07

Lin, J. S., Yang, C. W., Wang, D. W., and Wu-Hsieh, B. A. (2005). Dendritic cells cross-present exogenous fungal antigens to stimulate a protective CD8 T cell response in infection by *Histoplasma capsulatum*. *J. Immunol*. 174, 6282–6291. doi: 10.4049/jimmunol.174.10.6282

Martins, R. P., Finan, J. D., Guilak, F., and Lee, D. A. (2012). Mechanical regulation of nuclear structure and function. *Annu. Rev. Biomed. Eng*. 14, 431–455. doi: 10.1146/annurev-bioeng-071910-124638

Medeiros, A. I., Bonato, V. L., Malheiro, A., Dias, A. R., Silva, C. L., and Faccioli, L. H. (2002). *Histoplasma capsulatum* inhibits apoptosis and Mac-1 expression in leucocytes. *Scand. J. Immunol*. 56, 392–398. doi: 10.1046/j.1365-3083.2002.01142.x

Meinke, P., Nguyen, T. D., and Wehnert, M. S. (2011). The LINC complex and human disease. *Biochem. Soc. Trans*. 39, 1693–1697. doi: 10.1042/BST20110658

Morris, G. E., and Randles, K. N. (2010). Nesprin isoforms: are they inside or outside the nucleus? *Biochem. Soc. Trans*. 38, 278–280. doi: 10.1042/BST0380278

Newman, S. L., Lemen, W., and Smulian, A. G. (2011). Dendritic cells restrict the transformation of *Histoplasma capsulatum* conidia into yeasts. *Med. Mycol*. 49, 356–364. doi: 10.3109/13693786.2010.531295

Ostlund, C., Folker, E. S., Choi, J. C., Gomes, E. R., Gundersen, G. G., and Worman, H. J. (2009). Dynamics and molecular interactions of linker of nucleoskeleton and cytoskeleton (LINC) complex proteins. *J. Cell Sci*. 122, 4099–4108. doi: 10.1242/jcs.057075

Pitangui, N. S., Sardi, J. C., Silva, J. F., Benaducci, T., Moraes da Silva, R. A., Rodríguez-Arellanes, G., et al. (2012). Adhesion of *Histoplasma capsulatum* to pneumocytes and biofilm formation on an abiotic surface. *Biofouling* 28, 711–718. doi: 10.1080/08927014.2012.703659

Randles, K. N., Lam, I. T., Sewry, C. A., Puckelwartz, M., Furling, D., Wehnert, M., et al. (2010). Nesprins, but not sun proteins, switch isoforms at the nuclear envelope during muscle development. *Dev. Dyn*. 239, 998–1009. doi: 10.1002/dvdy.22229

Sá-Nunes, A., Medeiros, A. I., Nicolete, R., Frantz, F. G., Panunto-Castelo, A., Silva, C. L., et al. (2005). Efficacy of cell-free antigens in evaluating cell immunity and inducing protection in a murine model of histoplasmosis. *Microbes Infect*. 7, 584–592. doi: 10.1016/j.micinf.2004.12.017

Sahaza, J. H., Suárez-Alvarez, R., Estrada-Bárcenas, D. A., Pérez-Torres, A., and Taylor, M. L. (2015). Profile of cytokines in the lungs of BALB/c mice after intra-nasal infection with *Histoplasma capsulatum* mycelial propagules. *Comp. Immunol. Microbiol. Infect. Dis*. 41, 1–9. doi: 10.1016/j.cimid,.2015.05.003

Sardi, J. C., Duque, C., Mariano, F. S., Marques, M. R., Höfling, J. F., and Gonçalves, R. B. (2012). Adhesion and invasion of *Candida albicans* from periodontal pockets of patients with chronic periodontitis and diabetes to gingival human fibroblasts. *Med. Mycol*. 50, 43–49. doi: 10.3109/13693786.2011.586133

Sebghati, T. S., Engle, J. T., and Goldman, W. E. (2000). Intracellular parasitism by *Histoplasma capsulatum*: fungal virulence and calcium dependence. *Science* 290, 1368–1372. doi: 10.1126/science.290.5495.1368

Sepúlveda, V. E., Williams, C. L., and Goldman, W. E. (2014). Comparison of phylogenetically distinct Histoplasma strains reveals evolutionarily divergent virulence strategies. *MBio* 5, e01376–e01314. doi: 10.1128/mBio.01376-14

Singh, N. P., McCoy, M. T., Tice, R. R., and Schneider, E. L. (1988). A simple technique for quantitation of low levels of DNA damage in individual cells. *Exp. Cell Res*. 175, 184–191. doi: 10.1016/0014-4827(88)90265-0

Strasser, J. E., Newman, S. L., Ciraolo, G. M., Morris, R. E., Howell, M. L., and Dean, G. E. (1999). Regulation of the macrophage vacuolar ATPase and phagosome-lysosome fusion by *Histoplasma capsulatum*. *J. Immunol*. 162, 6148–6154.

Tagliari, L., Toledo, M. S., Lacerda, T. G., Suzuki, E., Straus, A. H., and Takahashi, H. K. (2012). Membrane microdomain components of *Histoplasma capsulatum* yeast forms, and their role in alveolar macrophage infectivity. *Biochim. Biophys. Acta* 1818, 458–466. doi: 10.1016/j.bbamem.2011.12.008

Taranum, S., Vaylann, E., Meinke, P., Abraham, S., Yang, L., Neumann, S., et al. (2012). LINC complex alterations in DMD and EDMD/CMT fibroblasts. *Eur. J. Cell Biol*. 91, 614–628. doi: 10.1016/j.ejcb.2012.03.003

Thewes, S., Moran, G. P., Magee, B. B., Schaller, M., Sullivan, D. J., and Hube, B. (2008). Phenotypic screening, transcriptional profiling, and comparative genomic analysis of an invasive and non-invasive strain of *Candida albicans*. *BMC Microbiol*. 8:187. doi: 10.1186/1471-2180-8-187

Tronchin, G., Pihet, M., Lopes-Bezerra, L. M., and Bouchara, J. P. (2008). Adherence mechanisms in human pathogenic fungi. *Med. Mycol*. 46, 749–772. doi: 10.1080/13693780802206435

Villena, S. N., Pinheiro, R. O., Pinheiro, C. S., Nunes, M. P., Takiya, C. M., DosReis, G. A., et al. (2008). Capsular polysaccharides galactoxylomannan and glucuronoxylomannan from *Cryptococcus neoformans* induce macrophage apoptosis mediated by Fas ligand. *Cell Microbiol*. 10, 1274–1285. doi: 10.1111/j.1462-5822.2008.01125.x

Wu-Hsieh, B. A., Chen, W., and Lee, H. J. (1998). Nitric oxide synthase expression in macrophages of *Histoplasma capsulatum*-infected mice is associated with splenocyte apoptosis and unresponsiveness. *Infect. Immun*. 66, 5520–5526.

Yang, G., Zhong, L., Jiang, L., Geng, C., Cao, J., Sun, X., et al. (2011). 6-gingerol prevents patulin-induced genotoxicity in HepG2 cells. *Phytother. Res*. 25, 1480–1485. doi: 10.1002/ptr.3446

Zhang, Q., Bethmann, C., Worth, N. F., Davies, J. D., Wasner, C., Feuer, A., et al. (2007). Nesprin-1 and -2 are involved in the pathogenesis of Emery Dreifuss muscular dystrophy and are critical for nuclear envelope integrity. *Hum. Mol. Genet*. 16, 2816–2833. doi: 10.1093/hmg/ddm238

**Conflict of Interest Statement:** The authors declare that the research was conducted in the absence of any commercial or financial relationships that could be construed as a potential conflict of interest.

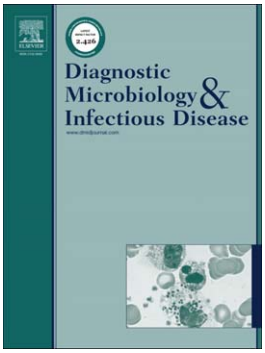


# Synthesis, antifungal activity of caffeic acid derivative esters, and their synergism with fluconazole and nystatin against *Candida* spp.

Janaína de Cássia Orlandi Sardi, Fernanda Patrícia Gullo, Irlan Almeida Freires, Nayla de Souza Pitangui, Maicon Petrônio Segalla, Ana Marisa Fusco-Almeida, Pedro Luiz Rosalen, Luís Octávio Regasini, Maria José Soares Mendes-Giannini

PII: S0732-8893(16)30239-5
DOI: doi: 10.1016/j.diagmicrobio.2016.08.002
Reference: DMB 14156

To appear in: *Diagnostic Microbiology and Infectious Disease*

Received date: 7 March 2016
Revised date: 11 July 2016
Accepted date: 5 August 2016

Please cite this article as: de Cássia Orlandi Sardi Janaína, Gullo Fernanda Patrícia, Freires Irlan Almeida, de Souza Pitangui Nayla, Segalla Maicon Petrônio, Fusco-Almeida Ana Marisa, Rosalen Pedro Luiz, Regasini Luís Octávio, Mendes-Giannini Maria José Soares, Synthesis, antifungal activity of caffeic acid derivative esters, and their synergism with fluconazole and nystatin against *Candida* spp., *Diagnostic Microbiology and Infectious Disease* (2016), doi: 10.1016/j.diagmicrobio.2016.08.002

# Synthesis, antifungal activity of caffeic acid derivative esters, and their synergism with fluconazole and nystatin against *Candida* spp.

Janaína de Cássia Orlandi Sardi[1,3,#], Fernanda Patrícia Gullo[1,#], Irlan Almeida Freires[3], Nayla de Souza Pitangui[1] Maicon Petrônio Segalla[2], Ana Marisa Fusco-Almeida[1], Pedro Luiz Rosalen[3], Luís Octávio Regasini[2,4], Maria José Soares Mendes-Giannini[1,*]

[1.] *Department of Clinical Analysis, Laboratory of Clinical Mycology, Faculty of Pharmaceutical Sciences, UNESP – Univ Estadual Paulista, Araraquara, SP, 14801-902 Brazil.*

[2] *Institute of Chemistry, Department of Biochemistry and Chemical Technology, UNESP – Univ Estadual Paulista, Araraquara, SP 14800-060, Brazil*

[3] *Department of Physiological Sciences, Piracicaba Dental School, University of Campinas, Piracicaba, SP, 13414-90, Brazil*

[4] *Institute of Biosciences, Letters and Exact Sciences, Department of Chemistry and Environmental Sciences, São José do Rio Preto, SP 15054-000, Brazil*

[#] *These authors contributed equally to this work.*

Correspondence to:

*Dr. Maria José Soares Mendes Giannini, Faculty of Pharmaceutical Sciences of Department of Clinical Analysis, Laboratory of Clinical Mycology, Univ Paulista (UNESP), R. Expedicionários do Brasil, 1621, CEP. 14801-902, Araraquara, São Paulo, Brazil
Tel: +55 – 16 – 3301 - 5716
e-mail: gianninimj@gmail.com / janasardi@gmail.com

**Key words:** Synergism, *Candida albicans*, Caffeic acid, Antifungal

**Abstract**

We tested the antifungal potential of caffeic acid and eight of its derivative esters against *C. albicans* ATCC 90028 and nine clinical isolates, and carried out a synergism assay with fluconazole and nystatin. Propyl caffeate (**C3**) showed the best antifungal activity against the tested strains. When in combination, **C3** markedly reduced the MIC of fluconazole and nystatin with synergistic effect up to 64-fold. Finally, **C3** showed a high $IC_{50}$ value and Selective Index (SI) against oral keratinocytes, demonstrating low toxicity against this cell type and selectivity for yeast cells. Further research should confirm its antifungal potential for development of combined therapy to treat *C. albicans* infections.

**Introduction**

Oral candidiasis is one of the most common opportunistic infections afflicting humans, with *Candida albicans* as the major causative agent of this disease (Garcia-Cuesta *et al*., 2014). The complexity of interactions between *Candida* and other microorganisms in the host, mainly bacteria, suggest that several mechanisms are involved in yeast fitness to the oral cavity. Some studies have shown that *Candida* spp. can co-aggregate with bacteria in dental plaque. This feature may be an important factor for the onset of oral candidiasis as well as fungal colonization of carious cavities and periodontal pockets (Sardi *et al*., 2012; Thurnheer *et al*., 2015). The presence of yeasts in subgingival regions may contribute to the pathogenesis of periodontal disease or increase the chance of candidemia, especially in cases of immunosuppression (Hannula *et al*., 2001; Reynaud *et al*., 2001; Al Mubarak *et al*., 2013). In addition, it has been well documented that systemic diseases such as diabetes and AIDS; physiological conditions such as pregnancy, infancy or old age; nutritional factors; treatment with broad-spectrum antibiotics; use of immunosuppressive drugs and corticosteroids; xerostomia, and use of dentures, may predispose the individual to develop candidiasis (Soll, 2002; Tekeli *et al*., 2004; Manfredi *et al*., 2006).

The current therapy with antifungals has serious drawbacks, in particular due to toxic effects to human cells and adverse effects (Epstein *et al*., 2002; Gabler *et al*., 2008). As the drugs used to treat candidiasis are not always specific and properly prescribed (targeting the causative agent of infection), there has been a significant increase in resistance of *Candida* spp. to traditional antifungal drugs. The increasing microbial resistance rates may also be a result of long-term drug exposure or selection of strains with

intrinsic resistance mechanisms (Ying *et al*., 2013; Fernandez-Ruiz *et al*., 2015; Liao *et al*., 2015; Seifi *et al*., 2015; Freitas *et al*., 2015). Therefore, the development of novel strategies to minimize the toxic effects of current antifungals and improve their effectiveness, has been strongly encouraged.

Natural products have continued to be a rich source of new drugs with clinically significant biological targets. Over the past 34 years, 49% of FDA-approved chemotherapeutic drugs were either natural products or directly derived therefrom (Newman & Cragg, 2016). There is a great interest of the pharmaceutical industry in the discovery of new molecules of natural origin or even their combination with existing drugs, in order to improve efficacy, potency, safety, tolerability, and decrease production costs, side effects and selection of resistant strains (Svetaz *et al*., 2016). A number of studies in the literature have established the value of combined antifungal therapy against resistant strains, in particular standard drugs with naturally-occurring agents (Pippi *et al*., 2015; Han *et al*., 2016).

Caffeic acid (3,4-dihydroxycinnamic acid) is an important phenolic compound commonly found in plants, foods and propolis samples, particularly in the form of caffeic acid phenethyl ester (CAPE) (Paracatu *et al*., 2014; Rzepecka-Stojko *et al*., 2015). It is better known for its pharmacological properties, including antimicrobial, antioxidant, anti-inflammatory and anticancer (Balachandran *et al*., 2012; Kuo *et al*., 2015). Nevertheless, modifications of the caffeic acid structure into esters or amides, for instance, may generate novel analog molecules with enhanced and desired biological activity (Touaibia *et al*., 2011), particularly as antimicrobials (Fu *et al*., 2010).

Herein, we investigated the antifungal potential of caffeic acid and eight of its derivative esters against *C. albicans* ATCC 90028 and nine oral clinical isolates. The most active molecule, propyl caffeate (**C3**), was selected for a synergism assay with fluconazole and nystatin against the *C. albicans* strains, and tested for its toxicity on oral keratinocytes (NOK cells).

## Material and Methods

***Synthesis of Esters.*** Caffeic acid (0.2 mM) solution and corresponding alcohols (20 mM) were prepared at 5°C with a solution of *N*, *N*′-dicyclohexylcarbodiimide (DCC, 1.0 mM) in *p*-dioxane (3.0 mL). After the solution was stirred for 48 h, the solvent was removed under reduced pressure. The residue was partitioned three-times with EtOAc and filtered. The

filtrate was serially washed with saturated aqueous citric acid solution (three times), saturated aqueous $NaHCO_3$ (three-times), water (two-times), dried over $MgSO_4$, and evaporated under reduced pressure. The crude products were purified over a silica gel column using an isocratic system of $CHCl_3$–MeOH (98:2). The modifications made in caffeic acid molecule are shown in Table 1.

***Microorganisms.*** *Candida albicans* ATCC 90028 strain and nine highly virulent clinical isolates of *C. albicans* obtained from the oral cavity of patients with diabetics and periodontitis (Sardi *et al*., 2012), were used in this study. This study was approved by the research ethics committee at Piracicaba Dental School, University of Campinas, Piracicaba, SP, Brazil (protocol no. 062/2008).

***Determination of Antifungal Activity.*** The Minimum Inhibitory Concentration (MIC) of caffeic acid and its eight derivatives against *C. albicans* ATCC 90028 was determined using 96-well microplates based on the protocol M27-A3 of the CLSI (2008), with modifications. The esters that showed the lowest MIC values against *C. albicans* ATCC 90028 (C3, C4 and C6) were then tested against nine clinical isolates of *C. albicans*. The synthetic compounds of caffeic acid were diluted in DMSO and tested in concentrations ranging from 250 µg/mL to 0.48 µg/mL (Scorzoni *et al*., 2007). The inoculum was prepared (λ 530 nm, Abs 0.08-0.1) and diluted to 2.5 x $10^3$ CFU/mL. The plates were incubated at 35°C for 24 h. The $MIC_{100}$ was determined as the lowest concentration of the compound inhibiting visible fungal growth as indicated by 0.1% resazurin (Sigma-Aldrich, St. Louis, MO, USA). Aliquots from the wells corresponding to the MIC and higher concentrations were sub-cultured on Sabouraud Dextrose Agar (Difco®, Detroit, MI, USA) for determination of the Minimum Fungicidal Concentration (MFC). The MFC was defined as the lowest concentration of the compound causing no visible growth on the agar plate.

***Combinatorial Antifungal Activity (Synergism Assay).*** The ester which showed the best activity against *C. albicans* strains (**C3**) was combined with conventional antifungals commonly used for the treatment of candidiasis, fluconazole and nystatin. Their combinatorial antifungal activity was determined through the checkerboard method using 96-well microplates (Dai *et al*., 2015). A mathematical calculation was used to generate the fractional inhibitory concentration index (FICI), as follows: FICI = (MIC compound 1 in combination / MIC compound 1 alone) + (MIC compound 2 in combination / MIC compound 2 alone). The combinations were classified as synergistic (FICI ≤ 0.5), additive

(0.5 < FICI ≤ 1.0), indifferent (1.0 < FICI < 4.0) and antagonistic (FICI ≥ 4.0) (Soares *et al*., 2014).

***Cytotoxic Effects on Oral Keratinocytes.*** The most active ester derivative (**C3**) as well as fluconazole and nystatin were tested for their cytotoxicity against keratinocytes from the oral mucosa of humans (NOK cells) provided by the Department of Medicine at Harvard Medical School (Dr. Karl Munger). NOK cells were maintained in culture medium for keratinocytes without fetal bovine serum (Gibco, Life Technologies) at 36.5ºC and 5% $CO_2$. Cells were seeded onto a 96-well plate at a density of 5 x $10^4$ cells/well for 24 h. Then the cells were exposed to the treatments (**C3**, Fluconazole, Nystatin, and their combinations) for 24 h. Cell viability was determined by adding aliquots of 10µL of MTT solution (5 mg/mL) (Sigma-Aldrich, St. Louis, MO) to each well. The plates were incubated at 37ºC for 4 h to allow for visualization of precipitated formazan crystals. Aliquots of 100 µL of isopropyl alcohol were added *per* well and absorbance was read using a spectrophotometer at 560 nm (Mosmann *et al*., 1983). Hydrogen peroxide (10%) was used as a positive control for cytotoxicity and untreated cells were considered as the negative control. Based on this cell viability assay, we next determined the half maximal inhibitory concentration ($IC_{50}$) for the esters, standard-drugs and their combinations. The IC50 was defined as the effective concentration of the compound able to inhibit 50% of the NOK cells. The establishment of this concentration was essential to calculate the selectivity index (SI) (IC50/MIC ratio), which was used as an indicator of potential toxicity against normal cells lines at the effective therapeutic concentration for each strain. Hence, the selectivity index (SI) indicated the relationship between drug toxicity against *C. albicans* and the host cells (Gullo et al., 2012; Mora-Navarro et al., 2016).

***Statistical Analysis.*** All assays were performed in triplicate of independent experiments. The data were analyzed on Graphpad Prism 5.0 (San Diego, CA, USA) by one-way analysis of variance (ANOVA) followed by Bonferroni's multiple comparison test, with a significance level of 5%.

## Results

***Structure-Activity Relationship of Caffeic Acid Derivatives.*** A screening for antifungal activity of caffeic acid and eight derivative esters against *C. albicans* was carried out.

These esters differ by the number of constituent carbons in the molecule, as shown in Table 1. Caffeic acid and all of its synthesized derivatives showed a fungicidal activity against *C. albicans* ATCC 90028 and presented a structure-activity relationship. As seen in Table 2, the caffeic acid molecule (**C0**) without structural change and the derived **C1** showed MIC and MFC values of 125 µg/mL. The derivatives **C2**, **C5**, **C7** and **C8** showed MIC and MFC values of 31.25 µg/mL. **C3** and **C4** showed strong fungicidal activity against *C. albicans* ATCC 90028, with MIC and MFC values of 15.62 µg/mL, together with **C6** which showed MIC and MFC equal to 7.81 µg/mL. Thus, the compounds **C3**, **C4** and **C6** – which were better than their originating caffeic acid molecule – were further tested against nine oral clinical isolates of *C. albicans.* As shown in Table 3, the compound **C3** demonstrated the best activity when compared with the other caffeic acid derivatives (**C4** and **C6**), with MIC and MFC values ranging between 7.81 and 62.5 µg/mL. The MIC and MFC of **C4** and **C6** ranged between 31.25-125 µg/mL and 7.81-≥250 µg/mL, respectively.

***Combinatorial Antifungal Activity with Standard Drugs.*** Given the strong antifungal activity of **C3** against *C. albicans* strains, we next investigated its combinatorial activity with the standard drugs fluconazole and nystatin. A synergistic activity was observed for the combination between **C3** and fluconazole against most strains, with FICI values ranging from 0.06 to 0.5. Indifferent activity was observed against two clinical isolates, with FICI values close to 2.0. When comparing the MIC values of **C3** and fluconazole alone and combined, we observed a decrease in their MIC and potentiation of fluconazole of 2 to 64-fold (Table 4). The combination of **C3** with nystatin was advantageous (synergistic) against three out of the ten strains when compared with the MIC values of the compounds tested alone, with potentiation of nystatin by 8- to 64-fold. Additive activity was observed against four clinical isolates and *C. albicans* ATCC 90028 strain, with FICI values ranging from 0.53 to 1.0. The additive activity of the combination showed potentiation of nystatin between 32- and 64-fold.

***Toxic Effects on Oral Keratinocytes.*** A viability assay was carried out to evaluate the toxicity of **C3** and standard drugs alone and in combination, against NOK cells. The antifungal compound **C3** showed low toxicity at the tested concentrations, with a high $IC_{50}$ value of 420 µg/mL. Likewise, fluconazole and nystatin showed high $IC_{50}$ values of 320

µg/mL and 400 µg/L, respectively. When combined, both **C3** and the antifungals had their SI value increased, indicating selectivity for yeasts rather than NOK cells (Table 5).

Figure 1 shows the percentage of cell viability of NOK cells treated with the antifungal compounds at different concentrations. The data showed that treatment with **C3**, fluconazole and nystatin maintained over 80% cell viability at all tested concentrations. Hydrogen peroxide, used as a positive control, markedly affected cell viability, with a significant difference when compared to **C3** and standard drugs ($P < 0.05$).

## Discussion

Opportunistic infections caused by *Candida* spp. have still been considered a recurrent health issue with high burden worldwide (Rodriguez-Tudela *et al*., 2015; Denning & Gugnani, 2015). Thus, novel therapeutic approaches are much needed to treat *Candida* infections, including the use of naturally-occurring agents. In this study, we demonstrate the antifungal potential of caffeic acid derivatives against *C. albicans* and their successful synergism with antifungals commercially available.

Caffeic acid is commonly found in fruits (Balachandran *et al*., 2012) and propolis samples (Freires *et al*., 2016) used in daily life products and folk medicine. We showed that caffeic acid molecule has fungicidal activity against *C. albicans* ATCC 90028. Nevertheless, the structural modifications performed in this study rendered the caffeic acid molecule much more effective in terms of fungicidal activity, showing a structure-activity relationship. The addition of 2 to 8 carbon atoms in the caffeic acid molecule increased its anti-*Candida* activity. Other studies have also demonstrated the relationship between the number of carbons and the antifungal activity of the molecule (Nihei *et al*., 2003; Soares *et al*., 2014). Among the synthesized compounds, **C3** showed better activity when compared with other caffeic acid derivatives (**C4** and **C6**), showing lower minimum inhibitory and fungicidal concentrations against most strains. Balachandran *et al*. (2012) isolated methyl caffeate from *Solanum torvum* plant and showed antibacterial activity against Gram-negative and Gram-positive bacteria, in addition to antifungal activity against *C. albicans* and *Apergillus flavus*. These findings confirm the antimicrobial potential of caffeic acid derivatives.

Of note, the clinical isolates used in this study showed lower susceptibility to nystatin and fluconazole when compared with the reference strain of *C. albicans* ATCC

90028. This could be due to acquisition of resistance mechanisms as the isolates belonged to diabetic patients. A recent study showed that this group of patients is prone to develop *Candida* infections in cases of poor glycemic control (Zomorodian *et al*., 2016).

Microbial resistance has raised concern over the last decades as the investment in antibiotic discovery is declining considerably over time when compared to high-priced drugs such as chemotherapeutics (Bax & Green, 2015). To make it worse, failure in prescribing the appropriate drug, misuse, and long hospital stay have led to the emergence of azole-resistant isolates, particularly in cases of invasive infections (Liao *et al*., 2015; Sanguinetti, Posteraro & Lass-Flörl, 2015). This opens avenues for the development of combined antifungal therapy, in which drugs with different mechanisms of action (or not) are combined to enhance their antifungal potency and avoid selection of resistant strains. Here, we demonstrated the successful combination of propyl caffeate (**C3**) with fluconazole and nystatin against *C. albicans* strains. A study performed by Lee & Han (2005) demonstrated the synergistic effect of the combination between amphotericin B and berberine (alkaloid) against *C. albicans*. These authors also tested this combination in mice with candidemia and observed that the combined treatment prolonged the lives of mice in 22 days compared to those treated with amphotericin B alone. Other studies have reported the successful combination of essential oils with conventional drugs, including nystatin, fluzonazole and micafugin (Aprotosoaie *et al*., 2008; Rosato *et al*., 2009; Rodrigues *et al*., 2012; Stringaro *et al*., 2014).

With the purpose of future clinical use, we also investigated the effects of **C3** against oral keratinocytes and compared them with those of the standard drugs. NOK cells were chosen for this study as they constitute the main epithelial cell type lining the oral mucosa, which would be highly exposed in case of administration of an oral suspension or a solution for oral candidiasis. Overall, low toxicity was found for **C3**, fluconazole and nystatin, with $IC_{50}$ values higher than their MIC/MFC. These agents also showed a high SI value, which means that if the index is greater than 10.0 the compound exhibits selectivity for killing yeasts rather than the host's cells. The combination between **C3** and fluconazole led to a considerable increase in their SIs, highlighting their selectivity for yeast cells.

Collectively, our findings indicate that the propyl ester modification of caffeic acid molecule (**C3**) has strong fungicidal activity and potentiated the effects of fluconazole and nystatin against *C. albicans* strains, with little effects against oral keratinocytes. Further

studies should focus on the effects of these combinations against *Candida* biofilms and establish **C3** mechanism(s) of action.

The authors declare no conflict of interest.

**References**

Al Mubarak S, Robert AA, Baskaradoss JK, Al-Zoman K, Al Sohail A, Alsuwyed A, Ciancio S (2013) The prevalence of oral *Candida* infections in periodontitis patients with type 2 diabetes mellitus. J Infect Public Health. 6: 296-301.

Aprotosoaie AC, Hăncianu M, Poiată A, Tuchiluş C, Spac A, Cioană O, Gille E, Stănescu U (2008) In vitro antimicrobial activity and chemical composition of the essential oil of *Foeniculum vulgare Mill*. Rev Med Chir Soc Med Nat Iasi. 112: 832-836.

Balachandran C, Duraipandiyan V, Al-Dhabi NA, Balakrishna K, Kalia NP, Rajput VS, Khan IA, Ignacimuthu S (2012) Antimicrobial and Antimycobacterial Activities of Methyl Caffeate Isolated from *Solanum torvum Swartz*. Fruit Indian J Microbiol. 52: 676-681.

Bax R, Green S (2015) Antibiotics: the changing regulatory and pharmaceutical industry paradigm. J Antimicrob Chemother. 70: 1281-1284.

Clinical and Laboratory Standards Institute (CLSI) (2008) Protocol M27-A3. Reference Method for Broth Dilution Antifungal Susceptibility Testing of Yeasts. 3.ed. Pennsylvania: CLSI.

Cordeiro RA, Teixeira CE, Brilhante RS, Castelo-Branco DS, Alencar LP, de Oliveira JS, Monteiro AJ, Bandeira TJ, Sidrim JJ, Moreira JL, Rocha MF (2015) Exogenous tyrosol inhibits planktonic cells and biofilms of *Candida* species and enhances their susceptibility to antifungals. FEMS Yeast Res 15: doi: 10.1093/femsyr/fov012.

Dai L, Zang C, Tian S, Liu W, Tan S, Cai Z, Ni T, An M, Li, R, Gao Y, Zhang D, Jiang Y (2015) Design, synthesis, and evaluation of caffeic acid amides as synergists to sensitize fluconazole-resistant *Candida albicans* to fluconazole. Bioorg Med Chem Lett 25:34-37.

Denning DW, Gugnani HC (2015) Burden of serious fungal infections in Trinidad and Tobago. Mycoses. 58: 80-84.

Epstein JB. Dawson JR, Buivids IA, Wong B, Le ND (2002) The effect of a disinfectant/coolant irrigant on microbes isolated from dental unit water lines. Spec Care Dentist 22:137-141.

Fernández-Ruiz M, Puig-Asensio M, Guinea J, Almirante B, Padilla B, Almela M, Díaz-Martín A, Rodríguez-Baño J, Cuenca-Estrella M, Aguado JM, CANDIPOP Project; GEIH-GEMICOMED (SEIMC); REIPI. (2015) *Candida tropicalis* bloodstream infection: Incidence, risk factors and outcome in a population-based surveillance. J Infect 71: 385-394.

Freires IA, Queiroz VC, Furletti VF, Ikegaki M, de Alencar SM, Duarte MC, et al. (2016) Chemical composition and antifungal potential of Brazilian propolis against *Candida* spp. J Mycol Med. doi: 10.1016/j.mycmed.2016.01.003.

Freitas EM, Monteiro LC, Fernandes MB, Martelli Junior H, Bonan PR, Nobre SA (2015) Antifungal susceptibility in vitro determined by the Etest® for *Candida* obtained from the oral cavity of irradiated and elderly individuals. Braz Dent J 26: 99-104.

Fu J, Cheng K, Zhang Z, Fang R, Zhu H (2010) Synthesis, structure and structure–activity relationship analysis of caffeic acid amides as potential antimicrobials. Eur J Med Chem 45:2638-2643.

Gabler IG, Barbosa AC, Velela RR, Lyon S, Rosa CA (2008) Incidence and anatomic localization of oral candidiasis in patients with AIDS hospitalized in a public hospital in Belo Horizonte, MG, Brazil. J Appl Oral Sci 16: 247-250.

Garcia-Cuesta C, Sarrion-Pérez MG, Bagán JV (2014) Current treatment of oral candidiasis: A literature review. J Clin Exp Dent 6: e576-82.

Gullo FP, Sardi JC, Santos VA, Sangalli-Leite F, Pitangui NS, Rossi SA, de Paula E Silva AC, Soares LA, Silva JF, Oliveira HC, Furlan M, Silva DH, Bolzani VS, Mendes-Giannini MJ, Fusco-Almeida AM (2012) Antifungal activity of maytenin and pristimerin. Evid Based Complement Alternat Med 2012:340787.

Han Y, Lee JH (2005) Berberine synergy with amphotericin B against disseminated candidiasis in mice. Biol Pharm Bull 28: 541-544.

Han B, Chen J, Yu Y, Cao Y, Jiang Y (2016) Antifungal activity of *Rubus chingii* extract combined with fluconazole against fluconazole-resistant *Candida albicans.* Microbiol Immunol 60: 82-92.

Hannula J, Dogan B, Slots J, Okte E, Asikainen S (2001) Subgingival strains of *Candida albicans* in relation to geographical origin and occurrence of periodontal pathogenic bacteria. Oral Microbiol Immunol 16: 113-118.

Kuo YY, Jim WT, Su LC, Chung CJ, Lin CY, Huo C, Tseng JC, Huang SH, Lai CJ, Chen BC, Wang BJ, Chan TM, Lin HP, Chang WS, Chang CR, Chuu CP (2015) Caffeic Acid phenethyl ester is a potential therapeutic agent for oral cancer Int J Mol Sci 16: 10748-10766.

Liao X, Qiu H, Li R, Guo F, Liu W, Kang M, Kang Y, China-SCAN Team (2015) Risk factors for fluconazole-resistant invasive candidiasis in intensive care unit patients: An analysis from the China Survey of Candidiasis study. J Crit Care 30: 862.e1-5.

Manfredi M, McCullough MJ, Al-Karaawi ZM, Vescovi P, Porter SR (2006) In vitro evaluation of virulence attributes of *Candida* spp. isolated from patients affected by diabetes mellitus. Oral Microbiol Immunol 21:183-189.

Mora-Navarro C, Méndez-Vega J, Caraballo-León J, Lee M-r, Palecek S, Torres-Lugo M, *et al*. (2016) Hydrophobicity of Antifungal β-Peptides Is Associated with Their Cytotoxic Effect on *In Vitro* Human Colon Caco-2 and Liver HepG2 Cells. PLoS ONE 11(3): e0149271. doi:10.1371/journal. pone.0149271.

Newman DJ, Cragg GM (2016) Natural Products as Sources of New Drugs over the 30 Years from 1981 to 20140. J Nat Prod. DOI: 10.1021/acs.jnatprod.5b01055. [In press].

Nihei K, Nihei A, Kubo I (2003) Rational design of antimicrobial agents: antifungal activity of alk(en)yl dihydroxybenzoates and dihydroxyphenyl alkanoates. Bioorg Med Chem Lett 13: 3993-3996.

Paracatu LC, Bonacorsi C, de Farias CM, Nazare AC, Petronio MS, Regasini LO, Silva DH, Raddi MS, da Fonseca LM, Ximenes VF (2014) Alkyl caffeates as anti-*Helicobacter pylori* and scavenger of oxidants produced by neutrophils. Med Chem. 10: 74-80.

Pippi B, Lana AJD, Moraes RC, Güez CM, Machado M, Oliveira LFS, *et al*. (2015) *In vitro* evaluation of the acquisition of resistance, antifungal activity and synergism of Brazilian red propolis with antifungal drugs on *Candida* spp. J Appl Microbiol. 118:839-850.

Reynaud AH, Nygaard-Østby B, Bøygard GK, Eribe ER, Olsen I, Gjermo P (2001) Yeasts in periodontal pockets. J Clin Periodontol 28: 860-864.

Rodrigues FF, Oliveira LG, Rodrigues FF, Saraiva ME, Almeida SC, Cabral ME, Campos AR, Costa JG (2012) Chemical composition, antibacterial and antifungal activities of essential oil from *Cordia verbenacea* DC leaves. Pharmacognosy Res 4: 161-165.

Rodriguez-Tudela JL, Alastruey-Izquierdo A, Gago S, Cuenca-Estrella M, León C, Miro JM, *et al.* (2015) Burden of serious fungal infections in Spain. Clin Microbiol Infect. 21: 183-189.

Rosato A, Vitali C, Piarulli M, Mazzotta M, Argentieri MP, Mallamaci R (2009) In vitro synergic efficacy of the combination of Nystatin with the essential oils of *Origanum vulgare* and *Pelargonium graveolens* against some *Candida* species. Phytomedicine 16: 972-975.

Rzepecka-Stojko A, Kabała-Dzik A, Moździerz A, Kubina R, Wojtyczka RD, Stojko R, Dziedzic A, Jastrzębska-Stojko Ż, Jurzak M, Buszman E, Stojko J (2015) Caffeic Acid phenethyl ester and ethanol extract of propolis induce the complementary cytotoxic effect on triple-negative breast cancer cell lines. Molecules 20: 9242-9262.

Sanguinetti M, Posteraro B, Lass-Flörl C (2015) Antifungal drug resistance among *Candida* species: mechanisms and clinical impact. Mycoses 58:2-13.

Sardi JC, Duque C, Höfling JF, Gonçalves RB (2012) Genetic and phenotypic evaluation of *Candida albicans* strains isolated from subgingival biofilm of diabetic patients with chronic periodontitis. Med Mycol 50: 467-475.

Scorzoni L, Benaducci T, Fusco-Almeida AM, Silva DHS, Bolzani VS, Mendes-Giannini MJS (2007) "The use of standard methodology for determination of antifungal activity of natural products against medical yeasts *Candida* sp and *Cryptococcus* sp. Brazilian Journal Microbiology 38: 391–397.

Seifi Z, Zarei-Mahmoudabadi A, Zarrin M (2015) Extracellular enzymes and susceptibility to fluconazole in *Candida* strains isolated from patients with vaginitis and healthy individuals. Jundishapur J Microbiol 8: e20162.

Soares LA, Gullo FP, Sardi Jde C, Pitangui Nde S, Costa-Orlandi CB, Sangalli-Leite F, Scorzoni L, Regasini LO, Petrônio MS, Souza PF, Silva DH, Mendes-Giannini MJ, Fusco-Almeida AM (2014) Anti-*trichophyton* activity of protocatechuates and their synergism with fluconazole. Evid Based Complement Alternat Med. 2014: 957860.

Soll DR (2002) *Candida* commensalism and virulence: the evolution of phenotypic plasticity. Acta Trop 81: 101-110.

Stringaro A, Vavala E, Colone M, Pepi F, Mignogna G, Garzoli S, Cecchetti S, Ragno R, Angiolella L (2014) Effects of *Mentha suaveolens* Essential Oil Alone or in Combination with Other Drugs in *Candida albicans*. Evid Based Complement Alternat Med. 2014:125904.

Svetaz LA, Postigo A, Butassi E, Zacchino SA, Sortino MA (2016) Antifungal drugs combinations: a patent review 2000-2015. Exp Opin Therapeut Patent. DOI: 10.1517/13543776.2016.1146693. [In press].

Tekeli A, Dolapci I, Emral R, Cesur S (2004) *Candida* carriage and *Candida dubliniensis* in oropharyngeal samples of type-1 diabetes mellitus patients. Mycoses 47: 315-318.

Thurnheer T, Bostanci N, Belibasakis GN (2015) Microbial dynamics during conversion from supragingival to subgingival biofilms in an in vitro model. Mol Oral Microbiol. doi: 10.1111/omi.12108.

Touaibia M, Jean-François J, Doiron J (2011) Caffeic Acid, A Versatile Pharmacophore: An Overview. Mini-Rev Med Chem 11:695-713.

Ying Y, Zhao Y, Hu X, Cai Z, Liu X, Jin G, Zhang J, Zhang J, Liu J, Huang X (2013) In vitro fluconazole susceptibility of 1,903 clinical isolates of *Candida albicans* and the identification of ERG11 mutations. Microb Drug Resist 19: 266-273.

Zomorodian K, Kavoosi F, Pishdad GR, Mehriar P, Ebrahimi H, Bandegani A, *et al*. (2016) Prevalence of oral Candida colonization in patients with diabetes mellitus. J Mycol Med. DOI:http://dx.doi.org/10.1016/j.mycmed.2015.12.008.

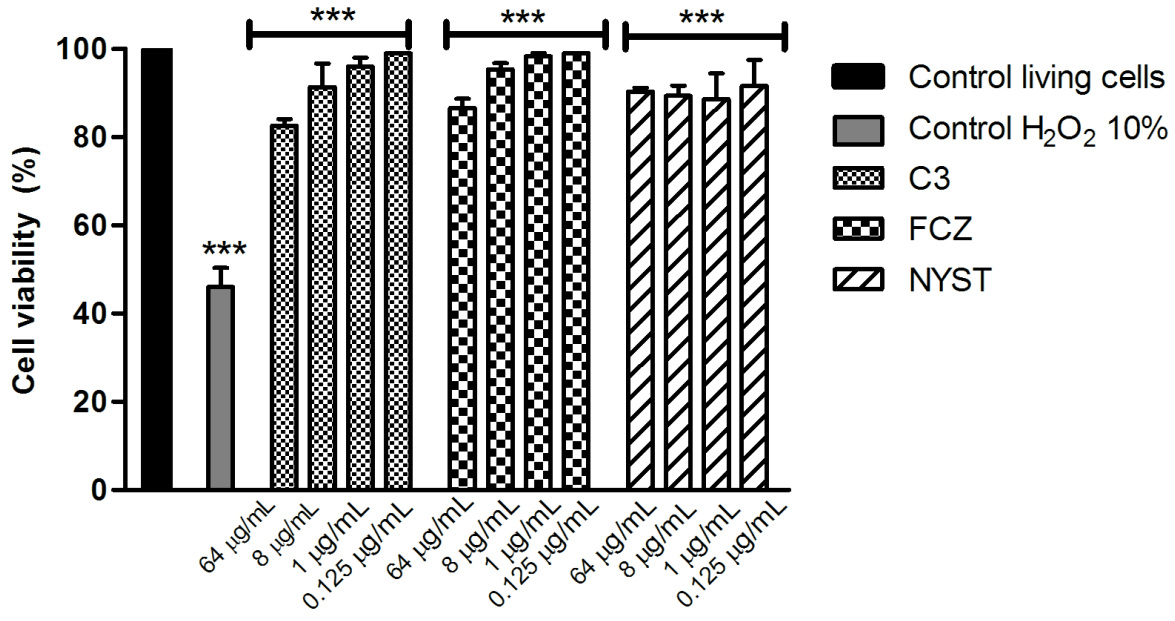


Figure 1

**Table 1.** Nomenclature, molecular formulas and the chemical structures of the caffeic acid derivative esters tested in this study.

| Code | Nomenclature | Molecular Formula | Chemical Structure |
|---|---|---|---|
| **C0** | Caffeic acid | $C_9H_8O_4$ | 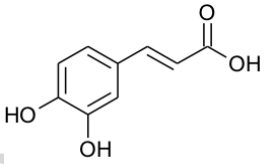 Caffeic acid |
| **C1** | Methyl caffeate | $C_{10}H_8O_4$ | 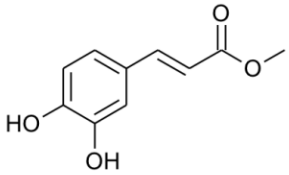 Methyl caffeate |
| **C2** | Ethyl caffeate | $C_{11}H_{12}O_4$ | 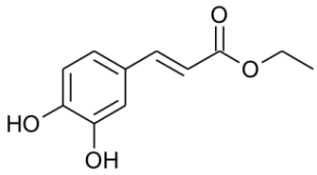 Ethyl caffeate |
| **C3** | Propyl caffeate | $C_{12}H_{14}O_4$ | 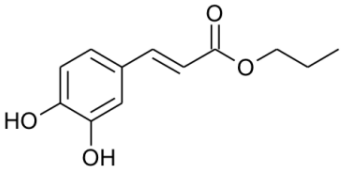 Propyl caffeate |
| **C4** | Butyl caffeate | $C_{13}H_{16}O_4$ | 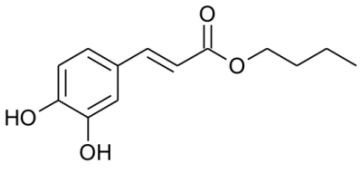 Butyl caffeate |
| **C5** | Pentyl caffeate | $C_{14}H_{18}O_4$ | 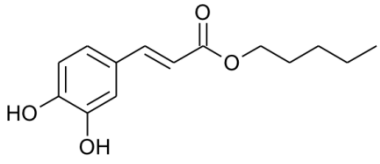 Pentyl caffeate |
| **C6** | Hexyl caffeate | $C_{15}H_{20}O_4$ | 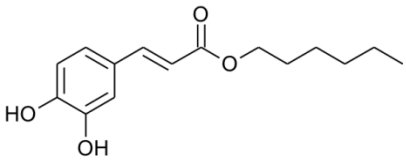 Hexyl caffeate |

| | | |
|---|---|---|
| **C7** | Heptyl caffeate | $C_{16}H_{22}O_4$ |

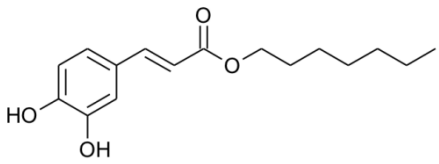


Heptyl caffeate

| | | |
|---|---|---|
| **C8** | Octyl caffeate | $C_{17}H_{24}O_4$ |

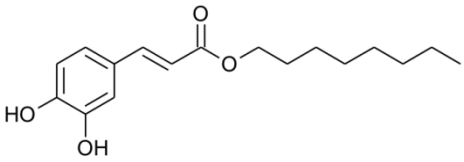


Octyl caffeate

**Table 2.** Antifungal activity of caffeic acid derivative esters against *Candida albicans* ATCC 90028.

| **Caffeic Acids Derivates** | ***Candida albicans* ATCC 90028** | |
|---|---|---|
| | **MIC (µg/mL)** | **MFC (µg/mL)** |
| **C0** | 125 | 125 |
| **C1** | 125 | 125 |
| **C2** | 31.25 | 31.25 |
| **C3** | 15.62 | 15.62 |
| **C4** | 15.62 | 15.62 |
| **C5** | 31.25 | 31.25 |
| **C6** | 7.81 | 7.81 |
| **C7** | 31.25 | 31.25 |
| **C8** | 31.25 | 31.25 |
| **Nystatin** | 4.0 | 4.0 |
| **Fluconazole** | 0.5 | 0.5 |

**Table 3**. Antifungal activity of caffeic acid derivative esters (**C3**, **C4** and **C6**) against nine oral clinical isolates of *Candida albicans*. MIC/MFC values are expressed in µg/mL.

| ***C. albicans*** | **C3** | | **C4** | | **C6** | | **Fluconazole** | | **Nystatin** | |
|---|---|---|---|---|---|---|---|---|---|---|
| **clinical isolates** | **MIC** | **MFC** | **MIC** | **MFC** | **MIC** | **MFC** | **MIC** | **MFC** | **MIC** | **MFC** |
| **Ca#22** | 7.81 | 7.81 | 31.25 | 31.25 | 7.81 | 7.81 | 8.0 | 8.0 | 8.0 | 8.0 |
| **Ca#25** | 31.25 | 31.25 | 62.50 | 62.50 | 125 | 125 | 8.0 | 8.0 | 8.0 | 8.0 |
| **Ca#45** | 15.62 | 15.62 | 31.25 | 31.25 | 125 | 125 | 8.0 | 8.0 | 8.0 | 8.0 |
| **Ca#50** | 31.25 | 31.25 | 125 | 125 | >250 | >250 | 2.0 | 2.0 | 4.0 | 4.0 |
| **Ca#61** | 31.25 | 31.25 | 62.50 | 62.50 | >250 | >250 | 0.5 | 0.5 | 8.0 | 8.0 |
| **Ca#62** | 7.81 | 7.81 | 31.25 | 31.25 | 7.81 | 7.81 | 8.0 | 8.0 | 8.0 | 8.0 |
| **Ca#63** | 31.25 | 31.25 | 62.50 | 62.50 | >250 | >250 | 8.0 | 8.0 | 8.0 | 8.0 |
| **Ca#105** | 31.25 | 31.25 | 125 | 125 | >250 | >250 | 8.0 | 8.0 | 8.0 | 8.0 |
| **Ca#124** | 62.50 | 62.50 | 125 | 125 | >250 | >250 | 4.0 | 4.0 | 8.0 | 8.0 |

**Table 4**. Antifungal effects of propyl caffeate (**C3**) combined with fluconazole and nystatin against *Candida albicans* ATCC 90028 and nine oral clinical isolates. MIC values are expressed in µg/mL.

| *C. albicans* strains | FCZ + C3 | | | | NYST + C3 | | | |
|---|---|---|---|---|---|---|---|---|
| | FCZ (MIC) | C3 (MIC) | FICI | Effect /Potentiation FCZ | NYST (MIC) | C3 (MIC) | FICI | Effect /Potentiation NYST |
| **ATCC 90028** | 0.25 | 0.12 | 0.50 | Synergistic /2X | 0.125 | 7.81 | 0.53 | Additive/32X |
| **Ca#22** | 0.125 | 15.62 | 2.01 | Indifferent/64X | 0.125 | 15.62 | 2.01 | Indifferent/64X |
| **Ca#25** | 0.5 | 0.12 | 0.06 | Synergistic/16X | 4.0 | 31.25 | 1.50 | Indifferent/2X |
| **Ca#45** | 1.0 | 0.12 | 0.13 | Synergistic/8X | 0.5 | 15.62 | 1.06 | Indifferent/16X |
| **Ca#50** | 0.5 | 3.90 | 0.37 | Synergistic/4X | 0.5 | 3.90 | 0.24 | Synergistic/8X |
| **Ca#61** | 0.25 | 0.12 | 0.50 | Synergistic/2X | 0.125 | 31.25 | 1.01 | Indifferent/64X |
| **Ca#62** | 0.125 | 15.62 | 2.01 | Indifferent/64X | 0.125 | 15.62 | 2.01 | Indifferent/64X |
| **Ca#63** | 1.0 | 1.95 | 0.18 | Synergistic/8X | 0.125 | 15.62 | 0.51 | Additive /64X |
| **Ca#105** | 0.5 | 0.48 | 0.07 | Synergistic/16X | 0.25 | 31.25 | 1.03 | Indifferent/32X |
| **Ca#124** | 0.5 | 0.12 | 0.12 | Siyergistic/ 8X | 0.25 | 15.62 | 0.28 | Synergistic/32X |

**Table 5.** $IC_{50}$ value and Selective Index (SI) of propyl caffeate (**C3**), fluconazole (FCZ) and nystatin (NYST) showing the toxicity of the compounds against yeasts in relationship to human oral keratinocytes (NOK cells).

| Compound | $IC_{50}$ (µg/mL) | SI (alone) | SI (combination) |
|---|---|---|---|
| **C3** | 420 | 13.5 | 26.9 (FCZ) / 13.5 (NYST) |
| **FCZ** | 320 | 40 | 320 |
| **NYST** | 400 | 50 | 100 |

## Highlights

- Caffeic acid and eight of its derivative esters were tested for their activity against *Candida* spp.
- Propyl caffeate (**C3**) was the most active compound against reference strain and clinical isolates.
- When combined, **C3** markedly reduced the MIC of fluconazole and nystatin up to 64-fold.
- **C3** showed low toxicity against oral keratinocytes and high selectivity for yeast cells.
- Further research should focus on its combined therapy to treat *C. albicans*-related infections.